

**Assessing the pharmacological properties of Novel  
Psychoactive Substances (NPS) identified online: *in  
silico* studies on designer benzodiazepines and  
novel synthetic opioids**

Submitted in partial fulfilment of the requirements of the  
University of Hertfordshire for the degree of PhD  
by Valeria Catalani

Supervisors: Prof Fabrizio Schifano  
Ass Prof Amira Guirguis  
Mr John Corkery  
Dr Michelle Botha

October 2022

**In loving memory of my Grandmother Luigia, I know you would be so  
proud of me**

## Acknowledgements

I would like to express my gratitude to my PhD supervisory team: Prof. Fabrizio Schifano , Associate Professor Amira Guirguis, Mr John Corkery and Dr Michelle Botha. Without their guidance, support and direction none of this would have been possible. Their immense knowledge, plentiful experience, dedication, and determination have kept me inspired and encouraged throughout my journey and my academic research. Thanks for supporting my research ideas and choices. A special thanks to my Prof Schifano who made me feel supported in all my decisions and has always been by my side.

I would like to thank Alessandro Vento and Damicon for giving me the opportunity to use *NPSfinder*<sup>®</sup> as an important part of my research project; the Chem Com group for their support and guidance with MOE<sup>®</sup> and Cresset for providing free access and support for their software Forge<sup>™</sup>.

Moreover, I am enormously thankful to Giuseppe Floresta and Al Ajamian for their continuous support in the computational analysis, their patience and their guidance which were essential for me.

I would like to extend thanks to the University of Hertfordshire and all the staff members within the Department of Clinical and Pharmaceutical Sciences who always provided me with support and patiently and professionally guided me through this journey.

Finally I would like to dedicate this thesis to my loving parents Antonella and Rolando, my sister Giulia, my auntie Nico and Bruce who have always supported and encouraged me and most importantly believed in me. Mum and Dad, without you I would not have achieved any of the goals I have so far, I am truly grateful.

## Abstract

### Background

By 2022, a total of 1,127 of Novel Psychoactive Substances (NPS) have been identified worldwide and officially reported by the United Nations Office on Drugs and Crime (UNODC) and the European Monitoring Centre for Drugs and Drug Addiction (EMCDDA). An analysis of the surface web via the use of a web crawler, *NPSfinder*<sup>®</sup>, indicated that the number of NPS could be almost four times higher than that known to both the UNODC and EMCDDA. This is of particular concern, especially if one considers the public health risks and harms associated with NPS use/abuse and the paucity of data related to their pharmacological/toxicity profiles. In particular, in the last few years two NPS classes, i.e. novel synthetic opioids (NSOs) and designer benzodiazepines (DBZDs) were associated with serious side-effects and life-threatening scenarios (i.e., fatalities and overdoses).

### Gaps in knowledge

Hence, with online NPS numbers exceeding those reported by official sources, there is a strong need to address the gap in knowledge concerning the discrepancies between the online and the evidence based NPS market(s); as well as the gap in knowledge concerning lack of pharmacological profiles for most of the newly-identified NPS.

### Objectives

This programme of research aimed to: use data available from *NPSfinder*<sup>®</sup>, the UNODC and EMCDDA to assess the current general NPS scenarios, and in particular for DBZDs and NSOs; use *in silico* computational techniques to predict the biological activity of the emerging NPS; use the predicted values to infer possible health threats associated with the consumption of these substances, underscoring which of the NPS identified online could indeed represent a serious threat to public health; assess the potential of *in silico* methodologies as preliminary risk assessment tools; and subsequently inform relevant stakeholders about the risks associated with these new NPS.

### Methods

The *NPSfinder*<sup>®</sup> web crawler was used to identify NPS which are available/discussed online. A comparison with UNODC and EMCDDA databases was then carried out to assess the extent of the total NPS scenario, and the numbers of the NSOs and DBZDs classes. To appreciate and predict the biological activities of NSOs and DBZDs, *in silico* models (e.g., quantitative structure-activity relationship (QSAR), Molecular Docking (MD) and pharmacophore mapping) were used as reliable, time- and cost- effective alternatives to the classical approaches such as *in vivo*, *in vitro* or preclinical studies.



## Results and Discussion

A total of 4,231 NPS were identified on the surface web, almost four times the numbers reported by both UNDOC and EMCDDA databases (circa 1,127). These results suggest how the online content analysis should be considered as an important source for the assessment of the NPS scenario. The same discrepancy in the total NPS numbers was observed for each NPS class and a total of 115 DBZDs and 371 NSOs were identified compared to 33 and 123 reported by the UNODC respectively. To assess pharmacological profiles of these NSOs and DBZDs identified online, specific QSAR models were developed in MOE<sup>®</sup> and Forge<sup>™</sup>. For the prediction of biological activities of DBZDs, the  $\gamma$ -aminobutyric acid A receptor (GABA-AR) was used; the mu opioid receptor (MOR) was used for the NSOs. In addition, for the DBZDs, a set of new potential ligands resulting from “scaffold hopping” exercises conducted with MOE<sup>®</sup> was also evaluated.

The generated QSAR models returned good performance statistics confirming their strong reliability in predicting the biological activity of an unknown or a newly-identified molecule. The DBZDs predicted to be the most active were flubrotizolam, clonazolam, pynazolam and, fluclotizolam, consistently with reported literature and/or drug discussion forums. In particular with flubrotizolam and fluclotizolam, it was found they were discussed on drug fora but not previously identified either by the UNODC or EMCDDA (flubrotizolam only). This suggests the possible presence on the market of very potent NPS which are still unknown to international agencies, potentially representing a serious threat to public health. Worrisome results were also obtained for the class of NSOs, with the identification of new and potent analogues of carfentanyl (10,000 more potent than morphine), i.e., 2-methyl carfentanyl, n-methyl-carfentanyl and butyryl-carfentanyl. Moreover, the scaffold hopping exercise conducted for the DBZDs class, strongly suggested that structural replacement of the pendant phenyl moiety could increase biological activity and highlighted the existence of a still unexplored chemical space for this NPS class. The results obtained with QSAR analysis were supported by molecular docking exercises, which gave an indication of the binding affinity of these NPS towards their respective receptors. Moreover, the binding affinity of a set of DBZDs was assessed for the MOR, in an attempt to assess a possible multi-receptor activity of these molecules.

## Conclusions

The online identification of a great number of NPS, including very potent central nervous system depressants, represents a serious challenge, in particular if one considers that DBZDs and NSOs are usually consumed either together or in combination with stimulants for recreational purposes and self-medication. The high numbers of available molecules, their patterns of use and the paucity of pharmacological data could lead to worrisome outcomes, including the synergy of each NPS class

side-effects, which could (and are) increasing the likelihood of respiratory depression, coma, and deaths.

To retrieve an extensive picture of the current NPS drug scenario, the online analysis has proven very useful, if not fundamental. Its ability to identify novel mentioned NPS, in a timely manner, makes it a very important tool for a range of activities, including informing law-enforcement and public health stakeholders, supporting the European and United Nations Early Warning Systems impacting and influencing law-making and guiding monitoring/surveillance. Moreover, *in silico* methodologies, proven as reliable tools for a fast prediction of biological activity, could be used in describing the activity/toxicity profile of novel NPS, aiming at supporting both law enforcement in scheduling process and public health stakeholders in drafting treatment/management educational packages. Finally, the combination of online and *in silico* analysis could support and improve the risk assessment procedures currently in place for NPS.

### **Statement of authorship**

I, Valeria Catalani declares that this thesis and the work presented in it are my own and has been generated by me as the result of my own original research. I confirm that this work was done wholly while in candidature for a research degree at the University of Hertfordshire. No part of this thesis has previously been submitted for a degree or any other qualification at this University or any other institution. Where I have consulted the published work of others, this is always clearly attributed, and where I have quoted from the work of others, the source is always given. With the exception of such quotations, this thesis is entirely my own work. I have acknowledged all main sources of help. Where the thesis is based on work done by myself jointly with others, I have made clear exactly what was done by others and what I have contributed myself. Parts of this work have been published before submission as :

Catalani et al. (2022) In silico studies on recreational drugs: 3D-QSAR prediction of classified and de novo designer benzodiazepines. *Chemical biology and drug design* doi: 10.1111/cbdd.14119. Online ahead of print.

Catalani et al. (2022) Designer benzodiazepines' activity on opioid receptors: a docking study. *Current pharmaceutical design* 28.32:2639-2659 DOI: 0.2174/1381612828666220510153319.

Catalani et al. (2021) Identifying new/emerging psychoactive substances at the time of COVID-19; a web-based approach. *Frontiers in Psychiatry* 11. Frontiers: 1638. DOI: 10.3389/FPSYT.2020.632405.

Catalani et al. (2021) Psychonauts' psychedelics: A systematic, multilingual, web-crawling exercise. *European Neuropsychopharmacology* 49. Elsevier: 69–92. DOI: 10.1016/J.EURONEURO.2021.03.006.

Catalani et al. (2021) The psychonauts' benzodiazepines; quantitative structure-activity relationship (QSAR) analysis and docking prediction of their biological activity. *Pharmaceuticals* 2021, Vol. 14, Page 720 14(8). Multidisciplinary Digital Publishing Institute: 720. DOI: 10.3390/PH14080720.

## Table of Contents

Chapter 1 Introduction .....	1
1.1 Research Background.....	1
1.2 New Psychoactive Substances.....	1
1.2.1 What are NPS? .....	1
1.2.2 NPS Classification .....	3
1.2.3 NPS phenomenon.....	5
1.2.4 NPS legal status .....	6
1.2.5 NPS threats and challenges .....	8
1.2.6 NPS Risk Assessment .....	9
1.2.7 Behind the NPS popularity .....	10
1.2.8 NPS diffusion: the importance of online markets .....	11
1.2.9 NPS scenario to date (2022) and NPS classes investigated by the present study .....	13
1.3 NPSfinder® .....	14
1.4 <i>In silico</i> studies.....	15
1.4.1 Predictive models definition .....	16
1.4.2 In silico drug design (in silico pharmacology).....	17
1.4.3 Chemical similarity .....	18
1.4.4 Quantitative Structure Activity Relationship (QSAR).....	19
1.4.5 Molecular Docking .....	21
1.4.6 Pharmacophore Mapping .....	23
1.4.7 De novo (drug) design and Scaffold hopping .....	24
1.4.8 In silico pharmacology and NPS.....	25
1.5 Gap(s) in knowledge .....	26
1.6 Aims and objective of the research programme .....	27
1.6.1 General aims of research programme .....	27
1.6.2 General objectives of research programme.....	27
Chapter 2 Methodologies .....	28

2.1	NPSfinder <sup>®</sup> .....	28
2.1.1	Web crawler data extraction .....	28
2.1.2	Classification of identified NPS.....	29
2.1.3	Comparison between NPSfinder <sup>®</sup> , EMCDDA and UNODC databases .....	30
2.2	In silico methodologies .....	31
2.2.1	QSAR Training and test set .....	31
2.2.2	Outliers: identification and removal .....	32
2.2.3	Descriptors selection .....	33
2.2.4	Model Building .....	33
2.2.5	QSAR validation .....	34
2.2.6	Applicability domain.....	35
2.3	Molecular docking.....	36
2.3.1	Protein Data Bank and 3D receptor structures identification .....	36
2.3.2	MOE <sup>®</sup> receptors preparation.....	37
2.3.3	MOE <sup>®</sup> Identification of the binding site .....	38
2.3.4	Preparing a small molecule dataset.....	39
2.3.5	MOE <sup>®</sup> Docking .....	40
2.3.6	Protein ligand interaction fingerprint (PLIF) .....	42
	Protein ligand interaction fingerprint(.....	42
2.3.7	Docking Validation .....	43
2.4	Pharmacophore mapping.....	44
2.4.1	Generation of a pharmacophore query .....	44
2.4.2	Refinement of a pharmacophore query .....	46
2.4.3	The Pharmacophore Query editor in MOE <sup>®</sup> .....	47
2.4.4	Validation of a pharmacophore query.....	48
Chapter 3	NPSfinder <sup>®</sup> .....	50
3.1	Identification of current NPS scenarios: NPSfinder <sup>®</sup> .....	50
3.2	The NPSfinder <sup>®</sup> DBZDs, comparison with UNODC and EMCDDA database.....	51

3.3	The NPSfinder <sup>®</sup> NSOs, comparison with UNODC and EMCDDA database .....	56
3.4	The importance of the web in the NPS scenario .....	78
Chapter 4 Designer benzodiazepines overview and methods .....		81
4.1	Chemical class overview .....	81
4.2	Designer benzodiazepines .....	84
4.2.1	Designer benzodiazepines phenomenon .....	85
4.2.2	Chemical and pharmaceutical form .....	87
4.2.3	Pharmacological profile, the GABA system and receptors .....	88
4.2.4	Toxicological profile .....	90
4.2.5	Structure Activity Relationship (SAR) .....	91
4.2.6	Designer benzodiazepines drug design .....	92
4.3	In silico methods for designer benzodiazepines .....	94
4.3.1	QSAR with MOE <sup>®</sup> .....	94
4.3.2	MOE <sup>®</sup> Manual QSAR models .....	95
4.3.3	MOE <sup>®</sup> automatic QSAR models .....	96
4.3.4	QSAR with Forge <sup>™</sup> .....	98
4.3.5	Forge <sup>™</sup> Ligand specification and alignment .....	99
4.3.6	Forge <sup>™</sup> descriptors' selections .....	100
4.3.7	Forge <sup>™</sup> QSAR models .....	100
4.3.8	Molecular Docking .....	102
4.3.9	Pharmacophore .....	110
4.3.10	Scaffold Hopping studies .....	112
Chapter 5 Results and discussions of in silico studies on designer benzodiazepines .....		114
5.1	QSAR with MOE <sup>®</sup> .....	114
5.1.1	Training and test sets .....	114
5.1.2	Manual QSAR Models .....	114
5.1.3	AutoQSAR models .....	116
5.1.4	AutoQSAR model domain of applicability .....	125

5.2	QSAR with Forge™	126
5.2.1	Training and test sets	126
5.2.2	3D QSAR Model	126
5.2.3	Domain of applicability with Forge™	132
5.3	Scaffold hopping	133
5.4	Molecular docking	138
5.5	Pharmacophore mapping	141
5.6	Profiling of the ten DBZDs with the highest predicted biological activity	144
5.6.1	Flubrotizolam	144
5.6.2	Clonazolam	146
5.6.3	Pynazolam	148
5.6.4	Fluclotizolam	150
5.6.5	MP-III-02	152
5.6.6	Ro 09-9292	154
5.6.7	Ro 15-9270	156
5.6.8	3-Hydroxyphenazepam	157
5.6.9	Flunitrazolam	159
5.7	Novelty and importance of the <i>in silico</i> methodology applications on DBZDs	161
5.8	Limitations	163
Chapter 6 Novel synthetic opioids overview and methods		164
6.1	Chemical class overview	164
6.2	The opioids epidemic	168
6.3	Novel synthetic opioids	169
6.3.1	Novel synthetic opioids phenomenon	171
6.3.2	Forms and routes of administration	174
6.3.3	Pharmacological profile, the opioid system and receptors	176
6.3.4	Toxicological profile	179
6.3.5	Current Structure Activity Relationship	181

6.3.6	Novel synthetic opioids drug design.....	187
6.4	In silico methods for novel synthetic opioids.....	188
6.4.1	QSAR with Forge™.....	188
6.4.2	Forge™ Ligand specification and alignment.....	190
6.4.3	Forge™ descriptors' selection .....	190
6.4.4	Molecular Docking .....	191
6.4.5	Pharmacophore.....	203
Chapter 7	Results and discussions of in silico studies on novel synthetic opioids.....	204
7.1	QSAR with Forge™ for fentanyl-like NSOs .....	204
7.1.1	Training and test sets.....	204
7.1.2	3D QSAR Models .....	204
7.1.3	Domain of applicability with Forge™ .....	210
7.2	QSAR with Forge™ for morphine-like NSOs .....	212
7.2.1	Training and test sets.....	212
7.2.2	3D QSAR Models .....	212
7.2.3	Domain of applicability with Forge™ .....	216
7.2.4	Molecular docking .....	216
7.2.5	Fentanyl-like NSOs molecular docking.....	217
7.2.6	Morphine-like NSOs molecular docking .....	220
7.2.7	Nitazene-like NSOs molecular docking.....	225
7.3	Profiling of the NSOs with the highest predicted biological activity.....	229
7.3.1	Carfentanyl.....	229
7.3.2	N-methyl-carfentanyl.....	232
7.3.3	Butyryl-carfentanyl .....	234
7.3.4	Acetyl-carfentanyl.....	236
7.3.5	4-Methoxymethylfentanyl.....	237
7.4	Novelty and importance of the in silico methodology applications on NSOs .....	239
7.5	Limitations.....	242



Chapter 8 Designer benzodiazepines' activity on opioid receptors studies.....	243
8.1 Benzodiazepines activity on opioids receptor literature background.....	243
8.2 Methodology .....	245
8.2.1 DBZDs object of the study.....	245
8.2.2 Identification of reference compounds .....	245
8.2.3 Pharmacophore filtering.....	247
8.2.4 Molecular docking .....	247
8.3 Pharmacophore filtering results.....	247
8.4 Molecular docking results .....	249
8.5 A discussion on the potential of DBZDs to activate ORs .....	254
8.5.1 Limitations of the current study .....	258
8.6 Novelty and importance of the study .....	259
Chapter 9 General conclusion .....	260
Chapter 10 Future work .....	264
References .....	266
Appendix A.....	314
Appendix B .....	385
Achievements.....	390

## List of Figures

Figure 1.1 Distribution of NPS reported to the UNODC by effect group.....	3
Figure 1.2 Three steps for the NPS risk assessment (EMCDDA 2020a).....	9
Figure 1.3 Example of ligand-protein docking studies. ....	21
Figure 1.4. Visual representation of a structure based (left) and ligand based (right) pharmacophore map. ....	23
Figure 2.1 NPSfinder® database interface.....	29
Figure 2.2 Screenshot of the Quick Prep Panel in MOE.....	37
Figure 2.3 Workflow of a docking study carried out with MOE.....	40
Figure 2.4 The MOE dock panel.....	41
Figure 2.5 The three types of annotation points included in the Unified annotation scheme. ....	45
Figure 2.6 Pharmacophore query editor interface in MOE.....	47
Figure 4.1 Most common structure of benzodiazepines scaffolds.....	83
Figure 4.2 Number of benzodiazepines identified each year for the first time between 2007 and 2021 (the image is reproduced with the consent of EMCDDA) (EMCDDA 2022c).....	86
Figure 4.3 Other structure identified among DBZDs. The structures were designed with ChemDraw 20.1 .....	87
Figure 4.4 Examples of designer benzodiazepines identified on the market. ....	87
Figure 4.5 3D representation of the pentameric structure of the GABA-AR. ....	88
Figure 4.6 Structure activity relationship identified for benzodiazepines. ....	92
Figure 4.7 QuaSar model panel in MOE.....	96
Figure 4.8 Dataset upload panel in Forge™.....	98
Figure 4.9 Example of an alignment made by Forge™.....	100
Figure 4.10. Parameters adopted for the Field QSAR calculation method in Forge™.....	101
Figure 4.11 Screenshot of the 6HUO and X3X receptor from RCSB Protein Databank. ....	103
Figure 4.12 6HUP binding pocket 3D and 2D representations. ....	105
Figure 4.13 6X3X binding pocket 3D and 2D representations. ....	106
Figure 4.14 6HUO binding pocket 3D and 2D representations. ....	107
Figure 4.15 Pharmacophore query used for the docking placement with 6HUO .....	109
Figure 4.16 Pharmacophore query used for docking placement with 6HUP.....	109
Figure 4.17 Representation of the allosteric binding pocket of GABA-AR with diazepam bound in its active conformation (PDB6HUP (RCSB PDB, 2018b)). ....	113
Figure 4.18 Three major moieties (1,2 and 3) for the MedChem (green) and Scaffold Replacement (red) studies ..	113

<i>Figure 5.1 Correlation coefficient and correlation matrix for the top ten scoring descriptors.....</i>	<i>115</i>
<i>Figure 5.2 Correlation values (<math>r^2</math>) for the training and the test set were obtained using the five descriptors QSAR model generated by AutoQSAR. ....</i>	<i>118</i>
<i>Figure 5.3 Example of 2D molecules belonging to the high, medium and low activity bins. ....</i>	<i>122</i>
<i>Figure 5.4 Visual representation of the predicted (x axis) vs. experimental (y axis) log 1/c values for training (blue) and test (yellow) sets. ....</i>	<i>128</i>
<i>Figure 5.5 Visual representation of the generated 3D Field QSAR model.....</i>	<i>129</i>
<i>Figure 5.6 Ligand pharmacophore features taken into consideration for the scaffold hopping exercise. ....</i>	<i>134</i>
<i>Figure 5.7 MedChem and Scaffold Replacement top scoring moieties .....</i>	<i>135</i>
<i>Figure 5.8 3D representation of the new scaffold created for DBZDs. ....</i>	<i>136</i>
<i>Figure 5.9 The poses of the top ten DBZDs docked in PDB6X3X and PDB6HUO .....</i>	<i>140</i>
<i>Figure 5.10 Visual representation of the interactions (potential contacts) between the 102 DBZDs and the residues of the binding pocket of PDB6HUP. ....</i>	<i>140</i>
<i>Figure 5.11 Pharmacophore maps generated on the DBZDs alignment.....</i>	<i>142</i>
<i>Figure 5.12 Flubrotizolam interactions 3D and 2D representations. ....</i>	<i>145</i>
<i>Figure 5.13 Clonazolam interactions 3D and 2D representations. ....</i>	<i>147</i>
<i>Figure 5.14 Pynazolam interactions 3D and 2D representations. ....</i>	<i>149</i>
<i>Figure 5.15 Fluclotizolam interactions 3D and 2D representations.....</i>	<i>151</i>
<i>Figure 5.16 MP-III-02 interactions 3D and 2D representations. ....</i>	<i>153</i>
<i>Figure 5.17 Ro 09-9292 interactions 3D and 2D representations.....</i>	<i>155</i>
<i>Figure 5.18 Ro 15-9270 interactions 3D and 2D representations.....</i>	<i>156</i>
<i>Figure 5.19 3-Hydroxyphenazepam interactions, 3D and 2D representations.....</i>	<i>158</i>
<i>Figure 5.20 Flunitrazolam interactions 3D and 2D representations.....</i>	<i>160</i>
<i>Figure 6.1 Most common chemical structures identified among the class of opioids.....</i>	<i>166</i>
<i>Figure 6.2 Numbers and types of synthetic opioids notified for the first time to the EWS. The image is reproduced with the EMCDDA permission (EMCDDA 2021g) .....</i>	<i>171</i>
<i>Figure 6.3 NSOs chemical classes reported each year from 2009 to 2019.....</i>	<i>172</i>
<i>Figure 6.4 Latest chemical structure of the opioids class to be scheduled under the Narcotic Convention (1961)..</i>	<i>173</i>
<i>Figure 6.5 Some examples of NSOs found on the market. ....</i>	<i>175</i>
<i>Figure 6.6 3D representation of the pentameric structure of GABA-AR. ....</i>	<i>177</i>
<i>Figure 6.7 Structure activity relationship identified for the morphine-like NSOs. ....</i>	<i>182</i>
<i>Figure 6.8 Structure activity relationship identified for the fentanyl-like NSOs.....</i>	<i>184</i>

<i>Figure 6.9 Structure activity relationship identified for the nitazene-like NSOs.</i> .....	186
<i>Figure 6.10 Example of an alignment made by Forge™.</i> .....	190
<i>Figure 6.11. 2D structure of the co-crystallised ligands for the ORs identified for the docking studies.</i> .....	192
<i>Figure 6.12 PDB51CM binding pocket 3D and 2D representations.</i> .....	194
<i>Figure 6.13 Representation of the two polar interactions (light blue cylinder).</i> .....	195
<i>Figure 6.14 PDB6B73 binding pocket 3D and 2D representations.</i> .....	196
<i>Figure 6.15 PDB6B73 binding pocket 3D and 2D representations of the PDB6B73 binding pocket.</i> .....	197
<i>Figure 6.16 Pharmacophore query used for the docking placement with PDB6PT3 (left) and with PDB6B73 (right).</i> .....	201
<i>Figure 6.17 Pharmacophore query used for the docking placement with PDB5C1M</i> .....	201
<i>Figure 7.1 Visual representation of the predicted (x axis) vs. experimental (y axis) log 1/c values for the training (blue) and test (orange) sets.</i> .....	206
<i>Figure 7.2 3D and 2D visual representations of the generated 3D Field QSAR model for electrostatic features</i> .....	207
<i>Figure 7.3 3D and 2D visual representations of the generated 3D Field QSAR model for hydrophobic features</i> ....	208
<i>Figure 7.4 Visual representation of the predicted (x axis) vs. experimental (y axis) log 1/c values for the training (blue) and test (orange) sets. The graphs were built with Excel 2022.</i> .....	213
<i>Figure 7.5 3D and 2D visual representations of the generated 3D Field QSAR model for electrostatic features</i> .....	214
<i>Figure 7.6 The poses of the top ten fentanyl-like NSOs docked in PDB5C1M.</i> .....	218
<i>Figure 7.7 Visual representation of the interactions (potential contacts) between the 238 NSOs and the residues of the binding pocket of PDB5C1M.</i> .....	219
<i>Figure 7.8 The poses of the top morphine-like docked in PDB5C1M.</i> .....	223
<i>Figure 7.9 Visual representation of the interactions (potential contacts) between the 238NSOs and the residues of the binding pocket of PDB5C1M.</i> .....	224
<i>Figure 7.10 positioning of the phenethylpiperidines scaffold (purple) and phenantrenes scaffold (yellow) inside of the MOR binding pocket.</i> .....	225
<i>Figure 7.11 Downward (A) and upward (B) orientation of flunitazene (in purple).</i> .....	227
<i>Figure 7.12 The poses of the top morphine-like docked in PDB5C1M.</i> .....	228
<i>Figure 7.13 The 3D pose carfentanyl docked in PDB5C1M and 2D representations.</i> .....	231
<i>Figure 7.14 The 3D pose of N-methyl-carfentanyl docked in PDB5C1M and 2D representations.</i> .....	233
<i>Figure 7.15 The 3D pose of butyryl-carfentanyl docked in PDB5C1M and 2D representations.</i> .....	235
<i>Figure 7.16 The 3D pose of acetyl-carfentanyl docked in PDB5C1M and 2D representations.</i> .....	236
<i>Figure 7.17 The 3D pose of 4-Methoxymethylfentanyl docked in PDB5C1M and 2D representations.</i> .....	238
<i>Figure 8.1 Pharmacophore queries generated for KOR, DOR and MOR</i> .....	248

<i>Figure 8.2 Pharmacophore queries generated for KOR, DOR and MOR without the flexibly aligned ligand. ....</i>	<i>248</i>
<i>Figure 8.3 2D ligands interactions for the three top scoring DBZDs for DOR. ....</i>	<i>253</i>
<i>Figure 8.4 2D ligand interactions for the three top scoring DBZDs for KOR. ....</i>	<i>253</i>
<i>Figure 8.5 2D ligands interactions for the three top scoring DBZDs for MOR. ....</i>	<i>254</i>

## List of Tables

<i>Table 1.1. Number of identified NPS per class by the UNODC (2009-2020) and EMCDDA (2010-2020)*</i> .....	4
<i>Table 1.2 Challenges related to the NPS phenomenon grouped in form main categories (Orsolini et al., 2020; Schifano, 2018; Schifano et al., 2019)</i> .....	8
<i>Table 1.3 Classes of computational methods for the de novo design (Suryanarayanan et al. 2018)</i> .....	24
<i>Table 2.1 Type and number of classes used to identify NPS identified online by the NPSfinder®</i> .....	30
<i>Table 2.2 Type of contacts identifiable with the Ligand interactions panel</i> .....	38
<i>Table 2.3 Steps that should be followed for each of the pharmacophore mapping type, i.e. ligand based, complexed base and target based</i> .....	44
<i>Table 3.1 The number of unique molecules identified for each NPS class during the years of activity of the NPSfinder®, i.e. 2017-2020</i> .....	50
<i>Table 3.2 List of designer benzodiazepines identified by the NPSfinder® and comparison with the EMCDDA and UNODC databases</i> .....	52
<i>Table 3.3 List of fentanyl like NSO identified by the NPSfinder® and comparison with the EMCDDA and UNODC databases</i> .....	58
<i>Table 3.4 List of non-fentanyl like NSO identified by the NPSfinder® and comparison with the UNODC database</i> ..	73
<i>Table 3.5 List of nitazenes like NSO identified by the NPSfinder® and comparison with the UNODC database</i> .....	76
<i>Table 3.6 List of morphinan like NSOs identified by the NPSfinder®</i> .....	77
<i>Table 4.1 List of BDZ scheduled under the UN Convention on Psychotropic Substances of 1971</i> .....	82
<i>Table 4.2 Description of the three binding pockets identified for 6HUO and 6HUP</i> .....	104
<i>Table 4.3 Reference dataset composition</i> .....	108
<i>Table 5.1 QSAR models calculated with the manually selected descriptors</i> .....	115
<i>Table 5.2 Statistical value for the QSAR models</i> .....	115
<i>Table 5.3 Specification of the five descriptors included in the final QSAR model</i> .....	117
<i>Table 5.4 Mutual correlation values for the 5 descriptors chosen for the QSAR equation</i> .....	118
<i>Table 5.5 The top 20 predicted value of biological activity (log1/c) for the 102 DBZDs identified by NPSfinder®</i> ..	120
<i>Table 5.6 Values for the statistics obtained for the three calculated QSAR models</i> .....	127
<i>Table 5.7 Values of predicted log 1/c of the top ten DBZD The entries are ranked for decreasing values of pred log 1/c</i> .....	131
<i>Table 5.8 S values obtained via the pharmacophore constraint docking for the reference compounds</i> .....	138
<i>Table 5.9 The predicted binding affinity values of the ten DBZDs predicted to display the higher biological activity in Forge™</i> .....	139
<i>Table 6.1 Description of the two binding pockets identified for 6HUO and 6HUP</i> .....	193
<i>Table 6.2 Refence molecules for docking studies</i> .....	199

<i>Table 7.1 Values for the statistics obtained for the three calculated QSAR models .....</i>	<i>205</i>
<i>Table 7.2 Top ten fentanyl-like NSOs molecules reported in decreasing order of the predicted pKi values. ....</i>	<i>209</i>
<i>Table 7.3 Values for the statistics obtained for the three calculated QSAR models .....</i>	<i>212</i>
<i>Table 7.4 Values of pKi predicted for the 19 morphine-like NSOs identified online. ....</i>	<i>215</i>
<i>Table 7.5 Binding affinity values for the reference compounds. The latter are listed in alphabetical order. ....</i>	<i>216</i>
<i>Table 7.6 Predicted values of binding affinity (S) for the fentanyl-like NSOs predicted to show the highest biological activity. ....</i>	<i>217</i>
<i>Table 7.7 Predicted values of binding affinity (S) for the morphine-like NSOs predicted to show the highest biological activity. ....</i>	<i>222</i>
<i>Table 7.8 Predicted values of binding affinity (S) for the nitazenes NSOs predicted to show the highest biological activity. ....</i>	<i>226</i>
<i>Table 8.1 Five refence molecules for docking studies of DBZDs on ORs .....</i>	<i>246</i>
<i>Table 8.2 Most common interactions identified between the DBDZs ligands and the ORs .....</i>	<i>250</i>
<i>Table 8.3 Binding values (S) generated for those DBDZs that display the ionic interaction with the charged amine of the Asp residues in DOR, KOR and MOR. ....</i>	<i>251</i>

## *Abbreviations*

<b>NPS</b>	New psychoactive substances
<b>UNODC</b>	United Nations Office for Drugs and Crime
<b>EMCDDA</b>	European Monitoring Centre for Drugs and Drug Addiction
<b>CADD</b>	Computer Aided Drug Design
<b>cAMP</b>	Cyclic adenosine monophosphate
<b>CB1</b>	Cannabinoid 1 receptor
<b>CHO</b>	Chinese Hamster Ovary cell
<b>CNR1</b>	Cannabinoid Receptor 1
<b>DA</b>	Dopamine
<b>DAT</b>	Dopamine Transporter
<b>DRD</b>	Drug Related Deaths
<b>EFS</b>	Electrical Field Stimulation
<b>ELISA</b>	Enzyme Linked ImmunoSorbent Assay
<b>Hz</b>	Hertz
<b>IBMX</b>	3-Isobutyl-1-methylxanthine
<b>LDH</b>	Lactate Dehydrogenase
<b>MOE</b>	Molecular Operating Environment
<b>MTS</b>	(3-(4,5-dimethylthiazol-2-yl)-5-(3-carboxymethoxyphenyl)-2-(4-sulfophenyl)-2H-tetrazolium)
<b>NE</b>	Norepinephrine
<b>NET</b>	Norepinephrine Transporter
<b>Nm</b>	Nanometers
<b>NPS</b>	Novel/New Psychoactive Substances
<b>PLIF</b>	Protein-Ligand Interaction Fingerprint
<b>Pg</b>	Picogram
<b>QSAR</b>	Quantitative Structure Activity Relationship
<b>SC</b>	Synthetic cannabinoid
<b>SF</b>	Scoring function
<b>SER</b>	Serotonin
<b>SERT</b>	Serotonin Transporter
<b>T<sub>c</sub></b>	Tanimoto Coefficient
<b>VDW</b>	van der Waals



# Chapter 1 Introduction

## 1.1 Research Background

The Novel Psychoactive Substances (NPS) phenomenon with its current and future trends is the context within which this programme of research stands. Results obtained by an ongoing analysis of the surface web, started in November 2017, indicate that the number of NPS available online could be much higher than those reported by both the United Nations Office on Drugs and Crime (UNODC) and the European Monitoring Centre for Drugs and Drug Addiction (EMCDDA) via their evidence-based identification and early warning systems. These innovative results can be considered very worrisome evidence of, and suggestion for, internet-based knowledge to be used in assessing “real-world” NPS scenarios. Moreover, they highlight the need to develop a fast and reliable approach in evaluating the possible health treats associated with these NPS, for which very few information is available on pharmacological/toxicological profiles. Looking into the use of in silico methodologies could be of great relevance in finding alternative methods to the classical in vitro and in vivo pharmacology approaches

## 1.2 New Psychoactive Substances

### 1.2.1 *What are NPS?*

The term NPS, which was adopted in Europe in the early 2000 and used in 2005 in the new EU legislation (Council of the European Union, 2005; EMCDDA, 2022a), defines a general class of substances which were created to resemble/mimic the effects of classical drugs of abuse (e.g. cocaine, heroin, amphetamine, cannabis). NPS can be either analogues of existing controlled drugs or newly synthesized chemicals (Council of the European Union, 2005; EMCDDA, 2022a).

The UNODC defines these molecules as ‘substances of abuse, either in a pure form or a preparation, that are not controlled by international drug conventions, but which may pose a public health threat’ (UNODC, 2013); while the EMCDDA adopts a different definition: ‘a new narcotic or psychotropic drug, in pure form or in preparation, that is not controlled by the United Nations drug conventions, but which may pose a public health threat comparable to that posed by substances listed in these conventions’(EMCDDA, 2022b).

In this context, the term "novel" does not necessarily refer to new inventions but to substances that have newly become available in specific markets. Indeed, molecules deriving from old pharmaceutical patents or failed clinical studies are often being repurposed in the recreational drug

markets together with molecules already well established (decades) on the therapeutic market (UNODC, 2021a).

### 1.2.2 NPS Classification

At present 1,127 NPS have been reported by the UNODC, identified by 134 countries and territories worldwide (UNODC, 2022a), against the 880 NPS reported in Europe for the same period (EMCDDA, 2022c). Due to the high diversity of pharmacological profile and chemical structure that characterise this group of substances, the classification of NPS is a very difficult and complex task. The latter is complicated by the drug market highly dynamic nature which sees different molecules appearing every week and increases the difficulty of allocating one substance to a defined class with no overlap or confusion (UNODC, 2019a).

There are multiple ways in which an NPS can be categorised, for example, NPS can be grouped for their origin – whether natural (e.g. fungi or plant based) or synthetic, for their psychotropic effects, or for their chemical structure.

In the early days of the NPS emergence (for a timeline please refer to Ch 1.2.3), the UNODC noticed that these molecules seemed to mimic the effects of the six main groups of substances controlled under the international drug conventions (LSS/RAB/DPA/UNODC, 2016); and proceeded to use the pharmacological activity as a criterion for classification. The following classes were adopted: stimulants, opioids, synthetic cannabinoid receptor agonists, dissociatives, classic hallucinogens and sedatives/hypnotics. Any NPS reported that did not fit in any of these six classes were labelled as not yet assigned (UNODC, 2022a, 2022b). Here is reported the 2021 NPS distribution at the global level, by effect group as per UNODC data (Figure 1.1).

NPS reported by effect group (until December 2021)

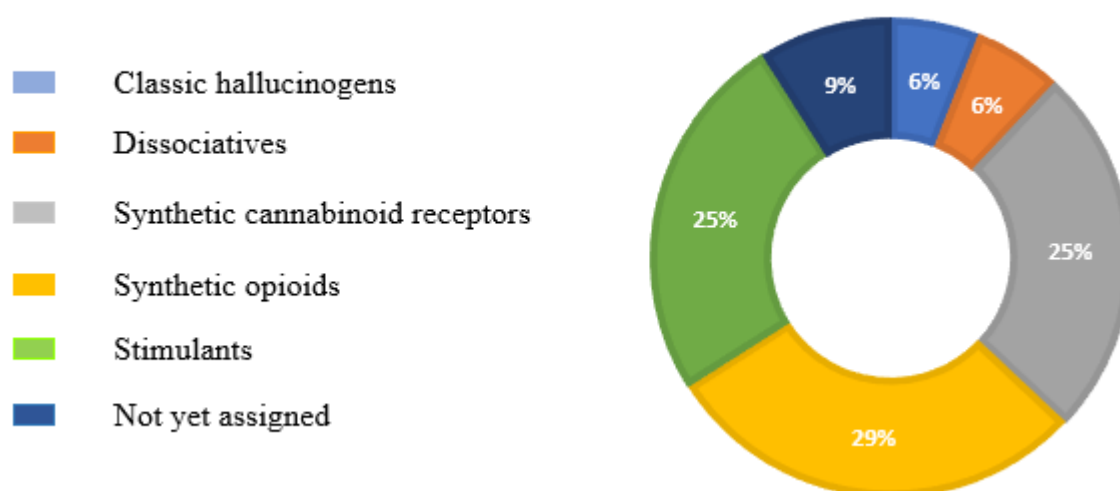


**Figure 1.1** Distribution of NPS reported to the UNODC by effect group.  
Data reproduced with permission of the UNODC (UNODC, 2022a)

The classification by effect adopted by the EMCDDA divides all the NPS into two categories: psychotropic substance or narcotic drug (EDND, 2021), in line with the Single Convention on Narcotic Drugs of 1961 and the Convention on Psychotropic Substances of 1971 (UNODC, 2022c). These two very different ways of categorising NPS substances could be considered the result of the highly independent work of these two international agencies.

Grouping NPS according to their pharmacological effects, however, can be a very challenging task, especially for newly identified substances, because no information regarding their pharmacology/toxicological profile is usually available. Hence, the UNODC and EMCDDA adopted an ulterior categorisation based on chemical structure. In particular the UNODC identifies a total of 11 NPS substance groups and the EMCDDA a total of 13 (Table 1.1). For clarity in this document we will refer to substance groups as classes.

*Table 1.1. Number of identified NPS per class by the UNODC (2009-2020) and EMCDDA (2010-2020)\*.*

UNODC		EMCDDA	
NPS Class	No (2009-2020)	NPS Class	No (2010-2020)
Aminoindanes	9	Aminoindanes	6
Fentanyl analogues	79	Arylalkylamines	41
Benzodiazepines	30	Arylcyclohexilamines	27
Phencyclidine-type substances	26	Benzodiazepines	33
Phenethylamines	176	Cannabinoids	224
Piperazines	27	Cathinones	162
Plant-based substances	22	Opioids	73
Synthetic cannabinoids	324	Phenethylamines	106
Synthetic cathinones	201	Piperazines	18
Tryptamines	60	Piperidines/pyrrolidines	15
Others (including opioids)	173	Plant-based	9
		Tryptamines	57
		Others	115

**\*The classes are listed in alphabetical order. To be noted that NPS opioids which are not fentanyl analogues have been included by the UNODC in the “others” class.**

### 1.2.3 NPS phenomenon

While records of NPS can be dated back to the mid-90s (Dargan and Wood, 2013), one could argue that the NPS phenomenon started in 1997 with the establishment of the EU Early Warning system and the ‘joint action concerning the information exchange, risk assessment and control of new synthetic drugs’ (Dargan and Wood, 2013; EMCDDA, 2022a). Indeed, in 1998 the first risk assessment on a NPS (MBDB (N-methyl-1-(1,3-benzodioxol- 5-yl)-2-butanamine)) was produced (EMCDDA, 1999). Between 1998 and 2007 however only a small number of NPS (roughly 60 in Europe) appeared on the market (EMCDDA, 2009a). These were then known as “new synthetic drugs” or “herbal highs” and were predominantly stimulants and hallucinogens/psychedelics molecules produced in small illicit European laboratories. In 2007 the appearance on the market of “Spice”, a mixture containing synthetic cannabinoids, and mephedrone started the era of “legal highs” and “research chemical”, which saw a rapid expansion of the number and type of NPS and the shift in production from the Europe to the China (EMCDDA, 2015, 2009b, 2009a). At that time, the term ‘legal highs’ was properly used to underscore the lack of any legal restriction concerning their possession, usage and marketing as well as implying the safety of the product. After this rapid expansion (EMCDDA, 2011), which, up to 2016, saw more than 800 “legal highs” and “research chemical” openly sold in physical shops and on the internet via very attractive marketing strategies (colourful packages, attractive names, and low prices) (Corazza et al., 2014b), the market(s) for NPS changed again towards different chemical classes, and towards a stabilisation in their numbers.

Stimulants (i.e., cathinones and phenethylamines), hallucinogens (mostly tryptamines), synthetic cannabinoid receptor agonists (SCRAs), synthetic benzodiazepines and opioids became the most popular NPS groups (UNODC, 2022b).

These new NPS contributed to a greater complexity of the markets characterised as well by the emergence of less but still highly potent NPS (in particular fentanyl-like and benzimidazole opioids and synthetic benzodiazepines), associated with more problematic patterns of use and more long-term, marginalised users (EMCDDA-Europol, 2019). Parallel to this, there was a growing integration between the NPS and the illicit drug markets, which showed predominantly in the use of NPS as counterfeit/falsified prescription drugs (e.g., Valium, Xanax (alprazolam)) (EMCDDA, 2022a). Another shift in the geography of production was observed as well, with India becoming one of the top manufacturing countries (Patil et al., 2016).

As a result, over the last decade a dramatic increase in the number of new psychoactive substances detected across the world has been observed, with a market that has been confirmed highly dynamic (UNODC 2022a). As of June 2022, the UNODC, through the Early Warning Advisory (EWA) on NPS (UNODC, 2022d), identified 1,127 individual new psychoactive substance reported by a total

of 134 countries (UNODC, 2022a), with an average of 100 substances reported by each country; while the EMCDDA via the Early Warning System (EWS) (EMCDDA, 2021a) reported a total of 884 NPS, of which 52 were formally notified in 2021 (EMCDDA, 2022a, 2022c).

The number of NPS notified in 2021 matches the trend of roughly 50 new molecules per year observed since 2016, down from the 100 identified in 2014 and 2015. Despite this decrease in numbers, at date the NPS class is still fast-evolving, very volatile and often diversified, and includes a variety of substances with different (il)legitimate use, composition and position in the global drug markets.

Differing from the controlled “traditional” drugs, NPS usually do not have established or long-lasting markets and they often display a rapid “life cycle” (Corkery et al., 2017). Indeed, the majority of NPS emerges and stays on the market only for a short period (e.g. months to a year), usually because they either do not generate enough interest (hence demand), are outshined by other rival NPS or are quickly banned due to their high potency often associated with high popularity (UNODC, 2022b) (EMCDDA, 2022a). However, for a small number of NPS, evidence of market stabilisation has been recently reported (i.e., synthetic opioids, synthetic benzodiazepines) (UNODC, 2021b, 2020a, 2020b, 2019b, 2019a, 2017a). Lower NPS turnover and a more stable markets could suggest how NPS have become more users targeted and a longer-term class of recreational drugs. However, despite the decrease of first-time detections, NPS still pose serious health risks worldwide with serious health emergencies (mass intoxications and deaths) reported due to synthetic opioids, designer benzodiazepines and synthetic cannabinoids (Adamowicz et al., 2019; Adams et al., 2017; Armenian et al., 2018; Darke et al., 2022; Elliott and Hernandez Lopez, 2018; EMCDDA, 2019a; Jalal and Burke, 2021; Koch et al., 2018).

#### *1.2.4 NPS legal status*

Per definition, NPS fall outside the global drug control system and are not included in the schedules of the 1961 or 1971 Conventions. As a result, the number and diversity of NPS identified worldwide in recent years have been posing considerable challenges for policymakers, both from international and national points of view.

At the national level, efforts in controlling the open sale of NPS has resulted in innovative legal responses and interventions designed to cover the time gap necessary for a permanent update on the drug law control. In particular, three types of responses can be identified (EMCDDA, 2016a, 2016b; UN, 2022):

- ‘Controls using consumer safety or medicines legislation’ (EMCDDA, 2016a), e.g. the requirement for which food and goods for sale need to be clearly labelled with their expected usage, the lack of which has been used to confiscate NPS
- ‘Extending and adapting existing laws and processes’ (EMCDDA, 2016a), e.g. the enact of temporary class drug orders to quickly control named NPS for a period up to one year.
- ‘Devising new legislation to tackle new substances’ (EMCDDA, 2016a), e.g. the enact of new laws, such as to control the sale of NPS. In particular three different types of new legislation were introduced: generic legislation including a precise definition of a family of substances; an analogue legislation including a more generic definition of activity/structure similarity; and a derivative legislation including NPS deriving from other well known drug of abuse.

In past years generic or “catchall” legislations have been widely (Australia, Germany, United Kingdom and China) adopted on NPS, which covered almost every possible variant if not all possible future variants of psychoactive substances (Corazza and Roman-Urrestarazu, 2017).

Currently in the UK, unless they are already controlled under the Misuse of Drugs Act 1971, NPS are caught by the Psychoactive Substances Act 2016, which came into force on 26 May 2016, and prohibits the sale, possession and possession with intent to sell of psychoactive compounds, including previously legal NPS, with provision for research institutions to be exempt from the 2016 Act (Home Office, 2018, 2016).

On a more international level, efforts have been directed towards discretionary provisional control measures (e.g. mephedrone (Commission on Narcotic Drugs, 2014)), and towards prioritizing only the most persistent, prevalent and harmful NPS for scheduling.

Of the 1,127 NPS identified so far, indeed only a total of 68, have been scheduled between 2015 and 2021 at the international level, including 21 under the 1961 Convention (mostly fentanyl analogues) and 47 under the 1971 Convention (UNODC, 2022c).

To help the scheduling decision process both the UNODC and the EMCDDA have legislative support in place and early warning systems (EMCDDA, 2020a; United Nations, 2022). The UNODC Early Warning Advisory (EWA) and the EMCDDA EWS indeed provide up to date reports on NPS, serving as global/European reference points, and aim to improve the development of evidence-based related policies.

Once information on an NPS not yet scheduled is available, which suggests the need for that substance to be added to any of the schedules of the Conventions, such information need to be notified to the Commission on Narcotic Drugs and the World Health Organization (WHO) (UNODC, 2013). The Expert Committee on Drug Dependence (ECDD) of the WHO is responsible

for carrying out a risk assessment on the substance, the results of which will guide the recommendations on control measures (i.e. adding, transferring, removing) (WHO, 2022, 2010).

### 1.2.5 NPS threats and challenges

NPS have been declared a serious threat to public health (UNODC, 2022b). The number of fatalities and drug poisonings attributed to NPS use/abuse has been constantly rising with more than 1500 toxicology cases, involving a total of 58 NPS, reported to the UNODC between October 2020 and April 2021 (UNODC, 2021b). Of these, 23% were classified as post-mortem (PM) and 55% as driving under the influence of drugs (DUID). Since their first emergence, NPS have challenged the traditional approaches to drug monitoring, surveillance, control, and public health responses aimed at reducing drug-related threat and harm. Despite, the many challenges linked to this class of substances, the latter can be mainly associated with: analytical identification; (risk) assessment; review, scheduling and regulatory status; and health responses (Table 1.2) (Orsolini et al., 2020; Schifano, 2018; Schifano et al., 2019b).

**Table 1.2 Challenges related to the NPS phenomenon grouped in form main categories (Orsolini et al., 2020; Schifano, 2018; Schifano et al., 2019)**

<b>Analytical Identification</b>
Large number of molecules classified as NPS; everchanging nature of available NPS on the market; speed at which they enter and exit the market; lack of available untargeted screening methods; low concentrations in both biological and non-biological specimens; lack of reference standards
<b>(Risk)Assessment</b>
Definition and classification; lack of pharmacology/toxicity profile information; different potency and risk profiles (dependence, abuse potential, severe side effects) despite chemical similarity (EMCDDA, 2010)
<b>Review, Scheduling and Regulatory status</b>
Pre-review; critical review; exempted preparations review; Expert Committee on Drug Dependence, recommendation (WHO, 2010)
<b>Health responses</b>
Polydrug use/consumption; untrained health personnel and emergency departments

It should be noted that the challenges relative to analytical identification and (risk) assessment should be seen as crucial for a proper understanding and assessment of the threat associated with the NPS phenomenon.



### 1.2.6 NPS Risk Assessment

Risk assessment can be defined as both the element of probability that some harm may occur (usually defined as ‘risk’) and the degree of seriousness of such a harm (usually defined as ‘hazard’) (Rausand and Haugen, 2020). NPS risk assessment is a crucial step in the legal framework designed to evaluate newly identified psychoactive substances and allow both the European Union (EU) and the WHO to rapidly detect, assess, and respond to health and social threats caused by these new drugs. In particular, it is the step on which any decision making on the prospect/need of scheduling/controlling is based (UNODC, 2019c). A risk assessment is usually requested after an initial report on the index NPS suggests that the substance could pose both severe public health risks and social risks (EMCDDA, 2010). The expert committee on drug dependence for the UNODC, and the Scientific Committee for the EMCDDA are tasked with the **medical and scientific review process** (EMCDDA, 2017a; UNODC, 2019c). The latter includes the evaluation of the **pharmacological profile and of the health and social risks associated to an NPS use/abuse** (Figure 1.2) (EMCDDA, 2020a).

#### NPS Risk Assessment

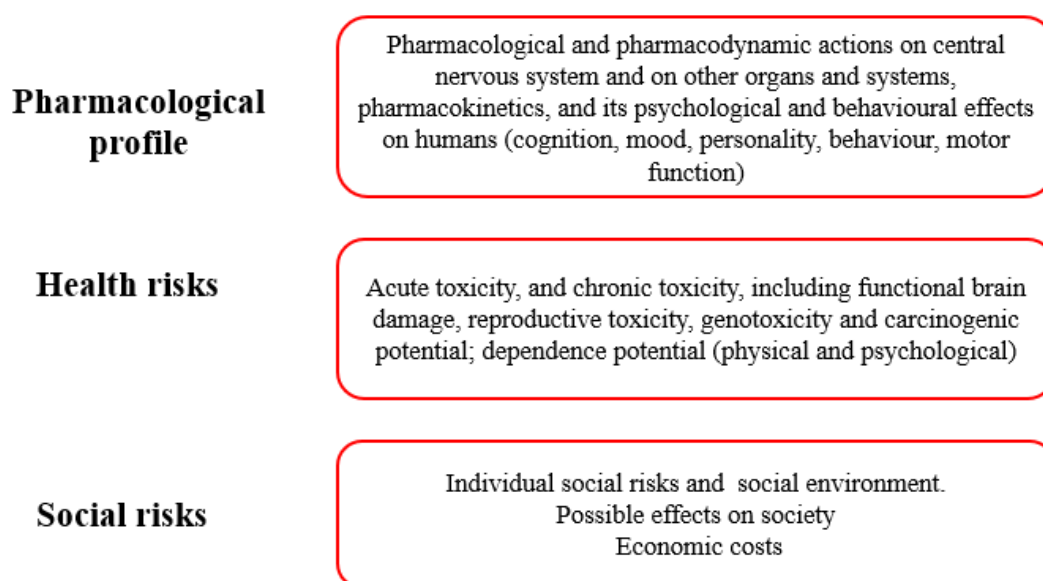


Figure 1.2 The three steps for the NPS risk assessment (EMCDDA, 2020a).

For the competent authority to provide an exhaustive risk assessment report, the latter should contain the available information on the pharmacological and toxicological properties of the assessed NPS. This would include the available scientific and law enforcement information and any other relevant scientific evidence, with particular regard to both *in vitro* and *in vivo* data. In particular, of great importance are any available data on the NPS receptor pharmacology

(EMCDDA, 2020a), and even more those on receptor implicated in substance dependence. As reported by the EMCDDA ‘In vitro and animal data demonstrating the toxicological properties are considered relevant for characterising the new psychoactive substance. Usually, human toxicological data are limited to case reports on serious adverse events such as acute poisonings and medico-legal death investigations’ (EMCDDA, 2020a) (pg. 12).

The EU risk assessment process was a very lengthy one, with roughly 26 weeks to be expected between the information collection and the risk assessment report completion. To tackle this issue in 2017, the EU proposed a new process with the intent of cutting the time frame down to 13/14 weeks (EMCDDA, 2018a; European Union, 2017). However, despite this effort still almost four months are needed between the time of the first identification/report of a new NPS and the relevant scheduling decision.

### *1.2.7 Behind the NPS popularity*

One of the main driving forces behind the popularity of NPS is the aura of their perceived legality. Many users have revealed how the term “legal highs” used to market these products and the fact that they were openly sold on the high street implied a “consequence-free” (no legal repercussion) drug use (Corazza et al., 2013b; Soussan and Kjellgren, 2016). Their perceived safety can be considered as another reason for their popularity, strictly intertwined with their legal status and their open sale/trade. Indeed, consumers perceive NPS as less dangerous than classic drugs of abuse, despite the fact that NPS differ only slightly, - small modification to the chemical structure, from their controlled, illegal counterpart (Home Office, 2020). Moreover, the potential health risks associated with NPS are reduced by disguising the presence of psychoactive molecules and not listing them on the package (Schifano et al., 2009).

Another important reason behind their popularity is represented by a high customer satisfaction in regard to ease of access to NPS, low cost and high potency. The EMCDDA reported how some amphetamine-like NPS (e.g. N-Benzylpiperazine (BZP)), not only were almost ten times more potent than the latter but were sold for a quarter of the price (Corazza and Roman-Urrestarazu, 2018; UNODC, 2013).

Finally marketing strategy played an important role in the NPS popularity as well. Colourful and captivating packaging, and names/brands similar to known illicit drugs, popular movies, comics, animals, or landscapes were/are frequently used (Corazza et al., 2014a). In relation to movies, the brand “Black Mamba” and “Clockwork Orange” were used to market two synthetic cannabinoids, AM-2201 and 5F-AKB48; in relation to Cinema, “Mad Alice” and “Krypton”

were used to market a psychedelic herbal blend and an opioid O-Desmethyltramadol (O-DT) (Corazza et al., 2014a).

### *1.2.8 NPS diffusion: the importance of online markets*

A major role in the NPS phenomenon and its different phases has been played by the rapid changes in technology, globalisation and the Internet observed since 2005 (Alalwan et al., 2017; Appel et al., 2020; Corazza et al., 2011). In the last seventeen years the Internet has defined the evolution of a new drug market with the emergence of new technologies (EMCDDA, 2016c; Walsh, 2011). Indeed before the advent of e-commerce, drug markets were identified more with physical spaces and in-person interactions, while after the introduction of online commerce they transformed more into virtual ones (Mackey, 2018; Miliano et al., 2018; UNODC, 2017b). This totally changed the scale of the drug trade from a more domestic to a global reach. The web, with its easily changeable and sometimes unruly structure, offers the perfect drug market structure: a 24/7 shopping experience with the ability to select vendors and interact with them, protected identities, electronic currencies, anonymous transactions and a huge variety and quality of available substances (ACMD, 2009; EMCDDA, 2014; Forman, 2006; Forman et al., 2006; Orsolini et al., 2017a).

Three types of virtual markets can be identified: the clear or surface web (Barratt et al., 2013), the deep/dark web, and those which operate on both the surface and the deep web (grey marketplaces) (Adrian, 2011; Barratt et al., 2014). As reported by the EMCDDA, the surface web is mostly associated with supply of either legal/non-controlled substances (NPS) or substances that are subject to different legal controls between countries (medicines, precursor chemicals, etc. (EMCDDA-Europol, 2016; EMCDDA, 2019a).

Recent legislative measures (EMCDDA, 2017b, 2016b; UNODC, 2021c, 2015), including the Psychoactive Substances Act 2016 (UK Parliament, 2016), have caused restrictions in the surface web sale and distribution of NPS and counterfeit medicines (Schmidt et al., 2011; Wadsworth et al., 2018a, 2018b), driving manufacturers, traders and buyers more towards the deep web (Jurásek et al., 2021; Van Hout and Hearne, 2017). Nevertheless, the surface web still remains an important medium for the sale of NPS and misused medicines (EMCDDA, 2017c; UNODC, 2019b).

Previous studies have shown how the Internet has become a crucial source of information about drugs and drug use (Barratt et al., 2013; Corazza et al., 2013a; Quintero and Bundy, 2011; Walsh, 2011) and have demonstrated the contribution and elucidated the role that social networks can have in this regard. In particular, platforms such as Twitter® (Buntain and Golbeck, 2015; Mackey et al., 2018; Mackey, 2018), Facebook® or YouTube®, facilitate communications, usually with short messages via smartphone, laptop or tablet and offer the chance to share links, information and more

important personal experiences and opinions related to the use availability and purchase of NPS and other drugs (Burns et al., 2014; Del Vigna et al., 2016; Miliano et al., 2018).

Alongside these well-known platforms, a huge number of fora, web pages and on-line communities were created in order to discuss the pros and cons of NPS, sometime to advise against their use, sometime to promote it. The ones that promote it, referred to as pro-drug websites (Orsolini et al., 2015b), include diverse website types (blogs, fora, vending and informational platforms) reporting various degrees of scientifically proven information.

Among these web pages and on-line communities, great following is received by e-psychonauts' blogs (Orsolini et al., 2015a, 2015b). E-psychonauts are typically middle-high class, very well educated individuals who possess the necessary technical knowledge (chemical, pharmacological and pharmacodynamical) to provide trustworthy information on various drugs, especially NPS (Davey et al., 2012; Orsolini et al., 2017b, 2015c; Schifano et al., 2006). Psychonauts define themselves as 'shamans' (Labate and Jungaberle, 2011), 'chaos magickians' (Booth, 2000), 'sailors of the mind/ soul', who typically explore their inner universe with psychedelic/NPS and share the experience on line (Orsolini et al., 2015b). They voluntarily experiment with new drugs in order to reach new and deeper states of mind, and they post their experiences with thorough details regarding dosage, time of action and effects. Psychonauts, as 'modern drug influencers', may help shape and populate online drug scenarios with a huge number of new substances not yet seized or officially detected.

Moreover, the spread of NPS and the Internet can be considered strongly interlinked, with the latter allegedly being a strong influencing voice in defining and feeding the markets for the former (Orsolini et al., 2015b; Schifano et al., 2003).

In light of the facts mentioned above, the Internet can be considered both a major challenge to monitoring agencies, law enforcement, and public health due to the rapidity with which is changing the drug market (EMCDDA, 2019a); and the most important resource to draw on for an extensive analysis and assessment of the current NPS scenario (Corazza et al., 2011; Corkery et al., 2017; Orsolini et al., 2020).

### *1.2.9 NPS scenario to date (2022) and NPS classes investigated by the present study*

In June 2022, the UNODC and EMCDDA reported that the trend observed for the previous years, in term of popularity, number and type of NPS was continuing in 2022 (UNODC, 2022b). In particular, the persistence of benzodiazepine-type NPS (designer benzodiazepines, DBDZ) and new synthetic opioids (NSO) have been observed, alongside a great number of synthetic cannabinoid receptor agonists (SCRAs), and stimulants. Of particular interest are the class of DBZD and NSO (EMCDDA, 2022c; UNODC, 2022b). The latter, which are per se very dangerous and potent CNS depressant, are even more of concern due to their reported co-use which could increase the likelihood of overdose and death (EMCDDA, 2022c; UNODC, 2022b). As reported by the UNODC, NSO are the ‘potentially the most harmful group of NPS’ which, in contrast to the general stabilisation of the number of NPS, has continued to grow, with 22 new molecules reported in 2020 and nine in 2021. NSO, representing 29% of the total NPS currently identified, included both fentanyl analogues and other opioids. Parallel to the increased availability of NSO, an increase in NPS with sedative and hypnotic effects, most of which are benzodiazepine-type NPS, have been reported. DBZD are very often sold at very low prices, sometimes as counterfeit existing medicines, varying greatly in dosage, composition and often adulterated with potent NSO (UNODC, 2021b). These trends have been confirmed by the 1500 NPS toxicology case reported to the UNODC in 2021, which see the persistence of DBZD and NSO among the 58 NPS identified. In particular, NSO accounted 14% and DBZD for 49% of the post-mortem cases reported in 2020-21. Moreover, in all the instance reported for NPS DBZD were found in 69% of the toxicological cases, while of all cases in which NSO were identified, 81% were reported as fatalities. The increase of numbers and complexity for DBZD and NSO contribute as well to the health threat and risks associated with poly drug use, which continues to be an important element in NPS casework (UNODC, 2021b, 2021d) .

Following the data reported by both the UNODC and the EMCDDA the DBZD and NSO classes and the concern/risk associated with the use/abuse of these NPS (Brunetti et al., 2021; EMCDDA, 2021b; Greenblatt and Greenblatt, 2019; Lovrecic et al., 2019; UNODC, 2020c, 2017a), the latter were chosen as objects of this research project.

### 1.3 NPSfinder<sup>®</sup>

As reported in Section 1.2.8 previous studies have underlined the importance of the web as a crucial source of information about drugs and drug use (Barratt et al., 2013; Corazza et al., 2013a; Quintero and Bundy, 2011; Walsh, 2011), in particular so for NPS. Moreover, the importance of analysing the web for an extensive analysis and assessment of the current NPS scenario (Corazza et al., 2011; Corkery et al., 2017; Orsolini et al., 2020) has been reported. These data stand behind the creation of a web crawler, the NPSfinder<sup>®</sup>. The latter is the product of a collaboration project between the Psychopharmacology, Drug Misuse and Novel Psychoactive Substances Research Unit of the University of Hertfordshire and Damicon, an Italian IT (information technology) enterprise. In 2017, Damicon designed a web crawler able to scan the surface web to identify NPS mentioned across a variety of websites (Appendix A). For full details and methodology please refer to Section 2.1. Emerging results, based on an on-going analysis of records retrieved during a 3-year period between November 2017 and October 2020, indicate that the number of NPS molecules across a range of different chemical classes is substantially higher than that known to and reported by both the UNODC and the EMCDDA.

These results seemed not to be in line with the stabilisation of the yearly number of newly identified NPS as reported by both EMCDDA and UNODC (EMCDDA, 2022a; UNODC, 2022b), and raised suspicions about a phenomenon that is either apparently stabilising or is evolving so fast that the only evidence-based approach used to assess the number and type of NPS cannot match the growing pace of the market. Indeed, the data presented by the two organisations result only from evidence-based identification for each of the NPS reported.

#### 1.4 *In silico* studies

As discussed above, among the challenges presented by the NPS, the lack of defined pharmacological/toxicological profiles is one of the most worrisome. Indeed, when novel NPS are discovered, only very limited scientific data are available on the activity/toxicity profile, the assessment of which is mandatory to evaluate the potential threats and risk associated with their recreational use/abuse (Sec. 1.2.6). However, carrying out *in vitro* and preclinical studies on these molecules may constitute an extremely time-consuming and very expensive exercise, especially if one considered the thousands of available NPS. To overcome this issue, the use of *in silico* models, also referred to as predictive or computational models (e.g., quantitative structure-activity relationship/QSAR and Molecular Docking) have been suggested. These models are able to predict the possible biological activity of an unknown molecule (NPS) towards a known receptor (e.g. serotonin, dopamine, opioids receptors) and to provide information on its mechanism of action in a time and cost efficient way. Binding affinity and interaction pattern can be analysed for a variety of receptors resulting in pharmacological profile predictions.

At date, the potential of *in silico* models is well established in the pharmaceutical sector, and successfully/extensively used in the drug development process. Recently, *in silico* models have been applied already to the study of NPS, i.e. designer benzodiazepines (Artemenko et al., 2009; Waters et al., 2018), synthetic cannabinoids (Durdagi et al., 2007a, 2007b; Floresta et al., 2018a), opioids (Floresta et al., 2019), hallucinogenic phenylalkylamines (Zhang et al., 2007), and tryptamines (Schulze-Alexandru et al., 1999) and phenethylamines (Guariento et al., 2018; Wu et al., 2019).

#### 1.4.1 Predictive models definition

A predictive model is a model that use statistics to predict outcomes. The model is usually applied to predict the future of the topic being studied/investigated (Geisser, 2017) and tries to guess the probability of an outcome given a set amount of data. Models can also try to determine the probability of a set of data belonging to another set. When used and distributed commercially, predictive models are referred to as predictive analytics, and are often a synonym for Machine Learning (ML) (Finlay, 2014).

Predictive analytics uses data analysis techniques such as data mining, machine learning and artificial intelligence.

ML focus on how computers can learn from sets of data (Burrell, 2016; Finlay, 2014), and can be :

- Supervised. The algorithm has both the set of input data and the outcome of interest and needs to find the relationship between the two (Lo et al., 2018).
- Unsupervised. The algorithm has only the set of input data and needs to find naturally occurring patterns or groupings within them (Lloyd et al., 2013).
- Semi-supervised. The algorithm has the outcome of interest and the set of data from which it will need to understand the respective correlation, but it will also erase the outcome of interest and find new types of clusters/correlations among the data (Kingma et al., n.d.).
- Reinforcement learning. The algorithm learns from interaction with the environment to achieve a goal and try to explore the best ways to earn the greatest reward (Popova et al., 2018).
- Neural networks and deep learning. The algorithm captures complex non-linear relationships between input variables and an outcome and can address some of the limitations of traditional analytics (Jing et al., 2018).

Predictive modelling/analytics is widely used in the pharmaceutical industry, where it is referred to more commonly as *in silico* methodologies. Adopted from computerised molecular modelling to clinical trial forecasting and drug approval prediction it has a high significance especially in the drug discovery process. In the latter, its applications include prediction of interaction, inhibition and toxicity (Lampa et al., 2016). Predictive models are applied to predict the structure of a future lead compound, hence used at the beginning of the development phase, or to predict the activity/toxicity of known compounds and, therefore, used later in the evaluation phase of a new drug.



#### 1.4.2 *In silico* drug design (*in silico* pharmacology)

The computer-based methods used in drug discovery are commonly referred to as computer-aided drug design (CADD) or *in silico* pharmacology. *In silico* technologies are powerful tools used to speed up the whole drug discovery process, reducing the time it takes for a new molecule to enter the market, and to reduce associated costs.

*In silico* is a modern term, related to the well-known biological terms *in vivo* and *in vitro*, and define experimentation performed by computer. Despite some uncertainty, the origin of the term can be retraced to Danchin (Danchin et al., 1991; Ekins et al., 2007):

*'[I]nformatics is a real aid to discovery when analyzing biological functions.... I was convinced of the potential of the computational approach, which I called in silico, to underline its importance as a complement to in vivo and in vitro experimentation'*.

*In silico* pharmacology is at date a growing discipline adopted worldwide to capture, analyse and combine medical data (experimental). This data can be then utilised in the creation of computational models to predict, suggest and provide medical/therapeutic discoveries. (Ekins, 2014; Ekins et al., 2007). *In silico* technology is able to virtually simulates every aspect of drug discovery and development, helping us to handle enormous amount of data, picking ideas and taking decision (Swaan and Ekins, 2005). It is basically a virtual shortcut to identify lead drug molecules and predict their effectiveness/toxicity (Leelananda and Lindert, 2016). *In silico* technology is usually used throughout the whole discovery process: screening of large libraries to extract a small number of putative active compounds to send for testing (Subhash et al., 2015); growing new future lead compounds; optimising the ADME (Absorption, Distribution, Metabolism, and Excretion) properties and investigating the potential toxicity of lead compounds (Bajorath, 2015).

Machine learning methods have been widely used in *in silico* pharmacology of small molecules since 1960, when the concept of quantitative relationships between chemical structure and pharmacodynamics and pharmacokinetics began to be uncovered (Ekins, 2014).

*In silico* technologies can be divided in structure-based drug design (SBDD) (Reich and Webber, 1993) or ligand-based drug design (LBDD) (Shim and MacKerell, 2011) methods. Usually SBDD is used when information on the 3D (three dimensional) target structure is available or can be retrieved while LBDD is used when such information is lacking (Shim and MacKerell, 2011). SBDD analyses the 3D structural information of a specific target, to identify key sites or cavities that are relevant to its biological activity. This information can be utilised to identify specific protein-ligand interaction(s). Popular approaches used in SBDD are molecular docking (MD), high throughput docking and *de novo* (anew) ligand design.

Conversely, LBDD analyses a group of known ligands for a specific target and tries to extrapolate which psychochemical properties, shared by the ligands, are essential for their biological activity. This is referred to as structure-activity relationship (SAR) and can be used either to direct de novo design of drugs or to optimise already known ones (Ramírez, 2016). Popular approaches used in LBDD are quantitative structure activity relationship (QSAR), quantitative structure-property relationship (QSPR) (Chen et al., 2012; Svetnik et al., 2003; Tropsha, 2010) and pharmacophore mapping (Leelananda and Lindert, 2016; Loew et al., 1993; Mason et al., 2005).

For the scope of this research programme, QSAR, molecular docking, pharmacophore mapping and scaffold hopping studies were chosen as considered the most appropriate to predict the biological activity (QSAR), the possible receptor interaction (molecular docking and pharmacophore mapping) and the possible future chemical modification for the DBZD and NSO classes.

### 1.4.3 Chemical similarity

Chemical similarity is a key concept in cheminformatics, which is another term for *in silico* techniques, and in all those studies which apply computer and information science techniques to chemistry (Bender and Glen, 2004). Chemical similarity identifies with the similarity of chemical elements and structures (i.e. molecules and compounds) either with respect to structural characteristics or to functional characteristics (Dean. M. P., 1995). The latter identify the effect that a molecule has on a biological system (i.e. receptor, enzymes, etc). The biological activity of a compound is the variable which is used to quantify and identify the functional similarity among a set of compounds. The chemical similarity instead is the variable which evaluates the “inverse of a measure of distance in descriptor space” (Johnson et al., 1990). Descriptors, which are going to be discussed in full in the next section are numbers which are used to describe the structure of a molecule and assess the similarity of the latter towards other. The chemical similarity concept is very important because it is at the base of the modern drugs design studies. These studies indeed are based on the similar property principle of Johnson and Maggiora (Johnson et al., 1990), which states: *similar compounds have similar properties*. To assess the molecular similarity, molecules are usually represented by structural keys or molecular fingerprints, based on both their 2D and 3D properties. 2D fingerprints have been reported as the most used tool to assess similarity specially to compare large databases. The most popular similarity measure based on fingerprints is the Tanimoto (or Jaccard) coefficient  $T_c$  (Bajusz et al., 2015a). Both coefficient measures similarity between two sample sets via the analysis of the size of the intersection (of these two sample set) divided by the size of the union of the sample sets. Tanimoto though, differently from Jaccard uses the ratio of bitmaps, where each bit of a fixed-size array represents the presence or absence of a

characteristic (Tanimoto, 1958). The ratio is calculated as is the number of common bits, divided by the number of bits set (i.e. nonzero) in either sample (Tanimoto, 1958).

#### 1.4.4 *Quantitative Structure Activity Relationship (QSAR)*

QSAR is an LBDD method that works on the principle of similar structure similar activity (Floris et al., 2014) known as the Similar Property Principle published by Johnson et al (Johnson et al., 1990). The similarity principle is the “observation that structurally similar molecules tend to have similar properties”, i.e. small changes to the chemical structure of an active compound should maintain the biological activity against a receptor (O’Boyle and Sayle, 2016). QSAR is a computer calculated mathematical model which tries to statistically correlate the structure and the function of a molecule using chemometric techniques (EL-Gindy and Hadad, 2012). The function of a molecule is the biological activity and it is often expressed as the half maximal inhibitory concentration ( $IC_{50}$ ) or the inhibition constant ( $K_i$ ). The structure instead is expressed using molecular descriptors. The latter are numbers that represents all biological, physical, and chemical properties. These descriptors can derive from knowledge-based, molecular or quantum-mechanical tools (Marrero-Ponce et al., 2012). They are classified according to the “dimensionality” of the property from which they are calculated in 1D, 2D and 3D. The 1D are derived from the molecular formula (molecular weight, number of heteroatoms, etc.), the 2D from the bond order (hydrogen bond donors/ acceptors, rotatable bonds/ bond order, etc) and the 3D from the spatial arrangement of the atoms (molecular/ polar surface area, chiral centre, volume, etc.) (Balaban, 2012). According to the type of descriptors used, QSAR methods are also classified as 1D, 2D, 3D and so on (Lewis and Wood, 2014). It should be noted that currently QSAR methods are classified up to the 6D level, where other properties of the molecule are considered such ligand configuration, induced fit models, etc. (Damale et al., 2014; Myint and Xie, 2010). QSAR models can also be classified as linear or nonlinear according to the calculation methods used. Linear methods use multiple linear regression (MLR), partial least-squares (PLS) and principal component analysis/regression (PCA/PCR) while nonlinear use artificial neural networks (ANN) and Bayesian neural networks (Becker et al., 2006).

Usually QSAR studies start from a dataset of biologically active compounds (preferably not less than 100) (Gad, 2014) for which experimentally derived biological activities are available. Once the dataset is finalised, it is divided into a training set and a test set, typically including, respectively, the 80% and 20% of whole dataset. The training set is used to build the mathematical model, while the test set is used to assess its predictivity and generalisability.

The resulting mathematical model shows how the activity of a molecule on a specific target is the consequence of the structural attributes of the molecule itself (molecular descriptors). QSAR is generally represented by a linear equation (Equation 1.1):

*Equation 1.1 Example of a QSAR mathematical model. The equation represents the biological activity, i.e. the dependent variable, as the function of three sets of data, a constant, i.e. Const; a set of descriptors, identified by the letter “P”, and their respective coefficient identified by the letter “c”. The “P” parameters are calculated for each molecule whose biological activity needs to be calculated, in the series and the coefficients “c” are calculated by fitting variations in the parameters and the biological activity.*

$$\text{Biological Activity} = \text{Const} + (c_1 \times P_1) + (c_2 \times P_2) + (c_3 \times P_3) + \dots + (c_n \times P_n)$$

Where  $P_1 \dots n$  represent the descriptors and  $c_1 \dots n$  their respective coefficients. Once calculated it is used to predict the activity of unknown compounds and new drug analogues (Verma et al., 2010).



Homepage,” 2021). These databases contain millions of biologically relevant small molecules and hundreds of thousands of protein structures (Sterling and Irwin, 2015; Wishart, 2006).

Once the 3D target structure is known and identified, MD software proceeds to identify the most appropriate target binding site (pocket) through either geometry or energy lead algorithms. Once the binding site is identified, MD proceed to generate different orientations of the ligands, known as poses, inside the pocket itself. Scoring functions are used to estimate the strength of these poses, i.e. for each pose a value of predicted binding affinity is returned, usually in Kcal/mol. Scoring is a method that uses a scoring function to rank the various ligand-target complex predicted in order to identify which is the most viable. The scoring functions are categorised into force-field based, knowledge-based, empirical-based and consensus-based (Ramírez, 2016). These functions are a crucial part of the algorithm and the more accurate they are the better the docking results.

There are two types of docking: rigid and flexible. Rigid docking assumes that compounds are inflexible, and the ligand will rearrange itself (3D) to best match the binding pocket; flexible docking instead identifies conformations for the receptor and ligand molecules as they exist in the complex (Huang et al., 2006). While rigid docking is more in line with the "lock-and-key model" proposed by Fischer in 1894, that see the ligand as a substrate which is inserted into the active site of a protein as a key is inserted into a lock, flexible docking embrace the theory of an induced-fit (Dias and de Azevedo Jr., 2008). This theory, proposed by Daniel Koshland in 1958, see both the ligand and target able to undergo modest conformational changes and adapt to each other until an ideal match is reached (Dias and de Azevedo Jr., 2008).

Molecular Docking can be used for various purposes: virtual screening of large libraries of compounds; propose structural hypotheses of how the ligands bind to the receptor, i.e. location and relative position of a ligand's interaction to a protein (also referred to as the binding mode or pose) which is invaluable in lead optimisation; and predict the binding affinity of unknown ligands towards know receptors (Raval and Ganatra, 2022).

### 1.4.6 Pharmacophore Mapping

Pharmacophore mapping (PM) is an LBDD technique that works on the same “similarity principle” of QSAR but focuses on the structure of the ligand more than on its biological activity. The term *pharmacophore* was first coined in 1909 by Paul Ehrlich to indicate ‘a molecular framework that carries (*phoros*) the essential features responsible for a drug's (*pharmacon*) biological activity’ (Güner and Bowen, 2014). The International Union of Pure and Applied Chemistry (IUPAC) definition is more explanatory: ‘A pharmacophore is an ensemble of steric and electronic features that is necessary to ensure the optimal supramolecular interactions with a specific biological target and to trigger (or block) its biological response’ (Wermuth et al., 1998). The term *supramolecular* means noncovalent. In other words, a pharmacophore is a 3D model describing the type and location of the binding interactions between a ligand and its target receptor, necessary to trigger or block the latter (Wermuth et al., 1998). Typical pharmacophoric features include hydrogen bond donor, hydrogen bond acceptor, hydrophobic, and positively and negatively ionised areas. A pharmacophore can be defined also as a 3D spatial arrangement, a map of chemical features which are derived using mathematical algorithms (Wolber et al., 2008).

Pharmacophore mapping can be either ligand based, or structure based (Figure 1.4).

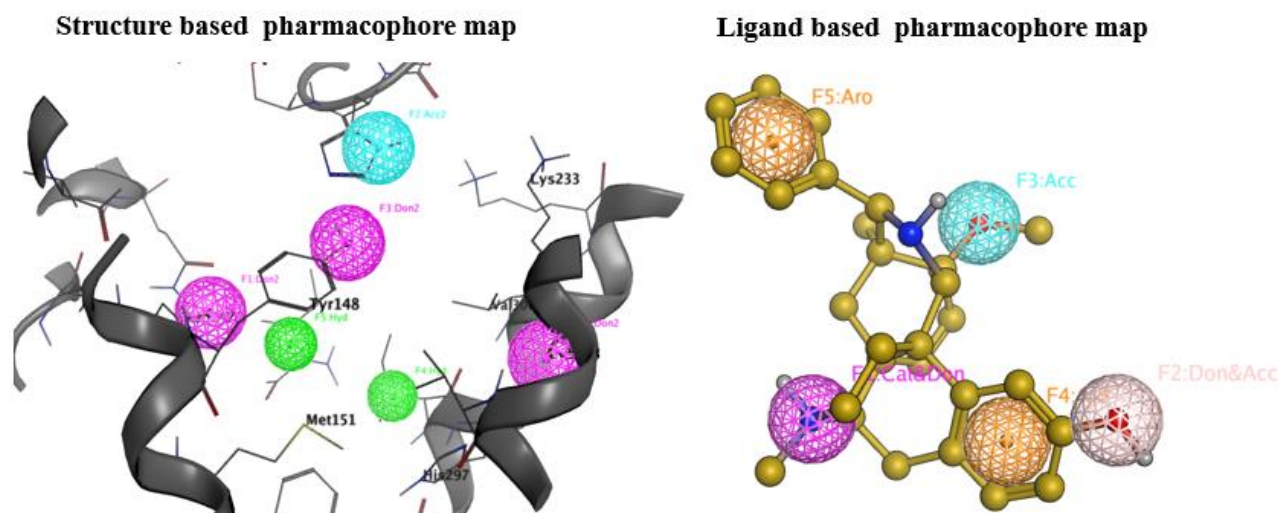


**Figure 1.4.** Visual representation of a structure based (left) and ligand based (right) pharmacophore map.

In order to obtain a ligand-based pharmacophore model a set of biologically active molecules need to be explored in terms of spatial conformations and superposed in a process that is called molecular alignment. From this superposing all the chemical features that are common across the molecules are extracted and use to design the pharmacophore (Yang, 2010). The alignment can be carried out either as a point-based (atoms, fragments, chemical features) or as a property-based approach

(molecular field descriptors). For structure-based pharmacophore mapping a 3D defined binding pocket needs to be available either with or without a complexed ligand. Every atom or chemical group in both the ligand and the structure can be labelled by chemical properties such as hydrogen bond donors or acceptors, aromatic, cationic, etc., and can be reduced to a pharmacophore fingerprint.

Once the pharmacophore model is ready, it then can be used to predict the affinity of unknown compounds and new drug analogues to a specified target through the screening of known libraries. (i.e. ZINC (Irwin et al., 2012; Sterling and Irwin, 2015; “ZINC,” 2021)).

#### 1.4.7 *De novo (drug) design and Scaffold hopping*

Among the in-silico technique, *de novo* design (DND) is a computational method used to generate novel molecular structures with desired pharmacological properties. *De novo* derives from Latin and means “from new,” “afresh,” or “a new-fangled” (Ramírez, 2016; Suryanarayanan et al., 2018). Six methods can be identified in the DND process (Suryanarayanan et al., 2018) Table 1.3.

**Table 1.3** *Classes of computational methods for the de novo design* (Suryanarayanan et al., 2018)

<b>Fragment positioning methods</b>
Identifies a specific position of atom or fragment in binding sites
<b>Site point connection methods</b>
Identifies a unique site location for placing fragments in the binding sites
<b>Fragment connection methods</b>
Connects the fragments at particular position within binding sites
<b>Library construction methods</b>
Builds a library of fragments with desirable information
<b>Molecule growth methods</b>
Keeps atoms or fragments at different places within binding sites of target and grows them by joining with other atoms/fragments with various coordination
<b>Random connection methods</b>
Connect the fragments in random way



DND can be used, beside finding new molecules, to produce novel chemical scaffolds or bioisosteric equivalents for already known structures (scaffold hopping) (Langdon et al., 2010). The notion of scaffold hopping was introduced by Schneider et al., as a 'technique to identify isofunctional molecular structures with significant different molecular backbones' (Schneider et al., 1999). Scaffold hopping, also known as lead hopping (Böhm et al., 2004), usually starts from the structure of known active compounds and tries to identify novel chemotypes while modifying their central core structure. Scaffold hopping modification can be classified as small, medium, and large-step, or according to the number of hops required (Sun et al., 2012):

- 1° hop for minor modifications, e.g., heteroatoms replacing in backbone rings
- 2° hop for more extensive modification, e.g., rings opening
- 3° hop for replacement of peptic moieties with non-peptic ones
- 4° hop for a totally new backbone.

Examples of scaffold replacement include morphine-tramadol, pheniramine-cyproheptadine and sildenafil-tadalafil (Sun et al., 2012).

#### 1.4.8 *In silico* pharmacology and NPS

Despite the fact that *in silico* methodologies were created/developed primarily for the pharmaceutical industry and are now well established, and successfully/extensively used tools in the drug development and discovery pipeline (de Ruyck et al., 2016; Valerio, 2012; Valerio and Choudhuri, 2012), they also have been used to better understand/predict the pharmacological profile of NPS. Indeed, computational models have already been applied to a great number of the NPS classes: 3D QSAR to predict the biological activity of DBZD (Artemenko et al., 2009; Waters et al., 2018); 3D QSAR and docking studies to predict synthetic cannabinoids with high affinity for the cannabinoid receptors (Durdagi et al., 2007b, 2007a; Floresta et al., 2018b; Tuccinardi et al., 2006); QSAR, docking and pharmacophore studies to predict NSO biological activity on opioids receptors (Ellis et al., 2018; Floresta et al., 2019; Jia et al., 2021; Vo et al., 2021; J Zhang et al., 2009); and 3D QSAR on hallucinogenic phenylalkylamines (Zhang et al., 2007) and phenethylamines and cathinones (Floresta and Abbate, 2021; Guariento et al., 2018; Isberg et al., 2013; Saha et al., 2015)

## 1.5 Gap(s) in knowledge

As reported by the UNODC and EMCDDA, NPS continue to pose serious health risks. They also present with numerous challenges in terms of detecting and monitoring, understanding patterns of use and harms caused and developing appropriate public health and legal responses. Despite the official sources (such as the UNODC and EMCDDA) reporting roughly 1,100 NPS, findings of an analysis of the surface web suggest how the number of NPS possibly available on the market is far (almost four times) higher. This is of particular concern if one considers that we are witnessing an upward trend, in terms of numbers and prevalence, of more potent NPS molecules. In particular, more potent synthetic opioids (e.g., fentanyl derivatives) and designer benzodiazepines are continually appearing on the market. The high potency of these drugs creates a life-threatening scenario, with very high chances of unintentional overdoses and increased health risks (EMCDDA, 2022a; UNODC, 2022b).

The assessing of an online NPS market that differ from the evidence based one, with online numbers exceeding the ones reported by official sources, represents a gap that need to be assessed.

Moreover, when novel NPS, are detected only very limited scientific data can be retrieved on the activity/toxicity profiles and the option of performing *in vivo* and *in vitro* studies on the latter (dozens to hundreds) may result in an extremely time consuming and very expensive task. A different approach, which could be of help in overcoming these issues, could consist in the use of computational models (e.g., quantitative structure-activity relationship/QSAR and Molecular Docking). These have indeed been suggested of help in providing levels of prediction of both biological activity and binding affinity of unknown molecules towards a known receptor in a quick and reliable way. This could help understand the threat associated with newly identified NPS and, in particular, with the classes of synthetic opioids and synthetic benzodiazepines which at present represent the most worrisome/challenging classes from legal and healthcare perspectives.

Given the numerous challenges posed by NPS, there is a strong need for multidisciplinary and international collaboration to enhance knowledge and understanding, strengthen best practice and improve the quality of information-sharing among professionals working in this area.

## 1.6 Aims and objective of the research programme

### 1.6.1 General aims of research programme

Against the above-described background, the aims of the projects within this programme of doctoral research were to: use the data available from the NPSfinder<sup>®</sup>, European and worldwide agencies to identify the current NPS online scenarios for DBZD and NSO; use *in silico* computational techniques to predict biological activity of these newly emerged NPS; use the predicted values to infer possible health threats associated with the consumption of these substances, underscoring which of the NPS identified online could indeed represent a serious threat to public health; assess the potential of *in silico* methodologies as a preliminary risk assessment tool; and subsequently inform relevant stakeholders with the risks associated with these new NPS.

### 1.6.2 General objectives of research programme

The objectives of the project were as follows:

- Assessing the current scenario for the DBZD and NSO NPS classes, with relevance to difference between the online and real word data (NPSfinder<sup>®</sup>, UNODC, EMCDDA and other official sources).
- Use the data from the point above to build computational predictive models with the use of Molecular Operating Environment (MOE<sup>®</sup>) and Forge<sup>™</sup>.
- Build Quantitative Structure Activity Relation (QSAR) models to predict biological activity of the DBZD and NSO classes of NPS identified online.
- Conduct docking studies with MOE<sup>®</sup> to validate/support the QSAR models results, and to understand the interaction patterns between NSO /DBZDs and corresponding receptors.
- Build Pharmacophore models on the molecules identified by NPSfinder<sup>®</sup> and predicted to be the most biologically active to analyse correlation between chemical feature and biological activity.
- Use the unique pharmacophore model to filter databases (i.e. ZINC) in order to discover new active structures for a determined target.
- Analyse the results obtained with the computational model to assess potential risky and worrisome future trend.
- Worldwide Spread of resulting knowledge, through seminars, conferences, papers, and reports to relevant stakeholders.

The following chapter will present an overview of the methodologies used, which will be then discussed in more details in Chapter 4 (DBZDs) and 6 (NSOs).

## Chapter 2 Methodologies

### 2.1 NPSfinder<sup>®</sup>

#### 2.1.1 Web crawler data extraction

The crawling/navigating software (i.e. NPSfinder<sup>®</sup>) was designed by Damicom, an IT enterprise based in Rome (Italy), to facilitate the process of early recognition of the increasing dissemination of NPS online and the variability of information sources. The NPSfinder<sup>®</sup> automatically scanned, from November 2017 to October 2020, the open/surface web for new/novel/emerging NPS using the current standard methodology in the IT Field (SQL Server; MYSQL; PHP/PYTHON; JAVASCRIPT for client side; 2 x Intel<sup>®</sup> Xeon<sup>®</sup> SP Gold 16-Core incl. Hyper-Threading Technology). It mapped on a 24/7 basis the variety of psychoactive molecules mentioned/discussed among a range of representative web pages, with particular attention to online psychonaut web sites/fora (Schifano et al., 2019). The scanned URLs were representative mostly of online psychonaut websites/fora but also of other NPS online resources (Appendix A). In particular the majority of the molecule were identified from isomerdesign.com (Isomer Design, 2021). The software reliability was validated before the start of the project with several pilot searches through Google<sup>®</sup> and other search engines. The key words used included: NPS, novel psychoactive substances, new psychoactive substances, emerging psychoactive substances, drugs online, buy new substances, psychonauts drug forums, prescribed medications, psychoactive plants, psychoactive herbs, image- and performance-enhancing drugs, etc. These pilot searches helped into shaping the list of URLs of interest. The predominant language used by the web crawler was English, but other languages were also used, including Spanish, German, Russian, Italian, Dutch, French, Swedish and Turkish.

From November 2017, NPSfinder<sup>®</sup> identified and extracted, contextually to the name of the molecule, a set of other information such as the chemical and street denomination, the chemical formula, the chemical structure, and any pharmacological information reported (when available). The data collected like so were imported and stored in a MYSQL database with an SSL security protocol and encrypted with asymmetric cryptographic procedures. The data were then stored in a virtual storage area, i.e. the NPSfinder<sup>®</sup> database. In this database, the interface of which is presented below (Figure 2.1), the NPS identified are listed in order of identification date, and each entry contains information about the substance family, the chemical characteristics, the commercial and street names, as well as information on pharmacology and toxicity, and suggestions on the clinical management of related intoxication.

NPS Finder  
WELDDME VALERIA CATALANI

HOME ► MOLECULES & PRODUCTS ► SETTINGS ►



⏪ Molecules & Products ADD NEW

Search:  Typology:

Family:  Order by:

Edited by:  Show hidden results:

4231 MOLECULES FOUND [ PAG 1 / 85 ]

#ID	IMAGE	INCLUSION DATE	FAMILY	NAME	OTHER NAMES	CHEMICAL COMPOSITION	SMILES KEY	INCHI KEY	DESCRIPTION	DETAILS
#21334		22/10/2020	Hallucinogens	1CP-MIPLA	1-Cyclopropionyl-N-ethyl-N-isopropyllyse	(6aR,9R)-1-Cyclopropionyl-N-methyl-N-isopropyl-7-methyl-4,6,6a,7,8,9-hexahydroindolo[4,3-fg]quinoline-9-carboxamide; (6aR,9R)-4-(cyclopropanecarbonyl)-N-isopropyl-N,7-dimethyl-4,6,6a,7,8,9-hexahydroindolo[4,3-fg]quinoline-9-carboxamide; C24H29N3O2	CN1C[C@@H](C=C2[C@H]1Cc1cn(c3c1c2ccc3)O(=O)C1CC1)O(=O)N(C(C)C)C	DBIYDHUGEKMIHZ-DYERRHJHSA-N	1cP-MIPLA is a novel psychedelic substance of the lysergamide class. 1cP-MIPLA is closely related to	

**Figure 2.1** NPSfinder® database interface.

All the data extracted by the web crawler from November 2017 to October 2020 were manually analysed by a group of trained medical professional. A further analysis, with particular regard to the class of DBZD and NSO was carried out for the scope of this research programme. Afterwards, a full assessment and editing of each NPSfinder® entry was carried out and the range of unique NPS was identified.

### 2.1.2 Classification of identified NPS

The molecules identified by the NPSfinder® were first searched for in Google®/ Google® Scholar (“Google,” 2019), PubMed (PubMed, 2020) and Wikipedia (“Wikipedia, the free encyclopedia,” 2022) to classify them according to their chemical description when available. PubChem (“PubChem,” 2021) and ChEMBL (EMBL-EBI, 2021) were used as well and, whenever possible IUPAC (IUPAC, 2019a, 2019b) name was also used/added to the description. Whenever there were errors in published IUPAC names, the software ChemDraw (PerkinElmer Informatics, 2022) was used as it enables the generation of chemical names from structures and vice versa. In order to achieve a more accurate identification of the NPSfinder® data entries, the latter were compared with those molecules reported by the EMCDDA EWS and the UNODC EWA databases. The classification adopted in the NPSfinder® identifies 17 classes of NPS (Schifano et al., 2015), which are reported in Table 2.1.

**Table 2.1** Type and number of classes used to identify NPS identified online by the NPSfinder<sup>®</sup>

NPSfinder <sup>®</sup>	
Aminoindanes	Phenethylamines
Cannabimimetics	Performance and Image Enhancing Drugs (PIEDs)
Cathinones	Piperazines
Fly	Plant-based
Gaba-ergics	Prescribed Drugs
Hallucinogens	Psychostimulant
NBOMe	Tryptamine
Opioids	Others
PCP-like	

All the information extracted by the web crawler were manually checked and corrected if necessary. Additional information collected for each substance from literature and scientific reports was added, when available, manually to each entry in the NPSfinder<sup>®</sup> database. Once all the available information were collected for each entry included in the NPSfinder<sup>®</sup> database, a further check was carried out to eliminate those molecules which were considered duplicate. To facilitate the process of unambiguous identification of the index NPS and minimise chances of duplicates, the International Chemical Identifier Key (InChIKey) was added to the single entries. InChIKey is a hashed representation of the full International Chemical Identifier (InChI) (Heller et al., 2013), created for the purpose of facilitating online searching of chemical compounds. For the purpose of this research programme, different salts of the same index NPS were considered as duplicates (Ch 2.2.1).

### 2.1.3 Comparison between NPSfinder<sup>®</sup>, EMCDDA and UNODC databases

For the DBZD and NSO classes, NPSfinder<sup>®</sup> entries were compared with those reported from both the EMCDDA European Database on New Drugs (EMCDDA, 2020b) and the UNODC Early Warning Advisory on NPS (UNODC, 2022d) databases. The comparison was conducted using the InChIKey to avoid any confusion due to the non-uniqueness of the other denominations (i.e. IUPAC, or common name).

## 2.2 In silico methodologies

Two software were used for the in silico studies, i.e. MOE<sup>®</sup> (Chemical Computing Group ULC, 2022) and 3D with Forge<sup>™</sup> (Cresset, 2021). These software in particular were chosen due to their high rate of citation in peer reviewed journal, patents and previous work conducted with NPS (Chemical Computing Group, 2022; Floresta et al., 2019, 2018b; Floresta and Abbate, 2021). In this section, an overview of the methodology which was used during this research project is presented. For detailed methodologies used for the two NPS classes analysed a more in-depth description can be found in the respective sections, i.e. 4.3 and 6.4.

### 2.2.1 QSAR Training and test set

The first step in building a QSAR model is the identification of a dataset (training and test set). For the definition of training and test set please refer to Section 1.4.3. As previously reported, the training set is the set of molecules used to build the mathematical model, while the test set is used to assess its predictivity and generalizability. The dataset in QSAR is the ensemble of two type of data: a 2D codified structure and the respective experimental value of biological activity towards a defined target. The 2D codified structure is usually represented by a simplified molecular-input line-entry system (SMILES), which is a line notation for describing the structure of chemical species using short ASCII strings (Weininger, 1988). Different biological activities values can be used to build a QSAR as long as they are experimental values. Without experimental biological activity available no QSAR model can be created.

To create a QSAR module that is reliable, i.e. predictive and robust, the dataset should be neither too small (e.g. < 50) nor too big (e.g. > 2000) and should include molecules with a similar structure to those in analysis (Gad, 2014). The higher limit is usually defined by the computing resources available and the lower limit by the number of training/test sets that need to be generated from the data set (Gad, 2014).

While we cannot identify an exact minimum number to generate a reliable QSAR model, we need to consider that training sets are used for model development, and if too small, the chances of correlation and overfitting (i.e. not predictive model) increase exponentially (Cherkasov et al., 2014; Tropsha, 2010). Indications can be taken from the literature: the number of compounds in the dataset for studies involving biological activity values should be more than 40, with the number of compounds in the test set reflecting an average of 10-20% of the latter (minimum value set to 5 (Tropsha, 2010)). The best situation would be a dataset comprising of 150-300 molecules and respective activity values.

Requirements apply also for the activity values: the total range of activities should be at least five times higher than the experimental error (when indicated); and no large gaps between two consecutive values, e.g. more than 10%–15% of the entire range of activities) should be allowed (Tropsha, 2010; Verma et al., 2010).

Moreover, because the QSAR models that can be generated may only be as good as the data itself, database curation is an essential step. In particular the portion of the dataset including inorganic and organometallic compounds and salts and mixtures should be eliminated, as well as any duplicate (Fourches et al., 2010).

### 2.2.2 *Outliers: identification and removal*

An outlier is per definition a data point that differs significantly from other observations. In QSAR outliers are compounds that have ‘unexpected biological activity and are unable to fit in a QSAR model’ (Verma and Hansch, 2005). When creating a dataset the main theory underlying QSAR, - similar compounds have similar biological activity, should be followed. However this is not always possible due to the presence of outliers (Johnson et al., 1990). The activity cliff is the term used to define this phenomenon, due to areas in the chemical structure, where very small modification (e.g. the addition or removal of a methyl group) will result in great variation in biological activity (Maggiora, 2006). Two types of outliers can be identified: structural outliers, i.e. singletons that can be identified in a dataset using available techniques described in statistical literature (e.g. Tanimoto coefficient (Tc) which assess the similarity between two molecular structures (Bajusz et al., 2015b) (Sec. 4.3.1)); and activity outliers defined as activity cliffs. Both outliers could be real or due to errors in representation and annotation but in any case, their presence could cause model unreliability. Hence, despite the fact that no official protocol to deal with outliers in QSAR is in place, the latter should be removed prior any calculations (Golbraikh et al., 2014; Maggiora, 2006).



### 2.2.3 Descriptors selection

Once the QSAR dataset is ready, descriptors (2D or 3D) can be calculated and correlated with the biological activity values. This process could be done either manually (MOE<sup>®</sup>) or automatically (Forge<sup>™</sup> and MOE<sup>®</sup>) according to the software utilised for the analysis, and usually returns a correlation coefficient ( $\rho$ ) for each of the descriptors. The closest  $\rho$  is to zero the less the correlation between the two variables, and vice versa. Usually only descriptors with high values of  $\rho$  are used to build the QSAR models (Hu and Bajorath, 2017). When building a QSAR model descriptors must be chosen in order to be as few as possible: the rule of thumb is to have a maximum of 1 descriptor for every 5 or more (better) molecule in the training set (Danishuddin and Khan, 2016). It is very important to assess the lack of correlation between descriptors (i.e. not correlated to each other), otherwise this will bias the model via a process called overfitting (Gad, 2014; IBM Cloud Education, 2021).

### 2.2.4 Model Building

Once descriptors have been calculated and selected (according to correlation with biological activity and non-mutual correlation), QSAR models (both 2D and 3D) are calculated. In order to build a reliable and robust QSAR methods, three statistical parameters need to be calculated and evaluated: the correlation coefficient ( $r^2$ ) (internal predictiveness) and the leave-one-out cross validation correlation ( $q^2$ ) (robustness) for the training set (internal validation); and  $r^2$  for the test set for external predictiveness (external validation). The  $r^2$  value defines the goodness of fit of the QSAR model,  $q^2$  defines the goodness of prediction (Golbraikh and Tropsha, 2000). A QSAR model is considered acceptable when it has an  $r^2$  value  $> 0.6$  and  $q^2 > 0.5$  for the training set (Beebe et al., 1998) and a  $r^2 > 0.5$  for the test set (Golbraikh and Tropsha, 2002). An error test is also necessary to evaluate the significance of the model, hence the root mean square errors (RMSEs) for the training and test sets are usually generated (Beebe et al., 1998).

### 2.2.5 QSAR validation

QSAR models are submitted to an internal and an external validation. The internal validation, or “leave one out “ cross validation, is carried out using the training set (Hawkins et al., 2003). This cross validation consists in removing (leave-out) one entry at a time from the training set during the model calculation, resulting in a new training set every time. The latter is used to calculate new models. All the entries of the dataset are removed once during this process, and all the models generated are compared to the original (complete training set). The differences observed among these methods are used to calculate  $q^2$ , i.e. the revised correlation coefficient. This type of internal validation gives an indication of how robust ( $q^2$ ) the model is, and if it is sensitive to small changes in the training set.

However, cross-validation tend to provide “overly optimistic estimates of the predictive power of the model, as the data are typically not a truly random sample of molecules” (Alexander et al., 2015). Indeed, while high values of  $q^2$  may suggest that the model fit the training set data well, it does not give any information on the ability of the model to predict activity of an external test set. Indeed, as reported by Alexander et al, “the use of an independent test set is considered the ‘gold standard’ for assessing the predictive power of models and is the most stringent approach”. The validity of this approach is reported as well in the guidance document on the validation of QSAR models used in regulatory applications (OECD, 2007). Here, the external validation is carried out with the use of a test set. This helps to evaluate the external predictive power for molecules to which the model was not previously exposed (test set). The value obtained,  $r^2$ , is an indication of the predictive power.

### 2.2.6 *Applicability domain*

The domain of applicability (or AD) is a very important concept in QSAR, which must be defined for each model as an additional step of the validation process. The applicability domain indeed allows to estimate ‘the uncertainty in the prediction of a particular molecule based on how similar it is to the compounds used to build the model’ (Weaver and Gleeson, 2008). The AD of a QSAR model has been defined as ‘the response and chemical structure space in which the model makes predictions with a given reliability’ (Netzeva et al., 2005; Roy et al., 2015a). It is important to highlight how a QSAR model is able to reliably predict the biological activity of a new compound, only when the latter falls within the AD of the model (Sahigara et al., 2012). If the new molecule falls within the AD, the prediction can be considered reliable (interpolation), if it falls outside the prediction is less reliable (extrapolation) (Roy et al., 2015a). The AD of a QSAR model can be determined in various methodologies, including but not limited to geometrical methods; distance-based methods, probability density distribution and ranges in the descriptor space. For the scope of this paper the distance based methods using the Tc evaluation will be used to assess the AD of the QSAR model generated with MOE<sup>®</sup> (Sahigara et al., 2012). Forge<sup>™</sup> instead calculates its own AD automatically.

## 2.3 Molecular docking

### 2.3.1 Protein Data Bank and 3D receptor structures identification

Molecular docking studies were used to evaluate the binding affinity between a ligand, the DBZD and NSO identified by *NPSfinder*<sup>®</sup>, and their respective receptor of which the 3D crystal structure is known, in particular the gamma-aminobutyric acid receptor A (GABA-AR) (Berman et al., 2000; Morris and Lim-Wilby, 2008; “RCSB PDB: Homepage,” 2021) and the delta ( $\delta$ ), kappa ( $\kappa$ ) and mu ( $\mu$ ) opioid receptors (DOR, KOR, MOR (Dhawan et al., 1996)).

The information required on ligands and target structures (protein) is publicly available and stored in many archives/databases such as PubChem (Kim et al., 2016), ZINC (Irwin et al., 2012), the Drug Bank (Wishart, 2006) and the Protein Data Bank (PDB) (Bernstein et al., 1977; “RCSB PDB: Homepage,” 2021). The latter was used in this study to retrieve 3D crystallised structures of the protein complexed with an active ligand (e.g. GABA-AR co crystallised with alprazolam).

The analysis of the Protein Data Bank database to retrieve the best 3D structures for the docking studies started with a query in the database, to which a list of putative structures was returned. The results were filtered according to both source organism (i.e. the organism from which the receptor was obtained, e.g. homo sapiens) and the experimental method (e.g. X-ray diffraction, electron microscopy, etc.) and refinement resolution used to generate the 3D structure (the resolution obtained in the 3D structure measured in Angstrom ( $\text{\AA}$ )). To each entry is associated a scientific paper that highlight details of the binding site and the key residues involved/essential for the binding of the ligands.

### 2.3.2 MOE<sup>®</sup> receptors preparation

Structural data often contain errors, hence additional preparatory steps are commonly required for the 3D structure of the receptor. MOE<sup>®</sup> was used to directly download the protein structure from PDB and then to proceed to a “Quick Prep” stage in which the protein is prepared for docking, with attention to the binding site. The Quick Prep tethers restraints to receptor, ligand, and/or solvent atoms and performs energy minimization on the system. The parameters used are presented in Figure 2.2.

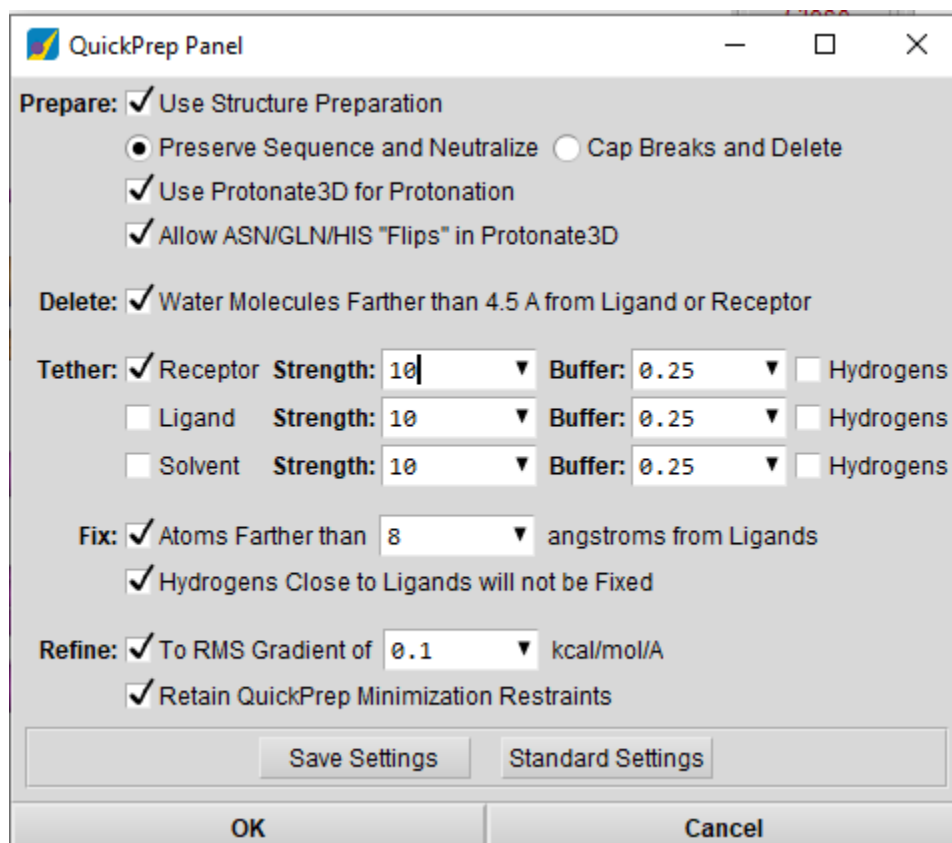


Figure 2.2 Screenshot of the Quick Prep Panel in MOE<sup>®</sup>

*Notes: Quick Prep function was used to carry out an initial refinement of the protein-ligand crystallised complex once downloaded in MOE<sup>®</sup>. Unprepared files, such as PDB files, may carry some structural errors as missing atoms or alternate geometry, due to the crystallisation process. Quick Prep was used to: rebuild missing atoms or loops or add hydrogens (Prepare); delete solvent uninteresting molecules (Delete); introduce tethers restrain for receptor (Tether); held fixed atoms far away from ligands for efficiency (Fix); and carry an energy minimisation on the structure prepared (Refine).*

### 2.3.3 MOE<sup>®</sup> Identification of the binding site

Once the protein is prepared, focus shifts to the ligand binding site and the residues responsible for the interaction. For small molecule docking, the binding pocket of the receptor must be specified. This can be done in different ways: specifying the atoms of the co-crystallised ligand; specifying the residues of a pocket or using MOE<sup>®</sup> Site Finder application to select site points (also defined as alpha sphere or "dummy" atoms). For all the receptors objects of the study, the presence of a co-crystallised ligand in the binding pocket was sufficient to define the size of the latter. To facilitate the view of the residues shaping the binding pocket, an ulterior analysis was carried out with the Site Finder application.

This application is able to identify all the possible active sites in a defined receptor using the 3D coordinates of the receptor itself (geometric methods) For further details please see Appendix B. For each site identified a Propensity for Ligand Binding (PLB) score was returned, indicating how likely that part of the receptor could act as a binding pocket (Krivák and Hoksza, 2015; Zheng et al., 2013). The more positive the PLB the higher the likelihood (Soga et al., 2007). The binding sites showing higher PLB were then compared to the one identified by the presence of the co-crystallise ligand to confirm size and composition of the binding pocket.

Once the binding pocket is confirmed, an analysis is carried out to assess the most important residues involved in the ligand interaction with the receptor. This step is carried out with the Ligand interaction application in MOE<sup>®</sup> (Appendix 3). The latter provides a diagrammatic (2D) visualisation of the active site, summarises a large amount of spatial data and can be used as a complement to 3D visualisation, as the 2D and 3D representations can be displayed alongside one another. Six types of contacts can be identified: Hydrogen bonds (H bond), Metal, Ionic, Arene, Covalent, and Van der Waals distance interactions (Table 2.2).

*Table 2.2 Types of contacts identifiable with the Ligand interactions panel*

<b>Contacts List</b>	
<b>distance</b>	Displays VdW distance interaction energies.
<b>covalent</b>	Displays covalent bonds. Principally these will consist of disulphide bridges but can also include peptide bonds if the sequence separation is set to 1.
<b>arene</b>	Displays arene interactions in the list, these include $\pi:\pi$ , $\pi$ -H, and $\pi$ :cation contacts
<b>ionic</b>	Displays ionic bond contacts in the list.
<b>metal</b>	Displays metal interactions which are bonded or are close enough to be within bonded distance.
<b>h-bond</b>	Displays hydrogen bond contacts.

#### 2.3.4 *Preparing a small molecule dataset*

Prior to starting the docking exercise with the DBZD and NSO datasets identified by NPSfinder<sup>®</sup>, a dataset of reference compounds was compiled for each receptor. This set comprises the co-crystallised ligand in the PDB structures chosen plus roughly ten molecules, well known to have a high potency towards the receptor (i.e., GABA-AR, KOR, MOR, and DOR). These datasets were manually created in Microsoft Excel (2019) and imported into MOE<sup>®</sup> via the Database Import Panel. Imported as 2D molecules the datasets were then processed as 3D structures. Generation of 3D structures, although not necessary for 2D applications, is crucial for applications such as docking, which requires a reasonable low-energy 3D conformation of the structure, possible minimised and with atomic partial charges set. For each molecule, a reasonable low energy 3D conformation with the most favourable tautomeric and protonation state was obtained. Correctly calculated partial charges (i.e. protonation state) are important to properly guide the binding interactions. For the calculation of the partial charges the forcefield Amber10:EHT was used (Gerber and Müller, 1995).

### 2.3.5 MOE<sup>®</sup> Docking

The docking process involves positioning various conformations of one molecule (NPS) with respect to another (PDB structure) and determining the optimal interaction geometry and its associated energy. All the steps associated with this process are presented in Figure 2.3.

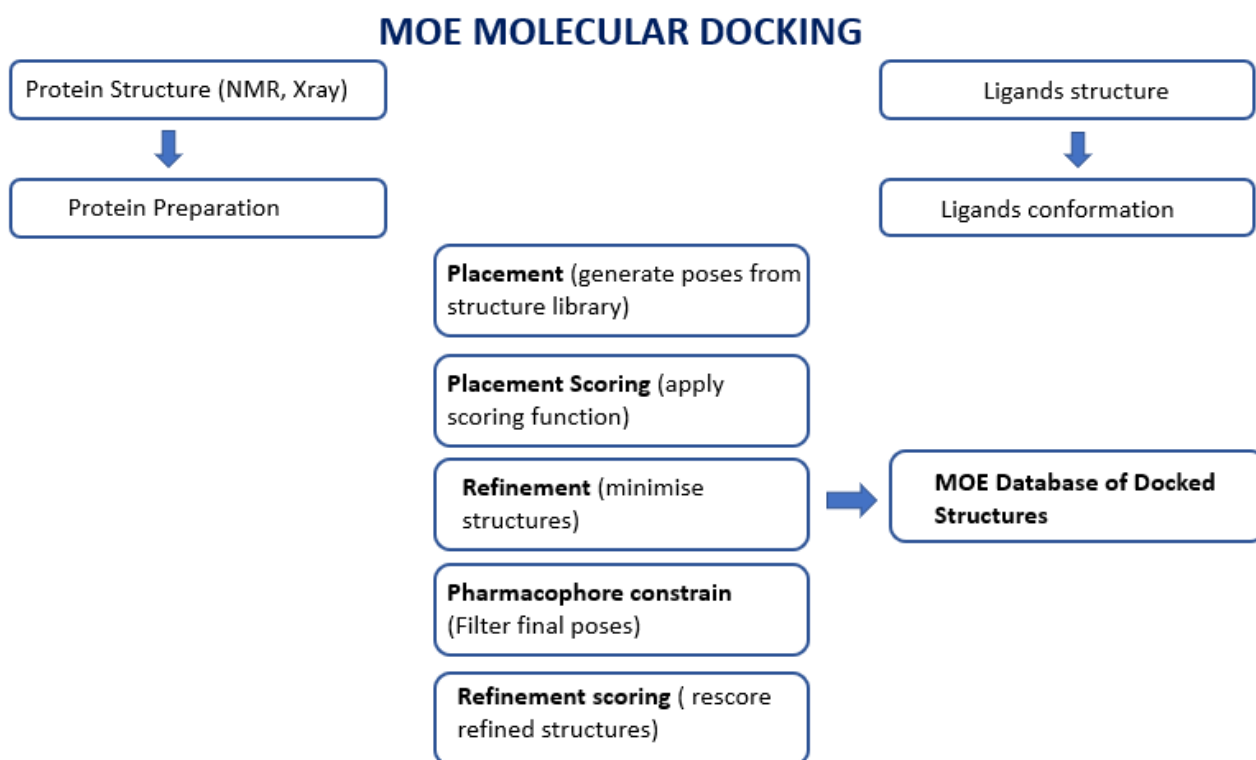


*Figure 2.3 Workflow of a docking study carried out with MOE<sup>®</sup>*

Once both protein and ligands are prepared as described above the first step is the placement, i.e. collection of poses is generated from the pool of ligand conformations using one of the placement methods and assigned a score (S). The dock panel is presented in Figure 2.4.



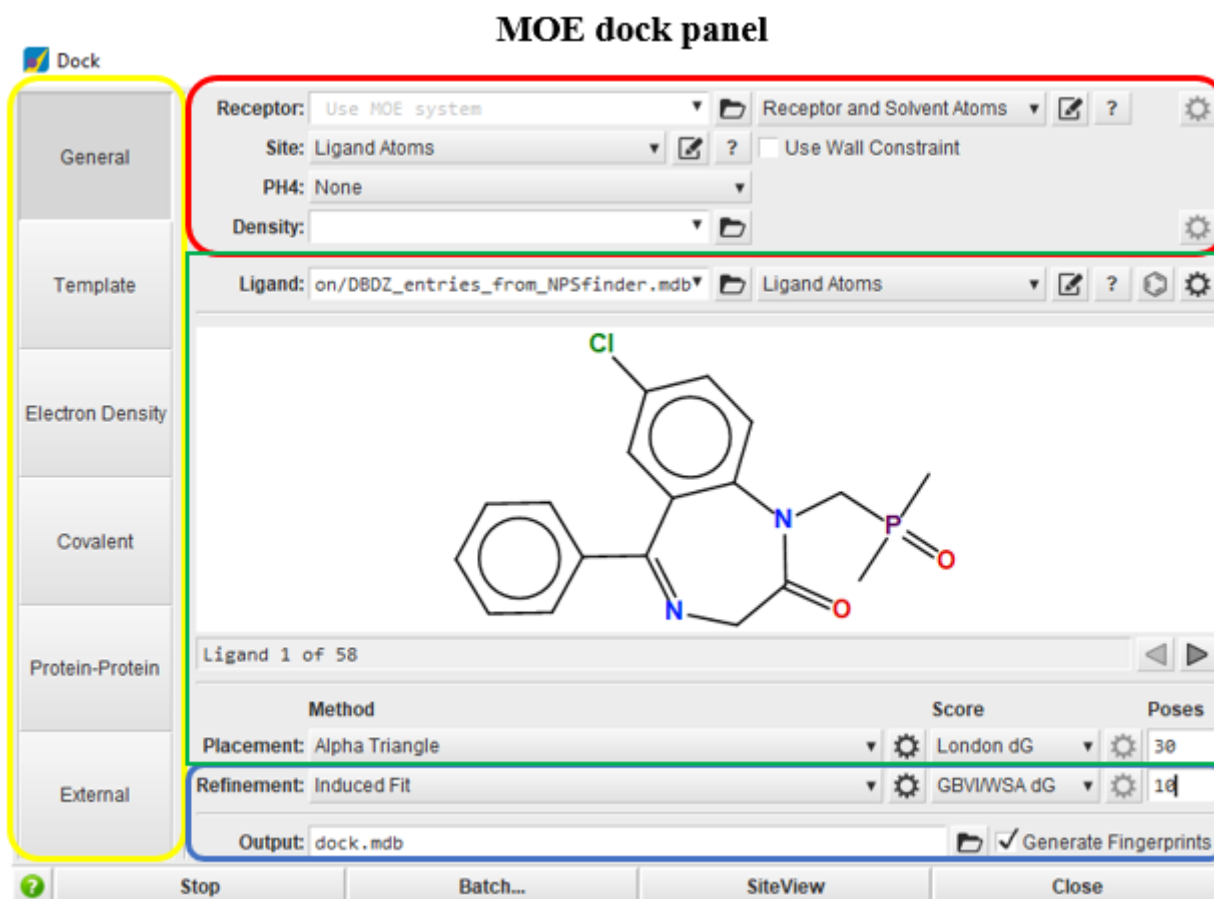


**Figure 2.4** The MOE<sup>®</sup> dock panel.

*Notes.* The panel, as seen in the image is divided into 4 sections. The first (yellow) is represented by the column on the left-hand side which indicated the various methods available for docking. The second (red) is at the top and is the area dedicated to specifying the characteristics of the receptor. The third one (green) is in the middle and is the ligand section where the ligands which will be docked can be specified. The fourth (blue) and last section is the one at the bottom that can be used to specify the parameters for the docking run, i.e. method, score, and poses, and where to store the output files. An option to generate fingerprints is available as well.

For the purpose of this study the general method was used, with the London dG scoring function for the placement and GBVI/WSA dG for the refinement. Both are the default scoring functions of the software. For a more detailed description of these scoring function please see the Appendix B. The induced fit, i.e., a non-rigid receptor structure was used as the refinement method. For each pose a fingerprint of the protein ligand interaction (PLIF) was generated as well. The docking run output is automatically saved in a MOE<sup>®</sup> database file and includes all the poses generated (the number of which is specified in the refinement stage Figure 2.4) and respective specifications among which the most important are:

- S, the final score (negative number), the more negative the better the binding
- RMSD, the root mean square deviation of the pose, expressed in Å, from the original ligand.
- rmsd\_refine, the root mean square deviation between the pose before and after refinement.
- E\_place, Score from the placement stage.

- **E\_refine**, Score from the refinement stage

All the poses can be analysed with the Database Browser application and the best one can be identified according to the S score, the ligand-receptor interactions and the active site residues involved in the binding.

### 2.3.6 *Protein ligand interaction fingerprint (PLIF)*

*Protein ligand interaction fingerprint (PLIF)* is a way of summarising the interactions between ligands and proteins using a fingerprint scheme. Interactions can be of two types: potential (energy-based) contacts and surface (patch) contacts. The first ones occur more in a protein ligand interaction setting and could be hydrogen bonds, ionic interactions and so on. Both potential and surface contacts are classified according to the residue of origin and built into a fingerprint scheme which is representative of a given database of protein-ligand complexes. Analysing the PLIF information reported in the docked database could be helpful to assess and understand the pattern of ligand-protein interaction. (Clark and Labute, 2007).

### 2.3.7 Docking Validation

There are different methods that can be used to validate docking studies (Hevener et al., 2009). One of these is the “pose selection “method. This method involves re-docking into the binding site, a compound with a known conformation and orientation (usually the co-crystallised ligand when present) and analysing the RMSD values for the returned poses. If the RMSD values are lower than the preselected value, usually of 1 or 2 units according to the size of the ligand, then the docking model is successful. Another method involves the use of a decoy set of compounds that are similar in physical properties with respect to the reference ligand but that may not bind effectively to the PDB receptor. The set can comprise both active and inactive compounds and is prepared to confound the software. The decoy set is usually docked and then analysed to understand if the dock protocol adopted can identify those compounds which are known not to bind the receptor. Usually, it is good practice as well to check the 3D structure used for the docking studies. The PDB database however carried these checks (e.g. Structure Analysis and Verification Server (SAVE) (UCLA, 2022) and structure evaluation (i.e. ERRAT (Colovos and Yeates, 1993) and Verify3D (Eisenberg et al., 1997) for each of the structure uploaded so no further work was necessary.

## 2.4 Pharmacophore mapping

### 2.4.1 Generation of a pharmacophore query

The pharmacophore mapping studies were carried out with MOE<sup>®</sup>, with which three different approaches can be followed according to the available data, and more precisely: ligand-based, complex-based and target-based.

The ligand-based approach can be used when a collection of ligands, both active and inactive are available. In this case no target information is either necessary or used. The complex-based can be used when structural data of protein ligand-complexes are available while the target-based when only the protein structure is available.

For each of these approaches different steps can/should be followed, as presented in Table 2.3

*Table 2.3 Steps that should be followed for each of the pharmacophore mapping type, i.e. ligand based, complexed base and target based*

<b>Ligand based</b>
<b>Flexible Alignment</b> (Flexibly align small molecules)
<b>Pharmacophore Consensus</b> (Obtain consensus features from aligned ligands)
<b>Pharmacophore Elucidation</b> (Automatically determine a pharmacophore query from ligands)
<b>Pharmacophore Query Editor</b> (Create new and edit existing pharmacophore queries)
<b>Complex based</b>
<b>PLIF</b> (Generate a pharmacophore query from a consensus of Protein Ligand Interaction Fingerprints)
<b>Pharmacophore Query Editor</b> (as above)
<b>Target based</b>
<b>Site Finder</b> (Locate binding cavities on a macromolecular structure)
<b>Feature Map</b> (electrostatic, interaction potential and non-bonded contact preferences)
<b>Pharmacophore Query Editor</b> (as above)

To create a pharmacophore model with MOE<sup>®</sup> four steps are usually followed: preparing the data, generating pharmacophore annotation points, selecting and refining the query (features to include in the pharmacophore, Sec.2.4.2). The data are prepared as described above, and if necessary conformations are generated. Once the data are ready, the Pharmacophore Query editor is used to identify regions of pharmacophoric importance. This application has different annotation scheme, but here the Unified scheme has been preferred because it is very comprehensive i.e. highest number/type of annotations features). Annotation points can be classified in atom, centroid or projected (Figure 2.5). Atom annotation points are located directly on an atom of a molecule, such as "H-bond acceptor" or "cation" and typically indicate a function related to protein-ligand binding.

Centroid annotations are located at the geometric centre of a subset of atoms, e.g. aromatic ring annotation located at the centroid of the atoms of the ring.

Projected Annotations are (typically) located along implicit lone pair directions or implicit hydrogen directions and are used to annotate the location of possible hydrogen bond partners or possible R-group atom locations.

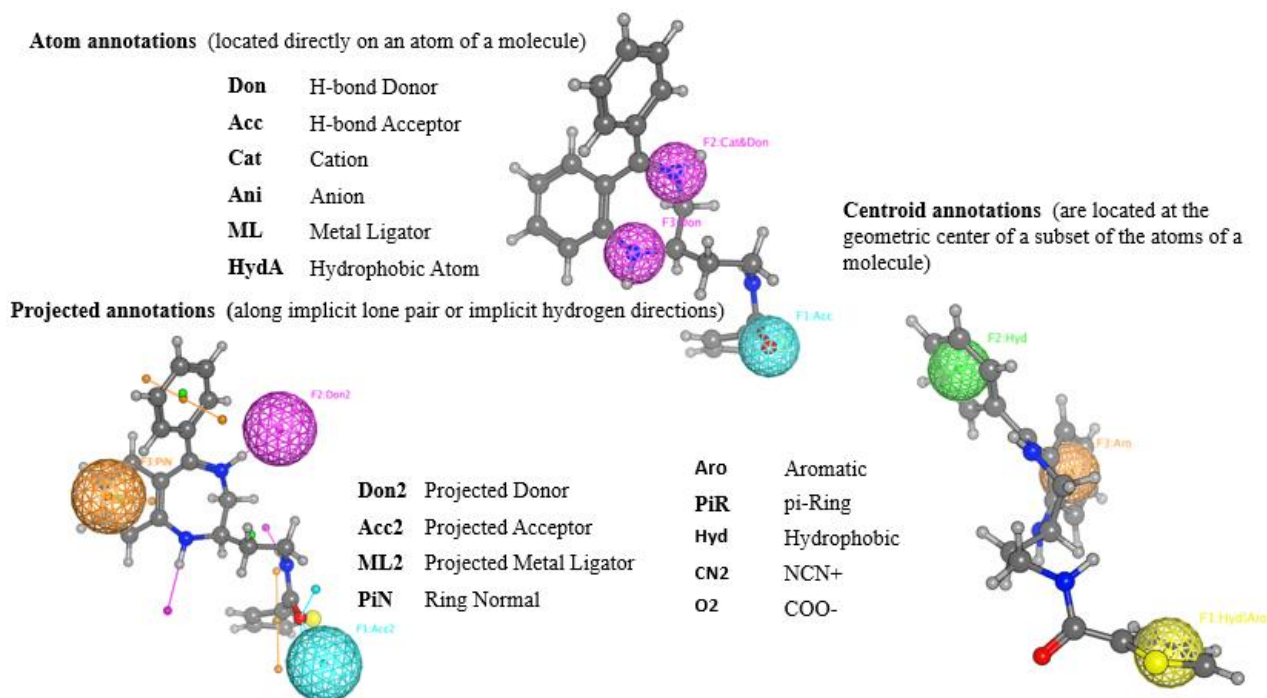


*Figure 2.5 The three types of annotation points included in the Unified annotation scheme.*

Using this annotation scheme the features which are thought to be responsible for the biological activity can be extracted either manually or with the use of the Pharmacophore Consensus panel, which is used to suggest a consensus set of pharmacophore features common to a set of ligands, or receptors. The features are scored based on the number of molecules in which they appear and are easily included in a pharmacophore query. The molecular conformations must have been precalculated and aligned and loaded into MOE®.

#### 2.4.2 *Refinement of a pharmacophore query*

The pharmacophore queries generated need to undergo an iterative cycle of refinement to obtain a reliable and representative query. Information of the binding pocket structure can be used to improve the query with steric and structural constrain, or with electrostatics and preferred contacts information. The strategies to refine pharmacophore queries, as presented in MOE, can include:

- using a large number of features to increase specificity
- dividing the features in essential and partial matching
- adjusting the position and the volume of the features
- examining the binding pocket to retrieve electrostatic information
- using the volumes of the binding pocket as space constrains

### 2.4.3 The Pharmacophore Query editor in MOE®

The Pharmacophore Query Editor (PQE) (Figure 2.6) is the primary MOE® interface for manually creating and editing pharmacophores queries, via the selection of annotation points (Figure 2.5) and conversion of the latter into pharmacophore features.

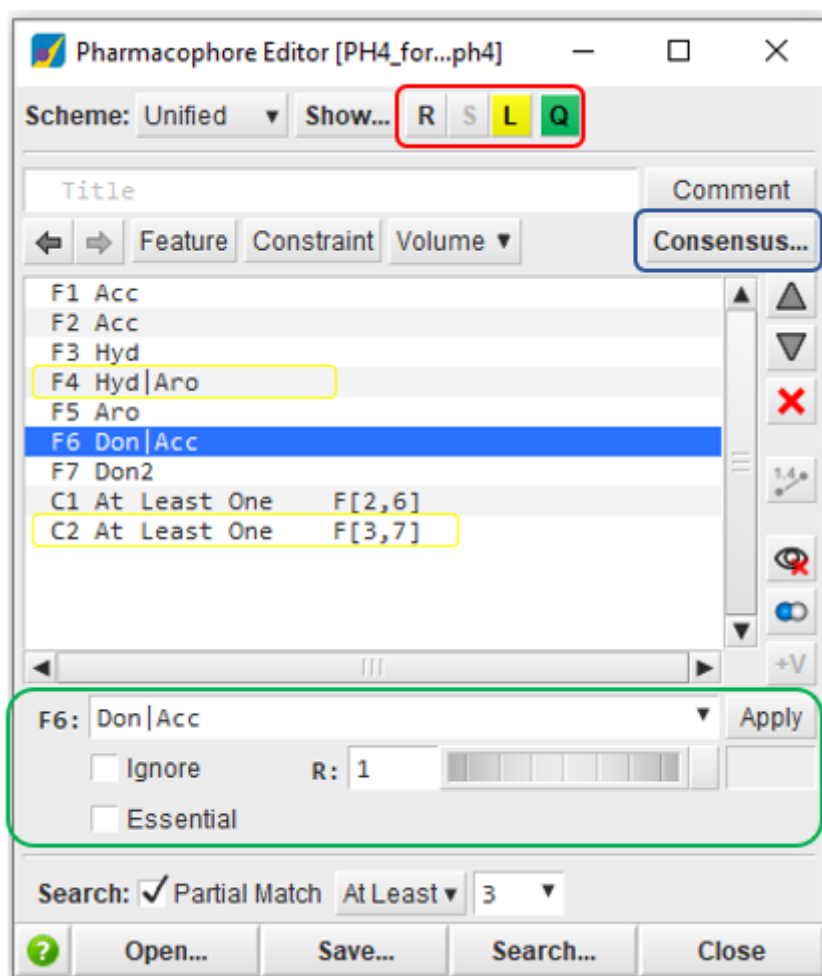


Figure 2.6 Pharmacophore query editor interface in MOE®

When the PQE is open in MOE®, annotations points are displayed automatically either for the ligand (L) or the receptor (R) according to which one is selected in the interface, i.e. yellow or green. These annotations points are then manually selected, and the corresponding feature defined (feature button).

Once pharmacophore features are defined these can be added or removed, their feature attributes (type and radius) modified, volumes constrained, and partial matching options added. PQE could be used as well to launch the Pharmacophore Consensus panel, which is used to suggest a consensus set of pharmacophore features. Each feature generated has a location in space, easily modifiable in the MOE® window, a radius controlled by the value of R in the panel; and a feature expression

including annotation point types and other information. A feature inherits its types from its generating annotation points.

When the pharmacophore query needs to be generated on multiple ligands for which the 3D conformation is known, it is possible to automate parts of the query generation process via the use of the Consensus model. The consensus model suggests features common to a set of aligned molecules and scores (%) them according to the number of molecules in which they appear. The consensus model is particularly useful when important common features across a set of ligands are to be assessed. Pharmacophore queries can be improved by an iterative cycle of refinement and with the inclusion of steric and other structural constraints from the binding pocket.

Some strategies include the use of constraints (volume or shape), the definition of essential features of partial matches, the determination of features from binding pocket analysis, and refining of feature radius and positions. Volume constraints are very helpful in improving the quality of the pharmacophore especially for docking studies because they ensure the avoidance of steric clashes with the receptor, confining hits to specific spatial regions, and the population of favourable contact regions with appropriate atoms.

For better practice, every pharmacophore query generated should be validated prior usage especially for pharmacophore search/filtering or screening exercises of known libraries.

#### *2.4.4 Validation of a pharmacophore query*

The validation of a pharmacophore query is a straightforward process which can use either a dataset of only active compounds (test set validation) or a dataset of active compounds mixed with decoys (decoy set validation) (Fei et al., 2013). These sets are screened with the pharmacophore maps, and a percentage of the matching molecules is returned. The percentage of the hits retrieved from the screening is an estimation of the validity of the pharmacophore query; however the meaning of the percentage varies according to the type of validations and scope of the study (Mason et al., 2005). For a decoy set validation including 2000 decoys and 10 active molecules, for example, a low percentage of hits (< 1.0%) is expected and can confirm the reliability of the pharmacophore map. For a test set validation instead, percentages closer to 100 suggest how the pharmacophore is able to match all the actives structures, while lower percentages indicate how the map could be more selective towards different biological activity values (e.g. matching only the most active compounds). Hence, there is no recommended value for the percentage of hits and each case needs to be considered individually (Yang, 2010).



In the following Chapter the results obtained with the *NPSfinder*<sup>®</sup> analysis of the surface web are reported together with a comparison between the NPS identified by the web crawler and those reported by the UNODC and EMCDDA.

## Chapter 3 NPSfinder®

### 3.1 Identification of current NPS scenarios: NPSfinder®

After more than three years of operation (November 2017 to October 2020), the overall number of unique NPS identified across the 17 families by the web crawler activities was 4,231. This number is substantially higher, almost four times, than that reported by both the UNODC and EMCDDA as a result of evidence-based identifications. Indeed as of June 2022, the UNODC identified 1,127 individual NPS reported by 134 countries (UNODC, 2022e), while the EMCDDA via the EWS (EMCDDA, 2022a) reported a total of 884 NPS, of which 52 were formally notified in 2021 (EMCDDA, 2022a, 2022c). The number of NPS identified for each family by the *NPSfinder*® are reported in Table 3.1

*Table 3.1 The number of unique molecules identified for each NPS class during the years of activity of the NPSfinder®, i.e. 2017-2020.*

Family	No. Molecules	%
Cannabimimetics	1261	29.8
Phenethylamines	1260	29.8
Opioids	405	9.6
Cathinones	228	5.4
Gabaergics	173	4.1
Prescription drugs	165	3.9
Plant-based	144	3.4
PIEDs	136	3.2
Other	131	3.1
Tryptamines	78	1.8
Psychostimulants	77	1.8
Hallucinogens	38	0.9
PCP-like	37	0.9
NBOMes	35	0.8
Piperazines	35	0.8
Flys	16	0.4
Aminoindanes	12	0.3

The results obtained with the *NPSfinder*® are clearly not in line with the reduced NPS growth (number of new NPS reported per year) reported by both agencies (EMCDDA, 2022c; UNODC, 2022b), but show concordance with the overall percentage of each NPS family (Table 1.1) presented by these stakeholders. Indeed, the numbers of NPS identified online matched the trends reported by the two international agencies, with cannabimimetics (29.8%), phenethylamines

(29.8%) (stimulants as well) and NSO (10%) representing the most conspicuous classes (Figure 1.1).

For each of the 4,231 molecules included in the database the following information were identified, reported and compiled, when available:

- inclusion date – online source
- family
- name- other names (i.e. main name and other common denominations)
- chemical composition (i.e. IUPAC name)
- SMILES string (Weininger, 1988) string, obtained either consulting PubChem or from the structure using Chewdraw12 Plus
- InChIKey (Heller et al., 2013; Pletnev et al., 2012)
- description (i.e. all the information available on pharmacokinetics, pharmacodynamics, toxicity, sought after and adverse effects, clinical management and legal status)

Once all the info were completed for each entry, for the scope of this research project, attention was given to the analysis of the DBZDs and NSOs classes. The class of psychedelics (i.e. phenethylamines, tryptamines and lysergamides) was analysed as well due to the high interest reported by UNODC and EMCDDA on psychedelic/stimulants NPS (Catalani et al., 2021c). An overview of the results is reported in Appendix B.

### **3.2 The NPSfinder<sup>®</sup> DBZDs, comparison with UNODC and EMCDDA database**

Due to the lack of a designated family for the classification of DBZDs in the NPSfinder<sup>®</sup>, the latter have been listed in two separated families, prescription drugs and gabaergics. In particular the benzodiazepines which were identified as approved medicines were included in the prescription drug class, while the gabaergics family comprised all those molecules active on the GABA system (e.g. benzodiazepine, Z drugs and barbiturates). These two families together totalled 338 entries. To identify the correct number of DBZDs reported by the web crawler, a further full assessment was conducted together with the editing of NPSfinder<sup>®</sup> entries- data when necessary. A screening was carried out to identify all the molecules which displayed one of the chemical structures included in Figure 4.1. Those molecules considered as DBZDs pro-drug or precursors were included as well. Forty-seven DBZDs were identified among the prescription drugs family and 96 among the GABAergic (i.e. 143). From these, the prescription benzodiazepines scheduled under international control, i.e. the Convention on Psychotropic Substances of 1971 (UNODC, 2022e), were excluded as they did not qualify as designer benzodiazepines (EMCDDA, 2020c). A total of 115 DBZS was identified. This number differs significantly from what officially reported by the EMCDDA, which

as of the 31st of December 2021 was monitoring 33 DBZDs, of which three notified in 2021 (EMCDDA, 2021c), as of what reported by the EWA of UNODC in August 2022, the current monitored DBZDs amount to a total of 40 (UNODC, 2022d)..

Despite the discrepancies in numbers, the percentage that DBZDs occupy on the total of NPS, i.e. 3%, is in line with what reported by EMCDDA - 4%, and UNODC - 3% (EMCDDA, 2022a, 2022c; UNODC, 2022d). The list of the 115 DBZD was compared with what reported by the UNODC and EMCDDA as per Table 3.2.

**Table 3.2 List of designer benzodiazepines identified by the NPSfinder® and comparison with the EMCDDA and UNODC databases**

*Note. The comparison of the three databases has been carried out using the InChIKey string. The data from the EMCDDA are older than those from the UNODC due to the exit of UK from the EU. The smiles were obtained from PubMed.*

Mol	SMILES	UNODC (2022)	EMCDDA (2021)
3-hydroxyphenazepam	<chem>BrC1cc2C(c3c(Cl)cccc3)=NC(O)C(=O)Nc2cc1</chem>	Y	Y
4'-chlorodiazepam	<chem>CN1C(=O)CN=C(C2=C1C=CC(=C2)Cl)C3=CC=C(C=C3)Cl</chem>	Y	Y
7-Aminoflunitrazepam	<chem>Fc1c(C2=NCC(=O)N(C)c3c2cc(N)cc3)cccc1</chem>	Y	N
7-BPDBD	<chem>BrC1cc2C(c3ccccc3)=NCC(=O)Nc2cc1</chem>	N	N
Adinazolam	<chem>CN(C)CC1=NN=C2N1C3=C(C=C(C=C3)Cl)C(=NC2)C4=CC=CC=C4</chem>	Y	Y
Alprazolam triazolobenzophenone derivative	<chem>CC1=NN=C(N1C2=C(C=C(C=C2)Cl)C(=O)C3=CC=CC=C3)CN</chem>	N	Y
Arfendazam	<chem>Clc1cc2N(c3ccccc3)C(=O)CCN(C(=O)OCC)c2cc1</chem>	N	N
Bentazepam	<chem>O=C1Nc2sc3c(c2C(c2ccccc2)=NC1)CCCC3</chem>	N	Y
Bromazolam	<chem>BrC1cc2C(c3ccccc3)=NCc3n(c(C)nn3)-c2cc1</chem>	Y	Y
Carburazepam	<chem>Clc1cc2C(N(C(=O)N)CC(=O)N(C)c2cc1)c1ccccc1</chem>	N	N
Ciclotizolam	<chem>BrC1sc2-n3c(C4CCCC4)nnc3CN=C(c3c(Cl)cccc3)c2c1</chem>	N	N
Cinazepam	<chem>BrC1cc2C(c3c(Cl)cccc3)=NC(OC(=O)CCC(=O)O)C(=O)Nc2cc1</chem>	N	Y
Cinolazepam	<chem>Clc1cc2C(c3c(F)cccc3)=NC(O)C(=O)N(CCC#N)c2cc1</chem>	N	N
Clazolam	<chem>Clc1cc2c(N(C)C(=O)CN3C2c2c(cccc2)CC3)cc1</chem>	N	N
Climazolam	<chem>Clc1c(C2=NCc3n(c(C)nc3)-c3c2cc(Cl)cc3)cccc1</chem>	N	N
Clonazolam	<chem>Clc1c(C2=NCc3n(c(C)nn3)-c3c2cc([N+](=O)[O-])cc3)cccc1</chem>	Y	Y
Cloniprazepam	<chem>Clc1c(C2=NCC(=O)N(CC3CC3)c3c2cc([N+](=O)[O-])cc3)cccc1</chem>	Y	Y
CP-1414S	<chem>O=[N+](O)c1cc2N(c3ccccc3)C(=O)CC(N)=Nc2cc1</chem>	N	N
Cyprazepam	<chem>Clc1cc2C(=[N+](O-))CC(NCC3CC3)=Nc2cc1)c1ccccc1</chem>	N	N
Deschloroetizolam	<chem>C(C)c1sc2-n3c(C)nnc3CN=C(c3ccccc3)c2c1</chem>	Y	Y
Desmethylnitrazolam	<chem>O=[N+](O)c1cc2C(c3ccccc3)=NCc3n(-c2cc1)cnn3</chem>	N	N

Desmethylniazepam	<chem>C1c(C2=NCc3n(-c4c2cc(Cl)cc4)cnn3)cccc1</chem>	N	N
Devazepide	<chem>O=C(NC1C(=O)N(C)c2c(C(c3cccc3)=N1)cccc2)c1[nH]c2c(c1)ccc2</chem>	N	N
Diclazepam	<chem>C1c(C2=NCC(=O)N(C)c3c2cc(Cl)cc3)cccc1</chem>	Y	Y
Difludiazepam	<chem>C1c1cc2C(c3c(F)cccc3F)=NCC(=O)N(C)c2cc1</chem>	Y	Y
Doxefazepam	<chem>C1c1cc2C(c3c(F)cccc3)=NC(O)C(=O)N(CCO)c2cc1</chem>	N	N
Elfazepam	<chem>C1c1cc2C(c3c(F)cccc3)=NCC(=O)N(CCS(=O)(=O)CC)c2cc1</chem>	N	N
Estazolam	<chem>C1C2=NN=CN2C3=C(C=C(C=C3)Cl)C(=N1)C4=CC=CC=C4</chem>	N	N
Ethyl Carfluzapate	<chem>C1c1cc2C(c3c(F)cccc3)=NC(C(=O)OCC)C(=O)N(C(=O)NC)c2cc1</chem>	N	N
Ethyl Dirazepate	<chem>C1c(C2=NC(C(=O)OCC)C(=O)Nc3c2cc(Cl)cc3)cccc1</chem>	N	N
Etizolam	<chem>C1c(C2=NCc3n(c(C)nn3)-c3sc(CC)cc23)cccc1</chem>	Y	Y
FG-8205	<chem>C1c1c2C(=O)N(C)C3c3(-c4nc(C(C)O)on4)nnc3-c2cc1</chem>	N	N
Fletazepam	<chem>C1c1cc2C(c3c(F)cccc3)=NCC(=O)N(CC(F)(F)F)c2cc1</chem>	N	N
Fluadinazolam	<chem>C1c1cc2C(c3c(F)cccc3)=NCc3n(c(CN(C)C)nn3)-c2cc1</chem>	N	N
Flualprazolam	<chem>C1c1cc2C(c3c(F)cccc3)=NCc3n(c(C)nn3)-c2cc1</chem>	Y	Y
Flubromazepam	<chem>Brc1cc2C(c3c(F)cccc3)=NCC(=O)Nc2cc1</chem>	Y	Y
Flubromazolam	<chem>Brc1cc2C(c3c(F)cccc3)=NCc3n(c(C)nn3)-c2cc1</chem>	Y	Y
Flubrotizolam	<chem>Brc1sc2-n3c(C)nnc3CN=C(c3c(F)cccc3)c2c1</chem>	Y	N
Fluclotizolam	<chem>C1c1sc2-n3c(C)nnc3CN=C(c3c(F)cccc3)c2c1</chem>	Y	Y
Fluetizolam	<chem>Fc1c(C2=NCc3n(c(C)nn3)-c3sc(CC)cc23)cccc1</chem>	N	N
Fluloprazolam	<chem>Fc1c(C2=NCC=3N(C(=O)C(=CN4CCN(C)CC4)N=3)c3c2cc([N+](=O)[O-])cc3)cccc1</chem>	N	N
Flunitrazolam	<chem>Fc1c(C2=NCc3n(c(C)nn3)-c3c2cc([N+](=O)[O-])cc3)cccc1</chem>	Y	Y
Flupyrzapon	<chem>Fc1c(C2=NCC(=O)N(C)c3n(C)nc(C)c23)cccc1</chem>	N	N
Flutazolam	<chem>C1c1cc2C3(c4c(F)cccc4)OCCN3CC(=O)N(CCO)c2cc1</chem>	N	N
Flutemazepam	<chem>C1c1cc2C(c3c(F)cccc3)=NC(O)C(=O)N(C)c2cc1</chem>	N	N
Flutoprazepam	<chem>C1c1cc2C(c3c(F)cccc3)=NCC(=O)N(CC3CC3)c2cc1</chem>	N	N
Fosazepam	<chem>C1c1cc2C(c3cccc3)=NCC(=O)N(CP(=O)(C)C)c2cc1</chem>	N	N
Gidazepam	<chem>Brc1cc2C(c3cccc3)=NCC(=O)N(CC(=O)NN)c2cc1</chem>	N	N
Imidazenil	<chem>Brc1c(C2=NCc3c(C(=O)N)nnc3-c3c2cc(F)cc3)cccc1</chem>	N	N
Iomazenil	<chem>Ic1c2C(=O)N(C)C3c3c(C(=O)OCC)nnc3-c2cc1</chem>	N	N
JQ1	<chem>C1c1ccc(C2=NC(CC(=O)OC(C)C)C)c3n(c(C)nn3)-c3sc(C)c(C)c23)cc1</chem>	N	N
Lofendazam	<chem>C1c1cc2N(c3cccc3)C(=O)CCNc2cc1</chem>	N	N
Lopirazepam	<chem>C1c1c(C2=NC(O)C(=O)Nc3c2nc(Cl)cc3)cccc1</chem>	N	N
Meclonazepam	<chem>CC1C(=O)NC2=C(C=C(C=C2)[N+](=O)[O-])C(=N1)C3=CC=CC=C3Cl</chem>	Y	Y
Menitrazepam	<chem>O=[N+](O)c1cc2C(C3=CCCC3)=NCC(=O)N(C)c2cc1</chem>	N	N
Metaclazepam	<chem>Brc1cc2C(c3c(Cl)cccc3)=NCC(COC)N(C)c2cc1</chem>	N	N

Methyl Clonazepam	<chem>C1c1c(C2=NCC(=O)N(C)c3c2cc([N+](=O)[O-])cc3)cccc1</chem>	Y	Y
Metizolam	<chem>C1c1c(C2=NCc3n(-c4sc(CC)cc24)enn3)cccc1</chem>	Y	Y
Mexazolam	<chem>C1c1c(C23OCC(C)N2CC(=O)Nc2c3cc(Cl)cc2)cccc1</chem>	N	N
MP-III-022	<chem>Fc1c(C2=NC(C)c3c(C(=O)NC)ncn3-c3c2cc(C#C)cc3)cccc1</chem>	N	N
Nifoxipam	<chem>Fc1c(C2=NC(O)C(=O)Nc3c2cc([N+](=O)[O-])cc3)cccc1</chem>	Y	Y
Nitrazolam	<chem>O=[N+](O)c1cc2C(c3ccccc3)=NCc3n(c(C)nn3)-c2cc1</chem>	Y	Y
N-Methylbromazepam	<chem>Brc1cc2C(c3ncccc3)=NCC(=O)N(C)c2cc1</chem>	N	N
Norfludiazepam	<chem>C1C(=O)NC2=C(C=C(C=C2)Cl)C(=N1)C3=CC=CC=C3F</chem>	Y	Y
Phenazepam	<chem>Brc1cc2C(c3c(Cl)cccc3)=NCC(=O)Nc2cc1</chem>	Y	Y
Phenazolam	<chem>Brc1cc2C(c3c(Cl)cccc3)=NCc3n(c(C)nn3)-c2cc1</chem>	Y	N
Pivoxazepam	<chem>C1c1cc2C(c3ccccc3)=NC(OC(=O)C(C)(C)C(=O)Nc2cc1</chem>	N	N
Premazepam	<chem>O=C1Nc2c(c(C)n(C)c2)C(c2ccccc2)=NC1</chem>	N	N
PWZ-029	<chem>C1c1cc2C(=O)N(C)Cc3c(COC)ncn3-c2cc1</chem>	N	N
Pyclazolam	<chem>C1c1cc2C(c3ncccc3)=NCc3n(c(C)nn3)-c2cc1</chem>	N	N
Pyeazolam	<chem>C(C)c1cc2C(c3ncccc3)=NCc3n(c(C)nn3)-c2cc1</chem>	N	N
Pynazolam	<chem>O=[N+](O)c1cc2C(c3ncccc3)=NCc3n(c(C)nn3)-c2cc1</chem>	N	N
Pyrazolam	<chem>Brc1cc2C(c3ncccc3)=NCc3n(c(C)nn3)-c2cc1</chem>	Y	Y
QH-II-066	<chem>O=C1N(C)c2c(C(c3ccccc3)=NC1)cc(C#C)cc2</chem>	N	N
Quazepam	<chem>C1c1cc2C(c3c(F)cccc3)=NCC(=S)N(CC(F)(F)F)c2cc1</chem>	N	N
Reclazepam	<chem>C1c1c(C2=NCCN(C=3OCC(=O)N=3)c3c2cc(Cl)cc3)cccc1</chem>	N	N
Remimazolam	<chem>Brc1cc2C(c3ncccc3)=NC(CCC(=O)OC)c3n(c(C)cn3)-c2cc1</chem>	N	N
Ripazepam	<chem>O=C1Nc2c(C)nn(CC)c2C(c2ccccc2)=NC1</chem>	N	N
Ro 05-3590	<chem>C1C(=O)NC2=C(C=C(C=C2)[N+](=O)[O-])C(=N1)C3=CC=CC=C3C(F)(F)F</chem>	N	N
Ro 05-4435 (Desemethylflunitrazepam)	<chem>Fc1c(C2=NCC(=O)Nc3c2cc([N+](=O)[O-])cc3)cccc1</chem>	Y	Y
Ro 05-4608	<chem>C1c1c(C2=NCC(=O)N(C)c3c2cccc3)cccc1</chem>	N	N
Ro 05-6822	<chem>CN1C(=O)CN=C(C2=C1C=CC(=C2)F)C3=CC=CC=C3F</chem>	N	N
Ro 07-3953	<chem>C1c1cc2C(c3c(F)cccc3F)=NCC(=O)Nc2cc1</chem>	N	N
Ro 07-5193	<chem>C1c1c(c(F)ccc1)C1=NCC(=O)Nc2c1cc(Cl)cc2</chem>	N	N
Ro 07-5220	<chem>C1c1c(c(Cl)ccc1)C1=NCC(=O)N(C)c2c1cc(Cl)cc2</chem>	N	N
Ro 07-9749	<chem>Ic1cc2C(c3c(F)cccc3)=NCC(=O)Nc2cc1</chem>	N	N
Ro 07-9957	<chem>CN1C(=O)CN=C(C2=C1C=CC(=C2)I)C3=CC=CC=C3F</chem>	N	N
Ro 09-9212	<chem>C1c1c(C2=NCC(=O)Nc3sc(Cl)cc23)cccc1</chem>	N	N
Ro 11-4878	<chem>O=C1NC2=CC=C(Cl)C=C2C(C3=CC=CC=C3F)=NC1C</chem>	N	N
Ro 13-3780	<chem>Brc1cc2C(c3c(F)cccc3F)=NCC(=O)N(C)c2cc1</chem>	N	N
Ro 14-3074	<chem>C1C(=O)NC2=C(C=C(C=C2)N=[N+]=[N-])C(=N1)C3=CC=CC=C3F</chem>	N	N

Ro 15-4941	<chem>C1c2C(=O)N3C(c4c(C(=O)OCC)ncn4-c2ccc1)CCC3</chem>	N	N
Ro 15-9270	<chem>C1c1c(C=2c3c(-n4c(C)nc4CC=2)ccc([N+](=O)[O-])c3)cccc1</chem>	N	N
Ro 17-1812	<chem>C1c1c2C(=O)N3C(c4c(C(=O)OCC5CC5)ncn4-c2ccc1)CC3</chem>	N	N
Ro 20-2533	<chem>CCC1=CC2=C(C=C1)NC(=O)CN=C2C3=CC=CC=C3</chem>	N	N
Ro 20-2541	<chem>CN1C(=O)CN=C(C2=C1C=CC(=C2)C#N)C3=CC=CC=C3F</chem>	N	N
Ro 20-3053	<chem>CC(=O)C1=CC2=C(C=C1)NC(=O)CN=C2C3=CC=CC=C3F</chem>	N	N
Ro 20-5747	<chem>C=CC1=CC2=C(C=C1)NC(=O)CN=C2C3=CC=CC=C3</chem>	N	N
Ro 20-8065	<chem>C1c1c(Cl)cc2NC(=O)CN=C(c3c(F)cccc3)c2c1</chem>	N	N
Ro 20-8552	<chem>C1c1c(C)cc2C(c3c(F)cccc3)=NCC(=O)Nc2c1</chem>	N	N
Ro 21-8137	<chem>C1c1cc2C(c3c(F)cccc3)=NCc3c(C(=O)N)ncn3-c2cc1</chem>	N	N
Ro 48-6791	<chem>Fe1cc2C(=O)N(C)Cc3c(-c4nc(CN(CCC)CCC)on4)ncn3-c2cc1</chem>	N	N
Ro 48-8684	<chem>Fe1cc2C(=O)N(C)Cc3c(-c4oc(CN(CCC)CCC)en4)ncn3-c2cc1</chem>	N	N
SH-053-R-CH3-2'F	<chem>Fe1c(C2=NC(C)c3c(C(=O)OCC)ncn3-c3c2cc(C#C)cc3)cccc1</chem>	N	N
Sulazepam	<chem>C1c1cc2C(c3cccc3)=NCC(=S)N(C)c2cc1</chem>	N	N
Thionordazepam	<chem>C1c1cc2C(c3cccc3)=NCC(=S)Nc2cc1</chem>	Y	Y
Tofisopam	<chem>O(C)c1c(OC)ccc(C2=NN=C(C)C(CC)c3c2cc(OC)c(OC)c3)c1</chem>	N	Y
Tolufazepam	<chem>C1c1c(C2=NCC(=O)N(CCS(=O)(=O)c3ccc(C)cc3)c3c2cc(Cl)cc3)cccc1</chem>	N	N
Triflubazam	<chem>FC(F)(F)c1cc2N(c3cccc3)C(=O)CC(=O)N(C)c2cc1</chem>	N	N
Triflunordazepam	<chem>FC(F)(F)c1cc2C(c3cccc3)=NCC(=O)Nc2cc1</chem>	N	N
Tuclazepam	<chem>C1c1c(C2=NCC(CO)N(C)c3c2cc(Cl)cc3)cccc1</chem>	N	N
Uldazepam	<chem>C1c1c(C2=NCC(NOCC=C)=Nc3c2cc(Cl)cc3)cccc1</chem>	N	N
Zapizolam	<chem>C1c1c(C2=NCc3n(-c4c2nc(Cl)cc4)cnm3)cccc1</chem>	Y	N
Zomebazam	<chem>O=C1N(C)c2n(C)nc(C)c2N(c2cccc2)C(=O)C1</chem>	N	N
Zometapine	<chem>C1c1cc(C2=NCCNc3n(C)nc(C)c23)ccc1</chem>	N	N

Of the 33 DBZDs reported by the UNODC, 29 were found to be common to the *NPSfinder*<sup>®</sup> database as well, the same number identified among those reported by the EMCDDA. The UNODC reported a total of four DBZDs which were not identified by *NPSfinder*<sup>®</sup> - i.e. deschloroclotizolam, desalkylgidazepam, 2-ethyl-4-phenyl-6H-thieno[3,2-f][1,2,4]triazolo[4,3-a][1,4]diazepine, norflurazepam, and bretazenil. On the same line, the web crawler identified a total of 79 molecules, which, after careful analysis, seem to be uniquely reported.

The 115 DBZDs so identified were further analysed to understand which core structure was the most represented. For each of the core structure, which are presented in Figure 4.1Figure 4.3, the percentage on the total was calculated. The majority of them – 63 out of 115 (55%) – were 1,4-benzodiazepines, followed by the triazolobenzodiazepines (17%), imidazodiazepines (12%) and thienotriazolodiazepines (7%). These percentage are in line with what reported by the two international agencies UNODC and EMCDDA (EMCDDA, 2022a; UNODC, 2022a). The rest of

the molecules were 1,5-benzodiazepines (3%), imidazodiazepines (3%), thiodiazepines (2%) and 2,3-diazepine (1%). Only one molecule was found not to match with any of the core structures, i.e. the alprazolam triazolobenzophenone derivative, and moreover not to possess a diazepine ring. For this reason, this entry was removed from the dataset in analysis during the computational studies.

### 3.3 The NPSfinder<sup>®</sup> NSOs, comparison with UNODC and EMCDDA database

The number of NSOs identified by the NPSfinder<sup>®</sup> totalled 371 molecules. The opioids of natural/plant origin and the opiates were not included in the list. A first screening was carried out to classify the substances according to their chemical structure (e.g. fentanyl, non-fentanyl analogues). The IUPAC name of each entry as well as the 2D representation of the chemical structure were taken into consideration. To help in the classification process the UNODC and EMCDDA database were consulted alongside to the International Narcotics Control Board (INCB) “Yellow List” (International Narcotics Control Board, 2021), and the fentanyl and synthetic non-fentanyl opioids with no known legitimate uses INCB report (International Narcotic Control Board, 2018). The 396 molecules were divided, for easiness of data analysis in: fentanyl-like (239), non-fentanyl-like (88), morphinan-like (38), nitazene-like (7),. A second screening was carried out to underscore which molecules, among these 396 are scheduled under the Narcotic Drug convention of 1961 (International Narcotics Control Board, 2021), because as per definition, NPS are molecules which are not controlled by neither of the two drug conventions - i.e. 1961 and 1971 (UNODC, 2022c). More than half of the molecules included in the morphinan-like group, i.e. 37 out of 60, and half of those included in the non-fentanyl-like group, i.e. 44 out of 88, were found to be included in the list of narcotic drugs under international control. It is important to note, that among the scheduled non-fentanyl analogues, there are molecules which can be classified as NSOs to all intents being them scheduled only recently, i.e. buprenorphine and U-47700 (DEA, 2018; Home Office, 2022a, 2022b),). From the fentanyl-like group, out of 239 molecules it seems like only 21 are currently scheduled, while of the nitazene group three out of seven are scheduled (UNODC, 2022a, 2022c). With the changes in scheduling and legal status of substances the classification of an opioid as an NPS can be a challenging task, especially if the substance is a previously approved medicine. At least for the opioids class one should be considered if and how the use of the latter has been changed over time. As per the end of 2021 the EMCDDA was monitoring a total of 73 new opioids identified on the drug market in Europe as the fourth-largest group of substances monitored. Of the 73 NSO, six were notified during 2021 (please note that the full list is not available, due to the exit of the UK from EU) (EMCDDA, 2022c). While the EMCDDA classify the NSOs in one class only, the UNODC separates them in two, fentanyl analogues and others, the latter including synthetic opioids



as U-47700. At the end of 2021, the UNODC reported 79 molecules in the first class and a total of 44 in the second (UNODC, 2022d).

As per the class of DBZDs, overall the *NPSfinder*<sup>®</sup> detected a larger number of NSOs, i.e. three times more than those listed by the international databases, with particular regard to fentanyl and non-fentanyl molecules which are reported below. However, as per the DPDZs, the percentage on the total of the fentanyl class is similar across the *NPSfinder*<sup>®</sup> = 6% and UNODC= 7%. The NSO identified by the web crawler were compared to those identified by the two international agencies. The comparison was made using the unique InChIKey, and for each subfamily identified, i.e. fentanyl, non-fentanyl, morphinan and nitazenes, is reported below.

Table 3.3 List of fentanyl like NSO identified by the NPSfinder® and comparison with the EMCDDA and UNODC databases\*.

MOL	SMILES	UNODC (2022)	EMCDDA (2019)
2,3-Secofentanyl	<chem>CCC(=O)N(C1=CC=CC=C1)C(C)CCN(C)CCC2=CC=CC=C2</chem>	N	N
2',2''-Difluorofentanyl	<chem>CCC(=O)N(C1CCN(CC1)CCC2=CC=CC=C2F)C3=CC=CC=C3F</chem>	Y	N
2'-Fluoro-Butyrylfentanyl	<chem>CCCC(=O)N(C1CCN(CC1)CCC2=CC=CC=C2)C3=CC=CC=C3F</chem>	N	N
2'-Fluoro-Isobutyrylfentanyl	<chem>CC(C)C(=O)N(C1CCN(CC1)CCC2=CC=CC=C2)C3=CC=CC=C3F</chem>	y	N
2'-Isopropyl-Furanylfentanyl	<chem>CC(C)C1=CC=CC=C1N(C2CCN(CC2)CCC3=CC=CC=C3)C(=O)C4=CC=CO4</chem>	Y	N
2-Fluorofentanyl	<chem>CCC(=O)N(C1CCN(C(C1)F)CCc1ccccc1)c1ccccc1</chem>	N	Y
2-Furanylbenzylfentanyl	<chem>c1ccc(cc1)CN1CCC(CC1)N(c1ccco1)c1ccccc1</chem>	Y	N
2-Methyl Carfentanil	<chem>CCC(=O)N(C1(CCN(CC1)CCc1ccccc1)C(=O)OC)c1ccccc1C</chem>	N	N
2-Methyl Crotonyl Fentanyl	<chem>CC(=CC(=O)N(C1CCN(CC1)CCC2=CC=CC=C2)C3=CC=CC=C3)C</chem>	Y	Y
2-Methylfentanyl	<chem>CCC(=O)N(C1CCN(C(C1)C)CCc1ccccc1)c1ccccc1</chem>	N	N
3,3-Dimethylfentanyl	<chem>CCC(=O)N(C1CCN(CC1(C)C)CCC2=CC=CC=C2)C3=CC=CC=C3</chem>	N	N
3,5-Dimethyl-Cyclopentylfentanyl	<chem>CC1CN(CCc2ccccc2)CC(C1N(C(=O)C1CCCC1)c1ccccc1)C</chem>	N	N
3,5-Dimethylfentanyl	<chem>CCC(=O)N(C1C(C)CN(CC1C)CCc1ccccc1)c1ccccc1</chem>	N	N
3'-4'-Dichloro-3''-Fluorofentanyl	<chem>CCC(=O)N(C1CCN(CC1)CCC2=CC(=CC=C2)F)C3=CC(=C(C=C3)Cl)Cl</chem>	N	N
3'-4'-Methylenedioxyfentanyl	<chem>CCC(=O)N(c1ccc2c(c1)OCO2)C1CCN(CC1)CCc1ccccc1</chem>	N	N
3'-Fluoro-Butyrylfentanyl	<chem>CCCC(=O)N(C1CCN(CC1)CCC2=CC=CC=C2)C3=CC(=CC=C3)F</chem>	Y	N
3'-Fluoro-Isobutyrylfentanyl	<chem>CC(C)C(=O)N(C1CCN(CC1)CCC2=CC=CC=C2)C3=CC(=CC=C3)F</chem>	Y	N
3'-Me-4f-Ibf	<chem>Fc1ccc(cc1)N(C(=O)C(C)C)C1CCN(CC1)CCc1cccc(c1)C</chem>	Y	N
3'-Methyl-Methoxyacetylfentanyl	<chem>CC1=CC(=CC=C1)N(C2CCN(CC2)CCC3=CC=CC=C3)C(=O)COC</chem>	N	N
3-Allylfentanyl	<chem>CCC(=O)N(C1CCN(CC1CC=C)CCC2=CC=CC=C2)C3=CC=CC=C3</chem>	N	N
3-Ethylfentanyl	<chem>CCC(=O)N(C1CCN(CC1CC)CCc1ccccc1)c1ccccc1</chem>	N	N
3-Fluorofentanyl	<chem>CCC(=O)N(C1CCN(CC1F)CCC2=CC=CC=C2)C3=CC=CC=C3</chem>	N	Y

3-Furanylfentanyl	<chem>C1CN(CCC1N(C2=CC=CC=C2)C(=O)C3=COC=C3)CCC4=CC=CC=C4</chem>	N	N
3-Methoxyfentanyl	<chem>CCC(=O)N(C1CCN(CC1OC)CCc1ccccc1)c1ccccc1</chem>	N	N
3-Methyl Phenoxy Acetylfentanyl	<chem>CC1CN(CCOc2ccccc2)CCC1N(c1ccccc1)C(=O)C</chem>	N	N
3-Methyl-Butyrylfentanyl	<chem>CCCC(=O)N(C1CCN(CC1C)CCc1ccccc1)c1ccccc1</chem>	y	N
3-Methylfentanyl	<chem>CCC(=O)N(C1CCN(CC1C)CCc1ccccc1)c1ccccc1</chem>	N	N
3-Methyl-Furanylfentanyl	<chem>CC1CN(CCC1N(C2=CC=CC=C2)C(=O)C3=CC=CO3)CCC4=CC=CC=C4</chem>	N	N
3-Methyl-Thiofentanyl	<chem>CCC(=O)N(C1CCN(CC1C)CCc1cccs1)c1ccccc1</chem>	N	N
3-Phenylpropanoylfentanyl	<chem>C1CN(CCC1N(C2=CC=CC=C2)C(=O)CCC3=CC=CC=C3)CCC4=CC=CC=C4</chem>	Y	Y
4-(M-Hydroxyphenyl)Fentanyl	<chem>CCC(=O)N(C1(CCN(CC1)CCc1ccccc1)c1cccc(c1)O)c1ccccc1</chem>	N	N
4''-Bromo-Ohmefentanyl	<chem>CCC(=O)N(C1CCN(CC1C)CC(c1ccc(cc1)Br)O)c1ccccc1</chem>	N	N
4'-Chloro-Butyrylfentanyl	<chem>CCCC(=O)N(C1CCN(CC1)CCC2=CC=CC=C2)C3=CC=C(C=C3)Cl</chem>	N	N
4'-Chloro-Cyclobutylylfentanyl	<chem>C1CC(C1)C(=O)N(C2CCN(CC2)CCC3=CC=CC=C3)C4=CC=C(C=C4)Cl</chem>	N	N
4'-Chloro-Cyclopropylfentanyl	<chem>C1CC1C(=O)N(C2CCN(CC2)CCC3=CC=CC=C3)C4=CC=C(C=C4)Cl</chem>	N	N
4'-Chlorofentanyl	<chem>CCC(=O)N(C1CCN(CC1)CCC2=CC=CC=C2)C3=CC=C(C=C3)Cl</chem>	y	N
4'-Fluoro-Butyrylfentanyl	<chem>CCCC(=O)N(C1CCN(CC1)CCC2=CC=CC=C2)C3=CC=C(C=C3)F</chem>	y	N
4'-Fluoro-Crotonylfentanyl	<chem>C/C=C/C(=O)N(c1ccc(cc1)F)C1CCN(CC1)CCc1ccccc1</chem>	N	N
4'-Fluoro-Cyclopentylfentanyl	<chem>C1CCC(C1)C(=O)N(C2CCN(CC2)CCC3=CC=CC=C3)C4=CC=C(C=C4)F</chem>	N	N
4'-Fluoro-Cyclopropylfentanyl	<chem>C1CC1C(=O)N(C2CCN(CC2)CCC3=CC=CC=C3)C4=CC=C(C=C4)F</chem>	N	Y
4''-Fluorofentanyl	<chem>CCC(=O)N(C1CCN(CC1)CCC2=CC=C(C=C2)F)C3=CC=CC=C3</chem>	N	N
4''-Fluoro-Ohmefentanyl	<chem>CCC(=O)N(C1CCN(CC1C)CC(c1ccc(cc1)F)O)c1ccccc1</chem>	N	N
4'-Hydroxybutyrylfentanyl	<chem>CCCC(=O)N(c1ccc(cc1)O)C1CCN(CC1)CCc1ccccc1</chem>	Y	Y
4''-Methoxyfentanyl	<chem>CCC(=O)N(c1ccccc1)C1CCN(CC1)CCc1ccc(cc1)OC</chem>	N	N
4''-Methyl-Acetylfentanyl	<chem>CC1=CC=C(C=C1)CCN2CCC(CC2)N(C3=CC=CC=C3)C(=O)C</chem>	y	N
4'-Methylfentanyl	<chem>CCC(=O)N(c1ccc(cc1)C)C1CCN(CC1)CCc1ccccc1</chem>	y	N
4''-Methylfentanyl	<chem>CCC(=O)N(c1ccccc1)C1CCN(CC1)CCc1ccc(cc1)C</chem>	N	N
4'-Methyl-Furanylfentanyl	<chem>CC1=CC=C(C=C1)N(C2CCN(CC2)CCC3=CC=CC=C3)C(=O)C4=CC=CO4</chem>	N	N

4'-Methyl-Methoxyacetylfentanyl	<chem>CC1=CC=C(C=C1)N(C2CCN(CC2)CCC3=CC=CC=C3)C(=O)COC</chem>	N	N
4'-Methyl-Tetrahydrofuranylfentanyl	<chem>CC1=CC=C(C=C1)N(C2CCN(CC2)CCC3=CC=CC=C3)C(=O)C4CCCO4</chem>	N	N
4''-Nitrofentanyl	<chem>CCC(=O)N(c1ccccc1)C1CCN(CC1)CCc1ccc(cc1)N(=O)=O</chem>	N	N
4-Anpp	<chem>C1CN(CCC1NC2=CC=CC=C2)CCC3=CC=CC=C3</chem>	y	N
4'-Chloro-Cyclopentylfentanyl	<chem>C1CCC(C1)C(=O)N(C2CCN(CC2)CCC3=CC=CC=C3)C4=CC=C(C=C4)Cl</chem>	N	N
4-Fluorofentanyl	<chem>CCC(=O)N(C1=CC=CC=C1)C2(CCN(CC2)CCC3=CC=CC=C3)F</chem>	N	N
4-Methoxymethylfentanyl	<chem>COCC1(CCN(CC1)CCc1ccccc1)N(c1ccccc1)C(=O)CC</chem>	N	N
4-Methylfentanyl	<chem>CCC(=O)N(C1(C)CCN(CC1)CCc1ccccc1)c1ccccc1</chem>	N	N
4-Phenylfentanyl	<chem>CCC(=O)N(C1=CC=CC=C1)C2(CCN(CC2)CCC3=CC=CC=C3)C4=CC=CC=C4</chem>	N	N
Acetyl-Carfentanil	<chem>COC(=O)C1(CCN(CC1)CCc1ccccc1)N(c1ccccc1)C(=O)C</chem>	N	N
Acetylfentanyl	<chem>CC(=O)N(C1CCN(CC1)CCC2=CC=CC=C2)C3=CC=CC=C3</chem>	Y	Y
Acetyl-Norfentanyl	<chem>CC(=O)N(C1CCNCC1)C2=CC=CC=C2</chem>	Y	N
Acrylfentanyl	<chem>C=CC(=O)N(C1CCN(CC1)CCC2=CC=CC=C2)C3=CC=CC=C3</chem>	N	Y
Alfentanil	<chem>CCC(=O)N(C1=CC=CC=C1)C2(CCN(CC2)CCN3C(=O)N(N=N3)CC)COC</chem>	N	N
Alphamethylfentanyl	<chem>CCC(=O)N(c1ccccc1)C1CCN(CC1)C(Cc1ccccc1)C</chem>	N	N
Benzodioxolefentanyl	<chem>C1CN(CCC1N(C2=CC=CC=C2)C(=O)C3=CC4=C(C=C3)OCO4)CCC5=CC=CC=C5</chem>	Y	Y
Benzofuranyl-Fentanyl	<chem>CCC(=O)N(c1ccccc1)C1CCN(CC1)CCc1ccc2c(c1)cco2</chem>	N	N
Benzoilolbenzylfentanil	N.a.	N	N
Benzoylbenzylfentanyl	<chem>C1CN(CCC1N(C2=CC=CC=C2)C(=O)C3=CC=CC=C3)CC4=CC=CC=C4</chem>	Y	Y
Benzoylfentanyl	<chem>C1CN(CCC1N(C2=CC=CC=C2)C(=O)C3=CC=CC=C3)CCC4=CC=CC=C4</chem>	Y	Y
Benzylfentanyl	<chem>CCC(=O)N(C1CCN(CC1)CC2=CC=CC=C2)C3=CC=CC=C3</chem>	Y	Y
Brifentanil	<chem>CCN1C(=O)N(N=N1)CCN2CCC(C(C2)C)N(C3=CC=CC=C3F)C(=O)COC</chem>	N	N
Butyryl-Carfentanil	<chem>CCCC(=O)N(C1=CC=CC=C1)C2(CCN(CC2)CCC3=CC=CC=C3)C(=O)OC</chem>	N	N
Butyrylfentanyl	<chem>CCCC(=O)N(C1CCN(CC1)CCC2=CC=CC=C2)C3=CC=CC=C3</chem>	N	Y
Butyrylremifentanil	<chem>CCCC(=O)N(C1=CC=CC=C1)C2(CCN(CC2)CCC(=O)OC)C(=O)OC</chem>	N	N
Carfentanil	<chem>CCC(=O)N(C1=CC=CC=C1)C2(CCN(CC2)CCC3=CC=CC=C3)C(=O)OC</chem>	Y	Y

Crotonylfentanyl	<chem>CC=CC(=O)N(C1CCN(CC1)CCC2=CC=CC=C2)C3=CC=CC=C3</chem>	Y	N
Cyclobutylfentanyl	<chem>C1CC(C1)C(=O)N(C2CCN(CC2)CCC3=CC=CC=C3)C4=CC=CC=C4</chem>	N	N
Cyclohexylfentanyl	<chem>C1CCC(CC1)C(=O)N(C2CCN(CC2)CCC3=CC=CC=C3)C4=CC=CC=C4</chem>	Y	N
Cyclopentenylfentanyl	<chem>C1CC=C(C1)C(=O)N(C2CCN(CC2)CCC3=CC=CC=C3)C4=CC=CC=C4</chem>	N	N
Cyclopentylfentanyl	<chem>C1CCC(C1)C(=O)N(C2CCN(CC2)CCC3=CC=CC=C3)C4=CC=CC=C4</chem>	Y	Y
Cyclopropylfentanyl	<chem>C1CC1C(=O)N(C2CCN(CC2)CCC3=CC=CC=C3)C4=CC=CC=C4</chem>	Y	Y
Despropionyl-3-Methylfentanyl	<chem>CC1CN(CCC1NC2=CC=CC=C2)CCC3=CC=CC=C3</chem>	N	N
Despropionyl-P-Fluorobenzylfentanyl	<chem>C1CN(CCC1NC2=CC=C(C=C2)F)CC3=CC=CC=C3</chem>	Y	N
Ethyl {4-[Phenyl(Propanoyl)Amino]-1-[2-(Thiophen-2-Yl)Ethyl]Piperidin-4-Yl}Methyl Carbonate	<chem>CCC(=O)N(C1=CC=CC=C1)C2(CCN(CC2)CCC3=CC=CC=C3)COC(=O)OCC</chem>	N	N
Ethyl 1-(2-Hydroxy-2-Phenylethyl)-3-Methyl-4-[Phenyl(Propanoyl)Amino]Piperidine-4-Carboxylate	<chem>CCOC(=O)C1(CCN(CC1C)CC(c1ccccc1)O)N(c1ccccc1)C(=O)CC</chem>	N	N
Fentanyl	<chem>CCC(=O)N(c1ccccc1)C1CCN(CC1)CCc1ccccc1</chem>	N	N
Fentranyl	<chem>CCC(=O)N(C1CCN(CC1)C2CC2C3=CC=CC=C3)C4=CC=CC=C4</chem>	N	N
Fluoropentyl-Norcarfentanil	<chem>FCCCCCN1CCC(CC1)(C(=O)OC)N(c1ccccc1)C(=O)CC</chem>	N	N
Furanylbenzylfentanyl	<chem>C1CN(CCC1N(C2=CC=CC=C2)C(=O)C3=CC=CO3)CC4=CC=CC=C4</chem>	Y	Y
Furanyl fentanyl	<chem>C1CN(CCC1N(C2=CC=CC=C2)C(=O)C3=CC=CO3)CCC4=CC=CC=C4</chem>	N	Y
Furanyl-Norfentanyl	<chem>O=C(N(c1ccccc1)C1CCNCC1)c1ccccc1</chem>	N	N
Hexanoyl Fentanyl	<chem>CCCCCC(=O)N(C1CCN(CC1)CCC2=CC=CC=C2)C3=CC=CC=C3</chem>	Y	N
Isobutyrylfentanyl	<chem>CC(C(=O)N(c1ccccc1)C1CCN(CC1)CCc1ccccc1)C</chem>	y	N
Isocarfentanil	<chem>COC(=O)C1CN(CCc2ccccc2)CCC1N(c1ccccc1)C(=O)CC</chem>	N	N
Isofentanyl	<chem>CCC(=O)N(C1CCN(CC1C)CC2=CC=CC=C2)C3=CC=CC=C3</chem>	N	N
Isovaleroylfentanyl	<chem>CC(CC(=O)N(c1ccccc1)C1CCN(CC1)CCc1ccccc1)C</chem>	y	N

Lofentaniil	<chem>CCC(=O)N(C1(CCN(CC1C)CCc1ccccc1)C(=O)OC)c1ccccc1</chem>	N	N
Methacroylfentanyl	<chem>CC(=C)C(=O)N(c1ccccc1)C1CCN(CC1)CCc1ccccc1</chem>	N	N
Methoxyacetylfentanyl	<chem>COCC(=O)N(C1CCN(CC1)CCC2=CC=CC=C2)C3=CC=CC=C3</chem>	N	Y
Methyl 1-(2-Hydroxy-2-Phenylethyl)-3-Methyl-4-[Phenyl(Propanoyl)Amino]Piperidine-4-Carboxylate	<chem>CCC(=O)N(C1(CCN(CC1C)CC(c1ccccc1)O)C(=O)OC)c1ccccc1</chem>	N	N
Methyl 1-[(2,3-Dihydro-1,4-Benzodioxin-2-Yl)Methyl]-4-[Phenyl(Propanoyl)Amino]Piperidine-4-Carboxylate	<chem>CCC(=O)N(C1=CC=CC=C1)C2(CCN(CC2)CC3COC4=CC=CC=C4O3)C(=O)OC</chem>	N	N
Methyl 1-[2-(2-Oxo-1,3-Benzoxazol-3(2h)-Yl)Ethyl]-4-[Phenyl(Propanoyl)Amino]Piperidine-4-Carboxylate	<chem>CCC(=O)N(C1=CC=CC=C1)C2(CCN(CC2)CCN3C4=CC=CC=C4OC3=O)C(=O)OC</chem>	N	N
Methyl 1-[2-(2-Oxo-2,3-Dihydro-1h-Indol-1-Yl)Ethyl]-4-[Phenyl(Propanoyl)Amino]Piperidine-4-Carboxylate	<chem>CCC(=O)N(C1(CCN(CC1)CCN1C(=O)Cc2c1ccccc2)C(=O)OC)c1ccccc1</chem>	N	N
Methyl 1-[2-(3-Oxo-2,3-Dihydro-4h-1,4-Benzothiazin-4-Yl)Ethyl]-4-[Phenyl(Propanoyl)Amino]Piperidine-4-Carboxylate	<chem>CCC(=O)N(C1(CCN(CC1)CCN1C(=O)CSc2c1ccccc2)C(=O)OC)c1ccccc1</chem>	N	N
Methyl 1-[2-(4-Methyl-1,3-Thiazol-5-Yl)Ethyl]-4-[Phenyl(Propanoyl)Amino]Piperidine-4-Carboxylate	<chem>CCC(=O)N(C1=CC=CC=C1)C2(CCN(CC2)CCC3=C(N=CS3)C)C(=O)OC</chem>	N	N

Methyl 1-[2-Hydroxy-2-(Thiophen-2-Yl)Ethyl]-4-[Phenyl(Propanoyl)Amino]Piperidine-4-Carboxylate	<chem>CCC(=O)N(C1=CC=CC=C1)C2(CCN(CC2)CC(C3=CC=CS3)O)C(=O)OC</chem>	N	N
Methyl 1-[2-Oxo-2-(Thiophen-2-Yl)Ethyl]-4-[Phenyl(Propanoyl)Amino]Piperidine-4-Carboxylate	<chem>CCC(=O)N(C1(CCN(CC1)CC(=O)c1cccs1)C(=O)OC)c1cccc1</chem>	N	N
Methyl 1-{2-[(1-Methyl-1h-Imidazol-2-Yl)Sulfanyl]Ethyl}-4-[Phenyl(Propanoyl)Amino]Piperidine-4-Carboxylate	<chem>CCC(=O)N(C1=CC=CC=C1)C2(CCN(CC2)CCSC3=NC=CN3C)C(=O)OC</chem>	N	N
Methyl 1-{2-[5-Methyl-2-(Methylsulfanyl)-6-Oxopyrimidin-1(6h)-Yl]Ethyl}-4-[Phenyl(Propanoyl)Amino]Piperidine-4-Carboxylate	<chem>CCC(=O)N(C1=CC=CC=C1)C2(CCN(CC2)CCN3C(=O)C(=CN=C3SC)C)C(=O)OC</chem>	N	N
Methyl 4-[Phenyl(Propanoyl)Amino]-1-[2-(1h-Pyrazol-1-Yl)Ethyl]Piperidine-4-Carboxylate	<chem>COC(=O)C1(CCN(CC1)CCn1cccn1)N(c1cccc1)C(=O)CC</chem>	N	N
Methyl 4-[Phenyl(Propanoyl)Amino]-1-[2-(1h-Pyrrol-1-Yl)Ethyl]Piperidine-4-Carboxylate	<chem>COC(=O)C1(CCN(CC1)CCn1cccc1)N(c1cccc1)C(=O)CC</chem>	N	N
Methyl 4-[Phenyl(Propanoyl)Amino]-1-[2-(2h-Tetrazol-2-Yl)Ethyl]Piperidine-4-Carboxylate	<chem>COC(=O)C1(CCN(CC1)CCn1nncn1)N(c1cccc1)C(=O)CC</chem>	N	N
Methyl 4-[Phenyl(Propanoyl)Amino]-	<chem>CCC(=O)N(C1(CCN(CC1)CCc1cccc1)C(=O)OC)c1cccc1</chem>	N	N

1-[2-(Pyridin-2-Y1)Ethyl]Piperidine-4-Carboxylate			
Methyl 4-[Phenyl(Propanoyl)Amino]-1-[2-(Thiophen-3-Y1)Ethyl]Piperidine-4-Carboxylate	<chem>COC(=O)C1(CCN(CC1)CCc1csc1)N(c1ccccc1)C(=O)CC</chem>	N	N
M-Fluoro-Methoxyacetylfentanyl	<chem>COCC(=O)N(C1CCN(CC1)CCC2=CC=CC=C2)C3=CC(=CC=C3)F</chem>	N	Y
Mirfentanil	<chem>C1CN(CCC1N(C2=NC=CN=C2)C(=O)C3=CC=CO3)CCC4=CC=CC=C4</chem>	N	N
M-Methylfentanyl	<chem>CCC(=O)N(c1ccccc1)C1CCN(CC1)CCc1ccccc1</chem>	N	N
N-(2-Fluorophenyl)-N-[1-(2-Hydroxy-2-Phenylethyl)-3-Methylpiperidin-4-Y1]Propanamide	<chem>CCC(=O)N(c1ccccc1F)C1CCN(CC1C)CC(c1ccccc1)O</chem>	N	N
N-(2-Fluorophenyl)-N-[1-(2-Phenylethyl)-4-(1,3-Thiazol-2-Y1)Piperidin-4-Y1]Propanamide	<chem>CCC(=O)N(C1(CCN(CC1)CCc1ccccc1)c1nccs1)c1ccccc1F</chem>	N	N
N-(2-Fluorophenyl)-N-[1-(2-Phenylethyl)-4-(Pyridin-2-Y1)Piperidin-4-Y1]Propanamide	<chem>CCC(=O)N(C1(CCN(CC1)CCc1ccccc1)c1ccccn1)c1ccccc1F</chem>	N	N
N-(2-Fluorophenyl)-N-[4-Phenyl-1-(2-Phenylethyl)Piperidin-4-Y1]Propanamide	<chem>CCC(=O)N(C1(CCN(CC1)CCc1ccccc1)c1ccccc1)c1ccccc1F</chem>	N	N
N-(2-Fluorophenyl)-N-{1-[2-(1h-Pyrazol-1-Y1)Ethyl]-4-(Pyridin-2-Y1)Piperidin-4-Y1}Propanamide	<chem>CCC(=O)N(C1=CC=CC=C1F)C2(CCN(CC2)CCN3C=CC=N3)C4=CC=CC=N4</chem>	N	N
N-(2-Fluorophenyl)-N-{1-[2-(4-Methyl-1,3-Thiazol-5-Y1)Ethyl]-4-Phenylpiperidin-4-Y1}Propanamide	<chem>CCC(=O)N(C1(CCN(CC1)CCc1snc1C)c1ccccc1)c1ccccc1F</chem>	N	N
N-(2-Fluorophenyl)-N-{4-(4-Methyl-	<chem>CCC(=O)N(C1=CC=CC=C1F)C2(CCN(CC2)CCN3C=CC=N3)C4=NC(=CS4)C</chem>	N	N



1,3-Thiazol-2-Yl)-1-[2-(1h-Pyrazol-1-Yl)Ethyl]Piperidin-4-Yl}Propanamide			
N-(2-Fluorophenyl)-N-{4-(4-Methyl-1,3-Thiazol-2-Yl)-1-[2-(4-Methyl-1,3-Thiazol-5-Yl)Ethyl]Piperidin-4-Yl}Propanamide	<chem>CCC(=O)N(C1=CC=CC=C1F)C2(CCN(CC2)CCC3=C(N=CS3)C)C4=NC(=CS4)C</chem>	N	N
N-(2-Fluorophenyl)-N-{4-(4-Methyl-1,3-Thiazol-2-Yl)-1-[2-(Thiophen-3-Yl)Ethyl]Piperidin-4-Yl}Propanamide	<chem>CCC(=O)N(C1=CC=CC=C1F)C2(CCN(CC2)CCC3=CSC=C3)C4=NC(=CS4)C</chem>	N	N
N-(2-Fluorophenyl)-N-{4-Phenyl-1-[2-(1h-Pyrazol-1-Yl)Ethyl]Piperidin-4-Yl}Propanamide	<chem>CCC(=O)N(C1(CCN(CC1)CCn1cccn1)c1ccccc1)c1ccccc1F</chem>	N	N
N-(2-Fluorophenyl)-N-{4-Phenyl-1-[2-(Thiophen-2-Yl)Ethyl]Piperidin-4-Yl}Propanamide	<chem>CCC(=O)N(C1=CC=CC=C1F)C2(CCN(CC2)CCC3=CC=CS3)C4=CC=CC=C4</chem>	N	N
N-(2-Fluorophenyl)-N-{4-Phenyl-1-[2-(Thiophen-3-Yl)Ethyl]Piperidin-4-Yl}Propanamide	<chem>CCC(=O)N(C1(CCN(CC1)CCc1ccsc1)c1ccccc1)c1ccccc1F</chem>	N	N
N-(3-Fluorophenyl)-N-[1-(2-Hydroxy-2-Phenylethyl)-3-Methylpiperidin-4-Yl]Propanamide	<chem>CCC(=O)N(C1CCN(CC1C)CC(c1ccccc1)O)c1ccccc1F</chem>	N	N
N-(4-Fluorophenyl)-N-[1-(2-Hydroxy-2-Phenylethyl)-3-Methylpiperidin-4-Yl]Propanamide	<chem>CCC(=O)N(C1CCN(CC1C)CC(c1ccccc1)O)c1ccc(cc1)F</chem>	N	N
N-[1-(2-Cyclopropyl-2-Hydroxyethyl)-3-Methylpiperidin-4-Yl]-N-Phenylpropanamide	<chem>CCC(=O)N(C1CCN(CC1C)CC(C1CC1)O)c1ccccc1</chem>	N	N

N-[1-(2-Hydroxy-2-Phenylethyl)-3-Methylpiperidin-4-Yl]-2-Methoxy-N-Phenylacetamide	<chem>COCC(=O)N(C1CCN(CC1C)CC(c1ccccc1)O)c1ccccc1</chem>	N	N
N-[1-(2-Hydroxy-2-Phenylethyl)-3-Methylpiperidin-4-Yl]-N-(3-Methoxyphenyl)Propanamide	<chem>CCC(=O)N(C1CCN(CC1C)CC(c1ccccc1)O)c1ccccc1OC</chem>	N	N
N-[1-(2-Hydroxy-2-Phenylethyl)-3-Methylpiperidin-4-Yl]-N-(Pyridin-2-Yl)Propanamide	<chem>CCC(=O)N(C1CCN(CC1C)CC(c1ccccc1)O)c1ccccc1</chem>	N	N
N-[1-(2-Hydroxy-2-Phenylethyl)-3-Methylpiperidin-4-Yl]-N-(Pyridin-3-Yl)Propanamide	<chem>CCC(=O)N(C1CCN(CC1C)CC(c1ccccc1)O)c1ccccc1</chem>	N	N
N-[1-(2-Hydroxy-2-Phenylethyl)-3-Methylpiperidin-4-Yl]-N-Phenylfuran-2-Carboxamide	<chem>OC(c1ccccc1)CN1CCC(C(C1)C)N(C(=O)c1ccoc1)c1ccccc1</chem>	N	N
N-[1-(2-Hydroxy-2-Phenylethyl)-3-Methylpiperidin-4-Yl]-N-Phenylfuran-3-Carboxamide	<chem>OC(c1ccccc1)CN1CCC(C(C1)C)N(C(=O)c1ccoc1)c1ccccc1</chem>	N	N
N-[1-(2-Hydroxy-2-Phenylethyl)-3-Methylpiperidin-4-Yl]-N-Phenylthiophene-2-Carboxamide	<chem>OC(c1ccccc1)CN1CCC(C(C1)C)N(C(=O)c1cccs1)c1ccccc1</chem>	N	N
N-[1-(2-Hydroxy-2-Phenylethyl)-3-Methylpiperidin-4-Yl]-N-Phenylthiophene-3-Carboxamide	<chem>OC(c1ccccc1)CN1CCC(C(C1)C)N(C(=O)c1ccsc1)c1ccccc1</chem>	N	N
N-[1-(2-Hydroxy-2-Phenylethyl)-4-(Methoxymethyl)-3-Methylpiperidin-4-Yl]-N-Phenylpropanamide	<chem>COCC1(CCN(CC1C)CC(c1ccccc1)O)N(c1ccccc1)C(=O)CC</chem>	N	N

N-[4-(4-Methyl-1,3-Thiazol-2-Yl)-1-(2-Phenylethyl)Piperidin-4-Yl]-N-Phenylpropanamide	<chem>CCC(=O)N(C1(CCN(CC1)CCc1ccccc1)c1scc(n1)C)c1ccccc1</chem>	N	N
N-{1-[(2r,3r)-3-Hydroxy-1,2,3,4-Tetrahydronaphthalen-2-Yl]-3-Methylpiperidin-4-Yl}-N-Phenylpropanamide	<chem>CCC(=O)N(C1CCN(CC1C)[C@@H]1Cc2ccccc2C[C@H]1O)c1ccccc1</chem>	N	N
N-{1-[2-(3,5-Dimethyl-1h-Pyrazol-1-Yl)Ethyl]-4-Phenylpiperidin-4-Yl}-N-(2-Fluorophenyl)Propanamide	<chem>CCC(=O)N(C1=CC=CC=C1F)C2(CCN(CC2)CCN3C(=CC(=N3)C)C)C4=CC=CC=C4</chem>	N	N
N-{1-[2-(4-Ethyl-5-Oxo-4,5-Dihydro-1h-Tetrazol-1-Yl)Ethyl]-4-(1,3-Thiazol-2-Yl)Piperidin-4-Yl}-N-(2-Fluorophenyl)Propanamide	<chem>CCC(=O)N(C1=CC=CC=C1F)C2(CCN(CC2)CCN3C(=O)N(N=N3)CC)C4=NC=CS4</chem>	N	N
N-{1-[2-(Furan-2-Yl)-2-Hydroxyethyl]-4-(Methoxymethyl)Piperidin-4-Yl}-N-Phenylpropanamide	<chem>COCC1(CCN(CC1)CC(c1ccco1)O)N(c1ccccc1)C(=O)CC</chem>	N	N
N-{1-[2-Hydroxy-2-(1-Methyl-1h-Pyrrol-2-Yl)Ethyl]-3-Methylpiperidin-4-Yl}-N-Phenylpropanamide	<chem>CCC(=O)N(C1CCN(CC1C)CC(c1cccn1C)O)c1ccccc1</chem>	N	N
N-{1-[2-Hydroxy-2-(Pyridin-3-Yl)Ethyl]-3-Methylpiperidin-4-Yl}-N-Phenylpropanamide	<chem>CCC(=O)N(C1CCN(CC1C)CC(c1cccn1)O)c1ccccc1</chem>	N	N
N-{1-[2-Hydroxy-2-(Pyridin-4-Yl)Ethyl]-3-Methylpiperidin-4-Yl}-	<chem>CCC(=O)N(C1CCN(CC1C)CC(c1ccncc1)O)c1ccccc1</chem>	N	N

N-Phenylpropanamide			
N-{1-[2-Hydroxy-2-(Thiophen-2-Y1)Ethyl]-3-Methylpiperidin-4-Y1}-N-(3-Methoxyphenyl)Propanamide	<chem>CCC(=O)N(C1CCN(CC1C)CC(c1cccs1)O)c1cccc(c1)OC</chem>	N	N
N-{3,5-Dimethyl-1-[2-(1h-Pyrazol-1-Y1)Ethyl]Piperidin-4-Y1}-2-Methoxy-N-Phenylacetamide	<chem>COCC(=O)N(C1C(C)CN(CC1C)CCn1cccn1)c1cccc1</chem>	N	N
N-Adamantyl-Fentanyl	<chem>CCC(=O)N(C12CC3CC(C2)CC(C1)C3)C1CCN(CC1)CCc1cccc1</chem>	N	N
N-Benzoxazolyl-Fentanyl	<chem>CCC(=O)N(c1ccc2c(c1)ocn2)C1CCN(CC1)CCc1cccc1</chem>	N	N
N-Benzyl-Acetylfentanyl	<chem>CC(=O)N(C1CCN(CC1)CC2=CC=CC=C2)C3=CC=CC=C3</chem>	Y	N
N-Benzyl-Butyrylfentanyl	<chem>CCCC(=O)N(C1CCN(CC1)CC2=CC=CC=C2)C3=CC=CC=C3</chem>	N	N
N-Benzylcarfentanil	<chem>CCC(=O)N(C1=CC=CC=C1)C2(CCN(CC2)CC3=CC=CC=C3)C(=O)OC</chem>	N	N
N-Benzyl-P-Fluoro-Isobutyrylfentanyl	<chem>O=C(C(c1ccc(cc1)F)C1CCN(CC1)Cc1cccc1)C(C)C</chem>	N	N
N-Furanylethylfentanyl	<chem>CCC(=O)N(c1cccc1)C1CCN(CC1)CCc1ccco1</chem>	N	N
N-Methyl Norfentanyl	<chem>CCC(=O)N(c1cccc1)C1CCN(CC1)C</chem>	Y	N
N-Methyl-Acetyl-Norfentanyl	<chem>CC(=O)N(C1CCN(CC1)C)C2=CC=CC=C2</chem>	N	N
N-Methyl-Butyrylfentanyl	<chem>CCCC(=O)N(C1CCN(CC1)C)C2=CC=CC=C2</chem>	N	N
N-Methyl-Carfentanil	<chem>CCC(=O)N(C1=CC=CC=C1)C2(CCN(CC2)C)C(=O)OC</chem>	N	N
N-Phenyl-N-[1-(2-Phenylethyl)-4-(1,3-Thiazol-2-Y1)Piperidin-4-Y1]Propanamide	<chem>CCC(=O)N(C1=CC=CC=C1)C2(CCN(CC2)CCC3=CC=CC=C3)C4=NC=CS4</chem>	N	N
N-Phenyl-N-{4-Phenyl-1-[2-(1h-Pyrazol-1-Y1)Ethyl]Piperidin-4-Y1}Propanamide	<chem>CCC(=O)N(C1=CC=CC=C1)C2(CCN(CC2)CCN3C=CC=N3)C4=CC=CC=C4</chem>	N	N
N-Phenyl-N-{4-Phenyl-1-[2-(Pyridin-2-Y1)Ethyl]Piperidin-4-	<chem>CCC(=O)N(C1=CC=CC=C1)C2(CCN(CC2)CCC3=CC=CC=N3)C4=CC=CC=C4</chem>	N	N

Y1}Propanamide			
N-Phenyl-N-{4-Phenyl-1-[2-(Thiophen-2-Y1)Ethyl]Piperidin-4-Y1}Propanamide	<chem>CCC(=O)N(C1=CC=CC=C1)C2(CCN(CC2)CCC3=CC=CS3)C4=CC=CC=C4</chem>	N	N
N-Phenyl-N-{4-Phenyl-1-[2-(Thiophen-3-Y1)Ethyl]Piperidin-4-Y1}Propanamide	<chem>CCC(=O)N(C1=CC=CC=C1)C2(CCN(CC2)CCC3=CSC=C3)C4=CC=CC=C4</chem>	N	N
N-Quinolinyl-Fentanyl	<chem>CCC(=O)N(c1cccc2c1nccc2)C1CCN(CC1)CCc1cccc1</chem>	N	N
Ocfentanyl	<chem>COCC(=O)N(c1cccc1F)C1CCN(CC1)CCc1cccc1</chem>	Y	Y
O-Fluoro-Despropionylfentanyl	<chem>C1CN(CCC1NC2=CC=CC=C2F)CCC3=CC=CC=C3</chem>	Y	N
Ohmefentanyl	<chem>CCC(=O)N(C1CCN(CC1C)CC(C2=CC=CC=C2)O)C3=CC=CC=C3</chem>	N	N
O-Methoxy-Furanylfentanyl	<chem>COc1cccc1N(C(=O)c1ccco1)C1CCN(CC1)CCc1cccc1</chem>	N	N
O-Methyl-Acetylfentanyl	<chem>CC1=CC=CC=C1N(C2CCN(CC2)CCC3=CC=CC=C3)C(=O)C</chem>	Y	Y
O-Methyl-Benzoylfentanyl	<chem>O=C(N(c1cccc1C)C1CCN(CC1)CCc1cccc1)c1cccc1</chem>	N	N
O-Methyl-Cyclopropylfentanyl	<chem>Cc1cccc1N(C(=O)C1CC1)C1CCN(CC1)CCc1cccc1</chem>	Y	N
O-Methylfentanyl	<chem>CCC(=O)N(c1cccc1C)C1CCN(CC1)CCc1cccc1</chem>	N	N
O-Methyl-Furanylfentanyl	<chem>CC1=CC=CC=C1N(C2CCN(CC2)CCC3=CC=CC=C3)C(=O)C4=CC=CO4</chem>	Y	N
P-Bromofentanyl	<chem>CCC(=O)N(c1ccc(cc1)Br)C1CCN(CC1)CCc1cccc1</chem>	Y	N
P-Chloro-Furanylfentanyl	<chem>C1CN(CCC1N(C2=CC=C(C=C2)Cl)C(=O)C3=CC=CO3)CCC4=CC=CC=C4</chem>	Y	N
P-Chloro-Isobutyrylfentanyl	<chem>CC(C)C(=O)N(C1CCN(CC1)CCC2=CC=CC=C2)C3=CC=C(C=C3)Cl</chem>	Y	Y
P-Chloro-Methoxyacetylfentanyl	<chem>COCC(=O)N(C1CCN(CC1)CCC2=CC=CC=C2)C3=CC=C(C=C3)Cl</chem>	N	N
P-Fluoro-Acetylfentanyl	<chem>CC(=O)N(C1CCN(CC1)CCC2=CC=CC=C2)C3=CC=C(C=C3)F</chem>	N	N
P-Fluoro-Acrylfentanyl	<chem>C=CC(=O)N(C1CCN(CC1)CCC2=CC=CC=C2)C3=CC=C(C=C3)F</chem>	N	N
P-Fluoro-Cyclopropylbenzylfentanyl	<chem>C1CC1C(=O)N(C2CCN(CC2)CC3=CC=CC=C3)C4=CC=C(C=C4)F</chem>	Y	N
P-Fluoro-Furan-3-Ylfentanyl	<chem>C1CN(CCC1N(C2=CC=C(C=C2)F)C(=O)C3=COC=C3)CCC4=CC=CC=C4</chem>	N	N
P-Fluoro-Furanylethylfentanyl	<chem>CCC(=O)C(c1ccc(cc1)F)C1CCN(CC1)CCc1ccco1</chem>	N	N

P-Fluoro-Furanylfentanyl	C1CN(CCC1N(C2=CC=C(C=C2)F)C(=O)C3=CC=CO3)CCC4=CC=CC=C4	Y	N
P-Fluoro-Furanylremifentanyl	COC(=O)C1(CCN(CC1)CCC(=O)OC)N(C(=O)c1cccc1)c1ccc(cc1)F	N	N
P-Fluoro-Isobutyrylfentanyl	CC(C)C(=O)N(C1CCN(CC1)CCC2=CC=CC=C2)C3=CC=C(C=C3)F	N	Y
P-Fluoro-Isopropylbenzylfentanyl	CC(C)C(=O)N(C1CCN(CC1)CC2=CC=CC=C2)C3=CC=C(C=C3)F	y	N
P-Fluoro-Methoxyacetylfentanyl	COCC(=O)N(C1CCN(CC1)CCC2=CC=CC=C2)C3=CC=C(C=C3)F	N	N
P-Fluoro-Tetrahydrofuranylfentanyl	Fc1ccc(cc1)N(C(=O)C1CCCO1)C1CCN(CC1)CCc1cccc1	N	N
P-Fluoro-Thiofentanyl	CCC(=O)N(c1ccc(cc1)F)C1CCN(CC1)CCc1cccc1	N	N
P-Fluoro-B-Hydroxy-Thiobutyrylfentanyl	CCCC(=O)N(c1ccc(cc1)F)C1CCN(CC1)CC(c1cccc1)O	N	N
Pharaohfentanyl	CCC(=O)N(C1(C)CCN(CC1)CC(c1cccc1)O)c1cccc1	N	N
Phenoxyethyl-Norfentanyl	CCC(=O)N(C1CCN(CC1)CCOC2=CC=CC=C2)C3=CC=CC=C3	N	N
Phenylacetylfentanyl	O=C(N(c1cccc1)C1CCN(CC1)CCc1cccc1)Cc1cccc1	N	N
Phenylpropyl-Norfentanyl	CCC(=O)N(c1cccc1)C1CCN(CC1)CCCc1cccc1	N	N
P-Iodofentanyl	CCC(=O)N(c1ccc(cc1)I)C1CCN(CC1)CCc1cccc1	N	N
Pivaloylfentanyl	O=C(C(C)(C)C)N(c1cccc1)C1CCN(CC1)CCc1cccc1	Y	N
P-Methoxy-Acetylfentanyl	COc1ccc(cc1)N(C(=O)C)C1CCN(CC1)CCc1cccc1	N	N
P-Methoxy-Butyrylfentanyl	CCCC(=O)N(C1CCN(CC1)CCC2=CC=CC=C2)C3=CC=C(C=C3)OC	Y	Y
P-Methoxyfentanyl	CCC(=O)N(c1ccc(cc1)OC)C1CCN(CC1)CCc1cccc1	Y	N
P-Methoxy-Furanylfentanyl	COc1ccc(cc1)N(C(=O)c1cccc1)C1CCN(CC1)CCc1cccc1	N	N
P-Methoxy-Methoxyacetylfentanyl	COCC(=O)N(c1ccc(cc1)OC)C1CCN(CC1)CCc1cccc1	N	N
P-Methoxy-Tetrahydrofuranylfentanyl	COC1=CC=C(C=C1)N(C2CCN(CC2)CCC3=CC=CC=C3)C(=O)C4CCCO4	N	N
P-Methoxy-Valerylfentanyl	CCCCC(=O)N(c1ccc(cc1)OC)C1CCN(CC1)CCc1cccc1	N	N
P-Methyl-Acetylfentanyl	Cc1ccc(cc1)N(C1CCN(CC1)CCc1cccc1)C(=O)C	N	N
P-Methyl-Cyclopropylfentanyl	Cc1ccc(cc1)N(C(=O)C1CC1)C1CCN(CC1)CCc1cccc1	Y	N
Propyl-Norfentanyl	CCCN1CCC(CC1)N(C2=CC=CC=C2)C(=O)CC	N	N
Psicofentanyl	CCC(=O)N(C1(CCN(CC1)CCc1c[nH]e2c1cccc2)C(=O)OC1CN2CCC1CC2)c1cccc1	N	N

P-Tfm-Fentanyl	<chem>CCC(=O)N(c1ccc(cc1)C(F)(F)F)C1CCN(CC1)CCc1ccccc1</chem>	N	N
Remifentanil	<chem>CCC(=O)N(C1=CC=CC=C1)C2(CCN(CC2)CCC(=O)OC)C(=O)OC</chem>	N	N
Remifentanil Bis Ethyl Ester	<chem>CCOC(=O)C1(CCN(CC1)CCC(=O)OCC)N(c1ccccc1)C(=O)CC</chem>	N	N
Sufentanil	<chem>COCC1(CCN(CC1)CCc1ccccc1)N(c1ccccc1)C(=O)CC</chem>	N	N
Tetrahydrofuranylfentanyl	<chem>C1CC(OC1)C(=O)N(C2CCN(CC2)CCC3=CC=CC=C3)C4=CC=CC=C4</chem>	Y	Y
Thenylfentanyl	<chem>CCC(=O)N(C1CCN(CC1)CC2=CC=CS2)C3=CC=CC=C3</chem>	N	N
Thiafentanil	<chem>COCC(=O)N(C1=CC=CC=C1)C2(CCN(CC2)CCC3=CC=CS3)C(=O)OC</chem>	N	N
Thiofentanyl	<chem>CCC(=O)N(c1ccccc1)C1CCN(CC1)CCc1ccccc1</chem>	N	N
Thiophenoylfentanyl	<chem>C1CN(CCC1N(C2=CC=CC=C2)C(=O)C3=CC=CS3)CCC4=CC=CC=C4</chem>	Y	N
Tmcp-F	<chem>CC1(C(C1(C)C)C(=O)N(C2CCN(CC2)CCC3=CC=CC=C3)C4=CC=CC=C4)C</chem>	Y	N
Trefentanil	<chem>CCC(=O)N(C1=CC=CC=C1F)C2(CCN(CC2)CCN3C(=O)N(N=N3)CC)C4=CC=CC=C4</chem>	N	N
Valerylfentanyl	<chem>CCCCC(=O)N(c1ccccc1)C1CCN(CC1)CCc1ccccc1</chem>	N	Y
A,3-Dimethylfentanyl	<chem>CCC(=O)N(C1CCN(CC1C)C(C)CC2=CC=CC=C2)C3=CC=CC=C3</chem>	N	N
A'-Methoxyfentanyl	<chem>COC(C(=O)N(c1ccccc1)C1CCN(CC1)CCc1ccccc1)C</chem>	N	N
A'-Methyl-Butyrylfentanyl	<chem>CCC(C(=O)N(c1ccccc1)C1CCN(CC1)CCc1ccccc1)C</chem>	N	N
A-Methyl-Acetylfentanyl	<chem>CC(N1CCC(CC1)N(c1ccccc1)C(=O)C)Cc1ccccc1</chem>	N	N
A-Methyl-Acrylfentanyl	<chem>C=CC(=O)N(c1ccccc1)C1CCN(CC1)C(Cc1ccccc1)C</chem>	N	N
A-Methyl-Butyrylfentanyl	<chem>CCCC(=O)N(C1CCN(CC1)C(C)CC2=CC=CC=C2)C3=CC=CC=C3</chem>	Y	N
A-Methyl-Isobutyrylfentanyl	<chem>CC(C)C(=O)N(C1CCN(CC1)C(C)CC2=CC=CC=C2)C3=CC=CC=C3</chem>	N	N
A-Methyl-P-Fluorofentanyl	<chem>CCC(=O)N(c1ccc(cc1)F)C1CCN(CC1)C(Cc1ccccc1)C</chem>	N	N
A-Methyl-Thiofentanyl	<chem>CCC(=O)N(c1ccccc1)C1CCN(CC1)C(Cc1ccccc1)C</chem>	N	N
B-Hydroxy-3-Methylfentanyl Carbamate	<chem>CCOC(=O)N(C1CCN(CC1C)CC(c1ccccc1)O)c1ccccc1</chem>	N	N
B-Hydroxy-3-Methyl-Thienylfentanyl	<chem>CCC(=O)N(C1CCN(CC1C)CC(c1ccccc1)O)c1ccccc1</chem>	N	N
B-Hydroxy-Carfentanil	<chem>CCC(=O)N(C1(CCN(CC1)CC(c1ccccc1)O)C(=O)OC)c1ccccc1</chem>	N	N
B-Hydroxyfentanyl	<chem>CCC(=O)N(c1ccccc1)C1CCN(CC1)CC(c1ccccc1)O</chem>	N	N

B-Hydroxy-P-Fluorofentanyl	<chem>CCC(=O)N(c1ccc(cc1)F)C1CCN(CC1)CC(c1ccccc1)O</chem>	N	N
B-Hydroxy-Sufentanil	<chem>COCC1(CCN(CC1)CC(c1cccs1)O)N(c1ccccc1)C(=O)CC</chem>	N	N
B-Hydroxy-Thiofentanyl	<chem>CCC(=O)N(c1ccccc1)C1CCN(CC1)CC(c1cccs1)O</chem>	N	N
B-Methylfentanyl	<chem>CCC(=O)N(c1ccccc1)C1CCN(CC1)CC(c1ccccc1)C</chem>	Y	N

**\*The comparison of the three databases has been carried out using the InChIKey string. The data from the EMCDDA are older than those from the UNODC due to the exit of UK from the EU. The SMILES were obtained from PubMed.**



Of 239 fentanyl-like NSOs, 64 were in common with the UNODC and EMCDDA, while 175 molecules seem to be unique to the NPSfinder<sup>®</sup> database. On the other hand, the UNODC EWA identified 33 NSOs which were not reported by the web crawler. The data here reported for the EMCDDA are not up to date and should not be considered as relevant to assess the European NSOs scenario. For the same reason, these data will not be commented or reported for the other NSO subfamilies.

The total of the non-fentanyl molecules identified amount to 88, of which only 17 are in common with the UNODC database (Table 3.4). While a total of 64 non-fentanyl NSOs seems to be unique to the NPSfinder<sup>®</sup>, the UNODC identified 33 molecules which were not detected by the web crawler (Appendix A).

**Table 3.4 List of non-fentanyl like NSO identified by the NPSfinder<sup>®</sup> and comparison with the UNODC database**

<b>Mol</b>	<b>SMILES</b>	<b>UNODC (2022)</b>
1-Phenethyl-4-Hydroxypiperidine	<chem>C1CN(CCC1O)CCC2=CC=CC=C2</chem>	N
2f-Viminol	<chem>CCC(C)N(CC(C1=CC=CN1CC2=CC=CC=C2F)O)C(C)CC</chem>	Y
3,4-Mdo-U-47700	<chem>CN(C)C1CCCCC1N(C)C(=O)C2=CC3=C(C=C2)OC3</chem>	Y
(2R,3R)-4-(Dimethylamino)-3-Methyl-1,2-Diphenyl-2-Butanyl Propionate	<chem>CN(C)C[C@@H](C)[C@](C1=CC=CC=C1)(OC(C)=O)CC2=CC=CC=C2</chem>	N
4-Phenylpiperidine-4-Carboxylic Acid	<chem>C1CNCCC1(C2=CC=CC=C2)C(=O)O</chem>	N
Acetoxymethylketobemidone	<chem>CC(=O)C1(CCN(CC1)C)C2=CC(=CC=C2)OC(=O)C</chem>	N
Acetylmethadol	<chem>CCC(C(CN(C)C)C)(C1=CC=CC=C1)C2=CC=CC=C2)OC(=O)C</chem>	N
Ah-7921	<chem>CN(C1(CCCCC1)CNC(=O)c1ccc(c(c1)Cl)Cl)C</chem>	Y
Allylprodine	<chem>CCC(=O)OC1(CCN(CC1CC=C)C)C2=CC=CC=C2</chem>	N
Alphacetylmethadol	<chem>CC[C@H](C(C[C@@H](C)N(C)C)(C1=CC=CC=C1)C2=CC=CC=C2)OC(=O)C</chem>	N
Alphameprodine	<chem>CC[C@@H]1CN(C)CC[C@@]1(OC(=O)CC)c1cccc1</chem>	N
Alphamethadol	<chem>CC[C@H](C(c1cccc1)(c1cccc1)C[C@H](N(C)C)C)O</chem>	N
Alphaprodine	<chem>CCC(=O)O[C@]1(CCN(C[C@H]1C)C)c1cccc1</chem>	N
Anileridine	<chem>CCOC(=O)C1(CCN(CC1)CCc1ccc(cc1)N)c1cccc1</chem>	N
Ap-237	<chem>CCCC(=O)N1CCN(CC1)CC=CC2=CC=CC=C2</chem>	Y
Ap-238	<chem>CCC(=O)N1C(CN(CC1)C)CC=CC2=CC=CC=C2)C</chem>	y
Bdpc	<chem>CN(C)C1(CCC(CC1)(CCC2=CC=CC=C2)O)C3=CC=C(C=C3)Br</chem>	N
Benzethidine	<chem>CCOC(=O)C1(CCN(CC1)CCOCc1cccc1)c1cccc1</chem>	N

Betacetylmethadol	<chem>CC[C@@H](C1CCCC1)(C1CCCC1)C[C@H](N(C)C)C)OC(=O)C</chem>	Y
Betameprodine	<chem>CC[C@H]1CN(C)CC[C@@]1(OC(=O)CC)c1cccc1</chem>	N
Betamethadol	<chem>CC[C@@H](C1CCCC1)(C1CCCC1)C[C@H](N(C)C)C)O</chem>	N
Betaprodine	<chem>CCC(=O)O[C@]1(CCN(C[C@H]1C)C)c1cccc1</chem>	N
Bezitramide	<chem>CCC(=O)n1c(=O)n(c2c1cccc2)C1CCN(CC1)CCC(c1cccc1)(c1cccc1)C#N</chem>	N
Bromadoline	<chem>CN(C)C1CCCC1NC(=O)C2=CC=C(C=C2)Br</chem>	N
Brorphine	<chem>CC(C1=CC=C(C=C1)Br)N2CCC(CC2)N3C4=CC=CC=C4NC3=O</chem>	Y
Carperidine	<chem>CCOC(=O)C1(CCN(CC1)CCC(=O)N)C2=CC=CC=C2</chem>	N
Desmethylmoramide	<chem>C1CCN(C1)C(=O)C(CCN2CCOCC2)(C3=CC=CC=C3)C4=CC=CC=C4</chem>	Y
Desmethylprodine	<chem>CCC(=O)OC1(CCN(CC1)C)C2=CC=CC=C2</chem>	N
Desmetramadol	<chem>CN(CC1CCCCC1(O)c1cccc(c1)O)C</chem>	N
Dextromoramide	<chem>CC(CN1CCOCC1)C(C2=CC=CC=C2)(C3=CC=CC=C3)C(=O)N4CCCC4</chem>	N
Dextropropoxyphene	<chem>CCC(=O)OC(CC1=CC=CC=C1)(C2=CC=CC=C2)C(C)CN(C)C</chem>	N
Diampromide	<chem>CCC(=O)N(CC(C)N(C)CCC1=CC=CC=C1)C2=CC=CC=C2</chem>	N
Diethylthiambutene	<chem>CCN(CC)C(C)C=C(C1=CC=CS1)C2=CC=CS2</chem>	N
Difenoxin	<chem>N#CC(c1cccc1)(c1cccc1)CCN1CCC(CC1)(C(=O)O)c1cccc1</chem>	N
Dimenoxadol	<chem>CCOC(C1=CC=CC=C1)(C2=CC=CC=C2)C(=O)OCCN(C)C</chem>	N
Dimethylthiambutene	<chem>CN(C(C=C(c1cccs1)c1cccs1)C)C</chem>	N
Dioxaphetyl Butyrate	<chem>CCOC(=O)C(c1cccc1)(c1cccc1)CCN1CCOCC1</chem>	N
Diphenoxylate	<chem>CCOC(=O)C1(CCN(CC1)CCC(c1cccc1)(c1cccc1)C#N)c1cccc1</chem>	N
Diphenpipenol	<chem>COC1=CC=CC=C1N2CCN(CC2)C(CC3=CC(=CC=C3)O)C4=CC=CC=C4</chem>	N
Dipipanone	<chem>CCC(=O)C(CC(C)N1CCCCC1)(C2=CC=CC=C2)C3=CC=CC=C3</chem>	N
Eluxadoline	<chem>CC1=CC(=CC(=C1)CC(C(=O)N(CC2=CC(=C(C=C2)OC)C(=O)O)C(C)C3=NC=C(N3)C4=CC=CC=C4)N)C)C(=O)N</chem>	N
Embutramide	<chem>OCCCC(=O)NCC(c1cccc(c1)OC)(CC)CC</chem>	N
Ethoheptazine	<chem>CCOC(=O)C1(CCCN(CC1)C)c1cccc1</chem>	N
Ethylmethylthiambutene	<chem>CCN(C(C=C(c1cccs1)c1cccs1)C)C</chem>	N
Etoxidine	<chem>OCCOCCN1CCC(CC1)(C(=O)OCC)c1cccc1</chem>	N
Furethidine	<chem>CCOC(=O)C1(CCN(CC1)CCOCC1CCCO1)c1cccc1</chem>	N
Hydroxypethidine	<chem>CCOC(=O)C1(CCN(CC1)C)C2=CC(=CC=C2)O</chem>	N
Isomethadone	<chem>CCC(=O)C(C1=CC=CC=C1)(C2=CC=CC=C2)C(C)CN(C)C</chem>	Y
Isopropyl-U-47700	<chem>CC(C)N(C1CCCCC1N(C)C)C(=O)C2=CC(=C(C=C2)Cl)Cl</chem>	Y
Levacetylmethadol	<chem>CCC(C(CC(C)N(C)C)(C1=CC=CC=C1)C2=CC=CC=C2)OC(=O)C</chem>	N
Levomoramide	<chem>CC(CN1CCOCC1)C(C2=CC=CC=C2)(C3=CC=CC=C3)C(=O)N4CCCC4</chem>	N
Loperamide	<chem>CN(C)C(=O)C(CCN1CCC(CC1)(C2=CC=C(C=C2)Cl)O)(C3=CC=CC=C3)C4=CC=CC=C4</chem>	N
Meprodine	<chem>CCC1CN(CCC1(C2=CC=CC=C2)OC(=O)CC)C</chem>	N
Metethoheptazine	<chem>CCOC(=O)C1(CCCN(CC1)C)C2=CC=CC=C2</chem>	N
Methadone	<chem>CCC(=O)C(c1cccc1)(c1cccc1)CC(N(C)C)C</chem>	N

Metheptazine	<chem>COC(=O)C1(CCCN(C(C1)C)C)c1cccc1</chem>	N
Mt-45	<chem>C1CCC(CC1)N2CCN(CC2)C(CC3=CC=CC=C3)C4=CC=CC=C4</chem>	N
N-Benzylpethidine	<chem>CCOC(=O)C1(CCN(CC1)CC2=CC=CC=C2)C3=CC=CC=C3</chem>	N
N-Methyl U-47931e	<chem>CN(C)C1CCCCC1N(C)C(=O)C2=CC=C(C=C2)Br</chem>	N
Noracymethadol	<chem>CCC(C(CC(C)NC)(C1=CC=CC=C1)C2=CC=CC=C2)OC(=O)C</chem>	N
Normethadone	<chem>CCC(=O)C(CCN(C)C)(C1=CC=CC=C1)C2=CC=CC=C2</chem>	N
Norpiprane	<chem>CCC(=O)C(CCN1CCCCC1)(C2=CC=CC=C2)C3=CC=CC=C3</chem>	N
Nortilidine	<chem>CCOC(=O)C1(CCC=CC1NC)C2=CC=CC=C2</chem>	N
Nsi-189	<chem>CC(C)CCNC1=C(C=CC=N1)C(=O)N2CCN(CC2)CC3=CC=CC=C3</chem>	Y
Oxpheneridine	<chem>CCOC(=O)C1(CCN(CC1)CC(C2=CC=CC=C2)O)C3=CC=CC=C3</chem>	N
Pepap	<chem>CC(=O)OC1(CCN(CC1)CCC2=CC=CC=C2)C3=CC=CC=C3</chem>	N
Pethidine	<chem>CCOC(=O)C1(CCN(CC1)C)c1cccc1</chem>	N
Pethidinic Acid	<chem>CN1CCC(CC1)(C2=CC=CC=C2)C(=O)O</chem>	N
Phenadoxone	<chem>CCC(=O)C(C(C)N1CCOCC1)(C2=CC=CC=C2)C3=CC=CC=C3</chem>	N
Phenampromide	<chem>CCC(=O)N(C1=CC=CC=C1)C(C)CN2CCCCC2</chem>	N
Phenoperidine	<chem>CCOC(=O)C1(CCN(CC1)CCC(c1cccc1)O)c1cccc1</chem>	N
Piminodine	<chem>CCOC(=O)C1(CCN(CC1)CCCNC2=CC=CC=C2)C3=CC=CC=C3</chem>	N
Piritramide	<chem>C1CCN(CC1)C2(CCN(CC2)CCC(C#N)(C3=CC=CC=C3)C4=CC=CC=C4)C(=O)N</chem>	N
Proheptazine	<chem>CCC(=O)OC1(CCCN(CC1)C)C2=CC=CC=C2</chem>	N
Properidine	<chem>CC(C)OC(=O)C1(CCN(CC1)C)C2=CC=CC=C2</chem>	N
Propiram	<chem>CCC(=O)N(c1ccccc1)C(CN1CCCCC1)C</chem>	N
Racemoramide	<chem>CC(C(C(=O)N1CCCC1)(c1cccc1)c1cccc1)CN1CCOCC1</chem>	N
Tapentadol	<chem>CCC(C1=CC(=CC=C1)O)C(C)CN(C)C</chem>	N
Tilidine	<chem>CCOC(=O)[C@]1(CCC=C[C@@H]1N(C)C)c1cccc1</chem>	N
Tmcp-F	<chem>CC1(C(C1(C)C)C(=O)N(C)CCN(CC2)CCC3=CC=CC=C3)C4=CC=CC=C4)C</chem>	N
Tramadol	<chem>COc1cccc(c1)C1(O)CCCCC1CN(C)C</chem>	N
Trimeperidine	<chem>CCC(=O)OC1(CC(C)N(CC1)C)c1cccc1</chem>	N
U-47700	<chem>CN(C)C1CCCCC1N(C)C(=O)C2=CC(=C(C=C2)Cl)Cl</chem>	Y
U-48800	<chem>CN(C)C1CCCCC1N(C)C(=O)CC2=C(C=C(C=C2)Cl)Cl</chem>	Y
U-49900	<chem>CCN(CC)C1CCCCC1N(C)C(=O)C2=CC(=C(C=C2)Cl)Cl</chem>	Y
U-51754	<chem>CN(C)C1CCCCC1N(C)C(=O)CC2=CC(=C(C=C2)Cl)Cl</chem>	Y
W-15	<chem>Clc1ccc(cc1)S(=O)(=O)N=C1CCCCN1CCc1cccc1</chem>	Y
W-18	<chem>Clc1ccc(cc1)S(=O)(=O)N=C1CCCCN1CCc1ccc(cc1)N(=O)=O</chem>	Y

\*The comparison of the two databases has been carried out using the InChIKey string. The SMILES were obtained from PubMed.

Of the seven nitazene NSOs identified, four were found to be included in the UNODC databases, which however reported a higher number of molecules in this class with a total of nine molecules, hence five which were unique.

*Table 3.5 List of nitazenes like NSO identified by the NPSfinder® and comparison with the UNODC database\*.*

Mol	SMILES	UNODC (2022)
Butonitazene	<chem>O=[N+](O)c1cc2nc(Cc3ccc(OCCCC)cc3)n(CC[NH+](CC)CC)c2cc1</chem>	Y
Clonitazene	<chem>Clc1ccc(Cc2n(CCN(CC)CC)c3c(n2)cc([N+](=O)[O-])cc3)cc1</chem>	N
Etonitazene	<chem>O=[N+](O)c1cc2nc(Cc3ccc(OCC)cc3)n(CC[NH+](CC)CC)c2cc1</chem>	N
Flunitazene	<chem>Fc1ccc(Cc2n(CC[NH+](CC)CC)c3c(n2)cc([N+](=O)[O-])cc3)cc1</chem>	Y
Isotonitazene	<chem>O=[N+](O)c1cc2nc(Cc3ccc(OC(C)C)cc3)n(CC[NH+](CC)CC)c2cc1</chem>	Y
Metodesnitazene	<chem>O(C)c1ccc(Cc2n(CC[NH+](CC)CC)c3c(n2)cccc3)cc1</chem>	N
Etazene	<chem>O(CC)c1ccc(Cc2n(CC[NH+](CC)CC)c3c(n2)cccc3)cc1</chem>	Y

**\*The comparison of the two databases has been carried out using the InChKEY string. The SMILES were obtained from PubMed**

Of the 38 morphinan-like, only one was included in the UNODC database, i.e. the acetyldihydrocodeine. These entries were compared to the list of narcotic drugs scheduled under the 1961 Convention (UNODC, 2022c) and the 19 molecules which are not included in the latter are reported below.

**Table 3.6 List of morphinan like NSOs identified by the NPSfinder®**

Mol	SMILES
14-Hydroxymorphine	<chem>O[C@H]1[C@H]2Oc3c(O)ccc4c3C32C(O)([C@@H]([NH+](C)CC3)C4)C=C1</chem>
3-(0-Carboxymethyl)Morphine	<chem>O=C(Oc1c2O[C@@H]3[C@H](O)C=C[C@H]4[C@@H]5[NH+](C)CC[C@]34c2c(cc1)C5)C</chem>
3-Benzylmorphine	<chem>O[C@H]1[C@H]2OC=3C(O)(Cc4cccc4)CC=C4C=3C32[C@H]([C@@H]([NH+](C)CC3)C4)C=C1</chem>
3-Carboxymethyl Morphine	<chem>O=C([O-])COc1c2O[C@@H]3[C@H](O)C=C[C@H]4[C@@H]5[NH+](C)CCC34c2c(cc1)C5</chem>
3-MAM	<chem>O=C(Oc1c2O[C@@H]3[C@H](O)C=C[C@H]4[C@@H]5[NH+](C)CCC34c2c(cc1)C5)C</chem>
6-MDDM	<chem>Oc1c2O[C@H]3C(=C)CC[C@H]4[C@@H]5[NH+](C)CC[C@]34c2c(cc1)C5</chem>
6-MAM	<chem>O=C(O[C@@H]1[C@@H]2Oc3c(O)ccc4c3C32[C@@H]([C@H]([NH+](C)CC3)C4)C=C1)C</chem>
Nicodicodine	<chem>O=C(O[C@@H]1[C@@H]2Oc3c(OC)ccc4c3C32[C@H]([C@H]([NH+](C)CC3)C4)CC1)c1cncc1</chem>
Acetorphine	<chem>O=C(Oc1c2O[C@@H]3[C@]4(OC)[C@@H]([C@](O)(CCC)C)[C@@]5([C@@H]6[NH+](C)CC[C@]35c2c(cc1)C6)C=C4)C</chem>
Acetyldihydrocodeine	<chem>O=C(O[C@@H]1[C@@H]2Oc3c(OC)ccc4c3[C@@]32[C@H]([C@H]([NH+](C)CC3)C4)CC1)C</chem>
Buprenorphine	<chem>O(C)[C@]12[C@@H]([C@](O)(C(C)(C)C)C)C[C@@]3([C@@H]4[NH+](CC5CC5)CC[C@@]53[C@H]1O)c1c(O)ccc(c51)C4)CC2</chem>
Codeine-N-Oxide	<chem>O(C)c1c2O[C@@H]3[C@H](O)C=C[C@H]4[C@@H]5[N+](O)(C)CCC34c2c(cc1)C5</chem>
Cyprenorphine	<chem>O(C)[C@]12[C@@H](C(O)(C)C)C[C@@]3([C@@H]4[NH+](CC5CC5)CC[C@@]53[C@H]1O)c1c(O)ccc(c51)C4)C=C2</chem>
Isocodeine	<chem>O(C)c1c2O[C@@H]3[C@H](O)C=C[C@H]4[C@@H]5[NH+](C)CCC34c2c(cc1)C5</chem>
Levallorphan	<chem>Oc1cc2c(cc1)C[C@H]1[NH+](CC=C)CC[C@@]32[C@H]1CCCC3</chem>
Nalbuphine	<chem>O[C@@H]1[C@@H]2Oc3c(O)ccc4c3[C@@]32[C@](O)([C@H]([NH+](CC2CCC2)CC3)C4)CC1</chem>
Nalmefene	<chem>Oc1c2O[C@@H]3C(=C)CC[C@@]4(O)[C@@H]5[NH+](CC6CC6)CC[C@]34c2c(cc1)C5</chem>
Pentazocine	<chem>Oc1cc2[C@@]3(C)[C@@H](C)[C@H]([NH+](CC=C(C)C)CC3)Cc2cc1</chem>
Salvinorin B Methoxymethyl Ether	<chem>CC1CCC3C(=O)OC(CC3(C1C(=O)C(CC2C(=O)OC)OCOC)C)C4=COC=C4</chem>

### 3.4 The importance of the web in the NPS scenario

From the data presented above an unprecedented list of DBZDs and NSOs was generated by the activity of the *NPSfinder*<sup>®</sup> on the surface web. For these two NPS classes a total of more than 500 molecules with possible recreational/misuse potential (Corkery et al., 2018) was identified, predominantly across psychonauts' websites, chemical databases (i.e. isomerdesign.com), e-commerce platforms and users' forums. For these NPS only very limited information, if none at all, is available on their pharmacological/toxicological profile, so much so that sometimes when firstly discovered they are listed provisionally in the "others" class, as per UNODC database. This is true for both the molecules which were already listed in the international database, and for those identified unequivocally by the *NPSfinder*<sup>®</sup>.

The discrepancy between the numbers of various NPS classes found after the analysis of the *NPSfinder*<sup>®</sup> web activity and the number reported by official sources suggested that examining the online scenarios could be of great potential to assess the NPS phenomenon. Even if it is not possible to guarantee with 100% certainty that the NPS discussed online in fact exist and are being used, or the molecules sold are indeed those marketed on the ecommerce platforms (i.e. which molecule is actually in the final product) scanning and analysing the web can still be of help in predicting and assessing the real world NPS scenario (Corazza et al., 2013a; Schifano et al., 2015).

The significant differences between the *NPSfinder*<sup>®</sup> and the remaining databases can however be explained in considering that the online drug scenario is different from the reactive, event-based reporting of official databases (Schifano et al., 2003). Indeed, limitations and challenges encountered in the NPS identification (UNODC, 2013), e.g. including but not limited to appropriate analytical techniques, reference standards availability, lack of analytical libraries for novel substances, etc. (Ch 1.2.5), slow down the NPS identification process and reduce considerably the number of molecules actually detected and reported. These challenges are not encountered online, where information is very easily accessed and shared, in a fast and very often anonymous way. Aware of the limitations that surround the analytical NPS identification, one should not assume that the "real" drug market is described only by the substances that are officially reported and consider other sources to be used as supportive/integrative tools. The best resource could be the web, e.g. the virtual space/world where everything happens in the modern era, including drug-related activities (Corazza et al., 2013a).

The results presented here suggest a strong interest toward opioid and sedative drugs from that group of users identified as psychonauts (Sec. 1.2.8), interest which have been reported on previous studies both in social media and in dark net setting (Arillotta et al., 2020; Kim et al., 2017). This strong interest could be explained with the evolutionary role which has been reported in connection

to the *use of sedatives and hypnotics* with the main adaptive advantages represented by “an increased control of anxiety/fear, hence better coping strategies during life stressor events; an increased sexual disinhibition/availability for mating; and a better control of painful stimuli”(Catalani et al., 2021a; Orsolini et al., 2017b). Despite their strong interest towards CNS depressant NPS, psychonauts most favourable drugs seem to still be those with entheogenic/psychedelic properties (Móro et al., 2011; Orsolini et al., 2015b, 2015c). In fact if one compares the numbers identified here, with that from a parallel study conducted on psychedelics (Catalani et al., 2021c), it is noticeable how the number of hallucinogenic molecules identified raises above the thousand, much higher than that of NSOs and DBZDs. Indeed the psychonauts’ drug intake has been reported to shows high similarities with ancient shamanic ritual plant consumption (Orsolini et al., 2017b), i.e. psychedelics.

Another point of consideration related with the numbers of DBZDs and NSOs here reported is that very few data is available on the latter to assess the risk associated with their possible recreational use. Indeed, whilst some NPS possess pharmacological profiles similar to their ‘controlled’ pharmaceutical counterpart, i.e. prescription BZDs and opioids, the majority of current NSOs and DBZDs are not well-described. At present the majority of *in vitro* studies on DBZDs focuses on defining their metabolic pathways more than their biological activity (Huppertz et al., 2018; Moosmann et al., 2016; Wagmann et al., 2021), and *in vivo* studies are not available, mostly as clinical-pre clinical studies with NPS are considered unethical. The majority of information on their activity toxicity is stored online, with the users forums considered as “appreciable data source” (El Balkhi et al., 2020). The same applies to NSOs, for which the amount of information available on the activity/toxicity profile is higher but there is still lack of proper *in vitro/ in vivo* investigations.

The main risk associated with DBZDs and NSOs acute intoxications includes respiratory and central nervous system depression which could lead to death, symptoms more likely to occur when these substances are used in polydrug consumption (for more detail please refer to Sec 4.2.4 and 6.34)

If little knowledge is available for those NPS currently monitored by the international agencies, the situation is even worse for those molecules which, according to the online analysis have still to be “discovered”. On this basis, the findings highlighted by NPSfinder<sup>®</sup> can be considered a reason of concern, with the scientific world and health care institutions possibly facing complex behavioural and medical toxicity (Schifano et al., 2019a) without any ad hoc intervention and harm reduction strategies in place.

A final consideration to be made is that, while the number of substances listed between the two official databases provides a full overview of NPS historical data regarding the different NPS

appearance over the last 15 years or so, *NPSfinder*<sup>®</sup> reports a more dynamic, and possibly current, picture of their existence and diffusion. *NPSfinder*<sup>®</sup> ability to continuously scan the web and detect new psychedelics in ‘real time’ makes it more focused on the present time and can provided some levels of understanding about future trends (Corkery et al., 2017).

The following Chapter will present an overview of the DBZDs class, and the methodologies used to analyse this NPS class.



## Chapter 4 Designer benzodiazepines overview and methods

### 4.1 Chemical class overview

Benzodiazepines (BZDs) were introduced in the therapeutic world in the early 1960s as anxiolytics, sedative hypnotics, anticonvulsants, and muscle relaxants, and a safer alternative to barbiturates, but their abuse potential was recognised early on (EMCDDA, 2020c).

Indeed a high risk of misuse associated with BDZ was recognised, with could results in triggering of tolerance and dependence, and in severe and life-threatening withdrawal symptoms (Corkery et al., 2022; EMCDDA, 2021c). For these reasons, strict restrictions on medical prescription were put in place and 35 BZDs were placed under control by the UN Convention on Psychotropic Substances of 1971 (LSS/RAB/DPA/UNODC, 2016; UNODC, 2020d). The full list of scheduled BDZs is presented in Table 4.1.

The BDZ structure is usually represented by a (1,4)-diazepine core fused to a benzene ring, and a phenyl moiety is usually attached to this core (i.e, phenyl pendant). The most common variations of this structure are presented in Figure 4.1. BDZs express their mechanism of action as positive allosteric modulators of  $\gamma$ -aminobutyric acid receptor (GABA) -A receptor. BZDs can be classified according to their pharmacokinetic characteristics (duration of action, plasma half-life ( $t_{1/2}$ )) or according to their chemical structure. If classified by pharmacokinetic properties, they can be either short- (<24h) or long- (>24H) acting for the duration of action or ultra-short ( $t_{1/2}$ , <6 h), short ( $t_{1/2}$ , 6 h), intermediate( $t_{1/2}$  6-24 h), and long ( $t_{1/2}$  > 24 h) for the half-life (Greenblatt et al., 1983, 1981).

*Table 4.1 List of BDZ scheduled under the UN Convention on Psychotropic Substances of 1971*

<b>Name</b>	<b>Duration of action</b>	<b>Major trade name</b>
<b>Anxiolytics</b>		
Alprazolam	Short	Xanax®
Bromazepam	Long	Lexotan®
Camazepam		Albego®
Chlordiazepoxide	Long	Librium®
Clobazam	Long	Frisium®
Clonazepam	Intermediate	Rivotril®
Clorazepate	Long	Tranxene®
Clotiazepam	Short	Trecalmo®
Cloxazolam	Long	Sepazon®
Delorazepam	Long	En®
Diazepam	Long	Valium®
Ethyl loflazepate	Long	Meilax®
Fludiazepam	Short	Erispan®
Halazepam	Long	Pacinone®
Ketazolam	Long	Anseren®
Lorazepam	Short/Intermediate	Ativan®
Medazepam	Long	Nobrium®
Nordazepam	Long	Stilny®
Oxazepam	Short	Serax®
Oxazolam	Long	Tranquit®
Pinazepam	Long	Domar®
Prazepam	Long	Centrax®
Tetrazepam	Short	Clinoxan®
<b>Sedative/hypnotics</b>		
Brotizolam	Short	Lendormin®
Estazolam	Intermediate	Pro-Som®
Flunitrazepam	Short/Intermediate	Rohypnol®
Flurazepam	Long	Dalmane®
Haloxazolam	Long	Somelin®
Loprazolam	Intermediate	Dormonox®
Lormetazepam	Short	Noctamid®
Midazolam	Short	Versed®
Nimetazepam	Long	Erinin®
Nitrazepam	Intermediate	Mogadon®
Temazepam	Short	Normison®
Triazolam	Short	Halcion®

The classification by chemical structure considers the core structure. As previously reported, the most common structure encountered for BZD is 1,4-benzodiazepine, but 1,5-benzodiazepines and 2,3-benzodiazepines also exist. The addition of a heterocyclic structure to the 1,4-core results in triazolobenzodiazepine, imidazobenzodiazepine, and oxazolobenzodiazepine. Moreover, replacement of the benzene ring results in thienodiazepines and thienotriazolodiazepines Figure 4.1.

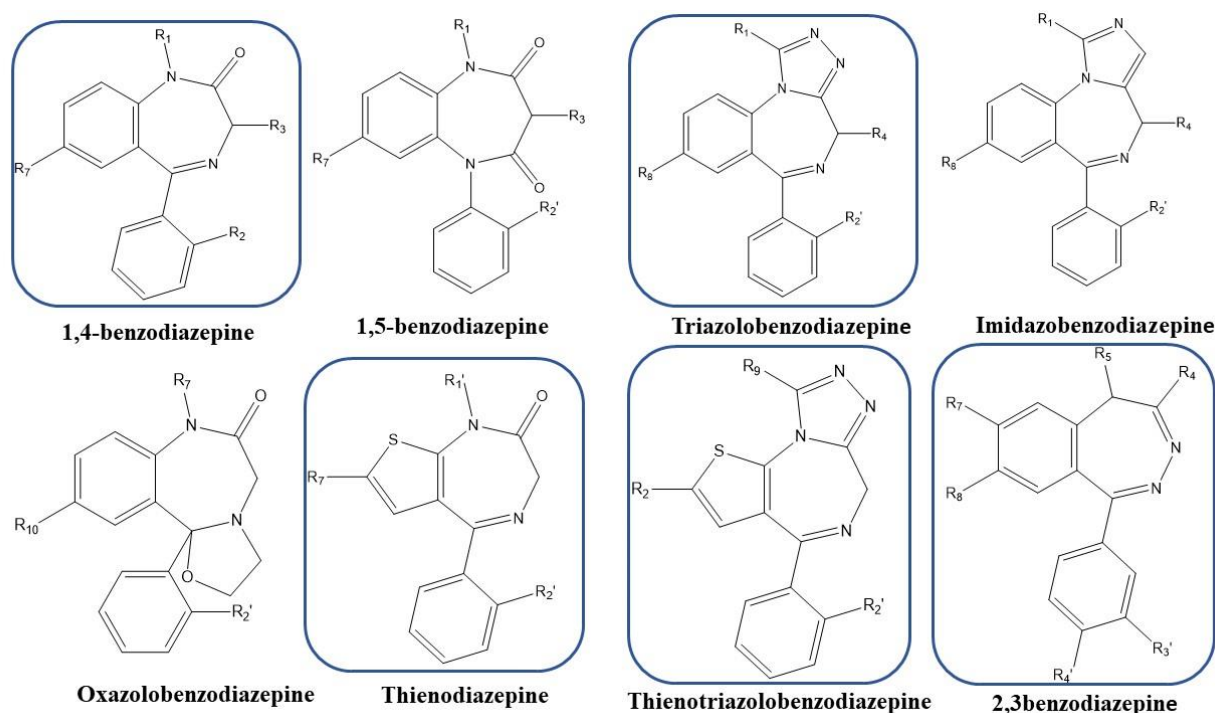


**Figure 4.1** Most common structure of benzodiazepines scaffolds

**Note.** The blue halos around the structures are used to identify the scaffold common to the DBZDs. The structures were designed with ChemDraw 20.1

Their activity as anxiolytics, sedative hypnotics, anticonvulsants, and muscle relaxants (with their low toxicity) made and still makes BDZs one of the most prescribed classes of drugs in the world (Drug Enforcement Administration, 2019).

BDZ are also used for other therapeutic purposes, including the treatment of alcohol withdrawal and drug-associated agitation, but due to the health concerns associated with long-period use, they are usually prescribed only for a short period of time (EMCDDA, 2021d). Parallel to their widespread medical use, BZDs represent the most used class of sedative for non-therapeutic purposes (EMCDDA, 2021d), as reported by 40 UN member states (UNODC, 2017a). Indeed, BDZs are often consumed in combination (poly-consumption, poly-use) with other psychoactive substances such as stimulants (usually to attenuate the “high” and enable re-dosing, or promote “come down” ),

opioids or alcohol (usually to prolong or enhance the “down” feeling) increasing exponentially the risk of non-fatal and fatal intoxication (EMCDDA, 2018b; Kataja et al., 2018; McAuley et al., 2022). The high demand for BZDs has attracted the interest of organised crime/criminals, with an increase on the market of diverted legitimate products, unlicensed, counterfeit ones, or new legal alternatives, i.e. DBZDs.

## **4.2 Designer benzodiazepines**

DBZDs are per definition NPS which contain a benzodiazepine or structurally similar (e.g. thienodiazepines) core, and are not controlled under the international drug control system (UNODC EWA, 2020). Generally, DBZDs seem to show the same pharmacological profile as the classical BDZs, acting as allosteric modulators at the GABA-AR (for detailed pharmacology see Section 4.2.3). Anxiolytic effects, muscle relaxation, sedation, anticonvulsant and sleep-inducing effects have indeed been reported (EMCDDA 2022b).

DBZDs are mainly produced in China as bulk powders, processed and sold either as legal replacements for commonly prescribed/therapeutic benzodiazepine or as legal alternatives (Corkery et al., 2022; EMCDDA-Europol, 2019; EMCDDA, 2022a). DBZDs are predominantly used for self-medication; sedative/hypnotic recreational use (often displaying higher potency than those of classical BDZs) (Orsolini et al., 2019); potentiation of other sedatives drugs, primarily opioids; promotion of ‘come down’ after stimulant use; or unintentionally, as counterfeits of prescription benzodiazepines (ACMD, 2020b). Low prices, ease of purchase (e.g., online vendors; without prescription), ease of use, and high availability can be considered as the main reasons for their popularity and continued emergence (EMCDDA, 2021b; Orsolini et al., 2020). In 2020, the UNODC reported an increase of benzodiazepine-like NPS in toxicological, post-mortem and driving under the influence medical reports. From data collected in 2019, DBZDs were found in the majority of these reports (UNODC, 2020e; UNODC EWA, 2020), often in a polydrug consumption scenario. DBZDs are strong CNS depressants and when used in combination with other drugs can cause serious toxicity with profound sedation, respiratory depression, coma, and death (Zawilska and Andrzejczak, 2015). The risks associated with their non-medical use is aggravated by the fact that for these DBZDs very few or no info at all on pharmacological and toxicological profile is available (UNODC, 2017a). This lack of pharmacological data represents a serious health threat, with unforeseeable risk especially in polydrug consumption scenarios or for high-risks opioid users (Policy, 2015). This phenomenon is even more worrisome if we consider that a big part of the DBZDs derive from molecules developed by the pharmaceutical industry but rejected as medications due to safety or efficacy issues (EMCDDA, 2022a).

#### 4.2.1 *Designer benzodiazepines phenomenon*

In the early 2000s the benzodiazepines identified on the drug market were usually diverted from both legal (false prescriptions, pharmacies) and illegal source (prescription BDZs from other countries) (Ibañez et al., 2013). However, after 2007 the first NPS benzodiazepines started to appear in seizures by customs and law enforcement agencies in Europe and USA (EMCDDA, 2022a). In particular phenazepam, and nimetazepam (2007) were the first to be identified on the Western Europe market as “legal highs” or counterfeit BDZs, followed by etizolam in 2011 (Maurer and Brandt, 2018). Since they were approved for medical use in some countries (i.e. Russia, Japan, Italy) (Ibañez et al., 2013) these molecules could not be classified as proper designer benzodiazepines (UNODC 2019d), the first of which, i.e. pyrazolam, was identified only years later in 2012 in Finland (EMCDDA-Europol, 2012). Pyrazolam was the first molecule of the benzodiazepines class, available on the market, not licensed in any part of the world nor under any national/international narcotic law (Maurer and Brandt, 2018).

Flubromazepam and diclazepam then followed by in 2013 (Łukasik-Głębocka et al., 2016; Moosmann and Auwärter, 2018) after a growing number of countries with high benzodiazepines misuse rates (e.g., Norway, and Finland) proceeded to scheduled phenazepam (2016) and etizolam (2019) (Moosmann and Auwärter, 2018; WHO, 2016, 2015).

Since their first emergence in 2012, an increasing number of different compounds were offered, for a total of 33 DBZDs reported in Europe as of December 2021 (EMCDDA, 2022a, 2022c), and a total of 40 reported by the UNODC (UNODC, 2022b). The numbers of DBZDs notified each year for the first time between 2007-2021 is reported in Figure 4.2. Despite the availability of more than 40 DBZDs reported, in the last couple of years the market has been dominated by just a handful of them, and in particular etizolam and flualprazolam (NPSdiscovery, 2022). This reflected on the latter accounting for almost 65 % of the total of DBZDs seizures in 2020 (i.e. 5% of the whole NPS seizures) (EMCDDA, 2021e; UNODC, 2021e).

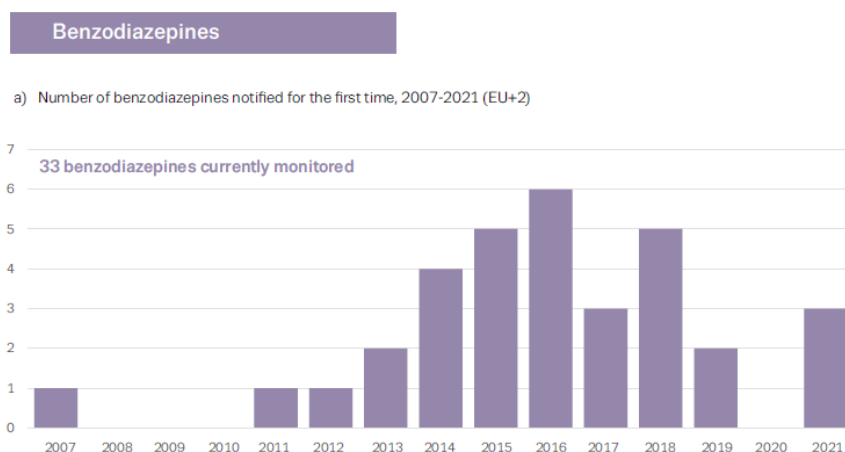


**Figure 4.2** Number of benzodiazepines identified each year for the first time between 2007 and 2021 (the image is reproduced with the consent of EMCDDA) (EMCDDA, 2022c)

Of the 40 plus DBZDs identified, only five are currently scheduled under the Single Convention on Narcotic Drugs of 1961: phenazepam (2016), flualprazolam, etizolam (2019), clonazolam and diclazepam (2021) (Commission on Narcotic Drugs, 2021; UNODC EWA, 2020).

Despite accounting for only a small percentage of the totality of NPS, DBZDs have been declared by the UNODC a serious threat to public health (UNODC, 2021b), being commonly mentioned worldwide (often with other drugs) in toxicological reports on drug-induced severe intoxications and deaths. In particular, in 2021 the UNODC identified them in 68% of the reported toxicological cases related to NPS (clinical admission, drug-facilitated sexual assault, driving under the influence (DUI)), and reported their presence in 49% of all instances of NPS within a fatality setting (CFSRE, 2022; Gevorkyan et al., 2021; UNODC, 2021e, 2021b). Several cases of acute poisoning and deaths related to DBZDs have been reported as well in northern Europe, especially in setting involving vulnerable groups and poly-drug consumption (Essink et al., 2022; Kriikku et al., 2020). In Scotland an upward trend of deaths attributable to the use of street benzodiazepines has been observed since 2015 (Scottish Government, 2022). In particular an increase from 58 fatalities (8.2%) of total drug related deaths (DRDs) to 879 in 2020 (66% of total DRDs) was reported (National Records of Scotland, 2021). All these data confirms how DBZDs should be considered as a -current primary threat for public health’ (UNODC, 2021b).

#### 4.2.2 Chemical and pharmaceutical form

At date, all DBZDs which have been identified on the market mostly belong to five of the aforementioned chemical scaffolds for the BDZs: 1,4-benzodiazepines, 2,3-benzodiazepines, thienodiazepines, thienotriazolodiazepines and triazolobenzodiazepines (Figure 4.1). However, other core structures have been observed: pyridotriazolodiazepine, a heterocyclic compound containing pyridine and triazole rings fused to a diazepine ring (zapizolam), 1,4-diazepinethione (thionordiazepam) and benzothiolodiazepine (Ali et al., 2011; Radinov et al., 1984) (Figure 4.3).

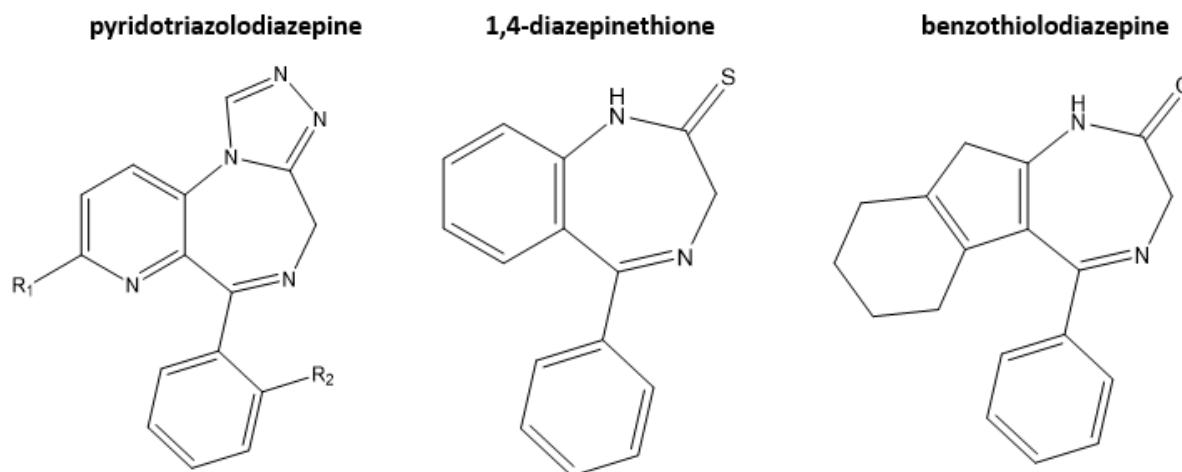


Figure 4.3 Other structure identified among DBZDs. The structures were designed with ChemDraw 20.1

Most DBZDs are described as white and odourless crystalline powders in their pure form and are usually sold as tablets, capsules or in blotter form (Figure 4.4).



Figure 4.4 Examples of designer benzodiazepines identified on the market.

The figure is reproduced with the permission of Moosman (2015), and is available at <http://www.munich2015.com/data/uploads/presentations/s4-01-bjoern-moosmann-nps-nov-2015.pdf> [Accessed 09 Dec 2019 (Moosmann and Auwärter, 2018)]



### 4.2.3 Pharmacological profile, the GABA system and receptors

BDZs express their mechanism of action as positive allosteric modulators of  $\gamma$ -aminobutyric acid (GABA)-A receptor (Griffin et al., 2013). BDZs have their own binding site in a specific pocket at the intersection of the  $\alpha$  and  $\gamma$  subunit, that differs from the GABA (endogen ligand) binding site (Kandasamy et al., 2021). They are defined as allosteric modulators because once bound to the receptor, they determine conformational changes of the latter that increase the affinity of GABA for its own agonist site without acting directly on the GABA pathway (Griffin et al., 2013). The increased affinity eases the GABA-A receptor activation which leads to hyperpolarisation, and inhibition of neurotransmission.

The GABA-A receptor is a ligand-gated ion channels built of five heteromeric protein subunits (5 glycoprotein). Despite the fact that 16 different GABA-A receptors and seven distinct subunit types have been identified ( $\alpha$  1–6,  $\beta$  1–3,  $\gamma$  1–3,  $\rho$ ,  $\delta$ ,  $\epsilon$  and  $\theta$ ), the majority comprise 2  $\alpha$ , 2  $\beta$  and 1  $\gamma$  subunit (Zhu et al., 2018) (Figure 4.5).

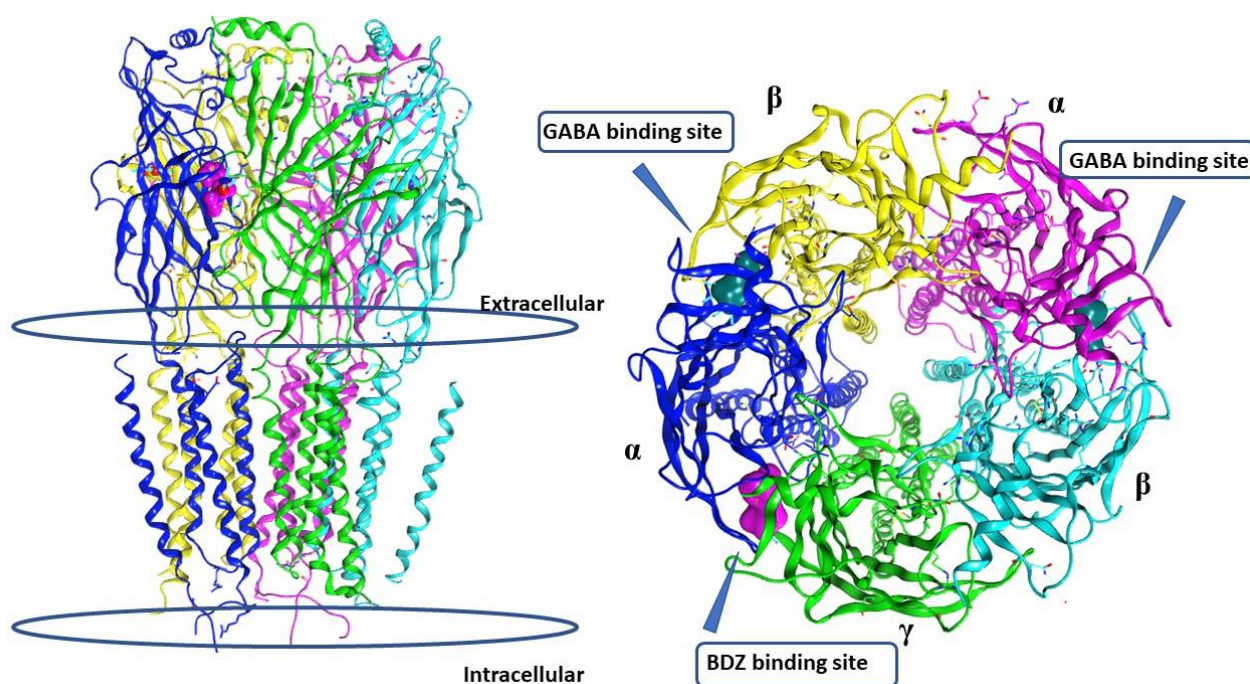


**Figure 4.5** 3D representation of the pentameric structure of the GABA-AR.

*On the left is presented the view of the receptor in the cell membrane; on the right is presented a view section from the top which helps identifying the five subunits and the binding site of the endogenous ligand GABA in dark green and the BDZ in purple. of the five subunits. The 3D images were created with MOE®, while the structure was taken from the PDB6HUP (RCSB PDB, 2018a)*

The  $\alpha$ ,  $\beta$  and  $\gamma$  subunits isoforms are responsible for the diverse affinity noted for BDZs; while receptors carrying the  $\gamma$ 2 subunit are more sensitive to BDZs, it is the  $\alpha$  subunits which influence the activity. Indeed to a different  $\alpha$  isoform correspond a different receptor activity:  $\alpha$ 1 receptors are



responsible for sedative, anterograde amnesic, anticonvulsant actions and addictive potential;  $\alpha 2$  for the anxiolytic effect and  $\alpha 2, 3, 5$  for myorelaxant actions (Rudolph et al., 1999; Tan et al., 2011). Of the various isoforms of the  $\alpha$  subunit, 1, 2, 3 and 5 are the ones that show higher affinity towards BDZs (Davies et al., 2002; Kelly et al., 2002). It should be noted that BDZs do not bind  $\alpha 4$  and  $\alpha 6$  (Davies et al., 2002).

Although information about receptor affinities and subtype specificity is widely available for BDZ, data on DBZDs are scarce, which make the prediction of their pharmacological effects a challenge. However, it has been observed that flumazenil is able to reverse the effects caused by DBZDs, suggesting how their action profile in humans is similar to the classical benzodiazepines (Bohnenberger and Liu, 2019).

#### 4.2.4 Toxicological profile

While data on the toxicological profile on DBZDs are scarce, similarities with the BDZ toxicity profile can be assumed. Despite BDZs being well known for their high therapeutic index, the use/abuse of the latter is associated with several side effects such as drowsiness, dizziness, fatigue, dysarthria, loss of coordination, headache and amnesia. Moreover, the prolonged use of BDZs (i.e. 4 to 6 weeks) has been proven, in clinical trials, to show strong addictive potential and induce tolerance and severe withdrawal symptoms. According to the UNODC and EMCDDA the emergence of DBZDs aggravated the side effects associated with their non-medical use, in particular when in co-consumption with opioids, by producing stronger sedation and amnesia, as well as increasing the risk of respiratory depression (Zawilska and Wojcieszak, 2019). Indeed, when these molecules are used in high doses and in combination with opioids or other CNS depressants the risk of death by respiratory suppression (i.e. suppression of medullary respiratory centers) exponentially increases (Horsfall and Sprague, 2017; Webster and Karan, 2020).

The risks associated with recreational use are strictly linked to their potency, which varies on a large scale, with the most potent ones (e.g. clonazepam and flubromazepam) requiring doses well below 1 mg to produce strong effects (a common dose of diazepam dosage varies from 2 to 10 mg). Their onset of action, which could vary according to the route of administration and the absorption rate (Brunetti et al., 2021), is also important for a risk assessment, with longer onset times increasing the chance of overdosing. Benzodiazepines overdose is characterised by extreme sedation, reduced reflexes, and altered mental status, and could induce respiratory depression resulting in coma and even death (Kang et al., 2022).

Due to the lack of in vitro and in vivo studies for the majority of DBZDs, usually data on side effects and toxicological profile is collected anecdotally via the analysis of trip report or users' forums online. Some examples of side effects are insomnia, delirium, and psychotic episodes for high doses of phenazepam; blackouts, sedation and short-term memory loss for flubromazepam; strong sedation and memory loss with severe respiratory failure, CNS depression and brain damage for flubromazepam (Orsolini et al., 2020).

The toxicity profile of each DBZDs could be further affected by the concomitant use of these substances with other drugs, resulting in several and unpredictable risks, particularly amongst high-risk opioid users (EMCDDA, 2018b).

#### 4.2.5 Structure Activity Relationship (SAR)

Previous studies conducted by Sternbach et al (1971) and Hester et al (1971,1979), identified some correlations between the structure of the 1,4-benzodiazepines and triazolobenzodiazepines and their activity on the GABA-AR (Figure 4.6.) (Hester et al., 1971; Hester and Von Voigtlander, 1979; Sternbach, 1971)

In particular, it was observed how:

- triazolobenzodiazepines are generally way more potent than their 1,4 counterparts (yellow box in Figure 4.6)
- at position N1 of 1,4-benzodiazepines, and respective C1 of the triazolobenzodiazepines, small substituents (CH<sub>3</sub>) increase the activity, while bulky ones (phenyl) decrease the activity (yellow box in Figure 4.6)
- at position C3 substituents generally decrease the potency (red box in Figure 4.6)
- at position C5 the phenyl appears to be the best option
- at position C6, C8 and C9 substituents lower the activity (red box in Figure 4.6)
- at position C7 the substitution has cardinal importance with electron-withdrawing substituent (e.g., halogen, CF<sub>3</sub>, or NO<sub>2</sub>) increasing the activity (green box in Figure 4.6)
- in the ortho position of the pendant phenyl, substitution with a halogen increases the activity (green box in Figure 4.6)
- at the para position of the pendant phenyl substituents exhibit strong steric repulsion at the GABAA receptor

## Structure Activity Relationship

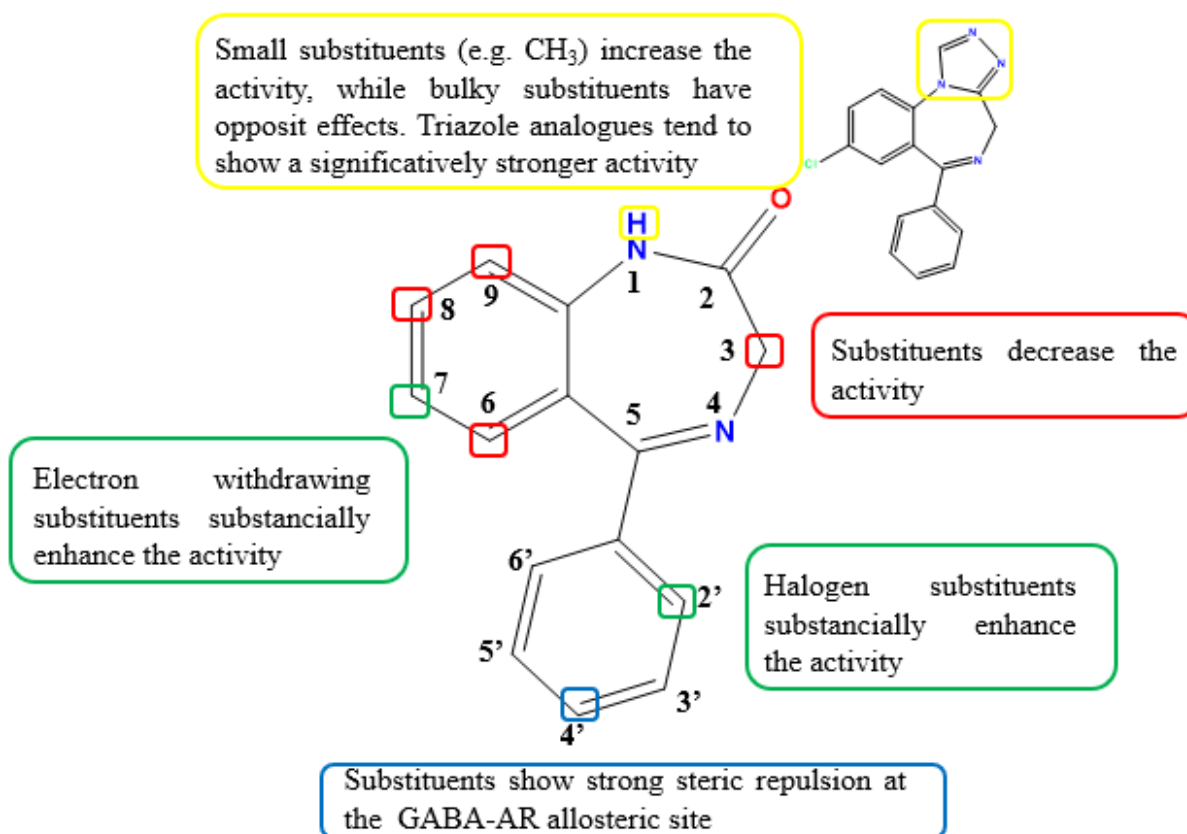


Figure 4.6 Structure activity relationship identified for benzodiazepines.

### 4.2.6 Designer benzodiazepines drug design

The production of DBZDs seems to follow four different strategies:

- identification of benzodiazepines reported in the scientific literature or patented, but never commercialised, or identification of appropriate substituents according to the known structure-activity relationships (SAR) in particular for the 1,4-benzodiazepine scaffold. Examples of these DBZDs are flubromazepam and some Ro compounds (e.g. Ro5-4864 and Ro7-4065) (Archer and Sternbach, 1968; Maurer and Brandt, 2018; Sternbach, 1971)
- identification of possible active metabolites, as seen per diazepam metabolites in the pharmaceutical sector. Examples of these DBZD include fonazepam, nimetazepam and 3-hydroxyphenazepam (Greenblatt et al., 1981).
- modifications of the first successful DBZPs. Examples include modification of the structure of etizolam with the synthesis of deschloroetizolam, and fluclozepam (Orsolini et al., 2020).

- identification of triazolo analogues of well-known 1,4-benzodiazepines. Examples include clonazolam, flubromazolam, flunitrazolam (Shafie et al., 2019).

### 4.3 In silico methods for designer benzodiazepines

#### 4.3.1 QSAR with MOE<sup>®</sup>

To create the dataset for this project, results from a previous study were considered (Hadjipavlou-Litina and Hansch, 1994; Waters et al., 2018). The information used was the logarithm of the reciprocal of concentration ( $\log 1/c$ ), where  $c$  is the molar inhibitory concentration ( $IC_{50}$ ), actually is the concentration of competing ligand which displaces 50% of the specific binding of the radioligand required to displace 50% of [3H]-diazepam from rat cerebral cortex. The  $\log 1/c$  data obtained from the literature (Hadjipavlou-Litina and Hansch, 1994) -were experimentally determined using spectrometric measurements of [3H]-diazepam displacement. The resulting data set included 77 1,4-benzodiazepines, triazolobenzodiazepines, imidazobenzodiazepines, and thienotriazolobenzodiazepines (Appendix A). The dataset did not include any benzodiazepine with a non-definitive binding value. A SMILES (Weininger, 1988) string was associated with each of the molecules included in the dataset, either obtained from PubChem or through ChemDraw 20.1.1. BZDs with provisional  $\log 1/c$  values or atypical atoms or substituents ( $T_c$  (Bajusz et al., 2015b)) were not taken into consideration.  $T_c$  values were calculated between all the molecules of the dataset, and average coefficients were used as a measure of similarity within the whole dataset.  $T_c$  are similarity coefficients, based on binary representation (Fernández-De Gortari et al., 2017) of a chemical structure, that can be calculated and used to measure how similar two molecules of a data set are. A binary representation is a machine-readable string built with binary vectors, where a 1 indicates the presence of a quality (i.e. chemical group or atoms) and a 0 indicates the absence. The  $T_c$  is expressed as a value from one to zero, where zero means no similarity and one mean complete similarity (same molecule). All the molecules that show a  $T_c$  equal or lower than 0.3 can be considered structure outliers. The  $T_c$  calculation use the following formula (Equation 4.1) and is usually software calculated, especially when large databases are compared.

**Equation 4.1 Tanimoto Coefficient Calculation.** *This equation represents mathematical formula used to calculate the  $T_c$ .*

$$T_c = N_{ab} / (N_a + N_b - N_{ab})$$

The  $N_a$  is the number of bits on a set in molecule A, the  $N_b$  the number of bits on a set in molecule B and  $N_{ab}$  the number of bits set on common to both molecules. This calculation was repeated for each pair of molecules. For the purpose of this study, in which 76 molecules needed to be compared, Open Bable 2.4.0. a software developed by SourceForce (California) (O'Boyle, 2012; O'Boyle et al., 2011; SourceForge, 2016) was used for the calculation. The average  $T_c$  cut off was set to 0.3, hence molecules showing values  $<0.3$  were re-moved from the latter as considered highly

dissimilar in structure. The dataset was subsequently divided into training and test sets taking into consideration the value of the similarity coefficient and the biological activity (Bajusz et al., 2015b; Bender and Glen, 2004; Godden et al., 2000).

The data set was split to obtain a ratio of roughly 80% in the training set and 20% in the test set (Leelananda and Lindert, 2016). The training set was used to build the mathematical model while the test set was used for its validation (external validation) (see section.....).

The SMILES strings and the  $\log_{10}1/c$  values were used to create a database in MOE<sup>®</sup> and then the SMILES strings were converted to molecule format. The conversion to molecule and their preparation with the Quick prep application was mandatory to be able to calculate the descriptors and build the QSAR models. QSAR models were built manually and automatically.

#### 4.3.2 MOE<sup>®</sup> Manual QSAR models

To build a manual QSAR model, the first step is to calculate the descriptors. In MOE<sup>®</sup> there are 435 descriptors available, belonging to four different 4 classes: **2D** (n= 206), which only use the atoms and connection information of the molecule; **i3D** (n= 138) which use the internal 3D coordinate information of the molecule; **x3D** (n=10) which use external 3D coordinate information but also require an absolute frame of reference (e.g. molecules docked into the same receptor); and **protein** (81) which use physicochemical protein properties. For lack of a reference frame and because working with small molecules and not proteins, only the 2D and i3D descriptors were calculated. The correlation to  $\log_{10}1/c$  was calculated and a number between zero (no correlation) and -1 (full negative correlation) or between zero (no correlation) and 1 (full positive correlation) was obtained. All descriptors that showed a value of less than -0.5 or more than 0.5 were brought further for evaluation and then ranked in descending order according to their absolute  $\rho$  values. The top ten descriptors were used in the initial building of the QSAR model using the Partial Least Squares method of the QuaSAR module in MOE<sup>®</sup> (Figure 4.7).

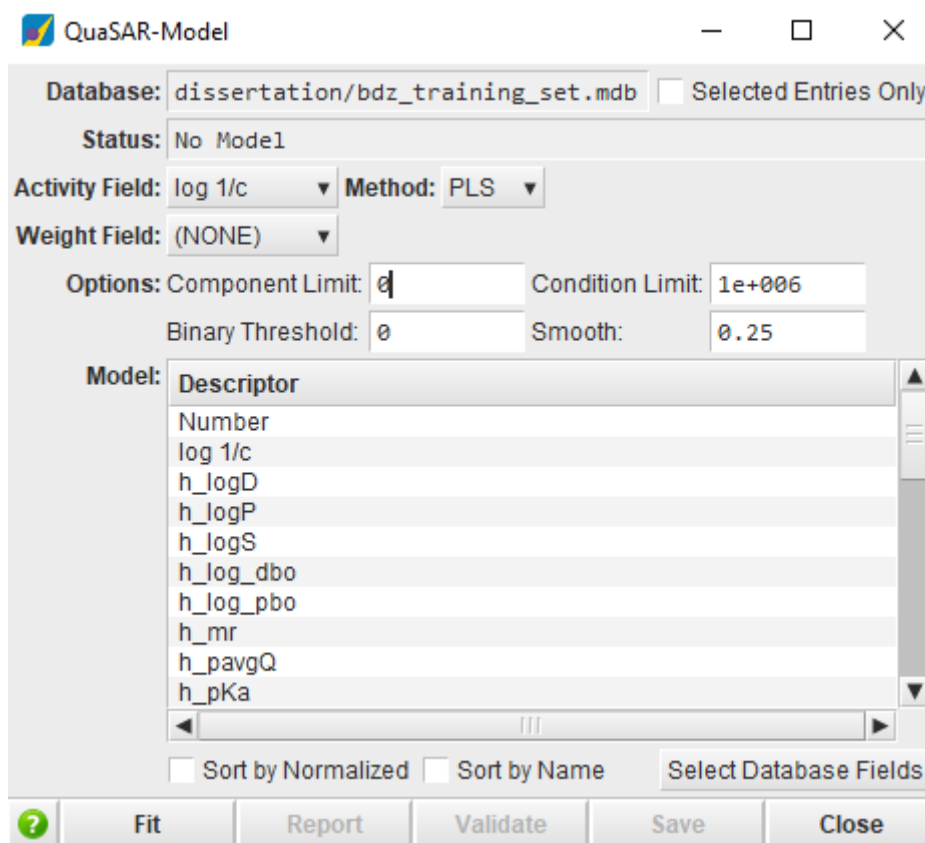


Figure 4.7 QuaSar model panel in MOE®.

*This panel enable the users to calculate a QSAR model while specifying the database object of the study, i.e. the list of molecules on which the model will be built; the activity field, i.e. the value used as biological activity, the method used to create the QSAR model (PLS) and the dercsitor which the users whats to include in the model.*

After that, a stepwise regression approach with repeated generations of the QSAR model was carried out until only 3 descriptors were left (minimum suggested number (Leelananda and Lindert, 2016)). All the calculated QSAR models were then submitted for cross validation with the QuaSAR Fit Validation application. For each QSAR models the correlation coefficient ( $r^2$ ), the RMSE value and  $xr^2$  (the cross validated  $r^2$ ) were generated. For data presentation homogeneity the value  $xr^2$  will be here identified with  $q^2$ . The closer  $r^2$  and  $q^2$  are to 1 the more predictive and robust the model.

The predictivity of the QSAR model was evaluated using the Evaluate function in MOE® which enables the calculation of predicted log 1/c values for the test set and the correlation Plot function that calculates the  $r^2$  for the test set.

#### 4.3.3 MOE® automatic QSAR models

The automatic QSAR models where generated using the partial least squares method of the AutoQSAR application in MOE®.



With this application the descriptors gets automatically calculated and refined after the software assesses their correlation to  $\log 1/c$ . To assess the latter, the QSAR-Contingency function, which is the MOE<sup>®</sup> statistical application designed for descriptors selection, was used. Descriptors which obtained a value  $< 0.5$ , i.e. did not correlate or were deemed non-contributory to were deleted. The limited cluster of descriptors chosen, was filtered to check for mutual collinearity (i.e., correlation values between two descriptors  $> 0.7$  resulted in rejected descriptors) and according to their relative importance towards  $\log 1/c$ . A stepwise regression approach with repeated QSAR model generations was carried out automatically by Auto QSAR, until an optimum model was generated. The suitability of the mathematical models was assessed by their respective values of  $r^2$ ,  $q^2$  (i.e., closest to 1 as possible) and the number of descriptors (i.e., roughly 1 for five entries in the training set) (Leelananda and Lindert, 2016; Tropsha, 2010). The final QSAR model was then validated using the test set, and then used to predict the  $\log 1/c$  values for the DBZDs identified online.

The same statistical parameters mentioned above were calculated: the correlation coefficient ( $r^2$ ) (goodness to fit) and the LOO correlation ( $q^2$ ) (robustness) for the training set (internal validation); and  $r^2$  for the test set (external validation).  $r^2$  defines the goodness-of-fit of the QSAR model, while  $q^2$  defines the goodness of prediction (Golbraikh and Tropsha, 2000). When  $r^2$  value  $> 0.6$  and  $q^2 > 0.5$  for the training set (Beebe et al., 1998) and a  $r^2 > 0.5$  for the test set (Golbraikh and Tropsha, 2002) the model can be considered acceptable. The stability of the latter is also assessed via the calculation of the root mean square errors (RMSEs) for the training and test sets (Beebe et al., 1998).

#### 4.3.4 QSAR with Forge™

The same dataset, or as referred to in Forge™ the ‘database molecules’, used in MOE® were used for the identification of the training and test set with Forge™. With this software, the identification is done automatically through a function called ‘partition of the Dataset’. The partition can be either random or activity stratified, i.e. depending on the log1/c. The user can choose the percentage of entries to allocate to each of the sets, starting from the default value of 20% for the test set.

To partition the data set into training and test set, the entries were loaded as a list of SMILES with corresponding log 1/c value indicated from a csv file. When loading the file into Forge™, the molecule role (training set) and the protonation state were specified by the user (Figure 4.8). Forge™ automatically convert all molecules to 3D. All the molecules were uploaded as training set and further divided into training and test set.

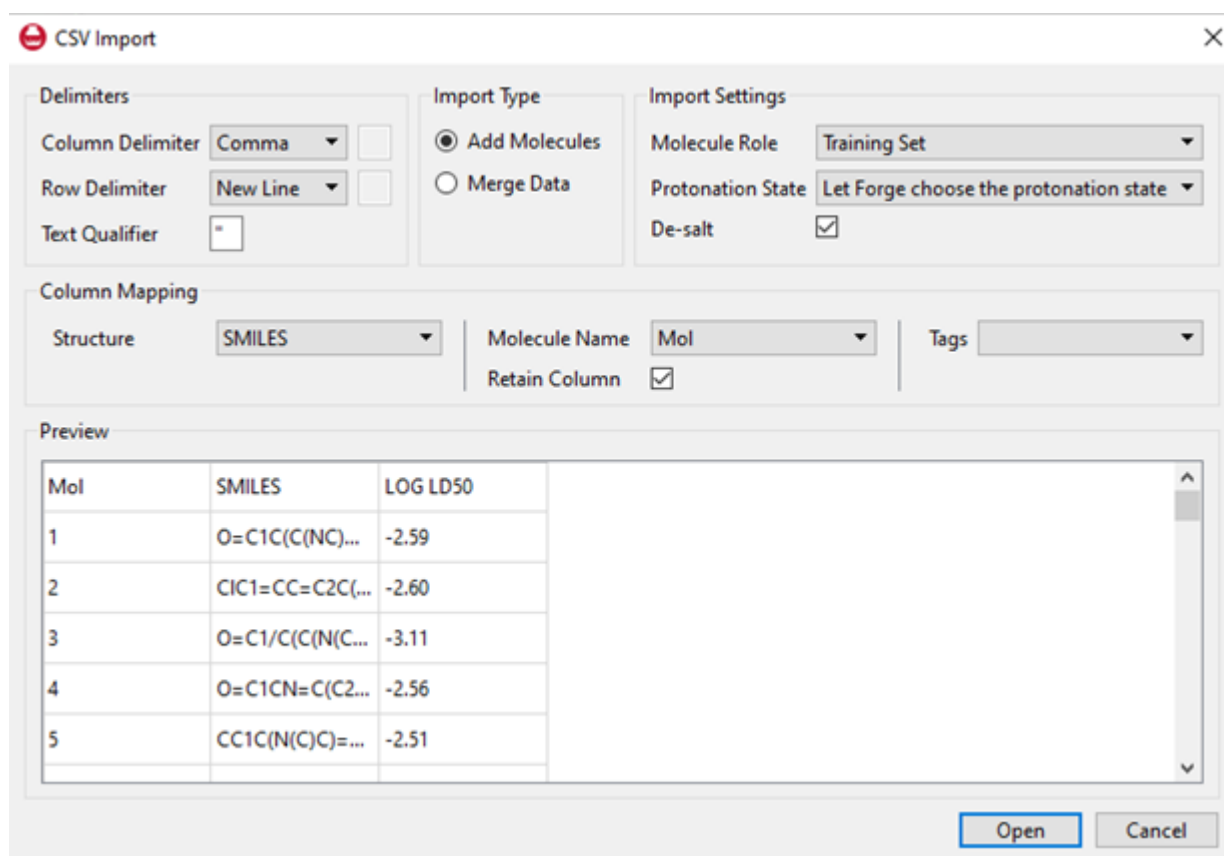


Figure 4.8 Dataset upload panel in Forge™

#### 4.3.5 *Forge™ Ligand specification and alignment*

Once the molecules are loaded, to generate a 3D QSAR model they need to be aligned to one or more reference molecule (i.e. ligands). Although using a single molecule is ok, using two or three pre aligned structures is usually recommended. In this way, a wider diversity of chemical features in the molecules that need to be aligned can be described, i.e. considered.

In *Forge™*, the alignment can be performed in two ways: normal (or protein centric view) or substructure based (or ligand centric view). For both methods, an initial alignment is generated and then further refined. Once the alignment is completed a list of alignment for each molecule is returned, and the most energy favourable one automatically displayed by the software (Figure 4.9). The user can browse through all the alignments generated and change that one which is displayed. Each alignment is returned with a similarity score (Sim) value that assesses the quality of the alignment itself (1 is 100% alignment). The alignment step is mandatory, and the 3D QSAR modelling is very sensitive to alignment noise and misalignment. Because this step is fully automatised by *Forge™*, a further visual inspection is recommended, and manual intervention can be used to improve the quality of the alignment itself.

Suitable reference molecules are highly active molecules, in their active 3D conformations when possible. These need to be chosen and loaded by the user as reference compounds. The ligands can be extrapolated from the 3D receptor structures available in the PDB database and saved as separate entities. In this way, one can be sure that the 3D conformations obtained are the active conformations.



**Figure 4.9** Example of an alignment made by Forge™.

On the right, the list of the possible 3D conformations automatically identified, and, on the left, the 3D structure of the one chosen by Forge™. The query molecule (oxazepam) is in green, while the two reference ligands (alprazolam and diazepam) are in light pink. The drop-down menu on the right identifies all the different possible alignments (in this case 10) of the oxazepam on the reference molecules.

#### 4.3.6 Forge™ descriptors' selections

Forge™ uses descriptors based on electrostatic molecular fields and steric properties to characterize each molecule and build the 3D-QSAR models. These descriptors are generated automatically from the alignments. Hence, no process of Descriptor selection is carried out by the user, and everything is done automatically by the software.

Molecular recognition occurs *via* electronic and surface properties: electrostatic and van der Waals forces.

When undertaking molecule design, it is therefore desirable to have a set of molecular descriptors that encode the aspects of a molecule which define its binding interactions. Such a set of descriptors would encode the surface, shape, electrostatic, and van der Waals properties of a molecule rather than its chemical connectivity. In other words, the descriptors would encode the molecular **fields** on and around the surface of the molecule, rather than a set of atoms and bonds.

#### 4.3.7 Forge™ QSAR models

Forge™ calculates the electrostatic and shape properties of each of the training-set molecules aligned to the reference ligands. From these properties, the software can identify sampling points which are used to investigate steric and electrostatic potential. All these sampling points (field points) are used to get an invariant set, which reduced the number of descriptors that must be considered. Electrostatic and steric properties were calculated using a distance of 1 Å between the

sample points. This ensures that all areas around the compounds that could contribute to the activity are effectively described.

The values obtained by these properties were automatically combined using Partial Least Squares (PLS) regression employing the SIMPLS algorithm which enables the use of as many descriptors as possible.. Differently to MOE<sup>®</sup>, Forge<sup>™</sup> does not display the mathematical algorithm of the chosen model, but a 3D representation through steric and electrostatic field points. The Field QSAR was chosen as the calculation method into the “Build Model” section of Forge<sup>™</sup> Processing (Figure 4.10) alongside other regression methods identified as “ machine learning models”. In Forge<sup>™</sup> there are four types of Machine Learning models: k-Nearest Neighbors (kNN), Random Forest, Support Vector Machines (SVM), and Relevance Vector Machines (RVM). Machine learning methods can be used to develop QSAR models by the electrostatic and shape properties of aligned molecules. Both regression and machine learning methods are really good when real values biological activity data (for example, pIC50, pKi) are available and the aim is to calculate a function that which can be used to predict further activity values.

The screenshot displays the 'Forge Processing' software interface, specifically the 'Build Model' tab. The 'Calculation Method' is set to 'Field QSAR'. The 'Activity' is set to 'log 1/C'. The 'Field QSAR model' section includes the following parameters: 'Maximum number of components' is 20, 'Sample point minimum distance' is 1.0 Å, and 'Number of Y scrambles' is 50. Under 'Fields to use', both 'Electrostatic' and 'Volume' are checked. The 'Weight molecules by similarity' option is unchecked, and the 'Weight ramp type' is set to 'Linear'. The 'Minimum similarity' is 0.00 and the 'Maximum similarity' is 1.00. The 'Cross-validation' section shows 'Cross-validation type' as 'Leave-one-out', 'Training set to use as validation data' as 20%, and 'Repeats' as 1000.

**Figure 4.10.** Parameters adopted for the Field QSAR calculation method in Forge<sup>™</sup>.

#### 4.3.8 Molecular Docking

##### Identification of the 3D protein structures


Molecular docking (MD) studies were used to evaluate the binding affinity between the DBZDs identified by the NPSfinder<sup>®</sup> and the 3D crystal structure of the GABA-AR identified in the PDB.

The analysis of the Protein Data Bank database to retrieve the best 3D structures for the docking included the use of several key words as ‘GABA-AR, benzodiazepine receptor, GABA receptor, diazepam, benzodiazepines’, etc. Only the structures of human receptors were considered. From the keywords search four structures of interest were identified:

- PDB6HUP – “CryoEM structure of human full-length alpha1beta3gamma2L GABA(A)R in complex with diazepam (Valium), GABA and megabody Mb38” (RCSB PDB, 2018a)
- PDB6HUO - “CryoEM structure of human full-length heteromeric alpha1beta3gamma2L GABA(A)R in complex with alprazolam (Xanax), GABA and megabody Mb38” (RCSB PDB, 2018b)
- PDB6D6U – “Human GABA-A receptor alpha1-beta2-gamma2 subtype in complex with GABA and flumazenil” (RCSB PDB, 2018c)
- PDB6X3X – “Human GABAA receptor alpha1-beta2-gamma2 subtype in complex with GABA plus diazepam” (RCSB PDB, 2020)

Of these, PDB6HUP, PDB6HUO and PDB6X3X were used for the docking studies, while the structure of the GABA-AR crystallised with flumazenil was left out as the latter is a competitive antagonist on the GABA-AR (Sigel et al., 1998). It is important to note that scientific literature report how agonist and antagonist ligands, when bound to their target, could cause a different rearrangement in the structure of the binding pocket and the whole receptor (An et al., 2019; Ng et al., 2014; Jianliang Zhang et al., 2009). Hence, to obtain more reliable results, it is advisable to use the 3D structure which is bound to the most similar molecule to those under evaluation (i.e. DBDZs), both structure and activity wise (Leelananda and Lindert, 2016).

The protein structures identified in the PDB database are crystallised structures of the  $\alpha 1\beta 2\gamma 2$  and  $\alpha 1\beta 3\gamma 2$  human GABA-AR in complex with a benzodiazepine in its biologically active conformation respectively, alprazolam (high potency and short-acting BDZ) and diazepam (low potency and long-acting). Despite PDB6X3X ( $\alpha 1\beta 2\gamma 2$ ) showing a better resolution than PDB HUP, i.e. 2.9 vs 3.6 Å, both were taken into consideration because displaying slightly different interaction patterns between diazepam and the binding pocket. Some characteristics, e.g., methods, organism, and macromolecule, of the PDB structures used, are reported in Figure 4.11 (please note the characteristics of 6HUP and 6HUO are the same).



[3D View](#)

### 6HUO

[Download File](#) [View File](#)

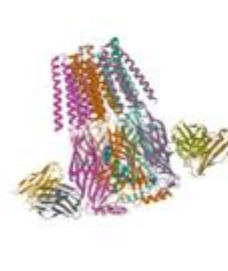
**CryoEM structure of human full-length heteromeric alpha1beta3gamma2L GABA(A)R in complex with alprazolam (Xanax), GABA and megabody Mb38.**

Masiulis, S., Desai, R., Uchanski, T., Sema Martin, I., Lavery, D., Karia, D., Malinauskas, T., Jasenko, Z., Pardon, E., Kotecha, A., Steyaert, J., Miller, K.W., Ancescu, A.R.

(2019) Nature 565: 454-459

<b>Released</b>	2019-01-02
<b>Method</b>	ELECTRON MICROSCOPY 3.26 Å
<b>Organisms</b>	Bos taurus Homo sapiens Lama glama
<b>Macromolecule</b>	Gamma-aminobutyric acid receptor subunit alpha-1, Gamma-aminobutyric acid receptor subunit alpha-1 (protein) Gamma-aminobutyric acid receptor subunit beta-3 (protein) Gamma-aminobutyric acid receptor subunit gamma-2 (protein)



[3D View](#)

### 6X3X

[Download File](#) [View File](#)

**Human GABAA receptor alpha1-beta2-gamma2 subtype in complex with GABA plus diazepam**

Kim, J.J., Gharpure, A., Teng, J., Zhuang, Y., Howard, R.J., Zhu, S., Novello, C.M., Walsh, R.M., Lindahl, E., Hibbs, R.E.

(2020) Nature 585: 303-308

<b>Released</b>	2020-09-09
<b>Method</b>	ELECTRON MICROSCOPY 2.92 Å
<b>Organisms</b>	Homo sapiens Mus musculus
<b>Macromolecule</b>	Gamma-aminobutyric acid receptor subunit alpha-1 (protein) Gamma-aminobutyric acid receptor subunit beta-2 (protein) Gamma-aminobutyric acid receptor subunit gamma-2 (protein) IgG2b Fab Heavy Chain (protein) Kappa Fab Light Chain (protein)

**Figure 4.11 Screenshot of the 6HUO and X3X receptor from RCSB Protein Databank.**

**Notes.** On the right side the resolution, method of crystallisation, source organism, the isoform of the receptor and the ligands complexed in the 3D crystal structure are indicated.

#### *Preparation of the PDB structures*

The PDB files were loaded into MOE<sup>®</sup> via the Load PDB File application and then prepared with the Quick Prep application (Figure 2.2). As reported in the method section (Sec. 2.3.2), Quick Prep corrected structural issues (e.g. missing atoms, chain break, protein chain C- or N-termini which need to be charged or capped) with Structure Preparation; protonated the structure (e.g. number of hydrogens, multiple rotamer and protomer states) with Protonate 3D; deleted the "unbound" water molecules; set tethers of different strengths on the receptor, ligand and solvent atoms; fixed atoms beyond 8Å from the active site and minimized the structure with the Amber10:EHT forcefield. The structures were then ready to be used as input in molecular docking.

### *Definition of the binding pocket and ligand interaction*

The co-crystallised ligands available in PDB6HUP, 6HUO and 6X3X were used to define the binding pocket/cavity and superposition target for docking calculations. All the residues included in a radius of 4.5 Å from the ligand were included in the binding pocket. Additionally, the Site finder application was used to define the characteristic of the whole pocket for each receptor (Table 4.2). The three binding pockets are, as expected, almost identical (Table 4.2).

**Table 4.2 Description of the three binding pockets identified for 6HUO and 6HUP\*.**

Receptor	Site	Size	PLB	Hyd	Side	Residues
6HUO	11	93	0.99	37	66	3:(ASP56 MET57 TYR58 ASN60 PHE77 PHE78 ALA79 MET130 ARG132 THR142 GLU189)4:(PHE100 HIS102 SER159 TYR160 VAL203 GLN204 SER205 SER206 THR207 TYR210)
6HUP	20	100	0.44	34	59	3:(ASP56 MET57 TYR58 PHE77 ALA79 MET130 THR142 GLU189)4:(PHE100 HIS102 GLY158 SER159 TYR160 VAL203 GLN204 SER205 SER206 THR207 TYR210 VAL211 VAL212)
6X3X	12	141	1.21	41	82	4:(PHE100 HIS102 ASN103 GLU138 PRO140 PRO154 LYS156 SER159 TYR160 ALA161 VAL203 GLN204 SER205 SER206 THR207 TYR210)5:(ASP56 MET57 TYR58 ASN60 SER61 PHE77 ALA79 MET130 THR142 SER186 GLU189 ASP192 SER195)

**\*The size column indicates the number of alpha spheres comprising the site; the PLB column indicates the Propensity for Ligand Binding score for the contact residues in the receptor; the Hyd column indicates the number of hydrophobic contact atoms, and the Side column indicates the number of sidechain contact atoms. The Residues column indicates the residues in the binding pocket in the format chain:residue-name.**

For each receptor, the 3D structure and the information contained in the scientific reference was used to explore ligands-protein interactions and identify the most important residues for the allosteric activation of the GABA-AR. The binding pockets, as visualised in MOE<sup>®</sup>, for 6HUP and 6X3X (diazepam) and 6HUO (alprazolam) are presented in Figure 4.12, 4.13 and 4.14 respectively. Similar interaction of the diazepam into the binding pocket are identified for 6X3X.



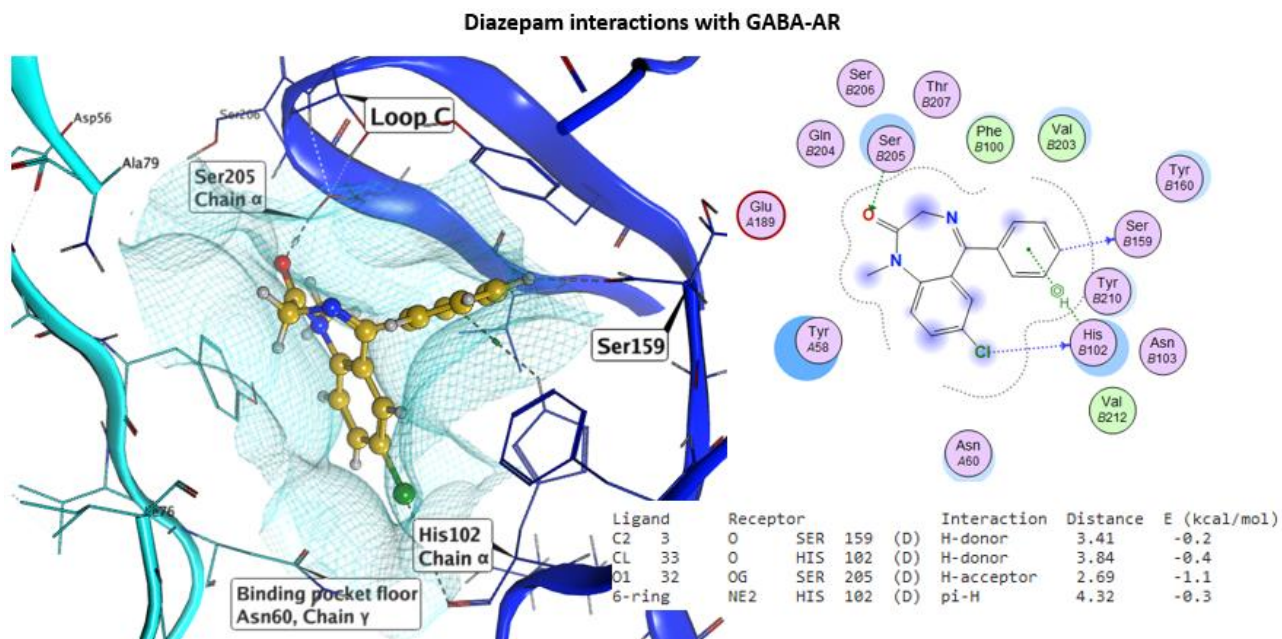


Figure 4.12 6HUP binding pocket 3D and 2D representations.

Notes: on the 3D left, the binding pocket representation with the co-crystallised ligand diazepam (yellow). The light blue portion represents the  $\gamma$  subunit of the receptor whilst the dark blue the  $\alpha$  subunit. The VDW interaction surface (transparent light grey) was added to increase visibility of the shape and size of the binding pocket. On the right, the 2D representation of the binding pocket and interactions between receptor residues and ligand are provided. Below, a report of the type of interactions, receptor residues and alprazolam atoms involved, and relative distance and energy parameter (kcal/mol) are outlined. Note that the letter (D) identifies the  $\alpha$  chain. The colours used to depict the residues in the 2D screenshot define different characteristics of the latter: light purple for polar residues and light green for hydrophobic ones; red circle indicates an acidic and blue a basic residue; and the light blue halo indicates solvent exposure both on the receptor and the ligand

### Diazepam interactions with GABA-AR (6X3X)

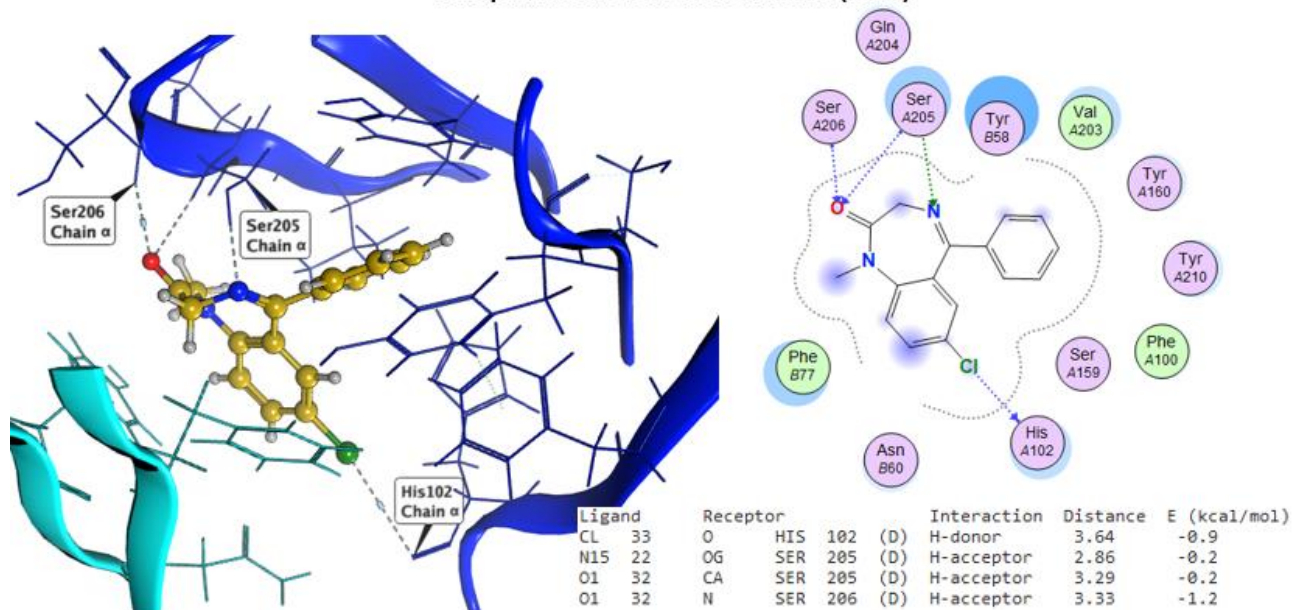


Figure 4.13 6X3X binding pocket 3D and 2D representations.

Notes: on the 3D left, the binding pocket representation with the co-crystallised ligand diazepam (yellow). The light blue portion represents the  $\gamma$  subunit of the receptor whilst the dark blue the  $\alpha$  subunit. The VDW interaction surface (transparent light grey) was added to increase visibility of the shape and size of the binding pocket. On the right, the 2D representation of the binding pocket and interactions between receptor residues and ligand are provided. Below, a report of the type of interactions, receptor residues and alprazolam atoms involved, and relative distance and energy parameter (kcal/mol) are outlined. Note that the letter (D) identifies the  $\alpha$  chain. The colours used to depict the residues in the 2D screenshot define different characteristics of the latter: light purple for polar residues and light green for hydrophobic ones; red circle indicates an acidic and blue a basic residue; and the light blue halo indicates solvent exposure both on the receptor and the ligand

### Alprazolam interactions with GABA-AR

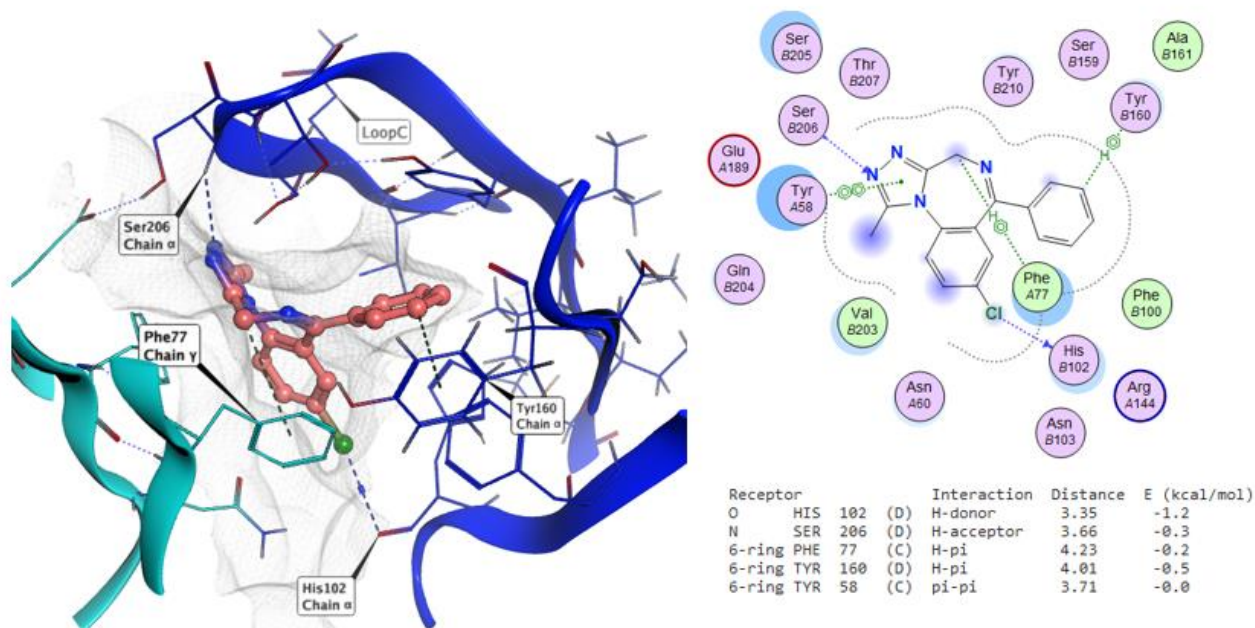


Figure 4.14 6HUO binding pocket 3D and 2D representations.

Notes: on the 3D left, the binding pocket representation with the co-crystallised ligand alprazolam (pink). The light blue portion represents the  $\gamma$  subunit of the receptor whilst the dark blue the  $\alpha$  subunit. The VDW interaction surface (transparent light grey) was added to increase visibility of the shape and size of the binding pocket. On the right, the 2D representation of the binding pocket and interactions between receptor residues and ligand are provided. Below, a report of the type of interactions, receptor residues and alprazolam atoms involved, and relative distance and energy parameter (kcal/mol) are outlined. Note that the letter (D) identifies the  $\alpha$  chain and the letter (C) the  $\gamma$  chain. The colours used to depict the residues in the 2D screenshot define different characteristics of the latter: light purple for polar residues and light green for hydrophobic ones; red circle indicates an acidic and blue a basic residue; and the light blue halo indicates solvent exposure both on the receptor and the ligand.

The scientific literature reports the fundamental role and importance of the  $\alpha$ 1His102 residue ( $\alpha$  chain) for the binding of classical BDZs at the allosteric site of GABA-AR. Indeed, the two chlorine atoms at the C8 and C7 positions in ALP and DZP (Figure 4.12 -Figure 4.14), are reported to interact as a hydrogen bond donor (i.e. through a hydrogen bond) with the  $\alpha$ 1His102 side chain. The importance of this bond has been confirmed over the years by cross-linking studies, which saw the loss of activity when the His residue was substituted with a Cys residue; and by the fact that BDZs do not bind to the GABA-AR showing the  $\alpha$ 4 and  $\alpha$ 6 subunits, in which the His position is occupied by Arg residues (Wieland et al., 1992). The Arg larger side chain indeed seem to sterically clash with ALP and DZP preventing the binding (Rudolph et al., 1999). Other important interactions have been reported to be the hydrogen bond with Ser205 or Ser206 ( $\alpha$  chain), mediated by the oxygen atom (C=O) of diazepam (Figure 4.12) and the nitrogen atom of the triazolo moiety of the alprazolam (Figure 4.14) (Masiulis et al., 2019; Sigel and Ernst, 2018). Other interactions include

arene-arene interactions with Tyr58 ( $\gamma$  chain), the hydrogen-arene interaction with Phe77 ( $\gamma$  chain) and Tyr160 ( $\alpha$  chain) and the hydrogen bond with Ser159 ( $\alpha$  chain).

#### *Ligands reference dataset*

A reference data set for the docking studies was prepared with the aim of including the two co-crystallised ligands (DZP and ALP) and some of the classical BDZs, which are well known in literature as a highly potent agonist for the GABA-AR (both short- and long lasting) (Chouinard, 2004). A total of six molecules were identified.

**Table 4.3 Reference dataset composition**

<b>Low-potency and long-acting benzodiazepines</b> (weak with a prolonged effect):	
Diazepam (Valium)	<chem>CN1C(=O)CN=C(C2=C1C=CC(=C2)Cl)C3=CC=CC=C3</chem>
<b>High-potency and short-acting benzodiazepines</b> (strong with short effects):	
Triazolam (Halcion)	<chem>CC1=NN=C2N1C3=C(C=C(C=C3)Cl)C(=NC2)C4=CC=CC=C4Cl</chem>
Alprazolam (Xanax)	<chem>CC1=NN=C2N1C3=C(C=C(C=C3)Cl)C(=NC2)C4=CC=CC=C4</chem>
Lorazepam (Ativan)	<chem>C1=CC=C(C(=C1)C2=NC(C(=O)NC3=C2C=C(C=C3)Cl)O)Cl</chem>
<b>High-potency and long-acting benzodiazepines</b> (strongest benzos):	
Clonazepam (Klonopin)	<chem>C1C(=O)NC2=C(C=C(C=C2)[N+](=O)[O-])C(=N1)C3=CC=CC=C3Cl</chem>
Flunitrazepam (Rohypnol)	<chem>CN1C(=O)CN=C(C2=C1C=CC(=C2)[N+](=O)[O-])C3=CC=CC=C3F</chem>

#### *Molecular Docking approaches*

The molecules in Table 4.3 were docked along with the molecule identified by NPSfinder<sup>®</sup> (Table 3.2), using the general docking panel in MOE<sup>®</sup>. It is important to underscore that, when available, information on the active placement (i.e. presence of the co-crystallised ligand) and fundamental interactions should be taken into high consideration to proceed to a more informed docking study. To include information available on the fundamental interactions, a pharmacophore query can be defined. The latter can then be added to guide the placement of the DBZDs in the analysis in addition to the superposition points represented by the co-crystallised alprazolam and diazepam (Figure 2.4). The pharmacophore queries for alprazolam and diazepam were generated with the Pharmacophore Query Panel (Sec. 4.3.9) and are reported in Figure 4.15 and Figure 4.16.



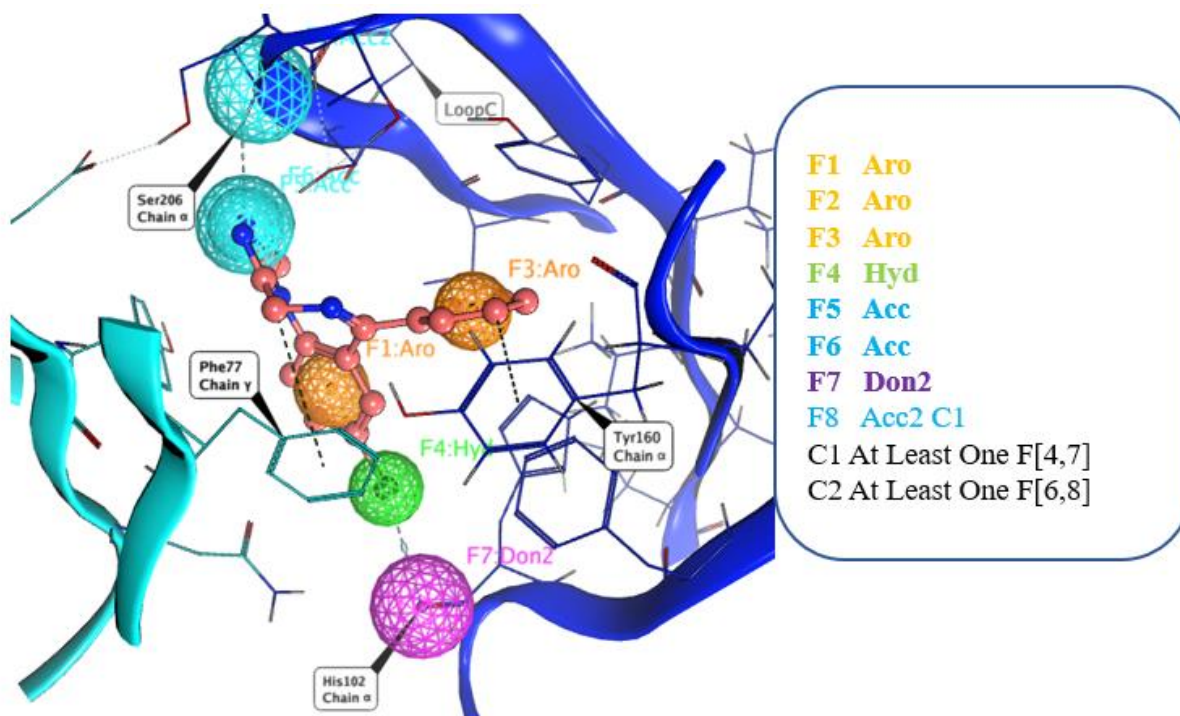


Figure 4.15 Pharmacophore query used for the docking placement with 6HUO

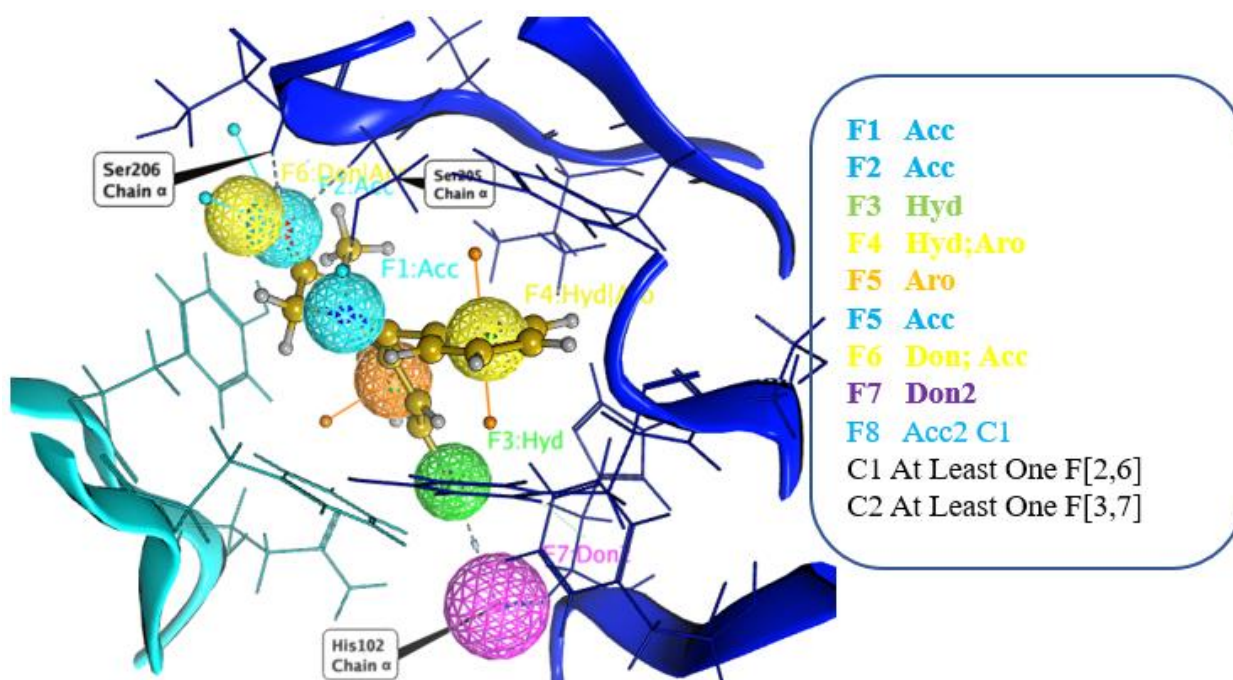


Figure 4.16 Pharmacophore query used for docking placement with 6HUP

The pharmacophore query thus designed takes into consideration both the ligand and the receptor properties. In particular two constrains (C1 and C2) were highlighted to ensure the presence of a ligand hydrogen feature in proximity of the protein donor features (His102) and the presence of an acceptor feature on the ligand in proximity of the acceptor residue of Ser205/206 on the receptor.

The generated pharmacophore queries were used both for placement and refinement of the poses. In particular, each docking run was done in triplicate, with 50 poses for each entry returned by the placement and ten poses returned by the refinement.

The poses were then analysed and filtered according to the S value and rmsd\_refine (i.e. the root mean square deviation between the pose before and after refinement), the E\_refine score from the refinement stage. For each pose, a PLIF was calculated as well.

#### *Protein ligand interaction fingerprint*

The PLIF was calculated automatically during the generation of the docking poses. As per Section 2.3.6 the PLIF could be representative of two types of interaction, i.e. potential or surface contacts. The potential contacts are used to characterize the binding of a small molecule in a well-defined binding site, whereas surface contacts are used to characterize protein-protein interfaces. For this study, the potential contacts were used in generating the PLIF. MOE<sup>®</sup> evaluated nine types of contacts: sidechain hydrogen bonds (donor or acceptor), backbone hydrogen bonds (donor or acceptor), solvent hydrogen bonds (donor or acceptor), ionic interactions, metal binding interactions and  $\pi$  interactions.

#### *4.3.9 Pharmacophore*

The 3D conformations obtained from the molecular docking studies were used to carry out a pharmacophore mapping exercise to define pharmacophore features common to those DBDZs predicted to show the highest log 1/c values. In particular for the purpose of this study only those conformations showing the best binding affinity value (i.e. more negative) were taken into consideration (Figure 4.12Figure 4.14). The latter were processed with the flexible alignment application in MOE<sup>®</sup> using the force field Amber10:EHT, resulting in a set of alignments each characterised by a final score. The final score (S) quantifies the quality of the alignment in terms of both internal strain (U score) and overlap of molecular features (F value) (Chan and Labute, 2010). The lower the S value, the better the quality of the alignments. The best alignment was used to generate a pharmacophore query, with the use of the pharmacophore editor application in the consensus mode. The consensus mode linked annotation points (e.g., H-bond donor, H-bond acceptor, etc.) to the 3D alignment of the DBZDs, generating the corresponding pharmacophore features. The consensus mode is so called because identify a % for each feature, that indicate how common that feature is. Only the features with 70% or higher were included in the final pharmacophore map. The pharmacophore map was validated on the 77 BDZs used as dataset for the

QSAR model. Once validated, it was used for virtual screening studies of databases included in Zinc.

#### 4.3.10 Scaffold Hopping studies

To explore the chemical space of the class of DBZDs, scaffold hopping studies were carried out with the use of the Fragment application tools in MOE<sup>®</sup> (Appendix B). This application contains different functions which can be used for this purpose, i.e. the MedChem, Scaffold Replacement, and Add Group to Ligand transformation functions. MedChem transformations uses bioisosteric replacements, on existing ligands to generate, hence discover novel chemical structures. Usually, functional groups or individual part of ring systems get substituted with bioisosters whilst preserving the rest of the ligand. These transformations can be applied iteratively and generate cumulative changes (Langdon et al., 2010). Scaffold Replacement instead is used to obtain improved ligands via the replace of bigger portion of the scaffold, e.g. entire rings system. The Add Group to Ligand has the same scope as Scaffold Replacement but operates in a different way. No replacement is carried out and only the addition of a substituent or the extension of a ligand is performed. For this purpose, MOE<sup>®</sup> has proprietary linker database which can be used. All the transformation were carried out on diazepam scaffold (Sec. 4.3.9), as this molecule was deemed a good starting point for optimisation. Moreover diazepam is bound in its active conformation (RCSB PDB, 2018a) – see Figure 4.17, enabling the steric hindrance of the binding pocket (van der Waals interaction surface) and its electrostatic properties to be taken into consideration and included in the scaffold hopping studies.

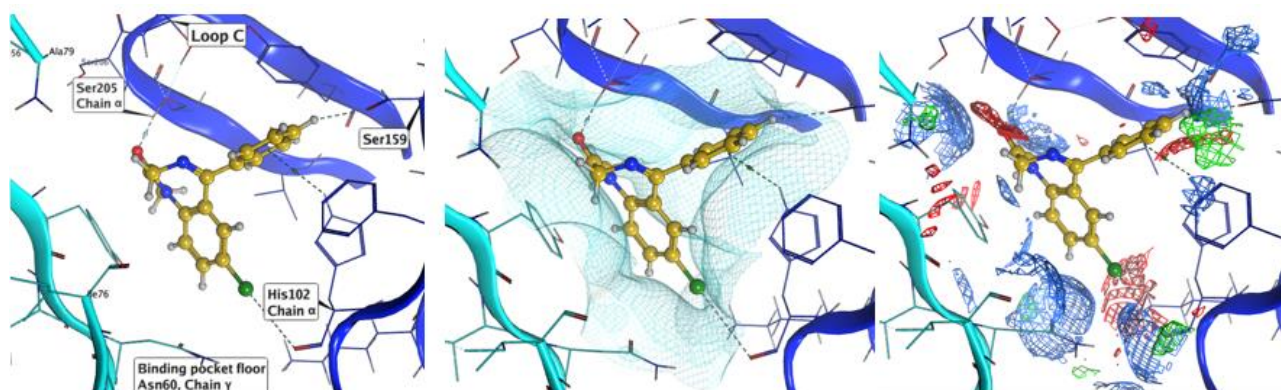




Figure 4.17 Representation of the allosteric binding pocket of GABA-AR with diazepam bound in its active conformation (PDB6HUP (RCSB PDB, 2018b)).

is presented, with the subunit  $\alpha 1$  identified in blue and the subunit  $\gamma 2$  identified in light blue. On the left side, the interactions with the binding pocket are visualised; in the middle, the electrostatic properties of the pocket and on the right, the van der Waals interactions surface are presented. The electrostatic properties are identified with three different colours: green for the hydrophobic portion, red for the H-bond acceptor, and blue for the H-bond donor-like portion. All of these were retrieved from the analysis of the crystallised structure.

To carry out the MedChem and Scaffold Replacement studies, and after evaluation of the benzodiazepine SAR (Sec 4.2.5), diazepam was divided into three major moieties, as shown in Figure 4.18.

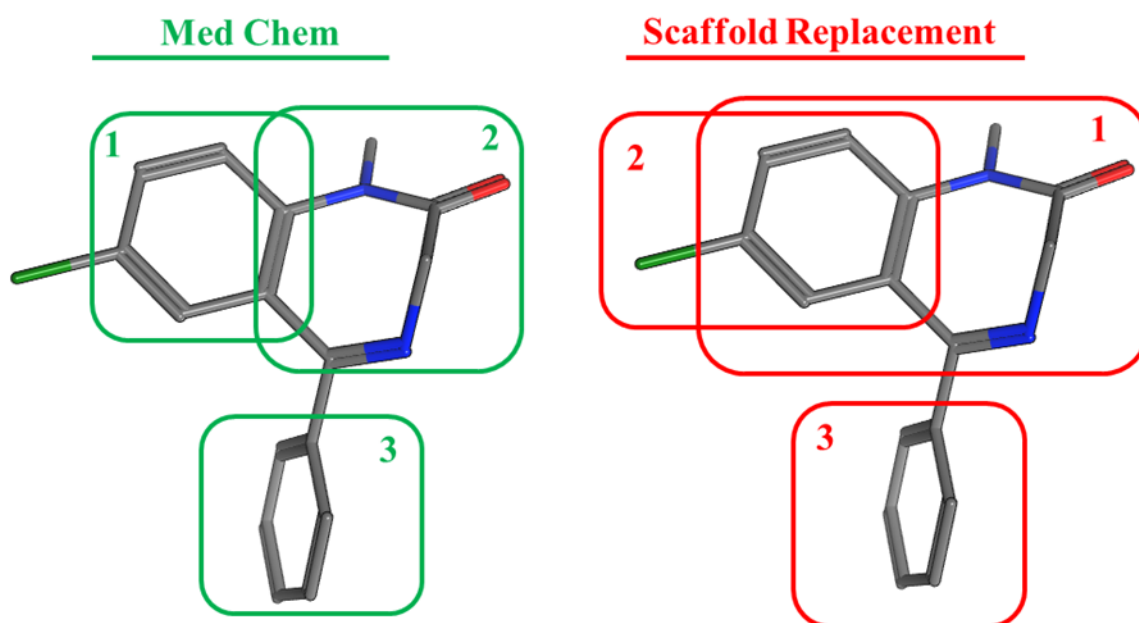


Figure 4.18 Three major moieties (1,2 and 3) for the MedChem (green) and Scaffold Replacement (red) studies

Notes. The green moieties include the benzene ring (1), the diazepine ring (2), and the pendant phenyl ring (3). The red moieties include the whole benzodiazepine ring (1), the benzene ring (2), and the pendant phenyl ring (3).

Only the Med Chem and Scaffold Replacement studies were performed at the beginning, with The Add Group to Ligand function used only subsequently. This was due to the fact that the purpose of the study was to explore diverse chemical structures rather than growing existing ones. The MOE<sup>®</sup> proprietary linker database containing 46000 linkers, was used. The default MOE<sup>®</sup> descriptor parameters were used to constrain the search and generated structures were energy-minimized.

The following Chapter will present the results obtained with the *in silico* studies on the DBZDs class.

## Chapter 5 Results and discussions of in silico studies on designer benzodiazepines

### 5.1 QSAR with MOE®<sup>1</sup>

#### 5.1.1 Training and test sets

The 77 BDZs discussed in Section 4.3.1 (Hadjipavlou-Litina and Hansch, 1994; Waters et al., 2018) were divided into a training (68) and a test set (9), and a SMILES string was generated for each molecule (Appendix A). As per Section 4.3.1, the training set and test set compositions were determined by similarity and activity sampling (Golbraikh and Tropsha, 2002). As discussed in Section 2.2.1, the training set is used to build the mathematical model, while the test set is used for the external validation of such model. i.e. to assess its predictivity and generalizability (Verma et al., 2010). The 77 molecules presented experimental values of log<sub>1/c</sub> between 6.05 and 8.92, where the higher values correspond to higher biological activity (Waters et al., 2018). The molecules were prepared as per the Methods section 4.3.1.

The training and test sets identified (Appendix A) were used in the manual (QuaSAR) and automatic (AutoQSAR) calculation of QSAR models. These model when then used to predict the biological activity of the set of DBZDs (115) identified by the NPSfinder® (Section 3.2). However, due to the fact that some of these 115 DBZDs were also listed among those molecules included either within the training or the test set, only 102 DBZDs out of the 115 (Section 3.2) were used for biological activity prediction.

#### 5.1.2 Manual QSAR Models

The evaluation and selection of the descriptors was done as explained in Section 4.3.2. Once the descriptors were ranked according to their absolute correlation coefficient ( $\rho$ ) value with log 1/c, a correlation matrix was developed to assess their mutual correlation with the correlation function in MOE® Figure 5.1.

---

<sup>1</sup> The results here presented have been previously published in Catalani V, Botha M, Corkery JM, et al. (2021) The psychonauts' benzodiazepines; quantitative structure-activity relationship (QSAR) analysis and docking prediction of their biological activity. *Pharmaceuticals* 2021, Vol. 14, Page 720 14(8). Multidisciplinary Digital Publishing Institute: 720. DOI: 10.3390/PH14080720 as part of VC PhD programme.

Descriptor	log 1/c		1	2	3	4	5	6	7	8	9	10	11
a_ICM	0.53	1. log 1/c	100										
a_nH	-0.57	2. a_ICM	53	100									
BCUT_PEOE_0	0.54	3. a_nH	-57	42	100								
BCUT_SLOGP_0	0.57	4. BCUT_PEOE_0	54	35	-77	100							
dens	0.55	5. BCUT_SLOGP_0	57	21	-53	76	100						
density	0.57	6. dens	55	77	47	35	34	100					
GCUT_SMR_2	0.51	7. density	57	77	-47	37	34	99	100				
PEOE_VSA_FNEG	0.51	8. GCUT_SMR_2	51	36	-44	40	50	59	59	100			
PEOE_VSA_FPOS	-0.51	9. PEOE_VSA_FNEG	51	64	-45	34	30	70	70	71	100		
vsurf_IW6	0.58	10. PEOE_VSA_FPOS	-42	-21	80	-48	-30	-32	-33	45	-42	100	
		11. vsurf_IW6	54	38	24	27	42	53	53	42	48	-21	100

Figure 5.1 Correlation coefficient and correlation matrix for the top ten scoring descriptors.

On the left-hand side is reported the correlation between the descriptor and the log 1/c value, on the right hand side the correlation between descriptors.

Analysing the results of the correlation studies, only four descriptors were found not to be mutually correlated, i.e. not correlating with each other. These descriptors, a\_nH, BCUT\_SLOGP\_0, density and vsurf\_IW6 were then used to develop the QSAR models. With the four descriptors obtained, two QSAR model were calculated with the QuaSAR application ( Table 5.1).

Table 5.1 QSAR models calculated with the manually selected descriptors

<b>QuaSAR-Model (PLS) 4 descriptors</b>
$\log 1/C = 8.48609 - 0.07418 * a\_nH + 1.03718 * BCUT\_SLOGP\_0 + 2.18721 * density + 0.17983 * vsurf\_IW6$
<b>QuaSAR-Model (PLS) 3 descriptors</b>
$\log 1/C = 10.21688 - 0.09289 * a\_nH + 0.98396 * BCUT\_SLOGP\_0 + 0.22810 * vsurf\_IW6$

For each of the models, the statistics parameters (training set  $r^2$  and  $q^2$ , test set  $r^2$  and the RMSE value, Sec. 4.3.1) for model predictiveness and robustness evaluation were calculated and are reported below (Table 5.2).

Table 5.2 Statistical value for the QSAR models

4 Descriptors QSAR model			
Training set			Test set
$r^2$	RMSE	$q^2$	$r^2$
0.59	0.47	0.51	0.60
3 Descriptors QSAR model			
Training set			Test set
$r^2$	RMSE	$q^2$	$r^2$
0.57	0.48	0.50	0.51

From the data in Table 5.2, it can be seen that the QSAR model identified by the four descriptors seems to be slightly more predictive than the one with three descriptors , with a test set  $r^2$  value of

0.60 which is higher than 0.51. The same model seems to be as well more robust, showing a LOO cross-validation value ( $q^2$ ) of 0.51 which is higher than 0.50. As reported in Section 2.2.4 a QSAR model is considered acceptable when it has an  $r^2$  value  $> 0.6$  and  $q^2 > 0.5$  for the training set (Beebe et al. 1998) and a  $r^2 > 0.5$  for the test set (Golbraikh and Tropsha 2002). Despite the four descriptors model matches these requirements, its statistics are just above the cut off values and very low if compared to what reported in literature ( $r^2 > 0.9$  (Waters et al., 2018)).

Further attempts to improve this statistic based on the evaluation of different combination of training and test sets were carried out (Appendix A). It was noted that, across the various training and test sets, the same combination/type of descriptors were identified as correlated to the biological activity. This is because descriptors are calculated on the molecule structure which did not change.

To better understand the reasons behind these low values and assess if more predictive QSAR models could be generated, a methodology different from the manual approach, i.e., the AutoQSAR application (Sec. 5.1.3), was investigated.

### 5.1.3 AutoQSAR models<sup>2</sup>

The AutoQSAR application generated 80 QSAR models from the 260 2D descriptors calculated. To assess the reliability and quality of the dataset further, the “ignore outliers” function was taken into consideration. The latter managed to identify one compound (Ro 06-9098) as an outlier, which was removed from the dataset and not included for the model building. After the removal of the outlier the training set was composed of 67 molecules only. Ro 06-9098 was flagged as an outlier after the evaluation of his \$Z-SCORE value which was higher than 2.5. The \$Z-SCORE value is "the number of standard deviations away from the mean" and is automatically calculated as validation parameter during the generation of QSAR model. MOE<sup>®</sup> explain this value as ‘the absolute difference between the value of the model and the activity field, divided by the square root of the mean square error of the data set’. The eighty QSAR equations generated were then manually analysed to identify the best model, i.e high values ( $>0.7$ ) of  $r^2$  (goodness of fit), high values ( $>0.6$ ) for  $q^2$  (robustness) and fewer descriptors. The model chosen was a five descriptors equation with an  $r^2$  of 0.75 and an  $q^2$  of 0.69 (Equation 5.1.)). The number of descriptors in the model chosen was in

---

<sup>2</sup> The results here presented have been previously published in Catalani V, Botha M, Corkery JM, et al. (2021) The psychonauts' benzodiazepines; quantitative structure-activity relationship (QSAR) analysis and docking prediction of their biological activity. *Pharmaceuticals* 2021, Vol. 14, Page 720 14(8). Multidisciplinary Digital Publishing Institute: 720. DOI: 10.3390/PH14080720.

line with the general recommendation or roughly one descriptor for every ten molecules included in the training set as discussed in sec. 2.2.3 (Danishuddin and Khan, 2016). The chosen model went then, through the external validation process, i.e., test set evaluation (i.e., prediction of log 1/c values for the test set). The "Model-Evaluate" function was used to predict the log1/c values for the test set. An  $r^2$  of 0.66, calculated using the correlation plot function, and an RMSE value of 0.65 were obtained. The same "ignore outliers" function was used on the test set and after the removal of two outliers (Ro 05-4336, Ro 05-2921), as suggested in the literature (Roy et al., 2016), a better RSME value of 0.36 was achieved.

**Equation 5.1 QSAR Equation identified with AutoQSAR application**

$$\log 1/C = 9.45416 + 0.77505 * h\_log\_pbo + 1.24990 * KierFlex - 0.03382 * Q\_VSA\_HYD - 0.01507 * SlogP\_VSA7 - 0.03849 * vsa\_pol$$

The five descriptors included in the model correlate with logP (octanol/water partition coefficient) (SlogP\_VSA7), the strength of  $\pi$ -electron bonds (h\_log\_pbo), the total hydrophobic van der Waals surface area (Q\_VSA\_HYD), the polar van der Waals surface area (vsa\_pol), and the molecular flexibility (KierFlex). This means that these 2D molecular descriptors are strictly linked to the biological activity of the molecules object of the study. For each descriptor, the single code detailed description and the relative importance is reported in Table 5.3.

**Table 5.3 Specification of the five descriptors included in the final QSAR model\*.**

Code	Description	RI
h_log_pbo	Sum of log (1 + pi bond order) for all bonds	0.65
KierFlex	Kier molecular flexibility index: (KierA1) (KierA2)/n	0.68
Q_VSA_HYD	Total hydrophobic van der Waals surface area	1.00
SlogP_VSA7	Approximate accessible van der Waals surface area contribution to logP(o/w)	0.25
vsa_pol	Approximation to the sum of VDW surface areas (Å <sup>2</sup> ) of polar atoms	0.29

**\*In the code column is reported the descriptor name, in the description column a brief explanation of what that descriptor represents as reported in the MOE® manual user, and in the RI column the relative importance \*i.e. correlation with log 1/c) of the descriptor**

As per methods section these descriptors were checked for mutual correlation. No value higher than 0.7 was found confirming the lack of any correlation (Table 5.4). It is of great importance to check this issue to eliminate the risk of overfitting the model (Gad, 2014) as explained in sec. 2.2.3, and reduce the chance of inaccurate predictions.

**Table 5.4 Mutual correlation values for the 5 descriptors chosen for the QSAR equation**

	KierFlex	h_log_pbo	Q_VSA_HYD	vsa_pol	SlogP_VSA7
KierFlex	1.00				
h_log_pbo	0.13	1.00			
Q_VSA_HYD	0.65	0.30	1.00		
vsa_pol	0.07	0.11	-0.12	1.00	
SlogP_VSA7	-0.25	0.53	-0.09	0.07	1.00

The predicted  $\log 1/c$  values for training and test set are listed in the supplementary information (Appendix A), while the correlation between experimental and predicted data are visualised in Figure 5.2.

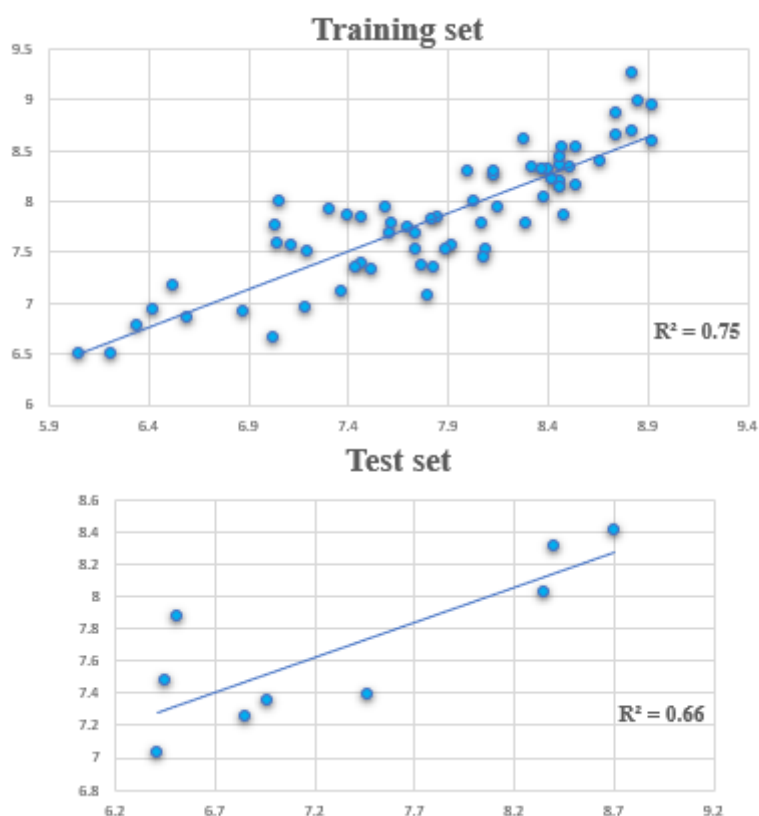


**Figure 5.2** Correlation values ( $r^2$ ) for the training and the test set were obtained using the five descriptors QSAR model generated by AutoQSAR.

**Note:** In the two graphs, the experimentally derived values of  $\log 1/c$  (x axis) are plotted against the values predicted by the QSAR model (y axis). The  $r^2$  defines the goodness of fit of the QSAR model. A QSAR model is considered acceptable when it has an  $r^2$  value  $>0.6$  for the training set and an  $r^2 > 0.5$  for the test set. This model has, respectively, an  $r^2$  of 0.75 and 0.66 for the training and test set.

The QSAR model displayed in Equation 5.1 was used to obtain a prediction of the biological activity data for the DBZDs identified by *NPSfinder*<sup>®</sup> (Appendix A). As per sec. 5.1.1, those DBZDs identified by the *NPSfinder* but present also in the training or test sets (13 molecules) were excluded, resulting in a total of 102 DBZDs used for both the QSAR predictions and docking studies. The predicted  $\log 1/c$  values were used to define three biological activity groups: low (5.80–6.99), medium (7.00–7.99) and high ( $\geq 8.00$ ). These values were chosen after the assessment of biological activity values available for four BDZs reported in literature as high potency ones, i.e. triazolam (Halcion,  $\log 1/c = 8.40$ ), lorazepam (Ativan,  $\log 1/c = 8.46$ ), clonazepam (Klonopin,  $\log 1/c = 8.74$ ) and flunitrazepam (Rohypnol,  $\log 1/c = 8.42$ ). The conservative choice of including in the high activity group all those DBZDs with  $\log 1/c$  values  $> 8.0$  was taken to account for error in the predicted values.

In Table 5.5 the top twenty DBZDs are reported according to their predicted biological activities. The calculated 2D descriptors, that were not part of the final QSAR model, but are considered by default important to describe the drug-likeness of these DBZDs, are reported in Appendix A. No evaluation of pharmacokinetics profile (PK) or absorption, distribution, metabolism, excretion and toxicity (ADMET) properties was conducted.

**Table 5.5 The top 20 predicted value of biological activity (log1/c) for the 102 DBZDs identified by NPSfinder®\*.**

<b>Molecule</b>	<b>SMILES</b>	<b>Predicted log1/c</b>
Ro 09-9212	<chem>Clc1c(C2=NCC(=O)Nc3sc(Cl)cc23)cccc1</chem>	9.40
Ro 07-5193	<chem>Clc1c(c(F)ccc1)C1=NCC(=O)Nc2c1cc(Cl)cc2</chem>	9.06
Ro 20-8065	<chem>Clc1c(Cl)cc2NC(=O)CN=C(c3c(F)cccc3)c2c1</chem>	9.04
Ro 07-5220	<chem>Clc1c(c(Cl)ccc1)C1=NCC(=O)N(C)c2c1cc(Cl)cc2</chem>	8.95
Ro 07-3953	<chem>Clc1cc2C(c3c(F)cccc3F)=NCC(=O)Nc2cc1</chem>	8.81
Fluclotizolam	<chem>Clc1sc2-n3c(C)nnc3CN=C(c3c(F)cccc3)c2c1</chem>	8.77
Ciclotizolam	<chem>Brc1sc2-n3c(C4CCCC4)nnc3CN=C(c3c(Cl)cccc3)c2c1</chem>	8.77
Flubrotizolam	<chem>Brc1sc2-n3c(C)nnc3CN=C(c3c(F)cccc3)c2c1</chem>	8.67
Phenazepam	<chem>Brc1cc2C(c3c(Cl)cccc3)=NCC(=O)Nc2cc1</chem>	8.61
Ro 07-9749	<chem>Ic1cc2C(c3c(F)cccc3)=NCC(=O)Nc2cc1</chem>	8.60
Clonazolam	<chem>Clc1c(C2=NCc3n(c(C)nn3)-c3c2cc([N+](=O)[O-])cc3)cccc1</chem>	8.58
Ro 15-9270	<chem>Clc1c(C=2c3c(-n4c(C)nnc4CC=2)ccc([N+](=O)[O-])c3)cccc1</chem>	8.52
Climazolam	<chem>Clc1c(C2=NCc3n(c(C)nc3)-c3c2cc(Cl)cc3)cccc1</chem>	8.49
Flunitrazolam	<chem>Fc1c(C2=NCc3n(c(C)nn3)-c3c2cc([N+](=O)[O-])cc3)cccc1</chem>	8.47
Ro 20-8552	<chem>Clc1c(C)cc2C(c3c(F)cccc3)=NCC(=O)Nc2c1</chem>	8.42
Methyl Clonazepam	<chem>Clc1c(C2=NCC(=O)N(C)c3c2cc([N+](=O)[O-])cc3)cccc1</chem>	8.40
Reclazepam	<chem>Clc1c(C2=NCCN(C=3OCC(=O)N=3)c3c2cc(Cl)cc3)cccc1</chem>	8.39
Uldazepam	<chem>Clc1c(C2=NCC(NOCC=C)=Nc3c2cc(Cl)cc3)cccc1</chem>	8.39
Zapizolam	<chem>Clc1c(C2=NCc3n(-c4c2nc(Cl)cc4)cnn3)cccc1</chem>	8.38
Ethyl Dirazepate	<chem>Clc1c(C2=NC(C(=O)OCC)C(=O)Nc3c2cc(Cl)cc3)cccc1</chem>	8.35

**\*Log1/c represents the logarithm of the reciprocal of the molar inhibitory concentration (IC50) (nM) required to remove 50% of [3H]-diazepam from rats' cerebral cortex. The molecules are listed in decreasing order of predicted log1/c. The higher log1/c values should correspond to a higher biological activity**



The number of DBZDs that show predicted  $\log_{1/c}$  values between 7.00 and 7.99, i.e. medium activity was 43 (42%), while the ones showing predicted  $\log_{1/c} > 8.00$ , i.e. high activity were 42 (41%). Seventeen molecules (17%) showed predicted  $\log_{1/c}$  values lower than 7.00, i.e. low indicating a low predicted biological activity. Among the top scoring DBZDs, a series of Ro molecules (Gardner and Hedgecock, 1989) was identified, as well as phenazepam (WHO, 2015), ciclotizolam (Weber et al., 1985), fluclozizolam (Binder et al., 1974), and flubrotizolam .

The three activity groups were visually assessed to identify any pattern of communality among chemical features. The double substitutions in position C7 and C2', mainly with halogens (i.e. Cl, Br and F) and  $\text{NO}_2$  was identified as a common feature in the "high activity" group. This was found to be the case also for the presence of a substitute thiazole ring replacing the benzene of the benzodiazepines scaffold and the presence of a triazolo/imidazole ring (N1-C2) fused in the core structure (Figure 5.3, Sec. 4.2.5). The "medium activity" group was characterised mostly by one single substitution with halogens (i.e. Br and F), either in position C2' or C7. Another recurrent structural characteristic was the presence of bulky substituents either on the imidazo/triazole ring or at position N1 (Figure 5.3, Sec. 4.2.5). The lack of the pendant phenyl was also observed in this group. The same substitution pattern of the bulky chains on N1 was observed in the "low activity" group as well, together with the presence of pyrrole or imidazole rings as substitutes of the benzene ring (Figure 5.3, Sec. 4.2.5). It should be noted that no clear or defined pattern/correlation could not be established.

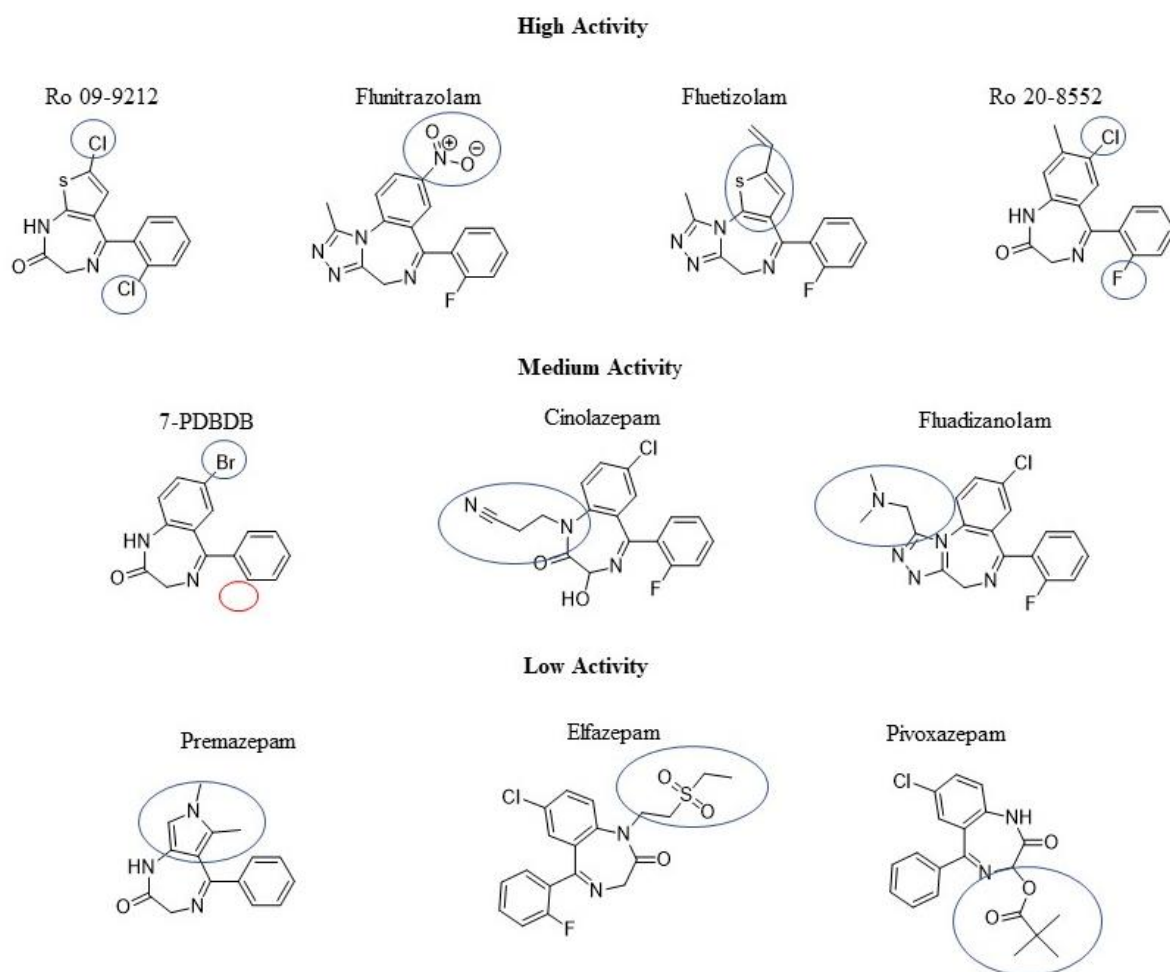


**Figure 5.3** Example of 2D molecules belonging to the high, medium and low activity bins.

**Notes:** In the figure, common chemical features across each activity bin are highlighted with a blue circle. Instead, the red circle indicates the lack of a substituent.

The best 2D QSAR model obtained with MOE<sup>®</sup> (Chemical Computing Group ULC, 2022), i.e. the one developed with the AutoQSAR application, was used to predict the biological activity of previously reported and unreported DBZDs. The validation process underwent also confirm the reliability of the model to predict the biological activity of new DBZDs and the possibility of using it for a fast evaluation as soon as a new molecule emerges online or on the real-world markets.

Despite these predictions are only educated guesses, with no experimental supporting data, the validation carried out on the QSAR model should suffice for the predicted biological activities to be regarded as valid, reliable and very useful for the initial assessment of novel DBZDs.

The statistic parameters reported for the model, i.e training test  $r^2$  (0.75) and  $q^2$  (0.69), prove goodness-of-fit and robustness (internal validation). The goodness-of-fit, or internal predictivity ( $r^2 = 0.75$ ) indicates how well the model predicts biological activity for molecules used to build the model itself but cannot predict the efficacy of the model for compounds that were not used to train

the model. Hence, the predictivity of the model need to be assessed by external validation (test set). This external validation returned values for  $r^2$  (0.66) and RMSE (0.36) which suggest a good productivity capacity of the algorithm. The  $r^2$  value indicates that the QSAR model was able to predict 66% of the activity values of the test set, while the RSME value instead indicates the confidence of the model. While the closer the  $r^2$  value is to 1 the higher the predictivity of the model, for RSME value is the opposite, being the latter a measure of the error of the prediction. However, differently from  $r^2$ , for RMSE there is no maximum cut-off (Consonni et al., 2010) and the lower the value the better the measure confidence (Alexander et al., 2015; Golbraikh et al., 2014; Tropsha, 2010; Worachartcheewan et al., 2018). Often RMSE is considered a more helpful gauge of a model's usefulness than  $r^2$  (Alexander et al., 2015).

These statistical values were refined after the identification and elimination of the outliers from the dataset. A compound is as a true outlier when the predicted log/c value is 2.5 units higher (Z-score) than the experimental one. True outliers are compounds that show unexpected biological activity or are unable to fit into a QSAR model (Verma and Hansch, 2005); eliminating true outliers from a training set is good practice to increase the quality of the model and avoid unnecessary bias (Furusjö et al., 2006).

It should be noted that this model will keep its good predictivity only when applied to new molecule which belong to the domain of applicability (Sec 5.2.3) of the model, i.e. are structurally classifiable as BZDs (Figure 4.1 and Figure 4.3). Indeed it cannot be used for a reliable prediction of the activity of other chemical classes on GABA-AR (e.g. Z-drugs) (Gunja, 2013).

The QSAR model here generated indicate a strong correlation between some physiochemical characteristics of DBZDs and their biological activity (Maddalena and Johnston, 1995; Thakur et al., 2004; Waters et al., 2018). LogP, or partition coefficient, which identify the ability of a molecule to permeate a membrane, the hydro-phobic surface and the polar surface are described by the QSAR model as very important properties in this regard for an index, unknown, DBZD. The same seems to apply to its molecular flexibility.

The total hydrophobic van der Waals (vdW) surface area (i.e. Q\_VSA\_HYD) is the descriptor mostly correlated with log1/c value (Table 5.3). Q\_VSA\_HYD, together with SlogP\_VSA7 (van der Waals surface area contribution to logP) and vsa\_pol (vdW polar surface areas), describe very important electrostatic molecular surface properties which are usually the most important for receptor interaction potential, i.e biological activity, and were also proved to influence the membrane permeability (Wildman and Crippen, 1999). KierFlex, the second most important

descriptor (Table 5.3), suggest the importance of the molecule flexibility for its biological activity (Hall and Kier, 1991). This could be explained if one considered the very tight binding pocket of the GABA-AR (Sec. 5.4). The sum of hydrogen bond donor strengths of carbon atoms, i.e.,  $h\_log\_pbo$ , appears to be the third most important descriptor in the QSAR model generated (Table 5.3). The importance of this descriptor could be explained if one takes into consideration that the majority of the interactions documented with the docking studies (Sec 5.4) are represented by hydrogen donor/acceptor bonds (Wang et al., 2019). Hence, the ability of a molecule to generate this type of bond could strongly correlate with its level of activity.

Parallel to the information displayed in the QSAR model which could be used to increase the knowledge on DBZDs, the predicted values of the  $log1/c$  represent the most interesting outcome of the QSAR study. As reported above (sec 5.1.3), molecules with  $log1/c >$  higher than 8.0 should display high potency in line with lorazepam and clonazepam, (respectively  $log1/c$  of 8.46 and 8.74 (Appendix A)).

Among the DBZDs ( $n = 102$ ) identified by the web crawler, a total of 41% show value of  $log1/c > 8.00$  (high potency). Etizolam (which is being prescribed in some countries, but still classified as DBZD in others), and flualprazolam, two of the most popular DBZDs worldwide (EMCDDA, 2020d; Public Health England, 2020) are included in this 41%, with predicted  $log 1/c$  values between 8.10 and 8.40. The top ten predicted  $log1/c$  values identified) are ten times higher than those predicted for etizolam and flualprazolam. This is of particular concern seeing that these two DBZDS have been connected to multiple fatalities and near misses (UNODC EWA, 2020). Phenazepam and fluclozepam are also predicted among the top ten DBZDs (ACMD, 2020a; Moosmann and Auwärter, 2018; UNODC, 2017a; WHO, 2015) together with lesser known DBZDs

Although these results need to be interpreted as speculative conclusions, hence not experimentally determined, they may still present a reason for concern. Indeed the QSAR results tentatively suggested that about half of the 102 DBZDs identified may possess high to very-high activity on the GABA-AR. Moreover, the  $log1/c$  values are calculated for the  $\alpha 1$  isoform of the GABA-AR, the one responsible for the addiction potential of BZDs (Tan et al., 2011). Therefore, it could be concluded that almost half of the DBZDs here assessed may be both potent and associated with a strong addiction potential (Brunetti et al., 2021; El Balkhi et al., 2020; Orsolini et al., 2020).

#### 5.1.4 *AutoQSAR model domain of applicability*

The applicability domain for the AutoQSAR model has been calculated accordingly to the structure similarity ( $T_c$ ). This means that all new molecules which shows a  $T_c=0.5$  (average) when compared to the whole dataset used to train and validate the QSAR model could be predicted by this model.

## 5.2 QSAR with Forge<sup>TM3</sup>

### 5.2.1 Training and test sets

The three-dimensional structures of 77 BZDs in the data set were prepared in MOE<sup>®</sup> with the molecular force field Amber10:EHT. The optimised 3D structures were uploaded to Forge<sup>TM</sup> for the 3D-QSAR studies. The 77 structures were divided with the activity stratify function into the training set (65) and a test set (12) (Appendix A). The splitting process was carried out multiple times and all the resulting combinations were used to assess reproducibility. The resulting training and test sets composition are dissimilar to the one obtained with MOE<sup>®</sup> because calculated in a different way.

Once uploaded in Forge<sup>TM</sup> each molecule was assigned with a set of field points which describe the complex three-dimensional electrostatic/van der Waals properties. The field points were calculated with the application of the extended electron distribution force field (XED). For each molecule Forge<sup>TM</sup> explored the electrostatically positive and negative van der Waals attractive and hydrophobic features. Each feature was identified with a sphere, whose size was proportional to the amount that, that feature is predicted to energetically influence the biological activity. The BDZs were then aligned on the 3D active conformations of diazepam and alprazolam in the crystallised protein ( Figure 4.12 and Figure 4.13) (RCSB PDB, 2018a, 2018b), and then submitted to the Forge<sup>TM</sup> processing application (i.e. conformation search, alignment, and model building calculations).

### 5.2.2 3D QSAR Model

A 3D-Field QSAR, and two machine learning models, a Random Forest, and a Relevant Vector Machine (RVM) models were created (Sec. 4.3.7). Detailed information on the methodology is presented in Appendix B.

The 3D Field QSAR was generated via a partial least squares (PLS) analysis (Wold et al., 2001), specifically with the use of the SIMPLS algorithm (de Jong, 1993). Twenty models were automatically generated, from which the number of PLS components defined as optimal (8, for this dataset) was identified. The chosen method displayed an  $r^2$  (coefficient of determination) of 0.98 and  $q^2$  (cross-validated coefficient of determination) of 0.75 as seen in Table 5.6. The parameter for the other methods are reported in Appendix A.

---

<sup>3</sup> The results here presented have been published in Catalani V, Floresta G, Corkery JM, et al. (2022) In silico studies on recreational drugs: 3D-QSAR prediction of classified and de novo designer benzodiazepines. *Chemical biology and drug design* (Accepted)

**Table 5.6 Values for the statistics obtained for the three calculated QSAR models\*.**

Model	r <sup>2</sup>	q <sup>2</sup>	r <sup>2</sup> Test	RMSE	Tau
3D Field QSAR	0.98	0.75	0.82	0.34	NA
Random Forest	0.91	0.51	0.46	0.53	0.55
RVM	0.98	0.72	0.86	0.40	0.71

**\*In particular are presented the coefficient of determination (r<sup>2</sup>) which indicates the goodness of fit; the cross-validated coefficient of determination (q<sup>2</sup>) which indicates the robustness; the coefficient of determination for the test set (r<sup>2</sup> test), which indicates the predictive power; the root mean square error (RMSE) as reliability measure; and Tau as a further parameter to assess the predictivity of the model. As r<sup>2</sup>, the closer the value of Tau is to one, the better the model <sup>4</sup>.**

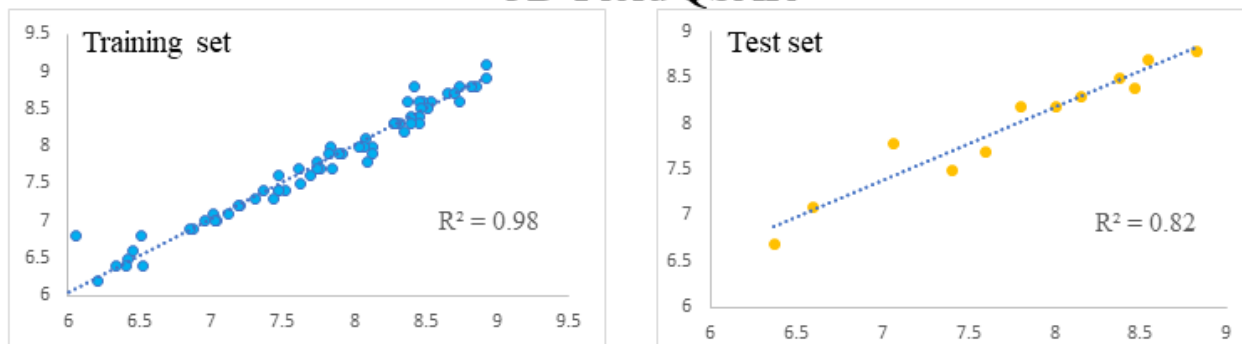
q<sup>2</sup> is the validation parameter obtained with the leave one out cross-validation (LOO CV) used in Forge™ as internal method validation, and ‘evaluates to which degree the prediction of a model is better compared to a null one’ (Catalani et al., 2022; Golbraikh and Tropsha, 2002). The root mean squared error (RMSE) values are reported as well as assessment of error forecast of the prediction. The value 0.34 reported for the final QSAR model can be considered a good result. As explained above (sec. 2.2.4), there is no RSME cut off value for model acceptance, and the lower the value the smaller the error and the better the model. The 8 components model was externally validated with the test set (12 molecules). The external validation returned an r<sup>2</sup> of 0.82 (as explained in sec 2.2.4, the closer the r<sup>2</sup> value is to the unity the better the model).

The two machine learning models returned very different statistic. The RVM performed better than Random Forest (Table 5.6). A visual representation of the predicted vs. experimental values for training and test sets is reported in Figure 5.4.

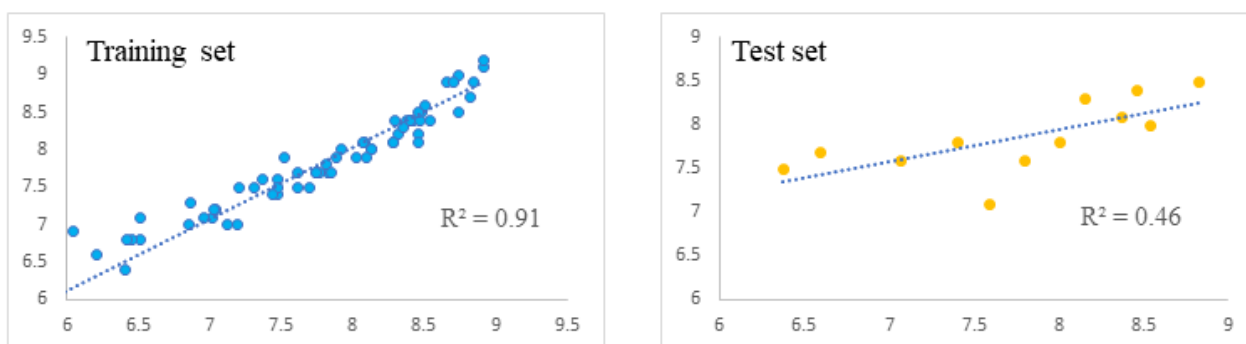
---

<sup>4</sup> The table has been published in Catalani V, Floresta G, Corkery JM, et al. (2022) In silico studies on recreational drugs: 3D-QSAR prediction of classified and de novo designer benzodiazepines. *Chemical biology and drug design* (Accepted)

## 3D-Field QSAR



## Random Forest



## Relevance Vector Machine

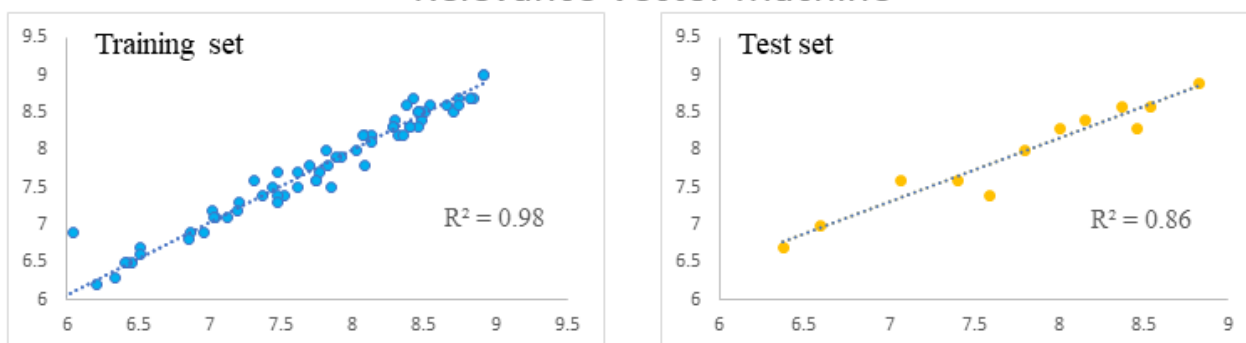


**Figure 5.4** Visual representation of the predicted (x axis) vs. experimental (y axis) log 1/c values for training (blue) and test (yellow) sets.

The graphs were built with Excel 2022. From the trend line associated to each set of data, and corresponding  $r^2$  values, it should be noted how the predictivity ability for the 3D Field QSAR and RVM models is really good both for the training sets (both  $r^2 = 0.98$ ) and the test sets (both  $r^2 > 0.8$ ). The same can not be noted with the test set of the RF model, which display a very low  $r^2$  value for the test set which fall beneath the acceptance cutoff for QSAR models<sup>5</sup>.

---

<sup>5</sup> The figure has been published in Catalani V, Floresta G, Corkery JM, et al. (2022) In silico studies on recreational drugs: 3D-QSAR prediction of classified and de novo designer benzodiazepines. *Chemical biology and drug design* (Accepted)



The visual interpretation of the 3D Field QSAR model is presented in Figure 5.5 .

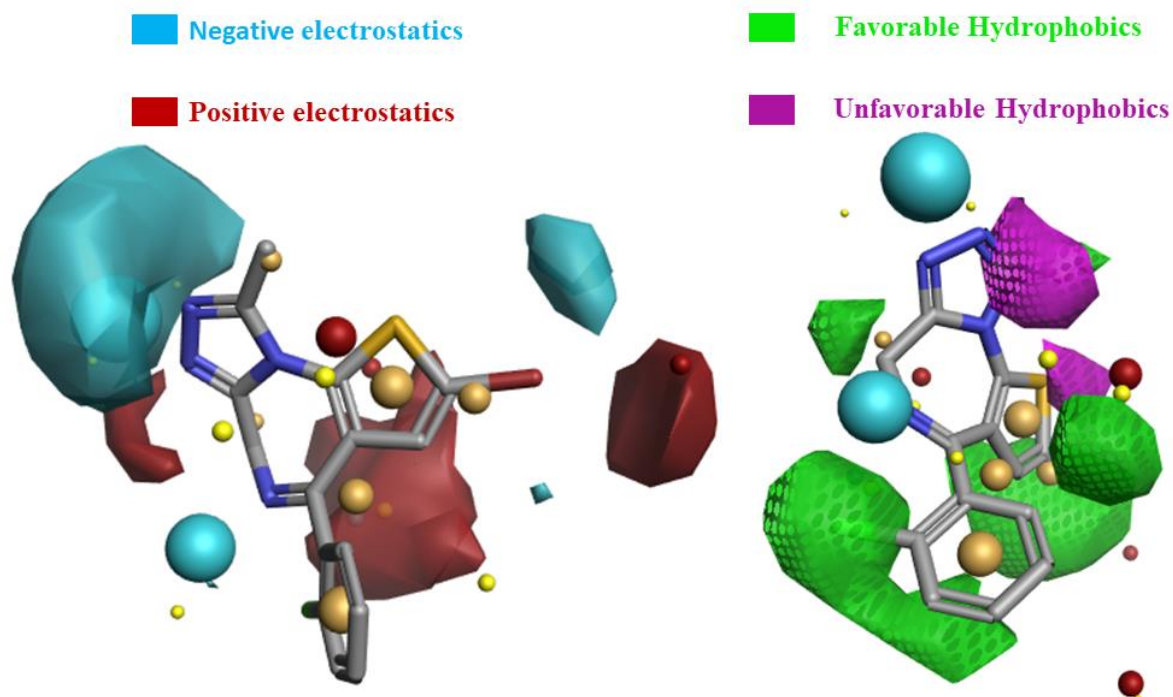


**Figure 5.5** Visual representation of the generated 3D Field QSAR model

*Notes. The electrostatic properties are identified by the red (positive) and blue (negative) colours, whereas the green and violet, respectively, identify areas of favourable and unfavourable hydrophobics. Red indicates areas of favourable positive electrostatic interactions, while blue negative. The green and violet areas instead indicate how the presence of a hydrophobic interaction in that region would increase (green) or decrease (violet) the activity. This model representation was created by Forge™<sup>6</sup>.*

In Figure 5.5 the blue and red, and the green and violet colours identify the most important electrostatic and hydrophobic features for the biological activity. In particular, the red and blue shapes indicate the space around the molecule in which more positive electrostatic interaction (red) or more negative electrostatic interaction (blue) will be beneficial (i.e. increase) for the activity. More positive interactions (red) could mean that placing strong H-bond donors in that region improves the activity or could mean as well that putting strong H-bond acceptors will worsen the activity, and vice versa with blue. This means that a triazolo ring fused to the core scaffold (i.e. strong H-bond acceptor) in correspondence with the big blue negative patch, as seen with alprazolam, will see a positive contribution to the biological activity. The same applies for those DBZDs similar to clonazepam (e.g. 4'-chlorodiazepam, 7-BPDBD, difludiazepam, etc.) showing a

---

<sup>6</sup> The figure has been published in Catalani V, Floresta G, Corkery JM, et al. (2022) In silico studies on recreational drugs: 3D-QSAR prediction of classified and de novo designer benzodiazepines in *Chemical biology and drug design*

carbonyl substitution in C2. Substitution with a NO<sub>2</sub> group in position C7 (e.g. meclonazepam) instead matches both the negative and positive electrostatic interactions (Figure 5.5).

Instead, the green and violet areas instead indicate how the presence of a hydrophobic interaction in that region would increase (green) or decrease (violet) the activity. It is interesting to note how the hydrophobic features identified by the 3D Field QSAR model are in line with the electrostatic surface derived via the receptor study with MOE<sup>®</sup> (Figure 4.17). Relevant hydrophobic interaction areas are identified around the pendant phenyl ring and in correspondence with a meta substituent. DBZDs showing halogenated substitution in meta (e.g. brotizolam and etizolam) indeed show a higher biological activity compared to those of less hydrophobic substituted molecules. Another hydrophobic interaction area is identified between the acceptor/donor features and the scaffold molecule in correspondence of C7. This may suggest an increased activity when a strong H-bond donor is connected to the core structure via a short aliphatic chain, instead of a direct bond with the carbon atoms of the scaffold.

Due to the fact that the value obtained for the test set  $r^2$  of the RF model fall beneath the cut off value for acceptance in QSAR (i.e. =0.5, sec 2.2.1), this model was not used to predict the biological activity of the identified DBZDs. Despite the very low level obtained for RF model is still under investigation, it should be noted that great discordance between the training and test set  $r^2$  values (as per Figure 5.5) when using machine learning algorithms (i.e. RF) have been reported before. This is usually due either to the fact that a small data set was used or to the tendency of the machine learning algorithms to overfit the training model, (Brownlee, 2018).

The two QSAR models identified above (Table 5.6) were used to predict the biological activity of the DBZDs identified online (the majority of which were retrieved from isomerdesign.com (Isomer Design, 2021)) (Appendix A). In summary the top ten DBZDs are reported inTable 5.7.

**Table 5.7 Values of predicted log 1/c of the top ten DBZD The entries are ranked for decreasing values of pred log 1/c.**

*Note. In addition to the predicted value of log 1/c, other parameters important to evaluate each entry are included, i.e. the distance to model, which indicates how distant is the structure of the query DBZDs to those in the model; the Sim which gives an indication of the quality of the alignment (1 is 100% alignment); and the logP which is an indication of the ability of that DBZDs to cross the brain barriers<sup>7</sup>.*

Title	3D Field QSAR	Distance to model	RVM	Sim	SlogP
Flubrotizolam	9.6	Excellent	9.5	0.9	4.2
Clonazolam	9.5	Excellent	9.4	0.9	3.4
Pynazolam	9.4	Good	9.4	0.9	2.1
Fluclotizolam	9.1	Excellent	9.1	0.9	4.1
MP-III-022	9.1	Good	9	0.6	3.6
Ro 09-9212	9	Excellent	9	0.9	3.9
Ro 15-9270	8.9	Good	8.3	0.8	4
3-Hydroxyphenazepam	8.9	Excellent	8.5	0.8	3.7
Flunitrazolam	8.8	Excellent	8.7	0.9	3.1

Their biological activity on the GABA-AR has already been reported for the 2D AutoQSAR model in The QSAR model displayed in Equation 5.1 was used to obtain a prediction of the biological activity data for the DBZDs identified by NPSfinder® (Appendix A). As per sec. 5.1.1, those DBZDs identified by the NPSfinder but present also in the training or test sets (13 molecules) were excluded, resulting in a total of 102 DBZDs used for both the QSAR predictions and docking studies. The predicted log1/c values were used to define three biological activity groups: low (5.80–6.99), medium (7.00–7.99) and high ( $\geq 8.00$ ). These values were chosen after the assessment of biological activity values available for four BDZs reported in literature as high potency ones, i.e. triazolam (Halcion, log 1/c= 8.40), lorazepam (Ativan, log 1/c= 8.46 ), clonazepam (Klonopin, log 1/c= 8.74) and flunitrazepam (Rohypnol, log 1/c= 8.42). The conservative choice of including in the high activity group all those DBZDs with log1/c values  $> 8.0$  was taken to account for error in the predicted values.

In Table 5.5 the top twenty DBZDs are reported according to their predicted biological activities. The calculated 2D descriptors, that were not part of the final QSAR model, but are considered by default important to describe the drug-likeness of these DBZDs, are reported in Appendix A. No evaluation of pharmacokinetics profile (PK) or absorption, distribution, metabolism, excretion and toxicity (ADMET) properties was conducted.

<sup>7</sup> The table has been published in Catalani V, Floresta G, Corkery JM, et al. (2022) In silico studies on recreational drugs: 3D-QSAR prediction of classified and de novo designer benzodiazepines in *Chemical biology and drug design*

**Table 5.5.** The latter presented predictive statistics which were indeed good ( a five descriptors equation with an  $r^2$  of 0.75 and an  $q^2$  of 0.69), but inferior if compared to the 3D models described above in Table 5.6 (Catalani et al., 2022, 2021b), suggesting how the data predicted with Forge™ could be considered more reliable.

From the fact that using the 3D spatial steric and electronic coordinates of the DBZDs better prediction are achieved – i.e. higher values of  $r^2$ ,  $q^2$  and test  $r^2$ , one could infer a weak correlation between the 2D properties of the benzodiazepines scaffold and their activity. With these predicted values, even a greater percentage of DBZDs, i.e. 55%, is included in the high activity group ( $\log 1/c > 8.0$ ), with 38% include in the medium activity group and the remaining 8 % in the low activity group.

The DBZDs showing the highest biological activity were: flubrotizolam ( $\log 1/c = 9.6$ ), clonazolam (9.5), pynazolam (9.4) and fluclozizolam (9.1). Flunitrazolam (8.8) and flubromazolam (8.7) followed with slightly lower values, together with other DBZDs. These results seem to be in line with what is reported in the literature and some drug discussion fora (El Balkhi et al., 2020; reddit, 2021a). Clonazolam for example was reported as the as the most active compound in his series (i.e. *6-phenyl-4H-s-triazolo[4,3-a][1,4]benzodiazepines*) (Hester et al., 1971) and has been sold online as a designer drug (Huppertz et al., 2015). Flunitrazolam, has also been sold online as a designer drug, and it was reported as a potent hypnotic and sedative drug similarly to the related compounds flunitrazepam, clonazolam and flubromazolam (EMCDDA and Europol, 2016). A detailed description for DBZD listed in **Error! Reference source not found.** is reported in sec. 5.6. The fact that the predicted most potent DBZDs are indeed described as such, suggest how the prediction carried out on unknown DBZDs could be reliable and of high relevance.

The QSAR methods predicted a strong biological activity for some DBZDs that have recently been recommended for inclusion in Schedule 1 of the Misuse of Drugs Regulations 2001 (ACMD, 2020b), and in particular flunitrazolam (8.8) and flualprazolam (8.3) . It is interesting to note that the presence of a triazole ring seems to be a structural feature that consistently increases the activity of the index molecule.

### 5.2.3 Domain of applicability with Forge™

The applicability domain, for each QSAR model generated with Forge™ is automatically calculated and reported in the 'Distance to Model' column for all the entries, being them in the training, test and prediction set. The distance to model is reported with values as “excellent”, “good”, “ok”, “poor” and “bad”, and identified whether the molecule has any field points or features (Sec. 4.3.5)

which are displayed by the training set molecules. Values as “excellent”, “good” and “ok” indicate that the predicted activity is reliable because all or most of the features in that particular molecule were indeed present in the training set. With values as “poor” and “bad” instead, the prediction should not be considered valid due to the fact that the molecule has features in regions (3D spatial point of the molecule) that the model has not seen before. The model is then not trained to understand the requirement for the activity in those regions, hence is not able to predict the activity. For example, the molecule may extend in a new direction. The model does not know anything about the requirements for activity in that region and therefore may predict a high activity for the molecule.

### 5.3 Scaffold hopping

To assess the possibility of enlarging the chemical diversity of designer benzodiazepines, MedChem and Scaffold Replacement studies were conducted. Roughly 4000 results were generated when the calculation were carried out taking into consideration only the steric hindrance of the receptor’s binding pocket for each of the transformations (Figure 4.17). Hence to generate more informed results, decision was taken to include the electrostatic properties of both the receptor and ligand into the study. The latter were assessed with the use of the pharmacophore editor function in MOE®. The following pharmacophore features were identified: an aromatic/hydrophobic feature in correspondence of the pendant phenyl which engages in an arene-hydrogen bond with His102, an interaction proven essential for receptor activation (Amundarain et al., 2021; Wieland et al., 1992); two hydrophobic features on the receptor pocket in proximity of Tyr160 and Tyr210 (Figure 5.6a) (Richter et al., 2012); an aromatic/hydrophobic feature at the centre of the benzene ring fused to the diazepine, the importance of which was previously reported (Catalani et al., 2021b; Davies et al., 2002; Sigel et al., 1998; Sigel and P. Luscher, 2012) (Figure 5.6b); an hydrophobic feature in proximity to the chlorine atom, the presence of which has been proven to increase the activity; and the acceptor feature on the C=O of the diazepine together with the feature identified by the oxygen lone pair projection on the receptor in proximity of Ser205 and Ser206 (Figure 5.6C).

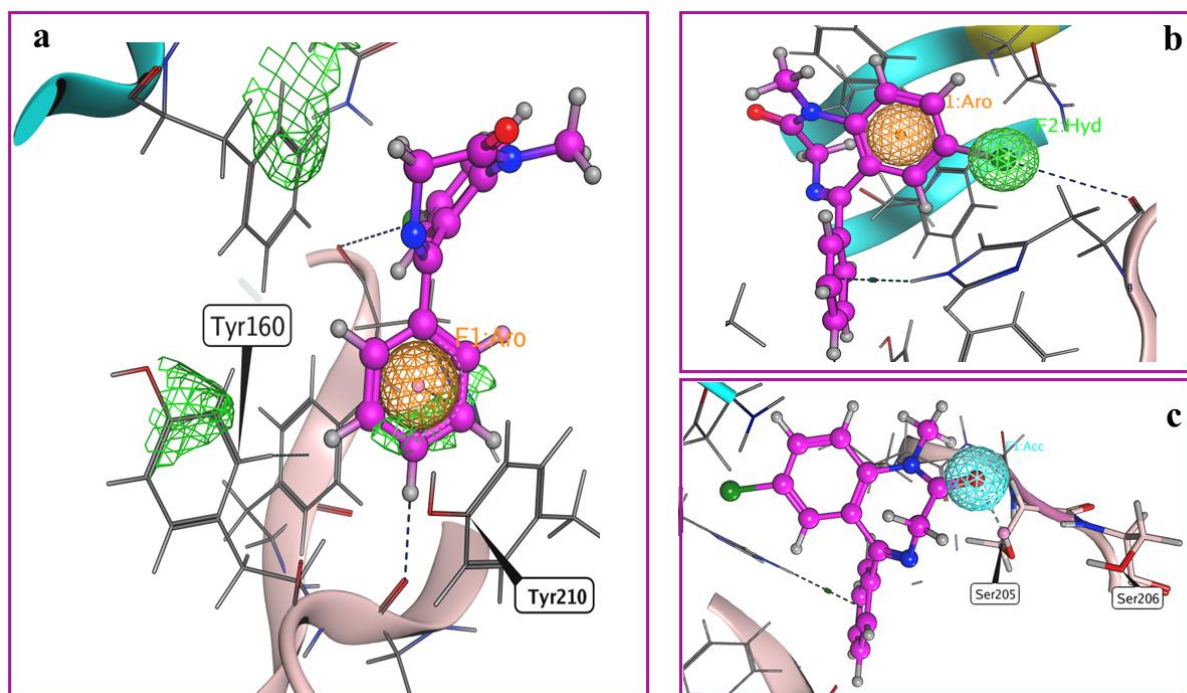


**Figure 5.6** Ligand pharmacophore features taken into consideration for the scaffold hopping exercise.

*The coloured spheres represent the pharmacophore features. The hydrophobic and aromatic features are presented in orange, while the H bond acceptor feature is presented in light blue. The electrostatic properties of the binding pocket are also presented: in green the hydrophobic, in red the H-bond acceptor and in blue the H-bond donor<sup>8</sup>*

The scaffold hopping studies performed taking into consideration the pharmacophore features just described, produced 477 results (364 Scaffold replacement and 113 MedChem, respectively). For the obtained structures, the inclusion in the applicability domain (AD) was automatically assessed by Forge™ through the “distance to model” function. Those structures flagged as outside the AD (57% of the Scaffold Replacement) were discarded. Only the top scoring modifications are reported in Figure 5.7.

<sup>8 8</sup> The figure has been published in Catalani V, Floresta G, Corkery JM, et al. (2022) In silico studies on recreational drugs: 3D-QSAR prediction of classified and de novo designer benzodiazepines in *Chemical biology and drug design*

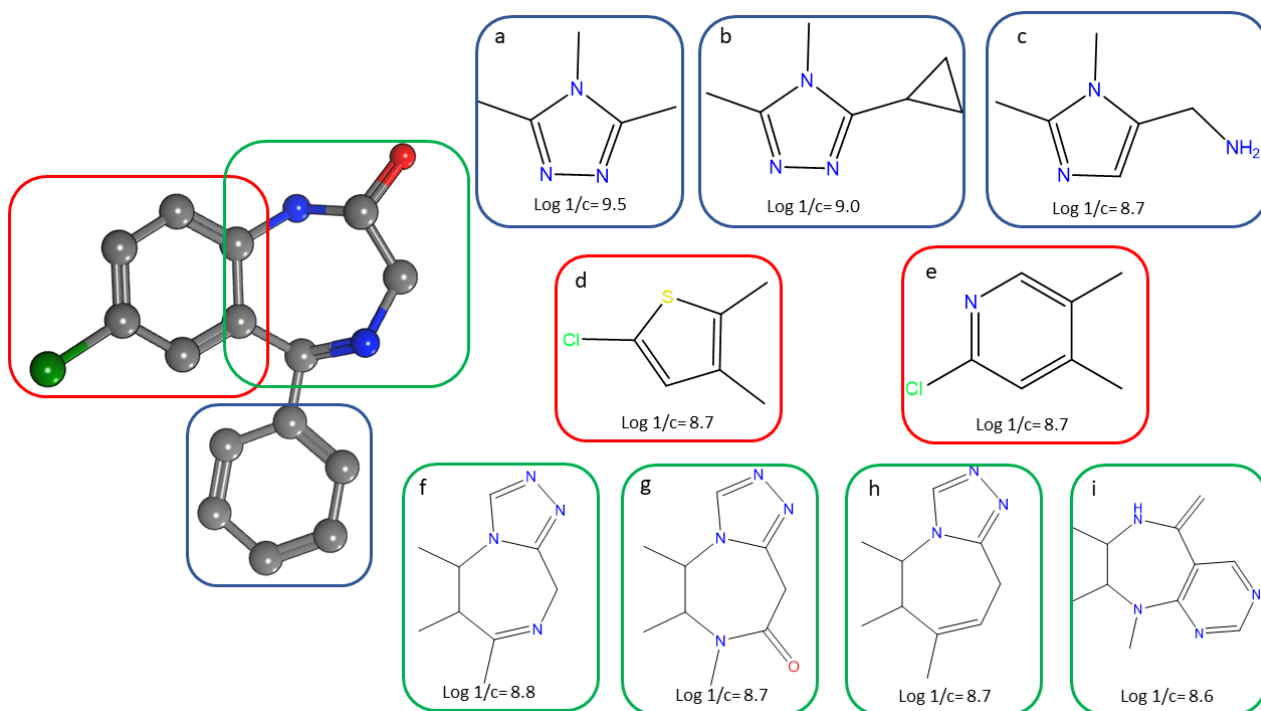


**Figure 5.7 MedChem and Scaffold Replacement top scoring moieties**

**The top scoring moieties are: (a, b) triazole; (c) imidazole; (d) triazole; (e) pyridine; (f, g, h) triazolobenzodiazepines; (i) pyrimidine<sup>9</sup>**

The top scoring moieties suggested as replacement by MOE® include some well-known DBZD scaffolds, as the triazole (Figure 5.7h), and thieno (6d) moieties. These two moieties have been identified, according to UNODC reports, in the majority of novel DBZDs recently identified (e.g. clonazolam, etizolam, flualprazolam, flubromazepam, flubromazolam) (UNODC, 2021b, 2020b). This finding is extremely important because it suggests that computational studies are reliable and could be used to predict future NPS scaffolds together with their biological activity.

However it should be noted that the molecule with the highest values of predicted  $\log 1/c$  obtained with these studies were those which applied transformation on the pendant phenyl ring. The latter was replaced by other aromatic five-membered rings, which matched the pharmacophore feature previously identified (Catalani et al., 2021b). The five-membered rings that showed the highest predicted activity values were the 1,3,4-triazole (Figure 5.7a, 5.7b), and the imidazole (5.7c). Interestingly, the binding pocket cavity that accommodates the pendant phenyl is very narrow and leaves very little room for chemical modification/growth. Indeed, SAR studies in the literature report how meta- and para- substitutions (small groups) on the ring are not beneficial for the activity (Davies et al., 2002; Hadjipavlou-Litina and Hansch, 1994). The suggestion/prediction that the use

<sup>9</sup> The figure has been published in Catalani V, Floresta G, Corkery JM, et al. (2022) In silico studies on recreational drugs: 3D-QSAR prediction of classified and de novo designer benzodiazepines in *Chemical biology and drug design*



of a smaller aromatic ring could increase the activity is indeed very interesting for further chemical space investigation. As per Figure 5.8a, the five-membered ring seems to still be able to engage in the hydrophobic interaction with His102. Moreover, the reduced size of the pendant moiety gives opportunity for a greater number of ring substitutions, either in position two or five of the triazole.

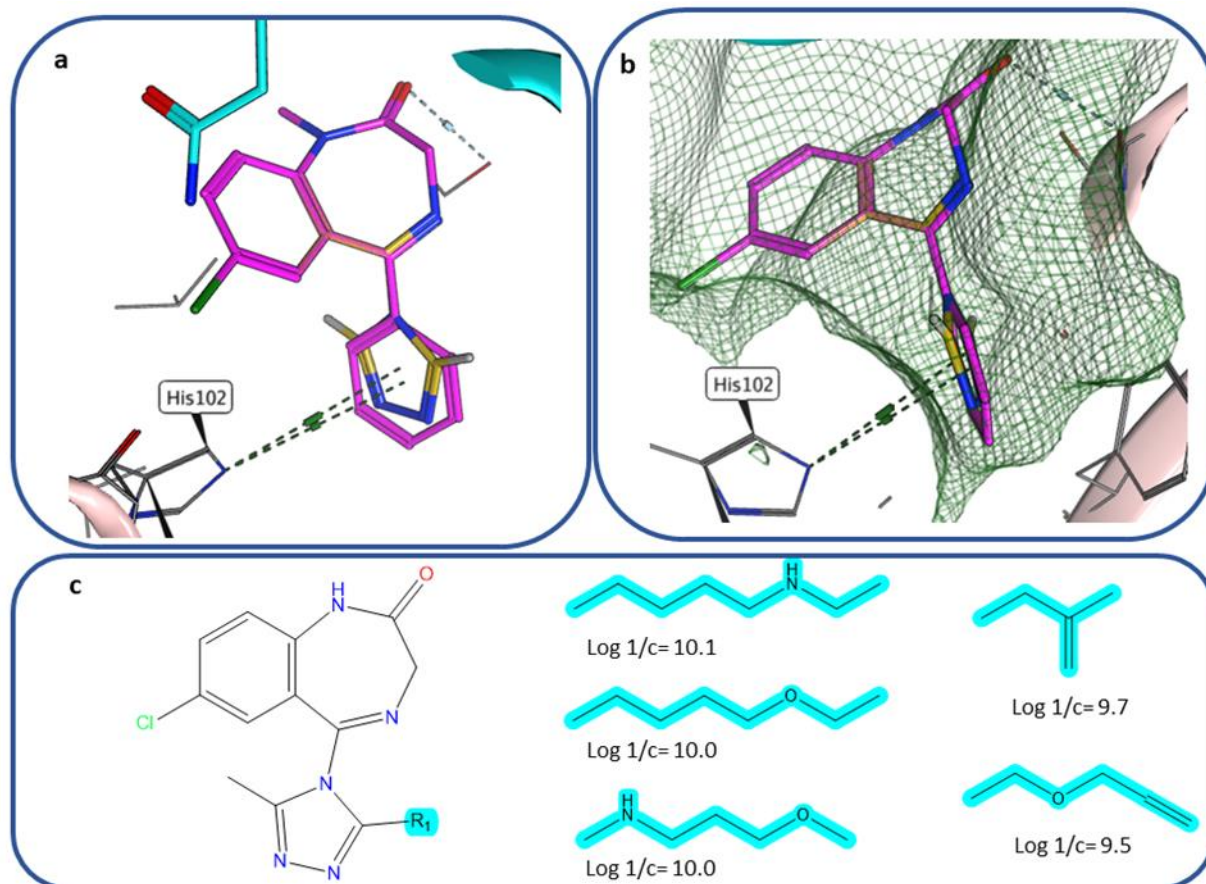


**Figure 5.8** 3D representation of the new scaffold created for DBZDs.

*Its adopted conformation inside the binding pockets which maintains the hydrophobic interaction with His102 is presented; b) same representation with the addition of the vanderWaal interaction surface which shows how narrow is the portion of the pocket which host the pendant aromatic ring; c) the predicted activities retrieved from “Add Group to Ligand” exercise on the C2 of the triazole pendant ring (R1)*



It should be noted that the substitution with a bulky chain (hydrophobic, more favourable) is preferred only at position 2 due to the steric hindrance of the receptor creating a very tight pocket near position 5 (Figure 5.8b).

Further substitutions in position 2 were explored with the “Add Group to Ligand” function in MOE®. A very high number of entries (> 2000) was generated and analysed. Among them, some high biological activities ( $\log 1/c \Rightarrow 9.5$ ) were predicted. Examples are shown in Figure 5.8c.

A set of halogenated substituents (that is, Br, Cl, F, CF<sub>3</sub>, etc.) in R<sub>1</sub> (Figure 5.8c) was also investigated but returned lower predicted biological activities ( $\log 1/c \Leftarrow 8.0$ ). The results obtained suggest that changes in the benzo or diazepine moieties of the molecule may have a smaller impact on biological activity compared to modification of the pendant phenyl. In fact, the new scaffolds for series 1-2 (Figure 4.18) show  $\log 1/c$  values lower than 9, suggesting still a high predicted biological activity, but more in line with the DBZDs currently on the market. Instead, a new scaffold for series 3 suggests the possibility of creating very potent DBZDs,  $\log 1/c$  values higher 9.5, for which the harm risk should be assessed.

## 5.4 Molecular docking

The 102 DBZDs identified by NPSfinder<sup>®</sup>, were docked as described in section 4.3.8. In particular those DBZDs showing the triazole moiety were docked in PDB6HUO using the pharmacophore placement in Figure 4.15, while the others were docked in PDB6X3 using the one in Figure 4.16. The S value for a set of high potency benzodiazepines (sec. 4.3.8) was calculated as a reference. This set included alprazolam and diazepam (co-crystallised ligands), and the obtained S values were used as a reference for good binding affinity towards PDB6HUO and PDB6X3X.

*Table 5.8 S values obtained via the pharmacophore constraint docking for the reference compounds*

Molecule	6HUO S (Kcal/mol)	6HUO rmsd	6X3X S (Kcal/mol)	6X3X rmsd
Triazolam (Halcion)	-7.2	1.4	-7.2	0.4
Lorazepam (Ativan)	-6.5	1.5	-6.8	1.4
Clonazepam (Klonopin)	-7.2	1.8	-7.2	2.1
Flunitrazepam (Rohypnol)	-7.4	1.2	-7.4	2.7
Alprazolam (Xanax)	-7.0	1.2		
Diazepam			-6.6	1.0

For each molecule, several conformations with different S values (Kcal/mol) were returned. The ones showing the lowest S value (i.e., the lower the value, the more potent the binding) as well as the interaction with His102 were identified. The rmsd value was taken into consideration as well, during the analysis of the docking pose choice. This value measures the root mean square deviation between the pose before refinement and the pose after refinement, giving an idea of how the refined pose is close to the one suggested by the docking superposition points (i.e. co-crystallised ligands). In other words, it is a measure of how much a molecule needs to be constrained to occupy a particular spatial conformation in the binding pocket, i.e. how energetically favoured a pose is. The obtained S values are reported in Appendix A. For brevity, here are presented only the S values obtained for those DBZDs predicted by the 3Q QSAR model as the most biologically active (sec. 5.2.2.).

**Table 5.9** The predicted binding affinity values of the ten DBZDs predicted to display the higher biological activity in Forge™.

Title	3D Field QSAR	Distance to model	S (Kcal/mol)	rsmd
Flubrotizolam	9.6	Excellent	-7.1	1.3
Clonazolam	9.5	Excellent	-7.2	1
Pynazolam	9.4	Good	-7.7	0.9
Fluclozizolam	9.1	Excellent	-6.5	1.6
MP-III-022	9.1	Good	-5.6	1.8
Ro 09-9212	9	Excellent	-5.4	0.9
Ro 15-9270	8.9	Good	-7.1	2
3-Hydroxyphenazepam	8.9	Excellent	-6.6	1.2
Flunitrazolam	8.8	Excellent	-7.8	0.8

It is important to clarify here that QSAR and docking studies are not necessarily linearly correlated, hence a high biological activity does not necessarily correspond to a high binding affinity and vice versa (Chen, 2015). Furthermore, the prediction of the binding affinity for a particular substance per se does not give much information about the molecule/receptor interaction (e.g., agonist; partial agonist; antagonist) activity. However, docking results can be used to support QSAR analysis, hence, the predicted binding affinity values of the ten DBZDs predicted to display the highest biological activity via the use of Forge™ 3D QSAR models, (Table 5.9) were further analysed. When compared with the docking S values obtained for alprazolam (S= -7.0) and diazepam (S = -6.6), the majority of these DBZDs display a lower S value (i.e. better affinity). These results suggested satisfactory binding affinity levels for the  $\alpha 1\beta 2\gamma 3$  human GABA-AR. One should note that, as per the literature, the majority of these compounds display the triazole moiety, identified already as a chemical characteristic responsible of increasing the biological activity (sec 4.2.5). Only two of them, MP-III-02 and Ro 09-9292 showed higher value suggesting a lower binding affinity. The low value of binding affinity of MP-III-02 is in line with its activity, as reported in literature, as a positive allosteric modulator of GABAA receptors containing the  $\alpha 5$  subunit. A more in-depth evaluation of each of the ten top scoring DBZDs is reported in Section 5.6 (Stamenić et al., 2016).

While the docking can give an evaluation of the binding affinity, no specific information on the actual agonist/antagonist role of these DBZDs can be extrapolated, even though the docking was performed using the active conformation of two agonist BZDs as superposition points (alprazolam and diazepam).

The poses of the top ten DBZDs docked in PDB6X3X and PDB6HUO are reported in Figure 5.9.

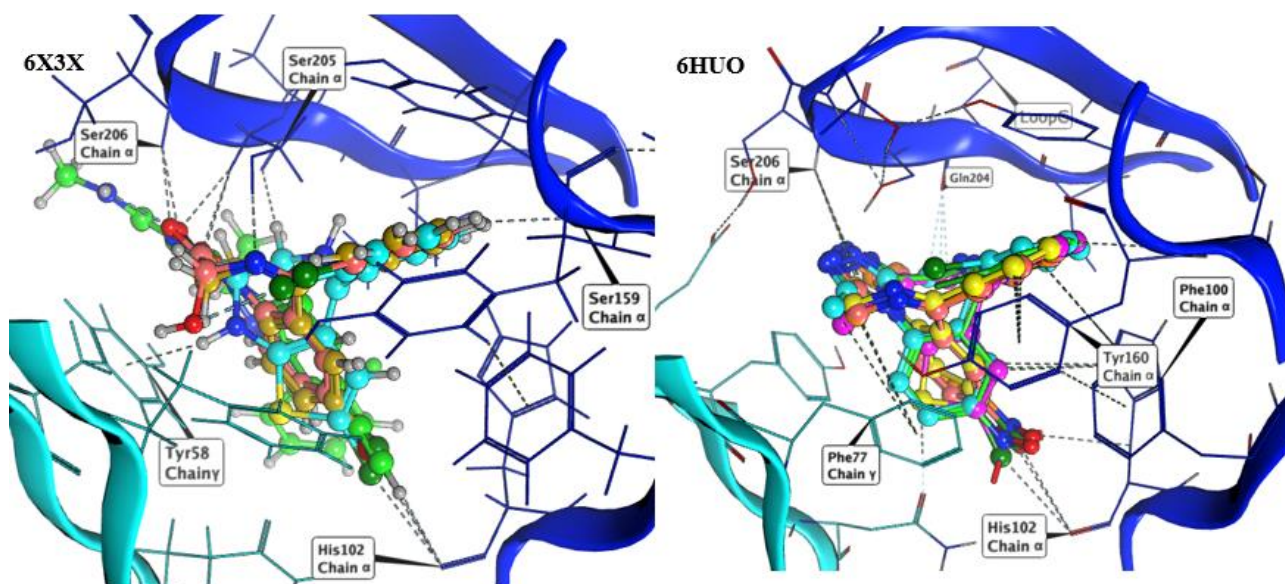


**Figure 5.9** The poses of the top ten DBZDs docked in PDB6X3X and PDB6HUO

For each of the poses generated for the 102 DBZDs a PLIF was calculated and analysed. The analysis of the PLIFs is presented below.



**Figure 5.10** Visual representation of the interactions (potential contacts) between the 102 DBZDs and the residues of the binding pocket of PDB6HUP.

This figure represents the interactions between the molecules and the receptor pocket with the use of barcodes. The number of bars is proportional to the frequency of the interactions with that ligand, suggesting how much a ligand is involved in the binding. On the horizontal axis the binding pocket's residues involved in the interactions are represented in different colours. The colours are randomly assigned. On the vertical axis the molecules docked, i.e. involved in the interaction, are represented by grey and white lines. A black bar is drawn every time a molecule interacts with a receptor residue.

This representation is called the barcode display and represents the entries (DBZDs) and the selected fingerprints as a matrix in which a set bit is drawn as a black rectangle. On the X-axis are displayed the numbers and code for those residues which are involved in the interaction with the ligands. The number of black rectangles displayed for each residue are a measure of the frequency

of the interactions with that ligand, i.e the higher the number the higher the frequency. The letter which is included next to the residue numbers represents the chain to which the residue belongs.

The results presented in Figure 5.10 and Figure 5.10 are able to confirm the importance of the  $\alpha$ His102 residue ( $\alpha$  chain) for the binding of DBDZs as observe for the classical BDZs (Wieland et al., 1992). The other residues which seems to be more often included in the ligand interactions are  $\alpha$ Ser205 and  $\alpha$ Ser206, the importance of which has been reported in the literature. (Masiulis et al., 2019; Sigel and Ernst, 2018). Other interactions include  $\gamma$ Tyr58,  $\gamma$ Phen100,  $\alpha$ Ser159 and  $\alpha$ Gln204. The analysis of the PLIF confirm that the pattern of ligand interactions between the GABA-AR and DBZDs highly resemble those identified for Alprazolam and Diazepam.

Docking results can be extremely useful in assessing the way a ligand interacts with the residues of the binding pocket of the GABA-R (Sec 4.3.8). As reported in Figure 5.10 the majority of the interactions involve the  $\alpha$  subunit of the GABA-AR binding pocket, and in particular the residue His102 ( $\alpha$  subunit), via hydrogen bonds usually with DBZDs halogenated substituents (C2'). Another hydrogen bond interaction, namely with Ser 206 and Ser 205 ( $\alpha$  subunit) seem to be a recurrent one as well as the aromatic interaction ( $\pi$ - $\pi$ ) with Tyr 58 ( $\gamma$  subunit). Although the receptor residues involved in the binding tend to stay consistent across the different DBZDs, the moiety of the molecule to which they bind seems to change according to the spatial pose of the latter. The presence of a side-chain substituent or an additional/diverse fused ring on the main core structure (e.g., triazolo, thiophene) seems to in-fluence the orientation and positioning inside the pocket resulting in a change of the interaction pattern (Figures 5–8).

This is observable when comparing, for example, alprazolam with Ro 09-9212 (Figure 5). The presence of a thiophene ring seems to shift the molecule in the binding pocket, and the repositioning seems to be driven by the hydrogen bond between the S atom of Ro09-9212 and the Tyr 160. This results in an aromatic interaction between the pendant phenyl ring and Tyr 58, a hydrogen bond between the halogen substituent and the Ser 159, instead of the HisIS102, and a further hydrogen bond between N1 and Thr 142. This change in residue interaction can be observed as well when compounds are docked in 6X3X.

Further molecular dynamics analysis will need to be conducted to understand if this different interaction pattern will be observable for new DBZDs showing side chain substituents (Noha et al., 2017; Sliwoski et al., 2014).

## 5.5 Pharmacophore mapping

The conformations obtained in the docking studies were used to produce a pharmacophore query. The conformations were aligned as per Section 4.3.9, including the structure docked both in

PDB6HUO and PDB6X3X. Two pharmacophore queries were generated (Figure 5.11) as described in Section 4.3.9, with the pharmacophore editor application used in the consensus mode.

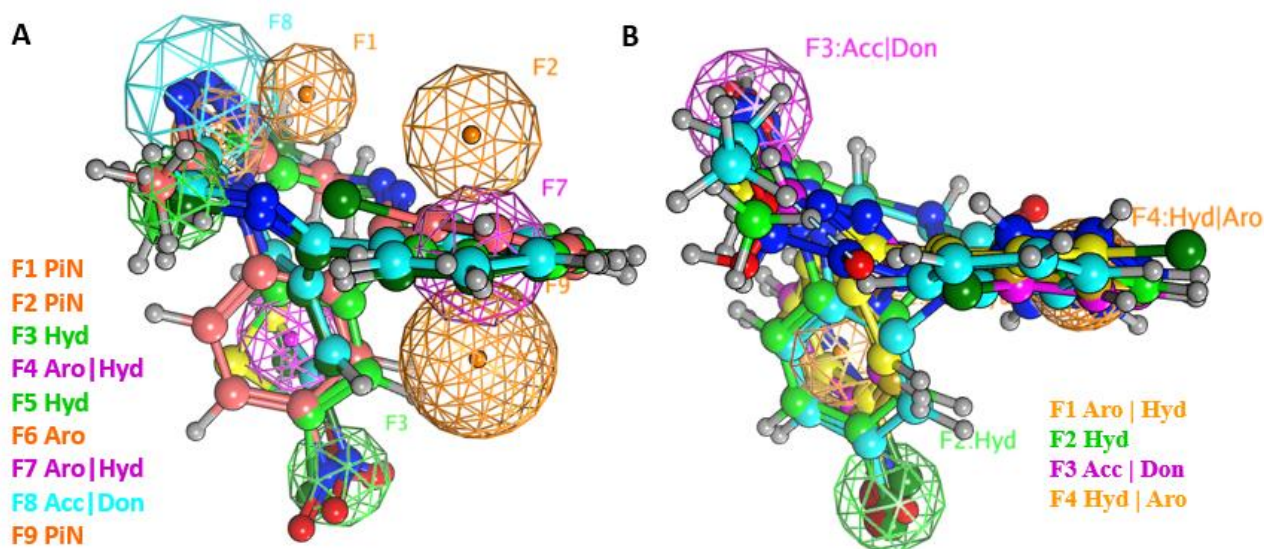


*Figure 5.11 Pharmacophore maps generated on the DBZDs alignment*

One pharmacophore query (Figure 5.11A) includes all the features which were found to be common to the top ten DBZDS (i.e. more detailed), the other (Figure 5.11B) includes all the features which were common to the larger DBZDs database (i.e. less detailed). This is reflected on the fact that to a higher number of structures correspond a smaller number of common features. Despite a slightly difference when comparing the features identified in proximity of the triazole moiety, an Acc group vs an Acc/Donor (Figure 5.11), the two pharmacophore maps both highlight the importance of two big aromatic functions and one hydrogen bond acceptor function. The aromatics features were identified in correspondence with the benzodiazepine ring the pendant phenyl ring, and the hydrogen bond acceptor in position C7.

These pharmacophore maps support the 3D Field QSAR results (Figure 5.5 and the importance of the hydrophobic van der Waals surface area (aromatic functions in Figure 5.11), and the polar van der Waals surface area (hydrogen bond acceptor and donor functions in Figure 5.11) in defining the biological activity of a DBDZ (Thakur et al., 2004). The identified pharmacophore highlighted the recurring presence of both two big aromatic groups and an hydrophobic acceptor areas in those molecules showing good receptor binding affinity levels and high biological activity (Sigel and P. Luscher, 2012).

The pharmacophore queries so generated were validated with the use of the QSAR dataset (77 molecules) and the pharmacophore search application. Pharmacophore A was able to match only a total of 7 out of 77 molecules (9%), while pharmacophore B matched a total of 66 out of 77 (86%). The results are in line with the way the two pharmacophores were built, and suggest how the use of

pharmacophore A, i.e a more detailed one, could be useful in the screening of big libraries (millions of compounds) to obtain new lead compounds in the quest for new GABA-AR allosteric modulator. It has indeed been used, so far to filter two databases from Zinc15, the of ion channel ligands (25376 entries) and the G-protein-coupled receptors (*GPCR*)-A ligands ([127728](#) entries). Of the total 46058 entries only a total of 12 among the ion channel ligands and 4 among the *GPCR*-A ligands were found to match the pharmacophore A (Appendix A). Further studies, starting with docking, will be necessary to assess their potential as GABA-AR binders (please see Chapter 10 Future work)

## 5.6 Profiling of the ten DBZDs with the highest predicted biological activity

### 5.6.1 Flubrotizolam

Flubrotizolam is the DBZDs predicted to have the highest biological activity, i.e.  $\log 1/c = 9.6$ . The docking results ( $S = -7.1$ ) seems to support this result, suggesting a strong affinity towards the  $\alpha 1\beta 3\gamma 2$  GAB-AR. The molecule is a thienotriazolodiazepines for which limited data are available. Never approved as a medication, it seems to be available for forensic and research application only (Weber et al., 1977). It was identified online by the web crawler activity (Catalani et al., 2022, 2021b) but is not yet reported by the UNODC or the EMCDDA. Its values of predicted biological activity and binding affinity for the  $\alpha 1\beta 3\gamma 2$  GAB-AR suggest how this molecule has the potential to be a high potency DBZD. The molecule has been discussed online in drug fora since 2021 and is better known as 'Fanax'. The *in silico* findings seem to be supported by what reported online. Flubrotizolam is indeed commercialised and marketed as four to five times more potent than etizolam ("Buy FANAX - Flubrotizolam | Chemical Planet," n.d., "Buy Flubrotizolam (Fanax) 2mg Pellets," n.d.). Anecdotal reports suggest how this molecule is predominantly a strong sedative/hypnotic and muscle relaxant with no euphoric effects. Reported potencies varies, but the general consent is that it seems to be slightly more potent than etizolam and in any case not recommended to get the "down" feel associated with the other DBZDs. The predicted interactions between flubrotizolam and the GABA-A allosteric binding site are presented, in detail, in Figure 5.12. The bromine atoms at the C7 position interacts via a hydrogen bond donor with the  $\alpha 1$ His102 side chain, which is the fundamental residue for the BDZs activity on the GABA-AR. All the other interactions, apart from the one with Phe77, as seen for alprazolam (Sec 4.3.8) are here identified as well. include arene-arene interactions with Tyr58 ( $\gamma$  chain), the hydrogen-arene interaction with Phe77 ( $\gamma$  chain) and Tyr160 ( $\alpha$  chain) and the hydrogen bond with Ser159 ( $\alpha$  chain).



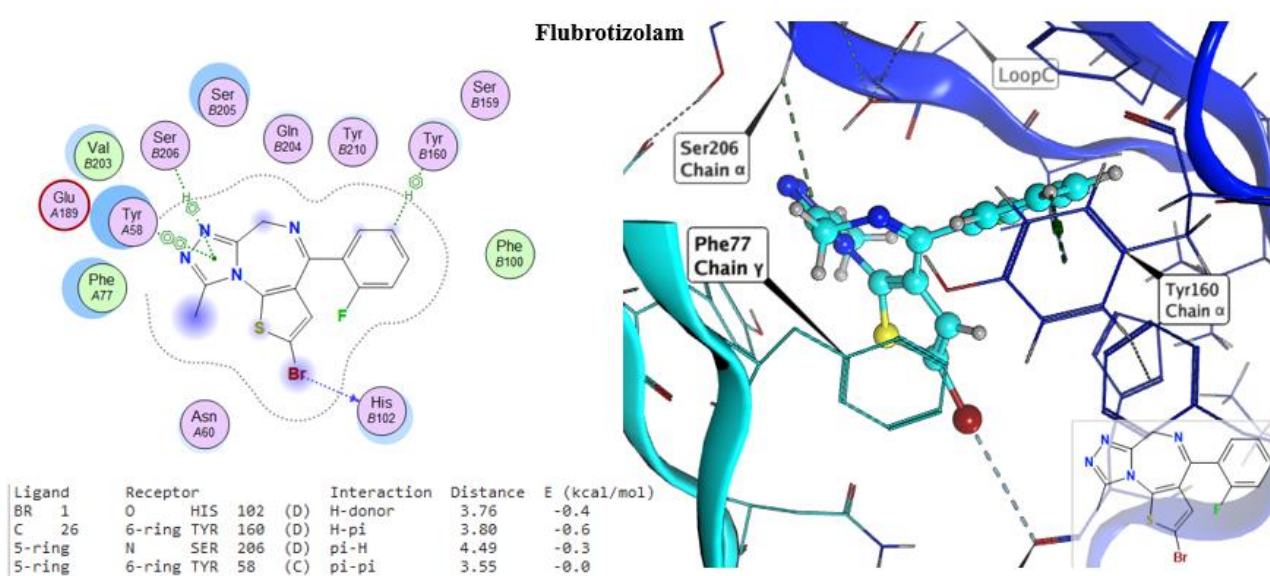


**Figure 5.12 Flubrotizolam interactions 3D and 2D representations.**

**Notes:** on the right, the binding pocket 3D representation with the docked ligand flubrotizolam (light blue). The light blue portion represents the  $\gamma$  subunit of the receptor whilst the dark blue the  $\alpha$  subunit. On the left, the 2D representation of the binding pocket and a report of the interactions between receptors residues and ligand are provided. Letter D identifies the  $\alpha$  chain and C the  $\gamma$  chain. The colours used to depict the residues in the 2D screenshot define different characteristics of the latter: light purple for polar residues and light green for hydrophobic ones; red circle indicates an acidic and blue a basic residue; and the light blue halo indicates solvent exposure both on the receptor and the ligand.

### 5.6.2 Clonazepam

Clonazepam is the DBZDZ predicted as the second most potent by the 3D QSAR models (Log 1/c= 9.5). It is the most potent of a series of triazolobenzodiazepines first reported in 1971 (Hester et al., 1971). It was never marketed and recently sold as a DBZDs, in particular as counterfeit prescription for diazepam and alprazolam (WHO, 2020a). Structurally, it is the chlorine (in the ortho position of the pendant phenyl) analogue of flubromazepam, with the addition of a nitro group on the C8 (Figure 5.13). Scheduled under schedule IV of the Convention on Psychotropic Substances (1971) in 2021 by the Commission on Narcotic Drugs (UNODC, 2021f), clonazepam is classified as a strong sedative. Due to its extremely high potency, it is often consumed on blotter paper or in liquid form (Orsolini et al., 2020). Indeed, due to its microgram-range potency, the use of powders is not recommended. Common side-effects of clonazepam poisoning include drowsiness, lethargy, slurred speech and tachycardia, strong sedation and multi-day blackouts (Orsolini et al., 2020). Between 2014 and 2017 the National Poison Data System (USA) reported clonazepam in 21% of BZD-related intoxications (Carpenter et al., 2019). Online, clonazepam is often referred to as “the beast” or “the heroin of benzodiazepines”. Serious episodes of blackouts are reported as well on drug discussion forums, where users despite the negative perception of this drug “keep coming back” and highlight the strong dependence and abuse potential of these DBZDs (reddit, 2018a). The predicted interactions between clonazepam and the GABA-A allosteric binding site are presented, in detail, in Figure 5.13. The NO<sub>2</sub> group in position C7 interacts via a hydrogen bond donor with the  $\alpha$ 1His102 side chain, which is the fundamental residue for the BDZs activity on the GABA-AR. All the other interactions, as seen for alprazolam (Sec 4.3.8), i.e. arene-arene interactions with Tyr58 ( $\gamma$  chain), the hydrogen-arene interaction with Phe77 ( $\gamma$  chain) and Tyr160 ( $\alpha$  chain) and the hydrogen bond with Ser159 ( $\alpha$  chain) are here identified as well. In addition clonazepam displays a hydrogen bond with Gly204 ( $\alpha$  chain), arene-arene interactions with Tyr210 ( $\alpha$  chain), and a hydrogen-arene interaction with Phe100 ( $\alpha$  chain). The increased number of interactions may translate in an increase stability of the binding complex and in an increase biological activity.

### Clonazepam

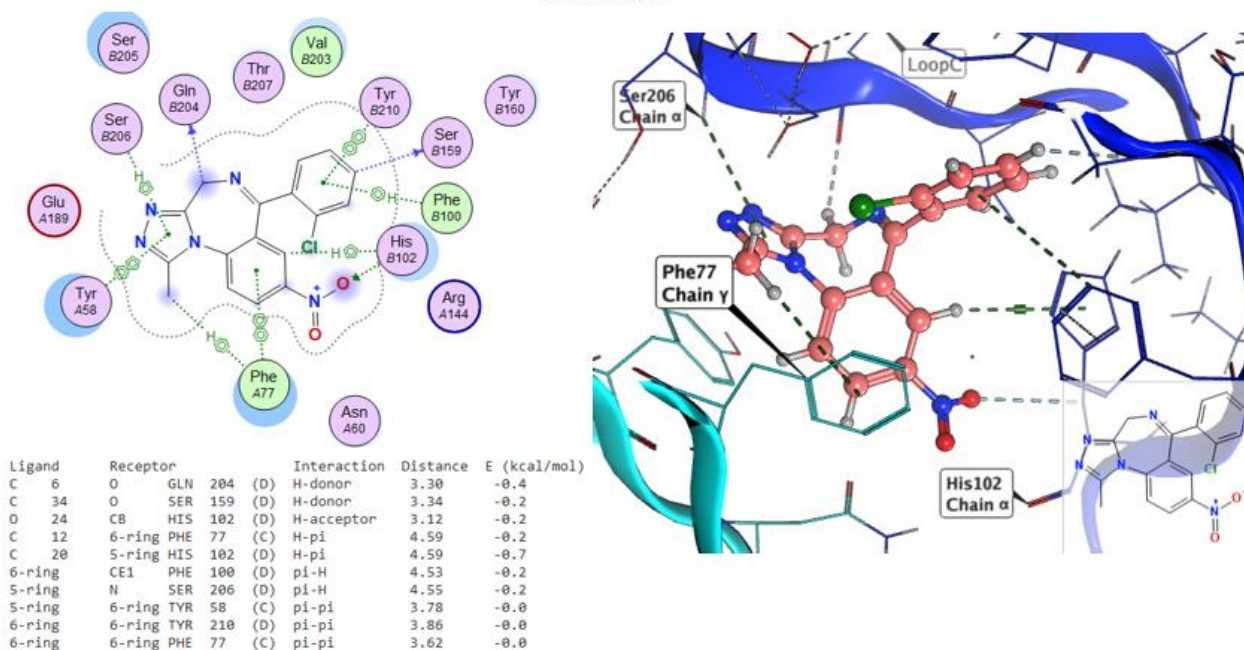


Figure 5.13 Clonazepam interactions 3D and 2D representations.

Notes: on the right, the binding pocket 3D representation with the docked ligand clonazepam (pink). The light blue portion represents the  $\gamma$  subunit of the receptor whilst the dark blue the  $\alpha$  subunit. On the left, the 2D representation of the binding pocket and a report of the interactions between receptors residues and ligand are provided. Letter D identifies the  $\alpha$  chain and C the  $\gamma$  chain. The colours used to depict the residues in the 2D screenshot define different characteristics of the latter: light purple for polar residues and light green for hydrophobic ones; red circle indicates an acidic and blue a basic residue; and the light blue halo indicates solvent exposure both on the receptor and the ligand.

### 5.6.3 Pynazolam

Pynazolam is another DBZD predicted to have a strong biological activity (9.4) towards the  $\alpha 1\beta 3\gamma 2$  GABA-AR and a strong binding affinity ( $S = -7.7$ ). The docking results seems to support the QSAR prediction, suggesting a strong affinity towards the  $\alpha 1\beta 3\gamma 2$  GABA-AR. Pynazolam is a thienotriazolodiazepine for which very limited data are available. First described in the US-3970664-A patent for the novel preparation of triazolobenzodiazepines (Sternbach and Walser, 1972), it was never approved as a medication and seems to be available for forensic and research application only. It seems to be mainly discussed in online fora as per flubrotizolam. When discussed by users, pynazolam recreational use is associated with a good “high” and euphoria similar to that of alcohol, with scarce hypnotic/sedating effects (reddit, 2018b). The majority of the discussion of the drugs fora seem to date back to 2016, suggesting that this DBZD could have had appeared on the market already, without being identified by either law enforcement or public health relevant stakeholders. The predicted interactions between pynazolam and the GABA-A allosteric binding site are presented, in detail, in Figure 5.14. The  $\text{NO}_2$  group in position C7 interacts via a hydrogen bond donor with the  $\alpha 1\text{His}102$  side chain, which is the fundamental residue for the BDZs activity on the GABA-AR. All the other interactions, as seen for alprazolam (Sec 4.3.8), i.e. arene-arene interactions with Tyr58 ( $\gamma$  chain), the hydrogen-arene interaction with Phe77 ( $\gamma$  chain) and Tyr160 ( $\alpha$  chain) and the hydrogen bond with Ser159 ( $\alpha$  chain) are here identified as well. No other interaction was identified.

### Pynazolam

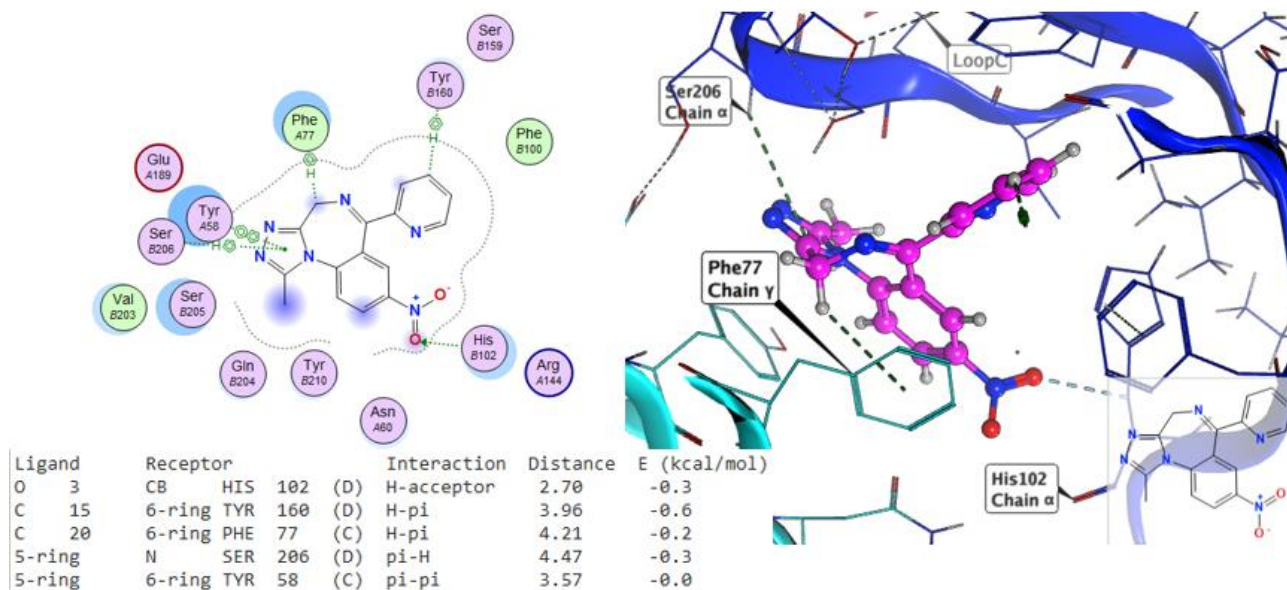
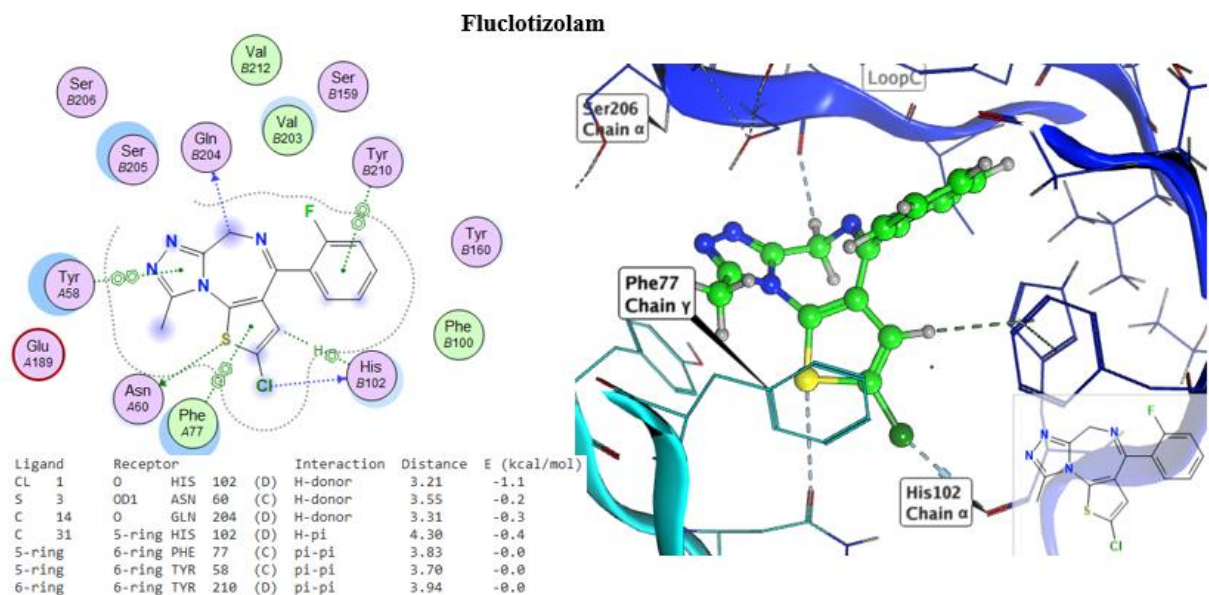


Figure 5.14 Pynazolam interactions 3D and 2D representations.

Notes: on the right, the binding pocket 3D representation with the docked ligand pynazolam (purple). The light blue portion represents the  $\gamma$  subunit of the receptor whilst the dark blue the  $\alpha$  subunit. On the left, the 2D representation of the binding pocket and a report of the interactions between receptors residues and ligand are provided. Letter D identifies the  $\alpha$  chain and C the  $\gamma$  chain. The colours used to depict the residues in the 2D screenshot define different characteristics of the latter: light purple for polar residues and light green for hydrophobic ones; red circle indicates an acidic and blue a basic residue; and the light blue halo indicates solvent exposure both on the receptor and the ligand.

#### 5.6.4 *Fluclotizolam*

Fluclotizolam is a thienodiazepine, having a diazepine ring fused to a thiophene, instead of to a benzene ring. Fluclotizolam was firstly mentioned in a 1974 patent on thienotriazolodiazepines (Binder et al., 1973), but was never marketed. It is not currently a controlled substance under the 1961 Single Convention on Narcotic Drugs. No clinical, pharmacological or toxicological data are reported. Online, it is reported as a recreational DBZD, with euphoric, sedating (enjoyable), disinhibition and sedating property, as observed for pynazolam. The timeline of the discussion goes from 2017 to 2021, suggesting either a long presence on the market or a recent re-introduction (reddit, 2021b, 2017). The predicted interactions between fluclotizolam and the allosteric binding site are presented, in detail, in Figure 5.15. The chlorine group in position C7 interacts via a hydrogen bond donor with the  $\alpha$ 1His102 side chain, as well as with an arene-arene bond, confirming the fundamental residue for the BDZs activity on the GABA-AR. Other interactions, as seen for alprazolam (Sec 4.3.8), i.e. arene-arene interactions with Tyr58 ( $\gamma$  chain), the hydrogen-arene interaction with Phe77 ( $\gamma$  chain) are here identified as well. In addition, fluclotizolam, as noted for clonazolam, displays a hydrogen bond with Gly204 ( $\alpha$  chain). It is interesting to note that the sulfur atoms present in the core scaffold engages as well in a hydrogen bond donor interaction with Asn60, interaction not reported before, which could be responsible for its increase biological activity.



**Figure 5.15** Fluclozotizolam interactions 3D and 2D representations.

*Notes: on the right, the binding pocket 3D representation with the docked ligand Fluclozotizolam (green). The light blue portion represents the  $\gamma$  subunit of the receptor whilst the dark blue the  $\alpha$  subunit. On the left, the 2D representation of the binding pocket and a report of the interactions between receptors residues and ligand are provided. Letter D identifies the  $\alpha$  chain and C the  $\gamma$  chain. The colours used to depict the residues in the 2D screenshot define different characteristics of the latter: light purple for polar residues and light green for hydrophobic ones; red circle indicates an acidic and blue a basic residue; and the light blue halo indicates solvent exposure both on the receptor and the ligand.*

### 5.6.5 MP-III-02

MP-III-02 is an imidazobenzodiazepine for which very few data seem available. It was obtained by the substitution of the ester moiety of the imidazobenzodiazepine SH-053-2'F-R-CH<sub>3</sub> with an amide group, during studies conducted on a series of imidazobenzodiazepines to improve the affinity towards the  $\alpha 5$  GABA-AR (Stamenić et al., 2016). Indeed it showed improved selectivity, efficacy, and kinetic behaviour as a positive modulator of GABAA receptors containing the  $\alpha 5$  subunit (Simeone et al., 2020). MP-III-022 was reported to have an efficacy of 300% at 100 nM in  $\alpha 5\beta 3\gamma 2$  GABA-AR, while being non- ( $\alpha 1$ ) or only weakly modulatory at  $\alpha 2$ - and  $\alpha 3$ -containing receptors (Simeone et al., 2020). These experimental values support the results obtained with the *in silico* approaches. The QSAR model and the docking predictions match the high efficacy with high values of biological activity –  $\log 1/c = 9.1$ , and the non  $\alpha 1$  modulation, with a very low binding affinity value –  $S = 5.6$ . While no data on this DBZD were found online in users forums, one could not exclude the possibility of it being used or commercialised, even under other names or as a counterfeit of classical BZD. The predicted interactions between MP-III-02 and the GABA-A allosteric binding site are presented in detail in Figure 5.16. MP-III-02 seems to interact with the  $\alpha 1$ His102 side chain through its ethynyl group (i.e. -CCH) instead of its fluorine atoms. Other interactions, as seen for alprazolam (Sec 4.3.8), i.e. arene-arene interactions with Tyr58 ( $\gamma$  chain), the hydrogen-arene interaction with Ser205 ( $\alpha$  chain) and an additional interaction with Asp192 ( $\gamma$  chain). The latter has not been reported before.



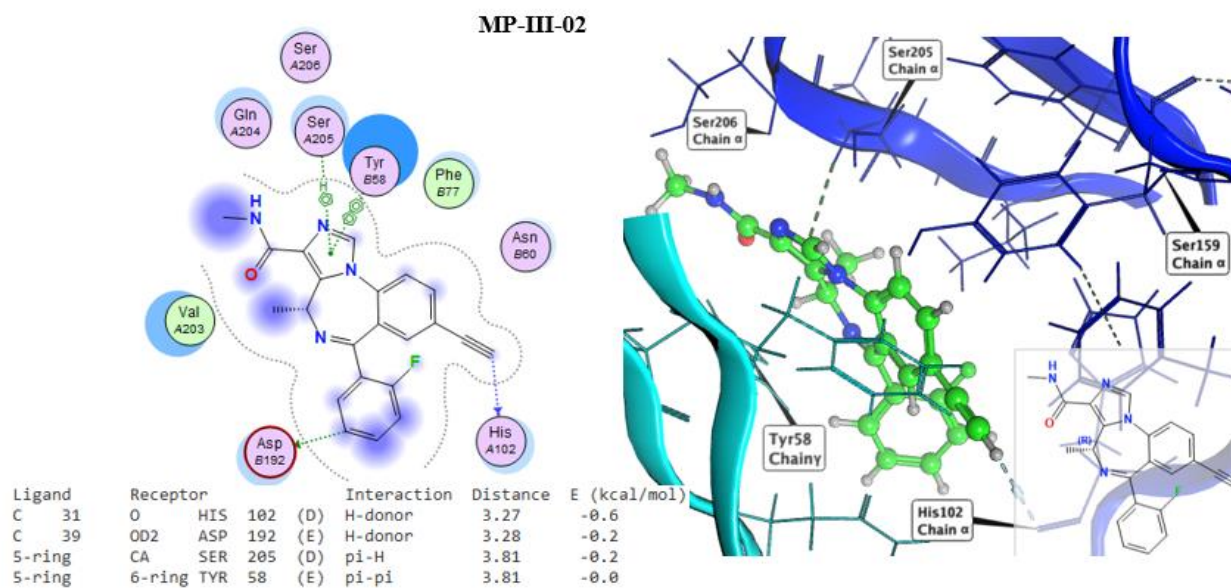


**Figure 5.16 MP-III-02 interactions 3D and 2D representations.**

**Notes:** on the right, the binding pocket 3D representation with the docked ligand MP-III-02 (green). The light blue portion represents the  $\gamma$  subunit of the receptor whilst the dark blue the  $\alpha$  subunit. On the left, the 2D representation of the binding pocket and a report of the interactions between receptors residues and ligand are provided. Letter D identifies the  $\alpha$  chain and C the  $\gamma$  chain. The colours used to depict the residues in the 2D screenshot define different characteristics of the latter: light purple for polar residues and light green for hydrophobic ones; red circle indicates an acidic and blue a basic residue; and the light blue halo indicates solvent exposure both on the receptor and the ligand.

### 5.6.6 Ro 09-9292

Ro 09-9292 is a thienodiazepine derivative which seems to display sedative and anxiolytic effects. The only one reference found on this molecule was in the Hofmann La Roche thienotriazolodiazepine derivatives patent US4155913A (Binder et al., 1974). While no data on this DBZDs were found online in users fora, one could not exclude the possibility of it being used or commercialised, even under other names or as a counterfeit of classical BZDs. The predicted interactions between Ro 09-9292 and the GABA-A allosteric binding site are presented, in detail, in Figure 5.17. As seen for fluclozepam, the chlorine group in position C7 interacts via a hydrogen bond donor with the  $\alpha$ 1His102 side chain, as well as with an arene-arene bond, confirming the fundamental residue for the BDZs activity on the GABA-AR. Other interactions include i.e. arene-arene interactions with Tyr58 ( $\gamma$  chain), the hydrogen bond with Gly204 ( $\alpha$  chain) and Ser205. The lack of the triazole moiety maybe responsible for the missed interaction with Asn60, as seen per fluclozepam.

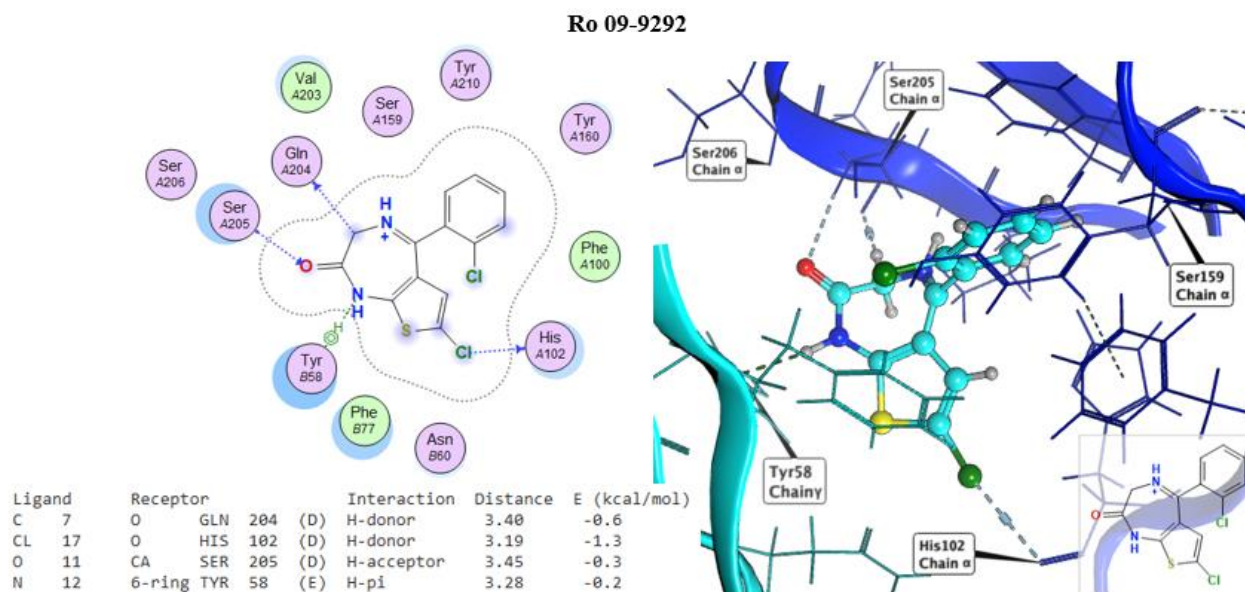


**Figure 5.17** Ro 09-9292 interactions 3D and 2D representations.

*Notes: on the right, the binding pocket 3D representation with the docked ligand Ro 09-9292 (light blue). The light blue portion represents the  $\gamma$  subunit of the receptor whilst the dark blue the  $\alpha$  subunit. On the left, the 2D representation of the binding pocket and a report of the interactions between receptors residues and ligand are provided. Letter D identifies the  $\alpha$  chain and C the  $\gamma$  chain. The colours used to depict the residues in the 2D screenshot define different characteristics of the latter: light purple for polar residues and light green for hydrophobic ones; blue circle indicates a basic residue; and the light blue halo indicates solvent exposure both on the receptor and the ligand.*

### 5.6.7 Ro 15-9270

Ro 15-9270 is a thienodiazepine derivative which seems to display sedative and anxiolytic effects. Only one reference found on this molecule was in the Hofmann La Roche thienotriazolodiazepine derivatives (US4155913A). While no data on this DBZDs were found online in users fora, one could not exclude the possibility of it being used or commercialised, even under other names or as a counterfeit of classical BZDs. The predicted interactions between Ro 15-9270 and the allosteric GABA-A binding site are presented, in detail, in Figure 5.18. The NO<sub>2</sub> group in position C7 interacts via a hydrogen bond donor with the  $\alpha$ His102 side chain, as well as with an arene-arene bond, confirming the fundamental residue for the BDZs activity on the GABA-AR. Other interactions, include arene-arene interactions with Tyr58 ( $\gamma$  chain) and Tyr210 ( $\alpha$  chain), the hydrogen-arene interaction with Ser205 and Ser 206 ( $\alpha$  chain). In addition, Ro 15-9270 as noted for flucotizolam, a hydrogen bond donor interaction with Asn60, is displayed.

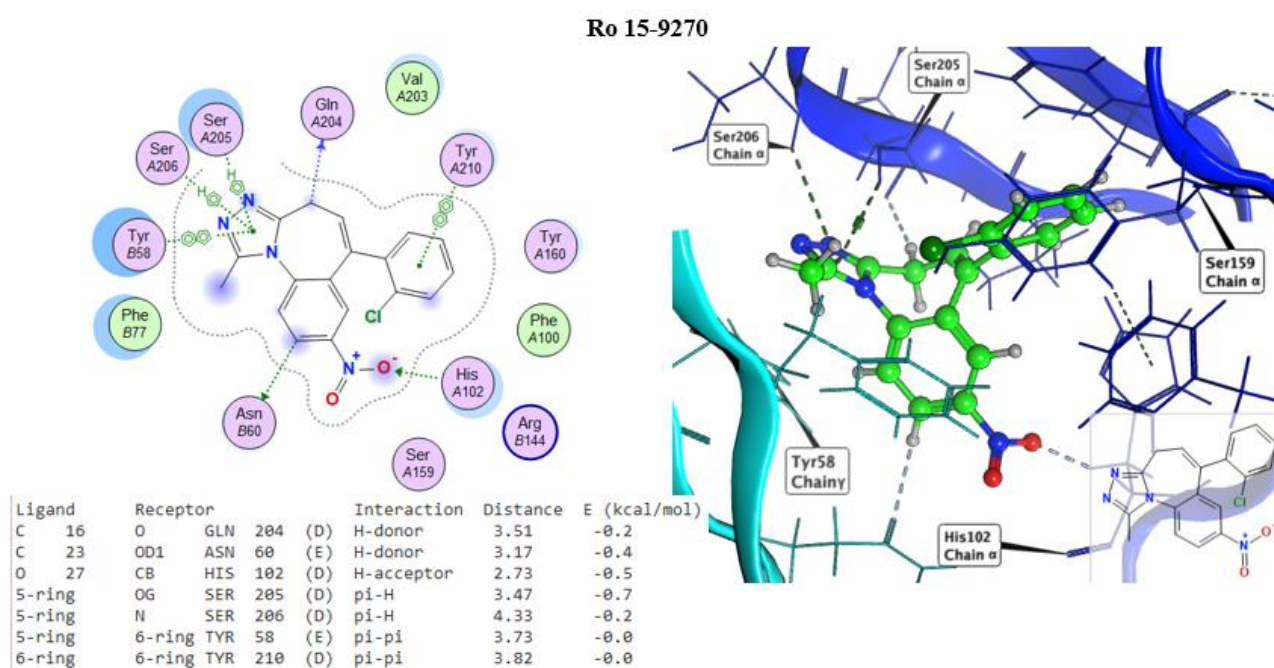


**Figure 5.18** Ro 15-9270 interactions 3D and 2D representations.

**Notes:** on the right, the binding pocket 3D representation with the docked ligand Ro 15-9270 ( green). The light blue portion represents the  $\gamma$  subunit of the receptor whilst the dark blue the  $\alpha$  subunit. On the left , the 2D representation of the binding pocket and a report of the interactions between receptors residues and ligand are provided. Letter D identifies the  $\alpha$  chain and C the  $\gamma$  chain. The colours used to depict the residues in the 2D screenshot define different characteristics of the latter: light purple for polar residues and light green for hydrophobic ones; blue circle indicates a basic residue; and the light blue halo indicates solvent exposure both on the receptor and the ligand.

### 5.6.8 *3-Hydroxyphenazepam*

3-Hydroxyphenazepam is an active metabolite of both phenazepam and cinazepam and acts as a full allosteric modulator of the GABA-AR. Discovered during metabolomic studies, it was never patented and has been sold as a DBZD (Valdman and Sandle, 1986). It is not currently controlled under either the 1971 United Nations Convention on Psychotropic Substances or the 1961 Single Convention on Narcotic Drugs (Orsolini et al., 2020). In comparison with phenazepam it has been reported to have diminished myorelaxant properties, showing however similar sedative, anxiolytic, anticonvulsant and hypnotic properties. It is a very discussed DBZD on drug forums, reported more as an anxiolytic than a euphoric one, with very different effects if compared to the parent drug phenazepam (reddit, 2020, 2018c). The predicted interactions between 3-hydroxyphenazepam and the GABA-A allosteric binding site are presented in detail in Figure 5.19. 3-hydroxyphenazepam engages with the with the  $\alpha$ 1His102 side chain through the bromine atom in position C7, as well as with Ser205 and Ser 206 and Ser159 ( $\alpha$  chain) via hydrogen-bond mediated interaction.

### 3-hydroxyphenazepam

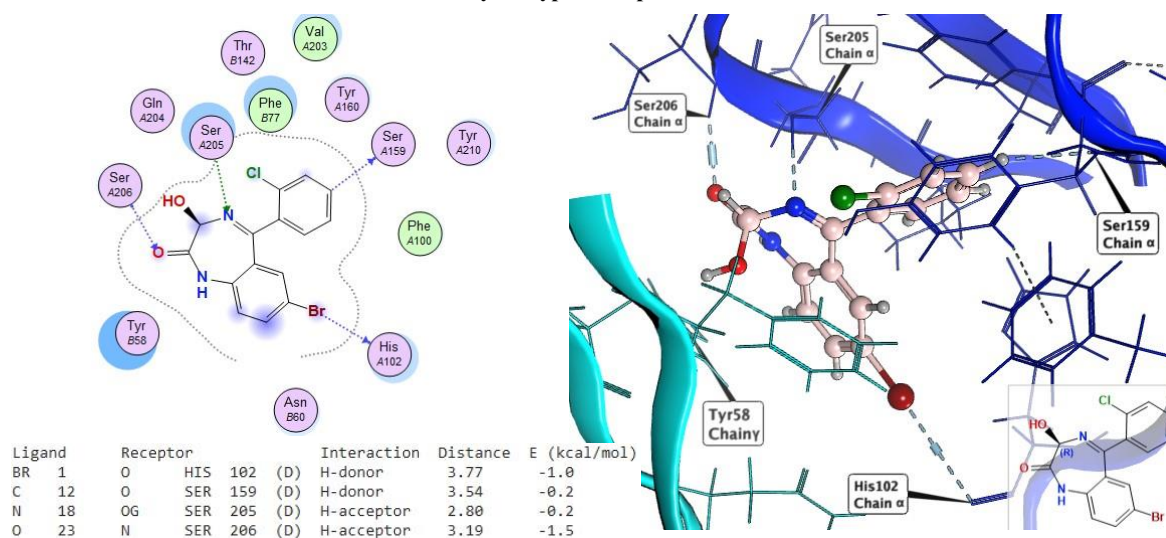


Figure 5.19 3-Hydroxyphenazepam interactions, 3D and 2D representations.

Notes: on the right, the binding pocket 3D representation with the docked ligand 3-Hydroxyphenazepam (pink). The light blue portion represents the  $\gamma$  subunit of the receptor whilst the dark blue the  $\alpha$  subunit. On the left, the 2D representation of the binding pocket and a report of the interactions between receptors residues and ligand are provided. Letter D identifies the  $\alpha$  chain and C the  $\gamma$  chain. The colours used to depict the residues in the 2D screenshot define different characteristics of the latter: light purple for polar residues and light green for hydrophobic ones; red circle indicates an acidic and blue a basic residue; and the light blue halo indicates solvent exposure both on the receptor and the ligand.

### 5.6.9 *Flunitrazolam*

Flunitrazolam is a triazolo DBZDs and a fluorinated analogue of the previously notified clonazolam. It also the triazole version of flunitrazepam. Not reported in the any patent or in literature, it was first identified in 2016 and reported to the EMCDDA EWS. It has been sold on line as a DBZD with strong hypnotic and sedative properties, much like clonazolam and flubromazolam. No information about its activity/toxicity profile is available at present. Flunitrazolam is not currently controlled either under the 1961 and 1971 international conventions. Online, flunitrazolam has mixed reviews, but is commonly presented as a potent short action DBZD, optimal for recreational purposes with a strong euphoric action. The predicted interactions between clonazolam and the allosteric binding site are presented in detail in Figure 5.20. The NO<sub>2</sub> group in position C7 interacts via a hydrogen bond donor with the  $\alpha$ 1His102 side chain, which is the fundamental residue for the BDZs activity on the GABA-AR. All the other interactions, as seen for alprazolam (Sec 4.3.8), i.e. arene-arene interactions with Tyr58 ( $\gamma$  chain), the hydrogen-arene interaction with Phe77 ( $\gamma$  chain) and Tyr160 ( $\alpha$  chain) and the hydrogen bond with Ser206 ( $\alpha$  chain) are here identified as well.



### Flunitrazolam

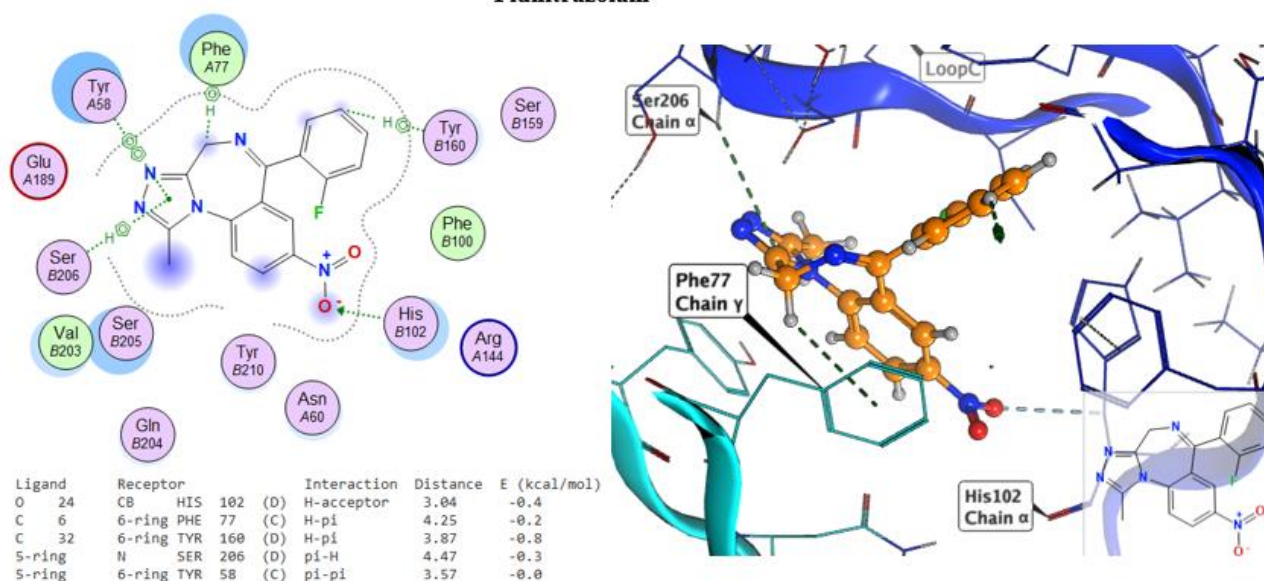


**Figure 5.20 Flunitrazolam interactions 3D and 2D representations.**

**Notes:** on the right, the binding pocket 3D representation with the docked ligand flunitrazolam (orange). The light blue portion represents the  $\gamma$  subunit of the receptor whilst the dark blue the  $\alpha$  subunit. On the left, the 2D representation of the binding pocket and a report of the interactions between receptors residues and ligand are provided. Letter D identifies the  $\alpha$  chain and C the  $\gamma$  chain. The colours used to depict the residues in the 2D screenshot define different characteristics of the latter: light purple for polar residues and light green for hydrophobic ones; red circle indicates an acidic and blue a basic residue; and the light blue halo indicates solvent exposure both on the receptor and the ligand.

All the data presented here seems to support the results obtained via both the QSAR and docking studies conducted, confirming the potential support of *in silico* methodologies for a quick evaluation and risk assessment of activity/toxicity profile of newly identified DBZDs.



### 5.7 Novelty and importance of the *in silico* methodology applications on DBZDs

Despite DBZDs represent only a small fraction (2%) of the total number of identified NPS, as reported in the latest UNODC reports (UNODC, 2022b, 2021b), they are molecules of great interest for intravenous drug misusers, being associated with fatalities worldwide (EMCDDA, 2021c; UNODC, 2022b). Indeed, they are increasingly being reported in polydrug consumption scenarios, usually with other central nervous system depressants (e.g., opiates and opioids) or stimulants. The concomitant use of more than one substance, especially of strong depressants, usually leads to a synergistic enhancement of the adverse effects of both substances, potentially leading to extremely severe side-effects including respiratory depression and death (Orsolini et al., 2020). The threat associated with polydrug consumption (in particular opioids and benzodiazepines, whether novel or not) is actual and is even more worrying if one considers that for the majority of NPS constantly introduced on the market, very limited data on their safety/toxicity profile are available (El Balkhi et al., 2020).

Hence, it is extremely important to assess as much as possible the extent of the DBZDs phenomenon, and more so with regards to their pharmacology. The novel approach of *in silico* methodology has proven very helpful in doing so. The 3D-QSAR models identified here seem to be very reliable in their predictive power. They identified as most potent, DBZDs such as flubromazolam, clonazolam, pynazolam and fluclotizolam, which were indeed reported as such, both in the scientific literature and by users. Moreover, the molecule predicted as the most potent, flubrotizolam, is a new DBZD for which no data are available in the literature (to the best of our knowledge). These findings, and in particular the assessment of unknown DBZDs, underscore the importance and the need for these computational models to be used. Their potential as preventive and informative tools need to be taken in consideration when dealing with NPS.

Indeed, these models could be used to assess, in a rapid and cost-effective way, the biological activity profile of a new DBZD, as soon as the latter is identified on the illegal market. Moreover, they could be of use to better discriminate between the various DBZDs, for which large differences exist between their pharmacokinetic parameters despite their structural and chemical similarity. *In silico* approaches should be used as the first evaluation step to better understand the possible harms associated with the recreational use of the substance and to draft a preliminary risk assessment. The latter could then be used as a starting point for pre-emptive legal measures and further investigations (e.g. *de novo* chemical synthesis; *in vitro* studies; preclinical studies).

The results obtained with the scaffold hopping exercise are also very promising because, despite suggesting the existence of a wider chemical landscape for this NPS class, they could be used as an effective tool in the prediction of the latter. It should be noted that among the new structures

generated are some very well-known and potent scaffolds. According to the predicted biological activity values, further modifications to the classical core structure could significantly increase the biological activity of an index molecule, and hence they need to be carefully investigated.

Finally, this study could be considered as the first step towards the creation of computational libraries that regulatory bodies can use as support tools for risk assessment and scheduling procedures.

The following Chapter will present an overview of the NSO class, and the methodologies used to analyse this NPS class.

## 5.8 Limitations

The major limitation for the QSAR studies is represented by the size of the data-set (training and test) used for the computational studies. The recommended size for a robust QSAR model varies but should be no less than 100 entries (Fourches et al., 2010; Golbraikh et al., 2014). However, to the best of our knowledge, no other experimental data comparable to the ones used here are available in the literature. That is, no other  $IC_{50}$  values were found for benzodiazepines-like structures at the GABA-AR, calculated as displacement of 50% of [3H]-diazepam, hence a bigger dataset could not be compiled. This means that if the QSAR analysis was to be done again the same limitation will apply and could not be overcome.

Other limitations include the use of only one crystallised structure of the GABA-AR for alprazolam, because that was the only 3D crystallised structure available; and the fact that MOE<sup>®</sup> uses force field methodology only for the energy minimisation of the molecules analysed, which could give slightly less accurate conformations if compared to semi empirical calculations.

## Chapter 6 Novel synthetic opioids overview and methods

### 6.1 Chemical class overview

Opioids are the most famous and effective class of therapeutics for the treatment of pain (Schifano et al., 2020). They are considered the standard of care almost worldwide for the management of acute and chronic, moderate to severe pain often related to advanced medical diseases or to medical procedures. Opioids encompass a large class of molecules structurally related to the natural alkaloids derived from the resin of the opium poppy or *Papaver somniferum* (DOJ and DEA, 2020). Opium has been known for millennia. Firstly cultivated around 3400 BC by the Sumerians in Mesopotamia, it spread throughout the world (Europe and Asia) to all main civilisations (CBN, 2022). Since the beginning, opium use was associated with strong addiction potential and tolerance (DOJ and DEA, 2020). Despite being known to relieve pain and used in surgical analgesia for several centuries, its use in the management of postoperative pain was described only since the 18<sup>th</sup> century (Ba et al., 2000). The therapeutic use of opium changed further in the early 19<sup>th</sup> century, when morphine was firstly isolated from the plant (Sertürner, 1817). This event, i.e. the first isolation of a natural product, was a ground-breaking event which influenced the history of the modern pharmacology. After its isolation, morphine started to get sold but it was not until the invention of the subcutaneous needle that its use became widespread (Ba et al., 2000). However, with the drug came the same addiction potential and tolerance identified for opium. Indeed almost immediately after morphine commercialisation, the abuse potential, addiction, and withdrawal syndrome associated with its use were described (Rosenblum et al., 2008). Since then, several morphine-like drugs have been synthesised in the quest of safer alternatives (i.e. reduced adverse effects and abuse potential). This led to the synthesis of heroin, in 1898, followed by meperidine in 1939 and methadone in 1949, which opened the road to all the other semisynthetic and synthetic opioids (e.g. oxycodone, meperidine, (Latta et al., n.d.; Stanley, 1992)). During the 1960s, this quest for safer opioid analgesics, opened the way for the synthesis and testing of a series of molecules by the pharmaceutical company Janssen Pharmaceutica. Among these new molecules fentanyl (which is 50-100 times stronger than morphine (Armenian et al., 2017; DEA, 2022a)) was synthesised, followed by dozen more of structurally similar analgesic, which altogether were named the “fentanyls” (Stanley, 1992) Some of the fentanyls, i.e. fentanyl, alfentanil, sufentanil and remifentanil, were approved for pain management treatment and broadly used, while others were used as veterinary medicines due to their elevated potency, i.e. carfentanyl and thiafentanyl (Stanley, 1992).

The new synthesised opioids however, showed the same abuse potential if not stronger than that observed with morphine. For these reasons, strict restrictions on medical prescription were put in

place and opioids were placed under control by the UN Convention on Narcotics of 1961 (UNODC 2022a).

This led to a long lasting debate between the need to take advantage of the medicinal properties of these drugs and the acknowledgement of their abuse and addiction potential as possible threats for society (Musto, 1973). Indeed, at present the use of opioids for chronic non-malignant pain (CNMP) is still controversial due to their high abuse and dependence potential, their low therapeutic index and their very severe side-effects (Tseng, 2018).

The term opioid defines all those molecules that act on the opioid receptors, both within and outside the CNS. These receptors include delta ( $\gamma$ ), kappa ( $\kappa$ ) and mu ( $\mu$ ) opioid receptors (DOR, KOR and MOR), and occur predominantly in areas and tracts of the CNS associated with pain perception (Schumacher et al., 2017). The activation of the mu opioid receptor is considered the most important for both analgesic and euphoric effects (Contet et al., 2004), and it is also responsible for the abuse and dependence potential. These receptors are discussed in detail in Section 6.3.3.

Opioids can be classified according to their source in endogenous (endorphins, enkephalins, dynorphins), natural (opiates), semisynthetic (e.g. heroin and oxycodone), and synthetic opioids (e.g. fentanyl and propoxyphene) (Alam et al., 2019).

They can also be classified according to their activity and their chemical structure. If classified by their activity they can be divided into full agonist (codeine and morphine), partial agonist (buprenorphine), mixed agonist/antagonist (pentazocine and butorphanol) and antagonist (naloxone and naltrexone) (Alam et al., 2019). The agonists in turn are divided into strong (morphine, fentanyl, meperidine), moderate (oxycodone) and weak (propoxyphene) agonist (Schumacher et al., 2017).

If classified by their chemical structure they can be divided in phenanthrenes (e.g. morphine, codeine, heroin), benzomorphans (e.g. pentazocine), diphenylpropylamines (e.g. loperamide, methadone and propoxyphene), phenylpiperidines (meperidine), phenethylpiperidines or anilidopiperidines (e.g. fentanyl and analogues), oripavine derivatives (e.g. buprenorphine and etorphine), morphinan derivatives (butorphanol), ciclohexylphenols (tramadol) (Alam et al., 2019). The main difference which can be appreciated between these structures is the presence or absence of a fused ring core, usually referred to as the phenanthrene core. The latter gives a much more rigid structure to the molecule which differ consistently from the very flexible nature of scaffolds as diphenylpropylamines, phenylpiperidines and phenethylpiperidines. A general overview of the different chemical structures is presented in Figure 6.1.

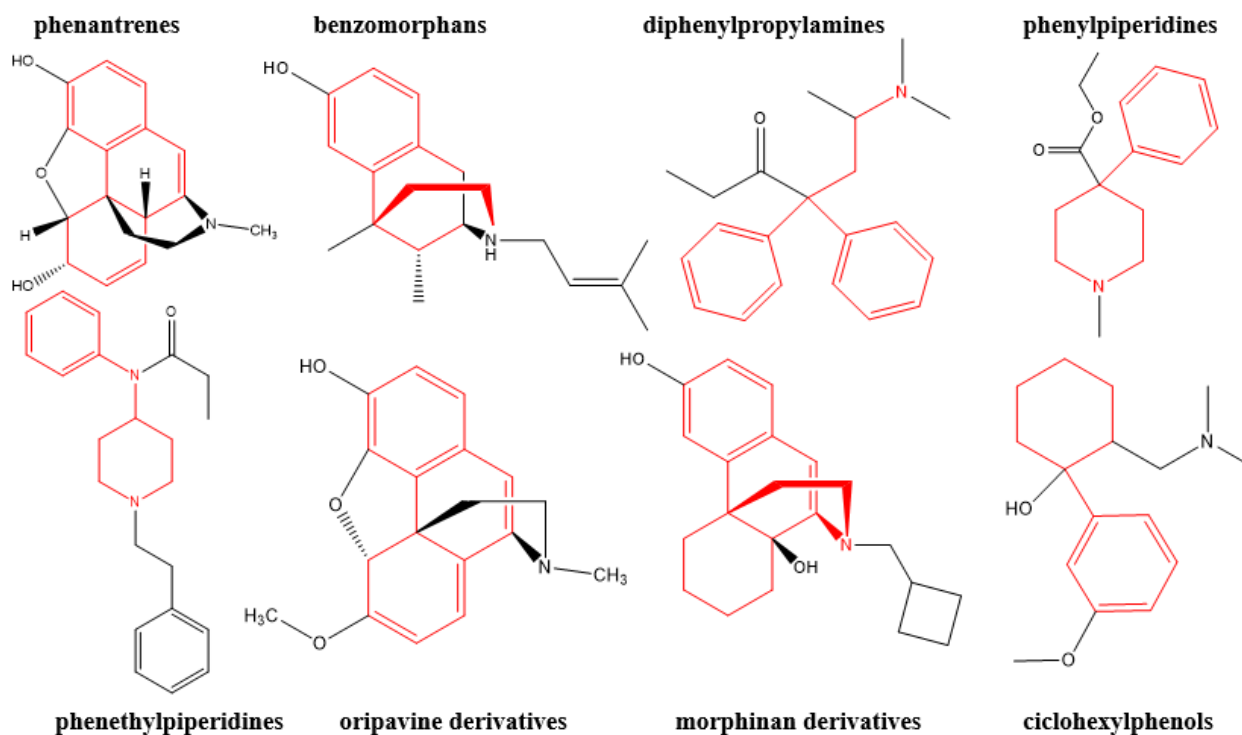


**Figure 6.1** Most common chemical structures identified among the class of opioids.

*The core structure which gives the name to the chemical class is highlighted in red. The structures were designed with ChemDraw 20.1.1 and were retrieved from PubChem.*

Medically opioids are primarily used for analgesia, i.e. pain relief (over-the-counter opioids as codeine, dihydrocodeine, and loperamide), treatment of acute pain (prescription opioids as hydrocodone, oxycodone, and morphine), and chronic terminal pain (prescription opioids as morphine, hydromorphone) (Department of Health and Services, n.d.; Dowell et al., 2016; Volkow et al., 2017). Their use in the management of non-malignant chronic pain, despite being controversial, has been growing and it has been associated with a new and rising problem of addiction and misuse (Stromgaard et al., 2009).

Opioids can also be used in anaesthesia (e.g. sufentanil, remifentanil, and alfentanil (Ferry and Dhanjal, 2022)), as antitussive (e.g. morphine, diamorphine, and codeine (Belvisi and Geppetti, 2004)), antidiarrhea (loperamide), in replacement therapy for opioid use disorder (e.g. buprenorphine or methadone (Dydyk et al., 2022)) or to reverse opioid overdose (e.g. naloxone and naltrexone (Theriot et al., 2022)). The mechanism of action of these opioids involves predominantly MOR, with KOR also involved in the action of opioids antitussives. Some of the opioids currently available as medicine are so potent that they are approved for veterinary use only (e.g. carfentanyl) (Clarke et al., 2019).

Opioids are very often used recreationally (i.e. non-medically) for their euphoric effects, to prevent/attenuate withdrawal or for self-medication. The most common side effects associated with

their use are, in the short term, itchiness, sedation, nausea, respiratory depression, constipation, and euphoria; tolerance, dependence and unpleasant withdrawal symptoms are observed instead in the long term. Opioids can be lethal if overdosed or co-used with other CNS depressants such as BDZ/DBZD, with death resulting from respiratory depression.

## 6.2 The opioids epidemic

Since the '90s, a rapid increase on the medical use, non-medical use, recreational use/abuse and overdose deaths attributed to opioids was registered in North America (Manchikanti et al., 2010), with significant medical, social and economic repercussion worldwide. This phenomenon was called the opioid epidemic or the opioid crisis (Volkow et al., 2019). The opioid epidemic started in North America mainly due to over-prescription of opioid analgesics encouraged by pharmaceutical companies 'marketing strategies (i.e. Purdue Pharma among others) based on the false advertisement of opioids (e.g. Oxycontin) as "safe" and non-addictive medications (Van Zee, 2009). It then evolved into different phases, presently culminating in high mortality rates caused by illicitly manufactured opioids (e.g. fentanyl, and fentanyl-like NSO) (DuPont, 2018). In the USA, almost 500,000 deaths were reported from opioids overdoses, both prescription and illicit opioids, between 1999 to 2019 (Mattson et al., 2021), with more than 56,000 deaths involving synthetic opioids reported in 2020 alone (CDC, 2021) and 100,000 in 2021 (Dyer, 2021).

Due to different opioids being involved across the years, three different phases (CDC, n.d.) of the opioid crisis were identified

- First phase (1990-2010). Increase in prescription opioids use in the 1990s, followed by increased related overdose deaths
- Second phase (2010-2013). Increase in overdose death related to heroin abuse
- Third phase (2013-2022) Significant increases in overdose deaths involving synthetic opioids, particularly illicitly manufactured fentanyl and analogues

At present, the crisis dynamics are strongly influenced by the presence and continuous introduction into the market of NSOs, whose chemical types and potencies vary constantly. This, and the fact that often NSOs are consumed as counterfeit prescription opioids and/or in combination with other drugs, i.e., heroin, benzodiazepines, cocaine, and methamphetamine (Gladden et al., 2019), are strongly increasing the lethal toll of the opioid epidemic. This is due to the fact that that combination of different drugs usually results in worsened side effects or accidentally overdoses with an increase likelihood of consequent fatalities.

To date, the nature of the opioid crisis seems to be caused, in particular in the northern hemisphere, by the adulteration of heroin products; substitution/counterfeit of prescription opioids with fentanyl, fentanyl analogues, and other NSOs by profit driven organised crime groups (Pardo et al., 2019); or by substitution of prescription opioids by users, who find NSOs cheaper and more easily accessible/purchasable .



Despite NSOs seeming to play a small role in Europe's drug market to date, there is growing concern about the availability of these substances (EMCDDA, 2021f). In the UK, the number of prescription opioids doubled in the period 1998 to 2018 suggesting the risk of a possible opioid crisis, even if on a different scale compared to the North American one (Alenezi et al., 2020). In 2021 an outbreak of poisonings and deaths was reported in the South of England due to heroin samples adulterated with isotonitazene (De Baerdemaeker et al., 2022). Indeed due to the increment of regulatory measure in Europe against fentanyl, different NSOs class, i.e. nitazenes, were increasingly identified (EMCDDA, 2021f).

The high demand for opioids driven by the opioid's epidemic, has attracted the interest of organised crime/criminals, with an increase on the market of diverted legitimate products, unlicensed, counterfeit ones, or new legal alternatives, i.e. NSOs.

### **6.3 Novel synthetic opioids**

Novel synthetic opioids represent a chemical diverse group of substances (e.g. fentanyl, derivatives of opiates, etc. (Figure 6.1 6.4) which act as central nervous system depressants and are not listed in the Narcotic or Psychotropic International Conventions on Narcotics (1961) or Psychotropics (1971) (UNODC, 2022c). NSOs possess structural features which allow them to bind specific opioid receptors (i.e., MOR, KOR and DOR), and produce effects which mimic those of morphine. Relaxation, euphoria, pain relief, and sedation have been reported (DEA, 2022b, 2022a; WHO, 2020b). They are predominantly sold as legal alternatives to illicit and prescription opioids, as counterfeit opioids or benzodiazepines, and as counterfeit heroin (Lovrecic et al., 2019). NSOs are predominantly used for self-medication - i.e. pain treatment and withdrawal, and for recreational use (Rauschert et al., 2022), very often by vulnerable and marginalised users and people who inject drugs (PWID) (Armenian et al., 2017; Specka et al., 2022). They are also used in poly-drug consumption with other CNS depressants to potentiate the "down" effects or with stimulants to 'offset the effects of each drug, or experience an enhanced, synergistic or more euphoric high' (Fogger, 2019; UNODC, 2022b).

As with other NPS, the production of NSOs and, in particular, fentanyl analogues seems to originate from companies in China and South East Asia, with very few reports of illicit production in Europe and North America (UNODC, 2021e, 2017c).

Of all the 2021 NPS intoxication cases reported by the UNODC, in which NSOs were reported, 81% were fatalities, 63% of which was connected to acetyl fentanyl and 11% to carfentanyl. While fentanyl and fentanyl analogues are predominantly reported in fatalities and intoxication cases, buprenorphine and isotonitazene were reported as well in clinical admission cases and fatalities, even if to a lesser extent (UNODC, 2021b). This could be due more to the lack of related validated

analytical methods for their detection than to a small extension of their diffusion. In fact, in 2020-2021 a shift away from fentanyl was observed with an increase in use and detection of benzimidazole opioids (Ujváry et al., 2021).

NSOs are strong CNS depressants and when used alone or in combination with other drugs can cause serious toxicity with profound sedation, respiratory depression, coma, and death (Fogarty et al., 2022; Tabarra et al., 2019). The risks associated with their nonmedical use is aggravated by the fact that for these NSOs very little or no information at all on pharmacological and toxicological profile is available (Prekupec et al., 2017; Wilde et al., 2019). In addition to scarcely described profile for the majority of the NSOs, some of those identified on the market tend to be very potent, indeed animal tests conducted by the Janssen Pharmaceutica on fentanyls showed how cis-3-methyl fentanyl and carfentanyl were respectively 7000 and 10000 more potent than morphine (EMCDDA, n.d.; Jalal and Burke, 2021). These findings suggest that very small doses, i.e. microgram ( $\mu\text{g}$ ), or even accidental exposure to these molecules, could represent a lethal health threat (EMCDDA, n.d.). Due to their extreme potency, relatively small amounts of NSOs (i.e. hundreds of grams) can produce many thousands of doses (EMCDDA, 2021f). This makes them easy both easy to transport and conceal and difficult to identify, turning them into a serious challenge for drug control agencies and forensic laboratories. A new area of concern is the appearance of novel dosage forms, such as nasal sprays and e-liquids for vaping in electronic cigarettes, meaning that some new opioids may be relatively easy to use and possibly considered more socially acceptable than established opioids such as heroin, although the risks of inadvertent exposure may be greater.

This and the lack of pharmacological data on NSOs represent a serious health threat, with unforeseeable risks, especially in polydrug consumption scenarios (EMCDDA, 2021f). This phenomenon is even more troubling if we consider that the majority of NSOs originate from molecules developed by the pharmaceutical industry but rejected as medications due to safety or efficacy issues (Raffa et al., 2017).

### 6.3.1 Novel synthetic opioids phenomenon

Novel synthetic opioids can potentially represent the most dangerous class of NPS. Their number, in contrast with the stabilisation trend reported for other NPS in the last couple of years, has been constantly increasing, so much so that a total of 87 fentanyl and 44 non-fentanyl NSOs have been reported in 2022 (UNODC, 2022d) by the UNODC. The first NSO, i.e., O-desmethyltramadol (the main metabolite of tramadol), was identified on the market in 2009 (UNODC, 2020c). The growth of this class appeared very slow at first, with only 14 NSOs reported between 2009 and 2015. However in the following four years the numbers grew to 56 (2019) and up to 87 in 2020, at which point NSOs represented the third-largest group in terms of number of substances reported by UN members (UNODC, 2022a). In 2020, the NSOs were the NPS groups with the highest number (22) of molecules identified by year (UNODC, 2022b). A similar growth trend was observed in the EU, as reported in Figure 6.2.

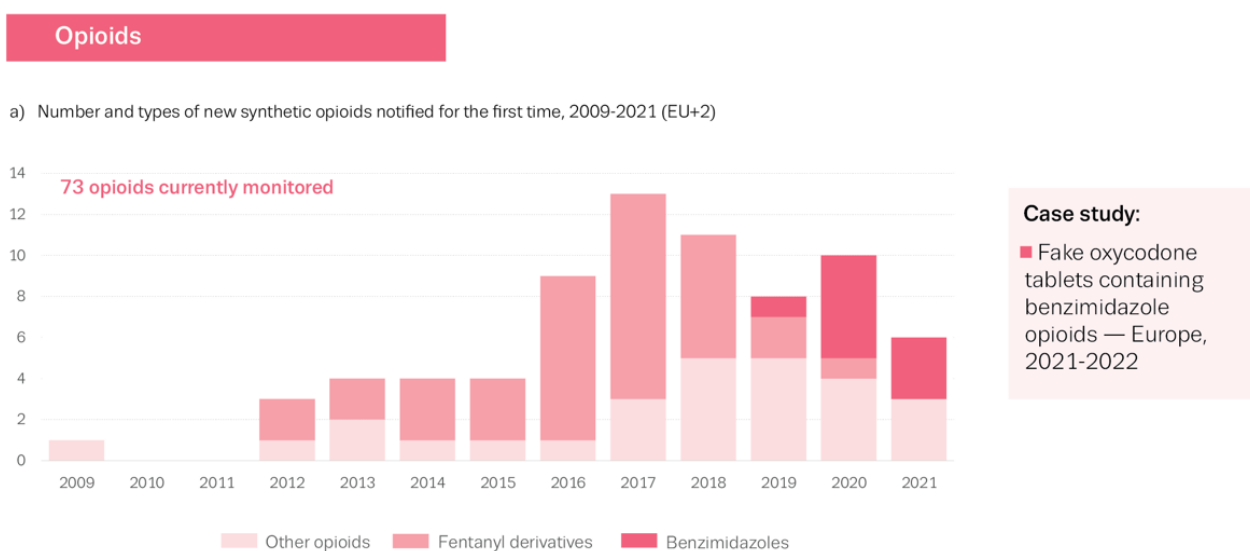


**Figure 6.2** Numbers and types of synthetic opioids notified for the first time to the EWS. The image is reproduced with the EMCDDA permission (EMCDDA, 2021g)

Parallel to the increase of the numbers, a diversification of the chemical structure has been observed as well. In 2012, UNODC reports only four chemical classes of NSOS, which became five in 2015. Between 2015 and 2019, a further increase in chemical diversity was observed, with a total of 8 chemical classes reported (UNODC, 2020c). The chemical classes identified each year are reported in Figure 6.3.

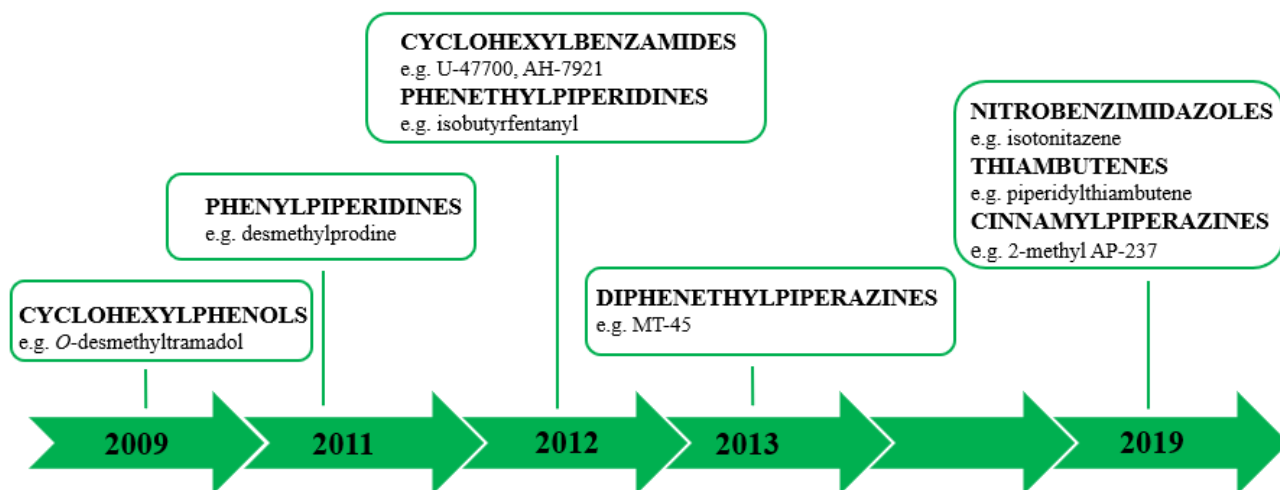


*Figure 6.3 NSOs chemical classes reported each year from 2009 to 2019.*

*This timeline was retrieved from the UNODC report “The growing complexity of the opioid crisis”, 2020*

The UNODC indeed reported, between 2009 and 2015, “a proliferation in the diversity of chemical classes of NPS with opioid effects in the global market” (UNODC, 2020c). Four of these eight chemical classes, i.e. cyclohexylbenzamides, diphenethylpiperazines, cinnamylpiperazines, and cyclohexylphenols (Figure 6.3) were included in the schedules of the 1961 Convention only after 2015. The structures of the NSOs classes identified after 2015 are reported in Figure 6.4 and Figure 6.1.

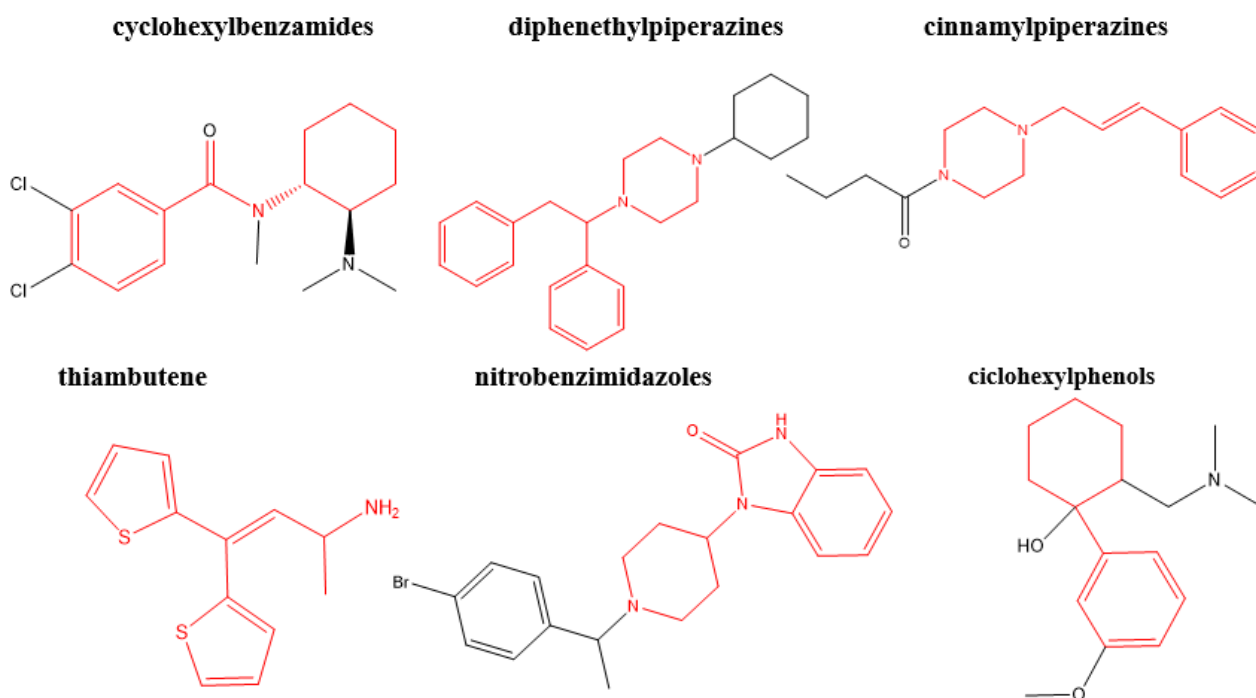


**Figure 6.4 Latest chemical structure of the opioids class to be scheduled under the Narcotic Convention (1961).**

*The core structure which gives the name to the chemical class is highlighted in red. Please note that the structure of ciclohexylphenols has been also reported in Figure 6.1.*

As a result of the rapid emergence and increasing prevalence of opioid NPS, coupled with a substantial increase in public health risks, the number of such substances placed under international control also increased. Between 2015 and 2020, almost one-third (17 out of 60) of the whole of the NPS scheduled were molecules with opioid effects. Despite them only representing a very low percentage (8%) of the total NPS identified (roughly 1,100), they are associated with the highest level of risk/harm.

Pushed by this aggressive scheduling process (DEA, 2021; USA Congress, 2021), and in particular after the generic legislation put in place in the USA by the DEA for fentanyl and fentanyl analogues, and the scheduling of isotonitazene in June 2020, a new fentanyl subclass was identified with bromphine. Despite the similarity with fentanyl, the phenethyl-piperidine-benzimidazolone structure fall outside the scope of the fentanyl analogues legislations.

The trends reported here seem to guide the NSOs market towards novel chemical classes every time the previous ones are put under legal control, i.e., scheduled under the two international conventions of 1961 and 1971. However, a lot of these novel opioids are not really novel and are either “failed” (e.g., metodesnitazene, fluorofentanyl, U-47700) or falsified/unregistered/unlicensed pharmaceuticals (e.g. etizolam, etonitazene, fluorofentanyl and AP-237) both classes of which were never approved for medical use. Moreover, other NSOs usually result from small modifications of

the chemical structure of the latter class, purposely to avoid the current legislation (Baumann et al., 2018).

These NSOs could display either similar or very different pharmacological potencies, if compared to fentanyl, which can lead to the creation of extremely potent compounds (Baumann et al., 2018; Prekupec et al., 2017). Opioids are in general known for their very narrow therapeutic index, which could cause , with a small variation in dosage, extremely potent adverse reaction including death (Beardsley and Zhang, 2018).

### 6.3.2 *Forms and routes of administration*

As mentioned above, NSOs can be sold as stand-alone products, adulterants (mainly in heroin), or constituents of counterfeit prescription opioids. NSOs have been found in a variety of physical and dosage forms throughout the world, which seems to vary according to which family they belong to. Non-medical and illicitly manufactured fentanyl has been found predominantly as powders but also detected in liquids, , e-liquids and tablets for oral or sublingual administration (UNODC, 2020c). They were also found as oral transmucosal lozenges, sublingual sprays, and as injectable formulations and transdermal patches (Lovrecic et al., 2019).

The new fentanyl derivatives and new generation NSOs (nitazenes or cinnamylpiperazines) are often sold as powders, tablets (e.g. counterfeit pills), nasal sprays, and liquids (Solimini et al., 2018). In particular, when sold as powders, they often contain cutting agents (such as mannitol, lactose, and paracetamol) and other drugs such as heroin and other fentanyls/opioids and, to a lesser extent cocaine or other stimulants (UNODC, 2020c). NSOs have been reported as well in blotters and plant material in which they were not disclosed as ingredients (EMCDDA, 2022a).

NSOs are usually taken orally (tablets and lozenges) or by sublingual application; snorted and insufflated (powders); smoked or inhaled via burning powder on aluminium foil or via a “vaporizer, injected either intramuscular or intravenous or taken intrarectally (Lovrecic et al., 2019; Prekupec et al., 2017).



**Figure 6.5** Some examples of NSOs found on the market.

*In clockwise order from the left a picture of buprenorphine also known as purple heroine (Michigan Poison Center, 2020); a mix of pills of coloured fentanyl, also known as rainbow fentanyl; counterfeit prescription, fentanyl laced, pills mimicking the look of prescription opioids like oxycodone using similar shapes and symbols; counterfeit hydromorphone prescription pills containing isotonitazene. The “M” and the number “8” make the pills virtually identical to Dilaudid (8mg). No information on the meaning of the purple colour for buprenorphine is available, while the rainbow colour of fentanyl pills ‘appears to be a new method used by drug cartels to sell highly addictive and potentially deadly fentanyl made to look like candy to children and young people’ (DEA, 2022c).*

### 6.3.3 *Pharmacological profile, the opioid system and receptors*

Opioid receptors are a group of inhibitory G protein-coupled receptors predominantly located at the synaptic complex in the CNS but found also in the spinal cord, on peripheral neurons, and in the digestive tract. In particular they belong to the large superfamily of seven transmembrane (7TM) G protein-coupled receptors (GPCRs) (Waldhoer et al., 2004) (Figure 4.5) and their endogenous ligands are dynorphins, enkephalins, endorphins, endomorphins and nociceptin. In 1967 the presence of multiple OR receptor types was suggested with the identification of ( $\mu$ ,  $\kappa$ , and  $\delta$ ) MOR, KOR, and DOR (Martin, 1967). A fourth OR, i.e. the nociceptin opioid peptide receptor (NOP), was identified, and despite sharing high aminoacidic sequence similarity with the other ORs, it was found not to have affinity for opioid peptides or morphine-like compounds (Butour et al., 1997). For this reason, it will not be described further in this work.

MOR, which takes its name from its agonist morphine, is mainly found in the brain and it is responsible for the well-known sought-after opioid effects, i.e. analgesia and euphoria. However, its activation produces many other effects associated with the use of opioids as miosis, reduced GI mobility, respiratory depression (Dhaliwal and Gupta, 2021; Kandasamy et al., 2021; Piotr F.J. Lipiński et al., 2019; Olson et al., 2019) and it particular seems to be the OR responsible for the abuse potential and physical dependence (Kieffer and Evans, 2002; Negus and Freeman, 2018; Pasternak and Pan, 2013). Three isoforms of the MOR (i.e.  $\mu$ 1,  $\mu$ 2, and  $\mu$ 3) have been identified (Pasternak and Pan, 2013).

KOR and DOR, which are the least studied of the OR family, are predominantly found in the brain tissue and similarly to MOR have, respectively, three and two isoforms (Wilde et al., 2019). When activated, KOR seems to produce similar effects to MOR, i.e. antinociception and analgesia, but also aversive and psychotomimetic effects (hallucination and dissociation) (Paton et al., 2020).

DOR activation has been associated with analgesia but in particular with, anxiolytic and antidepressant effects (Gendron et al., 2016; Zhou et al., 2021). Due to MOR being responsible for triggering the brain reward systems and initiating the addictive behaviours of opioids (Butelman et al., 2015) (Butelman et al., 2015), in recent years KOR and DOR have emerged as alternative molecular targets for the creation of safer analgesics (Bruchas and Roth, 2016).



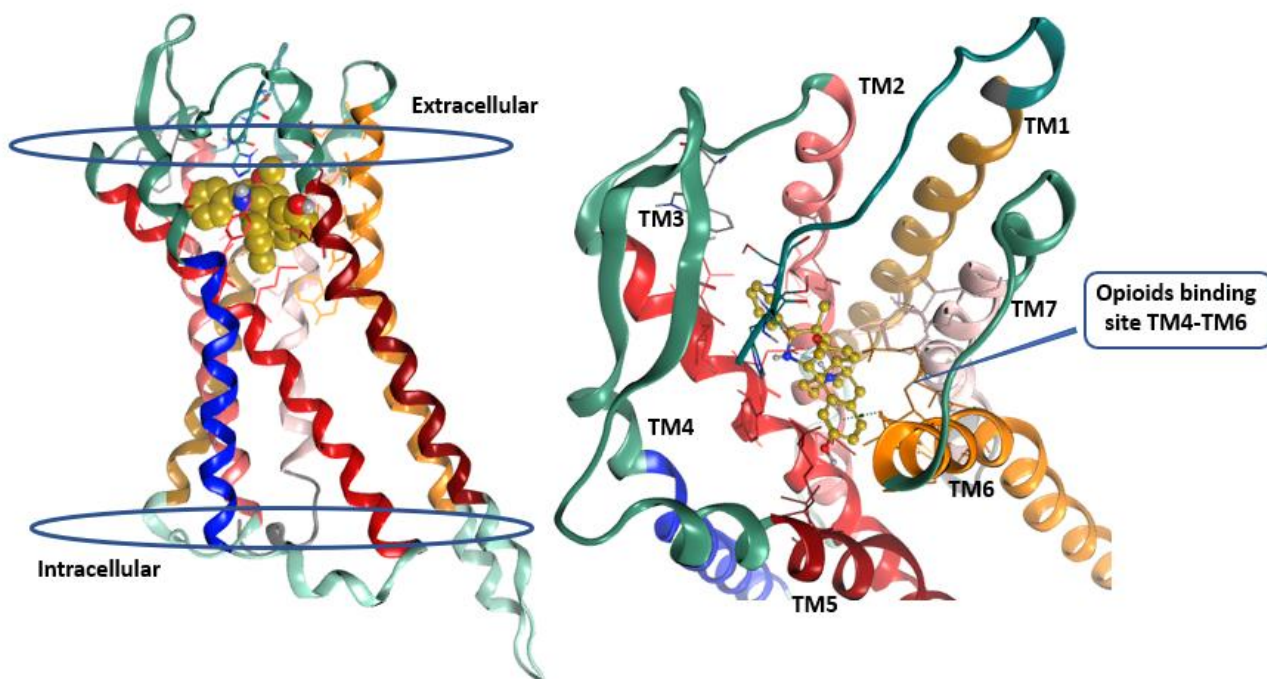


**Figure 6.6** 3D representation of the pentameric structure of GABA-AR.

On the left is presented the view of the receptor in the cell membrane; on the right is a section from the top which helps identifying the five subunits and the binding site of the endogenous ligand GABA in dark green and the BDZ in purple. The 3D images were created with MOE®, and the 3D structure here represented is the PDB51CM (RCSB PDB, 2015).

The activation of these G protein-coupled receptor (GPCR) could mediate a different array of cellular signalling through both G protein-dependent (through four major G-protein sub-classes: Gs, Gi / o, Gq/11 and G12/13) and independent pathways involving, for example, arrestin and ion channels (Hodavance et al., 2016). This phenomenon, by which ‘distinct downstream pathways can be preferentially activated by agonists working through the same receptor’, is defined as biased signalling (Uprety et al. 2021). This biased signalling is very important for ORs because the  $\beta$ -arrestin activation appears to be involved in the insurgence of severe, and potentially lethal, respiratory depression associated with use of opioid agonists (Mafi et al., 2020; Shang and Filizola, 2015). However, recently the role of  $\beta$ -arrestin signalling in opioid-induced respiratory depression has been refuted and evidence that G proteins could be involved in the latter through action on respiratory-controlling brainstem neurons has been proposed (Bateman and Levitt, 2021; Varga et al., 2020).

Although information about receptor affinities and subtype specificity is widely available for classical opioids, data on NSOs are scarce. Moreover, it is very difficult to predict their pharmacological effects and potency, because as seen with fentanyl and carfentanyl, a small change on the scaffold of an NSO could determine a drastic change in activity. Despite limited available information, it has been observed that naloxone and naltrexone are capable of reversing the effects

caused by NSOs, suggesting that their action profile in humans is similar to that of classical opioids (Lovrecic et al., 2019).

#### 6.3.4 Toxicological profile

The side effects associated with NSOs intoxication are reduced level of consciousness, ranging from drowsiness to stupor, which resembles that produced by more classic opioid agents (Fareed et al., 2011). Under conditions of overdose, NSOs induce an opioid toxidrome associated with loss of consciousness, bradycardia, respiratory depression, cyanosis, and miosis (Holstege and Borek, 2012; Zimmerman, 2014). Additional clinical features may include hypotension, pulmonary edema, ileus, nausea, vomiting, and pruritus. Death is usually from respiratory depression. Because many NSOs display chemical structures that are closer to those of fentanyl rather than morphine, it is expected that the properties of these substances would be more akin to those of fentanyl as well (Abdulrahim and Bowden-Jones, 2018). Thus, one would predict low oral bioavailability, high potency, and short duration of action, especially with the fentanyl analogues (MacKenzie et al., 2016).

New opioids may also present risks not only to those who use them (sometimes unknowingly), but also to others, such as postal workers, couriers, police and customs officers, families, and friends of users, who may be accidentally exposed to them.

The risks associated with NSO recreational use are linked to their potency, which varies over a large scale, with the most potent ones (e.g., carfentanyl ) requiring doses well below 1 mg to produce strong effects (a common diazepam dosage varies from 2 to 10 mg); and to their onset of action which could vary according to route of administration and absorption rate (Brunetti et al., 2021). Recent studies conducted by Vandeputte et al. show how the nitazene class potency seems to be in line with the fentanyl analogues, suggesting a similar toxicological profile (Vandeputte et al., 2021). Fogarty et al (2022) instead reported a lower potency for the class of cinnamylpiperazines compared with fentanyl.

Due to limited *in vitro* and *in vivo* studies for the majority of NSOs (Fogarty et al., 2022; Vandeputte et al., 2021), usually data on side-effects and toxicological profile are collected anecdotally via the analysis of trip reports or users' fora online (Arillotta et al., 2020; Bowen et al., 2019; Catalani et al., 2021a; Kjellgren et al., 2016; Moeller and Svensson, 2020; Spadaro et al., 2022).

It should be noted that the toxicity profile of each NSO could be further affected by the concomitant use of these substances with other drugs, resulting in several and unpredictable risks (UNODC, 2020c).

Due to very few *in vitro* and *in vivo* studies for the majority of NSOs, usually data on side effects and toxicological profile are collected anecdotally via the analysis of trip reports or users' forums

online (Arillotta et al., 2020; Bowen et al., 2019; Catalani et al., 2021a; Kjellgren et al., 2016; Moeller and Svensson, 2020; Spadaro et al., 2022).

It should be noted that the toxicity profile of each NSO could be further affected by the concomitant use of these substances with other drugs, resulting in several and unpredictable risks (UNODC, 2020c).

### 6.3.5 Current Structure Activity Relationship

The majority of studies of the SAR on opioids are conducted with respect to the mu opioid receptors. For this reason and considering the importance of the MOR in analgesia and rewarding opioid processes, the discussion below will focus on this receptor.

#### *Morphine like*

Previous studies (Elison et al., 1963; Feinberg et al., 1976; Portoghese, 1992) identified some correlations between the structure of the morphine and its activity on the MOR (Figure 4.6.).

In particular, it was observed how:

- The presence of a free phenol group at position C3 of the morphinan scaffold is essential for the activity. When the -OH is substituted by other groups that decrease the activity (yellow box in Figure 4.6), e.g. codeine
- In position C6 substituents as -OH or OCOCH<sub>3</sub> increase activity (e.g. heroin), while substituents such as -H or -CO decrease the activity (red box in Figure 4.6)
- The saturation of the double bond C7 = C8, that is, the substitution of 7,8 dihydro, increases activity (blue box in Figure 4.6). This is true even in the presence of a C=O group in position 6, i.e. hydromorphone.
- At C14, substitution with an OH -OH in  $\beta$  configuration, that is, above the phenanthrene ring, increases activity (oxymorphone) (green box in Figure 4.6)
- Alkyl substitution in N17 shows the same agonist activity if the number of carbon atoms is <3 or an increase in agonist activity when the number is >5. If the number of C atoms is between 3-5 the activity change to antagonist/ partial agonist, e.g. nalorphine and naloxone (pink box in Figure 4.6).

## Morphine Structure Activity Relationship

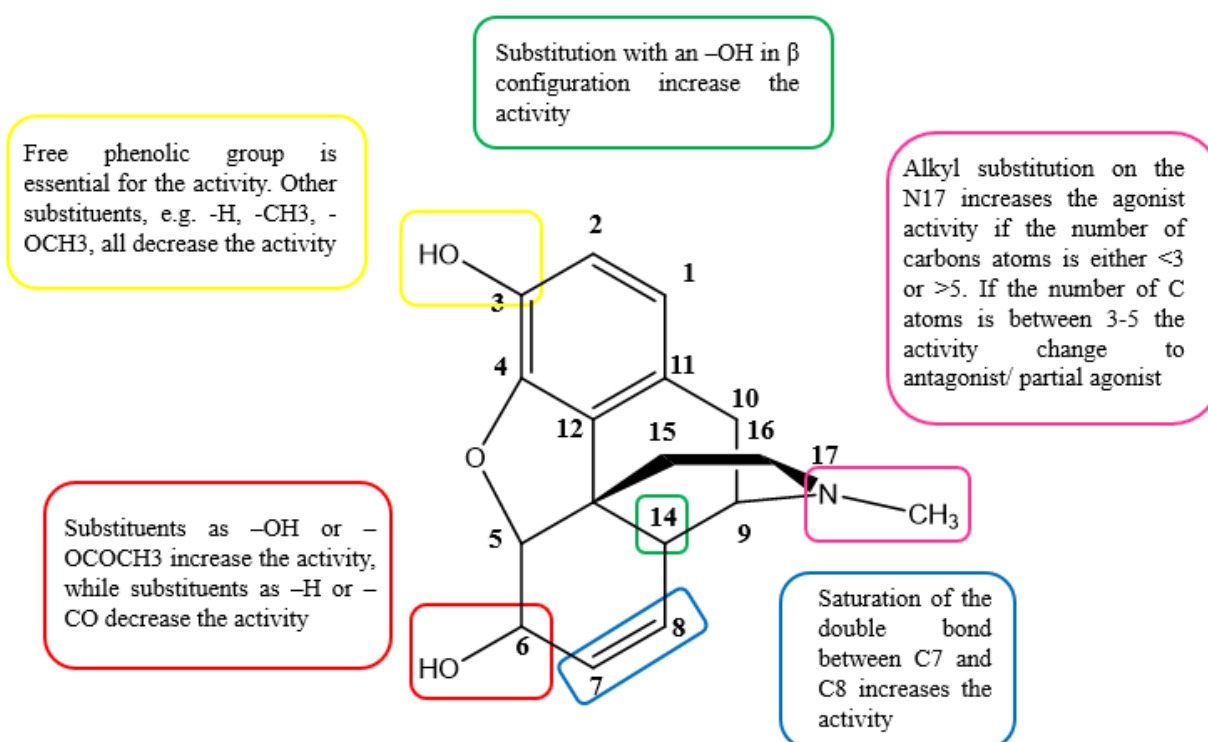


Figure 6.7 Structure activity relationship identified for morphine-like NSOs.

Each part of the chemical scaffold whose modification is linked with biological activity changes has been highlighted with a coloured box. A brief description of the SAR for each box is included in the figure as well. For the full description please see Section 6.3.5

### *Fentanyl like*

Previous studies (Casy and Parfitt, 1986; Higashikawa and Suzuki, 2008; Janssen and Van Daele, 1977; Vuckovic et al., 2009; Wilde et al., 2019) identified how small changes on the fentanyl structure could drastically affect the activity on the MOR. For the purpose of a structure activity analysis fentanyl molecule can be divided into 4 different moieties as per Figure 6.8. The majority of the research on the fentanyl SAR has been carried out on the piperidine moiety (Vasudevan et al., 2020), with very few studies conducted at the propanamide moiety (Wilde et al., 2019), variations of which have been recently made available on the market.

In particular, it was observed how:

- The aromaticity of the anilino phenyl moiety is a characteristic necessary to the activity (Casy and Parfitt, 1986).
- Changes in the length of the chain connecting the anilino phenyl to the nitrogen of the carboxamide chain, i.e., the insertion of a methyl or ethyl decrease fentanyl activity (Casy and Parfitt, 1986).
- Substitution of the same ring in para position decreases activity. However, the resulting fentanyl analogues still displays a potency higher than that of morphine, in decreasing order for F, I and CH<sub>3</sub>.
- Substitution on the C3 of the piperidine moiety with an alkyl group increases activity when the group is in the cis position more than trans (Vuckovic et al., 2009). Methyl substitution results in the larger increase in activity, while longer substituents would result in a less active substance, suggesting a steric hindrance. Despite this, substitution with a carboxy group strongly increases activity.
- Substitutions at position C4 of the piperidine ring with a group such as -CH<sub>2</sub>COOH or -CH<sub>2</sub>OH drastically increases binding and potency, i.e., carfentanyl (Dosen-Micovic et al., 2006; Vasudevan et al., 2020). In particular it has been observed that the chemical nature of the substituent is not important, and every substituent seems to increase activity (Janssen and Van Daele, 1977).
- Substitution of the phenyl moiety in  $\beta$  with an -OH increases activity (Wilde et al., 2019).
- For carboxamide, substitution of the moiety substitution with open and closed alkyl chains showed a decrease in activity with the increasing number of carbon atoms in the chain/ring (Vasudevan et al., 2020).

## Fentanyl Structure Activity Relationship

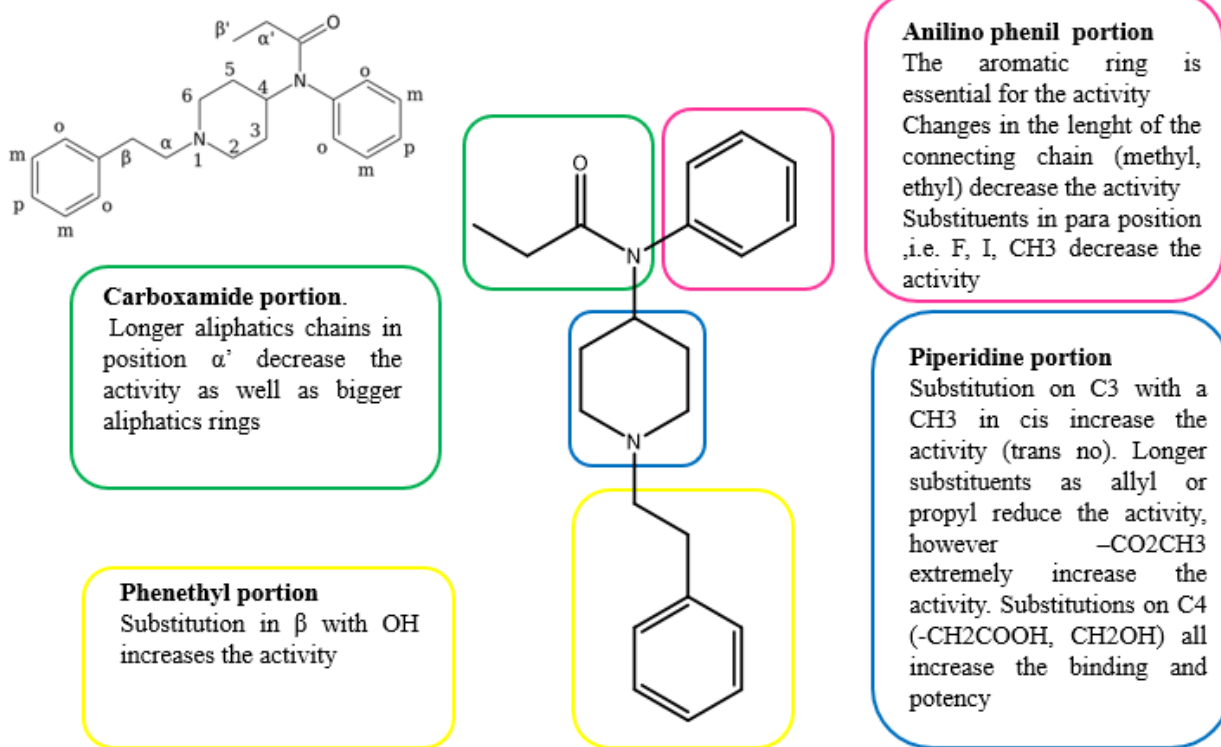


Figure 6.8 Structure activity relationship identified for fentanyl-like NSOs.

The fentanyl structure is here divided into its main four core components identified with coloured boxes (Vasudevan et al., 2020). A brief description of the SAR for each box is included in the figure as well. For the full description please see Section 6.3.5



### *Nitazene like NSOs*

Very little information is available on the SAR of the benzimidazole NSOs class, i.e., the nitazenes. This is mainly due to the fact that these compounds are relative new entries into the NSO market, being introduced in the recreational market only in 2020. SAR evaluation on this class seemed to have been reported only by Vandeputte et al. (2021), as a result of *in vitro* activity assay on the MOR (Vandeputte et al., 2021). The main findings are reported below:

- The length of the para-alkoxy side chain seems to influence activity. In particular, the paraethoxy substituent in etonitazene seems to have the highest potency followed by isopropoxy, suggesting how small or compact chain substitutions results in optimal MOR activation.
- Replacement of the para-alkoxy tail with halogens – e.g. chlorine (clonitazene) and fluorine (flunitazene) drastically decreased potency.
- Removal of the NO<sub>2</sub> group seems to reduce the activity suggesting an important role for the 5-nitro group in the MOR activity.
- The role of dealkylation on the tertiary amine has not been fully comprehended to date.

## Isotonitazene Structure Activity Relationship

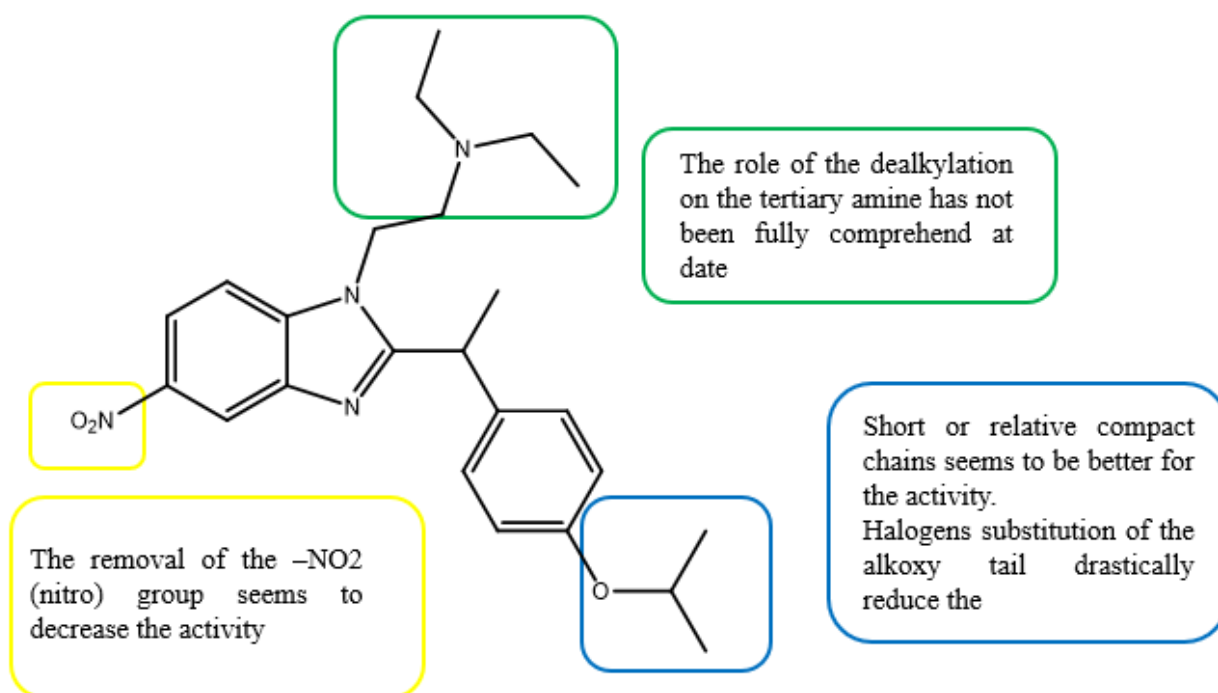


Figure 6.9 Structure activity relationship identified for nitazene-like NSOs.

Each part of the chemical scaffold whose modification is linked with biological activity changes has been highlighted with a coloured box. A brief description of the SAR for each box is included in the figure as well. For the full description please see Section 6.3.5

### 6.3.6 *Novel synthetic opioids drug design*

As previously reported for DBZDs, the production of NSOs seems to follow three main strategies:

- Identification of NSOs reported in the scientific literature or patented, but never commercialised. Examples are U-47700, an opioid analgesic of the class of cyclohexylbenzamides first developed in 1970 (Szmuszkovicz, 1976); MT-45 and opioid analgesic of the diphenyl-ethyl-piperazine class (Nishimura et al., 1976); desmethylprodine an opioid analgesic drug developed in the 1940s by Hoffmann-La Roche (Schmidle and Mansfield, 1954); acetylfentanyl was first disclosed in patents by the Belgian company Janssen in the early 1960s (EMCDDA-Europol, 2005); the AH-family first studies in the UK company Allen and Hanburys Limited (Brittain et al., 1973).
- Modifications of scheduled NSOs. e.g. U-49900 and 3,4-Methylenedioxy-U-47700 as novel structural analogues of U-47700 (Sharma et al., 2019).
- Emergence of new chemical classes. After the recent scheduling actions towards the fentanyl family of NSOs across the world, the emergence and interest towards new classes of “legal” opioids have been registered (Fogarty et al., 2022). These classes, which are structurally dissimilar to fentanyl, include cinnamylpiperazines and thiambutene.

## 6.4 In silico methods for novel synthetic opioids

From the analysis of the results obtained for the QSAR studies on DBZDs described above, the 3D QSAR model approach and the use of machine learning algorithms was found to be more reliable, i.e., produced better statistics, and more useful to predict the biological activity of unknown compounds. The 3D QSAR approach indeed employs different methodologies (e.g. machine learning and artificial neural networks) and different descriptor selection approaches which makes it more powerful than 2D QSAR. In particular it calculates/derives descriptor from the 3D spatial coordinate of the molecule which are more informative and more descriptive than the 2D coordinates only (Doweyko, 2007; Roy et al., 2015b; Tropsha, 2007). For this reason, for the class of NSOs, only the 3D QSAR models were calculated with the use of Forge™.

Moreover, due to the key role that MOR plays in both the strong analgesic property and the addiction and abuse potential which distinguishes the NSO class (sec 6.3.3), the study focused on evaluating firstly QSAR models for the prediction of biological activity on MOR.

### 6.4.1 QSAR with Forge™

The chemical structures of all the molecules used for the generation of the QSAR models with Forge™ were retrieved from the ChEMBL database selecting only those tested for their affinity for the human MOR (available online: <https://www.ebi.ac.uk/chembl/target/inspect/CHEMBL233>). For this target (ChEMBL, 2021a), i.e. CHEMBL233, various activity values are available, however only the Ki values were analysed and used. The biological activity Ki is identified as the ‘inhibition constant’ and indicates how potent a ligand is in inhibiting a process; Ki is the concentration required to produce half the maximum inhibition (Neubig et al., 2003). Ki is expressed in molar units (M), where 1 M is equivalent to 1 mol/L (Neubig et al., 2003). Only molecules for which the displacement of the radioligand [3H]DAMGO from the human MOR was used to determine of all of the Ki values, were selected. The binding data were converted to their negative decimal logarithm pKi ( $pKi = -\log Ki$ ).

As discussed previously (Ch 4.3.4), when building a QSAR model, attention should be paid to the similarity between the molecules used to train the model and those for which a prediction of activity is necessary. In this regard, the 2868 molecules available in ChEMBL were filtered with the use of Tc to produce two different datasets, one for fentanyl-like and one for morphine-like NSOs. Due to the paucity of experimentally derived biological activities for nitazene-like structures (Vandeputte et al., 2021), no QSAR model was built for the this NSO class. A total of 115 and 96 molecules was identified respectively for the dataset of fentanyl-like NSOs and of the morphine-like ones (Appendix A).

The two datasets were partitioned into training and test according to the activity, i.e. activity stratified. The default value of 20% was used to allocate entries in the test set.

To partition the data set into training and test set, the entries were loaded as a list of SMILES with corresponding  $K_i$  value from a csv file. When loading the file into Forge™, the molecule role (training set) and the protonation state were specified by the user. Forge™ automatically converted all molecules to 3D structures. All the molecules were uploaded (Figure 4.8) as a training set and further divided into a training and test set.

### 6.4.2 Forge™ Ligand specification and alignment

Once the molecules were loaded, they were aligned to the reference molecule (i.e. ligands). In Forge™, the alignment can be done in two ways: normal (or protein centric view) or substructure based (or ligand centric view). As reported above in paragraph 4.3.5, one or more molecule could be used as reference compounds for the alignment including the 3D structure of the receptor for a volume/steric evaluation guidance of the alignment (Floresta et al., 2019). For more details on the methodology please refer to Section 4.3.5. For the NSOs alignment, a combination of normal and structure based methods was used, due to the high flexibility of the molecules in analysis. An example of alignment made by Forge™ for the morphinan class is presented in Figure 4.9

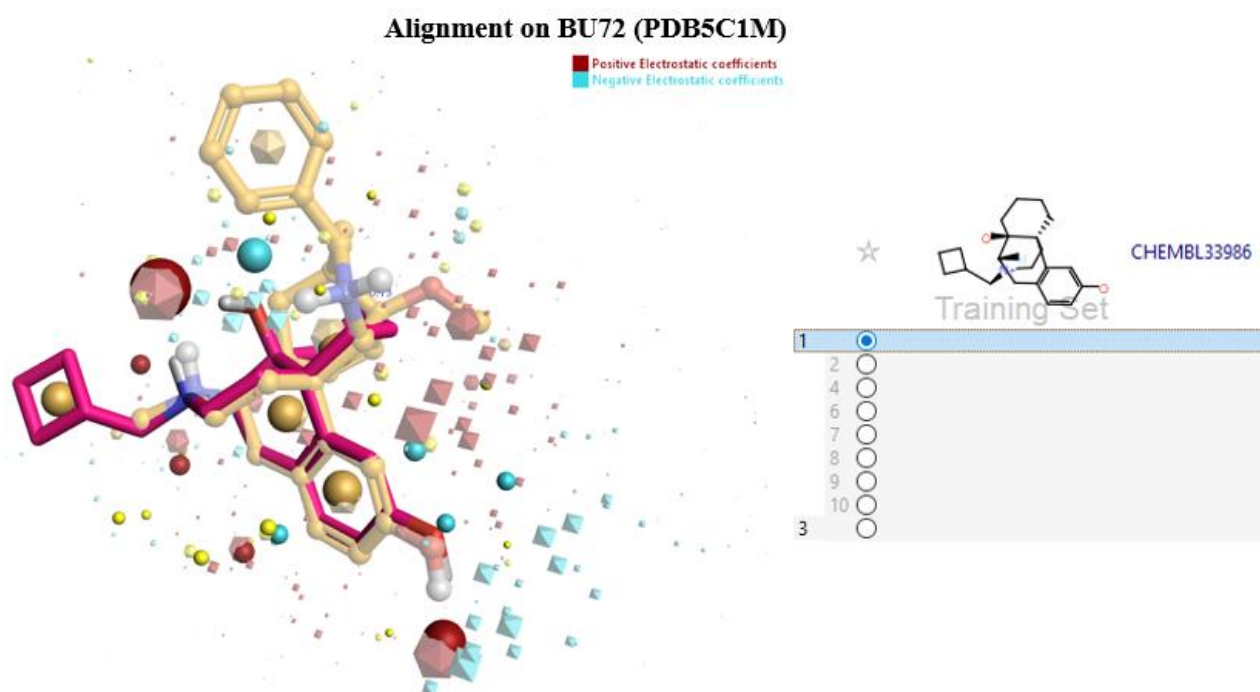


**Figure 6.10** Example of an alignment made by Forge™.

*On the right, the list of the possible 3D conformations automatically identified, and on the left, the 3D structure of the alignment proposed by Forge™ as the most energetic favourable by Forge™. The query molecule (CHEMBL33986) is in purple, while the reference ligand (BU72) is in light yellow. The drop-down menu on the right identifies all the different possible alignments (in this case 9) of the CHEMBL33986 on the reference molecule.*

### 6.4.3 Forge™ descriptors' selection

For detailed methodology of the descriptors selection in Forge™ please refer to Section 4.3.6

#### 6.4.4 Molecular Docking

##### *Identification of the 3D protein structures*

Molecular docking (MD) studies were used to evaluate the binding affinity between the NSOs identified by the NPSfinder<sup>®</sup> and the 3D crystal structure of the MOR identified in the PDB database. The crystallised structure of the KOR and DOR were used for the study reported in Chapter 8.

The analysis of the PDB database to retrieve the best 3D structures for the docking included the use of several key words as ‘opioid receptors, morphine, fentanyl, opioids, morphine-like, etc. Only the structures of human receptors were considered. From the keywords search three structures of interest were identified:

- PDB5C1M – ‘Crystal structure of active mu-opioid receptor bound to the agonist BU72’ (RCSB PDB, 2015)
- PDB6PT3 - ‘Crystal structure of the active delta opioid receptor in complex with the small molecule agonist DPI-287’ (RCSB PDB, 2019)
- PDB6B73 – ‘Crystal Structure of a nanobody-stabilized active state of the kappa-opioid receptor’ (RCSB PDB, 2018d)

As reported in section 4.3.8, agonist and antagonist ligands could cause a different rearrangement in the structure of the binding pocket and the whole receptor (An et al., 2019; Ng et al., 2014; Jianliang Zhang et al., 2009). Hence to obtain more reliable results, it is advisable to use the 3D structure which is bound to the most similar molecule to those under evaluation (i.e. DBDZs), both structure- and activity-wise (Leelananda and Lindert, 2016).

The protein structures identified in the PDB database are crystallised structures of the ORs in complex with the agonist BU72, DPI-287 and MP1104 (Figure 6.11).

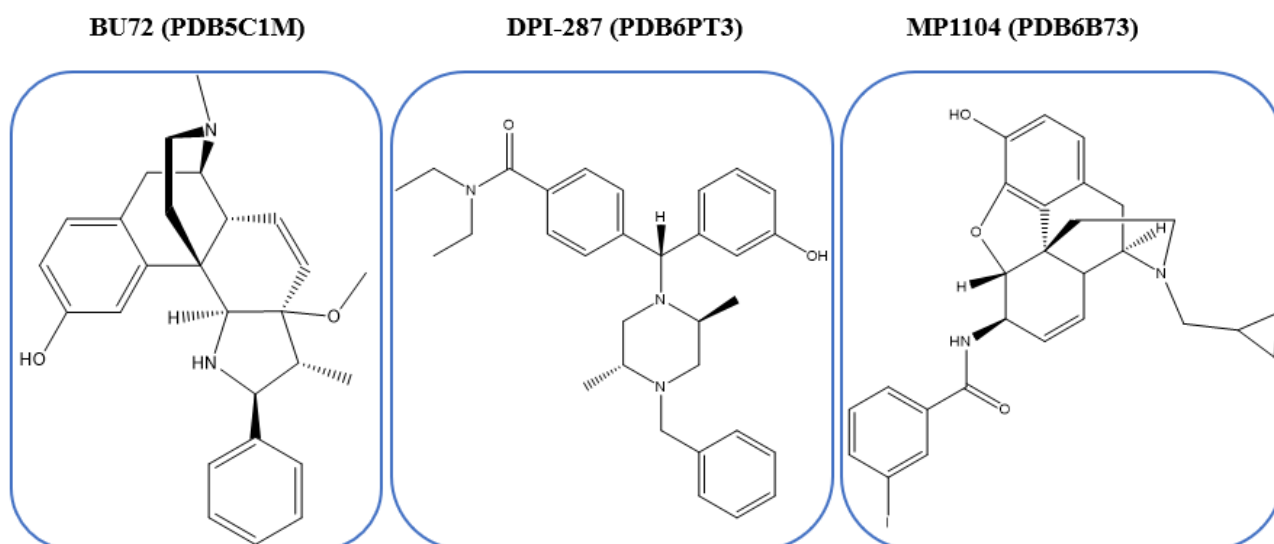


*Figure 6.11. 2D structure of the co-crystallised ligands for the ORs identified for the docking studies.*

*From the figure it can be observed that BU72 shows a phenanthrene scaffold, MP1104 a morphine like structure and DPI-287 a structure derivative of the benzlamides and phenylpiperazine.*

BU72 is an extremely potent opioid, showing a very high affinity for the MOR. Although it was found as a potent analgesic in animal studies, with a slow onset and long duration of action, it was never marketed (Neilan et al., 2004). It is used to model the activation process of MOR (Che et al., 2018). DPI-287 is a highly selective opioid agonist for DOR showing antidepressant like effects with reduced side effects (i.e. convulsion) (E. M. Jutkiewicz, 2006). MP1104, an analogue 3-iodobenzoyl naltrexamine, is a potent dual full agonist at DOR and KOR (Atigari et al., 2021, 2019).

#### *Preparation of the PDB structures*

The PDB files were loaded into MOE<sup>®</sup> via the Load PDB File application (see Appendix 4 for more details) and then prepared with the Quick Prep application as presented in Section 4.3.8. The structures were then ready to be used as input for molecular docking.



### Binding pocket and ligand interaction definition

The co-crystallised ligands available in PDB5C1M, PDB6PT3 and PDB6B73 were used to define the binding pocket/cavity and superposition target for docking calculations. All the residues included in a radius of 4.5 Å from the ligand were included in the binding pocket. Additionally, the Site finder application was used to define the characteristic of the whole pocket for each receptor (Table 4.2). The three binding pockets appear to be slightly different in terms of size and hydrophobic surface, with PDB6B73 showing a larger pocket (Table 4.2). This is due to a slightly different aminoacidic residues composition of the binding site consistent with the ORs belonging to three different subfamilies.

**Table 6.1 Description of the two binding pockets identified for 6HUO and 6HUP \*.**

Receptor	Site	Size	PLB	Hyd	Side	Residues
5C1M	1	204	3.64	74	128	1:(GLY52 SER53 HIS54 SER55 YCM57 TYR75 ALA117 THR120 GLN124 ASN127 TYR128 TRP133 VAL143 ILE144 ASP147 TYR148 ASN150 MET151 LYS209 CYS217 THR218 LEU219 THR220 PHE221 THR225 GLU229 LEU232 LYS233 VAL236 PHE237 TRP293 ILE296 HIS297 TYR299 VAL300 ILE301 LYS303 ALA304 TRP318 HIS319 CYS321 ILE322 GLY325 TYR326)
6B73	1	315	3.28	102	164	1:(VAL108 THR111 PHE114 GLN115 VAL118 TYR119 ASN122 SER123 TRP124 VAL134 LEU135 ASP138 TYR139 MET142 LYS200 ARG202 ASP204 VAL205 VAL207 ILE208 GLU209 CYS210 SER211 LEU212 GLN213 PHE214 PRO215 ASP216 SER220 TRP221 TRP222 ASP223 MET226 LYS227 VAL230 TRP287 ILE290 HIS291 PHE293 ILE294 GLU297 ALA298 THR302 SER303 HIS304 SER305 ALA308 LEU309 TYR312 TYR313 CYS315 ILE316 GLY319 TYR320 SER323)
6PT3	1	215	3.67	77	130	2:(ALA98 THR101 GLN105 ASP108 TRP114 VAL124 LEU125 ILE127 ASP128 TYR129 SER131 MET132 ARG192 ASP193 VAL197 CYS198 MET199 LEU200 GLN201 PHE202 SER206 TRP207 ASP210 THR211 THR213 LYS214 VAL217 PHE218 TRP274 ILE277 HIS278 PHE280 VAL281 ILE282 TRP284 THR285 LEU300 CYS303 ILE304 GLY307 TYR308 SER311)

\*The size column indicates the number of alpha spheres comprising the site; the PLB column indicates the Propensity for Ligand Binding score for the contact residues in the receptor; the Hyd column indicates the number of hydrophobic contact atoms, and the Side column indicates the number of sidechain contact atoms. The Residues column indicates the residues in the binding pocket in the format chain:residue-name.

For each receptor, the 3D structure as analysed and the information contained in the scientific paper of reference were used to explore the ligand interactions and identify the most important residues for the agonist allosteric activation of the OR. The binding pockets as visualised in MOE<sup>®</sup> for each OR are presented in Figure 4.12, 6.14 and 6.15.

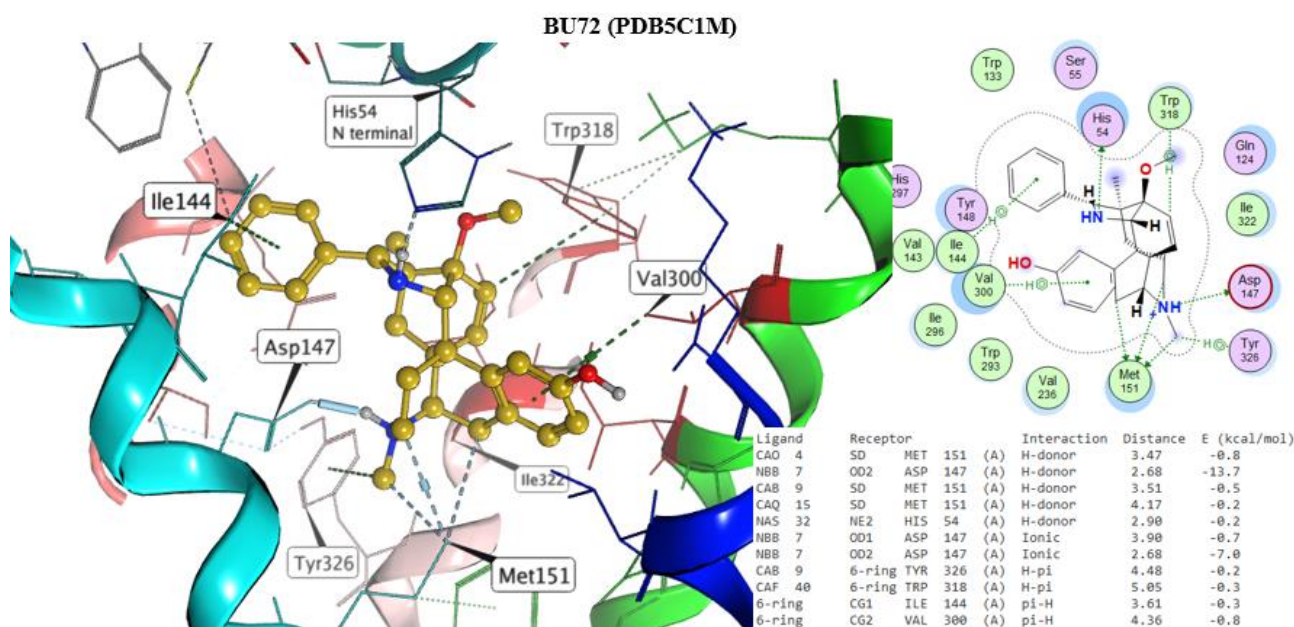


**Figure 6.12 PDB51CM binding pocket 3D and 2D representations.**

**Notes:** On the left, the binding pocket 3D representation with the co-crystallised ligand BU72 (gold). Light blue was used to identify the receptor TM3 helix, green for the TM6 helix, pink for the TM7 helix, dark blue for the TM5 helix and lobster pink for the TM2 helix. On the right, the 2D representation of the binding pocket and interactions between receptor residues and ligand are provided. Below a report of the type of interactions, the receptor residues and the BU72 atoms involved, and relative distance and energy parameter (kcal/mol) is outlined. The colours used to depict the residues in the 2D screenshot define different characteristics of the latter: light purple for polar residues and light green for hydrophobic ones; red circle indicates an acidic and blue a basic residue; and the light blue halo indicates solvent exposure both on the receptor and the ligand

Most of the interactions observed between BU72 and active  $\mu$ OR are hydrophobic or aromatic in nature, with only two conserved polar interactions. These two polar interactions are the ionic interaction between the morphinan tertiary amine and Asp1473, an interaction that is observed both for agonist and antagonist (Manglik et al., 2012); and a water-mediated interaction between the hydroxyl group on the phenolic ring and His297 (Huang et al., 2015) .

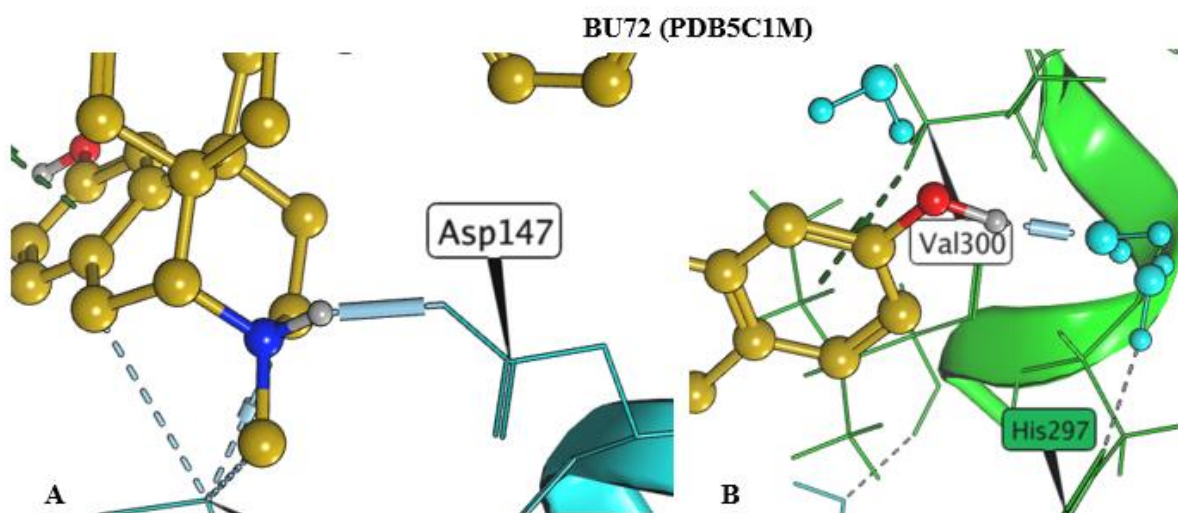


*Figure 6.13 Representation of the two polar interactions (light blue cylinder).*

*A is the ionic interaction between the morphinan tertiary amine and Asp1473, an interaction that is observed both for agonist and antagonist (Manglik et al. 2012); and B the water-mediated polar interaction between the hydroxyl group on the phenolic ring and His297 (Huang et al. 2015).*

Similar interaction patterns were observed for KOR (Figure 4.13).

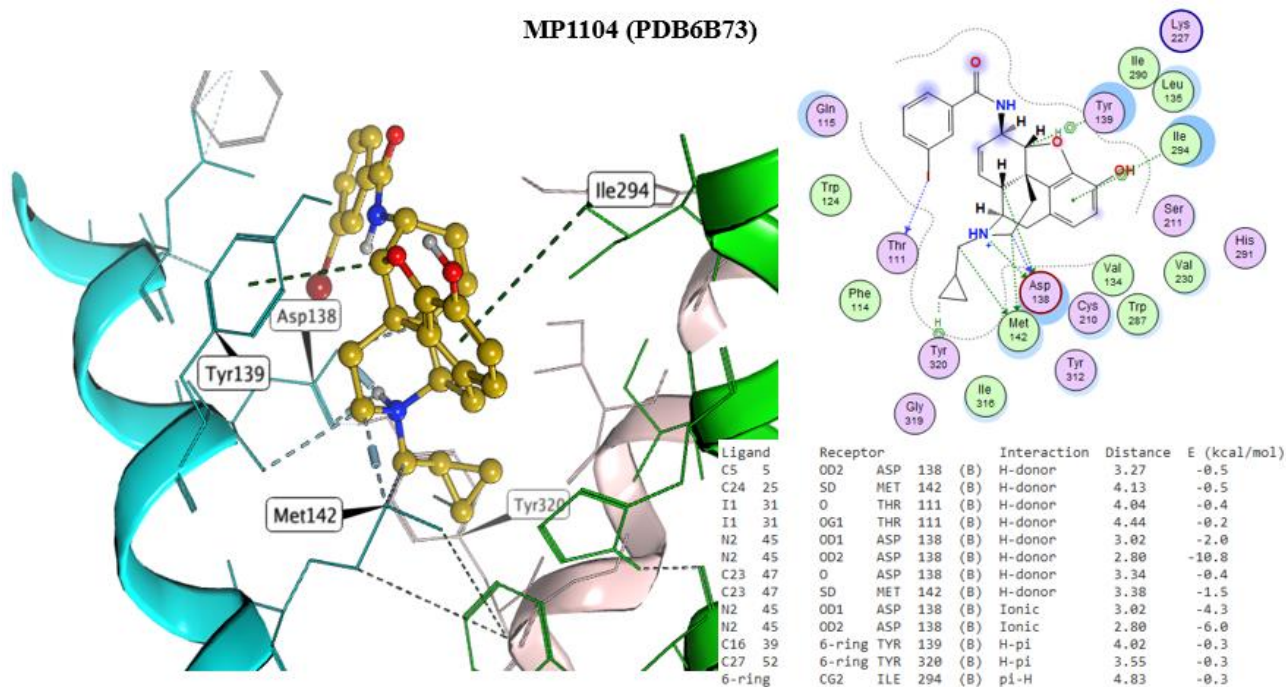


**Figure 6.14** PDB6B73 binding pocket 3D and 2D representations.

**Notes:** on the left, the 3D binding pocket representation with the co-crystallised ligand MP1104 (gold). Light blue was used to identify the receptor TM3 helix, green for the TM6 helix, pink for the TM7 helix. On the right, the 2D representation of the binding pocket and interactions between receptor residues and ligand are provided. Below a report of the type of interactions, the receptor residues and the MP1104 atoms involved, and relative distance and energy parameter (kcal/mol) are outlined. The colours used to depict the residues in the 2D screenshot define different characteristics of the latter: light purple for polar residues and light green for hydrophobic ones; red circle indicates an acidic and blue a basic residue; and the light blue halo indicates solvent exposure both on the receptor and the ligand

The pose assumed by the MP1104 core scaffolds showed common features typical for opioid ligands: i.e. the salt bridge between the ligand tertiary amine and Asp 138; H-bond donor interaction with Met142 and interactions with TM3/7 via chemically diverse moieties (Figure 4.13) (Che et al., 2018). In particular, the larger distance of the salt bridge (3.0) compared to BU72 suggest a weaker interaction between MP1104 and KOP (Che et al., 2018). For this compound, Che et al. report further interactions which cannot be appreciated by the analysis of the 3D structure, i.e. water-mediated hydrogen bonds between the phenolic group and the Lys227 (TM5). It is interesting how the cyclopropyl moiety of MP1104 occupies a hydrophobic pocket, previously thought to be responsible of the agonist/antagonist discrimination (Huang et al., 2015). Various interaction with this pocket and MP1104 have been reported (Che et al., 2018), i.e. the ones between the cyclopropyl and the side chain of Trp287, the backbone of Gly197 and the aromatic side chain of Tyr207 (the only one visible in Figure 4.13).



The interaction pattern of DOR is presented in Figure 4.14.

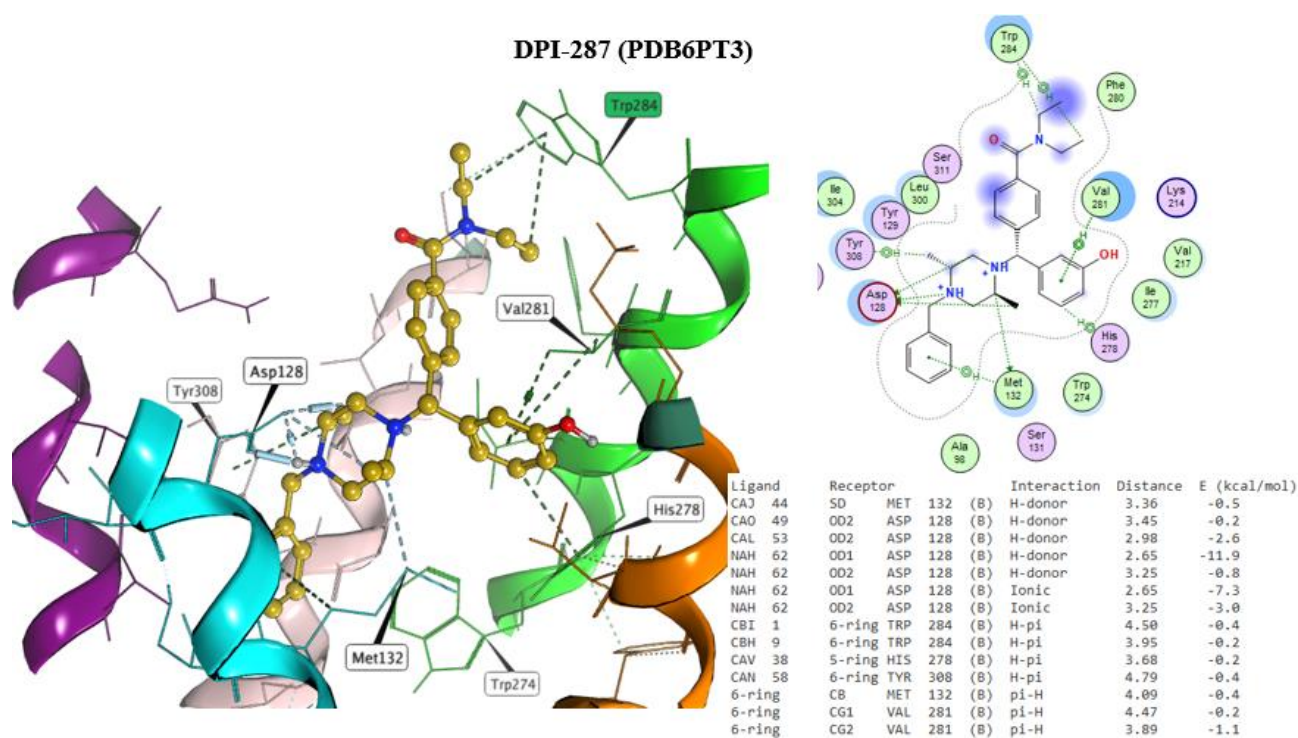


Figure 6.15 PDB6B73 binding pocket 3D and 2D representations of the PDB6B73 binding pocket.

Notes: on the 3D left, the binding pocket representation with the co-crystallised ligand DPI-287 (gold). Light blue was used to identify the receptor TM3 helix, green for the TM6 helix, pink for the TM7 helix, orange for the TM5 helix and purple for the TM2 helix. On the right, the 2D representation of the binding pocket and interactions between receptor residues and ligand are provided. Below, a report of the type of interactions, the receptor residues and DPI-287 atoms involved, and relative distance and energy parameter (kcal/mol) is outlined. The colours used to depict the residues in the 2D screenshot define different characteristics of the latter: light purple for polar residues and light green for hydrophobic ones; red circle indicates an acidic and blue a basic residue; and the light blue halo indicates solvent exposure both on the receptor and the ligand

DPI-287 shows the same protonated nitrogen atom mediated salt-bridge interaction to Asp128 observed for the other ORs ligands. The Asp128 is itself part of a polar network together with Tyr308, Thr101, and Gln105, which connects the TM2, TM3 and TM7 helices. Tyr308 shows additional aromatic static interactions with the unsubstituted benzyl moiety of DPI-287. Claff et al. argued that the polar network around the Asp residue plays an ‘essential role in agonist-induced activation at DOP’ and proposed that the positioning of the basic amine deeper into the binding pocket, as opposed to antagonist, is a symbol of opioid agonist activity (Claff et al., 2019). The interaction between His278 and the phenol moiety (conserved in many ligands of OR peptides and small molecules) is another important one for DOR activation. This interaction, as reported by Claff et al, indeed connects DPI-287 to TM3, TM5, and TM6 helices (Claff et al., 2019). Other interactions include hydrogen-bond donor with Met132, as observed in MOR and KOR; H-pi interactions with Tyr308 and Trp284; and pi-H interaction with Val281.

### *Ligands reference datasets*

A reference data set for the docking studies was prepared with the aim of including the co-crystallised ligand for each OR and some reference compounds among those identified in ChEMBL as potent agonist. A total of five molecules for each OR including the co-crystallised ligand were extrapolated from the literature according to their strong activity as agonist binders and used as reference molecules for docking studies (Table 6.2).

Table 6.2 Reference molecules for docking studies\*

<b>MOR</b>		
<b>Molecule</b>	<b>SMILESs</b>	<b>S (Kcal/mol)</b>
<b>BU72</b>	<chem>O(C)[C@]12[C@]3(C)[C@@H](c4ccccc4)[NH2+][C@H]1[C@@]14c5c(ccc(O)c5)C[C@@H]([NH+](C)CC1)[C@@]4(C=C2)C3</chem>	-10.15
fentanyl	<chem>O=C(N(c1ccccc1)C1CC[NH+](CCc2ccccc2)CC1)CC</chem>	-8.44
carfentanyl	<chem>O=C(N(c1ccccc1)C1(C(=O)OC)CC[NH+](CCc2ccccc2)CC1)CC</chem>	-9.59
$\alpha$ -methylfentanyl	<chem>O=C(N(c1ccccc1)C1CC[NH+](C[C@@H](Cc2ccccc2)C)CC1)CC</chem>	-8.99
$\beta$ -hydroxyfentanyl	<chem>O=C(N(c1ccccc1)C1CC[NH+](C[C@@H](O)c2ccccc2)CC1)CC</chem>	-8.79
<b>KOR</b>		
<b>MP11 04</b>	<chem>C1CC1CN2CC[C@]34[C@@H]5[C@H]2CC6=C3C(=C(C=C6)O)O[C@H]4[C@@H](C=C5)NC(=O)C7=CC(=CC=C7)I</chem>	-9.79
CHEMBL503080	<chem>Clc1cc2c(CC(=O)N3[C@H](C[NH+]4CCCC4)CN(c4ccccc4)CC3)csc2cc1</chem>	-9.00
CHEMBL526933	<chem>Clc1c(Cl)ccc(N(CC(=O)N2[C@H](C[NH+]3CCCC3)CN(S(=O)(=O)C)CC2)C)c1</chem>	-9.24
CHEMBL499351	<chem>Clc1c(Cl)ccc(N(CC(=O)N2[C@H](C[NH+]3CCCC3)CN(S(=O)(=O)c3cc(Cl)ccc3)CC2)C)c1</chem>	-9.74
CHEMBL525457	<chem>Clc1cc2N(CC(=O)N3[C@H](C[NH+]4CCCC4)CN(S(=O)(=O)c4cc(OC)c(OC)cc4)CC3)C(=O)Oe2cc1</chem>	-9.81
<b>DOR</b>		
<b>DPI-287</b>	<chem>O=C(N(CC)CC)c1ccc([C@@H](N2[C@@H](C)C[NH+](CC=C)[C@H](C)C2)c2cc(O)ccc2)cc1</chem>	-8.58
CHEMBL2151735	<chem>O=C(N([C@@H](C(=O)N[C@@H]1C(=O)N(CC(=O)N)Cc2c(cccc2)C1)C)C)[C@@H]([NH3+])Cc1c(C)cc(O)cc1C</chem>	-9.44
CHEMBL8234	<chem>O=C([O-])[C@@H](NC(=O)[C@@H](NC(=O)CNC(=O)CNC(=O)[C@@H]([NH3+])Cc1ccc(O)cc1)Cc1ccccc1)CC(C)C</chem>	-10.43
CHEMBL3758292	<chem>O=C([C@@H]([NH3+])Cc1c(C)cc(O)cc1)N1[C@@H](C(=O)NCc2[nH]c3c(n2)ccccc3)Cc2c(cccc2)C1</chem>	-9.70
CHEMBL2113666	<chem>Clc1c(/C=C/C(=O)N[C@]23[C@@H]4[NH+](C)CC[C@@]52[C@H](C(=O)CC3)Oe2c5c(ccc2)C4)cccc1</chem>	-7.26

\*Reference molecules for docking studies. A total of five potent agonist was identified including the co-crystallised ligand and four molecules identified in the ChEMBL target page for each OR. For each molecule, the SMILES was retrieved from ChEMBL.

### *Molecular Docking Approaches*

The molecules in Table 4.3 were docked alongside the molecule identified by NPSfinder<sup>®</sup> (Table 3.2), using the general docking panel in MOE<sup>®</sup>. It is important to underscore that, when available, information on the active placement (i.e. presence of the co-crystallised ligand) and fundamental interactions should be taken into high consideration to proceed to a more informed docking study. To include information available on fundamental interactions, a pharmacophore was defined as described in Section 4.3.8. Because of differences in the structure of some of the ligands, i.e. fentanyl-like and nitazenes, compared to the morphinan-like structures of the MOR and DOR ligands, only few features were included in the pharmacophore query. This differs from what was developed for the DBZDs, for which the pharmacophore queries were more detailed due to the similarity of structure between the DBZDs and the co-crystallised molecule. The pharmacophores obtained for MOR, DOR and KOR are reported in Figure 4.15 and Figure 4.16.



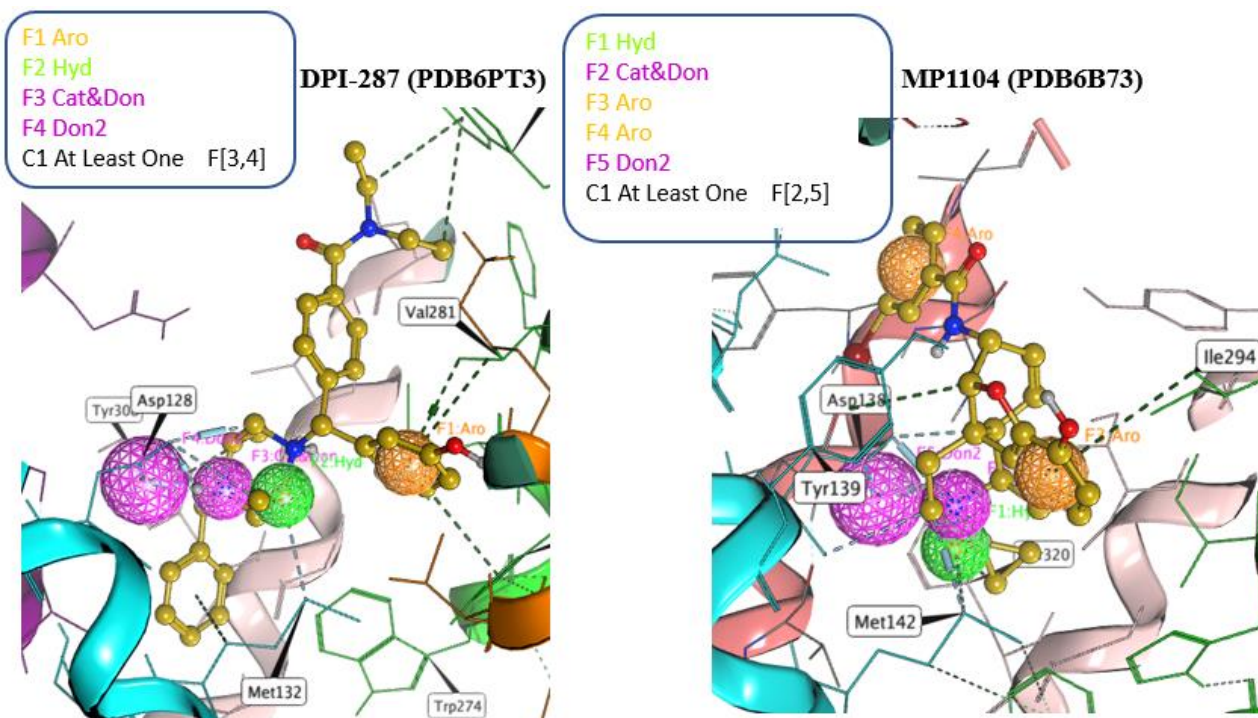


Figure 6.16 Pharmacophore query used for the docking placement with PDB6PT3 (left) and with PDB6B73 (right).

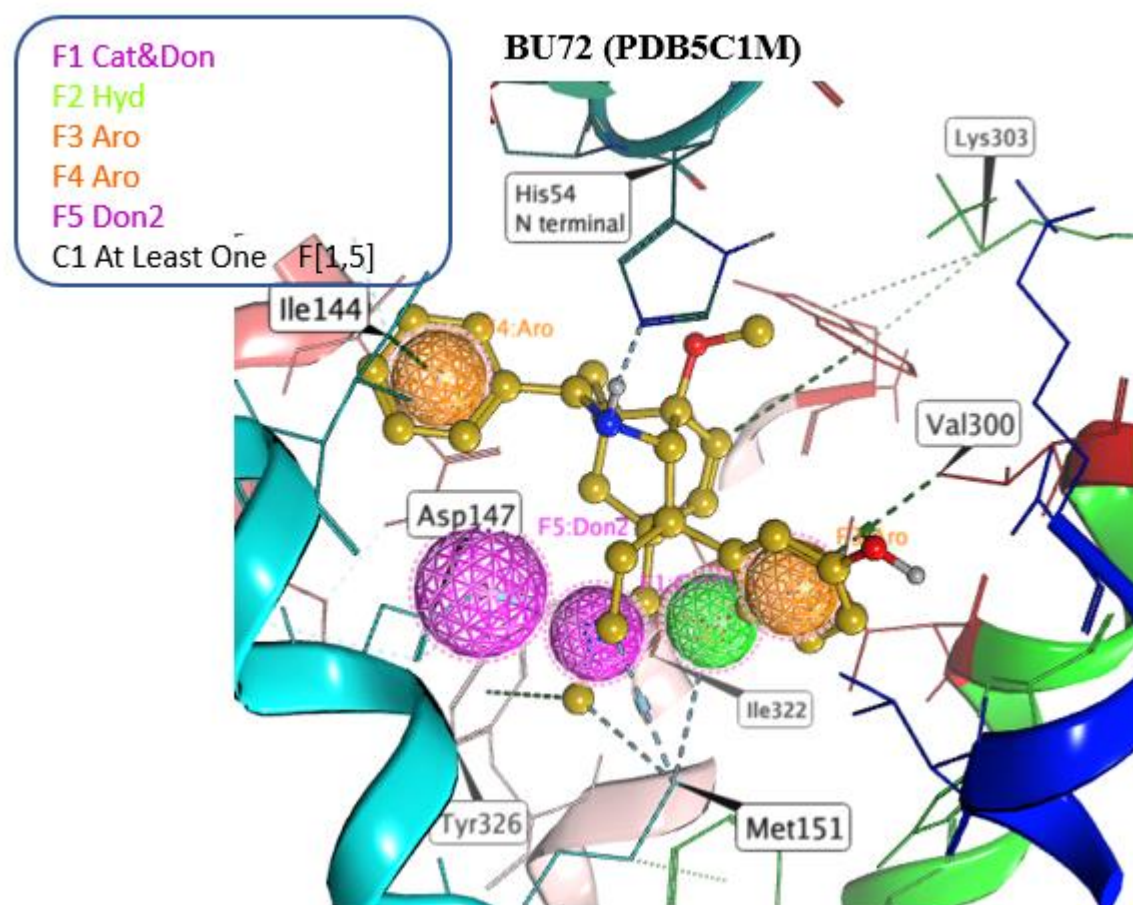


Figure 6.17 Pharmacophore query used for the docking placement with PDB5C1M

The so-designed pharmacophore query takes into consideration both the ligand and the receptor properties. In particular a constrain (C1 and C2) was highlighted to ensure the presence of a cation/donor ligand feature in proximity of the Asp residue in all the ORs. The other highlighted features were: two aromatic features in proximity to the phenolic ring and unsubstituted phenyl and a hydrogen one next to the ligand charged amine and in proximity to the Met residue.

The generated pharmacophore queries were used both for the placement and refinement of the poses. In particular, each docking run was done in triplicate, with 50 poses for each entry returned by the placement and ten poses returned by the refinement.

The poses were then analysed and filtered according to the S value and rmsd\_refine (i.e. the root mean square deviation between the pose before and after refinement), the E\_refine score from the refinement stage. For each pose, a PLIF was also calculated.

#### *Protein ligand interaction fingerprint*

The PLIF was calculated automatically during the generation of the docking poses. For further details, please refer to Section 4.3.8.

#### 6.4.5 Pharmacophore

For the pharmacophore mapping study's methodology carried on the ORs please refer to Section 4.3.9 and 8.2.3.

In the following Chapter the results of the *in silico* studies on NSOs are reported.

## Chapter 7 Results and discussions of in silico studies on novel synthetic opioids

As discussed in Section 6.4.1 two different models were created for the fentanyl-like and morphine-like NSOs.

### 7.1 QSAR with Forge™ for fentanyl-like NSOs

#### 7.1.1 Training and test sets

The same methodology presented in Section 5.2.1 was used here to define the training and the test set used for the QSAR studies. The total of 115 structures were divided according to their pKi value into a training set (94) and a test set (21) (Appendix A). The aim was to obtain two sets, both representative of the activity values space in the analysis. pKi values ranged from 10.2 and 5.1 across the whole database.,

A set of field points as described in Section 5.2.1 was calculated with regards to electrostatically positive and negative van der Waals attractive and hydrophobic features. The 115 3D structures were aligned in Forge™ on the previously reported active conformations of BU72 in the crystallised MOR structure ( Figures 4.12 and 4.13) (RCSB PDB, 2018a, 2018b), and then submitted to the Forge™ processing application. The alignment process used was a mix of normal and substructure.

Normal alignment is based on the on the field point overlay technique and it is the standard Cresset alignment method (Cresset, 2021). The substructure alignment instead aligns all molecules to one of the references. i.e. BU72 according to a Maximum Common Substructure (MCS). This step is followed by a conformation hunt applied to the remaining atoms, and the resulting conformers are scored in this aligned orientation (Cresset, 2021). The field score is used only to select orientations for any side chains.

#### 7.1.2 3D QSAR Models

Three different model building calculations were used similarly to the DBZDs project, i.e. 3D-Field QSAR, Random Forest, and Relevant Vector Machine (RVM) models (Ch 4.3.7). Detailed information on the methodology is presented in Appendix B.

The 3D Field QSAR was generated via a partial least squares (PLS) analysis (Wold et al., 2001), specifically with the use of the SIMPLS algorithm (de Jong, 1993). The number of components of PLS defined as optimal (5) was identified in 20 automatically generated, with a reported  $r^2$  (coefficient of determination) of 0.97 and  $q^2$  (cross-validated coefficient of determination) of 0.75 as seen in Table 5.6. The statistics for the 20 methods are reported in Appendix A.

**Table 7.1 Values for the statistics obtained for the three calculated QSAR models\***

Model	r <sup>2</sup>	q <sup>2</sup>	r <sup>2</sup> Test	RMSE	Tau
3D Field QSAR	0.97	0.75	0.94	0.51	0.86
Random Forest	0.91	0.7	0.81	0.27	0.82
RVM	0.95	0.76	0.97	0.24	0.81

**\*Here are presented the statistic for the QSAR models generated in the form of: the coefficient of determination (r<sup>2</sup>) which indicates the goodness of fit; the cross-validated coefficient of determination (q<sup>2</sup>) which indicates the robustness; the coefficient of determination for the test set (r<sup>2</sup> test), which indicates the predictive power; the root mean square error (RMSE) as reliability measure; and Tau as a further parameter to assess the predictivity of the model. As r<sup>2</sup>, the closer the value of Tau is to one, the better the model.**

The cross-validated coefficient of determination is the validation parameter obtained with the leave one out cross-validation (LOO CV) used in Forge<sup>TM</sup> as internal method validation, and evaluates to which degree the prediction of a model is better compared to a null one (Golbraikh and Tropsha, 2002). To further assess the reliability of the method, the forecast of the measurements of the root mean squared error (RMSE) are reported, and in particular a value of 0.51 was identified for the final QSAR model. External validation was carried out on the test set (21 molecules), obtaining an r<sup>2</sup> of 0.94. The two machine learning models' performance was found to be comparable with the Field QSAR one. With Forge<sup>TM</sup>, an additional variable is used to describe the reliability of the models, i.e. the Kendall's Tau, which predicts the ability of a model to rank molecules (sec 5.2.2 ) (Kendall, 1938). The Tau values obtained for the models are higher than 0.8, suggesting a good predictivity for all of them.

A visual representation of the predicted vs. experimental values for training and test sets is reported in Figure 7.1.

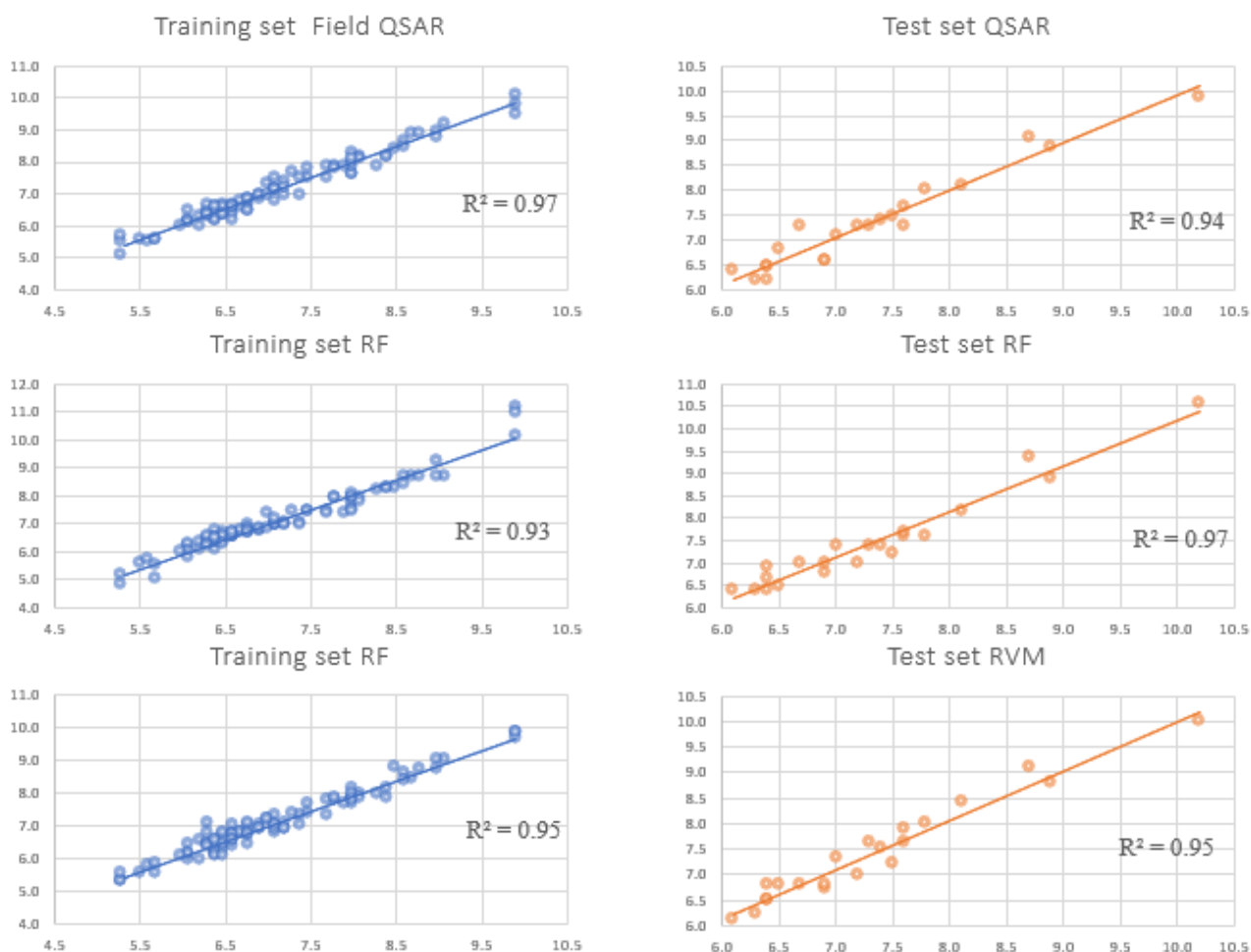


**Figure 7.1** Visual representation of the predicted (x axis) vs. experimental (y axis) log 1/c values for the training (blue) and test (orange) sets.

*The graphs were built with Excel 2022.*

The 3D Field QSAR analysis returned a linear relationship ( $r^2= 0.97$  for training set and 0.94 for test set) between the descriptors and the activity confirming a high correlation and predictivity and provided a visual interpretation of the QSAR model. Positive and negative electrostatic features are reported in Figure 7.2, while favourable and unfavourable hydrophobic features are reported in Figure 7.3.

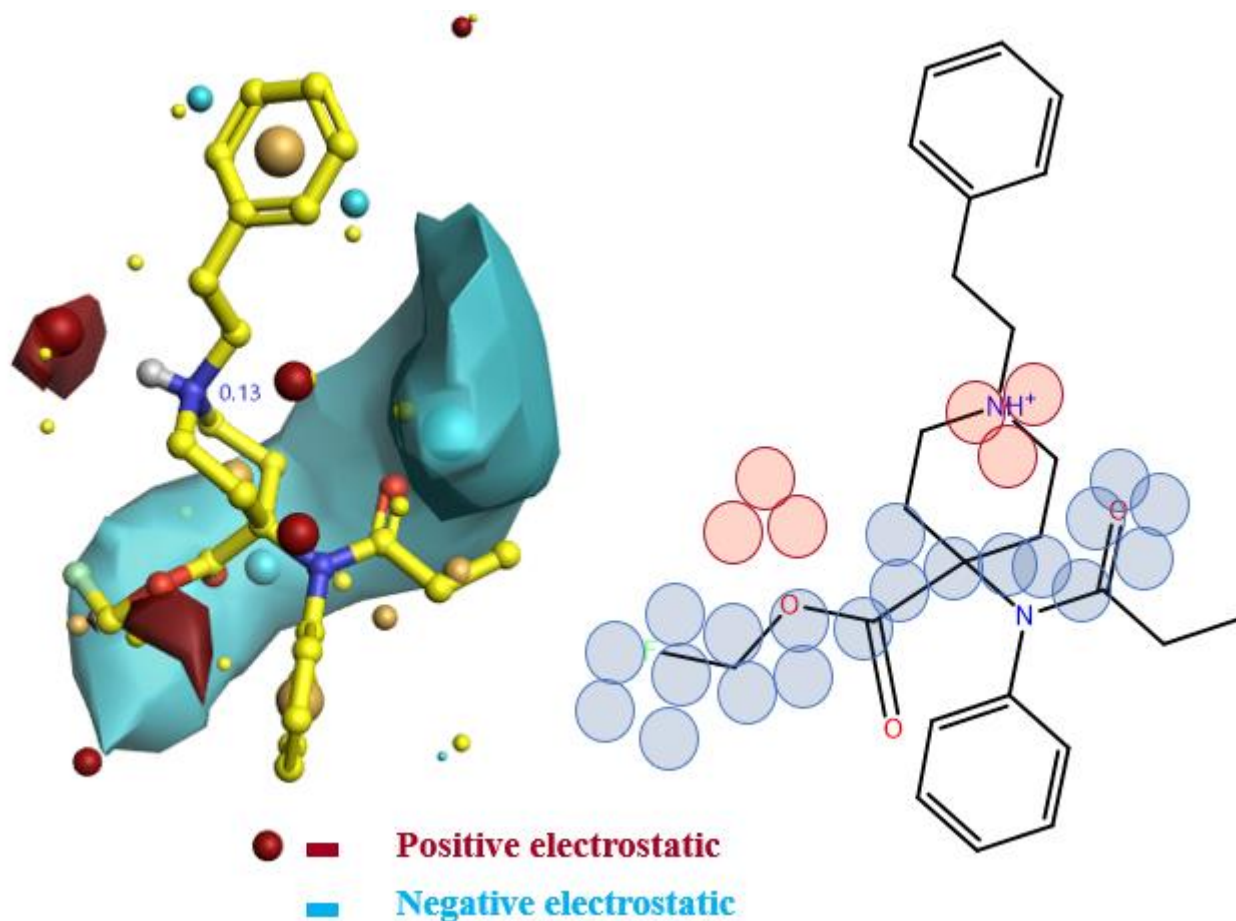


*Figure 7.2 3D and 2D visual representations of the generated 3D Field QSAR model for electrostatic features*

*Notes Electrostatic properties are identified by the red (positive) and blue (negative) colours. In particular, the red and blue shapes indicate the space around the molecule in which more positive electrostatic interaction (red) or more negative electrostatic interaction (blue) will be beneficial (i.e. increase) for the activity. More positive interactions (red) could mean that placing strong H-bond donors in that region improves activity or could mean as well that putting strong H-bond acceptors will worsen activity, and vice versa with blue. The green and violet areas instead indicate how the presence of a hydrophobic interaction in that region would increase (green) or decrease (violet) activity.*



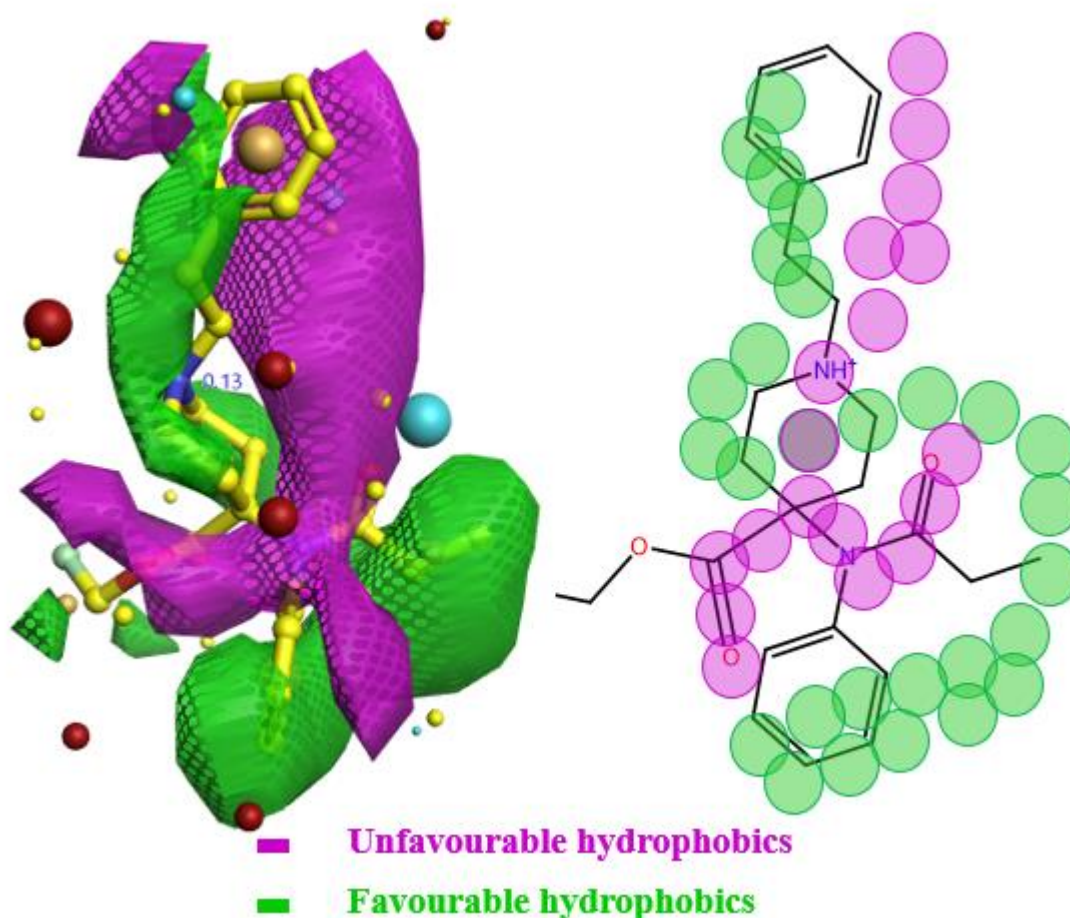


*Figure 7.3 3D and 2D visual representations of the generated 3D Field QSAR model for hydrophobic features*

*Notes The favourable and unfavourable hydrophobics are identified by the green and violet colours. The green and violet area indicate how the presence of a hydrophobic interaction-prone group in that region would increase (green) or decrease (violet) activity.*

From the 3D and 2D maps presented above (Figures 7.2 and 7.3), it is clear how hydrophobic interactions seem to play an important role in the definition of the activity of the molecule. This is in line with what was reported in Section 6.4.4, about the fact that the majority of the interactions observed between BU72 and the active MOR are hydrophobic or aromatic in nature, with only two conserved polar interactions (Huang et al., 2015). The positive electrostatic interactions (red shapes) cover a very small area of the whole molecule and can be found mainly in correspondence with the tertiary amine positively charged of the molecule. This means that a strong H-bond donor in that region is expected to improve activity. The blues shapes instead, i.e., negative electrostatic interaction, run along the lateral chains of the compound, i.e., the fluoromethoxycarbonil and the propyl amido, where the oxygen atoms are displayed. In fact, the blue shape indicates how a strong H-bond acceptor would increase activity. This is in line with what reported for the SAR of the carboxamide moiety of fentanyl in Section 6.3.5, i.e., aliphatic chains decrease activity, and for



aliphatic chains decrease the activity, and for the piperidine portion C4 substitution, i.e. increase of activity with R groups containing oxygen atoms (Vasudevan et al., 2020).

The green areas instead indicate how hydrophobic interactions are important for biological activity. Indeed relevant hydrophobic interaction areas are identified around the anilino phenyl and phenethyl moiety in agreement with the aromaticity of the anilino phenyl moiety as necessary to the activity (Casy and Parfitt, 1986). These hydrophobic patches which run alongside the whole molecule seems to be disrupted only in proximity to the nitrogen atoms (purple areas).

The three QSAR models identified above were used to predict the biological activity of the 238 NSOs identified online (the majority of which were retrieved from isomer design (Isomer Design, 2021) (Appendix A). As discussed in section 6.1.4 the biological activity  $K_i$  is the ‘inhibition constant’ (Neubig et al., 2003), is expressed in molar units (M), and calculated as the displacement of the radioligand [3H]DAMGO from the human MOR.

During the analysis of the predicted p $K_i$  values, it was noted that the RF models tend to over-predict values for some of the NSOs listed, hence only the Field QSAR and the RVM values were averaged to obtain a final prediction. For brevity, only the top ten NSOs listed according to their decrescent predicted biological activity value (Field QSAR) are reported below (**Error! Not a valid bookmark self-reference.**). The full table is in Appendix A.

*Table 7.2 Top ten fentanyl-like NSOs molecules reported in decreasing order of predicted p $K_i$  values\**

Title	p $K_i$ pred	Dist to model	Sim
N-(2-fluorophenyl)-n-[1-(2-phenylethyl)-4-(pyridin-2-yl)piperidin-4-yl]propanamide	10.2	Excellent	0.7
Methyl 4-[phenyl(propanoyl)amino]-1-[2-(1h-pyrrol-1-yl)ethyl]piperidine-4-carboxylate	10.1	Good	0.6
2-methyl carfentanil	10.0	Good	0.7
Carfentanil	10.0	Excellent	0.7
N-methyl-carfentanil	10.0	Excellent	0.6
Butyryl-carfentanil	10.0	Excellent	0.7
Acetyl-carfentanil	9.9	Excellent	0.7
N-{1-[2-(4-ethyl-5-oxo-4,5-dihydro-1h-tetrazol-1-yl)ethyl]-4-(1,3-thiazol-2-yl)piperidin-4-yl}-n-(2-fluorophenyl)propanamide	9.9	Excellent	0.6
4-methoxymethylfentanyl	9.9	Excellent	0.7
N-(2-fluorophenyl)-n-{1-[2-(1h-pyrazol-1-yl)ethyl]-4-(pyridin-2-yl)piperidin-4-yl}propanamide	9.9	Excellent	0.6

\*The reported p $K_i$  values are the average of Field QSAR and RVM predicted values.

The same methods were used to predict the p $K_i$  of fentanyl which returned a value of 9.2. This value together with the one obtained for carfentanil were used as a gauge of the relationship between predicted p $K_i$  and potency. In line with this, the final predictions were used to divide the NSOs into three groups as seen for the DBZDs, i.e. the high activity group (p $K_i$  > 9.0), the medium

activity group ( $pK_i < 9.0$  and  $>8.0$ ), and the low activity group ( $pK_i < 8.0$ ). Values of  $pK_i > 10$  can be considered prediction of very high biological activity. It was found that 40% of the 238 NSOs were predicted to display a high biological activity, 45% a medium and 15% a low biological activity. For the scope of this study a low biological activity is considered compared to fentanyl, hence this mean that these compounds can still display a potency in the range of the morphine-like structure.

The NSOs showing the highest biological activity were N-(2-Fluorophenyl)-N-[1-(2-phenylethyl)-4-(pyridin-2-yl)piperidin-4-yl]propanamide ( $pK_i = 10.1$ ), carfentanyl (10.0), butyryl-carfentanyl (10.0), N-(2-Fluorophenyl)-N-[1-(2-phenylethyl)-4-(1,3-thiazol-2-yl)piperidin-4-yl]propanamide (10.0), 2-methyl carfentanyl (10.0), acetyl-carfentanyl (9.9), 4-methoxymethylfentanyl and N-quinolinyl-fentanyl (both 9.8).

These molecules, predicted as very potent by the QSAR studies, were not identified nor reported by the official sources/databases, and they do not seem to be discussed online yet as well. It is interesting to note how all these NSOs, but one, show a substitution on the C4 atom predominantly with a carboxylate group in line with the SAR reported for this NPS class (Sec. 6.3.5). Other common characteristics of these NSOs are a fluorine atom on the anilino phenyl portion (Figure 6.8) and the substitution of the latter with a piperidine or the substitution of the phenethyl moiety with a pyrrole. Once again it is observed how the fluorine atoms substitution is associated with an increased biological activity.

The predicted values of  $pK_i$  suggest the likelihood of these NSOs having a biological activity which is comparable to carfentanyl, one of, if not the most, potent NSO so far reported by the UNODC and EMCDDA (Elliott and Hernandez Lopez, 2018; EMCDDA, 2022a, 2017d; UNODC, 2019d). Carfentanyl is indeed 10000 times more potent than morphine and 100 times more potent than fentanyl (DEA, 2022d), and has been associated with the rise of overdose deaths registered in the United States associated with the opioid crisis and in north Europe (EMCDDA, 2019b; Jalal and Burke, 2021; Prekupec et al., 2017; Seyler et al., 2021; Wilcoxon et al., 2018). The high potency of carfentanyl means that this NSO is active in the microgram range (i.e.  $k_i = \text{sub nM}$ , with fentanyl having a  $k_i$  in the 0-100 nM) - making it a very dangerous substance for the recreational users (also for the opioid tolerant ones) and a possible lethal threat to first responders and law enforcement personnel who may come in contact with this substance (DEA, 2022d).

### 7.1.3 Domain of applicability with Forge™

The applicability domain, for each QSAR model generated with Forge™ was automatically calculated and reported in the 'Distance to Model' column for all the entries as discussed in Section

5.2.3. The distance to model for each of the 238 NSOs is reported in Appendix A. Prediction with a poor or bad distance should not be taken into consideration as unreliable.

## 7.2 QSAR with Forge™ for morphine-like NSOs

### 7.2.1 Training and test sets

The same methodology presented in Section 5.2.1 was used here to define the training and the test set used for the QSAR studies. The 96 structures were divided according to their pKi value into a training set (75) and a test set (21) (Appendix A). The pKi values ranged from 10.2 and 5.3 across the whole database, with higher values indicating stronger biological activity. The same methodology described in Section 7.1.1 was followed.

### 7.2.2 3D QSAR Models

Also for morphine/like NSO 3D-Field QSAR, RM, and RVM models were calculated (Sec 4.3.7). Detailed information on the methodology is presented in Appendix B.

The number of components of PLS defined as optimal (3) was identified among 20 models automatically generated, with a reported  $r^2$  (coefficient of determination) of 0.87 and  $q^2$  (cross-validated coefficient of determination) of 0.69 as seen in Table 7.3. The statistics for the 20 methods are reported in Appendix A.

**Table 7.3 Values for the statistics obtained for the three calculated QSAR models\***

Model	$r^2$	$q^2$	$r^2$ Test	RMSE	Tau
3D Field QSAR	0.87	0.69	0.85	0.39	0.61
Random Forest	0.93	0.57	0.75	0.65	0.79
RVM	0.90	0.66	0.79	0.63	0.74

\* Here are presented the statistic of the QSAR models generated in the form of: the coefficient of determination ( $r^2$ ) which indicates the goodness of fit; the cross-validated coefficient of determination ( $q^2$ ) which indicates the robustness; the coefficient of determination for the test set ( $r^2$  test), which indicates the predictive power; the root mean square error (RMSE) as reliability measure; and Tau as a further parameter to assess the predictivity of the model. As with  $r^2$ , the closer the value of Tau is to one, the better the model.

For further details on the statistical parameters please refer to Section 7.1.2. The statistics of the QSAR on the morphine-line structure are slightly worse compared to the one presented for the fentanyl-like ones (Sec. 7.1.1). This can be explained by the difficulties encountered while aligning these molecules, due to their very complicated fused ring scaffold which characterise them. A visual representation of the predicted vs. experimental values for training and test sets is reported in Figure 7.4.



**Figure 7.4** Visual representation of the predicted (x axis) vs. experimental (y axis) log 1/c values for the training (blue) and test (orange) sets. The graphs were built with Excel 2022.

The 3D Field QSAR analysis returned a linear relationship between the descriptors and the activity along the visual interpretation of the QSAR model. Positive and negative electrostatic features and favourable and unfavourable hydrophobic features are reported in Figure 7.5.

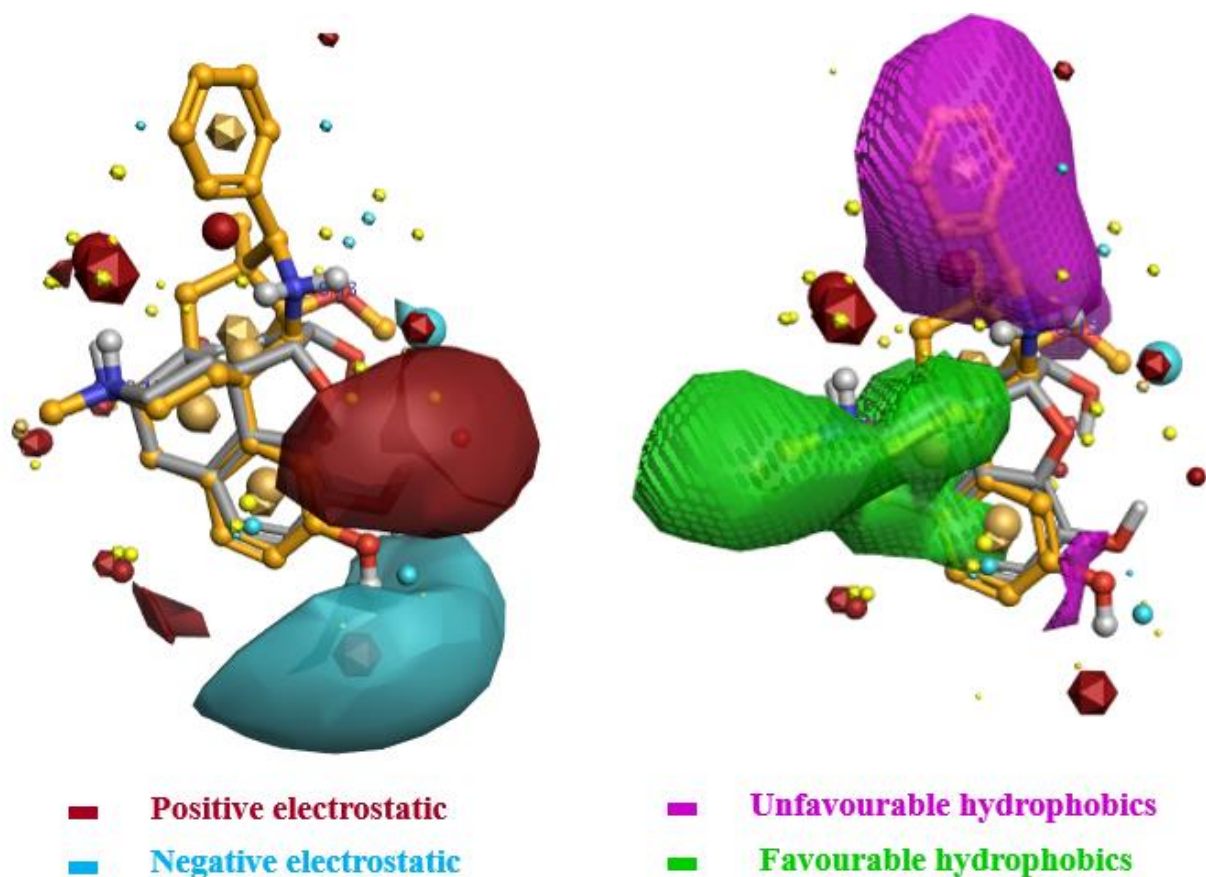


*Figure 7.5 3D and 2D visual representations of the generated 3D Field QSAR model for electrostatic features*

**Notes:** Electrostatic properties are identified by the red (positive) and blue (negative) colours. In particular, the red and blue shapes indicate the space around the molecule in which more positive electrostatic interaction (red) or more negative electrostatic interaction (blue) will be beneficial (i.e., increase) for the activity. More positive interactions (red) could mean that placing strong H-bond donors in that region improves the activity or could mean as well that putting strong H-bond acceptors will worsen the activity, and vice versa with blue. The green and violet areas instead indicate how the presence of a hydrophobic interaction in that region would increase (green) or decrease (violet) the activity.

Due to the difference between the reference molecule used for the alignment and the dataset, the resulting 3D Field QSAR model seems more difficult to explain if compared to the one retrieved for the fentanyl-like class. Indeed, analysing the alignment of the molecule, no direct correlation with the SAR reported in Section 6.3.5 was found. Still the model identified the portion of both the favourable and unfavourable hydrophobic as neatly separated by the one characterised by positive and negative electrostatic. This is in line with the fact that the MOR has a predominantly hydrophobic surface opposite to the Asp residue, the one responsible for the ionic interaction with the opioid's family.

The three QSAR models identified above were used to predict the biological activity of the 19 morphine-like NSOs identified online (the majority of which were retrieved from isomerdesign.com (Isomer Design, 2021)). However, the same issues experienced during the alignment of the training

and test set molecules were faced for the alignment of the morphine-like NSOs structures. As a result only 16 pKi values were predicted. These are reported in Table 7.4, in decreasing order of the average pKi values.

*Table 7.4 Values of pKi predicted for the 19 morphine-like NSOs identified online\*.*

Title	pKi average	Field QS AR	Dist to model	RF	RVM	Sim
Nalmefene	9.9	9.9	Excellent	9.7	10.1	0.26
3-Monoacetylmorphine (3-Mam)	8.9	8.9	Excellent	8.9	9	0.24
Levallorphan	8.9	8.8	Good	9.1	8.7	0.34
3-(0-Carboxymethyl)Morphine	8.5	8.6	Excellent	8.4	8.5	0.26
Isocodeine	8.5	8.7	Excellent	8.4	8.4	0.23
Acetyldihydrocodeine	8.4	8.3	Excellent	8.4	8.5	0.24
Cyprenorphine	8.4	8.8	Good	7.7	8.7	0.24
6-Methylenedihydrodesoxymorphine (6-Mddm)	8.0	7.8	Excellent	8.4	7.9	0.30
Pentazocine	8.0	7.9	Good	8.4	7.7	0.28
6-Monoacetylmorphine (6-Mam)	7.5	7.4	Excellent	7.8	7.4	0.24
3-Benzylmorphine	7.2	7.2	Good	7.3	7.2	0.21
Buprenorphine	7.2	7.4	Excellent	6.8	7.4	0.27
Acetorphine	7.2	7.3	Excellent	6.9	7.3	0.27
Codeine-N-Oxide	7.0	7.5	Excellent	6.2	7.3	0.17
3-Carboxymethyl Morphine	6.9	7	Excellent	7.1	6.7	0.16
14-Hydroxymorphine	NA	NA	NA	NA	NA	NA
6-Nicotinoyldihydrocodeine (Nicodicodine)	NA	NA	NA	NA	NA	NA
Nalbuphine	NA	NA	NA	NA	NA	NA
<b>Morphine</b>	<b>9.0</b>	<b>9.1</b>	<b>Excellent</b>	<b>9.4</b>	<b>8.8</b>	<b>0.26</b>

**\*Due to alignment issues these values were calculated only for 16 molecules.**

The predicted activity for morphine (9.0) is also presented. Among the morphine-like molecules predicted to have a high biological activity were some antagonists, i.e. nalmefene, and mixed agonist/antagonist, i.e. cyprenorphine. This is an example of the fact that QSAR cannot discern between the agonist and antagonist nature of the ligand. These molecules, which due to their antagonist nature cannot be considered of interest for recreational use were not considered further in this study. Other morphine-like molecules, as 6-methylenedihydrodesoxymorphine (Abdel-Rahman et al., 1966), isocodeine (Makleit and Hosztafi, 2006), acetyldihydrocodeine (Braun, 1914) and pentazocine (Fischer and Ganellin Robin, 2006) instead could be of interest for recreational or self-medication purposes hence are further discussed in Section 7.3.2.

### 7.2.3 Domain of applicability with Forge™

Please refer to Section 7.1.3 where the distance to model approach for the domain of applicability is described.

### 7.2.4 Molecular docking

The total of NSOs identified by the *NPSfinder*<sup>®</sup> (Sec 3.3), were docked as described in Section 4.3.8 in PDB5C1M (MOR). The docking was carried out using the pharmacophore placement in Figure 4.16. The S values for a set of well-known opioid ligands was calculated as a reference, including BU72 (co-crystallised ligand). The S values obtained (Table 7.5) were used as a reference for good binding affinity towards PDB5C1M.

**Table 7.5 Binding affinity values for the reference compounds. The latter are listed in alphabetical order.**

Molecule	SMILES	S (Kcal/mol)	rmsd
Buprenorphine	<chem>O(C)[C@]12[C@@H]([C@](O)(C(C)(C)C)C)[C@@]3([C@@H]4[NH+](CC5CC5)CC[C@@]53[C@H]1O)c1c(O)ccc(c51)C4)CC2</chem>	-9.6	1.3
Carfentanyl	<chem>O=C(N(c1ccccc1)C1(C(=O)OC)CC[NH+](CCc2ccccc2)CC1)CC</chem>	-9.4	1.7
Codeine	<chem>O(C)c1c2O[C@H]3[C@@H](O)C=C[C@H]4[C@@H]5[NH+](C)CC[C@]34c2c(cc1)C5</chem>	-7.1	1.2
Fentanyl	<chem>O=C(N(c1ccccc1)C1CC[NH+](CCc2ccccc2)CC1)CC</chem>	-8.4	1.5
Hydromorphone	<chem>O=C1[C@@H]2Oc3c(O)ccc4c3[C@@]32[C@H]([C@H]([NH+](C)CC3)C4)CC1</chem>	-7.7	1.4
Fentanyl	<chem>O=C(N(c1ccccc1)C1(C(=O)OC)C(C)C[NH+](CCc2ccccc2)CC1)CC</chem>	-10.0	1.4
Meperidine	<chem>O=C(OCC)C1(c2ccccc2)CC[NH+](C)CC1</chem>	-6.5	1.3
Morphine	<chem>O[C@@H]1[C@@H]2Oc3c(O)ccc4c3[C@@]32[C@H]([C@H]([NH+](C)CC3)C4)C=C1</chem>	-7.6	1.1
Oxymorphone	<chem>O=C1C2Oc3c(O)ccc4c3C32C(O)(C([NH+](C)CC3)C4)CC1</chem>	-8.1	2.0
Propoxyphene	<chem>O=C(O[C@]([C@@H](C[NH+](C)C)C)(Cc1ccccc1)c1ccccc1)CC</chem>	-8.0	1.4

For each molecule, several conformations with different S values (Kcal/mol) were returned. The ones showing the lowest S value (i.e., the lower the value, the more potent the binding) as well as the ionic interaction with Asp147 were identified. The rmsd value was taken into consideration as well, during the analysis of the docking pose choice. This value measures the root mean square deviation between the pose before refinement and the pose after refinement, giving an idea of how the refined pose is close to the one suggested by the docking superposition points (i.e. co-crystallised ligands). In other words, is a measure of how much a molecule needs to be constrained to occupy a particular spatial conformation in the binding pocket, i.e., how energetically favoured a pose is. The obtained S values are reported in Appendix A. For brevity, only the S values obtained for those NSOs predicted by the QSAR models as the most biologically active are presented (Sec.5.2.2). A further docking study on the nitazene class is reported as well (Sec. 7.3.3).



### 7.2.5 Fentanyl-like NSOs molecular docking

The binding affinity values for the ten fentanyl-likes NSOs predicted to show the highest biological activity are reported in Table 7.6.

**Table 7.6 Predicted values of binding affinity (S) for the fentanyl-like NSOs predicted to show the highest biological activity\*.**

Molecule	Pred pKi	S (kcal/mol)	rsmd
N-(2-Fluorophenyl)-N-[1-(2-phenylethyl)-4-(1,3-thiazol-2-yl)piperidin-4-yl]propanamide	10.2	-9.2	2.0
Methyl 4-[phenyl(propanoyl)amino]-1-[2-(1h-pyrrol-1-yl)ethyl]piperidine-4-carboxylate	10.1	-8.3	2.0
2-Methyl carfentanyl	10.0	-8.9	2.1
Carfentanyl	10.0	-8.7	2.2
N-methyl-carfentanil	10.0	-7.1	1.9
Butyryl-carfentanyl	10.0	-9.2	1.8
Acetyl-carfentanyl	9.9	-8.6	1.6
N-{1-[2-(4-ethyl-5-oxo-4,5-dihydro-1h-tetrazol-1-yl)ethyl]-4-(1,3-thiazol-2-yl)piperidin-4-yl}-n-(2-fluorophenyl)propanamide	9.9	-8.2	1.2
4-Methoxymethylfentanyl	9.9	-8.8	2.3
N-(2-fluorophenyl)-n-{1-[2-(1h-pyrazol-1-yl)ethyl]-4-(pyridin-2-yl)piperidin-4-yl}propanamide	9.9	-8.9	1.8

\* **Rsm**d is a measure of the variance of the pose.

As discussed in Section 5.4, QSAR and docking studies are not necessarily linearly correlated (Chen, 2015). However docking can be used to support and integrates QSAR results analysis, adding information on the affinity and modality of binding towards the receptor for which the biological activity has been predicted.

When compared with the docking S values obtained for both morphine (S= -7.6) and fentanyl (S = -8.4), the majority of these NSOs display a lower, i.e. more negative, S value (i.e. better affinity). These results suggested satisfactory binding affinity levels for the human MOR. It should be noted that, as per the literature, the majority of these compounds display the fentanyl structure substituted in position C4, identified already as a chemical characteristic responsible of increasing the biological activity (Sec. 6.3.5). Only one NSO, N-methyl-carfentanyl, showed a higher value suggesting a lower binding affinity. The low value of binding affinity of N-methyl-carfentanyl is not in line with the predicted activity but it is in line with the low reported potency in the literature (Cometta-Morini et al., 1992). Moreover, from the data reported in Table 7.6, it can be noted that the rsmd values are slightly high. It is important here to reiterate how different ligands determine different movements and rearrangement of the binding pocket. Hence, these rsmd values could be explained with MOE<sup>®</sup> trying to fit the fentanyl-like ligands in a space determined by a ligand,

BU72 with a more compact chemical structure. A more in-depth evaluation of each of the ten top scoring NSOs is reported in section 7.3 (Stamenić et al. 2016).

Despite the docking results suggesting a high binding affinity for almost all the top ten NSOs, they cannot give any specific information on the actual agonist/antagonist role of the latter, even though the docking was performed using the active conformation of an agonist opioid, i.e. BU72.

The poses of the top ten NSOs docked in PDB5C1M are reported in Figure 5.9.

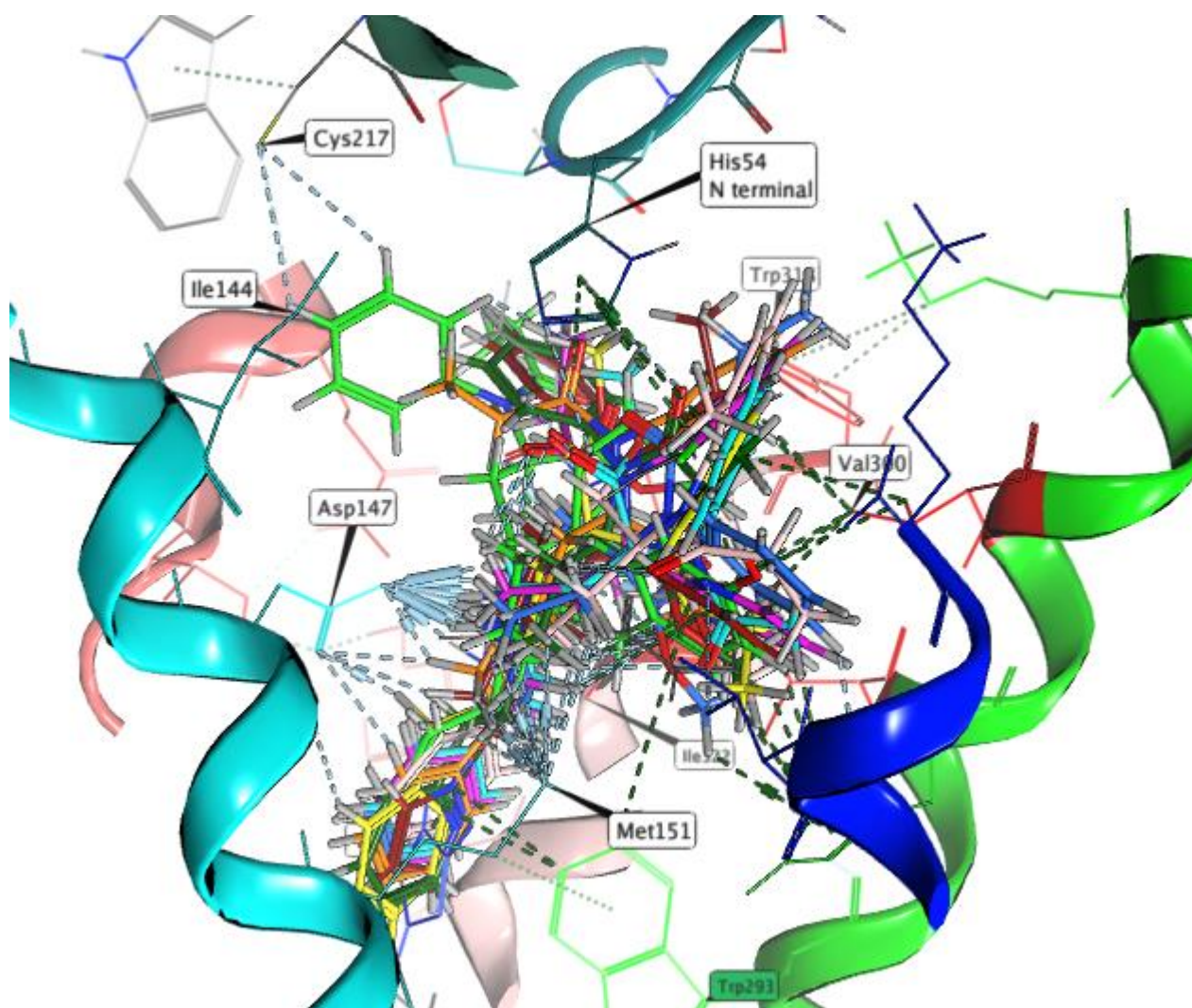


**Figure 7.6** The poses of the top ten fentanyl-like NSOs docked in PDB5C1M.

*The different TM helices are identified with different colours, light blue for TM3, dark blue for TM5 (which however is not involved in the binding), green for TM6, light pink for TM7; pink for TM2 and dark green for the N-terminal portion. The red colour visible in the TM6 identifies part the hydrophobic pocket characteristic of the ORs. The dotted lines show the interactions between the ligands and the pocket residues, and in particular, the light blue colour identifies both hydrogen-bond and ionic interactions, while the dark green identifies the H- $\pi$  bonds (aromatic interactions). The cylinder visible on some of the dotted line is a measure of the strength of the bonds, i.e. the bigger the cylinder the stronger the interaction.*

For each of the poses generated for the 238 NSOs, a PLIF was calculated and analysed. The analysis of the PLIFs is presented below.

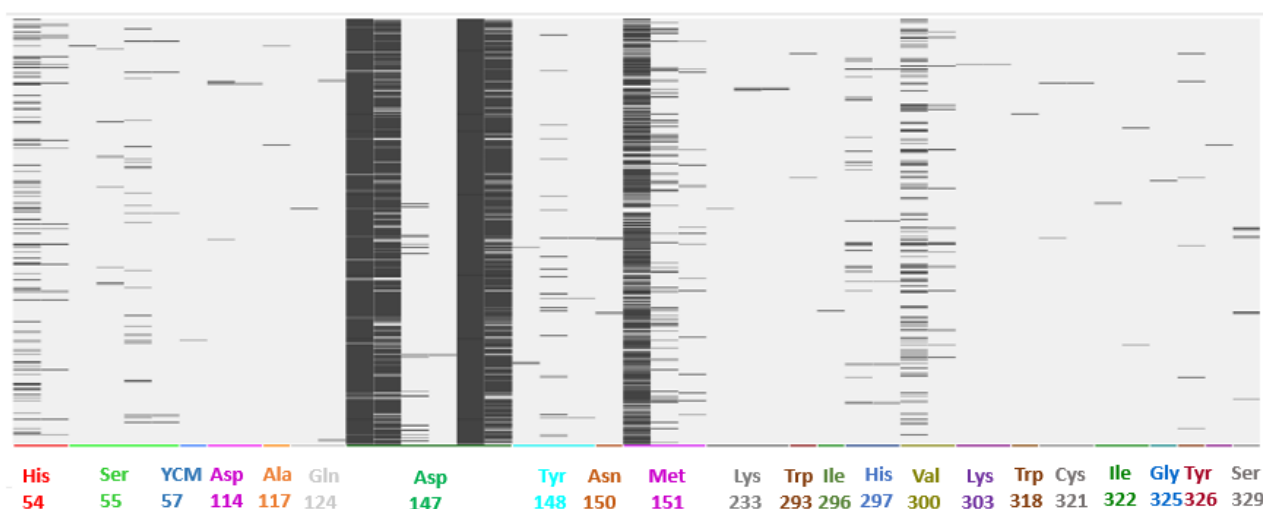


**Figure 7.7** Visual representation of the interactions (potential contacts) between the 238 NSOs and the residues of the binding pocket of PDB5C1M.

*This figure represents the interactions between the molecules and the receptor pocket with the use of barcodes. The number of bars is proportional to the frequency of the interactions with that ligand, suggesting how much a ligand is involved in the binding mode of a particular set of molecules.*

The barcode display represents the entries (NSOs) and the selected fingerprints of interactions as a matrix in which a set bit is drawn as a black rectangle. On the X-axis are displayed the numbers and code for those residues which are involved in the interaction with the ligands. The number of black rectangles displayed for each residue are a measure of the frequency of the interactions with that ligand, i.e the higher the number the higher the frequency.

The results presented in Figure 7.7 and Figure 7.9 confirm the importance of the Asp147 residue for the binding of NSOs as observed for the classical opioids (Kaserer et al., 2016; Piotr F. J. Lipiński et al., 2019; Piotr F.J. Lipiński et al., 2019).

Other residues which seem to be more often included in the ligand interactions are His 54, Val300 and Met151 (Kaserer et al., 2016; Piotr F. J. Lipiński et al., 2019; Piotr F.J. Lipiński et al., 2019; Masiulis et al., 2019; Sigel and Ernst, 2018). His297, the importance of which has been reported and studied for the recognition of fentanyl by the MOR (Vo et al., 2021), also appears to be involved in the interaction patten. However from Figure 7.7, it appears that its frequency of interaction is low. This could be explained by the fact that the side chain of His297 in this crystallised structure is not in the correct position to engage with the fentanyls-like structures, due to the conformational changes of the pockets generated by BU72. Unfortunately, this did not allow for a more in depth evaluation of the role of His297 in the binding of fentanyl-like NSOs.

Docking results can be very interesting in assessing the way a ligand interacts with the residues of the binding pocket (Figure 7.6). From the 3D ligand interactions, we can identify which residues are recurrently involved in the binding. It should be noted how the most important interaction happen

with the Asp147 of the TM3 subunit of the MOR binding pocket. The others transmembrane helices involved are TM6 with His297 and Val300, the N-terminal portion with His54 and occasionally TM7. The receptor residues involved in the binding tend to be recurrent across the different fentanyl-like NSOs, with the latter positioning almost vertically inside the binding pocket. While the phenethyl moiety seems to be always oriented towards the bottom of the binding pockets guiding the piperidine ring in proximity of the Asp147, the carboxamide and anilino-phenyl ones changes their orientation according to their side chain(s). The substitution in position C4 seems to play an important role. Often the anilino phenyl group is oriented towards the Val300, i.e. towards the hydrophobic pocket between TM6 and TM7, occupying a position almost perpendicular to the rest of the scaffold. The carboxamide group instead seems to be often oriented toward the extracellular side of the pocket. Despite observed variations (mainly due to the high flexibility of the fentanyl-like structure which complicates the docking process), the main positioning of the fentanyl-like NSOs found via the docking studies is in line with what is reported in the literature (Dosen-Micovic et al., 2006; Subramanian et al., 2000; Vo et al., 2021), a fact that support the validity of the results obtained.

#### 7.2.6 Morphine-like NSOs molecular docking

The binding affinity values for those morphine-likes NSOs predicted to show the highest biological activity are reported in This is because the probability of them being used as recreational drugs is very low.

Table 7.7. In this case, only those molecules showing a predicted  $pK_i < 8.0$  are presented. Indeed, as explained for the fentanyl-like NSOs, only values of  $pK_i > 8.00$  are considered as a medium/high biological activity. Moreover, those molecules included in the QSAR studies, which however were reported as full antagonist in literature, were not considered further even if displaying a high predicted biological activity. This is because the probability of them being used as recreational drugs is very low.

**Table 7.7 Predicted values of binding affinity (S) for the morphine-like NSOs predicted to show the highest biological activity.**

<b>Molecule</b>	<b>Pred pKi</b>	<b>Dist to model</b>	<b>S (kcal/mol)</b>	<b>rsmd</b>
3-Monoacetylmorphine	8.9	Excellent	-6.7	0.6
3-(0-Carboxymethyl)Morphine	8.5	Excellent	-6.7	0.6
Isocodeine	8.5	Excellent	-6.7	1.5
Acetyldihydrocodeine	8.4	Excellent	-7.6	1.5
Cyprenorphine	8.4	Good	-6.9	1.7
6-Methylenedihydrodesoxymorphine	8.0	Excellent	-6.6	1.2
Pentazocine	8.0	Good	7.5	1.9

Results presented in This is because the probability of them being used as recreational drugs is very low.



Table 7.7, suggest how the morphine-like NSOs display, a lower binding affinity (if compared to fentanyl-like NSOs) towards the MOR, together with a lower predicted biological activity. This is in line with what reported in the literature and in particular on the difference in potency between morphinans and fentanyls (UNODC, 2019e). Indeed, the prediction of the binding affinity for 3-monoacetylmorphine, matches what previously reported in the literature and the SAR morphine-like molecules (Sec 6.3.5), with the acetylation of the hydroxyl group resulting in a relatively weak affinity towards MOR (Houdi et al., 1996). The same applies to 3-(0-Carboxymethyl)Morphine (Köteles et al., 2021). Moreover, if compared to the reference molecules (Table 7.5), the values obtained for the binding affinity are lower than morphine (i.e. 7.6). The rmsd values are good (i.e. < 1.9), probably due to the similarity of these molecules to the chemical scaffold of BU72. As reported above, no information on agonist/antagonist activity can be inferred by the docking studies.

The poses of the morphine-like NSOs docked in PDB5C1M are reported in Figure 7.8

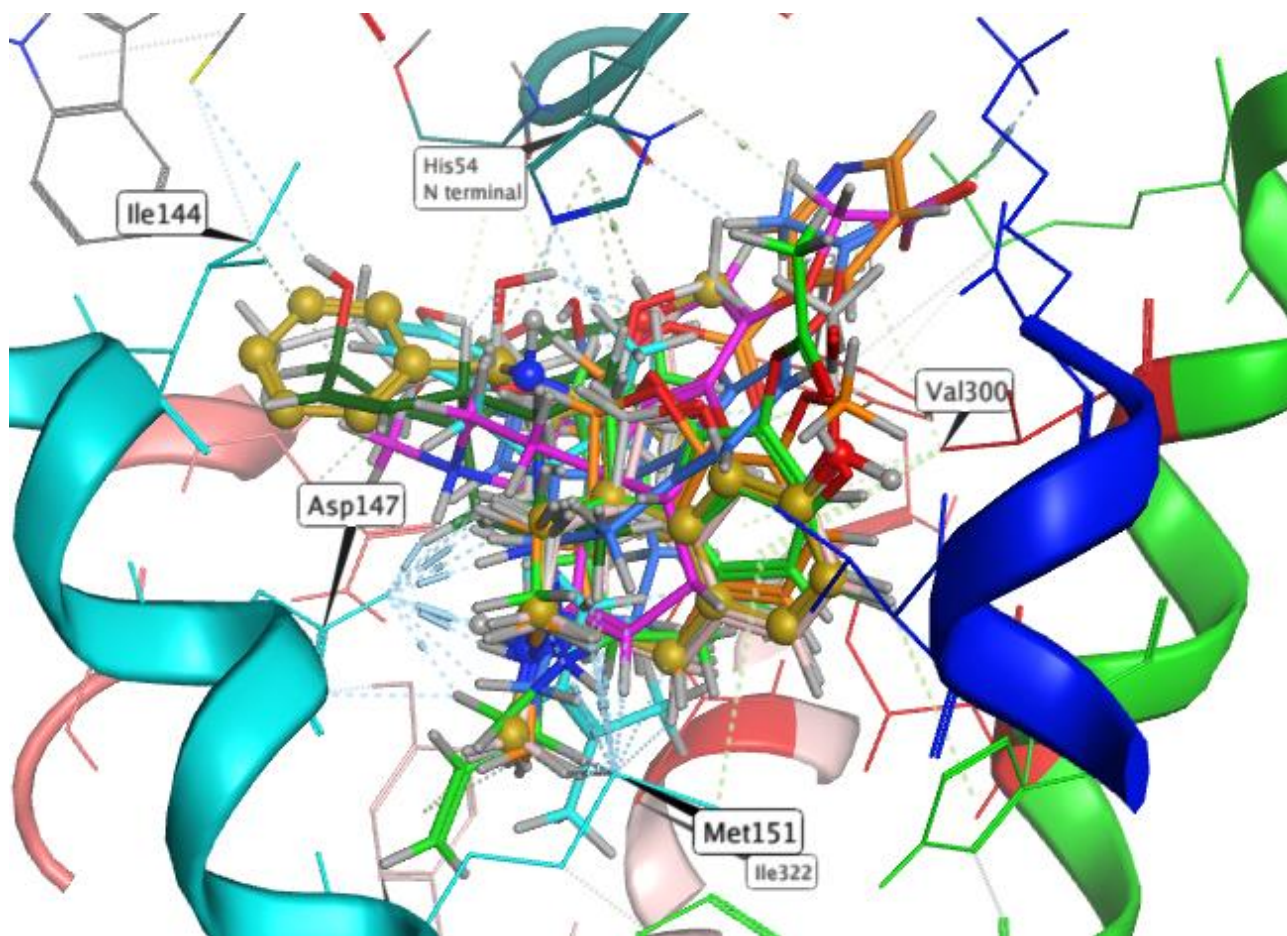


**Figure 7.8** The poses of the top morphine-like docked in PDB5C1M.

*The different TM helices are identified with different colours, light blue for TM3, dark blue for TM5 (which however is not involved in the binding), green for TM6, light pink for TM7; pink for TM2 and dark green for the N-terminal portion. The red colour visible in the TM6 identifies part the hydrophobic pocket characteristic of the ORs. The*

dotted lines show the interactions between the ligands and the pocket residues, and in particular, the light blue colour identifies both hydrogen-bond and ionic interactions, while the dark green identifies the H- $\pi$  bonds (aromatic interactions). The cylinder visible on some of the dotted line is a measure of the strength of the bonds, i.e. the bigger the cylinder the stronger the interaction.

For each of the poses generated for the 19 NSOs, a PLIF was calculated and analysed. The analysis of the PLIFs is presented below.

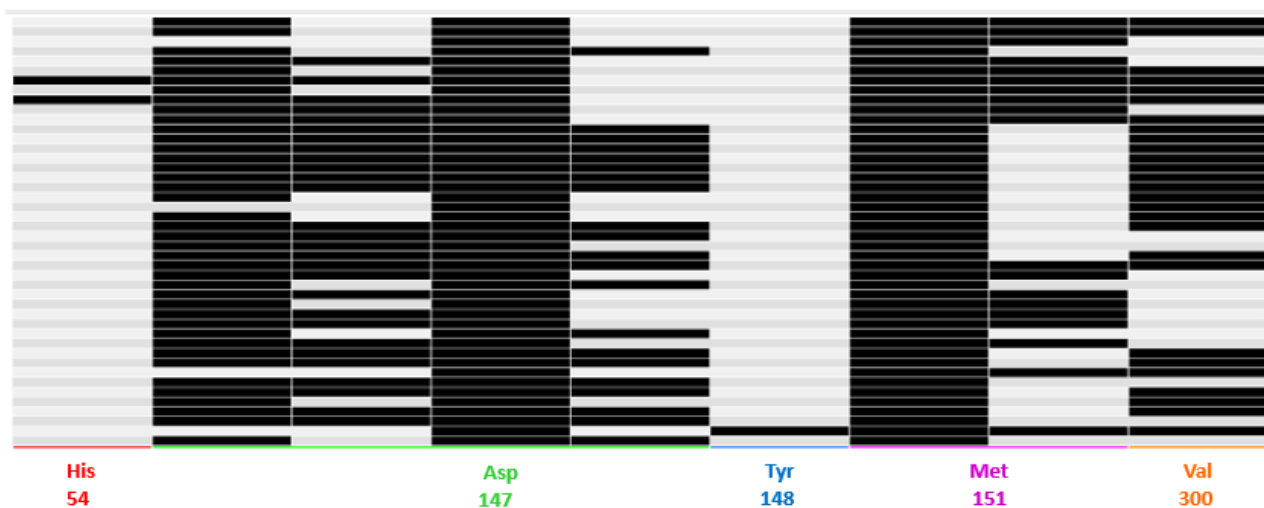


**Figure 7.9** Visual representation of the interactions (potential contacts) between the 238NSOs and the residues of the binding pocket of PDB5C1M.

*This figure represents the interactions between the molecules and the receptor pocket with the use of barcodes. The number of bars is proportional to the frequency of the interactions with that ligand, suggesting how much a ligand is involved in the binding mode of a particular set of molecules.*

The results presented in Figure 7.9 show a smaller number of residues involved in the binding of the morphine-like NSOs compared to the fentanyl-like (Figure 7.7). However as expected they engaged with all the residues considered important for the MOR activation. The difference in interactions pattern can be explained by the high flexibility of the fentanyl-like compared to the morphine-like structure which allows the former to connect to a greater number of residues side chains. For a discussion on the importance of these residues see Section 7.3.1.

Due to the low values of predicted pKi alongside low values of binding affinity for the mu receptor it could be inferred that the morphine-like NSOs identified online do not represent molecule of strong interest for recreational use. Despite this, 6-methylenedihydrodesoxymorphine (Abdel-Rahman et al., 1966), isocodeine (Makleit and Hosztafi, 2006), acetyldihydrocodeine (Braun, 1914) and pentazocine (Fischer and Ganellin Robin, 2006) will be further discussed in Section 7.4.

The same considerations on interaction patterns reported for the fentanyl-like NSOs ( Sec. 7.2.5) seems to apply also to the morphine-like NSOs with the compact phenanthrene structure positioned over the phenethylpiperidines at the centre of the binding pocket (Figure 7.10).



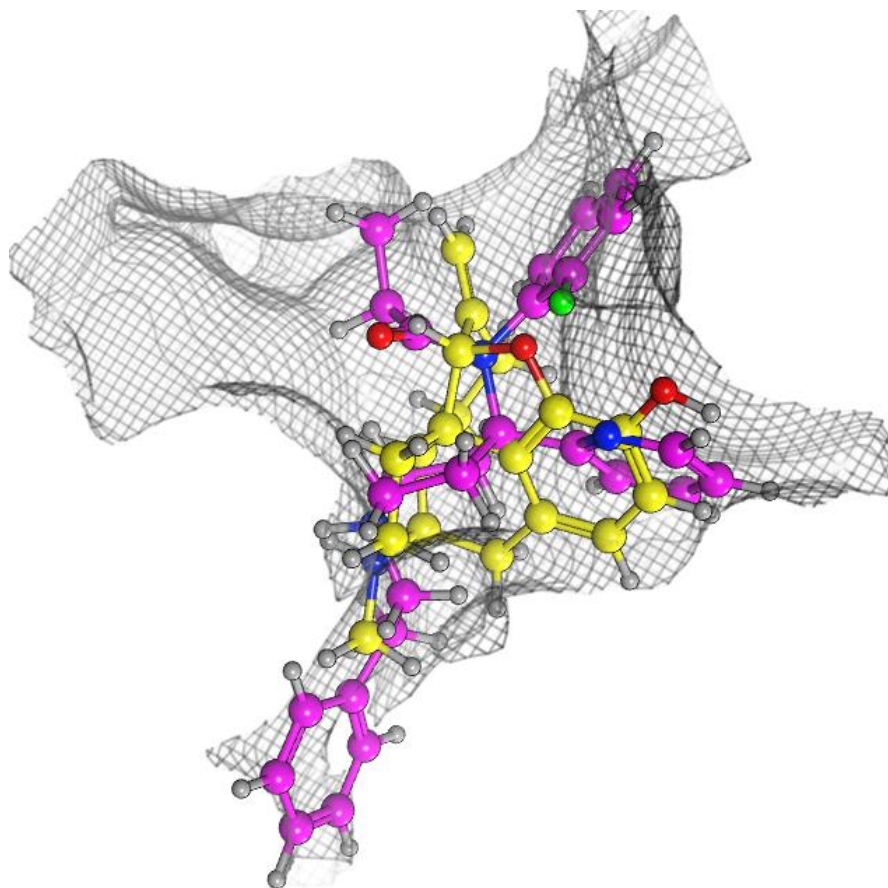


**Figure 7.10** positioning of the phenethylpiperidines scaffold (purple) and phenantrenes scaffold (yellow) inside of the MOR binding pocket.

*The molecular surface of the binding pocket is represented by the grey mesh*

#### 7.2.7 Nitazene-like NSOs molecular docking

While no QSAR study was conducted on the seven nitazenes identified by the web crawler (Table 3.5), a docking analysis was carried out to assess their possible methodology of binding to the MOR and predict their binding affinity values. Due to the fact that the nitazene class is a recent new entry on the NSO scene, the same reference compounds used to assess the S value obtained via the docking were the same used for the fentanyl-like and morphine-like NSOs. The only biological activity data available on nitazenes are those reported by Vandeputte et al., obtained via an *in vitro* study. In particular, the biological activity was assessed via two cell-based  $\beta$ -arrestin2/ mini-Gi recruitment assays monitoring  $\mu$ -opioid receptor (MOR) .

The values of predicted binding affinity for nitazenes are reported in Table 7.8.

**Table 7.8 Predicted values of binding affinity (S) for the nitazene-like NSOs predicted to show the highest biological activity.**

<b>Mol</b>	<b>S (kcal/mol)</b>	<b>rmsd</b>
Butonitazene	-9.4	1.76
Clonitazene	-8.4	1.32
Etonitazene	-8.8	1.67
Flunitazene	-7.9	1.15
Isotonitazene	-9.8	1.20
Metodesnitazene	-7.8	1.13
Etazene	-8.2	1.25

Results presented in Table 7.8, suggest how their binding affinity values is more in line with those reported for the fentanyl-like NSOs, and higher than the morphine-like ones. In particular butonitazene and isotonitazene display binding affinity higher than that calculated for carfentanyl (i.e  $s = -9.4$ ). This binding affinity values seems to be in line with the potency reported by Vandeputte et al, however, no direct or easy correlation which could help interpreting the data can be extrapolated. Moreover, once docked in MOR those nitazenes displaying the NO<sub>2</sub> group in their scaffold, i.e. all those in Table 7.8 but metodesnitazene and etazene seems to prefer two position inside the pocket, one with the nitro group facing towards the Val 300 (which will be referred to as the downward pose) and the other with the nitro group flipped in the other direction (upward pose). These two different orientations are presented in Figure 7.11.

### Downward and upward poses of flunitazene in the MOR

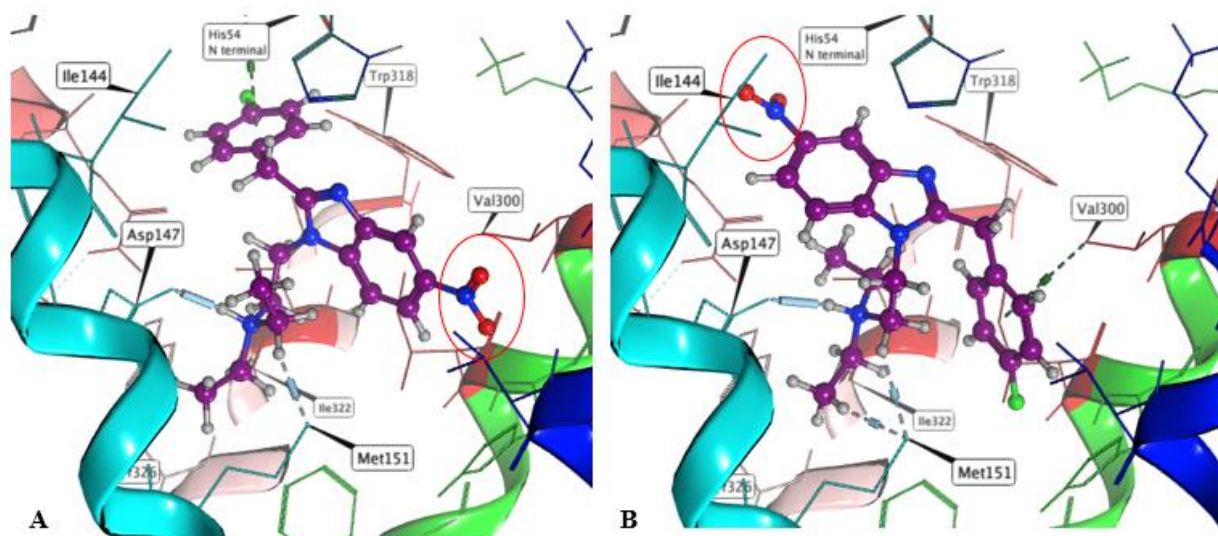


*Figure 7.11 Downward (A) and upward (B) orientation of flunitazene (in purple).*

*The nitro group which is depicted in red in the molecule scaffold is highlighted by the red circle. While the position of the positively charged tertiary amine does not change the rest of the molecules seems to be flipped around.*

Despite this dual orientation issue it seems like all nitazenes align to the co-crystallised ligand BU72, at the centre of the binding pocket Figure 7.12, with a more horizontal orientation similar to the morphine-like NSOs Figure 7.8, and different to the more vertical one of the fentanyl-like NSOs Figure 7.6.

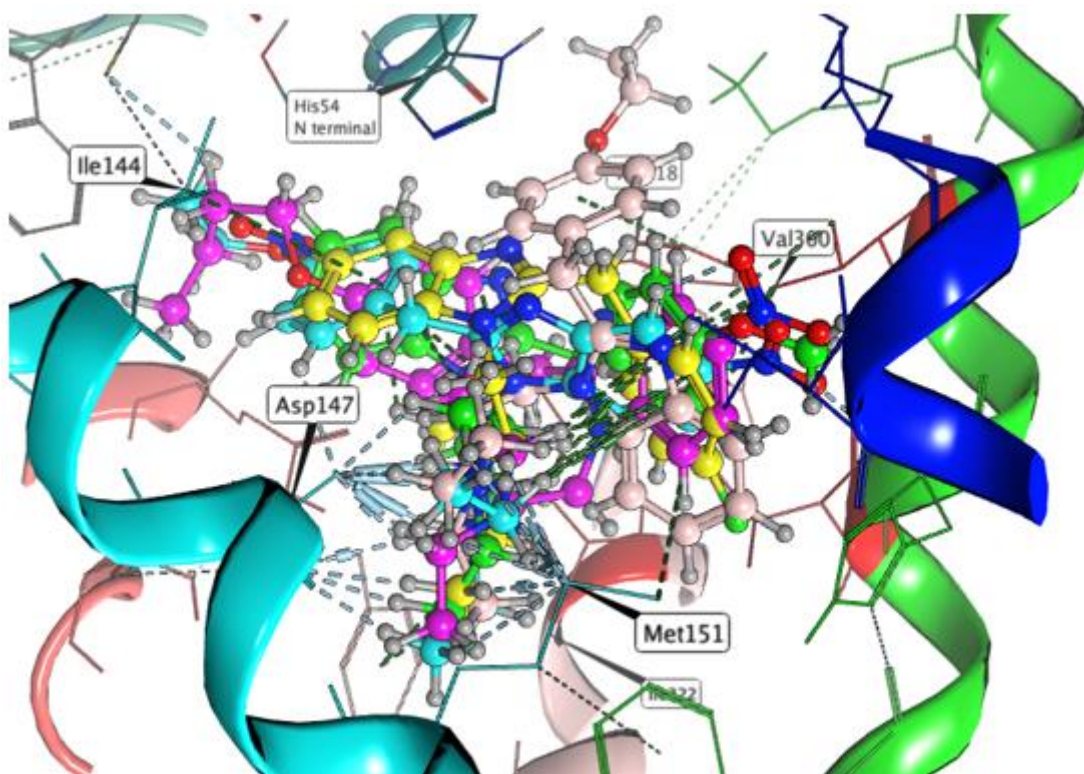


*Figure 7.12 The poses of the top morphine-like docked in PDB5C1M.*

*The different TM helices are identified with different colours, light blue for TM3, dark blue for TM5 (which however is not involved in the binding), green for TM6, light pink for TM7; pink for TM2 and dark green for the N-terminal portion. The red colour visible in the TM6 identifies part the hydrophobic pocket characteristic of the ORs. The dotted lines show the interactions between the ligands and the pocket residues, and in particular, the light blue colour identifies both hydrogen-bond and ionic bond.*

Further studies involving molecular dynamics (Chapter 10, future work) will be needed to address this dual orientation issue and understand the optimal interaction patter. Without a better understanding of the latter no further discussion can be carried out.

### 7.3 Profiling of the NSOs with the highest predicted biological activity

Of the top ten fentanyl-like NSOs (During the analysis of the predicted pKi values, it was noted that the RF models tend to over-predict values for some of the NSOs listed, hence only the Field QSAR and the RVM values were averaged to obtain a final prediction. For brevity, only the top ten NSOs listed according to their decrescent predicted biological activity value (Field QSAR) are reported below (**Error! Not a valid bookmark self-reference.**). The full table is in Appendix A.

Table 7.2) no information was retrieved on N-(2-Fluorophenyl)-N-[1-(2-phenylethyl)-4-(1,3-thiazol-2-yl)piperidin-4-yl]propanamide (pKi= 10.2), Methyl 4-[phenyl(propanoyl)amino]-1-[2-(1h-pyrrol-1-yl)ethyl]piperidine-4-carboxylate (pKi= 10.1), 2-Methyl carfentanyl (pKi= 10.0), N-{1-[2-(4-ethyl-5-oxo-4,5-dihydro-1h-tetrazol-1-yl)ethyl]-4-(1,3-thiazol-2-yl)piperidin-4-yl}-n-(2-fluorophenyl)propanamide (pKi= 9.9) and N-(2-fluorophenyl)-n-{1-[2-(1h-pyrazol-1-yl)ethyl]-4-(pyridin-2-yl)piperidin-4-yl}propanamide (pKi= 9.9). The other NSOs are discussed below in decreasing order of biological activity.

#### 7.3.1 Carfentanyl

Carfentanyl is one of the most known and potent NSO so far identified on the market. Its predicted biological activity, i.e. pKi= 10.0, and a binding affinity (S= -8.7) are in line with what reported in literature for this substance (EMCDDA, 2017d). Carfentanyl, which was scheduled under the 1961 Convention on Narcotics in 2018 (The Commission on Narcotic Drugs, 2018; WHO, 2017), was first synthesised in 1974 by Janssen Pharmaceutica and introduced into veterinary anesthesia practice for very large animals. Due to its extreme potency, i.e. 10,000 times greater than morphine and 100 times greater than fentanyl, carfentanyl has never been approved for human use; however, since 2016 it has emerged on the recreational drug market. Its use has been commonly reported for injection, insufflation, or inhalation, and has been associated with fatalities worldwide alone or in combination with other drugs (Elliott and Hernandez Lopez, 2018; Fomin et al., 2018; Jalal and Burke, 2021; Swanson et al., 2017). In particular hundreds of deaths resulted from the use of carfentanyl adulterated heroin in North America (Sanburn, 2016).

The recreational effects of carfentanyl in humans are similar to those of other opioids and include euphoria, relaxation, and pain relief. The side effects are similar as well but stronger proportionally to the potency and include drowsiness, sedation, slowed heart rate, low blood pressure, lowered body temperature, loss of consciousness, and suppression of breathing (Casale et al., 2017; EMCDDA, 2017d).

It is very interesting to note that, in fact, the NSO which has been reported as the most powerful opioid so far on the market, has been identified as such by the results of both QSAR and docking studies, supporting the reliability of the latter.

In Figure 7.11 are presented, in detail, the predicted interactions between carfentanyl and the MOR binding site. Interactions with Asp14, Met151 and His54 can be identified, together with the lack of interaction with His297.



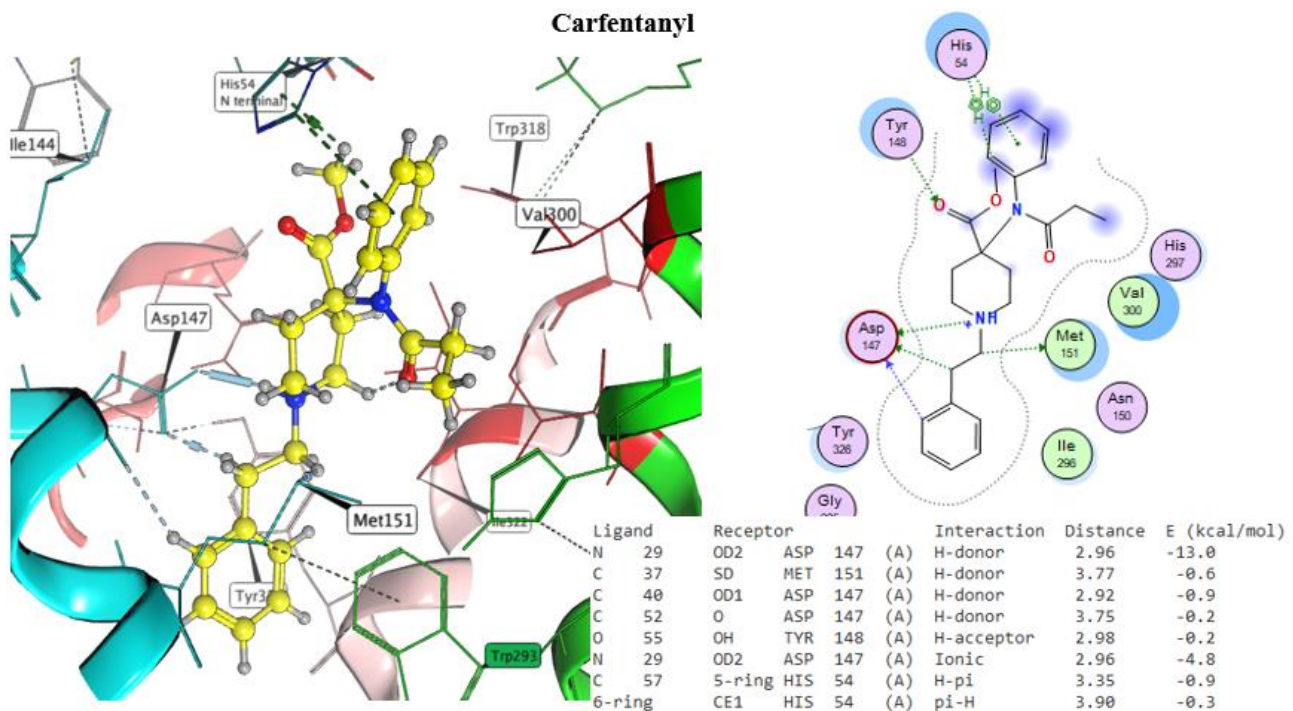


**Figure 7.13** The 3D pose carfentanyl docked in PDB5C1M and 2D representations.

*Notes: on the 3D representation on the left, the binding pocket with the docked ligand carfentanyl (yellow). The different TM helices are identified with different colours, light blue for TM3, green for TM6, light pink for TM7. The red colour visible in the TM6 identifies part the hydrophobic pocket characteristic of ORs. The dotted lines show the interactions between the ligands and the pocket residues, and in particular, the light blue colour identifies both hydrogen-bond and ionic interactions, while the dark green identifies the H-pi bonds (aromatic interactions). The cylinder visible on some of the dotted line is a measure of the strength of the bonds, i.e. the bigger the cylinder the stronger the interaction. On the right, the 2D representation of the binding pocket and a report of the interactions between receptor residues and ligand are provided. The colours used to depict the residues in the 2D screenshot define different characteristics of the latter: light purple for polar residues and light green for hydrophobic ones; red circle indicates an acidic and blue a basic residue; and the light blue halo indicates solvent exposure both on the receptor and the ligand.*

### 7.3.2 *N-methyl-carfentanyl*

N-methyl-carfentanyl, is predicted to have a biological activity, i.e.  $pK_i = 10.0$ , similar to that of carfentanyl. The docking results ( $S = -7.1$ ) however seems to be discordant, presenting this molecule as a weak binder to MOR. The molecule, also known as N-methyl norcarfentanyl, is indeed weaker if compared to carfentanyl, and only slightly stronger than morphine (Cometta-Morini et al., 1992). It was first synthesised during SAR studies supervised by Paul Janssen at Janssen Pharmaceutica, which highlighted the importance of the phenethyl group. The removal of the latter indeed almost nulled the opioids activity in fentanyl, while it retained reasonable opioid receptor activity in carfentanyl (Cometta-Morini et al., 1992). This molecule is very seldom discussed online, with opioids users' suggesting it as the perfect next NSOs, especially for its low potency. Despite no pharmacological profile has been reported for this NSO, it could be assumed that its side effects would be similar to those of fentanyl and morphine including itching, nausea and possibly serious and life-threatening respiratory depression (Prekupec et al., 2017). In Figure 7.12 are presented, in detail, the predicted interactions between N-methyl-carfentanyl and the MOR binding site. As per the QSAR results this NSO is supposed to have a biological activity compared with carfentanyl, data which are not in line with what experimentally reported (Cometta-Morini et al., 1992). From Figure 7.12 it could be noted that the molecule is still able to establish interactions with Asp147 and Val300 similarly to morphine, but due to its position in the pocket the 4-carbomethoxy group is not able to engage in interactions.



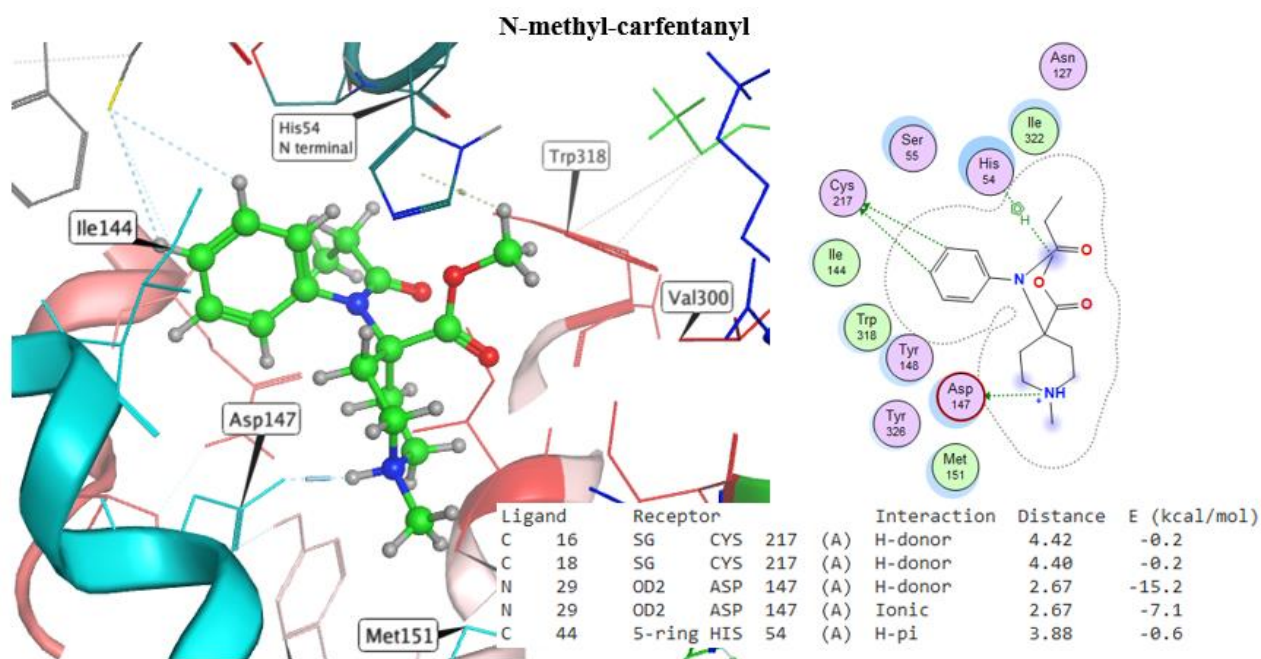


**Figure 7.14** The 3D pose of N-methyl-carfentanyl docked in PDB5C1M and 2D representations.

**Notes:** On the left, the binding pocket 3D representation with the docked ligand N-methyl-carfentanyl (green). The different TM helices are identified with different colours, light blue for TM3, green for TM6, light pink for TM7. The red colour visible in the TM6 identifies part the hydrophobic pocket characteristic of ORs. The dotted lines show the interactions between the ligands and the pocket residues, and in particular, the light blue colour identifies both hydrogen-bond and ionic interactions, while the dark green identifies the H-pi bonds (aromatic interactions). The cylinder visible on some of the dotted line is a measure of the strength of the bonds, i.e. the bigger the cylinder the stronger the interaction. On the right, the 2D representation of the binding pocket and a report of the interactions between receptors residues and ligand are provided. The colours used to depict the residues in the 2D screenshot define different characteristics of the latter: light purple for polar residues and light green for hydrophobic ones; red circle indicates an acidic and blue a basic residue; and the light blue halo indicates solvent exposure both on the receptor and the ligand.

### 7.3.3 *Butyryl-carfentanyl*

Butyryl-carfentanyl, is predicted to have a biological activity, i.e.  $pK_i = 10.0$ , similar to that of carfentanyl, alongside a stronger binding affinity ( $S = -9.2$ ) towards MOR.

No information was retrieved on butyryl-carfentanyl in literature. It can be considered an analogue of butyrylfentanyl which is a very potent and short-acting NSO, scheduled in 2017 by WHO for its abuse potential and side effects profile (WHO, 2018). The addition of a butyryl group to fentanyl seems to decrease the potency to a quarter of the starting one. However it could not be assumed that this would be the case also for the carfentanyl series, and indeed the predicted activity suggest otherwise. Moreover, the predicted biological activity of butyryl-carfentanyl is higher than that of butyrylfentanyl, ( $pK_i = 9.4$ , Appendix A). If one considered that the use/abuse of the latter has been associate with fatalities worldwide, the higher activity predicted should be regarded as highly worrisome (Bowen et al., 2019; Poklis et al., 2016; UNODC, 2020a). In Figure 7.13 are presented, in detail, the predicted interactions between N-methyl-carfentanyl and the MOR binding site. As per the QSAR results this NSO is supposed to have a biological activity comparable with carfentanyl. From Figure 7.13 it could be noted that the molecule is still able to establish interactions with Asp147 and Val300 similarly to morphine, as well as interactions between the 4-carbomethoxy group and His297.

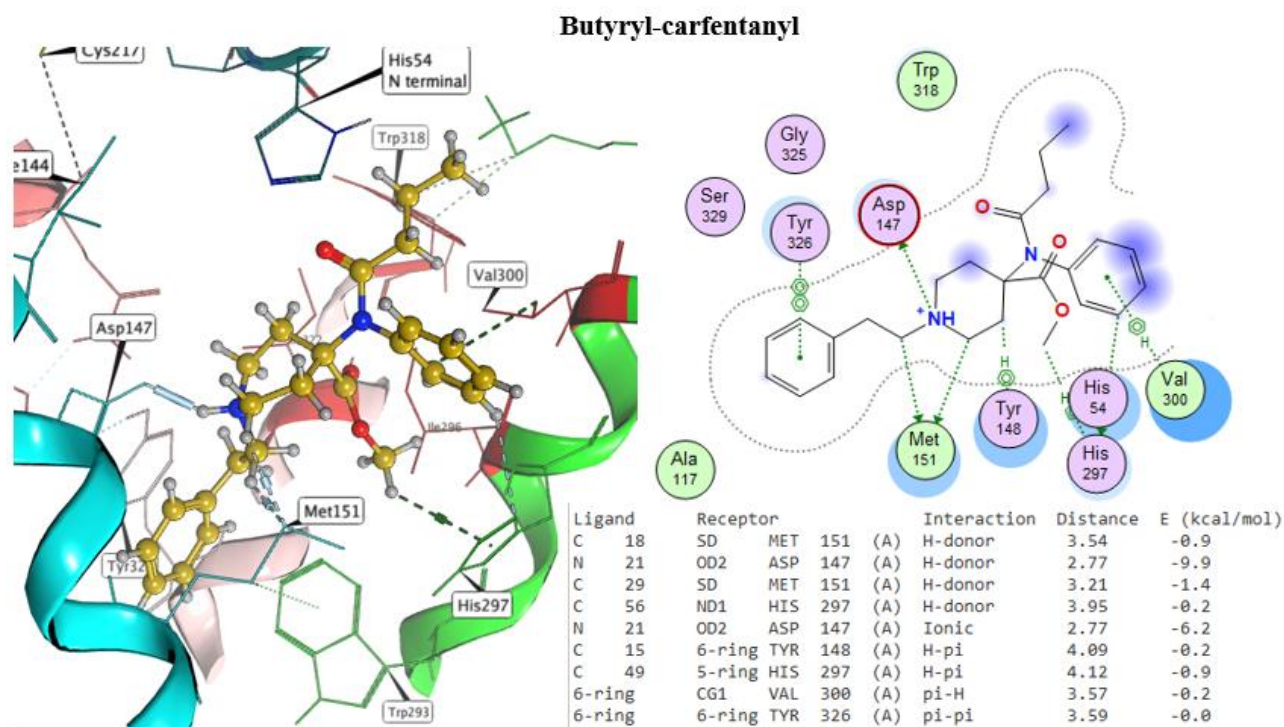
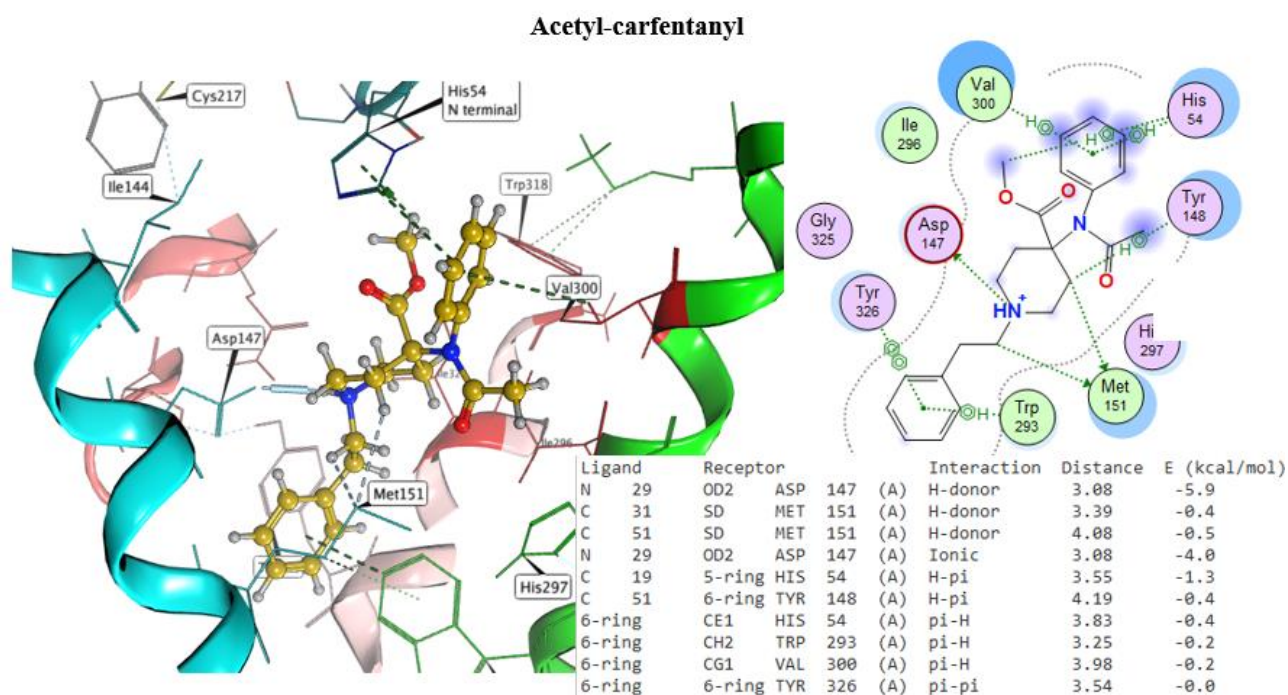


Figure 7.15 The 3D pose of butyryl-carfentanyl docked in PDB5C1M and 2D representations.

Notes: on the left, the binding pocket 3D representation with the docked ligand butyryl-carfentanyl (gold). The different TM helices are identified with different colours, light blue for TM3, green for TM6, light pink for TM7. The red colour visible in the TM6 identifies part the hydrophobic pocket characteristic of ORs. The dotted lines show the interactions between the ligands and the pocket residues, and in particular, the light blue colour identifies both hydrogen-bond and ionic interactions, while the dark green identifies the H-pi bonds (aromatic interactions). The cylinder visible on some of the dotted line is a measure of the strength of the bonds, i.e. the bigger the cylinder the stronger the interaction. On the right, the 2D representation of the binding pocket and a report of the interactions between receptors residues and ligand are provided. The colours used to depict the residues in the 2D screenshot define different characteristics of the latter: light purple for polar residues and light green for hydrophobic ones; red circle indicates an acidic and blue a basic residue; and the light blue halo indicates solvent exposure both on the receptor and the ligand.

### 7.3.4 Acetyl-carfentanyl

Acetyl-carfentanyl, is predicted to have a biological activity, i.e.  $pK_i = 9.9$ , similar to that of carfentanyl, alongside a comparable binding affinity ( $S = -8.9$ ) towards MOR. No information was retrieved on this molecule, apart from it being characterised as an impurity in two exhibits. According to the authors, acetyl-carfentanyl ‘presumably arises from the clandestine synthesis of carfentanyl, similar to that of acetylfentanyl in illicit fentanyl exhibits’ (Casale et al., 2017). The latter has been estimated to be more potent than heroin, suggesting the same for the carfentanyl analogue, in line with what is predicted here by QSAR and docking studies. As per butyryl-fentanyl several fatalities are connected to the use/abuse of acetyl-fentanyl (Drummer and Odell, 2001), raising concern on the possible availability of acetyl-carfentanyl on the NPS market. In Figure 7.16 are presented, in detail, the predicted interactions between acetyl-carfentanyl and the MOR binding site.



**Figure 7.16** The 3D pose of acetyl-carfentanyl docked in PDB5C1M and 2D representations.

**Notes:** on the left, the binding pocket 3D representation with the docked ligand acetyl-carfentanyl (gold). The different TM helices are identified with different colours, light blue for TM3, green for TM6, light pink for TM7. The red colour visible in the TM6 identifies part the hydrophobic pocket characteristic of ORs. The dotted lines show the interactions between the ligands and the pocket residues, and in particular, the light blue colour identifies both hydrogen-bond and ionic interactions, while the dark green identifies the H-pi bonds (aromatic interactions). The cylinder visible on some of the dotted line is a measure of the strength of the bonds, i.e. the bigger the cylinder the stronger the interaction. On the right, the 2D representation of the binding pocket and a report of the interactions between receptors residues and ligand are provided. The colours used to depict the residues in the 2D screenshot define different characteristics of the latter: light purple for polar residues and light green for hydrophobic ones; red circle indicates an acidic and blue a basic residue; and the light blue halo indicates solvent exposure both on the receptor and the ligand.

### 7.3.5 4-Methoxymethylfentanyl

4-methoxymethylfentanyl, is predicted to have a biological activity, i.e.  $pK_i = 9.9$ , similar to that of carfentanyl, alongside a comparable binding affinity ( $S = -8.8$ ) towards MOR. This NSO, also known as R-30490, was firstly synthesised by Janssen Pharmaceutica as seen for N-methyl-carfentanyl (Vardanyan and Hruby, 2014) and was found to display a potency slightly lower than that of carfentanyl. 4-methoxymethylfentanyl, which was found to be the agonist most selective towards MOR. It was never approved for medical use in humans, despite being very similar to sufentanil. Side-effects for this NSO are supposedly in line with those of fentanyl and other NSO opioids. Despite no information being available on its pharmacology, this substance was found to be discussed in drug fora which date back to 2018 (reddit, 2018d). There are discordant opinions on the fact that it was actually sold/ available on the market, but the users who report its consumption describe 4-methoxymethylfentanyl as being better than carfentanyl, with a relative lower potency, less breathing depression, more euphoria, and slightly longer effects. In Figure 7.17 are presented, in detail, the predicted interactions between acetyl-carfentanyl and the MOR binding site.



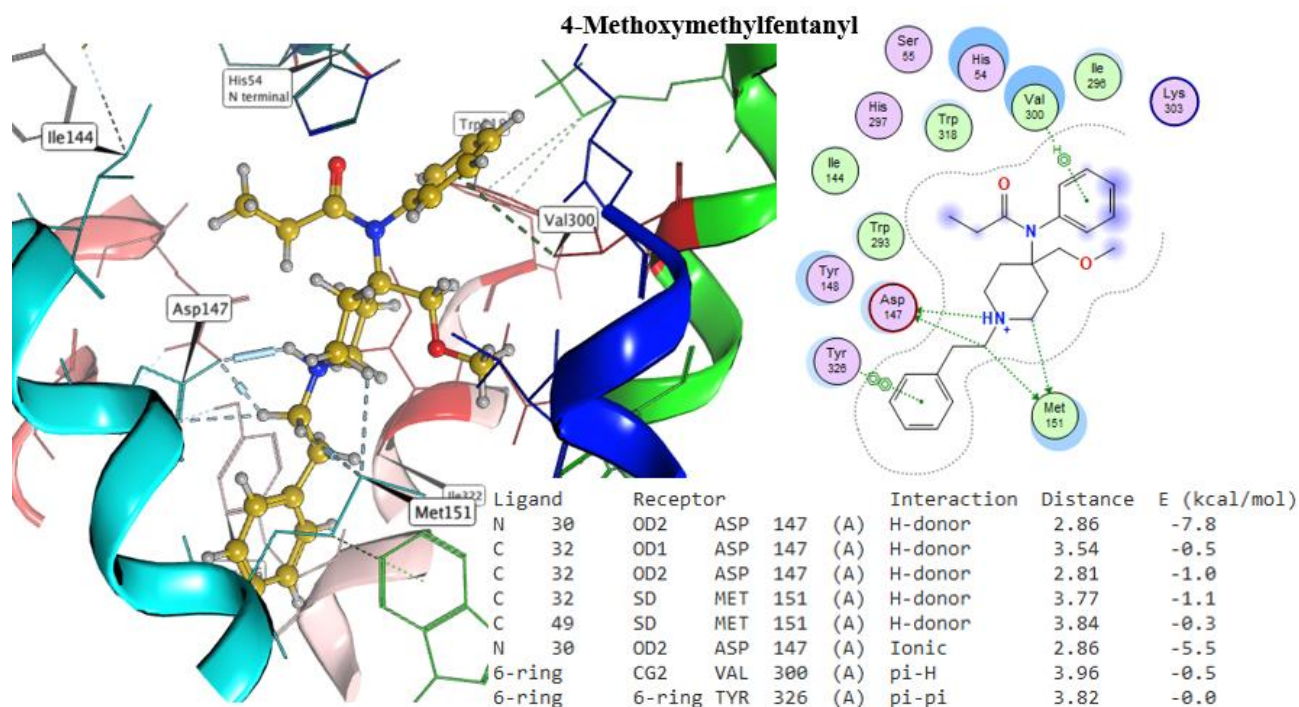


**Figure 7.17** The 3D pose of 4-Methoxymethylfentanyl docked in PDB5C1M and 2D representations.

**Notes:** on the 3D representation of the left, the binding pocket with the docked ligand 4-Methoxymethylfentanyl (gold). The different TM helices are identified with different colours, light blue for TM3, green for TM6, light pink for TM7. The red colour visible in the TM6 identifies part the hydrophobic pocket characteristic of ORs. The dotted lines show the interactions between the ligands and the pocket residues, and in particular, the light blue colour identifies both hydrogen-bond and ionic interactions, while the dark green identifies the H-pi bonds (aromatic interactions). The cylinder visible on some of the dotted line is a measure of the strength of the bonds, i.e. the bigger the cylinder the stronger the interaction. On the right, the 2D representation of the binding pocket and a report of the interactions between receptor residues and ligand are provided. The colours used to depict the residues in the 2D screenshot define different characteristics of the latter: light purple for polar residues and light green for hydrophobic ones; red circle indicates an acidic and blue a basic residue; and the light blue halo indicates solvent exposure both on the receptor and the ligand.

#### 7.4 Novelty and importance of the in silico methodology applications on NSOs

As reported in the latest UNODC reports (UNODC, 2022b, 2021b), NSOs are potentially the most dangerous class of NPS, being responsible for 100,000 deaths in North America in 2021 alone (Dyer, 2021). Moreover, the EMCDDA reported that, of the 5,800 fatalities involving one or more illicit drugs registered in 2020 in the European Union, opioids were involved in more than three-quarters, with fentanyl and its analogues contribution underestimated in some countries (EMCDDA, 2022c).

In particular, NSOs seems to be responsible, to date, for the third wave of the opioid epidemic, i.e., a significant increase in overdose deaths involving, in particular, illicitly manufactured fentanyl and analogues (Gladden et al., 2019; Mattson et al., 2021). As reported above, the scenario is deeply complicated by the constant increase in the NSOs identified, i.e., available on the market, in the last couple of years. Indeed, in contrast to the stabilisation trend reported for other NPS, the class of NSOs has been growing since 2016 (**Error! Reference source not found.**) reaching a total of 131 officially reported molecules in 2022, i.e., roughly 11% of the total NPS identified.

NSOs in general, but more so the fentanyl-like class, are characterised by very strong potencies, which can be equated to 10000 that of morphine (Beardsley and Zhang, 2018; Ellis et al., 2018; EMCDDA, 2017d; Piotr F. J. Lipiński et al., 2019), which flag them as serious threats for public health both for recreational users and frontline staff (i.e. law enforcement, border police, health care personnel, etc) (U.S. Customs and Border Protection U.S. Customs and Border Protection, 2022; US Fire Administration, 2021; USA House of Representatives, 2021).

While NSOs are extremely dangerous on their own, the risk associated with their use/abuse increase exponentially and became more complicated within the increasingly reported polydrug consumption scenarios (EMCDDA, 2022c; UNODC, 2022b). The latter see NSOs used very often in combination with other central nervous system depressants (e.g., BDZs and DBDZs) or stimulants (i.e. methamphetamine) (Elliott et al., 2019; Fogger, 2019; Frisoni et al., 2018; Jones et al., 2020; Mattson et al., 2021). As discussed for DBDZs, the concomitant use of more than one substance, especially strong depressants, usually leads to a synergistic enhancement of the adverse effects of both substances, potentially leading to extremely severe side effects including respiratory depression and death (Abdulrahim and Bowden-Jones, 2018; Arillotta et al., 2020; Orsolini et al., 2020).

The threat associated with NSOs is actual and is even more worrisome if one considers the paucity of safety/toxicity data available for the majority of NPS, with particular regard to the new ones

identified on the market, i.e. nitazenes and cinnamylpiperazines. Consequently, it is extremely important to assess as much as possible the extent of the NSOs phenomenon, and more so with regard to their pharmacology.

In this regard, both *in vitro* studies have been carried out to possibly assess the relative potency of NSOs to morphine, towards MOR (Fogarty et al., 2022; Krotulski et al., 2021; Vandeputte et al., 2021; Vasudevan et al., 2020), along with a few *in silico* approaches (Ellis et al., 2018; Floresta et al., 2019; Noha et al., 2017).

The novel approach of *in silico* methodologies has proven very helpful in doing so. The 3D-QSAR models identified here seem to be very reliable in their predictive power. They identified NSO analogues of fentanyl and carfentanyl as the most potent, i.e., N-methyl-carfentanyl, butyryl-carfentanyl, acetyl-carfentanyl, and 4-Methoxymethylfentanyl, for the majority of which no information was retrieved in the scientific literature. The only prediction confirmed by available experimental data was that for 4-methoxymethylfentanyl. The lack of information on these NSOs highlights the importance and the need for *in silico* approaches to be used as preventive and informative tools.

As discussed for the DBZD class, these models could be used to assess, in a rapid and cost-effective way, the biological activity profile of a new NSO, as soon as the latter is identified on the illegal market. Moreover, they could be of use to better discriminate between the various NSOs, for which large differences in structures/chemical scaffolds, could result in great biological activity disparity. *In silico* approaches could and should be used as support methodologies for the drafting of preliminary risk assessments and the proposal of temporary bans / schedules. It has been witnessed, especially for NSOs how the scheduling of a substance resulted in an immediate change in the availability of the latter. Therefore, the ability to quickly assess the activity profile of a new NSO, proceeding to a temporary ban of the latter, could potentially result in an important decrease in related intoxication cases and fatalities. *In silico* methodologies could be used as a starting point for pre-emptive legal measures and further investigations (e.g., *de novo* chemical synthesis; *in vitro* studies; preclinical studies).

The results obtained with the scaffold hopping exercise carried out for DBZDs suggest how the same should be done for the other NPS classes to assess the existence of a possibly wider chemical landscape for these molecules and to draft computational libraries that regulatory bodies could use as support tools for risk assessment and scheduling procedures.

The following Chapter will present the study carried out to assess the possible activity of DBZDs on ORs.





## 7.5 Limitations

The major limitation is represented by the chemical structure variety of the class of NSOs, which led to the design of two different QSAR models, one for fentanyl-like molecules and the other for morphine-like molecules. Due to the lack of a reliable number of experimental values for nitazenes (i.e. only 14 (Vandeputte et al., 2021)), a QSAR model for predicting their biological activity could not be created. Other limitations include the uncertainty measure of the experimental value of pKi identified across datasets (training and test) used for the computational studies, as well as the fact that the pKi values do not come from the same experimental assay. Despite the diverse assays were chosen as and deemed comparable this inevitably add measure uncertainty. The measure uncertainty is, however, common in QSAR and is not considered to affect strongly the reliability of the final model (Fourches et al., 2010; Golbraikh et al., 2014). The highly structural flexibility of the class of fentanyl-like molecules alongside the very complex ring system of the morphine-like NSOs represented a challenge for the alignment process conducted with Forge™, especially if one considered that no similar co-crystallised 3D structure was available as reference molecule. This resulted in issues with the alignment of some morphine-like NOSs identified by the NPS finder whose values of pKi were not predicted. Please refer to the Chapter 10, i.e. Future work, for this issue.

Other limitations include the use of one crystallised structure of the MOR, whose co-crystallised ligand has a different structure of the molecules in the analysis. This could affect the geometry of the binding pocket, influencing the interactions pattern of the NOSs analysed. However, the PLIFs obtained for both classes suggest that this influence, if happening, does not have a substantial effect. The use of force field methodology only for the energy minimisation of the molecules analysed, which could give slightly less accurate conformations if compared to semi empirical calculations, could be included among the limitations on this study.

## Chapter 8 Designer benzodiazepines' activity on opioid receptors studies

The work discussed in this chapter was published in Current pharmaceutical design as Catalani et al. (2022) *Designer benzodiazepines' activity on opioid receptors: a docking study*, and it was presented (oral presentation) at the VIII International NPS Conference held online in November 2021 (International Society for the Study of Emerging Drugs (ISSED), n.d.).

### 8.1 Benzodiazepines activity on opioids receptor literature background

As discussed above BZDs (Sec 4.1) are one of the most prescribed classes of drugs across the world (EMCDDA, 2020c, 2018b) Historically prescribed as anxiolytics, sedatives, hypnotics, anticonvulsants, and muscle relaxants (EMCDDA, 2020c) they also have been prescribed to heroin/opioid users to minimise withdrawal symptoms (EMCDDA, 2020c). However, recently, this particular therapeutic indication has become controversial due to the reported increase of co-abuse disorders and addiction potential between the two classes of substances (De Wet et al., 2004; EMCDDA, 2021c; Liu et al., 2021; National Institute on Drug Abuse (NIDA), 2021; UNODC, 2021e).

Previous studies have reported that BZDs seem to enhance euphoric, analgesic, and reinforcing properties of opioids in opioid users (Goodchild and Serrao, 1987; Navaratnam and Foong, 2008; Poisnel et al., 2009; Rattan et al., 1991). As a result, whilst BZDs' main mechanism of action is the allosteric modulation of the GABA-AR (Sec. 4.2.3), a direct effect on KOR, MOR, DOR has been postulated (Goodchild and Serrao, 1987; Rattan et al., 1991). Indeed, literature reports how both midazolam and diazepam have a direct effect on the spinal antinociceptive opioid receptors (KOR and DOR) (Cox and Collins 2001) with reinforcing properties. A reinforcing effect on ORs has been reported as well for the anxiolytic properties of the BZDs It has been observed that the systemic administration of non-selective opioid antagonists (i.e., naloxone, picrotoxin, and  $\beta$ -funaltrexamine), in both animal and human models, can interfere with the anxiety-reducing effects of BZDs (Billingsley and Kubena, 1978; Tsuda et al., 1996), hence their anxiolytic effects may indeed be mediated through the modulation of the endogenous opioid system (Primeaux et al., 2006). However, the exact mechanism of interaction, including the possible subtypes of opioid receptors involved, is still unclear (Primeaux et al., 2006). A role for amygdalar opioid receptor sites (MOR and DOR) in the anxiolytic effects of benzodiazepines has been postulated (Primeaux et al., 2006).

In addition to this, it was observed how naltrexone, a preferential antagonist of MOR, reduced the effects of diazepam on response latency in rats, suggesting that some of diazepam's effects could be caused by a mechanism sensitive to naltrexone (Herling, 1983; Richardson et al., 2005).

Moreover, in the quest for safe and effective antinociceptive agents, derivatives of 1,4-benzodiazepine (e.g., tifuladom) have been identified as possessing a selective affinity for KOR (Anzini et al., 2003; Cappelli et al., 1996).

The interactions postulated between BZDs and ORs could and should be considered also for the DBZDs, considering that for some of them an increased potency and a quick on set have been reported. Indeed such interactions could worsen the already complicated pharmacological profile in co-abuse scenarios in recreational drug settings, resulting in additive effects with increased risks of sedation, synergistic induction of respiratory depression, coma, and death (Afzal and Kiyatkin, 2019; Boon et al., 2020; Liu et al., 2021; Medicines and Healthcare products Regulatory Agency, 2020; National Institute on Drug Abuse (NIDA), 2021).

In light of the above, it is postulated that DBZDs could have a direct effect on OR receptors. This could complicate their already scarcely known pharmacodynamics and aggravate their safety/toxicity profiles. To date, the activity profile of DBZDs with ORs has not been assessed. Indeed, it is important to better understand the possible risks/harm associated with the use/abuse of DBZDs, assessing their mechanism of action and identifying the relative target receptor(s). While conducting preclinical studies with dozens or hundreds of molecules may constitute an extremely time-consuming and costly exercise, computational models could be used as fast and reliable preliminary assessment methodologies to investigate this mechanism of action.

This study aimed to computationally evaluate the binding affinity (or lack thereof) of the 115 DBZDs identified online towards KOR, MOR, and DOR, with the use of pharmacophore and docking studies, to assess if their mechanism of action could include activity on opioid receptors.

## 8.2 Methodology

### 8.2.1 DBZDs object of the study

The DBZDs object of the study were the 115 identified by the NPSfinder (please refer to Section 3.2).

### 8.2.2 Identification of reference compounds

Reference compounds necessary for pharmacophore filtering and for docking studies were obtained from the ChEMBL database (EMBL-EBI, 2021). Homo sapiens MOR, KOR, and DOR targets were searched for in the database and strong agonist binders for each of them were identified among the available activity data (ChEMBL, 2021b, 2021a, 2021c). The EC<sub>50</sub>, i.e. the concentration inducing half of the maximum effect, assessed as stimulation of [<sup>35</sup>S]GTPgammaS, binding was the activity type used. For each of the ORs, twenty potent (i.e., low value of EC<sub>50</sub>) agonists, including peptide and non-peptide ligands were identified and used (**Appendix A**). These were identified across the assays to minimise biases. The 20 compounds displaying low values of EC<sub>50</sub> were chosen to obtain a good variety of chemical structures.

Five additional molecules for each OR including the co-crystallized ligand were extrapolated from the literature according to their strong activity as agonist binders and used as reference molecules for docking studies (Table 8.1).

Table 8.1 Five reference molecules for docking studies of DBZDs on ORs

<b>MOR</b>		
<b>Molecule</b>	<b>SMILES</b>	<b>S (Kcal/mol)</b>
<b>BU72</b>	<chem>O(C)[C@]12[C@]3(C)[C@@H](c4cccc4)[NH2+][C@H]1[C@@]14c5c(ccc(O)c5)C[C@@H]([NH+](C)CC1)[C@@]4(C=C2)C3</chem>	-10.15
fentanyl	<chem>O=C(N(c1cccc1)C1CC[NH+](CCc2cccc2)CC1)CC</chem>	-8.44
carfentanyl	<chem>O=C(N(c1cccc1)C1(C(=O)OC)CC[NH+](CCc2cccc2)CC1)CC</chem>	-9.59
$\alpha$ -methylfentanyl	<chem>O=C(N(c1cccc1)C1CC[NH+](C[C@@H](Cc2cccc2)C)CC1)CC</chem>	-8.99
$\beta$ -hydroxyfentanyl	<chem>O=C(N(c1cccc1)C1CC[NH+](C[C@@H](O)c2cccc2)CC1)CC</chem>	-8.79
<b>KOR</b>		
<b>MP11 04</b>	<chem>C1CC1CN2CC[C@]34[C@@H]5[C@H]2CC6=C3C(=C(C=C6)O)[C@H]4[C@@H](C=C5)NC(=O)C7=CC(=CC=C7)I</chem>	-9.79
CHEMBL503080	<chem>Clc1cc2c(CC(=O)N3[C@H](C[NH+]4CCCC4)CN(c4cccc4)CC3)csc2cc1</chem>	-9.00
CHEMBL526933	<chem>Clc1c(Cl)ccc(N(CC(=O)N2[C@H](C[NH+]3CCCC3)CN(S(=O)(=O)C)CC2)C)c1</chem>	-9.24
CHEMBL499351	<chem>Clc1c(Cl)ccc(N(CC(=O)N2[C@H](C[NH+]3CCCC3)CN(S(=O)(=O)c3cc(Cl)ccc3)CC2)C)c1</chem>	-9.74
CHEMBL525457	<chem>Clc1cc2N(CC(=O)N3[C@H](C[NH+]4CCCC4)CN(S(=O)(=O)c4cc(OC)c(OC)cc4)CC3)C(=O)Oe2cc1</chem>	-9.81
<b>DOR</b>		
<b>DPI-287</b>	<chem>O=C(N(CC)CC)c1ccc([C@@H](N2[C@@H](C)C[NH+](CC=C)[C@H](C)C2)c2cc(O)ccc2)cc1</chem>	-8.58
CHEMBL2151735	<chem>O=C(N([C@@H](C(=O)N[C@@H]1C(=O)N(CC(=O)N)Cc2c(cccc2)C1)C)C)[C@@H]([NH3+])Cc1c(C)cc(O)cc1C</chem>	-9.44
CHEMBL8234	<chem>O=C([O-])[C@@H](NC(=O)[C@@H](NC(=O)CNC(=O)CNC(=O)[C@@H]([NH3+])Cc1ccc(O)cc1)Cc1cccc1)CC(C)C</chem>	-10.43
CHEMBL3758292	<chem>O=C([C@@H]([NH3+])Cc1c(C)cc(O)cc1C)N1[C@@H](C(=O)NCc2[nH]c3c(n2)cccc3)Cc2c(cccc2)C1</chem>	-9.70
CHEMBL2113666	<chem>Clc1c(/C=C/C(=O)N[C@]23[C@@H]4[NH+](C)CC[C@@]52[C@H](C(=O)CC3)Oe2c5c(ccc2)C4)cccc1</chem>	-7.26

### 8.2.3 *Pharmacophore filtering*

The flexible alignments and the pharmacophore mapping were carried out as explained in Section 4.3.9. The consensus mode was used for the pharmacophore mapping. The final pharmacophore maps generated for each OR was validated via the filtering of three databases of known MOR, KOR and DOR ligands which are reported in Appendix A.

### 8.2.4 *Molecular docking*

For a review of the molecular docking methodology, please refer to section 4.3.8. To perform the molecular docking studies, the same MOR, DOR and KOR structures discussed in section 6.4.4 were used.

As seen before, the co-crystallised ligand atoms of each receptor were used as the docking “site” in the General docking panel. No pharmacophore constraint was added due to the diversity between the co-crystallised ligands and the DBZDs under evaluation and to avoid forcing poses for the latter. If solvent molecules were present in the crystal structure, they were included in the docking process.

Reference compounds (i.e. selective and potent binders) for each of the receptors were docked to evaluate MOE<sup>®</sup> placement and scoring methods (Sec 4.3.8). Once the placement and scoring methods were chosen, they were applied to the docking studies on those DBZDs resulted by the pharmacophore filtering exercise together with the four reference compounds (i.e., strong agonist binders) and the co-crystallised ligand (BU72, DPI-287 and MP1104). For each DBZD the number of poses generated in the placement was increased from the default values of 30 to 100 to account for system variability (Ellis et al., 2018).

## **8.3 Pharmacophore filtering results**

The three pharmacophore consensus queries for KOR, MOR, and DOR were generated from the alignment showing the lowest S values and manually analysed (Figure 8.1Figure 8.2).

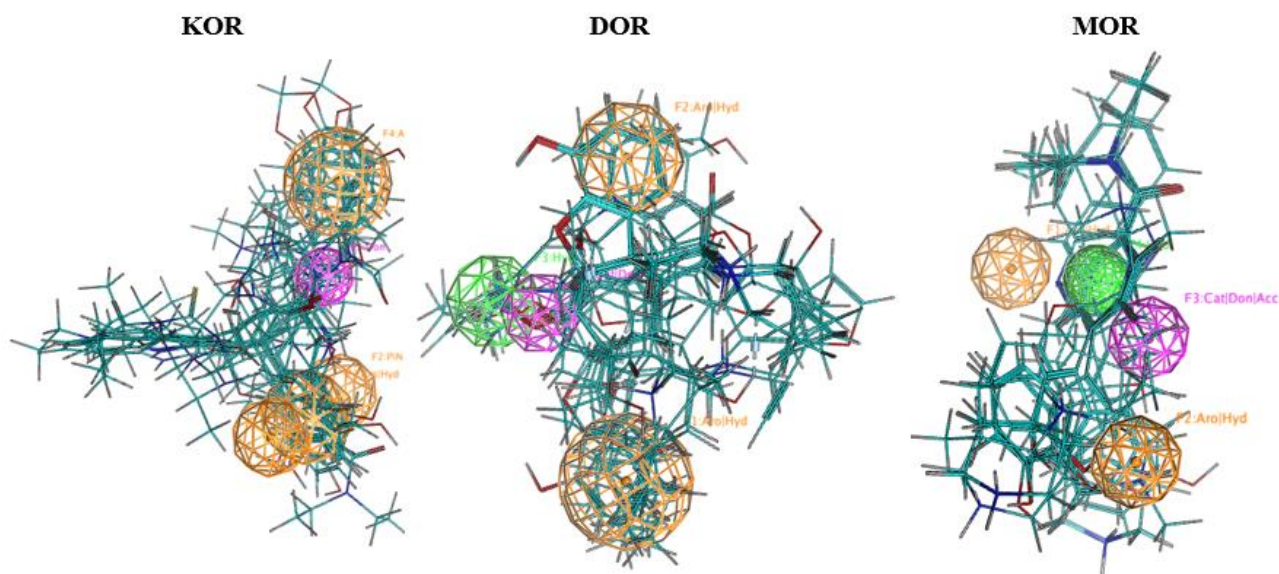


**Figure 8.1** Pharmacophore queries generated for KOR, DOR and MOR

*Notes.* The pharmacophore query and the flexible alignment of the strong agonist binders for each receptor are reported. Please note that for image clarity not all the twenty agonists used in the flexible alignment are displayed. It can be noted that different spatial coordinates may host more than one feature. In orange are represented the aromatic/hydrophobic centroids, in green the hydrophobic ones, and in purple the H-bond donor and cationic centroid.

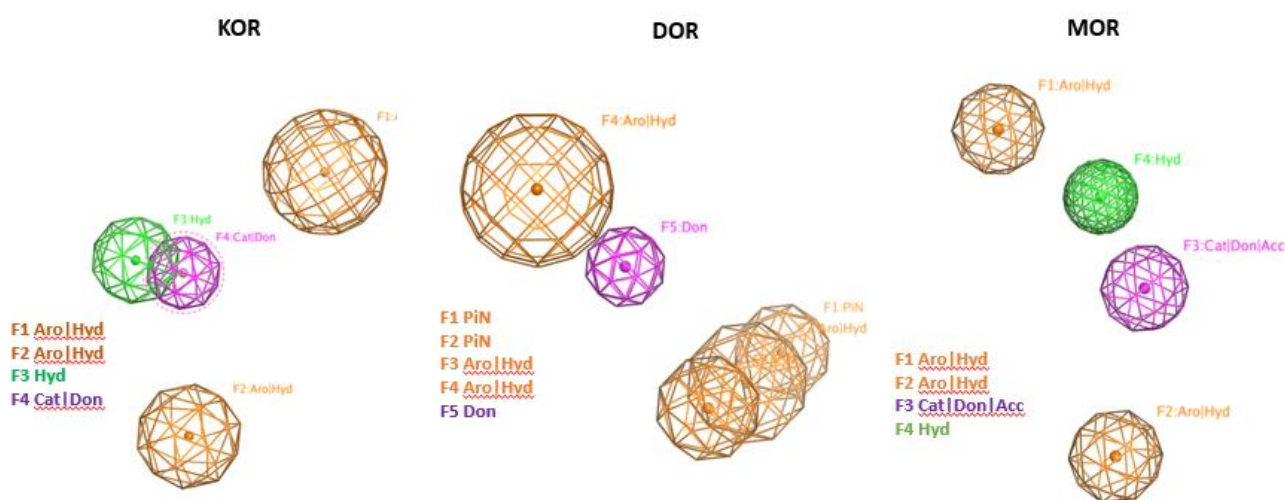


**Figure 8.2** Pharmacophore queries generated for KOR, DOR and MOR without the flexibly aligned ligand.

*Note.* Please note that for each pharmacophore, the list of features is displayed for clarity.

The resulting pharmacophore maps were “validated” through the filtering of the agonist ligands databases (validation sets) extrapolated from ChEMBL (76 ligands for each receptor, Appendix A). KOR pharmacophore matched 69 of the ligands (91%) in the validation set, MOR 62 ligands (81%) and DOR 36 ligands (47%). These data suggested how MOR and DOR were more comprehensive pharmacophore, matching compounds with higher values of biological activity, while KOR was more selective toward those with lower activity values, i.e. more potent. When



these queries were used to filter the list of 115 DBDZs identified by NPSfinder<sup>®</sup> on the surface web (isomerdesign.com (Catalani et al., 2021b; Isomer Design, 2021)), the resulting hits were: 16 molecules for KOR, 23 molecules for DOR, and 21 molecules for MOR (Appendix A).

#### **8.4 Molecular docking results**

PDB5C1M for MOR (Huang et al., 2015; RCSB PDB, 2015), PDB6PT3 for DOR (Claff et al., 2019; RCSB PDB, 2019), and PDB6B73 (Che et al., 2018; RCSB PDB, 2018d) for KOR were used for the docking studies (sec 6.4.4).

The characteristic agonists interactions, as identified in the literature, with aspartic acid (Asp128, 138, 147), methionine (Met132, 142, 151), and valine (Val281, 300) can be observed in Figures 6.12, 6.14 and 6.15 (Che et al., 2018; Claff et al., 2019; Huang et al., 2015).

London dG and GBVI/WSA dG (Chemical Computing Group ULC, 2022) were used as the scoring methods for placement (alpha triangle and refinement (induced fit)). For each molecule, the docking poses were analysed according to the S values and the type of interactions observable for that particular pose. The most common interactions identified between the DBZDs, and the binding pockets are presented in Table 8.2.

**Table 8.2 Most common interactions identified between the DBZDs ligands and ORs**

<b>Receptor</b>	<b>Residue</b>	<b>Interaction</b>
<b>MOR</b>	Asp 147	H-donor; ionic
	Met 151	H-donor
	Val300	hydrophobic
	His297	hydrogen bonds water mediated.
	Lys233	hydrogen bonds water mediated.
<b>DOR</b>	Asp 128	H-donor; ionic
	Met 132	H-donor
	Val 281	hydrophobic
	His 278	hydrophobic
<b>KOR</b>	Asp 138	H-donor; ionic
	Met 142	H-donor
	Ser 211	H- acceptor
	Leu 212	H- acceptor
	Glu 115	H- acceptor
	Tyr139	hydrophobic
	Ile 316	H- acceptor.

For the binding affinity, a cut-off point was chosen after evaluating the reference compounds *S* values and those for the co-crystallized ligands BU72 (*S*= -10.1), DPI-287 (*S*= -8.5) and MP1104 (*S*= -9.8) (Table 8.3). Consequently, DBZDs showing *S*< -8.0 (the lower the value, the stronger the binding), were considered putative strong binders. For the interactions patterns, particular regard was given to ionic and hydrogen-bond mediated interactions with Asp and to the hydrogen-bond mediated interactions with Met (Che et al., 2018; Claff et al., 2019; Huang et al., 2015). Indeed, as reported in Section 6.4.4, the ionic Asp bond is mandatory to infer the activation of the ORs (Krumm and Grisshammer, 2015; Shim et al., 2013). A total of six molecules for KOR, five for DOR and four for MOR meeting both criteria were identified (Table 8.3).

**Table 8.3 Binding values (S) generated for those DBZDs that display the ionic interaction with the charged amine of the Asp residues in DOR, KOR and MOR.**

*The S values of the co-crystallised ligand and the reference compounds for each ORs are reported as reference values. Only DBZDs showing a predicted S value < -8.0 were included in the table.*

DOR		
Molecule	SMILES	S (Kcal/mol)
CHEMBL8234	<chem>O=C([O-])[C@@H](NC(=O)[C@@H](NC(=O)CNC(=O)CNC(=O)[C@@H]([NH3+])Cc1cccc(O)cc1)Cc1cccc1)CC(C)C</chem>	-10.43
CHEMBL3758292	<chem>O=C([C@@H]([NH3+])Cc1c(C)cc(O)cc1C)N1[C@@H](C(=O)NCc2[nH]c3c(n2)cccc3)Cc2c(ccc2)C1</chem>	-9.70
CHEMBL2151735	<chem>O=C(N([C@@H](C(=O)N[C@@H]1C(=O)N(CC(=O)N)Cc2c(ccc2)C1)C)C)[C@@H]([NH3+])Cc1c(C)cc(O)cc1C</chem>	-9.44
DPI-287	<chem>O=C(N(CC)CC)c1ccc([C@@H](N2[C@@H](C)C[NH+](CC=C)[C@H](C)C2)c2cc(O)ccc2)cc1</chem>	-8.58
CHEMBL2113666	<chem>Clc1c/C=C/C(=O)N[C@]23[C@@H]4[NH+](C)CC[C@]52[C@H](C(=O)CC3)Oc2c5c(ccc2)C4)cccc1</chem>	-7.26
Ro 48-8684	<chem>Fc1cc2C(=O)N(C)Cc3c(-c4oc(C[NH+](CCC)CCC)cn4)ncn3-c2cc1</chem>	-8.70
Ro 48-6791	<chem>Fc1cc2C(=O)N(C)Cc3c(-c4nc(CN(CCC)CCC)on4)ncn3-c2cc1</chem>	-8.67
Fluloprazolam	<chem>Fc1c(C2=NCC=3N(C(=O)C(=CN4CC[NH+](C)CC4)N=3)c3c2cc([N+](=O)[O-])cc3)cccc1</chem>	-8.45
JQ1	<chem>Clc1cccc(C2=[NH+](C)CC(=O)OC(C)(C)C)c3n(c(C)nn3)-c3sc(C)c(C)c23)cc1</chem>	-8.12
Ciclotizolam	<chem>Brc1sc2-n3c(C4CCCC4)nc3C[NH+]=C(c3c(Cl)cccc3)c2c1</chem>	-8.07
KOR		
MP11 04	<chem>C1CC1CN2CC[C@]34[C@@H]5[C@H]2CC6=C3C(=C(C=C6)O)[C@H]4[C@@H](C=C5)NC(=O)C7=CC(=CC=C7)I</chem>	-9.79
CHEMBL499351	<chem>Clc1c(Cl)ccc(N(CC(=O)N2[C@H](C[NH+](C)CC4)N=3)c3c2cc([N+](=O)[O-])cc3)CC2)C)c1</chem>	-9.74
CHEMBL526933	<chem>Clc1c(Cl)ccc(N(CC(=O)N2[C@H](C[NH+](C)CC4)N=3)c3c2cc([N+](=O)[O-])cc3)CC2)C)c1</chem>	-9.24
CHEMBL526747	<chem>Clc1c(Cl)ccc(N(CC(=O)N2[C@H](C[NH+](C)CC4)N=3)c3c2cc([N+](=O)[O-])cc3)CC2)C)c1</chem>	-9.01
CHEMBL503080	<chem>Clc1cc2c(CC(=O)N3[C@H](C[NH+](C)CC4)N=3)c3c2cc([N+](=O)[O-])cc3)CC2)C)c1</chem>	-9.00
Ro 48-8684	<chem>Fc1cc2C(=O)N(C)Cc3c(-c4oc(C[NH+](CCC)CCC)cn4)ncn3-c2cc1</chem>	-8.74
JQ1	<chem>Clc1cccc(C2=[NH+](C)CC(=O)OC(C)(C)C)c3n(c(C)nn3)-c3sc(C)c(C)c23)cc1</chem>	-8.47
Ciclotizolam	<chem>Brc1sc2-n3c(C4CCCC4)nc3C[NH+]=C(c3c(Cl)cccc3)c2c1</chem>	-8.45
Cinazepam	<chem>Brc1cc2C(c3c(Cl)cccc3)=NC(OC(=O)CCC(=O)[O-])C(=O)Nc2cc1</chem>	-8.34
Fluloprazolam	<chem>Fc1c(C2=NCC=3N(C(=O)C(=CN4CC[NH+](C)CC4)N=3)c3c2cc([N+](=O)[O-])cc3)cccc1</chem>	-8.23
MOR		
BU72	<chem>O(C)[C@]12[C@]3(C)[C@@H](c4cccc4)[NH2+][C@H]1[C@@]14c5c(ccc(O)c5)C[C@@H]([NH+](C)CC1)[C@@]4(C=C2)C3</chem>	-10.15
Carfentanyl	<chem>O=C(N(c1cccc1)C1(C(=O)OC)CC[NH+](CCc2cccc2)CC1)CC</chem>	-9.59
$\alpha$ -methylfentanyl	<chem>O=C(N(c1cccc1)C1CC[NH+](C[C@@H](Cc2cccc2)C)CC1)CC</chem>	-8.99
$\beta$ -hydroxyfentanyl	<chem>O=C(N(c1cccc1)C1CC[NH+](C[C@@H](O)c2cccc2)CC1)CC</chem>	-8.79
Fentanyl	<chem>O=C(N(c1cccc1)C1CC[NH+](Cc2cccc2)CC1)CC</chem>	-8.44
JQ1	<chem>Clc1cccc(C2=[NH+](C)CC(=O)OC(C)(C)C)c3n(c(C)nn3)-c3sc(C)c(C)c23)cc1</chem>	-9.37
Ro 48-8684	<chem>Fc1cc2C(=O)N(C)Cc3c(-c4oc(C[NH+](CCC)CCC)cn4)ncn3-c2cc1</chem>	-9.08
Fluloprazolam	<chem>Fc1c(C2=NCC=3N(C(=O)C(=CN4CC[NH+](C)CC4)N=3)c3c2cc([N+](=O)[O-])cc3)cccc1</chem>	-8.89
Cyprazepam	<chem>C1CC1CN=C2CN(C(=C3C=C(C=CC3=N2)Cl)C4=CC=CC=C4)O</chem>	-8.09
Ciclotizolam	<chem>Brc1sc2-n3c(C4CCCC4)nc3C[NH+]=C(c3c(Cl)cccc3)c2c1</chem>	-8.07

Cinazepam, cyprazepam, ciclotizolam, fluloprazolam, Ro 48-6791, Ro 48-8684, and JQ1 were found to display good binding affinity and the mandatory ionic interaction with the Asp residues. In particular, ciclotizolam, fluloprazolam, Ro 48-8684, and JQ1 showed these characteristics consistently across the three receptor subtypes, displaying however different binding affinity for the ORs.

The 2D ligand interactions maps for the three top scoring DBZDs for each OR are reported in Figure 8.3, 8.4 and 8.5

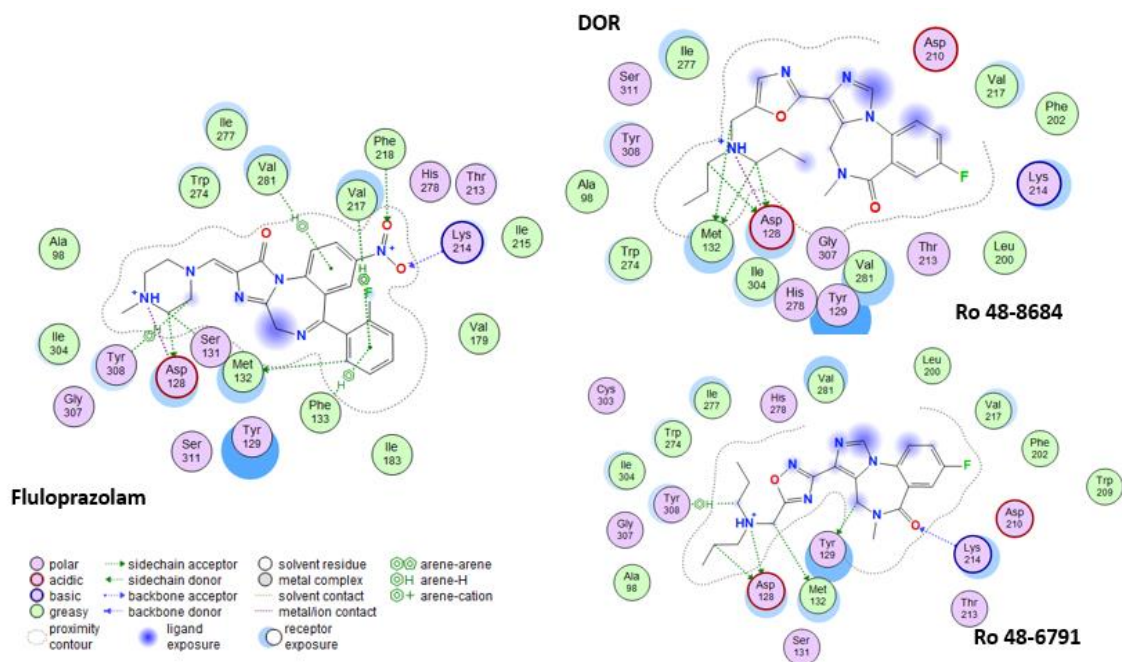


Figure 8.3 2D ligands interactions for the three top scoring DBZDs for DOR.

Notes. The colours used to depict the residues in the 2D screenshot define different characteristics of the latter: light purple for polar residues and light green for hydrophobic ones; red circles indicate an acidic and blue a basic residue; and the light blue halo indicates solvent exposure both on the receptor and the ligand

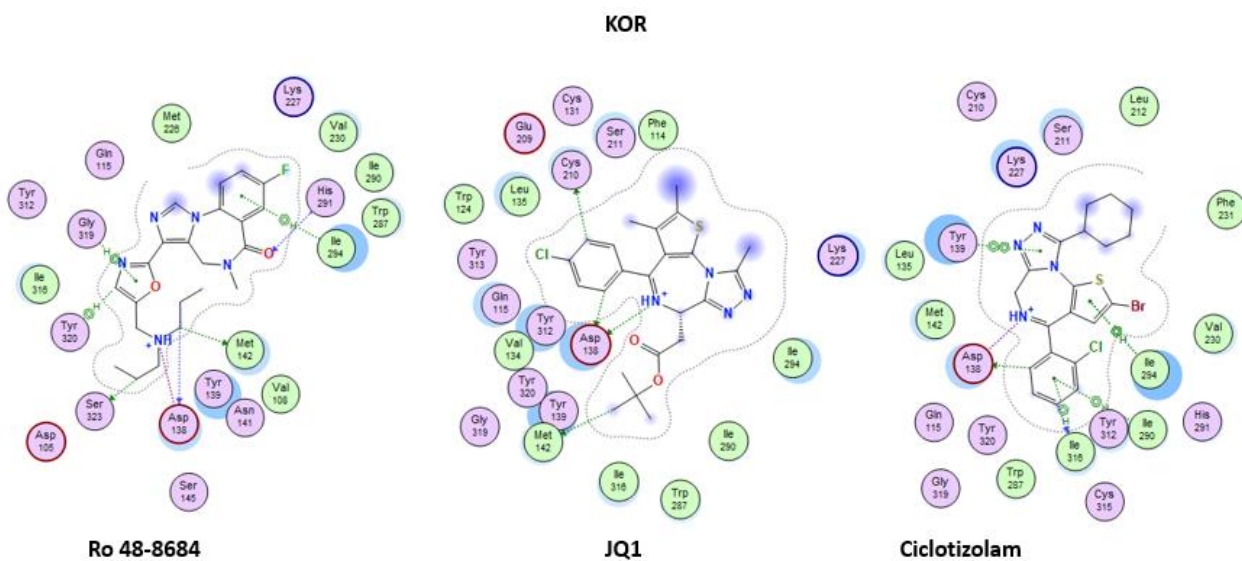
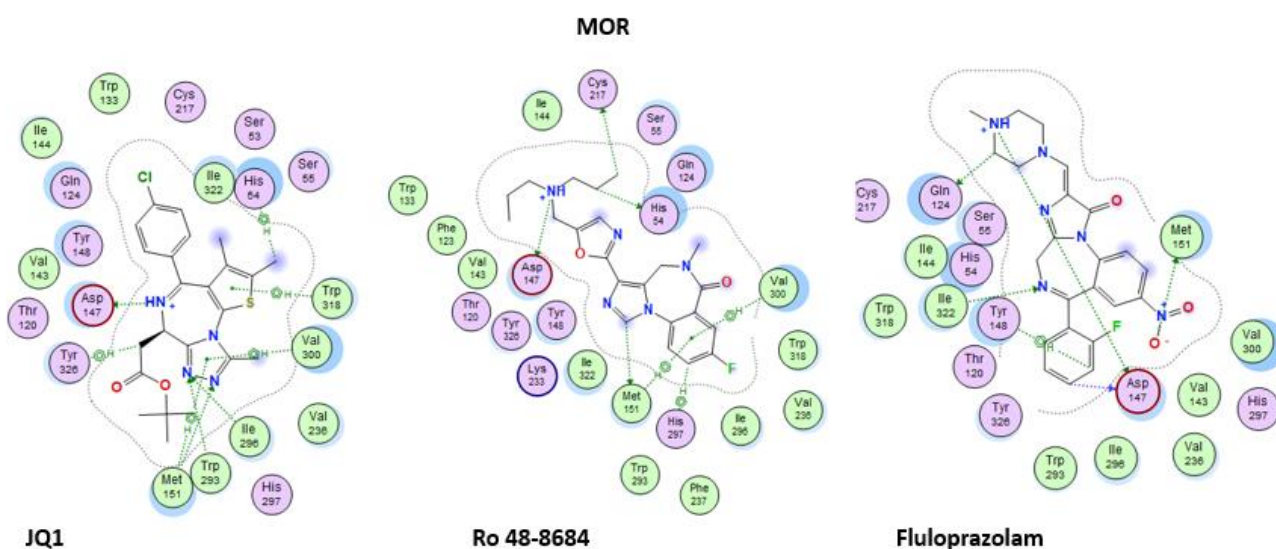


Figure 8.4 2D ligand interactions for the three top scoring DBZDs for KOR.

Notes. The colours used to depict the residues in the 2D screenshot define different characteristics of the latter: light purple for polar residues and light green for hydrophobic ones; red circles indicate an acidic and blue a basic residue; and the light blue halo indicates solvent exposure both on the receptor and the ligand



**Figure 8.5** 2D ligands interactions for the three top scoring DBZDs for MOR.

*Notes.* The colours used to depict the residues in the 2D screenshot define different characteristics of the latter: light purple for polar residues and light green for hydrophobic ones; red circles indicate an acidic and blue a basic residue; and the light blue halo indicates solvent exposure both on the receptor and the ligand

Detailed ligand interactions for Figure 8.3-8.5 are reported in Appendix A. Fluloprazolam, Ro 48-8684 and Ro 48-6791 seems to interact with Asp residue via the charged amine linked to the imidazole and oxazole moieties. None of the nitrogen atoms in benzodiazepine core structure seem to be involved in such interaction. JQ1 and ciclotizolam instead interact with the Asp via the charged nitrogen atom at position 4 of the diazepine core.

From Figure 8.2-8.5, it can be noted that all the DBZDs which seems to be able to interact with the ORs, shows either a triazolo or imidazole-benzodiazepine scaffold. The latter as stated in Chapter 5 seems to be associated with the highest values of biological activity and potency. If one looks at these structures from another point of view, benzotriazole and benzimidazole moieties could be identified. \this structure makes these DBZDs really similar to the one observed for the synthetic opioid class nitazenes (Vandeputte et al., 2021), supporting a possible interaction with ORs.

### 8.5 A discussion on the potential of DBZDs to activate ORs

To the best of our knowledge, this study is the first to evaluate the possible binding affinity between DBZDs and KOR, MOR, and DOR, giving an insight into their possible mechanism of action.

For each OR a pharmacophore map was designed to filter the DBZDs previously identified online. The resulting OR pharmacophores, in line with what is reported in literature (Shim et al., 2011; Singh et al., 2008; J Zhang et al., 2009), confirmed the importance and the recurring presence of two aromatic features and a more complex one including, across all three receptor subtypes, a cation, a hydrogen bond prone group and a hydrophobic centre. The latter identifies the important positively charged tertiary amine group, responsible for the ORs family activation (Casy and Parfitt, 254

1986; Manglik, 2020). Consistent with previous studies, the interaction between the charged amine and the aspartic acid residue can be mediated either by a hydrogen bond or ionic interaction (salt bridge), the latter being stronger and important for the activation of the receptor (Zimmerman and Leander, 1990).

Due to the similarity of the pharmacophores obtained for the ORs, the lists of the filtered DBZDs share similar entries (Appendix A), with ciclotizolam, fluloprazolam, JQ1, Ro 48-8684 and Ro 48-6791 matching all of them. These DBZDs are either partial agonists towards the GABA-AR (Tricklebank et al., 1990), characterised by fast pharmacokinetics (i.e., rapid onset and short half-life) (Krall et al., 2015), or “unknown” molecules, identified as DBZDs but lacking any further information on activity profile (e.g., fluloprazolam).

The pharmacophore filtered molecules were docked and further analysed according to the predicted binding affinity (*S*) and their engagement in ionic/hydrogen bond interactions with the Asp residue. The lack of the latter constituted a reason for rejecting the molecule as a putative OR binder. The cut-off for the *S* value was set to -8.0 (Kcal/ mol). Despite the fact that this cut-off is one order of magnitude lower than some of the very potent agonists/strong binders reference compounds (e.g., Leu-enkephalin, carfentanyl, etc.), DBZDs with such *S* values could still show good binding affinity. The five DBZDs that met both criteria are discussed as possible binders: JQ1, fluloprazolam, ciclotizolam, Ro 48-8684, and Ro 48-6791.

JQ1 is a thienotriazolobenzodiazepine that does not act as an agonist at the GABA-AR. It is not currently used in human clinical trials due to its very short half-life (Zhou et al., 2020).

Fluloprazolam seems to be an unknown DBZD, and only reference to a patent was retrieved from the literature (Prost-Marechal, 1982). Ciclotizolam is a very well-known low efficacy partial agonist of GABA-AR (Weber et al., 1985).

Ro 48-8684 and Ro 48-6791 are benzodiazepines developed by Hoffman-LaRoche in the 1990s (Godel et al., 1997) to achieve an improved replacement for midazolam. Unfortunately, they did not show advantages over the parent drug and were never developed as therapeutics (van Gerven et al., 1997).

Studies conducted with Ro 48-8684 and Ro 48-6791 (Hering et al., 1996; van Gerven et al., 1997; Wrigley et al., 2019) reported considerably shorter duration of action as well as faster recovery from the deep hypnotic effect. In particular, for Ro 48-8684 a reduced sensitivity was observed after repeated increasing dosage administration, due to undetermined factors (van Gerven et al., 1997).

These DBZDs show a short duration of action, in line with a partial agonist activity profile and the results predicted for their biological activity on GABA-AR (Catalani et al., 2021b). Indeed, previous QSAR studies (Catalani et al., 2021b) predicted very low biological activity for Ro 48-

8684, Ro 48-6791, JQ1, and fluloprazolam on the GABA-AR in line with their partial agonist activity profile. The only oddly predicted value was for ciclotizolam, indicating that the molecule may have a strong activity in contrast with it being a weak binder.

From the docking data presented it can be noted that JQ1, Ro 48-8684 and fluloprazolam display higher binding affinity toward MOR, with values similar or greater than those obtained for carfentanyl and fentanyl ( $S = -9.95, -8.44$ ) (Appendix A). They all show interactions with Asp147 and Met151, while none of them interacts with His297 (Figure 8.5), as observed for BU72. JQ1 and Ro 48-8684 display the hydrophobic bond with Val300 (Figure 8.5). This interaction has been observed, so far, in the binding of morphinan ligands only with the recruitment of a bigger hydrophobic surface including I296, W318, and I322 (Huang et al., 2015). It is interesting to note that JQ1, the top scoring DBZD, seems to interact with the Asp147 residue only, while Ro 48-8684 and fluloprazolam bind Met151 as well **Error! Reference source not found.**). The distance of the ionic bond (respectively, 3.20 (JQ1), 3.58 (fluloprazolam), and 3.35 (Ro 48-8684) Å) suggests a slightly stronger interaction than BU72 (3.53 Å) (Appendix A).

The same very strong binding affinity is not observed for KOR, towards which the DBZDs display  $S$  values that are roughly one unit lower than the reference compounds and the epoxymorphinan MP1104. It could be inferred that lower  $S$  values mean an activity threshold moved towards a greater order of magnitude when compared to MP1104. However, considering the latter has a picomolar KOR binding affinity (Che et al., 2018), one can assume the higher concentration required to activate a response (Ellis et al., 2018) will still fall in the lower nM range. Ro 48-8684 seems to be the most likely to bind KOR ( $S = -8.74$ ), followed by JQ1 and ciclotizolam. The distance of their ionic bond to Asp138, respectively, 3.91 and 3.02 and 3.35 Å, suggests a strength interaction similar to MP1104 (3.02 Å). The interactions for each molecule are presented in Figures 8.3-8.5, confirming binding to Asp138.

A similar profile of binding affinity is observed for DOR. The DBZDs seem to show less affinity when compared to the reference compounds (Table 8.3), but the same affinity of the co-crystallised ligand DPI-287 ( $S = -8.58$ ). Their interaction profile is presented in Figure 9.. Ro 48-8684 seems to be the molecule showing again the best affinity ( $S = -8.70$ ). The distance of its ionic interaction (3.20) (Appendix A) suggests it to be slightly weaker than DPI-287 (2.72), in line with the binding prediction (Table 8.3). This applies as well to Ro 48-6791 (3.11) and fluloprazolam (3.61).

It is interesting to note that all the top scoring DBZDs, being either triazolo or imidazole-benzodiazepines, show structural similarity to midazolam, which was shown to have a direct effect on the spinal antinociceptive opioid receptors (KOR and DOR) (Cox and Collins, 2001). To further validate the results obtained here midazolam and other five GABAergic currently used in the



anaesthesia diazepam and lorazepam (Miller and Gropper, 2019) were evaluated for their binding affinity towards ORs. Midazolam was the only anaesthetic showing any ionic interaction with Asp147 in MOR, with an S value of -7.33 which suggests a low binding affinity in line with the literature (Cox and Collins, 2001; Goodchild and Serrao, 1987; Rattan et al., 1991). Same ionic interactions were observed for KOR and DOR.

Compared to midazolam, the top scoring DBZDs seems to show higher binding affinity towards ORs.

These results suggest how those obtained for the DBZDs could be of value, especially if one considers the presence of benzotriazole and benzimidazole moieties in the scaffold of these molecules, and their similarity with the nitazenes class of synthetic opioids.

Despite the docking results obtained for each molecule being only an educated guess, a prediction of the binding affinity towards ORs, they can still be considered of value due to the comparison with those obtained for well-known strong agonist binders and the respective ORs co-crystallised ligands (Ellis et al., 2018). This comparison, together with the identification of ionic interactions and the fact that docking score function has been proven capable of predicting crystallographic binding orientations (Jakhar et al., 2019; Ramírez and Caballero, 2018), could support the thesis that these DBZDs may be able to act on ORs, and not just fit in the binding pocket. However, to confirm or refute this hypothesis, further and more sophisticated computational methodologies (molecular dynamics), and/or experimental (i.e. *in vitro* and *ex vivo*) approaches are needed.

Moreover binding affinity does not give information on the agonist or antagonist nature of the binding. Indeed docking *per se* does not provide a measure to discern between the two. Nevertheless, considering that the pharmacophores were built using agonist ligands, the likelihood of these DBZDs showing an agonist profile could be inferred.

These results give an interesting insight into the possible interactions and mechanisms of action of these five DBZDs. They all seem to possess low activity on GABA-AR (fluloprazolam excluded), however, expressing some of the agonist features (analgesic, antidepressant and anxiolytic), accompanied by fast pharmacodynamics.

Indeed, the two Ro compounds have a reported profile of action that differs from common BZDs, characterised by a rapid onset and rapid recovery from the deep hypnotic effect together with the development of tolerance.

It could be inferred that the particular pharmacodynamics observed, especially the fast onset and recovery timing, could be due to the recruitment and activation of opioids' transmission. Indeed, it has been reported that the binding pockets of the ORs analysed here are largely exposed to the

extracellular surface cavity and cause very fast dissociation half-lives of some extremely potent opioids (e.g., buprenorphine, carfentanyl, etorphine) (Manglik, 2020; Manglik et al., 2012).

Moreover, activation of the ORs produces effects similar to the activation of GABA-AR. In particular: activation of MOR results in sedation as well as tolerance and respiratory suppression, as seen for the  $\alpha 1$  isoform of GABA-AR (McKernan et al., 2000); activation of DOR results in anxiolytic and antidepressant-like effects (Dripps and Jutkiewicz, 2017; Gendron et al., 2016; E. Jutkiewicz, 2006) as seen for the activation of the  $\alpha 2$  isoform (Rudolph et al., 1999). Activation of KOR instead produces analgesic, hallucinogenic, and dysphoric effects (Che et al., 2018), which have not been observed with GABA-AR activation. Analgesic properties have previously been reported for BZDs; however, it is important to underscore that this could be due to other mechanisms than interaction with ORs. Indeed, it has been reported that the reduced complaints of pain following BZDs consumption is just an indirect effect of their depressant activity (Reddy and Patt, 1994). Further studies will be conducted on evaluating possible pharmacophore match between opioid and BZDs, to address the possibility of a common drug scaffold.

Finally, if one considers that the most powerful analgesic and addictive properties of opioids are mediated by MOR, the results obtained from the docking studies could suggest a reinforcement of the addiction potential of these DBZDs.

#### 8.5.1 *Limitations of the current study*

The major limitation of this study is the restricted size of the dataset (20 compounds for each receptor) used to develop the queries for the pharmacophore mapping/filtering exercise. Other limitations include the use of one receptor active conformation and co-crystallised ligand only, the lack of consensus docking; the lack of previous experimental data assessing the experimental binding affinity of DBZDs on ORs; and the lack of clear information on agonist /antagonist activity of the mentioned DBZDs despite the use of agonist binders for the creation of the pharmacophores. Further studies will include the evaluation of the binding pocket pharmacophore for each of the three ORs; *in vitro* assays to obtain experimental data on the EC50 or Ki (Vandeputte et al., 2021); and *ex vivo* assays to get insight in their possible G protein (or  $\beta$ -arrestin) pathways activation (Inoue et al., 2012).

## 8.6 Novelty and importance of the study

To the best of our knowledge this study is the first to assess the activity of DBZDs on ORs via the use of *in silico* methodologies. As stated above, while DBZDs represent only a small percentage of the NPSs identified worldwide they are increasingly being reported in acute and fatal intoxication often in poly consumption with other CNS depressants (e.g., opioids). The concomitant use of CNS depressants could lead to severe synergism of their adverse effects, especially so if they have the potential to activate the same receptor transmissions. Indeed NPS pharmacodynamics and activity/toxicity profiles are largely unknown, and complications could arise if one considered a possible multitarget action profile for these new DBZDs.

It is, therefore, relevant to assess as much as possible their profile of activity, including possible actions on multiple receptors. This is particularly true for DBZDs because an interaction with opioids' transmission has already been postulated (Goodchild and Serrao, 1987; Rattan et al., 1991) and molecules containing the BZD scaffold synthesised in the quest for selective ORs ligands (Anzini et al., 2003; Cappelli et al., 1996).

The *in silico* approaches here discussed, have been proven useful as a novel approach to elucidate the mechanism of action of these unknown molecules and help understand the possible associated health threats. Computational studies can provide quick and reliable predictions of activity and affinity for a biological target, helping researchers to focus and direct their efforts and studies (e.g. *in vitro*, preclinical) towards a smaller number of NPSs.

## Chapter 9 General conclusion

The programme of research discussed here represents a novel and successful approach in regard to two main challenges/issues closely related to the family of NPS, i.e. identification and risk assessment. Two research questions were highlighted at the beginning, i.e. would it be possible to use the internet and the analysis of the latter to improve the identification of new NPS, to obtain a more comprehensive picture of the NPS phenomenon, and to predict future drug scenarios? and would it be possible to utilise *in silico* technologies to develop a quick and reliable preliminary risk assessment procedure to guide legislative, law enforcement and public health responses and efforts against newly identified NPS?

The analysis of the internet, or surface web, forums, e-commerce platforms and chemical databases, via the use of a web crawler proved very valuable in assessing a NPS scenario different from the evidence based one presented by the UNODC and EMCDDA Early Warning Systems, as the preliminary research conducted on the topic suggested (Arillotta et al., 2020; Catalani et al., 2021c; Napoletano et al., 2020; Zangani et al., 2020). Indeed a total of 4,231 molecules were identified, a number almost four times the one reported by both the UNODC and EMCDDA as a result of evidence-based identifications. As of June 2022, the UNODC identified 1,127 individual NPS while the EMCDDA via the EWS (EMCDDA, 2022a) reported a total of 884 NPS. Moreover, the numbers of molecules identified for DBZDs (115) and NSOs (396) by NPSfinder<sup>®</sup> were found to be almost four times higher than those reported by the official databases, i.e., 33 and 78 respectively. This result highlights and confirms the importance of the analysis of the surface web and suggests how the web crawler activity may possess the potential to detect a broad range of novel or previously undescribed NPS. NPSfinder<sup>®</sup> could be used as a tool to predict future drug scenarios, i.e. to identify which NPS will be next available in the real market after assessing the virtual one. This was observed for example with flubrotizolam (Sec 5.6.1) a molecule not identified by the UNODC or EMCDDA databases which has been discussed online in drug fora since 2021 and is better known as ‘Fanax’, or fluclotizolam who was identified by the NPSfinder<sup>®</sup> before October 2020 and only identified in actual samples in 2021, as reported by the NPSDiscovery trend reports (NPSdiscovery, 2021).

Moreover, NPSfinder<sup>®</sup> can be used as an effective monitoring tool. Systematic monitoring, more so if global, is recognised by the UNODC as a powerful tool against drugs problems, as stated in the “Political Declaration and Plan of action on international cooperation towards an integrated and balanced strategy to counter the world Drug problem” (UNODC, 2009). The analysis of the surface web has no borders and could be used to keep the harms associated with NPS under surveillance

and review, even in those situations, as the recent COVID-19 pandemic, which could cause the disruption of the drug markets with a possible rise in online drugs purchases (Catalani et al., 2021a). Once novel NPS are identified very limited data is available on their pharmacological/toxicological profile, and the internet could also be used to retrieve such information if/when available (Orsolini et al., 2020). In the modern era, everything is discussed online including recreational drugs, and even more so if these recreational drugs attract the attention of drug enthusiastic/experimenter, the so called “psychonauts” (Orsolini et al., 2019, 2015a). This experience-sharing trend should be taken into high consideration as valuable for accessing anecdotal data on sought-after/side effects, as well as to potentially assess/ describe timelines for the emergence of a new substance (Corkery et al., 2017).

In support of this, more predictive data regarding NPS (i.e., a risk assessment) on pharmacology, acute and long-term related adverse effects and abuse potential could be generated with *in silico* methodologies. In this project, the latter have been once more confirmed to be reliable, cost- and time- effective tools which could be used to predict the pharmacology profile of an index NPS towards a set of receptors. Moreover, they could be used to assess a multi-target (i.e., receptors) profile of action. When applied to DBZDs, *in silico* methodologies predicted flubrotizolam, clonazolam, pynazolam and, fluclozotizolam as very active molecules, consistently with what reported in the literature and/or in drug discussion forums. In particular with flubrotizolam and fluclozotizolam it was found they were discussed on drug forums but not previously identified either by the UNODC or EMCDDA (flubrotizolam only). This suggests the possible presence on the market of very potent NPS representing a serious threat to public health. Moreover, the scaffold hopping exercise conducted for the DBZDs class, strongly suggested that structural replacement of the pendant phenyl moiety could increase biological activity and highlighted the existence of a still unexplored chemical space for this NPS class .

Worrisome results were also obtained for the class of NSOs, with the identification of new and potent analogues of carfentanyl (10,000 times more potent than morphine), i.e. 2-methyl carfentanyl, n-methyl-carfentanyl and butyryl-carfentanyl. The results obtained with the QSAR analysis were supported by molecular docking exercises, which gave an indication of the binding affinity of these NPS towards their respective receptors.

In addition, the use of *in silico* methodologies could be of use also for classification of new NPS. As reported in Section 1.2.2, the UNODC divide NPS into the main groups of substances controlled under the international drug conventions according to their pharmacological activity (Sec 1.2.2) (LSS/RAB/DPA/UNODC, 2016). It is indeed interesting to note that a good number of NPS reported by the UNODC are included in the “other” group. While the majority of the latter are

molecules for which the pharmacology is known, for some no data or very limited data is available. Even if their chemical structure is known and maybe similar to some other NPS, no pharmacological information is available. In this regard, *in silico* methodologies based on chemical similarity could be of extreme use in helping international authorities in classifying novel NPS. Paucity of experimental data could make *in silico* approaches, i.e. QSAR, difficult to carry out. However it is very likely that, if the new NPS are structurally similar to well-known NPS, then enough experimental data will be available. Also molecular docking, as seen for the study of DBZDs on ORs, could help in the classification via the assessment of binding affinities on different receptors (e.g. opioids, GABA-A, serotonin, B-adrenergic, etc).

In this research project attention was focused on two classes of NPS only, the ones which are deemed currently the most worrisome in terms of public health risks and harms associated with their usage (i.e., fatalities and overdoses). However a set of QSAR models, including more NPS classes, could be prepared and validated so that when a novel NPS is identified, the latter could be “run” through these models almost as a screening test procedure. This will help assessing its potential biological activity on a wide range of receptors and will support its classification process. If data are not available for QSAR, docking could come in support to describe any possible binding affinity of an index NPS towards a set of known (3D) receptor structures, e.g. beta adrenergic, dopaminergic and serotonergic.

The combination of online analysis and *in silico* methodologies could be considered as a very important tool for informing law enforcement agencies and public health stakeholders. The information which will be provided could potentially influence and impact other aspects related to NPS, such as treatment options, service provision, law-making, monitoring/surveillance and education. The latter, which should be considered of high importance in particular towards social and health prevention, could be of use also for both law enforcement agencies (e.g. which NPS to expect on the market and relative risk effect associated with accidental exposure) and for health professionals (e.g. for treatment option or professional formation). Potential and actual users could benefit also from information provided to increase awareness of the high risks associated with these new psychoactive substances.

To conclude this research project could be considered as a preliminary assessment on the creation of computational libraries that could represent important support tools for regulatory bodies in risk assessment and scheduling procedures.



## Chapter 10 Future work

QSAR studies (Chapters 5,7 and 8) identified a set of possibly very potent NSOs and DBZDs, via the prediction of their biological activity. However due to the fact that *in silico* approaches are only predictive methodologies, experimental studies will be necessary to assess and confirm the possible activity and scale of the latter on the GABA-AR for DBZDs and on the MOR for NSOs (De Luca et al., 2022; Loi et al., 2020). If more funding will become available collaboration with other Universities will be explored to carry out some *in vitro* and preclinical studies.

For the assessment of NSOs, a similar *in vitro* methodology as presented by Vandeputte et al., i.e. MOR- $\beta$ -arrestin2/mini-Gi Recruitment Bioassays, could be adopted to assess not only if these novel molecules are able to activate the MOR transmission, but also to understand their preferential pathway of activation, i.e. including the assessment of  $\beta$ -arrestin2 or mini-Gi (Vandeputte et al., 2021). Using this *in vitro* approach, it will be possible to compare the activity of the index NSO with fentanyl and morphine activity.

*In vitro* testing should be carried out also for the identified DBZDs to assess both their potency and their agonist/antagonist profile. An assay which could be used for this purpose is the one which assesses the agonist activity at recombinant human GABAA receptor  $\alpha 1\beta 1\gamma 2L$  expressed in *Xenopus laevis* oocytes incubated for 30 secs by electrophysiological method (Belelli et al., 1996; Sparling and DiMauro, 2017). Another assay which is reported for the evaluation of the efficacy on the GABA-AR is “Efficacy against human GABA  $\alpha$ -1 receptor expressed in mouse fibroblast L(tk-) cells by whole cell patch clamp method” (Jones et al., 2006). Studies which evaluate the binding of benzodiazepines to their receptor site under *in vivo* conditions have been reported also (Duka et al., 1979), via the injection of highly radiolabelled [ $^3H$ ]-flunitrazepam. This could help in evaluating the CNS barrier permeability of novel DBZDs.

Along these, *in vivo*/ preclinical studies could be performed for estimation of antinociceptive, sedative/anxiolytic and reinforcement properties of NSOs and DBZDs. For the estimation of analgesic and antinociceptive activity of NSOs, the tail flick test in mice could be used (Chen et al., 2007). The latter is indicative of pain sensitivity in an organism and of reduction of pain sensitivity produced by analgesics (Chen et al., 2007). It should be noted that, because many thermal tests are not able to distinguish between opioid agonists and mixed agonist-antagonists, a tail flick test for mice using cold water should be carried out instead (Pizziketti et al., 1985). There is however a great variety of animal models which can be used for the assessment of analgesia, and also measures of non-reflexive behaviours should be considered (Gregory et al., 2013).



To assess the sedative-hypnotic and muscle relaxant activity of the top scoring DBZDs, the following animal (mice) models could be used: thiopental sodium -induced sleeping time and sleep latency; the righting-reflex test and the rotarod test (Golovenko et al., 2020).

Finally self-administration-based animal models could be used to assess abuse potential and dependence connected with these novel NPS (Spanagel, 2017). Drug-induced reinforcement can indeed be evaluated in mice with a plethora of different tests which include non-operant procedures (restricted to oral self-administration procedure) and operant procedure based on the learning contingency defined as “positive reinforcement” (i.e. where a positive reinforcer is provided contingently to the conclusion of the programmed requirements) (Sanchis-Segura and Spanagel, 2006).

Another approach that could be considered is the one presented by Morbiato et al (2020) who used zebrafish larvae and mice models for the forensic toxicology screening of NPS, i.e. to ‘rapidly hypothesize potential aversive or beneficial effects of novel molecules’ via the assessment of spontaneous locomotor activity (Morbiato et al., 2020):

Future work including molecular dynamics studies on the nitazene NSO class should be carried out to confirm the orientation of the latter in the MOR binding pocket and assess the role and importance of the NO<sub>2</sub> group. Molecular dynamics analyse the movements of a ligand-receptor complex, allowing the latter to interact for a predetermined period of time (e.g. 1000 nanoseconds). Analysing these movements is it possible to understand which is the more stable orientation of the ligand and to get a view on the dynamic "evolution" of the system (Piotr F.J. Lipiński et al., 2019). This work has already been started in collaboration with the King’s College.

Future work could be conducted as well on the results of the scaffold hopping exercise if collaboration will be set up with a chemical synthesis lab (Chapter 7) (Wang and Ramírez-Hinestrosa, 2020). This work will assess the new DBZDs scaffold proposed via the scaffold hopping exercise for viable synthetic routes and if possible the compounds will be synthesised and characterised using standard analytical techniques such as nuclear magnetic resonance (NMR) and liquid chromatography mass spectroscopy (LCMS). The characterised molecules will then be examined for biological activity using the same methodology described for the others. Finally the scaffold hopping exercise will be also applied to the NSO class to assess the chemical space of the latter.

## References

- Volkow, N.D., Icaza, M.E.M., Poznyak, Vladimir, Saxena, S., Gerra, G., 2019. Addressing the opioid crisis globally. *World Psychiatry* 18, 231–232. <https://doi.org/10.1002/wps.20633>
- Abdel-Rahman, M.A., Elliott, H.W., Binks, R., Kung, W., Rapoport, H., 1966. Synthesis and Pharmacology of 6-Methylenedihydrodesoxymorphine. *J. Med. Chem.* 9, 1–6. [https://doi.org/10.1021/JM00319A001/ASSET/JM00319A001.FP.PNG\\_V03](https://doi.org/10.1021/JM00319A001/ASSET/JM00319A001.FP.PNG_V03)
- Abdulrahim, D., Bowden-Jones, O., 2018. The misuse of synthetic opioids: harms and clinical management of fentanyl, fentanyl analogues and other novel synthetic opioids Information for clinicians.
- ACMD, 2020a. Novel Benzodiazepines A review of the evidence of use and harms of Novel Benzodiazepines. London.
- ACMD, 2020b. Addendum to ACMD's report on novel benzodiazepines [WWW Document]. URL <https://www.gov.uk/government/publications/novel-benzodiazepines-prevalence-and-harms-in-the-uk/addendum-to-acmds-report-on-novel-benzodiazepines> (accessed 1.31.22).
- ACMD, 2009. Advisory Council on the Misuse of Drugs Annual Report Accounting Year 2009 - 2010.
- Adamowicz, P., Meissner, E., Maślanka, M., 2019. Fatal intoxication with new synthetic cannabinoids AMB-FUBINACA and EMB-FUBINACA. *57*, 1103–1108. <https://doi.org/10.1080/15563650.2019.1580371>
- Adams, A.J., Banister, S.D., Irizarry, L., Trecki, J., Schwartz, M., Gerona, R., 2017. “Zombie” Outbreak Caused by the Synthetic Cannabinoid AMB-FUBINACA in New York. *N. Engl. J. Med.* 376, 235–242. [https://doi.org/10.1056/NEJMOA1610300/SUPPL\\_FILE/NEJMOA1610300\\_DISCLOSURES.PDF](https://doi.org/10.1056/NEJMOA1610300/SUPPL_FILE/NEJMOA1610300_DISCLOSURES.PDF)
- Adrian, C., 2011. The Underground Website Where You Can Buy Any Drug Imaginable [WWW Document]. URL <https://gawker.com/the-underground-website-where-you-can-buy-any-drug-imag-30818160> (accessed 3.31.20).
- Afzal, A., Kiyatkin, E., 2019. Interactions of benzodiazepines with heroin: Respiratory depression, temperature effects, and behavior. *Neuropharmacology* 158. <https://doi.org/10.1016/J.NEUROPHARM.2019.107677>
- Alalwan, A.A., Rana, N.P., Dwivedi, Y.K., Algharabat, R., 2017. Social media in marketing: A review and analysis of the existing literature. *Telemat. Informatics* 34, 1177–1190.

<https://doi.org/10.1016/j.tele.2017.05.008>

- Alam, P., Borkokoty, S., Siddiqi, M.K., Ehtram, A., Majid, N., Uddin, M., Khan, R.H., 2019. DARK Classics in Chemical Neuroscience: Opium, a Friend or Foe. *ACS Chem. Neurosci.* 10, 182–189. <https://doi.org/10.1021/ACSCHEMNEURO.8B00546>
- Alenezi, A., Yahyouche, A., Paudyal, V., 2020. Current status of opioid epidemic in the United Kingdom and strategies for treatment optimisation in chronic pain. *Int. J. Clin. Pharm.* 2020 432 43, 318–322. <https://doi.org/10.1007/S11096-020-01205-Y>
- Alexander, D.L.J., Tropsha, A., Winkler, D.A., 2015. Beware of R2: Simple, Unambiguous Assessment of the Prediction Accuracy of QSAR and QSPR Models. *J. Chem. Inf. Model.* 55, 1316–1322. <https://doi.org/10.1021/acs.jcim.5b00206>
- Ali, S., Ashwell, M., Kelleher, E., Koerner, S., Lapierre, J.-M., Link, J., Liu, Y., Moussa, M., Palma, R., Tandon, M., Vensel, D., Westlund, N., Wu, H., Yang, R.-Y., 2011. WO2011123678 Substituted benzo-pyrido-triazolo-diazepine compounds. PCT/US2011/030774.
- Amundarain, M.J., Caffarena, E.R., Costabel, M.D., 2021. How does  $\alpha$ 1Histidine102 affect the binding of modulators to  $\alpha$ 1 $\beta$ 2 $\gamma$ 2 GABAA receptors? molecular insights from in silico experiments. *undefined* 23, 3993–4006. <https://doi.org/10.1039/D0CP05081D>
- An, X., Bai, Q., Bing, Z., Zhou, S., Shi, D., Liu, H., Yao, X., 2019. How Does Agonist and Antagonist Binding Lead to Different Conformational Ensemble Equilibria of the  $\kappa$ -Opioid Receptor: Insight from Long-Time Gaussian Accelerated Molecular Dynamics Simulation. *ACS Chem. Neurosci.* 10, 1575–1584. [https://doi.org/10.1021/ACSCHEMNEURO.8B00535/SUPPL\\_FILE/CN8B00535\\_SI\\_001.PDF](https://doi.org/10.1021/ACSCHEMNEURO.8B00535/SUPPL_FILE/CN8B00535_SI_001.PDF)
- Anzini, L., Canullo, M., Braile, C., Cappelli, A., Gallelli, A., Vomero, S., Menziani, M., De Benedetti, P., Rizzo, M., Collina, S., Azzolina, O., Sbacchi, M., Ghelardini, C., Galeotti, N., 2003. Synthesis, biological evaluation, and receptor docking simulations of 2-[(acylamino)ethyl]-1,4-benzodiazepines as kappa-opioid receptor agonists endowed with antinociceptive and anti-amnesic activity. *J. Med. Chem.* 46, 3853–3864. <https://doi.org/10.1021/JM0307640>
- Appel, G., Grewal, L., Hadi, R., Stephen, A.T., 2020. The future of social media in marketing. *J. Acad. Mark. Sci.* 48, 79–95. <https://doi.org/10.1007/s11747-019-00695-1>
- Archer, G.A., Sternbach, L.H., 1968. Chemistry of benzodiazepines. *Chem. Rev.* 68, 747–784. [https://doi.org/10.1021/CR60256A004/ASSET/CR60256A004.FP.PNG\\_V03](https://doi.org/10.1021/CR60256A004/ASSET/CR60256A004.FP.PNG_V03)
- Arillotta, D., Schifano, F., Napoletano, F., Zangani, C., Gilgar, L., Guirguis, A., Corkery, J.M., Aguglia, E., Vento, A., 2020. Novel Opioids: Systematic Web Crawling Within the e-

- Psychonauts' Scenario. *Front. Neurosci.* 14, 149. <https://doi.org/10.3389/fnins.2020.00149>
- Armenian, P., Darracq, M., Gevorkyan, J., Clark, S., Kaye, B., Brandehoff, N.P., 2018. Intoxication from the novel synthetic cannabinoids AB-PINACA and ADB-PINACA: A case series and review of the literature. *Neuropharmacology* 134, 82–91. <https://doi.org/10.1016/J.NEUROPHARM.2017.10.017>
- Armenian, P., Vo, K.T., Barr-Walker, J., Lynch, K.L., 2017. Fentanyl, fentanyl analogs and novel synthetic opioids: A comprehensive review. *Neuropharmacology*. <https://doi.org/10.1016/j.neuropharm.2017.10.016>
- Artemenko, A.G., Kuz'Min, V.E., Muratov, E.N., Polishchuk, P.G., Borisyuk, I.Y., Golovenko, N.Y., 2009. Influence of the structure of substituted benzodiazepines on their pharmacokinetic properties. *Pharm. Chem. J.* 43, 454–462. <https://doi.org/10.1007/s11094-009-0332-x>
- Atigari, D.V., Paton, K.F., Uprety, R., Váradi, A., Alder, A.F., Scouller, B., Miller, J.H., Majumdar, S., Kivell, B.M., 2021. The mixed kappa and delta opioid receptor agonist, MP1104, attenuates chemotherapy-induced neuropathic pain. *Neuropharmacology* 185. <https://doi.org/10.1016/J.NEUROPHARM.2020.108445>
- Atigari, D. V., Uprety, R., Pasternak, G.W., Majumdar, S., Kivell, B.M., 2019. MP1104, a mixed kappa-delta opioid receptor agonist has anti-cocaine properties with reduced side-effects in rats. *Neuropharmacology* 150, 217–228. <https://doi.org/10.1016/J.NEUROPHARM.2019.02.010>
- Ba, G.R.H., Baskett, T.F., Frcsc, M.B., 2000. History of Anesthesia In the arms of Morpheus: the development of mor-phine for postoperative pain relief. *CAN J ANESTH* 47, 4–367.
- Bajorath, J., 2015. Computer-aided drug discovery. *F1000Research* 4. <https://doi.org/10.12688/f1000research.6653.1>
- Bajusz, D., Rácz, A., Héberger, K., 2015a. Why is Tanimoto index an appropriate choice for fingerprint-based similarity calculations? *J. Cheminform.* 7, 1–13. <https://doi.org/10.1186/S13321-015-0069-3/FIGURES/7>
- Bajusz, D., Rácz, A., Héberger, K., 2015b. Why is Tanimoto index an appropriate choice for fingerprint-based similarity calculations? 7, 20. <https://doi.org/10.1186/s13321-015-0069-3>
- Balaban, A.T., 2012. Review of “Statistical Modelling of Molecular Descriptors in QSAR/QSPR” by Matthias Dehmer, Kurt Varmuza, and Danail Bonchev. *J. Cheminform.* 4, 36. <https://doi.org/10.1186/1758-2946-4-36>
- Barratt, M.J., Ferris, J.A., Winstock, A.R., 2014. Use of Silk Road, the online drug marketplace, in the United Kingdom, Australia and the United States. *Addiction* 109, 774–783. <https://doi.org/10.1111/add.12470>

- Barratt, M.J., Lenton, S., Allen, M., 2013. Internet content regulation, public drug websites and the growth in hidden Internet services 20, 195–202. <https://doi.org/10.3109/09687637.2012.745828>
- Bateman, J.T., Levitt, E.S., 2021. Evaluation of G protein bias and  $\beta$ -arrestin 2 signaling in opioid-induced respiratory depression. *Am. J. Physiol. - Cell Physiol.* 321, C681–C683. [https://doi.org/10.1152/AJPCELL.00259.2021/ASSET/IMAGES/LARGE/AJPCELL.00259.2021\\_F001.JPEG](https://doi.org/10.1152/AJPCELL.00259.2021/ASSET/IMAGES/LARGE/AJPCELL.00259.2021_F001.JPEG)
- Baumann, M.H., Majumdar, S., Le Rouzic, V., Hunkele, A., Uprety, R., Huang, X.P., Xu, J., Roth, B.L., Pan, Y.-X.X., Pasternak, G.W., 2018. Pharmacological characterization of novel synthetic opioids (NSO) found in the recreational drug marketplace. *Neuropharmacology* 134, 101–107. <https://doi.org/10.1016/j.neuropharm.2017.08.016>
- Beardsley, P.M., Zhang, Y., 2018. Synthetic opioids. *Handb. Exp. Pharmacol.* 252, 353–381. [https://doi.org/10.1007/164\\_2018\\_149](https://doi.org/10.1007/164_2018_149)
- Becker, O.M., Dhanoa, D.S., Marantz, Y., Chen, D., Shacham, S., Cheruku, S., Heifetz, A., Mohanty, P., Fichman, M., Sharadendu, A., Nudelman, R., Kauffman, M., Noiman, S., 2006. An integrated in silico 3D model-driven discovery of a novel, potent, and selective amidosulfonamide 5-HT<sub>1A</sub> agonist (PRX-00023) for the treatment of anxiety and depression. *J. Med. Chem.* 49, 3116–3135. <https://doi.org/10.1021/jm0508641>
- Beebe, R.K., Pell, J.R., Seasholts, M.B., 1998. *Chemometrics: A Practical Guide*. Wiley.
- Belelli, D., Callachan, H., Hill-Venning, C., Peters, J.A., Lambert, J.J., 1996. Interaction of positive allosteric modulators with human and *Drosophila* recombinant GABA receptors expressed in *Xenopus laevis* oocytes. *Br. J. Pharmacol.* 118, 563. <https://doi.org/10.1111/J.1476-5381.1996.TB15439.X>
- Belvisi, M.G., Geppetti, P., 2004. Cough • 7: Current and future drugs for the treatment of chronic cough. *Thorax* 59, 438–440. <https://doi.org/10.1136/THX.2003.013490>
- Bender, A., Glen, R.C., 2004. Molecular similarity: a key technique in molecular informatics. *Org. Biomol. Chem.* 2, 3204–3218. <https://doi.org/10.1039/B409813G>
- Berg, J.M., Tymoczko, J.L., Stryer, L., 2002. Three-Dimensional Protein Structure Can Be Determined by NMR Spectroscopy and X-Ray Crystallography, in: *Biochemistry*. W H Freeman, New York.
- Berman, H.M., Bhat, T.N., Bourne, P.E., Feng, Z., Gilliland, G., Weissig, H., Westbrook, J., 2000. The Protein Data Bank and the challenge of structural genomics. *Nat. Struct. Biol.* <https://doi.org/10.1038/80734>
- Bernstein, F.C., Koetzle, T.F., Williams, G.J., Meyer, E.F., Brice, M.D., Rodgers, J.R., Kennard,

- O., Shimanouchi, T., Tasumi, M., 1977. The Protein Data Bank. A computer-based archival file for macromolecular structures. *Eur. J. Biochem.* 80, 319–24. <https://doi.org/10.1111/j.1432-1033.1977.tb11885.x>
- Billingsley, M., Kubena, R., 1978. The effects of naloxone and picrotoxin on the sedative and anticonflict effects of benzodiazepines. *Life Sci.* 22, 897–906. [https://doi.org/10.1016/0024-3205\(78\)90614-8](https://doi.org/10.1016/0024-3205(78)90614-8)
- Binder, D., Hellerbach, J., Hromatka, O., Zeller, P., 1973. DE2405682A1 - Diazepin-derivate .
- Binder, D., Hellerbach, J., Hromatka, O., Zeller, P., Binder, D., 1974. US4155913A Thienotriazolodiazepine derivatives. US4155913A.
- Böhm, H.J., Flohr, A., Stahl, M., 2004. Scaffold hopping. *Drug Discov. Today Technol.* 1, 217–224. <https://doi.org/10.1016/J.DDTEC.2004.10.009>
- Bohnenberger, K., Liu, M.T., 2019. Flubromazolam overdose: A review of a new designer benzodiazepine and the role of flumazenil. *Ment. Heal. Clin.* 9, 133. <https://doi.org/10.9740/MHC.2019.05.133>
- Boon, M., van Dorp, E., Broens, S., Overdyk, F., 2020. Combining opioids and benzodiazepines: effects on mortality and severe adverse respiratory events. *Ann. Palliat. Med.* 9, 54257–54557. <https://doi.org/10.21037/APM.2019.12.09>
- Booth, M., 2000. *A magick life : a biography of Aleister Crowley*. Coronet Books.
- Bowen, D.A., O'Donnell, J., Sumner, S.A., 2019. Increases in Online Posts About Synthetic Opioids Preceding Increases in Synthetic Opioid Death Rates: a Retrospective Observational Study. *J. Gen. Intern. Med.* 34, 2702. <https://doi.org/10.1007/S11606-019-05255-5>
- Braun, v. J., 1914. Untersuchungen über Morphium-Alkaloide. *Berichte der Dtsch. Chem. Gesellschaft* 47, 2312–2330. <https://doi.org/10.1002/CBER.191404702149>
- Brittain, R.T., Kellett, D.N., Neat, M.L., Stables, R., 1973. Proceedings: Anti-nociceptive effects in N-substituted cyclohexylmethylbenzamides. *Br. J. Pharmacol.* 49, 158P.
- Brownlee, J., 2018. The Model Performance Mismatch Problem (and what to do about it) [WWW Document]. URL <https://machinelearningmastery.com/the-model-performance-mismatch-problem/> (accessed 2.24.22).
- Bruchas, M.R., Roth, B.L., 2016. New Technologies for Elucidating Opioid Receptor Function. *Trends Pharmacol. Sci.* 37, 279–289. <https://doi.org/10.1016/J.TIPS.2016.01.001>
- Brunetti, P., Giorgetti, R., Tagliabracchi, A., Huestis, M.A., Busardò, F.P., 2021. Designer Benzodiazepines: A Review of Toxicology and Public Health Risks. *Pharm.* 2021, Vol. 14, Page 560 14, 560. <https://doi.org/10.3390/PH14060560>
- Buntain, C., Golbeck, J., 2015. This is your twitter on drugs. any questions?, in: *WWW 2015*

- Companion - Proceedings of the 24th International Conference on World Wide Web. Association for Computing Machinery, Inc, New York, New York, USA, pp. 777–782. <https://doi.org/10.1145/2740908.2742469>
- Burns, L., Roxburgh, A., Bruno, R., Van Buskirk, J., 2014. Monitoring drug markets in the Internet age and the evolution of drug monitoring systems in Australia. *Drug Test. Anal.* 6, 840–845. <https://doi.org/10.1002/dta.1613>
- Burrell, J., 2016. How the machine ‘thinks’: Understanding opacity in machine learning algorithms. *Big Data Soc.* 3, 205395171562251. <https://doi.org/10.1177/2053951715622512>
- Butelman, E.R., Picetti, R., Reed, B., Yuferov, V., Kreek, M.J., 2015. Addictions, in: *Neurobiology of Brain Disorders: Biological Basis of Neurological and Psychiatric Disorders*. Academic Press, pp. 570–584. <https://doi.org/10.1016/B978-0-12-398270-4.00035-5>
- Butour, J.L., Moisand, C., Mazarguil, H., Mollereau, C., Meunier, J.C., 1997. Recognition and activation of the opioid receptor-like ORL1 receptor by nociceptin, nociceptin analogs and opioids. *Eur. J. Pharmacol.* 321, 97–103. [https://doi.org/10.1016/S0014-2999\(96\)00919-3](https://doi.org/10.1016/S0014-2999(96)00919-3)
- Buy FANAX - Flubrotizolam | Chemical Planet [WWW Document], n.d. URL <https://chemicalplanet.net/fanax-flubrotizolam-0-5mg-pellets> (accessed 10.2.22).
- Buy Flubrotizolam (Fanax) 2mg Pellets [WWW Document], n.d. URL <https://www.gr8researchchemicals-eu.com/flubrotizolam-2mg-pellets> (accessed 10.2.22).
- Cappelli, A., Anzini, M., Vomero, S., Menziani, M., De Benedetti, M., Sbacchi, P., Clarke, G., Mennuni, L., 1996. Synthesis, biological evaluation, and quantitative receptor docking simulations of 2-[(acylamino)ethyl]-1,4-benzodiazepines as novel tipluadom-like ligands with high affinity and selectivity for kappa-opioid receptors. *J. Med. Chem.* 39, 860–872. <https://doi.org/10.1021/JM950423P>
- Carpenter, J.E., Murray, B.P., Dunkley, C., Kazzi, Z.N., Gittinger, M.H., 2019. Designer benzodiazepines: a report of exposures recorded in the National Poison Data System, 2014–2017. *Clin. Toxicol.* 57, 282–286. <https://doi.org/10.1080/15563650.2018.1510502>
- Casale, J.F., Mallette, J.R., Guest, E.M., 2017. Analysis of illicit carfentanil: Emergence of the death dragon. *Forensic Chem.* 3, 74–80. <https://doi.org/10.1016/J.FORC.2017.02.003>
- Casy, A.F., Parfitt, R.T., 1986. *Opioid analgesics: chemistry and receptors*, 1st ed. Springer US, New York.
- Catalani, V., Arillotta, D., Corkery, J.M., Guirguis, A., Vento, A., Schifano, F., 2021a. Identifying new/emerging psychoactive substances at the time of COVID-19; a web-based approach. *Front. Psychiatry* 11, 1638. <https://doi.org/10.3389/FPSYT.2020.632405>
- Catalani, V., Botha, M., Corkery, J.M., Guirguis, A., Vento, A., Scherbaum, N., Schifano, F.,

- 2021b. The psychonauts' benzodiazepines; quantitative structure-activity relationship (QSAR) analysis and docking prediction of their biological activity. *Pharm.* 2021, Vol. 14, Page 720 14, 720. <https://doi.org/10.3390/PH14080720>
- Catalani, V., Corkery, J.M., Guirguis, A., Napoletano, F., Arillotta, D., Zangani, C., Vento, A., Schifano, F., 2021c. Psychonauts' psychedelics: A systematic, multilingual, web-crawling exercise. *Eur. Neuropsychopharmacol.* 49, 69–92. <https://doi.org/10.1016/J.EURONEURO.2021.03.006>
- Catalani, V., Floresta, G., Botha, M., Corkery, J.M., Guirguis, A., Vento, A., Abbate, V., Schifano, F., 2022. In silico studies on recreational drugs: 3D-QSAR prediction of classified and de novo designer benzodiazepines. *Chem. Biol. Drug Des.*
- CBN, 2022. Opium throughtout History [WWW Document]. URL <http://cbn.nic.in/html/opiumhistory1.htm> (accessed 8.17.22).
- CDC, 2021. Synthetic Opioid Overdose Data | Drug Overdose | CDC Injury Center [WWW Document]. URL <https://www.cdc.gov/drugoverdose/deaths/synthetic/index.html> (accessed 8.18.22).
- CDC, n.d. Understanding the Epidemic | Drug Overdose | CDC Injury Center [WWW Document]. 2022. URL <https://www.cdc.gov/drugoverdose/epidemic/index.html> (accessed 8.17.22).
- CFSRE, 2022. Bromazolam Prevalence Surging Across the United States Driven In Part by Increasing Detections Alongside Fentanyl [WWW Document]. URL <https://www.cfsre.org/nps-discovery/public-alerts/bromazolam-prevalence-surging-across-the-united-states-driven-in-part-by-increasing-detections-alongside-fentanyl> (accessed 11.27.22).
- Chan, S.L., Labute, P., 2010. Training a scoring function for the alignment of small molecules. *J. Chem. Inf. Model.* 50, 1724–1735. <https://doi.org/10.1021/ci100227h>
- Che, T., Majumdar, S., Zaidi, S.A., Ondachi, P., McCorvy, J.D., Wang, S., Mosier, P.D., Uprety, R., Vardy, E., Krumm, B.E., Han, G.W., Lee, M.Y., Pardon, E., Steyaert, J., Huang, X.P., Strachan, R.T., Tribo, A.R., Pasternak, G.W., Carroll, F.I., Stevens, R.C., Cherezov, V., Katritch, V., Wacker, D., Roth, B.L., 2018. Structure of the Nanobody-Stabilized Active State of the Kappa Opioid Receptor. *Cell* 172, 55-67.e15. <https://doi.org/10.1016/J.CELL.2017.12.011>
- ChEMBL, 2021a. Mu opioid receptor Target Report Card [WWW Document]. URL [https://www.ebi.ac.uk/chembl/target\\_report\\_card/CHEMBL233/](https://www.ebi.ac.uk/chembl/target_report_card/CHEMBL233/) (accessed 10.13.21).
- ChEMBL, 2021b. Delta opioid receptor Target Report Card [WWW Document]. URL [https://www.ebi.ac.uk/chembl/target\\_report\\_card/CHEMBL236/](https://www.ebi.ac.uk/chembl/target_report_card/CHEMBL236/) (accessed 10.18.21).
- ChEMBL, 2021c. Kappa opioid receptor Target Report Card [WWW Document]. URL



- [https://www.ebi.ac.uk/chembl/target\\_report\\_card/CHEMBL237/](https://www.ebi.ac.uk/chembl/target_report_card/CHEMBL237/) (accessed 10.13.21).
- Chemical Computing Group, 2022. Chemical Computing Group (CCG) | MOE citation [WWW Document]. URL <https://www.chemcomp.com/Research.htm> (accessed 10.5.22).
- Chemical Computing Group ULC, 2022. Molecular Operating Environment (MOE), 2022.02.
- Chen, B., Sheridan, R.P., Hornak, V., Voigt, J.H., 2012. Comparison of random forest and Pipeline Pilot Naïve Bayes in prospective QSAR predictions. *J. Chem. Inf. Model.* 52, 792–803. <https://doi.org/10.1021/ci200615h>
- Chen, X.J., Levedakou, E.N., Millen, K.J., Wollmann, R.L., Soliven, B., Popko, B., 2007. Proprioceptive Sensory Neuropathy in Mice with a Mutation in the Cytoplasmic Dynein Heavy Chain 1 Gene. *J. Neurosci.* 27, 14515–14524. <https://doi.org/10.1523/JNEUROSCI.4338-07.2007>
- Chen, Y.C., 2015. Beware of docking! *Trends Pharmacol. Sci.* 36, 78–95. <https://doi.org/10.1016/j.tips.2014.12.001>
- Cherkasov, A., Muratov, E.N., Fourches, D., Varnek, A., Baskin, I.I., Cronin, M., Dearden, J., Gramatica, P., Martin, Y.C., Todeschini, R., Consonni, V., Kuz'Min, V.E., Cramer, R., Benigni, R., Yang, C., Rathman, J., Terfloth, L., Gasteiger, J., Richard, A., Tropsha, A., 2014. QSAR modeling: Where have you been? Where are you going to? *J. Med. Chem.* 57, 4977–5010. <https://doi.org/10.1021/jm4004285>
- Chouinard, G., 2004. Issues in the clinical use of benzodiazepines: Potency, withdrawal, and rebound. *J. Clin. Psychiatry* 65, 7–12.
- Claff, T., Yu, J., Blais, V., Patel, N., Martin, C., Wu, L., Han, G.W., Holleran, B.J., Van der Poorten, O., White, K.L., Hanson, M.A., Sarret, P., Gendron, L., Cherezov, V., Katritch, V., Ballet, S., Liu, Z.J., Müller, C.E., Stevens, R.C., 2019. Elucidating the active  $\delta$ -opioid receptor crystal structure with peptide and small-molecule agonists. *Sci. Adv.* 5, eaax9115. <https://doi.org/10.1126/SCIADV.AAX9115>
- Clark, A.M., Labute, P., 2007. 2D depiction of protein-ligand complexes. *J. Chem. Inf. Model.* 47, 1933–1944. <https://doi.org/10.1021/CI7001473>
- Clarke, D.L., Drobotz, K.J., Korzekwa, C., Nelson, L.S., Perrone, J., 2019. Trends in Opioid Prescribing and Dispensing by Veterinarians in Pennsylvania. *JAMA Netw. Open* 2, e186950–e186950. <https://doi.org/10.1001/JAMANETWORKOPEN.2018.6950>
- Colovos, C., Yeates, T.O., 1993. Verification of protein structures: patterns of nonbonded atomic interactions. *Protein Sci.* 2, 1511–1519. <https://doi.org/10.1002/pro.5560020916>
- Cometta-Morini, C., Maguire, P.A., Loew, G.H., 1992. Molecular determinants of mu receptor recognition for the fentanyl class of compounds. | *Molecular Pharmacology. Mol. Pharmacol.*

January 41, 185–196.

- Commission on Narcotic Drugs, 2021. Implementation of the international drug control treaties: changes in the scope of control of substances. Vienna.
- Commission on Narcotic Drugs, 2014. ackground paper prepared by the United Kingdom of Great Britain and Northern Ireland related to its notification submitted on 23 January to the Secretary-General on the review of the scope of control of mephedrone.
- Consonni, V., Ballabio, D., Todeschini, R., 2010. Evaluation of model predictive ability by external validation techniques. *J. Chemom.* 24, 194–201. <https://doi.org/10.1002/cem.1290>
- Contet, C., Kieffer, B., Befort, K., 2004. Mu opioid receptor: a gateway to drug addiction. *Curr. Opin. Neurobiol.* 14, 370–378. <https://doi.org/10.1016/J.CONB.2004.05.005>
- Corazza, O., Assi, S., Simonato, P., Corkery, J., Bersani, F.S., Demetrovics, Z., Stair, J., Fergus, S., Pezzolesi, C., Pasinetti, M., Deluca, P., Drummond, C., Davey, Z., Blaszkowski, U., Moskalewicz, J., Mervo, B., Furia, L. Di, Farre, M., Flesland, L., Pisarska, A., Shapiro, H., Siemann, H., Skutle, A., Sferrazza, E., Torrens, M., Sambola, F., van der Kreeft, P., Scherbaum, N., Schifano, F., 2013a. Promoting innovation and excellence to face the rapid diffusion of novel psychoactive substances in the EU: the outcomes of the ReDNet project. *Hum. Psychopharmacol.* 28, 317–23. <https://doi.org/10.1002/hup.2299>
- Corazza, O., Demetrovics, Z., van den Brink, W., Schifano, F., 2013b. “Legal highs” an inappropriate term for “Novel Psychoactive Drugs” in drug prevention and scientific debate. *Int. J. Drug Policy* 24, 82–83. <https://doi.org/10.1016/J.DRUGPO.2012.06.005>
- Corazza, O., Martinotti, G., Bersani, F., Schifano, F., Bersani, G., 2014a. “Spice,” “Kryptonite,” “Black Mamba”: An Overview of Brand Names and Marketing Strategies of Novel Psychoactive Substances on the Web. *J. Psychoactive Drugs*.
- Corazza, O., Roman-Urrestarazu, A., 2018. Handbook of Novel Psychoactive Substances, Handbook of Novel Psychoactive Substances. Routledge. <https://doi.org/10.4324/9781315158082/HANDBOOK-NOVEL-PSYCHOACTIVE-SUBSTANCES-ORNELLA-CORAZZA-ANDRES-ROMAN-URRESTARAZU>
- Corazza, O., Roman-Urrestarazu, A., 2017. Novel psychoactive substances: Policy, economics and drug regulation, Novel Psychoactive Substances: Policy, Economics and Drug Regulation. Springer International Publishing. <https://doi.org/10.1007/978-3-319-60600-2>
- Corazza, O., Schifano, F., Farre, M., Deluca, P., Davey, Z., Drummond, C., Torrens, M., Demetrovics, Z., Di Furia, L., Flesland, L., Mervo, B., Moskalewicz, J., Pisarska, A., Shapiro, H., Siemann, H., Skutle, A., Pezzolesi, C., Van Der Kreeft, P., Scherbaum, N., 2011. Designer Drugs on the Internet: A Phenomenon Out-of-Control? The Emergence of Hallucinogenic

- Drug Bromo-Dragonfly. *Curr. Clin. Pharmacol.* 6, 125–129.  
<https://doi.org/10.2174/157488411796151129>
- Corazza, O., Simonato, P., Corkery, J., Trincas, G., Schifano, F., 2014b. “Legal highs”: Safe and legal “heavens”? A study on the diffusion, knowledge and risk awareness of novel psychoactive drugs among students in the UK. *Riv. Psichiatr.* 49, 89–94.  
<https://doi.org/10.1708/1461.16147>
- Corkery, J.M., Guirguis, A., Chiappini, S., Martinotti, G., Schifano, F., 2022. Alprazolam-related deaths in Scotland, 2004-2020. *J. Psychopharmacol.* 026988112211040.  
<https://doi.org/10.1177/02698811221104065>
- Corkery, J.M., Orsolini, L., Papanti, D., Schifano, F., 2018. Novel Psychoactive Substances (NPS) and Recent Scenarios: Epidemiological, Anthropological and Clinical Pharmacological Issues. *Compr. Ser. Photochem. Photobiol. Sci.* 17, 207–255. <https://doi.org/10.1039/9781788010344-00207>
- Corkery, J.M., Orsolini, L., Papanti, D., Schifano, F., 2017. From concept(ion) to life after death/the grave: The ‘natural’ history and life cycle(s) of novel psychoactive substances (NPS). *Hum. Psychopharmacol.* 32. <https://doi.org/10.1002/hup.2566>
- Council of the European Union, 2005. Council Decision 2005/387/JHA of 10 May 2005 on the information exchange, risk-assessment and control of new psychoactive substances . *Off. J. Eur. Union* 127, 32–37.
- Cox, R.F., Collins, M.A., 2001. The effects of benzodiazepines on human opioid receptor binding and function. *Anesth. Analg.* 93, 354–358. <https://doi.org/10.1213/00000539-200108000-00024>
- Cresset, 2021. Forge 10.6.
- Damale, M., Harke, S., Kalam Khan, F., Shinde, D., Sangshetti, J., 2014. Recent Advances in Multidimensional QSAR (4D-6D): A Critical Review. *Mini-Reviews Med. Chem.* 14, 35–55.  
<https://doi.org/10.2174/13895575113136660104>
- Danchin, A., Médigue, C., Gascuel, O., Soldano, H., Hénaut, A., 1991. From data banks to data bases. *Res. Microbiol.* 142, 913–916. [https://doi.org/10.1016/0923-2508\(91\)90073-J](https://doi.org/10.1016/0923-2508(91)90073-J)
- Danishuddin, Khan, A.U., 2016. Descriptors and their selection methods in QSAR analysis: paradigm for drug design. *Drug Discov. Today* 21, 1291–1302.  
<https://doi.org/10.1016/J.DRUDIS.2016.06.013>
- Dargan, P., Wood, D., 2013. *Novel Psychoactive Substances Classification, Pharmacology and Toxicology*, 1st ed. Elsevier.
- Darke, S., Peacock, A., Dufrou, J., Farrell, M., Lappin, J., 2022. Characteristics of fatal ‘novel’

- benzodiazepine toxicity in Australia. *Forensic Sci. Int.* 331, 111140. <https://doi.org/10.1016/J.FORSCIINT.2021.111140>
- Davey, Z., Schifano, F., Corazza, O., Deluca, P., 2012. E-Psychonauts: Conducting research in online drug forum communities. *J. Ment. Heal.* 21, 386–394. <https://doi.org/10.3109/09638237.2012.682265>
- Davies, M., Bateson, A.N., Dunn, S.M.J., 2002. Structural Requirements for Ligand Interactions at the Benzodiazepine Recognition Site of the GABAA Receptor. *J. Neurochem.* 70, 2188–2194. <https://doi.org/10.1046/j.1471-4159.1998.70052188.x>
- De Baerdemaeker, K.S.C., Dines, A.M., Hudson, S., Sund, L.J., Waters, M.L., Hunter, L.J., Blundell, M.S., Archer, J.R.H., Wood, D.M., Dargan, P.I., 2022. Isotonitazene, a novel psychoactive substance opioid, detected in two cases following a local surge in opioid overdoses. *QJM An Int. J. Med.* <https://doi.org/10.1093/QJMED/HCAC039>
- de Jong, S., 1993. SIMPLS: An alternative approach to partial least squares regression. *Chemom. Intell. Lab. Syst.* 18, 251–263. [https://doi.org/10.1016/0169-7439\(93\)85002-X](https://doi.org/10.1016/0169-7439(93)85002-X)
- De Luca, M.A., Tocco, G., Mostallino, R., Laus, A., Caria, F., Musa, A., Pintori, N., Ucha, M., Poza, C., Ambrosio, E., Di Chiara, G., Castelli, M.P., 2022. Pharmacological characterization of novel synthetic opioids: Isotonitazene, metonitazene, and piperidylthiambutene as potent MU opioid receptor agonists. *Neuropharmacology* 221, 109263. <https://doi.org/10.1016/J.NEUROPHARM.2022.109263>
- de Ruyck, J., Brysbaert, G., Blossey, R., Lensink, M.F., 2016. Molecular docking as a popular tool in drug design, an in silico travel. *Adv. Appl. Bioinforma. Chem.* <https://doi.org/10.2147/AABC.S105289>
- De Wet, C., Reed, L., Glasper, A., Moran, P., Bearn, J., Gossop, M., 2004. Benzodiazepine co-dependence exacerbates the opiate withdrawal syndrome. *Drug Alcohol Depend.* 76, 31–35. <https://doi.org/10.1016/J.DRUGALCDEP.2004.04.002>
- DEA, 2022a. Fentanyl [WWW Document]. URL <https://www.dea.gov/factsheets/fentanyl> (accessed 8.17.22).
- DEA, 2022b. U-47700 [WWW Document]. URL <https://www.dea.gov/factsheets/u-47700> (accessed 8.17.22).
- DEA, 2022c. DEA Warns of Brightly-Colored Fentanyl Used to Target Young Americans [WWW Document]. URL <https://www.dea.gov/press-releases/2022/08/30/dea-warns-brightly-colored-fentanyl-used-target-young-americans> (accessed 9.19.22).
- DEA, 2022d. Carfentanil: A Dangerous New Factor in the U.S. Opioid Crisis [WWW Document].
- DEA, 2021. 2021 - Placement of Four Specific Fentanyl-Related Substances in Schedule I [WWW

- Document]. URL [https://www.deadiversion.usdoj.gov/fed\\_regs/rules/2021/fr0504\\_4.htm](https://www.deadiversion.usdoj.gov/fed_regs/rules/2021/fr0504_4.htm) (accessed 10.10.22).
- DEA, 2018. 2018 - Final Order: Placement of Butyryl Fentanyl and U-47700 Into Schedule I [WWW Document]. URL [https://www.deadiversion.usdoj.gov/fed\\_regs/rules/2018/fr0420.htm](https://www.deadiversion.usdoj.gov/fed_regs/rules/2018/fr0420.htm) (accessed 8.10.22).
- Dean. M. P., 1995. *Molecular Similarity in Drug Design*, Molecular Similarity in Drug Design. Springer Netherlands. <https://doi.org/10.1007/978-94-011-1350-2>
- Del Vigna, F., Avvenuti, M., Bacciu, C., Deluca, P., Petrocchi, M., Marchetti, A., Tesconi, M., 2016. Spotting the diffusion of new psychoactive substances over the internet, in: *Lecture Notes in Computer Science (Including Subseries Lecture Notes in Artificial Intelligence and Lecture Notes in Bioinformatics)*. Springer Verlag, pp. 86–97. [https://doi.org/10.1007/978-3-319-46349-0\\_8](https://doi.org/10.1007/978-3-319-46349-0_8)
- Department of Health, U., Services, H., n.d. Opioids for Acute Pain What You Need to Know Types of Pain [WWW Document]. URL [www.cdc.gov/drugoverdose](http://www.cdc.gov/drugoverdose) (accessed 10.2.22).
- Dhaliwal, A., Gupta, M., 2021. Physiology, Opioid Receptor. StatPearls.
- Dhawan, B., Cesselin, F., Raghbir, R., Reisine, T., Bradley, P., Portoghesi, P., Hamon, M., 1996. International Union of Pharmacology. XII. Classification of opioid receptors. *Pharmacol. Rev.* 48.
- Dias, R., de Azevedo Jr., W., 2008. Molecular docking algorithms. *Curr. Drug Targets* 9, 1040–1047. <https://doi.org/10.2174/138945008786949432>
- DOJ, DEA, 2020. Opium Drug Fact Sheet.
- Dosen-Micovic, L., Ivanovic, M., Micovic, V., 2006. Steric interactions and the activity of fentanyl analogs at the  $\mu$ -opioid receptor. *Bioorg. Med. Chem.* 14, 2887–2895. <https://doi.org/10.1016/J.BMC.2005.12.010>
- Dowell, D., Haegerich, T.M., Chou, R., 2016. CDC Guideline for Prescribing Opioids for Chronic Pain—United States, 2016. *JAMA* 315, 1624–1645. <https://doi.org/10.1001/JAMA.2016.1464>
- Doweyko, A.M., 2007. Three-Dimensional Quantitative Structure–Activity Relationship: The State of the Art. *Compr. Med. Chem. II* 4, 575–595. <https://doi.org/10.1016/B0-08-045044-X/00266-2>
- Dripps, I.J., Jutkiewicz, E.M., 2017. Delta Opioid Receptors and Modulation of Mood and Emotion, in: *Handbook of Experimental Pharmacology*. Springer, Cham, pp. 179–197. [https://doi.org/10.1007/164\\_2017\\_42](https://doi.org/10.1007/164_2017_42)
- Drug Enforcement Administration, 2019. *Benzodiazepines*. Springfield.
- Drummer, O.H., Odell, M., 2001. *The forensic pharmacology of drugs of abuse*. Arnold.

- Duka, T., Höllt, V., Herz, A., 1979. In vivo receptor occupation by benzodiazepines and correlation with the pharmacological effect. *Brain Res.* 179, 147–156. [https://doi.org/10.1016/0006-8993\(79\)90498-0](https://doi.org/10.1016/0006-8993(79)90498-0)
- DuPont, R.L., 2018. The opioid epidemic is an historic opportunity to improve both prevention and treatment. *Brain Res. Bull.* 138, 112–114. <https://doi.org/10.1016/J.BRAINRESBULL.2017.06.008>
- Durdagi, S., Kapou, A., Kourouli, T., Andreou, T., Nikas, S.P., Nahmias, V.R., Papahatjis, D.P., Papadopoulou, M.G., Mavromoustakos, T., 2007a. The application of 3D-QSAR studies for novel cannabinoid ligands substituted at the C1' position of the alkyl side chain on the structural requirements for binding to cannabinoid receptors CB1 and CB2. *J. Med. Chem.* 50, 2875–2885. <https://doi.org/10.1021/jm0610705>
- Durdagi, S., Papadopoulou, M.G., Papahatjis, D.P., Mavromoustakos, T., 2007b. Combined 3D QSAR and molecular docking studies to reveal novel cannabinoid ligands with optimum binding activity. *Bioorganic Med. Chem. Lett.* 17, 6754–6763. <https://doi.org/10.1016/j.bmcl.2007.10.044>
- Dydyk, A.M., Jain, N.K., Gupta, M., 2022. Opioid Use Disorder. *StatPearls*.
- Dyer, O., 2021. A record 100 000 people in the US died from overdoses in 12 months of the pandemic, says CDC. *BMJ* 375, n2865. <https://doi.org/10.1136/bmj.n2865>
- EDND, 2021. EDND - Login page [WWW Document]. URL <https://ednd2.emcdda.europa.eu/ednd/login> (accessed 11.18.19).
- Eisenberg, D., Luthy, R., Bowie, J.U., 1997. Verify3D: Assessment of protein models with three-dimensional profiles. *Methods Enzymol.* 277, 396–404.
- Ekins, S., 2014. Progress in computational toxicology. *J. Pharmacol. Toxicol. Methods* 69, 115–140. <https://doi.org/10.1016/J.VASCN.2013.12.003>
- Ekins, S., Mestres, J., Testa, B., 2007. In silico pharmacology for drug discovery: methods for virtual ligand screening and profiling. *Br. J. Pharmacol.* 152, 9. <https://doi.org/10.1038/SJ.BJP.0707305>
- EL-Gindy, A., Hadad, G.M., 2012. Chemometrics in Pharmaceutical Analysis: An Introduction, Review, and Future Perspectives. *J. AOAC Int.* 95, 609–623. [https://doi.org/10.5740/jaoacint.sge\\_el-gindy](https://doi.org/10.5740/jaoacint.sge_el-gindy)
- El Balkhi, S., Monchaud, C., Herault, F., Géniaux, H., Saint-Marcoux, F., 2020. Designer benzodiazepines' pharmacological effects and potencies: How to find the information. *J. Psychopharmacol.* 34, 269881119901096. <https://doi.org/10.1177/0269881119901096>
- Elison, C., Elliott, H.W., Look, M., Rapoport, H., 1963. Some Aspects of the Fate and Relationship

- of the N-Methyl Group of Morphine to its Pharmacological Activity. *J. Med. Chem.* 6, 237–246. [https://doi.org/10.1021/JM00339A005/ASSET/JM00339A005.FP.PNG\\_V03](https://doi.org/10.1021/JM00339A005/ASSET/JM00339A005.FP.PNG_V03)
- Elliott, L., Haddock, C.K., Campos, S., Benoit, E., 2019. Polysubstance use patterns and novel synthetics: A cluster analysis from three U.S. cities. *PLoS One* 14, e0225273. <https://doi.org/10.1371/JOURNAL.PONE.0225273>
- Elliott, S.P., Hernandez Lopez, E., 2018. A Series of Deaths Involving Carfentanil in the UK and Associated Post-mortem Blood Concentrations. *J. Anal. Toxicol.* 42, e41–e45. <https://doi.org/10.1093/JAT/BKX109>
- Ellis, C.R., Kruhlak, N.L., Kim, M.T., Hawkins, E.G., Stavitskaya, L., 2018. Predicting opioid receptor binding affinity of pharmacologically unclassified designer substances using molecular docking. *PLoS One* 13. <https://doi.org/10.1371/journal.pone.0197734>
- EMBL-EBI, 2021. ChEMBL Database [WWW Document]. URL <https://www.ebi.ac.uk/chembl/> (accessed 10.1.21).
- EMCDDA-Europol, 2019. EU Drug Markets Report 2019.
- EMCDDA-Europol, 2016. EU Drug Markets Report 2016.
- EMCDDA-Europol, 2012. Annual Report on the implementation of Council Decision 2005/387/JHA.
- EMCDDA-Europol, 2005. EMCDDA-Europol Joint Report on a new psychoactive substance: N-phenyl-N-[1-(2-phenylethyl)piperidin-4-yl] acetamide (acetylfentanyl). Lisbon.
- EMCDDA, 2022a. New psychoactive substances: 25 years of early warning and response in Europe. <https://doi.org/10.2810/882318>
- EMCDDA, 2022b. New psychoactive substances (NPS) [WWW Document]. URL [https://www.emcdda.europa.eu/topics/nps\\_en](https://www.emcdda.europa.eu/topics/nps_en) (accessed 7.6.22).
- EMCDDA, 2022c. European Drug Report 2022: Trends and Developments. Lisbon.
- EMCDDA, 2021a. The EU Early Warning System on new psychoactive substances (NPS) [WWW Document]. URL [https://www.emcdda.europa.eu/publications/topic-overviews/eu-early-warning-system\\_en](https://www.emcdda.europa.eu/publications/topic-overviews/eu-early-warning-system_en) (accessed 10.23.19).
- EMCDDA, 2021b. New report highlights public health risks and increasing availability of ‘designer benzodiazepines’ in Europe [WWW Document]. URL [https://www.emcdda.europa.eu/news/2021/6/report-highlights-public-health-risks-and-increasing-availability-designer-benzodiazepines-europe\\_en](https://www.emcdda.europa.eu/news/2021/6/report-highlights-public-health-risks-and-increasing-availability-designer-benzodiazepines-europe_en) (accessed 1.31.22).
- EMCDDA, 2021c. New benzodiazepines in Europe – a review. Lisbon.
- EMCDDA, 2021d. Spotlight on... Non-medical use of benzodiazepines [WWW Document]. URL [https://www.emcdda.europa.eu/spotlights/non-medical-use-benzodiazepines\\_en](https://www.emcdda.europa.eu/spotlights/non-medical-use-benzodiazepines_en) (accessed

2.2.22).

EMCDDA, 2021e. European Drug Report 2021: Trends and Developments | [www.emcdda.europa.eu](http://www.emcdda.europa.eu). Lisbon.

EMCDDA, 2021f. Spotlight on... Fentanils and other new opioids [WWW Document]. URL [https://www.emcdda.europa.eu/spotlights/fentanils-and-other-new-opioids\\_en](https://www.emcdda.europa.eu/spotlights/fentanils-and-other-new-opioids_en) (accessed 8.21.22).

EMCDDA, 2021g. Infographic: opioids notifications to the Early Warning System and seizures | [www.emcdda.europa.eu](http://www.emcdda.europa.eu) [WWW Document]. URL [https://www.emcdda.europa.eu/media-library/infographic-opioids-notifications-early-warning-system-and-seizures\\_en](https://www.emcdda.europa.eu/media-library/infographic-opioids-notifications-early-warning-system-and-seizures_en) (accessed 8.17.22).

EMCDDA, 2020a. EMCDDA operating guidelines for the risk assessment of new psychoactive substances. Lisbon.

EMCDDA, 2020b. European Database on New Drugs [WWW Document]. URL <https://ednd2.emcdda.europa.eu> (accessed 9.4.20).

EMCDDA, 2020c. Benzodiazepines drug profile [WWW Document]. URL [http://www.emcdda.europa.eu/publications/drug-profiles/benzodiazepines\\_en](http://www.emcdda.europa.eu/publications/drug-profiles/benzodiazepines_en) (accessed 4.12.20).

EMCDDA, 2020d. New psychoactive substances: global markets, global threats and the COVID-19 pandemic — an update from the EU Early Warning System. Lisbon.

EMCDDA, 2019a. European Drug Report 2019: Trends and Developments. Lisbon.

EMCDDA, 2019b. Drug-related deaths and mortality in Europe RAPID COMMUNICATION.

EMCDDA, 2018a. New legislation, bringing faster response to new drugs, applies from today [WWW Document]. URL [https://www.emcdda.europa.eu/news/2018/8/new-legislation-brings-faster-response-to-new-psychoactive-substances\\_en](https://www.emcdda.europa.eu/news/2018/8/new-legislation-brings-faster-response-to-new-psychoactive-substances_en) (accessed 7.12.22).

EMCDDA, 2018b. Perspectives on drugs: the misuse of benzodiazepines among high-risk opioid users in Europe. Lisbon.

EMCDDA, 2017a. EMCDDA Scientific Committee [WWW Document]. URL [https://www.emcdda.europa.eu/about/sc\\_en](https://www.emcdda.europa.eu/about/sc_en) (accessed 7.12.22).

EMCDDA, 2017b. New legislation published today to bring faster response to new drugs [WWW Document]. URL [http://www.emcdda.europa.eu/news/2017/16/new-legislation-response-new-psychoactive-drugs\\_en](http://www.emcdda.europa.eu/news/2017/16/new-legislation-response-new-psychoactive-drugs_en) (accessed 4.20.20).

EMCDDA, 2017c. Drugs and the darknet: perspectives for enforcement, research and policy | [www.emcdda.europa.eu](http://www.emcdda.europa.eu). Lisbon.

EMCDDA, 2017d. Carfentanil Report on the risk assessment . Lisbon.



- EMCDDA, 2016a. Legal approaches to controlling new psychoactive substances I What policy challenges do new drugs pose? Lisbon.
- EMCDDA, 2016b. New psychoactive substances in Europe Legislation and prosecution-current challenges and solutions. <https://doi.org/10.2810/61905>
- EMCDDA, 2016c. The internet and drug markets. <https://doi.org/10.2810/324608>
- EMCDDA, 2015. New psychoactive substances in Europe. An update from the EU Early Warning System (March 2015) . Lisbon.
- EMCDDA, 2014. European Drug Report 2014: Trends and developments.
- EMCDDA, 2011. New drugs becoming available at ‘unprecedented pace’, says report [WWW Document]. URL [https://www.emcdda.europa.eu/news/2011/2\\_en](https://www.emcdda.europa.eu/news/2011/2_en) (accessed 7.11.22).
- EMCDDA, 2010. Risk assessment of new psychoactive substances — operating guidelines. Lisbon.
- EMCDDA, 2009a. The state of the drug problem in Europe, Annual report 2009. Lisbon.
- EMCDDA, 2009b. Understanding the “Spice” phenomenon . Lisbon.
- EMCDDA, 1999. Report on the risk assessment of MBDB in the framework of the joint action on new synthetic drugs . Lisbon.
- EMCDDA, n.d. Fentanyl drug profile [WWW Document]. 2022. URL [https://www.emcdda.europa.eu/publications/drug-profiles/fentanyl\\_en](https://www.emcdda.europa.eu/publications/drug-profiles/fentanyl_en) (accessed 8.21.22).
- EMCDDA, Europol, 2016. EMCDDA–Europol 2015 Annual Report on the implementation of Council Decision 2005/387/JHA.
- Essink, S., Nugteren-van Lonkhuyzen, J.J., van Riel, A.J.H.P., Dekker, D., Hondebrink, L., 2022. Significant toxicity following an increase in poisonings with designer benzodiazepines in the Netherlands between 2010 and 2020. *Drug Alcohol Depend.* 231, 109244. <https://doi.org/10.1016/J.DRUGALCDEP.2021.109244>
- European Union, 2017. Legislation. Off. J. Eur. Union.
- Fei, J., Zhou, L., Liu, T., Tang, X.Y., 2013. Pharmacophore Modeling, Virtual Screening, and Molecular Docking Studies for Discovery of Novel Akt2 Inhibitors. *Int. J. Med. Sci.* 10, 265. <https://doi.org/10.7150/IJMS.5344>
- Feinberg, A.P., Creese, I., Snyder, S.H., 1976. The opiate receptor: a model explaining structure-activity relationships of opiate agonists and antagonists. *Proc. Natl. Acad. Sci.* 73, 4215–4219. <https://doi.org/10.1073/PNAS.73.11.4215>
- Fernández-De Gortari, E., García-Jacas, C.R., Martínez-Mayorga, K., Medina-Franco, J.L., 2017. Database fingerprint (DFP): an approach to represent molecular databases. *J. Cheminform.* 9. <https://doi.org/10.1186/s13321-017-0195-1>
- Ferry, N., Dhanjal, S., 2022. Opioid Anesthesia. *StatPearls*.

- Finlay, S., 2014. Predictive analytics, data mining and big data: myths, misconceptions and methods. Palgrave Macmillan.
- Fischer, J., Ganellin Robin, 2006. Analogue-based Drug Discovery . Wiley-VCH.
- Floresta, G., Abbate, V., 2021. Machine learning vs. field 3D-QSAR models for serotonin 2A receptor psychoactive substances identification. RSC Adv. 11, 14587–14595. <https://doi.org/10.1039/D1RA01335A>
- Floresta, G., Apirakkan, O., Rescifina, A., Abbate, V., 2018a. Discovery of High-Affinity Cannabinoid Receptors Ligands through a 3D-QSAR Ushered by Scaffold-Hopping Analysis. Mol. 2018, Vol. 23, Page 2183 23, 2183. <https://doi.org/10.3390/MOLECULES23092183>
- Floresta, G., Apirakkan, O., Rescifina, A., Abbate, V., 2018b. Discovery of high-affinity cannabinoid receptors ligands through a 3D-QSAR ushered by scaffold-hopping analysis †. Molecules 23, 2183. <https://doi.org/10.3390/molecules23092183>
- Floresta, G., Rescifina, A., Abbate, V., 2019. Structure-based approach for the prediction of mu-opioid binding affinity of unclassified designer fentanyl-like molecules, in: International Journal of Molecular Sciences. MDPI AG, p. 2311. <https://doi.org/10.3390/ijms20092311>
- Floris, M., Manganaro, A., Nicolotti, O., Medda, R., Mangiatordi, G.F., Benfenati, E., 2014. A generalizable definition of chemical similarity for read-across. J. Cheminform. 6, 39. <https://doi.org/10.1186/s13321-014-0039-1>
- Fogarty, M.F., Vandeputte, M.M., Krotulski, A.J., Papsun, D., Walton, S.E., Stove, C.P., Logan, B.K., 2022. Toxicological and pharmacological characterization of novel cinnamylpiperazine synthetic opioids in humans and in vitro including 2-methyl AP-237 and AP-238. Arch. Toxicol. 2022 966 96, 1701–1710. <https://doi.org/10.1007/S00204-022-03257-7>
- Fogger, S.A., 2019. Methamphetamine Use: A New Wave in the Opioid Crisis? J. Addict. Nurs. 30, 219–223. <https://doi.org/10.1097/JAN.0000000000000298>
- Fomin, D., Baranauskaite, V., Usaviciene, E., Sumkovskaja, A., Laima, S., Jasulaitis, A., Minkuviene, Z.N., Chmieliauskas, S., Stasiuniene, J., 2018. Human deaths from drug overdoses with carfentanyl involvement-new rising problem in forensic medicine A STROBE-compliant retrospective study. Med. (United States) 97. <https://doi.org/10.1097/MD.00000000000013449>
- Forman, R.F., 2006. Narcotics on the net: The availability of web sites selling controlled substances. Psychiatr. Serv. <https://doi.org/10.1176/appi.ps.57.1.24>
- Forman, R.F., Marlowe, D.B., McLellan, A.T., 2006. The internet as a source of drugs of abuse. Curr. Psychiatry Rep. <https://doi.org/10.1007/s11920-006-0039-6>
- Fourches, D., Muratov, E., Tropsha, A., 2010. Trust, but verify: On the importance of chemical

- structure curation in cheminformatics and QSAR modeling research. *J. Chem. Inf. Model.* 50, 1189–1204. <https://doi.org/10.1021/ci100176x>
- Frisoni, P., Bacchio, E., Bilel, S., Talarico, A., Gaudio, R.M., Barbieri, M., Neri, M., Marti, M., 2018. Novel Synthetic Opioids: The Pathologist's Point of View. *Brain Sci.* 2018, Vol. 8, Page 170 8, 170. <https://doi.org/10.3390/BRAINSCI8090170>
- Furusjö, E., Svenson, A., Rahmberg, M., Andersson, M., 2006. The importance of outlier detection and training set selection for reliable environmental QSAR predictions. *Chemosphere* 63, 99–108. <https://doi.org/10.1016/j.chemosphere.2005.07.002>
- Gad, S.C., 2014. QSAR, in: Wexler, P. (Ed.), *Encyclopedia of Toxicology: Third Edition*. Elsevier, pp. 1–9. <https://doi.org/10.1016/B978-0-12-386454-3.00971-4>
- Gardner, C.R., Hedgecock, J.R., 1989. US4868176A Novel imidazobenzodiazepines.
- Geisser, S., 2017. Predictive inference: An introduction, *Predictive Inference: An Introduction*. CRC Press. <https://doi.org/10.1201/9780203742310>
- Gendron, L., Cahill, C.M., Zastrow, M. von, Schiller, P.W., Pineyro, G., 2016. Molecular Pharmacology of  $\delta$ -Opioid Receptors. *Pharmacol. Rev.* 68, 631. <https://doi.org/10.1124/PR.114.008979>
- Gerber, P., Müller, K., 1995. MAB, a generally applicable molecular force field for structure modelling in medicinal chemistry. *J. Comput. Aided. Mol. Des.* 9, 251–268. <https://doi.org/10.1007/BF00124456>
- Gevorkyan, J., Kinyua, J., Pearing, S., Rodda, L.N., 2021. A Case Series of Etizolam in Opioid-Related Deaths. *J. Anal. Toxicol.* 45, E4–E17. <https://doi.org/10.1093/JAT/BKAA146>
- Gladden, R.M., O'Donnell, J., Mattson, C.L., Seth, P., 2019. Changes in Opioid-Involved Overdose Deaths by Opioid Type and Presence of Benzodiazepines, Cocaine, and Methamphetamine — 25 States, July–December 2017 to January–June 2018. *MMWR. Morb. Mortal. Wkly. Rep.* 68, 737–744. <https://doi.org/10.15585/MMWR.MM6834A2>
- Godden, J.W., Xue, L., Bajorath, J., 2000. Combinatorial Preferences Affect Molecular Similarity/Diversity Calculations Using Binary Fingerprints and Tanimoto Coefficients. *J. Chem. Inf. Comput. Sci.* 40, 163–166. <https://doi.org/10.1021/ci990316u>
- Godel, T., Hunkeler, W., Stadler, H., Widmer, U., 1997. US5665718A Imidazodiazepines. US5665718A.
- Golbraikh, A., Muratov, E., Fourches, D., Tropsha, A., 2014. Data set modelability by QSAR. *J. Chem. Inf. Model.* 54, 1–4. <https://doi.org/10.1021/ci400572x>
- Golbraikh, A., Tropsha, A., 2002. Beware of q2! *J. Mol. Graph. Model.* 20, 269–276. [https://doi.org/10.1016/S1093-3263\(01\)00123-1](https://doi.org/10.1016/S1093-3263(01)00123-1)

- Golbraikh, A., Tropsha, A., 2000. Predictive QSAR modeling based on diversity sampling of experimental datasets for the training and test set selection. *Mol. Divers.* 5, 231–243. <https://doi.org/10.1023/A:1021372108686>
- Golovenko, M., Larionov, V., Reder, A., Valivodz, I., Tsapenko, Z., Bogatsky, A. V., 2020. Sedative-hypnotic and muscle relaxant activities of propoxazepam in animal models and investigation on possible mechanisms 14, 2020.
- Goodchild, C., Serrao, J., 1987. Intrathecal midazolam in the rat: evidence for spinally-mediated analgesia. *Br. J. Anaesth.* 59, 1563–1570. <https://doi.org/10.1093/BJA/59.12.1563>
- Google [WWW Document], 2019. URL <https://www.google.co.uk/> (accessed 10.24.19).
- Greenblatt, D.J., Divoll, M., Abernethy, D.R., Ochs, H.R., Shader, R.I., 1983. Clinical Pharmacokinetics of the Newer Benzodiazepines. *Clin. Pharmacokinet.* 8, 233–252. <https://doi.org/10.2165/00003088-198308030-00003>
- Greenblatt, D.J., Shader, R.I., Divoll, M., Harmatz, J.S., 1981. Benzodiazepines: a summary of pharmacokinetic properties. *J. clin. Pharmacol.* 1, 11–16.
- Greenblatt, H.K., Greenblatt, D.J., 2019. Designer Benzodiazepines: A Review of Published Data and Public Health Significance. *Clin. Pharmacol. Drug Dev.* 8, 266–269. <https://doi.org/10.1002/cpdd.667>
- Gregory, N.S., Harris, A.L., Robinson, C.R., Dougherty, P.M., Fuchs, P.N., Sluka, K.A., 2013. An overview of animal models of pain: disease models and outcome measures. *J. Pain* 14, 1255–1269. <https://doi.org/10.1016/J.JPAIN.2013.06.008>
- Griffin, C.E., Kaye, A.M., Rivera Bueno, F., Kaye, A.D., 2013. Benzodiazepine pharmacology and central nervous system-mediated effects. *Ochsner J.* 13, 214–223.
- Guariento, S., Tonelli, M., Espinoza, S., Gerasimov, A.S., Gainetdinov, R.R., Cichero, E., 2018. Rational design, chemical synthesis and biological evaluation of novel biguanides exploring species-specificity responsiveness of TAAR1 agonists. *Eur. J. Med. Chem.* 146, 171–184. <https://doi.org/10.1016/j.ejmech.2018.01.059>
- Güner, O.F., Bowen, J.P., 2014. Setting the record straight: The origin of the pharmacophore concept. *J. Chem. Inf. Model.* 54, 1269–1283. <https://doi.org/10.1021/CI5000533>
- Gunja, N., 2013. The Clinical and Forensic Toxicology of Z-drugs. *J. Med. Toxicol.* 9, 155–162. <https://doi.org/10.1007/s13181-013-0292-0>
- Hadjipavlou-Litina, D., Hansch, C., 1994. Quantitative Structure–Activity Relationships of the Benzodiazepines. A Review and Reevaluation. *Chem. Rev.* 94, 1483–1505. <https://doi.org/10.1021/cr00030a002>
- Hall, L.H., Kier, L.B., 1991. The Molecular Connectivity Chi Indexes and Kappa Shape Indexes in

- Structure-Property Modeling. John Wiley & Sons, Ltd, pp. 367–422.  
<https://doi.org/10.1002/9780470125793.ch9>
- Hawkins, D.M., Basak, S.C., Mills, D., 2003. Assessing model fit by cross-validation. *J. Chem. Inf. Comput. Sci.* 43, 579–586. <https://doi.org/10.1021/ci025626i>
- Heller, S., McNaught, A., Stein, S., Tchekhovskoi, D., Pletnev, I., 2013. InChI - The worldwide chemical structure identifier standard. *J. Cheminform.* 5, 7. <https://doi.org/10.1186/1758-2946-5-7>
- Hering, W., Ihmsen, H., Albrecht, S., Schwilden, H., Schüttler, J., 1996. [RO 48-6791--a short acting benzodiazepine. Pharmacokinetics and pharmacodynamics in young and old subjects in comparison to midazolam]. *Anaesthesist* 45, 1211–1214.  
<https://doi.org/10.1007/S001010050360>
- Herling, S., 1983. Naltrexone blocks the response-latency increasing effects but not the discriminative effects of diazepam in rats. *Eur. J. Pharmacol.* 88, 121–124.  
[https://doi.org/10.1016/0014-2999\(83\)90400-4](https://doi.org/10.1016/0014-2999(83)90400-4)
- Hester, J.B., Rudzik, A.D., Kamdar, B. V., 1971. 6-phenyl-4H-s-triazolo[4,3-a][1,4]benzodiazepines which have central nervous system depressant activity. *J. Med. Chem.* 14, 1078–1081. <https://doi.org/10.1021/JM00293A015>
- Hester, J.B., Von Voigtlander, P., 1979. 6-Aryl-4H-s-triazolo[4,3-a][1,4]benzodiazepines. Influence of 1-substitution on pharmacological activity. *J. Med. Chem.* 22, 1390–1398.  
<https://doi.org/10.1021/JM00197A021>
- Hevener, K.E., Zhao, W., Ball, D.M., Babaoglu, K., Qi, J., White, S.W., Lee, R.E., 2009. Validation of molecular docking programs for virtual screening against dihydropteroate synthase. *J. Chem. Inf. Model.* 49, 444–460.  
[https://doi.org/10.1021/CI800293N/SUPPL\\_FILE/CI800293N\\_SI\\_001.PDF](https://doi.org/10.1021/CI800293N/SUPPL_FILE/CI800293N_SI_001.PDF)
- Higashikawa, Y., Suzuki, S., 2008. Studies on 1-(2-phenethyl)-4-(N-propionylanilino)piperidine (fentanyl) and its related compounds. VI. Structure-analgesic activity relationship for fentanyl, methyl-substituted fentanyls and other analogues. *Forensic Toxicol.* 2008 261 26, 1–5.  
<https://doi.org/10.1007/S11419-007-0039-1>
- Hodavance, S.Y., Gareri, C., Torok, R.D., Rockman, H.A., 2016. G Protein-Coupled Receptor Biased Agonism. *J. Cardiovasc. Pharmacol.* 67, 193.  
<https://doi.org/10.1097/FJC.0000000000000356>
- Home Office, 2022a. Classification and scheduling of Brorphine and Metonitazene - GOV.UK [WWW Document]. URL <https://www.gov.uk/government/publications/classification-and-scheduling-of-brorphine-and-metonitazene> (accessed 8.10.22).

- Home Office, 2022b. Controlled drugs list-GOV.UK [WWW Document]. URL <https://www.gov.uk/government/publications/controlled-drugs-list--2> (accessed 8.9.22).
- Home Office, 2020. New Psychoactive Substances (NPS) - Resource pack for informal educators and practitioners.
- Home Office, 2018. Review of the Psychoactive Substances Act 2016. London.
- Home Office, 2016. Psychoactive Substances Act 2016. Queen's Printer of Acts of Parliament.
- Horsfall, J.T., Sprague, J.E., 2017. The Pharmacology and Toxicology of the 'Holy Trinity.' *Basic Clin. Pharmacol. Toxicol.* 120, 115–119. <https://doi.org/10.1111/BCPT.12655>
- Houdi, A.A., Kottayil, S., Crooks, P.A., Butterfield, D.A., 1996. 3-O-Acetylmorphine-6-O-sulfate: A potent, centrally acting morphine derivative. *Pharmacol. Biochem. Behav.* 53, 665–671. [https://doi.org/10.1016/0091-3057\(95\)02067-5](https://doi.org/10.1016/0091-3057(95)02067-5)
- Hu, Y., Bajorath, J., 2017. Entering the “big data” era in medicinal chemistry: molecular promiscuity analysis revisited. *Futur. Sci. OA* 3. <https://doi.org/10.4155/fsoa-2017-0001>
- Huang, N., Shoichet, B.K., Irwin, J.J., 2006. Benchmarking sets for molecular docking. *J. Med. Chem.* 49, 6789–6801. <https://doi.org/10.1021/JM0608356>
- Huang, W., Manglik, A., Venkatakrisnan, A., Laeremans, T., Feinberg, E., Sanborn, A., HE, K., KE, L., TS, T., RC, K., S, G., P, G., Husbands, S., Traynor, J., Weis, W., Steyaert, J., Dror, R., Kobilka, B., 2015. Structural insights into  $\mu$ -opioid receptor activation. *Nature* 524, 315–321. <https://doi.org/10.1038/NATURE14886>
- Huppertz, L.M., Bisel, P., Westphal, F., Franz, F., Auwärter, V., Moosmann, B., 2015. Characterization of the four designer benzodiazepines clonazolam, deschloroetizolam, flubromazolam, and meclonazepam, and identification of their in vitro metabolites. *Forensic Toxicol.* 2015 332 33, 388–395. <https://doi.org/10.1007/S11419-015-0277-6>
- Huppertz, L.M., Moosmann, B., Auwärter, V., 2018. Flubromazolam – Basic pharmacokinetic evaluation of a highly potent designer benzodiazepine. *Drug Test. Anal.* 10, 206–211. <https://doi.org/10.1002/DTA.2203>
- Ibañez, G.E., Levi-Minzi, M.A., Rigg, K.K., Mooss, A.D., 2013. Diversion of benzodiazepines through healthcare sources. *J. Psychoactive Drugs* 45, 48–56. <https://doi.org/10.1080/02791072.2013.764232>
- IBM Cloud Education, 2021. What is Overfitting? [WWW Document]. URL <https://www.ibm.com/cloud/learn/overfitting> (accessed 7.21.22).
- Inoue, A., Ishiguro, J., Kitamura, H., Arima, N., Okutani, M., Shuto, A., Higashiyama, S., Ohwada, T., Arai, H., Makide, K., Aoki, J., 2012. TGF $\alpha$  shedding assay: an accurate and versatile method for detecting GPCR activation. *Nat. Methods* 2012 910 9, 1021–1029.

<https://doi.org/10.1038/nmeth.2172>

- International Narcotic Control Board, 2018. Fentanyl-Related Substances with no known legitimate use [WWW Document]. URL [https://www.incb.org/incb/en/opioids\\_project/fentanyl-related-substances-with-no-known-legitimate-use.html](https://www.incb.org/incb/en/opioids_project/fentanyl-related-substances-with-no-known-legitimate-use.html) (accessed 8.9.22).
- International Narcotics Control Board, 2021. Yellow list-List of Narcotic Drugs Under International Control [WWW Document]. 60th. URL <https://www.incb.org/incb/en/narcotic-drugs/Yellowlist/yellow-list.html> (accessed 8.9.22).
- International Society for the Study of Emerging Drugs (ISSED), n.d. Novel Psychoactive Substances [WWW Document]. URL <https://www.novelpsychoactivesubstances.org/> (accessed 9.2.22).
- Irwin, J.J., Sterling, T., Mysinger, M.M., Bolstad, E.S., Coleman, R.G., 2012. ZINC: A free tool to discover chemistry for biology. *J. Chem. Inf. Model.* <https://doi.org/10.1021/ci3001277>
- Isberg, V., Paine, J., Leth-Petersen, S., Kristensen, J.L., Gloriam, D.E., 2013. Structure-activity relationships of constrained phenylethylamine ligands for the serotonin 5-HT<sub>2</sub> receptors. *PLoS One* 8. <https://doi.org/10.1371/JOURNAL.PONE.0078515>
- Isomer Design, 2021. Isomer Design [WWW Document]. URL <https://isomerdesign.com> (accessed 11.17.21).
- IUPAC, 2019a. Nomenclature [WWW Document]. URL <https://iupac.org/what-we-do/nomenclature/> (accessed 10.24.19).
- IUPAC, 2019b. IUPAC - International Union of Pure and Applied Chemistry: Project Details [WWW Document]. URL [https://web.archive.org/web/20120527162256/http://www.iupac.org/home/projects/project-db/project-details.html?tx\\_wfqbe\\_pi1%5Bproject\\_nr%5D=2000-025-1-800](https://web.archive.org/web/20120527162256/http://www.iupac.org/home/projects/project-db/project-details.html?tx_wfqbe_pi1%5Bproject_nr%5D=2000-025-1-800) (accessed 10.31.19).
- Jakhar, R., Dangi, M., Khichi, A., Chhillar, A.K., 2019. Relevance of Molecular Docking Studies in Drug Designing. *Curr. Bioinform.* 15, 270–278. <https://doi.org/10.2174/1574893615666191219094216>
- Jalal, H., Burke, D.S., 2021. Carfentanil and the rise and fall of overdose deaths in the United States. *Addiction* 116, 1593–1599. <https://doi.org/10.1111/ADD.15260>
- Janssen, P.A.J., Van Daele, G.H.P., 1977. N-(4-piperidiny)-N-phenylamides - Patent US-4179569-A - PubChem.
- Jia, X., Ciallella, H.L., Russo, D.P., Zhao, L., James, M.H., Zhu, H., 2021. Construction of a Virtual Opioid Bioprofile: A Data-Driven QSAR Modeling Study to Identify New Analgesic Opioids. *ACS Sustain. Chem. Eng.* 9, 3909–3919.

[https://doi.org/10.1021/ACSSUSCHEMENG.0C09139/SUPPL\\_FILE/SC0C09139\\_SI\\_003.XLSX](https://doi.org/10.1021/ACSSUSCHEMENG.0C09139/SUPPL_FILE/SC0C09139_SI_003.XLSX)

- Jing, Y., Bian, Y., Hu, Z., Wang, L., Xie, X.Q.S., 2018. Deep Learning for Drug Design: an Artificial Intelligence Paradigm for Drug Discovery in the Big Data Era. *AAPS J.* <https://doi.org/10.1208/s12248-018-0210-0>
- Johnson, M.A., Maggiora, G.M., American Chemical Society. Meeting (196th : 1988 : Los Angeles, C., 1990. Concepts and applications of molecular similarity. Wiley.
- Jones, C.M., Bekheet, F., Park, J.N., Alexander, G.C., 2020. The Evolving Overdose Epidemic: Synthetic Opioids and Rising Stimulant-Related Harms. *Epidemiol. Rev.* 42, 154–166. <https://doi.org/10.1093/EPIREV/MXAA011>
- Jones, P., Atack, J.R., Braun, M.P., Cato, B.P., Chambers, M.S., O'Connor, D., Cook, S.M., Hobbs, S.C., Maxey, R., Szekeres, H.J., Szeto, N., Wafford, K.A., MacLeod, A.M., 2006. Pharmacokinetics and metabolism studies on (3-tert-butyl-7-(5-methylisoxazol-3-yl)-2-(1-methyl-1H-1,2,4-triazol-5-ylmethoxy) pyrazolo[1,5-d][1,2,4]triazine, a functionally selective GABAA  $\alpha 5$  inverse agonist for cognitive dysfunction. *Bioorg. Med. Chem. Lett.* 16, 872–875. <https://doi.org/10.1016/J.BMCL.2005.11.012>
- Jurásek, B., Čmelo, I., Svoboda, J., Čejka, J., Svozil, D., Kuchař, M., 2021. New psychoactive substances on dark web markets: From deal solicitation to forensic analysis of purchased substances. *Drug Test. Anal.* 13, 156–168. <https://doi.org/10.1002/DTA.2901>
- Jutkiewicz, E., 2006. The antidepressant-like effects of delta-opioid receptor agonists. *Mol. Interv.* 6, 162–169. <https://doi.org/10.1124/MI.6.3.7>
- Jutkiewicz, E.M., 2006. The antidepressant-like effects of delta-opioid receptor agonists. *Mol. Interv.* 6, 162–169. <https://doi.org/10.1124/MI.6.3.7>
- Kandasamy, R., Hillhouse, T.M., Livingston, K.E., Kochan, K.E., Meurice, C., Eans, S.O., Li, M.H., White, A.D., Roques, B.P., McLaughlin, J.P., Ingram, S.L., Burford, N.T., Alt, A., Traynor, J.R., 2021. Positive allosteric modulation of the mu-opioid receptor produces analgesia with reduced side effects. *Proc. Natl. Acad. Sci. U. S. A.* 118. <https://doi.org/10.1073/PNAS.2000017118/-/DCSUPPLEMENTAL>
- Kang, M., Galuska, M.A., Ghassemzadeh, S., 2022. Benzodiazepine Toxicity. *StatPearls.*
- Kaserer, T., Lantero, A., Schmidhammer, H., Spetea, M., Schuster, D., 2016.  $\mu$  Opioid receptor: novel antagonists and structural modeling. *Nat. Publ. Gr.* <https://doi.org/10.1038/srep21548>
- Kataja, K., Törrönen, J., Hakkarainen, P., Tigerstedt, C., 2018. A virtual academy of polydrug use: Masters, novices and the art of combinations. *NAD Nord. Stud. Alcohol Drugs* 35, 413–427. <https://doi.org/10.1177/1455072518770351>



- Kelly, M.D., Smith, A., Banks, G., Wingrove, P., Whiting, P.W., Atack, J., Seabrook, G.R., Maubach, K.A., 2002. Role of the histidine residue at position 105 in the human  $\alpha 5$  containing GABA A receptor on the affinity and efficacy of benzodiazepine site ligands . *Br. J. Pharmacol.* 135, 248–256. <https://doi.org/10.1038/sj.bjp.0704459>
- Kendall, M.G., 1938. A New Measure of Rank Correlation. *Biometrika* 30, 81. <https://doi.org/10.2307/2332226>
- Kieffer, B.L., Evans, C.J., 2002. Opioid tolerance-in search of the holy grail. *Cell* 108, 587–590. [https://doi.org/10.1016/S0092-8674\(02\)00666-9](https://doi.org/10.1016/S0092-8674(02)00666-9)
- Kim, S., Thiessen, P.A., Bolton, E.E., Chen, J., Fu, G., Gindulyte, A., Han, L., He, J., He, S., Shoemaker, B.A., Wang, J., Yu, B., Zhang, J., Bryant, S.H., 2016. PubChem substance and compound databases. *Nucleic Acids Res.* 44, D1202–D1213. <https://doi.org/10.1093/nar/gkv951>
- Kim, S.J., Marsch, L.A., Hancock, J.T., Das, A.K., 2017. Scaling Up Research on Drug Abuse and Addiction Through Social Media Big Data. *J. Med. Internet Res.* 19, e353. <https://doi.org/10.2196/jmir.6426>
- Kingma, D.P., Rezende, D.J., Mohamed, S., Welling, M., n.d. Semi-supervised Learning with Deep Generative Models. 2014.
- Kjellgren, A., Jacobsson, K., Soussan, C., 2016. The quest for well-being and pleasure : experiences of the novel synthetic opioids AH-7921 and MT-45, as reported by anonymous users online. *J. Addict. Res. Ther.* 7. <https://doi.org/10.4172/2155-6105.1000287>
- Koch, K., Auwärter, V., Hermanns-Clausen, M., Wilde, M., Neukamm, M.A., 2018. Mixed intoxication by the synthetic opioid U-47700 and the benzodiazepine flubromazepam with lethal outcome: Pharmacokinetic data. *Drug Test. Anal.* 10, 1336–1341. <https://doi.org/10.1002/DTA.2391>
- Köteles, I., Mazák, K., Tóth, G., Horváth, P., Kiss, E., Tüz, B., Hosztafi, S., 2021. Synthesis of 3-O-Carboxyalkyl Morphine Derivatives and Characterization of Their Acid-Base Properties. *Chem. Biodivers.* 18, e2100135. <https://doi.org/10.1002/CBDV.202100135>
- Krall, J., Balle, T., Krosgaard-Larsen, N., Sørensen, T.E., Krosgaard-Larsen, P., Kristiansen, U., Frølund, B., 2015. GABAA receptor partial agonists and antagonists: structure, binding mode, and pharmacology. *Adv. Pharmacol.* 72, 201–227. <https://doi.org/10.1016/BS.APHA.2014.10.003>
- Kriikku, P., Rasanen, I., Ojanperä, I., Thelander, G., Kronstrand, R., Vikingsson, S., 2020. Femoral blood concentrations of flualprazolam in 33 postmortem cases. *Forensic Sci. Int.* 307. <https://doi.org/10.1016/J.FORSCIINT.2019.110101>

- Krivák, R., Hoksza, D., 2015. Improving protein-ligand binding site prediction accuracy by classification of inner pocket points using local features. *J. Cheminform.* 7, 12. <https://doi.org/10.1186/s13321-015-0059-5>
- Krotulski, A.J., Papsun, D.M., Noble, C., Kacinko, S.L., Logan, B.K., 2021. Brorphine— Investigation and quantitation of a new potent synthetic opioid in forensic toxicology casework using liquid chromatography-mass spectrometry. *J. Forensic Sci.* 66, 664–676. <https://doi.org/10.1111/1556-4029.14623>
- Krumm, B.E., Grisshammer, R., 2015. Peptide ligand recognition by G protein-coupled receptors. *Front. Pharmacol.* 6, 48. <https://doi.org/10.3389/FPHAR.2015.00048/BIBTEX>
- Kühlbrandt, W., 2014. The resolution revolution. *Science* (80-. ). <https://doi.org/10.1126/science.1251652>
- Labate, B.C., Jungaberle, H., 2011. *The Internationalization of Ayahuasca, Anthropology of Consciousness.* Lit Verlag.
- Lampa, S., Alvarsson, J., Spjuth, O., 2016. Towards agile large-scale predictive modelling in drug discovery with flow-based programming design principles. *J. Cheminform.* 8. <https://doi.org/10.1186/s13321-016-0179-6>
- Langdon, S.R., Ertl, P., Brown, N., 2010. Bioisosteric Replacement and Scaffold Hopping in Lead Generation and Optimization. *Mol. Inform.* 29, 366–385. <https://doi.org/10.1002/MINF.201000019>
- Latta, K., Ginsberg, B., Robert, L., n.d. Meperidine: A Critical Review [WWW Document]. *Am. J. Ther.* URL [https://journals.lww.com/americantherapeutics/Abstract/2002/01000/Meperidine\\_\\_A\\_Critical\\_Review.10.aspx](https://journals.lww.com/americantherapeutics/Abstract/2002/01000/Meperidine__A_Critical_Review.10.aspx) (accessed 9.5.22).
- Leelananda, S.P., Lindert, S., 2016. Computational methods in drug discovery. *Beilstein J. Org. Chem.* 12, 2694–2718. <https://doi.org/10.3762/bjoc.12.267>
- Lewis, R.A., Wood, D., 2014. Modern 2D QSAR for drug discovery. *Wiley Interdiscip. Rev. Comput. Mol. Sci.* 4, 505–522. <https://doi.org/10.1002/wcms.1187>
- Lipiński, Piotr F.J., Jarończyk, M., Dobrowolski, J.C., Sadlej, J., 2019. Molecular dynamics of fentanyl bound to  $\mu$ -opioid receptor. *J. Mol. Model.* 25, 1–17. <https://doi.org/10.1007/S00894-019-3999-2/FIGURES/16>
- Lipiński, Piotr F. J., Kosson, P., Matalińska, J., Roszkowski, P., Czarnocki, Z., Jarończyk, M., Misicka, A., Dobrowolski, J.C., Sadlej, J., 2019. Fentanyl Family at the Mu-Opioid Receptor: Uniform Assessment of Binding and Computational Analysis. *Mol.* 2019, Vol. 24, Page 740 24, 740. <https://doi.org/10.3390/MOLECULES24040740>

- Liu, E.Y., Tamblyn, R., Filion, K.B., Buckeridge, D.L., 2021. Concurrent prescriptions for opioids and benzodiazepines and risk of opioid overdose: protocol for a retrospective cohort study using linked administrative data. *BMJ Open* 11, 42299. <https://doi.org/10.1136/bmjopen-2020-042299>
- Lloyd, S., Mohseni, M., Rebstroff, P., 2013. Quantum algorithms for supervised and unsupervised machine learning [WWW Document]. URL <http://arxiv.org/abs/1307.0411> (accessed 2.5.20).
- Lo, Y.C., Rensi, S.E., Torng, W., Altman, R.B., 2018. Machine learning in chemoinformatics and drug discovery. *Drug Discov. Today*. <https://doi.org/10.1016/j.drudis.2018.05.010>
- Loew, G.H., Villar, H.O., Alkorta, I., 1993. Strategies for Indirect Computer-Aided Drug Design. *Pharm. Res. An Off. J. Am. Assoc. Pharm. Sci.* <https://doi.org/10.1023/A:1018977414572>
- Loi, B., Sahai, M.A., De Luca, M.A., Shiref, H., Opacka-Juffry, J., 2020. The Role of Dopamine in the Stimulant Characteristics of Novel Psychoactive Substances (NPS)-Neurobiological and Computational Assessment Using the Case of Desoxypipradrol (2-DPMP). *Front. Pharmacol.* 11. <https://doi.org/10.3389/FPHAR.2020.00806>
- Lovrecic, B., Lovrecic, M., Gabrovec, B., Carli, M., Pacini, M., Maremmani, A.G.I., Maremmani, I., 2019. Non-medical use of novel synthetic opioids: A new challenge to public health. *Int. J. Environ. Res. Public Health*. <https://doi.org/10.3390/ijerph16020177>
- LSS/RAB/DPA/UNODC, 2016. New psychoactive substances: overview of trends, challenges and legal approaches. Vienna.
- Łukasik-Głębocka, M., Sommerfeld, K., Tezyk, A., Zielińska-Psuja, B., Panieński, P., Zaba, C., 2016. Flubromazolam - A new life-threatening designer benzodiazepine. *Clin. Toxicol.* 54, 66–68. <https://doi.org/10.3109/15563650.2015.1112907>
- Mackey, T., Kalyanam, J., Klugman, J., Kuzmenko, E., Gupta, R., 2018. Solution to Detect, Classify, and Report Illicit Online Marketing and Sales of Controlled Substances via Twitter: Using Machine Learning and Web Forensics to Combat Digital Opioid Access. *J. Med. Internet Res.* 20, e10029. <https://doi.org/10.2196/10029>
- Mackey, T.K., 2018. Opioids and the Internet: Convergence of Technology and Policy to Address the Illicit Online Sales of Opioids. *Heal. Serv. Insights* 11. <https://doi.org/10.1177/1178632918800995>
- Maddalena, D.J., Johnston, G.A.R., 1995. Prediction of Receptor Properties and Binding Affinity of Ligands to Benzodiazepine/Gm& Receptors Using Artificial Neural Networks. *J. Med. Chem* 38, 715–724.
- Mafi, A., Kim, S.K., Goddard, W.A., 2020. Mechanism of  $\beta$ -arrestin recruitment by the  $\mu$ -opioid G protein-coupled receptor. *Proc. Natl. Acad. Sci. U. S. A.* 117, 16346–16355.

[https://doi.org/10.1073/PNAS.1918264117/SUPPL\\_FILE/PNAS.1918264117.SM04.MP4](https://doi.org/10.1073/PNAS.1918264117/SUPPL_FILE/PNAS.1918264117.SM04.MP4)

- Maggiore, G.M., 2006. On Outliers and Activity Cliffs Why QSAR Often Disappoints. *J. Chem. Inf. Model.* 46, 1535. <https://doi.org/10.1021/CI060117S>
- Makleit, S., Hosztafi, S., 2006. Application of the Mitsunobu Reaction for the Preparation of Isomorphine and Isocodeine Derivatives. <http://dx.doi.org/10.1080/00397919108016763> 21, 407–412. <https://doi.org/10.1080/00397919108016763>
- Manchikanti, L., Fellows, B., Ailinani, H., Pampati, V., 2010. Therapeutic use, abuse, and nonmedical use of opioids: A Ten-year perspective. *Pain Physician* 13, 401–435.
- Manglik, A., 2020. Molecular Basis of Opioid Action: From Structures to New Leads. *Biol. Psychiatry* 87, 6–14. <https://doi.org/10.1016/J.BIOPSYCH.2019.08.028>
- Manglik, A., Kruse, A.C., Kobilka, T.S., Thian, F.S., Mathiesen, J.M., Sunahara, R.K., Pardo, L., Weis, W.I., Kobilka, B.K., Granier, S., 2012. Crystal structure of the  $\mu$ -opioid receptor bound to a morphinan antagonist. *Nat.* 2012 4857398 485, 321–326. <https://doi.org/10.1038/nature10954>
- Marrero-Ponce, Y., Santiago, O.M., López, Y.M., Barigye, S.J., Torrens, F., 2012. Derivatives in discrete mathematics: a novel graph-theoretical invariant for generating new 2/3D molecular descriptors. I. Theory and QSPR application. *J. Comput. Aided. Mol. Des.* 26, 1229–1246. <https://doi.org/10.1007/s10822-012-9591-9>
- Martin, W.R., 1967. Opioid antagonists. *Pharmacol Rev.* 19, 463–521.
- Masiulis, S., Desai, R., Uchański, T., Serna Martin, I., Lavery, D., Karia, D., Malinauskas, T., Zivanov, J., Pardon, E., Kotecha, A., Steyaert, J., Miller, K.W., Aricescu, A.R., 2019. GABAA receptor signalling mechanisms revealed by structural pharmacology. *undefined* 565, 454–459. <https://doi.org/10.1038/S41586-018-0832-5>
- Mason, J., Good, A., Martin, E., 2005. 3-D Pharmacophores in Drug Discovery. *Curr. Pharm. Des.* 7, 567–597. <https://doi.org/10.2174/1381612013397843>
- Mattson, C.L., Tanz, L.J., Quinn, K., Kariisa, M., Patel, P., Davis, N.L., 2021. Trends and Geographic Patterns in Drug and Synthetic Opioid Overdose Deaths — United States, 2013–2019. *MMWR. Morb. Mortal. Wkly. Rep.* 70, 202–207. <https://doi.org/10.15585/MMWR.MM7006A4>
- Maurer, H.H., Brandt, S.D. (Eds.), 2018. *New Psychoactive Substances*, 1st ed, Handbook of Experimental Pharmacology. Springer International Publishing. <https://doi.org/10.1007/978-3-030-10561-7>
- McAuley, A., Matheson, C., Robertson, J.R., 2022. From the clinic to the street: the changing role of benzodiazepines in the Scottish overdose epidemic. *Int. J. Drug Policy* 100.

<https://doi.org/10.1016/J.DRUGPO.2021.103512>

- McKernan, R.M., Rosahl, T.W., Reynolds, D.S., Sur, C., Wafford, K.A., Atack, J.R., Farrar, S., Myers, J., Cook, G., Ferris, P., Garrett, L., Bristow, L., Marshall, G., Macaulay, A., Brown, N., Howell, O., Moore, K.W., Carling, R.W., Street, L.J., Castro, J.L., Ragan, C.I., Dawson, G.R., Whiting, P.J., 2000. Sedative but not anxiolytic properties of benzodiazepines are mediated by the GABAA receptor  $\alpha 1$  subtype. *Nat. Neurosci.* 2000 36 3, 587–592. <https://doi.org/10.1038/75761>
- Medicines and Healthcare products Regulatory Agency, 2020. Benzodiazepines and opioids: reminder of risk of potentially fatal respiratory depression. [WWW Document]. URL <https://www.gov.uk/drug-safety-update/benzodiazepines-and-opioids-reminder-of-risk-of-potentially-fatal-respiratory-depression> (accessed 10.11.21).
- Michigan Poison Center, 2020. Michigan Poison Center issues warning about “purple heroin” - School of Medicine News - Wayne State University [WWW Document]. URL <https://today.wayne.edu/medicine/news/2020/10/14/michigan-poison-center-issues-warning-about-purple-heroin-40724> (accessed 9.19.22).
- Miliano, C., Margiani, G., Fattore, L., De Luca, M.A., 2018. Sales and advertising channels of new psychoactive substances (NPS): Internet, social networks, and smartphone apps. *Brain Sci.* <https://doi.org/10.3390/brainsci8070123>
- Miller, R., Gropper, M., 2019. *Miller’s Anesthesia*, 9th ed, El sevier España,.
- Moeller, K., Svensson, B., 2020. “Shop Until You Drop”: Valuing Fentanyl Analogs on a Swedish Internet Forum: <https://doi.org/10.1177/0022042620964129> 51, 181–195. <https://doi.org/10.1177/0022042620964129>
- Moosmann, B., Auwärter, V., 2018. Designer benzodiazepines: Another class of new psychoactive substances, in: *Handbook of Experimental Pharmacology*. Springer New York LLC, pp. 383–410. [https://doi.org/10.1007/164\\_2018\\_154](https://doi.org/10.1007/164_2018_154)
- Moosmann, B., Bisel, P., Franz, F., Huppertz, L.M., Auwärter, V., 2016. Characterization and in vitro phase I microsomal metabolism of designer benzodiazepines — an update comprising adinazolam, cloniprazepam, fonazepam, 3-hydroxyphenazepam, metizolam and nitrazolam. *J. Mass Spectrom.* 51, 1080–1089. <https://doi.org/10.1002/JMS.3840>
- Morbiato, E., Bilel, S., Tirri, M., Arfè, R., Fantinati, A., Savchuk, S., Appolonova, S., Frisoni, P., Tagliaro, F., Neri, M., Grignolio, S., Bertolucci, C., Marti, M., 2020. Potential of the zebrafish model for the forensic toxicology screening of NPS: A comparative study of the effects of APINAC and methiopropamine on the behavior of zebrafish larvae and mice. *Neurotoxicology* 78, 36–46. <https://doi.org/10.1016/J.NEURO.2020.02.003>

- Móro, L., Simon, K., Bárd, I., Rácz, J., 2011. Voice of the psychonauts: Coping, life purpose, and spirituality in psychedelic drug users. *J. Psychoactive Drugs* 43, 188–198. <https://doi.org/10.1080/02791072.2011.605661>
- Morris, G.M., Lim-Wilby, M., 2008. Molecular docking. *Methods Mol. Biol.* 443, 365–382. [https://doi.org/10.1007/978-1-59745-177-2\\_19](https://doi.org/10.1007/978-1-59745-177-2_19)
- Musto, D.F., 1973. American disease - Origins of narcotic control| Office of Justice Programs. Yale University Press Address New Haven CT 06520, United States.
- Myint, K.Z., Xie, X.Q., 2010. Recent advances in fragment-based QSAR and multi-dimensional QSAR methods. *Int. J. Mol. Sci.* 11, 3846–3866. <https://doi.org/10.3390/ijms11103846>
- Napoletano, F., Schifano, F., Corkery, J., Guirguis, A., Arillotta, D., Zangani, C., Vento, A., 2020. The psychonauts' world of cognitive enhancers. *Front. psychiatry* 11. <https://doi.org/10.3389/FPSYT.2020.546796>
- National Institute on Drug Abuse (NIDA), 2021. Benzodiazepines and Opioids [WWW Document]. URL <https://www.drugabuse.gov/drug-topics/opioids/benzodiazepines-opioids> (accessed 11.16.21).
- National Records of Scotland, 2021. Drug-related deaths in Scotland in 2020, Report.
- Navaratnam, V., Foong, K., 2008. Opiate dependence—the role of benzodiazepines. <http://dx.doi.org/10.1185/03007999009112688> 11, 620–630. <https://doi.org/10.1185/03007999009112688>
- Negus, S.S., Freeman, K.B., 2018. Abuse Potential of Biased Mu Opioid Receptor Agonists. *Trends Pharmacol. Sci.* 39, 916. <https://doi.org/10.1016/J.TIPS.2018.08.007>
- Neilan, C.L., Husbands, S.M., Breeden, S., Ko, M.C., Aceto, M.D., Lewis, J.W., Woods, J.H., Traynor, J.R., 2004. Characterization of the complex morphinan derivative BU72 as a high efficacy, long-lasting mu-opioid receptor agonist. *Eur. J. Pharmacol.* 499, 107–116. <https://doi.org/10.1016/J.EJPHAR.2004.07.097>
- Netzeva, T.I., Worth, A.P., Aldenberg, T., Benigni, R., Cronin, M.T.D., Gramatica, P., Jaworska, J.S., Kahn, S., Klopman, G., Marchant, C.A., Myatt, G., Nikolova-Jeliazkova, N., Patlewicz, G.Y., Perkins, R., Roberts, D.W., Schultz, T.W., Stanton, D.T., Van De Sandt, J.J.M., Tong, W., Veith, G., Yang, C., 2005. Current status of methods for defining the applicability domain of (quantitative) structure-activity relationships. The report and recommendations of ECVAM Workshop 52. *Altern. Lab. Anim.* 33, 155–173. <https://doi.org/10.1177/026119290503300209>
- Neubig, R.R., Spedding, M., Kenakin, T., Christopoulos, A., 2003. International Union of Pharmacology Committee on Receptor Nomenclature and Drug Classification. XXXVIII. Update on Terms and Symbols in Quantitative Pharmacology.

<https://doi.org/10.1124/pr.55.4.4>

- Ng, H.W., Zhang, W., Shu, M., Luo, H., Ge, W., Perkins, R., Tong, W., Hong, H., 2014. Competitive molecular docking approach for predicting estrogen receptor subtype  $\alpha$  agonists and antagonists. *BMC Bioinformatics* 15, 1–15. <https://doi.org/10.1186/1471-2105-15-S11-S4/TABLES/8>
- Nishimura, H., Uno, H., Natsuka, K., Shimokawa, N., Shimizu, M., Nakamura, H., 1976. 1-substituted-4-(1,2-diphenylethyl)piperazine derivatives and their salts and the preparation thereof. US3957788A.
- Noha, S.M., Schmidhammer, H., Spetea, M., 2017. Molecular Docking, Molecular Dynamics, and Structure–Activity Relationship Explorations of 14-Oxygenated N-Methylmorphinan-6-ones as Potent  $\mu$ -Opioid Receptor Agonists. *ACS Chem. Neurosci.* 8, 1327. <https://doi.org/10.1021/ACSCHEMNEURO.6B00460>
- NPSdiscovery, 2022. Trend Report: Q2 2022 NPS Benzodiazepines in the United States.
- NPSdiscovery, 2021. Trend Report: Q4 2021 NPS Benzodiazepines in the United States.
- O’Boyle, N.M., 2012. Towards a Universal SMILES representation - A standard method to generate canonical SMILES based on the InChI. *J. Cheminform.* 4, 22. <https://doi.org/10.1186/1758-2946-4-22>
- O’Boyle, N.M., Banck, M., James, C.A., Morley, C., Vandermeersch, T., Hutchison, G.R., 2011. Open Babel: An Open chemical toolbox. *J. Cheminform.* 3, 33. <https://doi.org/10.1186/1758-2946-3-33>
- O’Boyle, N.M., Sayle, R.A., 2016. Comparing structural fingerprints using a literature-based similarity benchmark. *J. Cheminform.* 8, 1–14. <https://doi.org/10.1186/S13321-016-0148-0/FIGURES/11>
- OECD, 2007. Guidance Document on the Validation of (Quantitative) Structure-Activity Relationship [(Q)SAR] Models, OECD Series on Testing and Assessment. OECD, Paris. <https://doi.org/10.1787/9789264085442-en>
- Olson, K.M., Duron, D.I., Womer, D., Fell, R., Streicher, J.M., 2019. Comprehensive molecular pharmacology screening reveals potential new receptor interactions for clinically relevant opioids. *PLoS One* 14, e0217371. <https://doi.org/10.1371/JOURNAL.PONE.0217371>
- Orsolini, L., Chiappini, S., Corkery, J.M., Guirguis, A., Papanti, D., Schifano, F., 2019. The use of new psychoactive substances (NPS) in young people and their role in mental health care: a systematic review. *Expert Rev. Neurother.* 19, 1253–1264. <https://doi.org/10.1080/14737175.2019.1666712>
- Orsolini, L., Corkery, J.M., Chiappini, S., Guirguis, A., Vento, A., De Berardis, D., Papanti, D.,

- Schifano, F., 2020. "New/Designer Benzodiazepines": an analysis of the literature and psychonauts' trip reports. *Curr. Neuropharmacol.* 18(9), 809–837. <https://doi.org/10.2174/1570159X18666200110121333>
- Orsolini, L., Francesconi, G., Papanti, D., Giorgetti, A., Schifano, F., 2015a. Profiling online recreational/prescription drugs' customers and overview of drug vending virtual marketplaces. *Hum. Psychopharmacol.* 30, 302–318. <https://doi.org/10.1002/hup.2466>
- Orsolini, L., Papanti, D., Corkery, J., Schifano, F., 2017a. An insight into the deep web; why it matters for addiction psychiatry? *Hum. Psychopharmacol.* 32. <https://doi.org/10.1002/hup.2573>
- Orsolini, L., Papanti, G.D., Francesconi, G., Schifano, F., 2015b. Mind Navigators of Chemicals' Experimenters? A Web-Based Description of E-Psychonauts. *Cyberpsychology, Behav. Soc. Netw.* 18, 296–300. <https://doi.org/10.1089/cyber.2014.0486>
- Orsolini, L., Papanti, G.D., Francesconi, G., Schifano, F., 2015c. Navigating in the Virtual Mind of the Web': the E-psychonauts' Profiling. *Eur. Psychiatry* 30, 1045. [https://doi.org/10.1016/s0924-9338\(15\)30822-1](https://doi.org/10.1016/s0924-9338(15)30822-1)
- Orsolini, L., St John-Smith, P., McQueen, D., Papanti, D., Corkery, J.M., Schifano, F., 2017b. Evolutionary considerations on the emerging subculture of the e-psychonauts and the novel psychoactive substances: a comeback to the shamanism? *Curr. Neuropharmacol.* 15. <https://doi.org/10.2174/1570159x15666161111114838>
- Pardo, B., Taylor, J., Caulkins, J.P., Kilmer, B., Reuter, P., Stein, B.D., 2019. The Future of Fentanyl and Other Synthetic Opioids. *Futur. Fentanyl Other Synth. Opioids.* <https://doi.org/10.7249/RR3117>
- Pasternak, G.W., Pan, Y.X., 2013. Mu Opioids and Their Receptors: Evolution of a Concept. *Pharmacol. Rev.* 65, 1257. <https://doi.org/10.1124/PR.112.007138>
- Patil, V., Tewari, A., Rao, R., 2016. New psychoactive substances: Issues and challenges. *J. Ment. Heal. Hum. Behav.* 21, 98. <https://doi.org/10.4103/0971-8990.193427>
- Paton, K., Atigari, D., Kaska, S., Prisinzano, T.E., Kivell, B.M., 2020. Strategies for developing kappa opioid receptor agonists for the treatment of pain with fewer side-effects. *J. Pharmacol. Exp. Ther.* 375, 332–348. <https://doi.org/10.1124/JPET.120.000134>
- PerkinElmer Informatics, 2022. ChemDraw - Chemical Drawing Software.
- Pizziketti, R.J., Pressman, N.S., Geller, E.B., Cowan, A., Adler, M.W., 1985. Rat cold water tail-flick: A novel analgesic test that distinguishes opioid agonists from mixed agonist-antagonists. *Eur. J. Pharmacol.* 119, 23–29. [https://doi.org/10.1016/0014-2999\(85\)90317-6](https://doi.org/10.1016/0014-2999(85)90317-6)
- Pletnev, I., Erin, A., McNaught, A., Blinov, K., Tchekhovskoi, D., Heller, S., 2012. InChIKey



- collision resistance: An experimental testing. *J. Cheminform.* 4. <https://doi.org/10.1186/1758-2946-4-39>
- Poisnel, G., Dhilly, M., Le Boisselier, R., Barre, L., Debruyne, D., 2009. Comparison of five benzodiazepine-receptor agonists on buprenorphine- induced  $\mu$ -opioid receptor regulation. *J. Pharmacol. Sci.* 110, 36–46. <https://doi.org/10.1254/JPHS.08249FP>
- Poklis, J., Poklis, A., Wolf, C., Hathaway, C., Arbefeville, E., Chrostowski, L., Devers, K., Hair, L., Mainland, M., Merves, M., Pearson, J., 2016. Two Fatal Intoxications Involving Butyryl Fentanyl. *J. Anal. Toxicol.* 40, 703. <https://doi.org/10.1093/JAT/BKW048>
- Policy, N.D., 2015. National drug control strategy 2015.
- Popova, M., Isayev, O., Tropsha, A., 2018. Deep reinforcement learning for de novo drug design. *Sci. Adv.* 4. <https://doi.org/10.1126/sciadv.aap7885>
- Portoghese, P.S., 1992. The Role of Concepts in Structure-Activity Relationship Studies of Opioid Ligands. *J. Med. Chem.* 35, 1927–1937. [https://doi.org/10.1021/JM00089A001/ASSET/JM00089A001.FP.PNG\\_V03](https://doi.org/10.1021/JM00089A001/ASSET/JM00089A001.FP.PNG_V03)
- Prekupec, M.P., Mansky, P.A., Baumann, M.H., 2017. Misuse of Novel Synthetic Opioids: A Deadly New Trend. *J. Addict. Med.* 11, 256. <https://doi.org/10.1097/ADM.0000000000000324>
- Primeaux, S.D., Wilson, S.P., McDonald, A.J., Mascagni, F., Wilson, M.A., 2006. The role of delta opioid receptors in the anxiolytic actions of benzodiazepines. *Pharmacol. Biochem. Behav.* 85, 545. <https://doi.org/10.1016/J.PBB.2006.09.025>
- Prost-Marechal, J., 1982. Imidazobenzodiazepines and their salt. DE 3211243 A1 19821007. PubChem [WWW Document], 2021. URL <https://pubchem.ncbi.nlm.nih.gov/> (accessed 1.24.21).
- Public Health England, 2020. Evidence of harm from illicit or fake benzodiazepines.
- PubMed, 2020. PubMed [WWW Document]. URL <https://pubmed.ncbi.nlm.nih.gov/> (accessed 9.28.20).
- Quintero, G., Bundy, H., 2011. “Most of the time you already Know”: Pharmaceutical information assembly by young adults on the internet. *Subst. Use Misuse* 46, 898–909. <https://doi.org/10.3109/10826084.2011.570630>
- Radinov, R.N., Khaimova, M.A., Simova, E.M., 1984. 4H-pyrido[3,4-f]-1,2,4-triazolo[4,3-a]-1,4-diazepine — A new heterocyclic system. *Chem. Heterocycl. Compd.* 1984 202 20, 229–229. <https://doi.org/10.1007/BF00506304>
- Raffa, R.B., Jr, J.V.P., Ba, J.A.L., Jr, R.T., 2017. The fentanyl family : A distinguished medical history tainted by abuse 154–158. <https://doi.org/10.1111/jcpt.12640>
- Ramírez, D., 2016. Computational Methods Applied to Rational Drug Design. *Open Med. Chem. J.* 10, 7–20. <https://doi.org/10.2174/1874104501610010007>

- Ramírez, D., Caballero, J., 2018. Is It Reliable to Take the Molecular Docking Top Scoring Position as the Best Solution without Considering Available Structural Data? *Molecules* 23. <https://doi.org/10.3390/MOLECULES23051038>
- Rattan, A., McDonald, J., Tejwani, G., 1991. Differential effects of intrathecal midazolam on morphine-induced antinociception in the rat: role of spinal opioid receptors. *Anesth. Analg.* 73, 124–131. <https://doi.org/10.1213/00000539-199108000-00004>
- Rausand, M., Haugen, S., 2020. *Risk Assessment: Theory, Methods, and Applications*, 2nd Edition, 2nd ed, Risk Management. Wiley.
- Rauschert, C., Seitz, N.N., Olderbak, S., Pogarell, O., Dreischulte, T., Kraus, L., 2022. Abuse of Non-opioid Analgesics in Germany: Prevalence and Associations Among Self-Medicated Users. *Front. Psychiatry* 13, 589. <https://doi.org/10.3389/FPSYT.2022.864389/BIBTEX>
- Raval, K., Ganatra, T., 2022. Basics, types and applications of molecular docking: A review. *IP Int. J. Compr. Adv. Pharmacol.* 7, 12–16. <https://doi.org/10.18231/J.IJCAAP.2022.003>
- RCSB PDB: Homepage [WWW Document], 2021. URL <https://www.rcsb.org/> (accessed 2.4.21).
- RCSB PDB, 2020. 6X3X: Human GABAA receptor alpha1-beta2-gamma2 subtype in complex with GABA plus diazepam [WWW Document]. URL <https://www.rcsb.org/structure/6X3X> (accessed 8.2.22).
- RCSB PDB, 2019. 6PT3: Crystal structure of the active delta opioid receptor in complex with the small molecule agonist DPI-287 [WWW Document]. URL <https://www.rcsb.org/structure/6PT3> (accessed 10.12.21).
- RCSB PDB, 2018a. 6HUP: CryoEM structure of human full-length alpha1beta3gamma2L GABA(A)R in complex with diazepam (Valium), GABA and megabody Mb38. [WWW Document]. URL <https://www.rcsb.org/structure/6HUP> (accessed 3.8.21).
- RCSB PDB, 2018b. 6HUO: CryoEM structure of human full-length heteromeric alpha1beta3gamma2L GABA(A)R in complex with alprazolam (Xanax), GABA and megabody Mb38. [WWW Document]. URL <https://www.rcsb.org/structure/6HUO> (accessed 3.8.21).
- RCSB PDB, 2018c. 6D6U: Human GABA-A receptor alpha1-beta2-gamma2 subtype in complex with GABA and flumazenil, conformation A [WWW Document]. URL <https://www.rcsb.org/structure/6D6U> (accessed 8.2.22).
- RCSB PDB, 2018d. 6B73: Crystal Structure of a nanobody-stabilized active state of the kappa-opioid receptor [WWW Document]. URL <https://www.rcsb.org/structure/6B73> (accessed 10.12.21).
- RCSB PDB, 2015. 5C1M: Crystal structure of active mu-opioid receptor bound to the agonist

- BU72 [WWW Document]. URL <https://www.rcsb.org/structure/5C1M> (accessed 10.12.21).
- reddit, 2021a. reddit: the front page of the internet [WWW Document]. URL <https://www.reddit.com/> (accessed 10.8.20).
- reddit, 2021b. Fluclotizolam: first time review : researchchemicals [WWW Document]. URL [https://www.reddit.com/r/researchchemicals/comments/q9nb1m/fluclotizolam\\_first\\_time\\_review/](https://www.reddit.com/r/researchchemicals/comments/q9nb1m/fluclotizolam_first_time_review/) (accessed 8.26.22).
- reddit, 2020. Experiences with 3-Hydroxyphenazepam? : researchchemicals [WWW Document]. URL [https://www.reddit.com/r/researchchemicals/comments/sdi5d3/experiences\\_with\\_3hydroxyphenazepam/](https://www.reddit.com/r/researchchemicals/comments/sdi5d3/experiences_with_3hydroxyphenazepam/) (accessed 8.31.22).
- reddit, 2018a. God Damn Clonazepam Part Three : researchchemicals [WWW Document]. URL [https://www.reddit.com/r/researchchemicals/comments/a0eltx/god\\_damn\\_clonazepam\\_part\\_three/](https://www.reddit.com/r/researchchemicals/comments/a0eltx/god_damn_clonazepam_part_three/) (accessed 8.26.22).
- reddit, 2018b. Benzodiazepines (Etizolam, Diclazepam, Clonazepam, Flubromazepam, Flunitrazepam, Pyrazepam etc.) discussion thread : researchchemicals [WWW Document]. URL [https://www.reddit.com/r/researchchemicals/comments/7yb9rz/benzodiazepines\\_etizolam\\_diclazepam\\_clonazepam/](https://www.reddit.com/r/researchchemicals/comments/7yb9rz/benzodiazepines_etizolam_diclazepam_clonazepam/) (accessed 8.26.22).
- reddit, 2018c. 3-Hydroxyphenazepam: A report : researchchemicals [WWW Document]. URL [https://www.reddit.com/r/researchchemicals/comments/8w5ze7/3hydroxyphenazepam\\_a\\_report/](https://www.reddit.com/r/researchchemicals/comments/8w5ze7/3hydroxyphenazepam_a_report/) (accessed 8.26.22).
- reddit, 2018d. Anyone have experience with r30490 aka 4 methoxymethylfentanyl? : fentanyl [WWW Document]. URL [https://www.reddit.com/r/fentanyl/comments/9hbib5/anyone\\_have\\_experience\\_with\\_r30490\\_aka\\_4/](https://www.reddit.com/r/fentanyl/comments/9hbib5/anyone_have_experience_with_r30490_aka_4/) (accessed 10.3.22).
- reddit, 2017. Floclotizolam Report : researchchemicals [WWW Document]. URL [https://www.reddit.com/r/researchchemicals/comments/7214iw/floclotizolam\\_report/](https://www.reddit.com/r/researchchemicals/comments/7214iw/floclotizolam_report/) (accessed 8.26.22).
- Reddy, S., Patt, R.B., 1994. The benzodiazepines as adjuvant analgesics. *J. Pain Symptom Manage.* 9, 510–514. [https://doi.org/10.1016/0885-3924\(94\)90112-0](https://doi.org/10.1016/0885-3924(94)90112-0)
- Reich, S.H., Webber, S.E., 1993. Structure-based drug design (SBDD): Every structure tells a story... *Perspect. Drug Discov. Des.* 1, 371–390. <https://doi.org/10.1007/BF02174536>
- Richardson, D.K., Reynolds, S.M., Cooper, S.J., Berridge, K.C., 2005. Opioid agonists and benzodiazepine agonists each increase food intake. Both also increase hedonic “liking”

- reactions to sweet tastes in rats. Do opioids and benzodiazepines share overlapping mechanisms of hedonic impact? *Pharmacol. Biochem. Behav.* 81, 657–663. <https://doi.org/10.1016/J.PBB.2005.05.006>
- Richter, L., De Graaf, C., Sieghart, W., Varagic, Z., Mörzinger, M., De Esch, I.J.P., Ecker, G.F., Ernst, M., 2012. Diazepam-bound GABAA receptor models identify new benzodiazepine binding-site ligands. *Nat. Chem. Biol.* 8, 455. <https://doi.org/10.1038/NCHEMBIO.917>
- Rosenblum, A., Marsch, L.A., Joseph, H., Portenoy, R.K., 2008. Opioids and the Treatment of Chronic Pain: Controversies, Current Status, and Future Directions. *Exp. Clin. Psychopharmacol.* 16, 405. <https://doi.org/10.1037/A0013628>
- Roy, K., Das, R.N., Ambure, P., Aher, R.B., 2016. Be aware of error measures. Further studies on validation of predictive QSAR models. *Chemom. Intell. Lab. Syst.* 152, 18–33. <https://doi.org/10.1016/j.chemolab.2016.01.008>
- Roy, K., Kar, S., Ambure, P., 2015a. On a simple approach for determining applicability domain of QSAR models. *Chemom. Intell. Lab. Syst.* 145, 22–29. <https://doi.org/10.1016/J.CHEMOLAB.2015.04.013>
- Roy, K., Kar, S., Das, R.N., 2015b. Introduction to 3D-QSAR. *Underst. Basics QSAR Appl. Pharm. Sci. Risk Assess.* 291–317. <https://doi.org/10.1016/B978-0-12-801505-6.00008-9>
- Rudolph, U., Crestani, F., Benke, D., Brünig, I., Benson, J.A., Fritschy, J.M., Martin, J.R., Bluethmann, H., Möhler, H., 1999. Benzodiazepine actions mediated by specific  $\gamma$ -aminobutyric acid(A) receptor subtypes. *Nature* 401, 796–800. <https://doi.org/10.1038/44579>
- Saha, K., Partilla, J.S., Lehner, K.R., Seddik, A., Stockner, T., Holy, M., Sandtner, W., Ecker, G.F., Sitte, H.H., Baumann, M.H., 2015. “Second-Generation” Mephedrone Analogs, 4-MEC and 4-MePPP, Differentially Affect Monoamine Transporter Function. *Neuropsychopharmacology* 40, 1321–1331. <https://doi.org/10.1038/NPP.2014.325>
- Sahigara, F., Mansouri, K., Ballabio, D., Mauri, A., Consonni, V., Todeschini, R., 2012. Comparison of different approaches to define the applicability domain of QSAR models. *Molecules* 17, 4791–4810. <https://doi.org/10.3390/MOLECULES17054791>
- Sanburn, J., 2016. Heroin is being laced with a terrifying substance what to know about carfentanil [WWW Document]. URL <https://time.com/4485792/heroin-carfentanil-drugs-ohio/> (accessed 9.24.22).
- Sanchis-Segura, C., Spanagel, R., 2006. Behavioural assessment of drug reinforcement and addictive features in rodents: an overview. *Addict. Biol.* 11, 2–38. <https://doi.org/10.1111/J.1369-1600.2006.00012.X>
- Schifano, F., 2018. Recent changes in drug abuse scenarios: The new/novel psychoactive

substances (NPS) phenomenon. *Brain Sci.* <https://doi.org/10.3390/brainsci8120221>

- Schifano, F., Corazza, O., Deluca, P., Davey, Z., Furia, L. Di, Farre', M., Flesland, L., Mannonen, M., Pagani, S., Peltoniemi, T., Pezzolesi, C., Scherbaum, N., Siemann, H., Skutle, A., Torrens, M., Kreeft, P. Van Der, 2009. Psychoactive drug or mystical incense? Overview of the online available information on Spice products. <http://dx.doi.org/10.1080/17542860903350888> 2, 137–144. <https://doi.org/10.1080/17542860903350888>
- Schifano, F., Deluca, P., Baldacchino, A., Peltoniemi, T., Scherbaum, N., Torrens, M., Farrè, M., Flores, I., Rossi, M., Eastwood, D., Guionnet, C., Rawaf, S., Agosti, L., Di Furia, L., Brigada, R., Majava, A., Siemann, H., Leoni, M., Tomasin, A., Rovetto, F., Ghodse, A.H., 2006. Drugs on the web; the Psychonaut 2002 EU project. *Prog. Neuro-Psychopharmacology Biol. Psychiatry* 30, 640–646. <https://doi.org/10.1016/j.pnpbp.2005.11.035>
- Schifano, F., Leoni, M., Martinotti, G., Rawaf, S., Rovetto, F., 2003. Importance of cyberspace for the assessment of the drug abuse market: Preliminary results from the Psychonaut 2002 project. *Cyberpsychology Behav.* 6, 405–410. <https://doi.org/10.1089/109493103322278790>
- Schifano, F., Napoletano, F., Arillotta, D., Zangani, C., Gilgar, L., Guirguis, A., Corkery, J.M., Vento, A., 2020. The clinical challenges of synthetic cathinones. *Br. J. Clin. Pharmacol.* <https://doi.org/10.1111/bcp.14132>
- Schifano, F., Napoletano, F., Chiappini, S., Guirguis, A., Corkery, J.M., Bonaccorso, S., Ricciardi, A., Scherbaum, N., Vento, A., 2019a. New/emerging psychoactive substances and associated psychopathological consequences. *Psychol. Med.* 51, 30–42. <https://doi.org/10.1017/S0033291719001727>
- Schifano, F., Napoletano, F., Chiappini, S., Orsolini, L., Guirguis, A., Corkery, J.M., Bonaccorso, S., Ricciardi, A., Scherbaum, N., Vento, A., 2019b. New Psychoactive Substances (NPS), Psychedelic Experiences and Dissociation: Clinical and Clinical Pharmacological Issues. *Curr. Addict. Reports* 6, 140–152. <https://doi.org/10.1007/s40429-019-00249-z>
- Schifano, F., Orsolini, L., Duccio Papanti, G., Corkery, J.M., 2015. Novel psychoactive substances of interest for psychiatry. *World Psychiatry* 14, 15–26. <https://doi.org/10.1002/wps.20174>
- Schmidle, C.J., Mansfield, R., 1954. US2765314A Preparation of esters.
- Schmidt, M.M., Sharma, A., Schifano, F., Feinmann, C., 2011. “Legal highs” on the net-Evaluation of UK-based Websites, products and product information. *Forensic Sci. Int.* 206, 92–97. <https://doi.org/10.1016/j.forsciint.2010.06.030>
- Schneider, G., Neidhart, W., Giller, T., Schmid, G., 1999. “Scaffold-Hopping” by topological pharmacophore search: A contribution to virtual screening. *Angew. Chemie - Int. Ed.* 38, 2894–2896. [https://doi.org/10.1002/\(SICI\)1521-3773\(19991004\)38:19<2894::AID-](https://doi.org/10.1002/(SICI)1521-3773(19991004)38:19<2894::AID-)

ANIE2894>3.0.CO;2-F

Schulze-Alexandru, M., Kovar, K.-A., Vedani, A., 1999. Quasi-atomistic Receptor Surrogates for the 5-HT<sub>2A</sub> Receptor: A 3D-QSAR Study on Hallucinogenic Substances. *Mol. Inform.* 18, 548–560. [https://doi.org/10.1002/\(SICI\)1521-3838\(199912\)18:6<548::AID-QSAR548>3.0.CO;2-B](https://doi.org/10.1002/(SICI)1521-3838(199912)18:6<548::AID-QSAR548>3.0.CO;2-B)

QSAR548>3.0.CO;2-B

Schumacher, M., Basbaum, A., Naidu, R., 2017. Opioid Agonists & Antagonists, in: Bertram, E., Katzung, B. (Eds.), *Asic & Clinical Pharmacology*.

Scottish Government, 2022. Benzodiazepine use - current trends: evidence review - gov.scot.

Sertürner, F., 1817. Analyse de l'Opium. De la Morphine et de l'Acide méconique, considérés comme parties essentielles de l'Opium. *Ann. Chim. Phys.* 5, 21–42.

Seyler, T., Giraudon, I., Noor, A., Mounteney, J., Griffiths, P., 2021. Is Europe facing an opioid epidemic: What does European monitoring data tell us. *Eur. J. pain.*

Shafie, A., Mohammadi-Khanaposhtani, M., Asadi, M., Rahimi, N., Ranjbar, P.R., Ghasemi, J.B., Larijani, B., Mahdavi, M., Shafaroodi, H., Dehpour, A.R., 2019. Novel fused 1,2,3-triazolo-benzodiazepine derivatives as potent anticonvulsant agents: design, synthesis, in vivo, and in silico evaluations. *Mol. Divers.* 2019 241 24, 179–189. <https://doi.org/10.1007/S11030-019-09940-9>

Shang, Y., Filizola, M., 2015. Opioid receptors: Structural and mechanistic insights into pharmacology and signaling. *Eur. J. Pharmacol.* 763, 206–213. <https://doi.org/10.1016/J.EJPHAR.2015.05.012>

Sharma, K.K., Hales, T.G., Vaidya, ., Rao, J., Nicdaeid, N., Mckenzie, C., 2019. The search for the “next” euphoric non-fentanil novel synthetic opioids on the illicit drugs market: current status and horizon scanning 37, 1–16. <https://doi.org/10.1007/s11419-018-0454-5>

Shim, J., Coop, A., Mackerell, A.D., 2013. Molecular details of the activation of the  $\mu$  opioid receptor. *J. Phys. Chem. B* 117, 7907–7917. <https://doi.org/10.1021/JP404238N>

Shim, J., Coop, A., MacKerell, J.A.D., 2011. Consensus 3D Model of  $\mu$ -Opioid Receptor Ligand Efficacy Based on a Quantitative Conformationally Sampled Pharmacophore. *J. Phys. Chem. B* 115, 7487–7496. <https://doi.org/10.1021/JP202542G>

Shim, J., MacKerell, A.D., 2011. Computational ligand-based rational design: Role of conformational sampling and force fields in model development. *Medchemcomm.* <https://doi.org/10.1039/c1md00044f>

Sigel, E., Ernst, M., 2018. The Benzodiazepine Binding Sites of GABA<sub>A</sub> Receptors. *Trends Pharmacol. Sci.* 39, 659–671. <https://doi.org/10.1016/j.tips.2018.03.006>

Sigel, E., P. Luscher, B., 2012. A Closer Look at the High Affinity Benzodiazepine Binding Site on

- GABAA Receptors. *Curr. Top. Med. Chem.* 11, 241–246.  
<https://doi.org/10.2174/156802611794863562>
- Sigel, E., Schaerer, M.T., Buhr, A., Baur, R., 1998. The benzodiazepine binding pocket of recombinant  $\alpha 1\beta 2\gamma 2$   $\gamma$ -aminobutyric acid(A) receptors: Relative orientation of ligands and amino acid side chains. *Mol. Pharmacol.* 54, 1097–1105.  
<https://doi.org/10.1124/mol.54.6.1097>
- Simeone, X., Koniuszewski, F., Müllegger, M., Smetka, A., Steudle, F., Puthenkalam, R., Ernst, S., M., Scholze, P., 2020. A benzodiazepine ligand with improved GABA A receptor  $\alpha 5$ -subunit-selectivity driven by interactions with loop C. *Mol. Pharmacol. Fast Forw.*  
<https://doi.org/10.1124/molpharm.120.000067>
- Singh, N., Nolan, T., McCurdy, C., 2008. Chemical function-based pharmacophore development for novel, selective kappa opioid receptor agonists. *J. Mol. Graph. Model.* 27, 131–139.  
<https://doi.org/10.1016/J.JMGM.2008.03.007>
- Sliwoski, G., Kothiwale, S., Meiler, J., Lowe, E.W., 2014. Computational Methods in Drug Discovery. *Pharmacol. Rev.* 66, 334. <https://doi.org/10.1124/PR.112.007336>
- Soga, S., Shirai, H., Koborv, M., Hirayama, N., 2007. Use of amino acid composition to predict ligand-binding sites. *J. Chem. Inf. Model.* 47, 400–406. <https://doi.org/10.1021/ci6002202>
- Solimini, R., Pichini, S., Pacifici, R., Busardò, F.P., Giorgetti, R., 2018. Pharmacotoxicology of non-fentanyl derived new synthetic opioids. *Front. Pharmacol.* 9, 654.  
<https://doi.org/10.3389/FPHAR.2018.00654/BIBTEX>
- SourceForge, 2016. Open Babel 2.4.0.
- Soussan, C., Kjellgren, A., 2016. The users of Novel Psychoactive Substances: Online survey about their characteristics, attitudes and motivations. *Int. J. Drug Policy* 32, 77–84.  
<https://doi.org/10.1016/J.DRUGPO.2016.03.007>
- Spadaro, A., Sarker, A., Hogg-Bremer, W., Love, J.S., O'Donnell, N., Nelson, L.S., Perrone, J., 2022. Reddit discussions about buprenorphine associated precipitated withdrawal in the era of fentanyl. *Clin. Toxicol.* 60, 694–701.  
[https://doi.org/10.1080/15563650.2022.2032730/SUPPL\\_FILE/ICTX\\_A\\_2032730\\_SM2318.DOCX](https://doi.org/10.1080/15563650.2022.2032730/SUPPL_FILE/ICTX_A_2032730_SM2318.DOCX)
- Spanagel, R., 2017. Animal models of addiction. *Dialogues Clin. Neurosci.* 19, 247.  
<https://doi.org/10.31887/DCNS.2017.19.3/RSPANAGEL>
- Sparling, B.A., DiMauro, E.F., 2017. Progress in the discovery of small molecule modulators of the Cys-loop superfamily receptors. *Bioorg. Med. Chem. Lett.* 27, 3207–3218.  
<https://doi.org/10.1016/J.BMCL.2017.04.073>

- Specka, M., Kuhlmann, T., Bonnet, U., Sawazki, J., Schaaf, L., Kühnhold, S., Steinert, R., Grigoleit, T., Eich, H., Zeiske, B., Niedersteberg, A., Steiner, K., Schifano, F., Scherbaum, N., 2022. Novel Synthetic Opioids (NSO) Use in Opioid Dependents Entering Detoxification Treatment. *Front. Psychiatry* 0, 933. <https://doi.org/10.3389/FPSYT.2022.868346>
- Stamenić, T.T., Poe, M.M., Rehman, S., Santrač, A., Divović, B., Scholze, P., Ernst, M., Cook, J.M., Savić, M.M., 2016. Ester to amide substitution improves selectivity, efficacy and kinetic behavior of a benzodiazepine positive modulator of GABA A receptors containing the  $\alpha 5$  subunit. *Eur. J. Pharmacol.* 791, 433–443. <https://doi.org/10.1016/J.EJPHAR.2016.09.016>
- Stanley, T.H., 1992. The history and development of the fenatnyl series. *J. Pain Symptom Manag.* 7.
- Sterling, T., Irwin, J.J., 2015. ZINC 15 - Ligand Discovery for Everyone. *J. Chem. Inf. Model.* 55, 2324–2337. <https://doi.org/10.1021/acs.jcim.5b00559>
- Sternbach, L.H., 1971. 1,4-benzodiazepines. Chemistry and some aspects of the structure-activity relationship. *Angew. Chem. Int. Ed. Engl.* 10, 34–43. <https://doi.org/10.1002/ANIE.197100341>
- Sternbach, L.H., Walser, A., 1972. Preparation of triazolo benzodiazepines - Patent US-3970664-A - PubChem.
- Stromgaard, K., Krosgaard-Larsen, P., Madsen, U., 2009. *Textbook of Drug Design and Discovery, Fourth Edition.* CRC Press.
- Subhash, C.B., Marjan, V., Apurba, K.B., 2015. Editorial: Big Data and New Drug Discovery: Tackling “Big Data” for Virtual Screening of Large Compound Databases. *Curr. Comput. Aided-Drug Des.* 11, 197–201. <https://doi.org/10.2174/157340991103151124190920>
- Subramanian, G., Paterlini, M.G., Portoghese, P.S., Ferguson, D.M., 2000. Molecular docking reveals a novel binding site model for fentanyl at the mu-opioid receptor. *J. Med. Chem.* 43, 381–391. <https://doi.org/10.1021/JM9903702>
- Sugiki, T., Kobayashi, N., Fujiwara, T., 2017. Modern Technologies of Solution Nuclear Magnetic Resonance Spectroscopy for Three-dimensional Structure Determination of Proteins Open Avenues for Life Scientists. *Comput. Struct. Biotechnol. J.* <https://doi.org/10.1016/j.csbj.2017.04.001>
- Sun, H., Tawa, G., Wallqvist, A., 2012. Classification of Scaffold Hopping Approaches. *Drug Discov. Today* 17, 310. <https://doi.org/10.1016/J.DRUDIS.2011.10.024>
- Suryanarayanan, V., Panwar, U., Chandra, I., Singh, S.K., 2018. De novo design of ligands using computational methods. *Methods Mol. Biol.* 1762, 71–86. [https://doi.org/10.1007/978-1-4939-7756-7\\_5/TABLES/3](https://doi.org/10.1007/978-1-4939-7756-7_5/TABLES/3)



- Svetnik, V., Liaw, A., Tong, C., Christopher Culberson, J., Sheridan, R.P., Feuston, B.P., 2003. Random Forest: A Classification and Regression Tool for Compound Classification and QSAR Modeling. *J. Chem. Inf. Comput. Sci.* 43, 1947–1958. <https://doi.org/10.1021/ci034160g>
- Swaan, P.W., Ekins, S., 2005. Reengineering the pharmaceutical industry by crash-testing molecules. *Drug Discov. Today* 10, 1191–1200. [https://doi.org/10.1016/S1359-6446\(05\)03557-9](https://doi.org/10.1016/S1359-6446(05)03557-9)
- Swanson, D.M., Hair, L.S., Rivers, S.R.S., Smyth, B.C., Brogan, S.C., Ventoso, A.D., Vaccaro, S.L., Pearson, J.M., 2017. Fatalities Involving Carfentanil and Furanyl Fentanyl: Two Case Reports. *J. Anal. Toxicol.* 41, 498–502. <https://doi.org/10.1093/JAT/BKX037>
- Szmuszkowicz, J., 1976. Analgesic n-(2-aminocycloaliphatic)benzamides. US4098904A.
- Tabarra, I., Soares, S., Rosado, T., Gonçalves, J., Luís, Â., Malaca, S., Barroso, M., Keller, T., Restolho, J., Gallardo, E., 2019. Novel synthetic opioids—toxicological aspects and analysis. *Forensic Sci. Res.* <https://doi.org/10.1080/20961790.2019.1588933>
- Tan, K.R., Rudolph, U., Lüscher, C., 2011. Hooked on benzodiazepines: GABAA receptor subtypes and addiction. *Trends Neurosci.* 34, 188–197. <https://doi.org/10.1016/j.tins.2011.01.004>
- Tanimoto, T.T., 1958. An Elementary Mathematical theory of Classification and Prediction. New York.
- Thakur, M., Thakur, A., Sudele, P., 2004. Comparative QSAR and QPAR study of benzodiazepines. *Indian J. Chem.* 43, 976–982.
- The Commission on Narcotic Drugs, 2018. Decision 61/1 Inclusion of carfentanil in Schedules I and IV of the Single Convention on Narcotic Drugs of 1961 as amended by the 1972 Protocol .
- Theriot, J., Sabir, S., Azadfard, M., 2022. Opioid Antagonists.
- Tricklebank, M.D., Honore, T., Iversen, S.D., Kemp, J.A., Knight, A.R., Marshall, G.R., Rupniak, N.M.J., Singh, L., Tye, S., Watjen, F., Wong, E.H.F., 1990. The pharmacological properties of the imidazobenzodiazepine, FG 8205, a novel partial agonist at the benzodiazepine receptor. *Br. J. Pharmacol.* 101, 753–761. <https://doi.org/10.1111/J.1476-5381.1990.TB14152.X>
- Tropsha, A., 2010. Best Practices for QSAR Model Development, Validation, and Exploitation. *Mol. Inform.* 29, 476–488. <https://doi.org/10.1002/minf.201000061>
- Tropsha, A., 2007. Predictive Quantitative Structure–Activity Relationship Modeling. *Compr. Med. Chem. II* 4, 149–165. <https://doi.org/10.1016/B0-08-045044-X/00248-0>
- Tseng, K.S., 2018. Considerations in 2017–2018 for the Use of Opioids in Non-terminal Pain. *Curr. Anesthesiol. Reports* 2018 84 8, 342–347. <https://doi.org/10.1007/S40140-018-0289-Y>
- Tsuda, M., Suzuki, T., Misawa, M., Nagase, H., 1996. Involvement of the opioid system in the

- anxiolytic effect of diazepam in mice. *Eur. J. Pharmacol.* 307, 7–14.  
[https://doi.org/10.1016/0014-2999\(96\)00219-1](https://doi.org/10.1016/0014-2999(96)00219-1)
- Tuccinardi, T., Ferrarini, P.L., Manera, C., Ortore, G., Saccomanni, G., Martinelli, A., 2006. Cannabinoid CB2/CB1 selectivity. Receptor modeling and automated docking analysis. *J. Med. Chem.* 49, 984–994.  
<https://doi.org/10.1021/JM050875U/ASSET/IMAGES/MEDIUM/JM050875UN00001.GIF>
- U.S. Customs and Border Protection U.S. Customs and Border Protection, 2022. Fighting the Opioid Scourge [WWW Document]. URL <https://www.cbp.gov/frontline/fighting-opioid-scourge> (accessed 9.24.22).
- UCLA, 2022. SAVESv6.0 - Structure Validation Server [WWW Document]. URL <https://saves.mbi.ucla.edu/> (accessed 4.21.21).
- Ujváry, I., Christie, R., Evans-Brown, M., Gallegos, A., Jorge, R., De Morais, J., Sedefov, R., 2021. DARK Classics in Chemical Neuroscience: Etonitazene and Related Benzimidazoles. *ACS Chem. Neurosci.* 12, 1072–1092. <https://doi.org/10.1021/ACSCHEMNEURO.1C00037>
- UN, 2022. Rapid procedures to control NPS [WWW Document]. URL <https://syntheticdrugs.unodc.org/syntheticdrugs/en/legal/national/rapidprocedures.html> (accessed 7.11.22).
- United Nations, 2022. UN Toolkit on Synthetic Drugs, Legal Module [WWW Document]. URL <https://syntheticdrugs.unodc.org/syntheticdrugs/en/legal/index.html> (accessed 7.11.22).
- UNODC, 2022a. World Drug Report 2022. Vienna.
- UNODC, 2022b. World drug report 2022, Booklet 4, Drug market trends of Cocaine, Amphetamine-type stimulants and New Psychoactive Substances. Vienna.
- UNODC, 2022c. The International Drug Control Conventions [WWW Document].
- UNODC, 2022d. Early Warning Advisory (EWA) on New Psychoactive Substances (NPS) [WWW Document]. URL <https://www.unodc.org/LSS/Home/NPS> (accessed 2.4.21).
- UNODC, 2022e. January 2022 – UNODC-SMART: 1,124 NPS reported to UNODC from 134 countries and territories [WWW Document]. URL <https://www.unodc.org/LSS/Announcement/Details/40df1bf0-4f70-4862-844e-20536e0d95fd> (accessed 2.2.22).
- UNODC, 2021a. World Drug Report 2021, Booklet 2, Global overview of drug demand and drug supply. Vienna.
- UNODC, 2021b. Current NPS Threats Volume IV.
- UNODC, 2021c. SMART UPDATE VOLUME 2 5 Regional diversity and the impact of scheduling on NPS trends. Vienna.

UNODC, 2021d. News: November 2021 – UNODC EWA: Synthetic opioids increase and diversify rapidly [WWW Document]. URL <https://www.unodc.org/LSS/Announcement/Details/1746b9f3-24ca-45e7-a1db-3c16d39fc6fe> (accessed 2.4.22).

UNODC, 2021e. World Drug Report 2021. Vienna.

UNODC, 2021f. News: April 2021 – UNODC: Eight substances “scheduled” at the 64th Session of the Commission on Narcotic Drugs [WWW Document]. URL <https://www.unodc.org/LSS/Announcement/Details/dacec77f-b73c-48c2-bea0-25bb98a4aa9a> (accessed 8.26.22).

UNODC, 2020a. Current NPS Threats Volume II. Vienna.

UNODC, 2020b. Current NPS Threats Volume III. Vienna.

UNODC, 2020c. The growing complexity of the opioid crisis. Vienna.

UNODC, 2020d. Schedules of the Convention on Psychotropic Substances of 1971, as at 3 November 2020. New York.

UNODC, 2020e. Current NPS Threats [WWW Document]. URL <https://www.unodc.org/unodc/en/scientists/current-nps-threats.html> (accessed 4.10.20).

UNODC, 2019a. Current NPS Threats Volume I. Vienna.

UNODC, 2019b. World Drug Report 2019.

UNODC, 2019c. Legal Module - scheduling of substances [WWW Document]. URL <https://syntheticdrugs.unodc.org/syntheticdrugs/en/legal/system/scheduling.html> (accessed 7.12.22).

UNODC, 2019d. World Drug Report, Booklet 3 Depressants. Vienna.

UNODC, 2019e. Understanding the global opioid crisis. Vienna.

UNODC, 2017a. Non-medical use of benzodiazepines : a growing threat to public health ?, Global Smart Update. Vienna.

UNODC, 2017b. In Just Two Decades, Technology Has Become A Cornerstone Of Criminality [WWW Document]. URL <https://www.unodc.org/unodc/en/frontpage/2017/October/in-just-two-decades--technology-has-become-a-cornerstone-of-criminality.html> (accessed 7.7.22).

UNODC, 2017c. Global Synthetic Drugs Assessment. Vienna.

UNODC, 2015. GLOBAL SMART UPDATE Special Segment Legal responses to NPS: Multiple approaches to a multi-faceted problem.

UNODC, 2013. The challenge of new psychoactive substances, Global SMART Programme. Vienna.

UNODC, 2009. Political Declaration and Plan of Action on International Cooperation towards an Integrated and Balanced Strategy to Counter the World Drug Problem 11–12.

- UNODC EWA, 2020. March 2020- Recently scheduled benzodiazepines Flualprazolam and Etizolam associated with multiple post-mortem and DUID cases in UNODC EWA [WWW Document]. URL <https://www.unodc.org/LSS/Announcement/Details/ad0c279b-b4d4-49f3-b638-cd87755d2d42> (accessed 4.10.20).
- US Fire Administration, 2021. Protecting First Responders from Opioid Exposure [WWW Document]. URL <https://www.usfa.fema.gov/blog/ig-102121.html> (accessed 9.24.22).
- USA Congress, 2021. H.R.2630 - 117th Congress (2021-2022): Extending Temporary Emergency Scheduling of Fentanyl Analogues Act.
- USA House of Representatives, 2021. House Passes Congressman Kim's Bill to Highlight Dangers of Synthetic Opioids [WWW Document]. URL <https://kim.house.gov/media/press-releases/house-passes-congressman-kim-s-bill-to-highlight-dangers-of-synthetic-opioids> (accessed 9.24.22).
- Valdman, A.V., Sandle, M., 1986. Drug Dependence and Emotional Behavior. Springer US.
- Valerio, L.G., 2012. Application of advanced in silico methods for predictive modeling and information integration. *Expert Opin. Drug Metab. Toxicol.* <https://doi.org/10.1517/17425255.2012.664636>
- Valerio, L.G., Choudhuri, S., 2012. Chemoinformatics and chemical genomics: potential utility of in silico methods. *J. Appl. Toxicol.* 32, 880–889. <https://doi.org/10.1002/jat.2804>
- van Gerven, J., Roncari, G., Schoemaker, R., Massarella, J., Keesmaat, P., Kooyman, H., Heizmann, P., Zell, M., Cohen, A., Dingemans, J., 1997. Integrated pharmacokinetics and pharmacodynamics of Ro 48-8684, a new benzodiazepine, in comparison with midazolam during first administration to healthy male subjects. *Br. J. Clin. Pharmacol.* 44, 487–493. <https://doi.org/10.1046/J.1365-2125.1997.T01-1-00613.X>
- Van Hout, M.C., Hearne, E., 2017. New psychoactive substances (NPS) on cryptomarket fora: An exploratory study of characteristics of forum activity between NPS buyers and vendors. *Int. J. Drug Policy* 40, 102–110. <https://doi.org/10.1016/J.DRUGPO.2016.11.007>
- Van Zee, A., 2009. The Promotion and Marketing of OxyContin: Commercial Triumph, Public Health Tragedy. *Am. J. Public Health* 99, 221. <https://doi.org/10.2105/AJPH.2007.131714>
- Vandeputte, M.M., Van Uytfanghe, K., Layle, N.K., St. Germaine, D.M., Iula, D.M., Stove, C.P., 2021. Synthesis, Chemical Characterization, and  $\mu$ -Opioid Receptor Activity Assessment of the Emerging Group of “nitazene” 2-Benzylbenzimidazole Synthetic Opioids. *ACS Chem. Neurosci.* 12, 1241–1251. [https://doi.org/10.1021/ACSCHEMNEURO.1C00064/SUPPL\\_FILE/CN1C00064\\_SI\\_001.PDF](https://doi.org/10.1021/ACSCHEMNEURO.1C00064/SUPPL_FILE/CN1C00064_SI_001.PDF)

- Vardanyan, R.S., Hruba, V.J., 2014. Fentanyl-related compounds and derivatives: current status and future prospects for pharmaceutical applications. *Future Med. Chem.* 6, 385. <https://doi.org/10.4155/FMC.13.215>
- Varga, A.G., Reid, B.T., Kieffer, B.L., Levitt, E.S., 2020. Differential impact of two critical respiratory centres in opioid-induced respiratory depression in awake mice. *J. Physiol.* 598, 189–205. <https://doi.org/10.1113/JP278612>
- Vasudevan, L., Vandeputte, M., Deventer, M., Wouters, E., Cannart, A., Stove, C.P., 2020. Assessment of structure-activity relationships and biased agonism at the Mu opioid receptor of novel synthetic opioids using a novel, stable bio-assay platform. *Biochem. Pharmacol.* 177. <https://doi.org/10.1016/j.bcp.2020.113910>
- Verma, J., Khedkar, V., Coutinho, E., 2010. 3D-QSAR in Drug Design - A Review. *Curr. Top. Med. Chem.* 10, 95–115. <https://doi.org/10.2174/156802610790232260>
- Verma, R.P., Hansch, C., 2005. An approach toward the problem of outliers in QSAR. *Bioorganic Med. Chem.* 13, 4597–4621. <https://doi.org/10.1016/j.bmc.2005.05.002>
- Vo, Q.N., Mahinthichaichan, P., Shen, J., Ellis, C.R., 2021. How  $\mu$ -opioid receptor recognizes fentanyl. *Nat. Commun.* 2021 121 12, 1–11. <https://doi.org/10.1038/s41467-021-21262-9>
- Volkow, N., Benveniste, H., McLellan, A.T., 2017. Annual Review of Medicine Use and Misuse of Opioids in Chronic Pain. <https://doi.org/10.1146/annurev-med-011817>
- Vuckovic, S., Prostran, M., Ivanovic, M., Dosen-Micovic, L., Todorovic, Z., Nestic, Z., Stojanovic, R., Divac, N., Mikovic, Z., 2009. Fentanyl analogs: structure-activity-relationship study. *Curr. Med. Chem.* 16, 2468–2474. <https://doi.org/10.2174/092986709788682074>
- Wadsworth, E., Drummond, C., Deluca, P., 2018a. The adherence to UK legislation by online shops selling new psychoactive substances. *Drugs Educ. Prev. Policy* 25, 97–100. <https://doi.org/10.1080/09687637.2017.1284417>
- Wadsworth, E., Drummond, C., Deluca, P., 2018b. The Dynamic Environment of Crypto Markets : The Lifespan of New Psychoactive Substances ( NPS ) and Vendors Selling NPS. *Brain Sci.* <https://doi.org/10.3390/brainsci8030046>
- Wagmann, L., Manier, S.K., Felske, C., Gampfer, T.M., Richter, M.J., Eckstein, N., Meyer, M.R., 2021. Flubromazolam-Derived Designer Benzodiazepines: Toxicokinetics and Analytical Toxicology of Clobromazolam and Bromazolam. *J. Anal. Toxicol.* 45, 1014–1027. <https://doi.org/10.1093/JAT/BKAA161>
- Waldhoer, M., Bartlett, S.E., Whistler, J.L., 2004. Opioid Receptors. <http://dx.doi.org/10.1146/annurev.biochem.73.011303.073940> 73, 953–990. <https://doi.org/10.1146/ANNUREV.BIOCHEM.73.011303.073940>

- Walsh, C., 2011. Drugs, the Internet and change. *J. Psychoactive Drugs* 43, 55–63. <https://doi.org/10.1080/02791072.2011.566501>
- Wang, X., Ramírez-Hinestrosa, S., 2020. prova per mendely formatting. *Phys. Chem. Chem. Phys.* 22, 10624–10633. <https://doi.org/10.1039/C9CP05445F>
- Wang, Y., Liu, H., Fan, Y., Chen, X., Yang, Y., Zhu, L., Zhao, J., Chen, Y., Zhang, Y., 2019. In Silico Prediction of Human Intravenous Pharmacokinetic Parameters with Improved Accuracy. *J. Chem. Inf. Model.* 59, 3968–3980. <https://doi.org/10.1021/acs.jcim.9b00300>
- Waters, L., Manchester, K.R., Maskell, P.D., Haegeman, C., Haider, S., 2018. The use of a quantitative structure-activity relationship (QSAR) model to predict GABA-A receptor binding of newly emerging benzodiazepines. *Sci. Justice* 58, 219–225. <https://doi.org/10.1016/j.scijus.2017.12.004>
- Weaver, S., Gleeson, M.P., 2008. The importance of the domain of applicability in QSAR modeling. *J. Mol. Graph. Model.* 26, 1315–1326. <https://doi.org/10.1016/J.JMGM.2008.01.002>
- Weber, K.-H., Bauer, A., Danneberg, P., Kuhn, F.J., 1977. US4094984A 6-PHENYL-8-BROMO-4H-S-TRIAZOLO-(3,4C)-THIENO-(2,3E)-1,4-DIAZEPINES AND SALTS THEREOF. US4094984A.
- Weber, K.H., Kuhn, F.J., Böke-Kuhn, K., Lehr, E., Danneberg, P.B., Hommer, D., Paul, S.M., Skolnick, P., 1985. Pharmacological and neurochemical properties of 1,4-diazepines with two annelated heterocycles ('hetrazepines'). *Eur. J. Pharmacol.* 109, 19–31. [https://doi.org/10.1016/0014-2999\(85\)90535-7](https://doi.org/10.1016/0014-2999(85)90535-7)
- Webster, L.R., Karan, S., 2020. The Physiology and Maintenance of Respiration: A Narrative Review. *Pain Ther.* 9, 467–486. <https://doi.org/10.1007/S40122-020-00203-2/FIGURES/8>
- Weininger, D., 1988. SMILES, a Chemical Language and Information System: 1: Introduction to Methodology and Encoding Rules. *J. Chem. Inf. Comput. Sci.* 28, 31–36. <https://doi.org/10.1021/ci00057a005>
- Wermuth, C.G., Ganellin, C.R., Lindberg, P., Mitscher, L.A., 1998. Glossary of terms used in medicinal chemistry (IUPAC Recommendations 1998). *Pure Appl. Chem.* 70, 1129–1143. <https://doi.org/10.1351/pac199870051129>
- WHO, 2022. Expert Committee on Drug Dependence [WWW Document]. URL <https://www.who.int/groups/who-expert-committee-on-drug-dependence> (accessed 7.11.22).
- WHO, 2020a. Critical Review Report: CLONAZOLAM . Geneva.
- WHO, 2020b. Critical Review Report: ISOTONITAZENE Expert Committee on Drug Dependence Forty-third Meeting. Geneva.

- WHO, 2018. WHO Expert Committee on Drug Dependence Thirty-ninth report.
- WHO, 2017. WHO recommends the most stringent level of international control for synthetic opioid carfentanil [WWW Document]. URL <https://www.who.int/news/item/13-12-2017-who-recommends-the-most-stringent-level-of-international-control-for-synthetic-opioid-carfentanil> (accessed 9.24.22).
- WHO, 2016. WHO Expert Committee on Drug Dependence: thirty-seventh report. Geneva.
- WHO, 2015. Phenazepam Pre-Review Report Agenda item 5.8 Expert Committee on Drug Dependence Thirty-seventh Meeting. Geneva.
- WHO, 2010. Guidance on the WHO review of psychoactive substances for international control. Geneva.
- Wieland, H.A., Luddens, H., Seeburg, P.H., 1992. A single histidine in GABA(A) receptors is essential for benzodiazepine agonist binding. *J. Biol. Chem.* 267, 1426–1429. [https://doi.org/10.1016/S0021-9258\(18\)45961-3](https://doi.org/10.1016/S0021-9258(18)45961-3)
- Wikipedia, the free encyclopedia [WWW Document], 2022. URL [https://en.wikipedia.org/wiki/Main\\_Page](https://en.wikipedia.org/wiki/Main_Page) (accessed 4.2.20).
- Wilcoxon, R.M., Middleton, O.L., Meyers, S.E., Kloss, J., Love, S.A., 2018. The Elephant in the Room: Outbreak of Carfentanil Deaths in Minnesota and the Importance of Multiagency Collaboration. *Acad. Forensic Pathol.* 8, 729–737. <https://doi.org/10.1177/1925362118797746>
- Wilde, M., Pichini, S., Pacifici, R., Tagliabracci, A., Busardò, F.P., Auwärter, V., Solimini, R., 2019. Metabolic pathways and potencies of new fentanyl analogs. *Front. Pharmacol.* 10, 238. <https://doi.org/10.3389/FPHAR.2019.00238/BIBTEX>
- Wildman, S.A., Crippen, G.M., 1999. Prediction of physicochemical parameters by atomic contributions. *J. Chem. Inf. Comput. Sci.* 39, 868–873. <https://doi.org/10.1021/ci9903071>
- Wishart, D.S., 2006. DrugBank: a comprehensive resource for in silico drug discovery and exploration. *Nucleic Acids Res.* 34, D668–D672. <https://doi.org/10.1093/nar/gkj067>
- Wolber, G., Seidel, T., Bendix, F., Langer, T., 2008. Molecule-pharmacophore superpositioning and pattern matching in computational drug design. *Drug Discov. Today.* <https://doi.org/10.1016/j.drudis.2007.09.007>
- Wold, S., Trygg, J., Berglund, A., Antti, H., 2001. Some recent developments in PLS modeling. *Chemom. Intell. Lab. Syst.* 58, 131–150. [https://doi.org/10.1016/S0169-7439\(01\)00156-3](https://doi.org/10.1016/S0169-7439(01)00156-3)
- Worachartcheewan, A., Toropova, A.P., Toropov, A.A., Siritwong, S., Prapojanasomboon, J., Prachayasittikul, V., Nantasenamat, C., 2018. Quantitative Structure-activity Relationship Study of Betulinic Acid Derivatives Against HIV using SMILES-based Descriptors. *Curr. Comput. Aided. Drug Des.* 14, 152–159.

<https://doi.org/10.2174/1573409914666180112094156>

- Wrigley, P.J., Elliott, D.W., Blake, D., 2019. A Phase 2 Clinical Trial Comparing Ro 48-6791, a New Short-Acting Benzodiazepine, with Propofol for Induction of Anaesthesia: <https://doi.org/10.1177/0310057X9802600506> 26, 509–514.  
<https://doi.org/10.1177/0310057X9802600506>
- Wu, N., Feng, Z., He, X., Kwon, W., Wang, J., Xie, X.Q., 2019. Insight of Captagon Abuse by Chemogenomics Knowledgebase-guided Systems Pharmacology Target Mapping Analyses. *Sci. Rep.* 9. <https://doi.org/10.1038/s41598-018-35449-6>
- Yang, S.Y., 2010. Pharmacophore modeling and applications in drug discovery: Challenges and recent advances. *Drug Discov. Today*. <https://doi.org/10.1016/j.drudis.2010.03.013>
- Zangani, C., Schifano, F., Napoletano, F., Arillotta, D., Gilgar, L., Guirguis, A., Corkery, J.M., Gambini, O., Vento, A., 2020. The e-Psychonauts' 'Spiced' World; Assessment of the Synthetic Cannabinoids' Information Available Online. *Curr. Neuropharmacol.* 18. <https://doi.org/10.2174/1570159x18666200302125146>
- Zawilska, J.B., Andrzejczak, D., 2015. Next generation of novel psychoactive substances on the horizon - A complex problem to face. *Drug Alcohol Depend.* 157, 1–17. <https://doi.org/10.1016/j.drugalcdep.2015.09.030>
- Zawilska, J.B., Wojcieszak, J., 2019. An expanding world of new psychoactive substances—designer benzodiazepines. *Neurotoxicology* 73, 8–16. <https://doi.org/10.1016/j.neuro.2019.02.015>
- Zhang, J, Liu, G., Tang, Y., 2009. Chemical function-based pharmacophore generation of selective kappa-opioid receptor agonists by catalyst and phase. *J. Mol. Model.* 15, 1027–1041. <https://doi.org/10.1007/S00894-008-0418-5>
- Zhang, Jianliang, Xue, F., Chang, Y., 2009. Agonist- and antagonist-induced conformational changes of loop F and their contributions to the  $\rho 1$  GABA receptor function. *J. Physiol.* 587, 139. <https://doi.org/10.1113/JPHYSIOL.2008.160093>
- Zhang, Z., An, L., Hu, W., Xiang, Y., 2007. 3D-QSAR study of hallucinogenic phenylalkylamines by using CoMFA approach. *J. Comput. Aided. Mol. Des.* 21, 145–153. <https://doi.org/10.1007/s10822-006-9090-y>
- Zheng, X., Gan, L., Wang, E., Wang, J., 2013. Pocket-based drug design: Exploring pocket space. *AAPS J.* <https://doi.org/10.1208/s12248-012-9426-6>
- Zhou, S., Zhang, S., Wang, L., Huang, S., Yuan, Y., Yang, Jie, Wang, H., Li, X., Wang, P., Zhou, L., Yang, Jun, Xu, Y., Gao, H., Zhang, Y., Lv, Y., Zou, X., 2020. BET protein inhibitor JQ1 downregulates chromatin accessibility and suppresses metastasis of gastric cancer via



inactivating RUNX2/NID1 signaling. *Oncog.* 2020 93 9, 1–14. <https://doi.org/10.1038/s41389-020-0218-z>

Zhou, W., Li, Y., Meng, X., Liu, A., Mao, Y., Zhu, X., Meng, Q., Jin, Y., Zhang, Z., Tao, W., 2021. Switching of delta opioid receptor subtypes in central amygdala microcircuits is associated with anxiety states in pain. *J. Biol. Chem.* 296, 100277. <https://doi.org/10.1016/J.JBC.2021.100277>

Zhu, S., Noviello, C.M., Teng, J., Walsh, R.M., Kim, J.J., Hibbs, R.E., 2018. Structure of a human synaptic GABAA receptor. *Nature* 559, 67–88. <https://doi.org/10.1038/s41586-018-0255-3>

Zimmerman, D.M., Leander, J.D., 1990. Selective opioid receptor agonists and antagonists: research tools and potential therapeutic agents. *J. Med. Chem.* 33, 895–902. <https://doi.org/10.1021/JM00165A002>

ZINC [WWW Document], 2021. URL <https://zinc.docking.org/> (accessed 1.13.21).

## Appendix A

*Table A1 List of websites monitored by the NPSfinder® web crawler, November 2017- October 2020, surface web only. This list includes psychonauts fora, users' fora, chemical databases and e-commerce websites.*

N	Website name
1	Avalonmagicplants.com
2	Azarius.net
3	Bluelight.org
4	Bluemorphotours.com
5	Cannabis.net
6	Chemeurope.com
7	Committedpsychonaut.tumblr.com
8	Consolidated Index of Controlled Substances
9	Daath.hu/psychonauts
10	Dancesafe.org
11	Deviantart.com/psychonaut-a
12	Druglibrary.org
13	Drugs.tripsit.me
14	Drugs-forum.com
15	Drugs-plaza.com
16	Dutch-headshop.eu
17	Ecstasydata.org
18	Elephantos.com
19	Energycontrol.org
20	Entheogen-network.com/forums
21	Erowid.org
22	Eusynth.org
23	Everything2.com/title/Psychonaut
24	Fungifun.org
25	Hedweb.com
26	Hipforums.com/forum
27	Isomerdesign.com
28	Knehnv.home.xs4all.nl
29	Kratomshop.com
30	Legal-high-inhaltsstoffe.de
31	Mindstates.org
32	Mycotopia.net

33	Natmedtalk.com	
34	Npsproject.eu	
35	Peyote.com/peyolink.html	
36	Psychedelic-library.org	
37	Psychonaut.ca	
38	Psychonaut.fr	
39	Psychonautdocs.com	
40	Psychonautwiki.org	
41	Psyconauts.tripod.com	
42	Reddit.com and drug-related subreddits (e.g. Reddit.com/r/Psychonaut/; Reddit.com/r/shroomers/)	
43	Shayanashop.com	
44	Sjamaan.com	
45	Tripzine.com	
46	Tryptamind.com	
47	Urban75.net	
48	Wikipedia List of designer drugs	
49	Zamnesia.com	

**Table A.2 List of non-fentanyl-like NSOs identified univocally by the UNODC (i.e. not identified by the NPSfinder®) and reported by the UNODC Early Warning Advisory on New Psychoactive Substances**

UNODC	SMILES
2',5'-Dimethoxyfentanyl	SAQRGDVCSASPSH-UHFFFAOYSA-N
2-Chlorofentanyl	JPKVUHSMCMLOPC-UHFFFAOYSA-N
2-fluoroacrylfentanyl	ROBNYLIA YXEIFM-UHFFFAOYSA-N
2-Fluorobutyrfentanyl 2F-BF	NLSYMTDGNFMCMX-UHFFFAOYSA-N
2-Fluorofuranylfentanyl	QAURJPLHDYKGGHY-UHFFFAOYSA-N
2-Methoxyfuranylfentanyl 2-Meo-Fu-F	DCDCWVRDPIOMBB-UHFFFAOYSA-N
2-Methylmethoxyacetylfentanyl	JJNJOPCUJRZRG-UHFFFAOYSA-N
3',4'-Dimethoxyfentanyl	UAMWMLGPFPCSAP-UHFFFAOYSA-N
3-Chlorofentanyl	PEGQDTGCZUMBDF-UHFFFAOYSA-N
3-Fluorofentanyl	SLTQVWMQISKVDN-UHFFFAOYSA-N
3-Fluorofuranylfentanyl	NLTYWPGXHYUTRN-UHFFFAOYSA-N
3-Fluoromethoxyacetylfentanyl	GLYKZHGNYYYJLH-UHFFFAOYSA-N
3-Furanylfentanyl	AEDOTOMIDAMDFC-UHFFFAOYSA-N
4-Fluorobenzylfentanyl	PUFHNCRAVCTYOY-UHFFFAOYSA-N
4-Fluoroisobutyrfentanyl	OZDOSQNUJIXEOR-UHFFFAOYSA-N
4-Methoxyfuranylfentanyl	CCKUDBCTLAHGQ-UHFFFAOYSA-N
4-Methylacetylfentanyl	JNQPTABAZAHVEN-UHFFFAOYSA-N
Acrylfentanyl	RFQNLMWUIJJEQF-UHFFFAOYSA-N
alpha-Methylacetylfentanyl	OKTLVZBUKMRPLL-UHFFFAOYSA-N
beta-Hydroxythiofentanyl	GLAAETOTOUGGSB-UHFFFAOYSA-N
Butyrfentanyl	QQOMYEQWQJRKK-UHFFFAOYSA-N
Despropionyl 2-Methylfentanyl	UQFMMFWGILFTGJ-UHFFFAOYSA-N
Despropionyl 3-methylfentanyl	BRXORURFEVRTDI-UHFFFAOYSA-N
Despropionyl 4-fluorofentanyl	WWDHLOLWLHFBH-UHFFFAOYSA-N
Fentanyl carbamate	BPXVEPWHWMDYCP-UHFFFAOYSA-N
Furanylfentanyl Fu-F	FZJVHWISUGFFQV-UHFFFAOYSA-N
heptanoyl fentanyl	ZLPDQEYWTXBVRY-UHFFFAOYSA-N
Lofentanil	IMYHGORQCPYVBZ-NBGIEHNGSA-N
Methoxyacetylfentanyl	SADNVKRDSWWFTK-UHFFFAOYSA-N
N-methylcyclopropylnorfentanyl	QCCRFOCZMVDGGA-UHFFFAOYSA-N
Orthofluorofentanyl	BKUWDIVZCJNXRA-UHFFFAOYSA-N
Thienylfentanyl	JSOSWRYHPGIWGT-UHFFFAOYSA-N
Valerylfentanyl	VCCPXHWAJYWQMR-UHFFFAOYSA-N

*Table A.3 . Composition of the training and test set used to build the QSAR modes. The log 1/c data obtained from the literature (Hadjipavlou-Litina and Hansch, 1994) -were experimentally determined using spectrometric measurements of [3H]-diazepam displacement. The resulting data set included 77 1,4-benzodiazepines, triazolobenzodiazepines, imidazobenzodiazepines, and thienotriazolobenzodiazepines. The predicted values (AutoQSAR model from Sec. 5.1.3) of log1/c for each molecule are presented as well.*

Training set				
Molecule	Smile	log 1/C	PRED 1/C	log
Brotizolam	<chem>Brc1sc2-n3c(C)nnc3CN=C(c3c(Cl)cccc3)c2c1</chem>	8.92		8.94
Meclonazepam	<chem>Clc1c(C2=NC(C)C(=O)Nc3c2cc([N+](=O)[O-])cc3)cccc1</chem>	8.92		8.60
Ro 11-1465	<chem>Clc1c(C2=NCc3n(c(C)nn3)-c3sc(Cl)cc23)cccc1</chem>	8.85		8.99
Ro 05-4435	<chem>Fc1c(C2=NCC(=O)Nc3c2cc([N+](=O)[O-])cc3)cccc1</chem>	8.82		8.69
Ro 14-1636	<chem>Ic1sc2-n3c(C)nnc3CN=C(c3c(Cl)cccc3)c2c1</chem>	8.82		9.26
Clonazepam	<chem>Clc1c(C2=NCC(=O)Nc3c2cc([N+](=O)[O-])cc3)cccc1</chem>	8.74		8.86
Delorazepam	<chem>Clc1c(C2=NCC(=O)Nc3c2cc(Cl)cc3)cccc1</chem>	8.74		8.65
Ro 05-4082	<chem>Clc1c(C2=NCC(=O)N(C)c3c2cc([N+](=O)[O-])cc3)cccc1</chem>	8.66		8.40
Ro 07-9957	<chem>Ic1cc2C(c3c(F)cccc3)=NCC(=O)N(C)c2cc1</chem>	8.54		8.15
Ro 11-7800	<chem>Clc1c(C2=NCc3n(c(CN)nn3)-c3sc(Cl)cc23)cccc1</chem>	8.54		8.53
Etizolam	<chem>Clc1c(C2=NCc3n(c(C)nn3)-c3sc(CC)cc23)cccc1</chem>	8.51		8.34
Ro 11-5073	<chem>Clc1cc2C(c3c(F)cccc3)=NC(C)c3n(c(C)nn3)-c2cc1</chem>	8.48		7.87
Ro 11-5074	<chem>Clc1c(C2=NC(SC)c3n(c(C)nn3)-c3c2cc([N+](=O)[O-])cc3)cccc1</chem>	8.47		8.53
Lorazepam	<chem>Clc1c(C2=NC(O)C(=O)Nc3c2cc(Cl)cc3)cccc1</chem>	8.46		8.20
Ro 05-3590	<chem>FC(F)(F)c1c(C2=NCC(=O)Nc3c2cc([N+](=O)[O-])cc3)cccc1</chem>	8.46		8.35
Ro 11-4878	<chem>Clc1cc2C(c3c(F)cccc3)=NC(C)C(=O)Nc2cc1</chem>	8.46		8.14
Ro 17-4582	<chem>Clc1c(C2=NCc3n(c(C)nn3)-c3sccc23)cccc1</chem>	8.46		8.43
Flunitrazepam	<chem>Fc1c(C2=NCC(=O)N(C)c3c2cc([N+](=O)[O-])cc3)cccc1</chem>	8.42		8.21
Ro 11-6679	<chem>S(C)C1N=C(c2c(F)cccc2)c2c(-n3c(C)nnc13)ccc([N+](=O)[O-])c2</chem>	8.40		8.31
Hydroxytriazolam	<chem>Clc1c(C2=NCc3n(c(CO)nn3)-c3c2cc(Cl)cc3)cccc1</chem>	8.38		8.05
U-35005	<chem>Clc1c(C2=NCc3n(c(C)nn3)-c3c2cc(Cl)cc3)cccc1</chem>	8.37		8.31
Midazolam	<chem>Clc1cc2C(c3c(F)cccc3)=NCc3n(c(C)nc3)-c2cc1</chem>	8.32		8.33
Ro 05-6822	<chem>Fc1c(C2=NCC(=O)N(C)c3c2cc(F)cc3)cccc1</chem>	8.29		7.78
Ro 20-7078	<chem>Clc1cc2C(c3c(F)cccc3)=NC(Cl)C(=O)Nc2cc1</chem>	8.28		8.61
Ro 11-6896	<chem>Fc1c(C2=NC(C)C(=O)N(C)c3c2cc([N+](=O)[O-])cc3)cccc1</chem>	8.15		7.94
Ro 05-6820	<chem>Fc1c(C2=NCC(=O)Nc3c2cc(F)cc3)cccc1</chem>	8.13		8.26
Ro 21-5205	<chem>Clc1cc2C(c3c(F)cccc3)=NCc3c(C(=O)OC)n3-c2cc1</chem>	8.13		8.30
Diazepam	<chem>Clc1cc2C(c3cccc3)=NCC(=O)N(C)c2cc1</chem>	8.09		7.53
Ro 07-1986	<chem>C1N1C(=O)CN=C(c2c(F)cccc2)c2c1ccc(CCN)c2</chem>	8.08		7.45
Estazolam	<chem>Clc1cc2C(c3cccc3)=NCc3n(-c2cc1)cnn3</chem>	8.07		7.78
Nordiazepam	<chem>Clc1cc2C(c3cccc3)=NCC(=O)Nc2cc1</chem>	8.03		8.00
Nitrazepam	<chem>O=[N+](=[O-])c1cc2C(c3cccc3)=NCC(=O)Nc2cc1</chem>	8.00		8.29
Ro 22-1892	<chem>Clc1cc2C(c3cccc3)=NCc3c(C(=O)OC(C)C)n3-c2cc1</chem>	7.92		7.56
Ro 05-2904	<chem>FC(F)(F)c1cc2C(c3cccc3)=NCC(=O)Nc2cc1</chem>	7.89		7.52
Ro 16-0529	<chem>Clc1c2C(c3cccc3)=NCc3c(C(=O)OCC)n3-c2cc1</chem>	7.85		7.84
Flurazepam	<chem>Clc1cc2C(c3c(F)cccc3)=NCC(=O)N(CCN(CC)CC)c2cc1</chem>	7.83		7.36
Ro 15-8670	<chem>Clc1cc2C(c3cccc3)=NCc3c(C(=O)OCC)n3-c2cc1</chem>	7.82		7.82
Temazepam	<chem>Clc1cc2C(c3cccc3)=NC(O)C(=O)N(C)c2cc1</chem>	7.80		7.07

Ro 05-4865	<chem>Fc1cc2C(c3ccccc3)=NCC(=O)N(C)c2cc1</chem>	7.77	7.38
Oxazepam	<chem>C1c1cc2C(c3ccccc3)=NC(O)C(=O)Nc2cc1</chem>	7.74	7.53
Ro 20-3053	<chem>Fc1c(C2=NCC(=O)Nc3c2cc(C(=O)C)cc3)cccc1</chem>	7.74	7.69
Alprazolam	<chem>C1c1cc2C(c3ccccc3)=NCc3n(c(C)nn3)-c2cc1</chem>	7.70	7.75
Ro 20-5747	<chem>O=C1Nc2c(C(c3ccccc3)=NC1)cc(C=C)cc2</chem>	7.62	7.79
Ro 07-2750	<chem>C1c1cc2C(c3c(F)cccc3)=NCC(=O)N(CCO)c2cc1</chem>	7.61	7.68
Ro 21-8482	<chem>C1c1c(C2=NCc3c(C(=O)N)nc(C)n3-c3c2cc(Cl)cc3)cccc1</chem>	7.59	7.94
Ro 20-2541	<chem>Fc1c(C2=NCC(=O)N(C)c3c2cc(C#N)cc3)cccc1</chem>	7.52	7.34
Desmethyltetrazepam	<chem>C1c1cc2C(C3=CCCCC3)=NCC(=O)Nc2cc1</chem>	7.47	7.85
Tetrazepam	<chem>C1c1cc2C(C3=CCCCC3)=NCC(=O)N(C)c2cc1</chem>	7.47	7.40
Ro 20-2533	<chem>O=C1Nc2c(C(c3ccccc3)=NC1)cc(CC)cc2</chem>	7.44	7.35
Ro 05-3061	<chem>Fc1cc2C(c3ccccc3)=NCC(=O)Nc2cc1</chem>	7.40	7.86
Ro 08-9013	<chem>C1N1C(=O)CN=C(c2c(F)cccc2)c2c1ccc(CCOCC(=O)N)c2</chem>	7.37	7.12
Ro 06-7263	<chem>C1N1C(=O)C(C)N=C(c2ccccc2)c2c1ccc(Cl)c2</chem>	7.31	7.92
Ro 08-3026	<chem>C1c1c(C2=NCC(=O)Nc3c2cc(COCCN)cc3)cccc1</chem>	7.20	7.50
Ro 20-1815	<chem>Fc1c(C2=NCC(=O)N(C)c3c2cc(N)cc3)cccc1</chem>	7.19	6.95
Ro 05-4619	<chem>C1c1c(C2=NCC(=O)Nc3c2cc(N)cc3)cccc1</chem>	7.12	7.57
Ro 05-3328	<chem>C1c1cc2C(c3ccccc3)=NCC(=O)Nc2cc1</chem>	7.06	8.00
Halazepam	<chem>C1c1cc2C(c3ccccc3)=NCC(=O)N(CC(F)(F)F)c2cc1</chem>	7.04	7.58
Pinazepam	<chem>C1c1cc2C(c3ccccc3)=NCC(=O)N(CC#C)c2cc1</chem>	7.03	7.77
Ro 20-7736	<chem>Fc1c(C2=NCC(=O)N(C)c3c2cc(NO)cc3)cccc1</chem>	7.02	6.67
Adinazolam	<chem>C1c1cc2C(c3ccccc3)=NCc3n(c(CN(C)C)nn3)-c2cc1</chem>	6.87	6.92
Ro 17-2221	<chem>O=C1Nc2c(C(c3ccccc3)=NC1)cc(CCN)cc2</chem>	6.59	6.85
Ro 22-4683	<chem>Fc1c(C2=NCC(=O)N(C(C)(C)C)c3c2cc([N+](=O)[O-])cc3)cccc1</chem>	6.52	7.17
Ro 05-4528	<chem>O=C1N(C)c2c(C(c3ccccc3)=NC1)cc(C#N)cc2</chem>	6.42	6.94
Ro 12-6377	<chem>Fc1c(C2=NCC(=O)N(C)c3c2cc(NC(=O)NC)cc3)cccc1</chem>	6.34	6.77
Ro 20-1310	<chem>C1c1cc2C(c3ccccc3)=NCC(=O)N(C(C)(C)C)c2cc1</chem>	6.21	6.51
Camazepam	<chem>C1c1cc2C(c3ccccc3)=NC(OC(=O)N(C)C)C(=O)N(C)c2cc1</chem>	6.05	6.50
<b>Test set</b>			
<b>Molecule</b>	<b>Smile</b>	<b>log 1/C</b>	<b>PRED log 1/C</b>
Prazepam	<chem>C1c1cc2C(c3ccccc3)=NCC(=O)N(CC3CC3)c2cc1</chem>	6.96	7.36
Ro 05-2921	<chem>O=C1Nc2c(C(c3ccccc3)=NC1)cccc2</chem>	6.45	7.48
7-Aminonitrazepam	<chem>O=C1Nc2c(C(c3ccccc3)=NC1)cc(N)cc2</chem>	6.41	7.03
Norfludiazepam	<chem>C1c1cc2C(c3c(F)cccc3)=NCC(=O)Nc2cc1</chem>	8.70	8.41
Ro 05-4336	<chem>Fc1c(C2=NCC(=O)Nc3c2cccc3)cccc1</chem>	6.51	7.87
Ro 05-4520	<chem>Fc1c(C2=NCC(=O)N(C)c3c2cccc3)cccc1</chem>	7.47	7.39
Proflazepam	<chem>C1c1cc2C(c3c(F)cccc3)=NCC(=O)N(CC(O)CO)c2cc1</chem>	6.85	7.25
Triazolam	<chem>C1c1c(C2=NCc3n(c(C)nn3)-c3c2cc(Cl)cc3)cccc1</chem>	8.40	8.31
4-hydroxymidazolam	<chem>C1c1cc2C(c3c(F)cccc3)=NCc3n(c(CO)nc3)-c2cc1</chem>	8.35	8.03

**Table A.4 Training and test sets combinations for the evaluation of structural variability in the generation of 2D QSAR models. To understand if and how the structures variability present in the training and test set reported in Table A.3 could affect the statistic of the of the QSAR model generated (AutoQSAR model from Sec. 5.1.3) the 77 compounds were divided according to their chemical structure. 1,4-benzodiazepines were separated from the triazolo, imidazo and thienotriazolo benzodiazepines and other two sets of training and test set were prepared, i.e. the 1,4-BZD, and Other-BDZ training and test sets**

Training set 1,4 benzodiazepines		
Molecule	Smile	log 1/C
Camazepam	<chem>C1c1cc2C(c3ccccc3)=NC(OC(=O)N(C)C)C(=O)N(C)c2cc1</chem>	6.05
Clonazepam	<chem>C1c1c(C2=NCC(=O)Nc3c2cc([N+](=O)[O-])cc3)cccc1</chem>	8.74
Delorazepam	<chem>C1c1c(C2=NCC(=O)Nc3c2cc(Cl)cc3)cccc1</chem>	8.74
Demoxepam	<chem>ClC1=CC2=C(N(O)CC(=O)N=C2C=C1)c1ccccc1</chem>	6.51
Desmethyltetrazepam	<chem>C1c1cc2C(C3=CCCCC3)=NCC(=O)Nc2cc1</chem>	7.47
Diazepam	<chem>C1c1cc2C(c3ccccc3)=NCC(=O)N(C)c2cc1</chem>	8.09
Flunitrazepam	<chem>Fc1c(C2=NCC(=O)N(C)c3c2cc([N+](=O)[O-])cc3)cccc1</chem>	8.42
Flurazepam	<chem>C1c1cc2C(c3c(F)cccc3)=NCC(=O)N(CCN(CC)CC)c2cc1</chem>	7.83
Halazepam	<chem>C1c1cc2C(c3ccccc3)=NCC(=O)N(CC(F)(F)F)c2cc1</chem>	7.04
Lorazepam	<chem>C1c1c(C2=NC(O)C(=O)Nc3c2cc(Cl)cc3)cccc1</chem>	8.46
Meclonazepam	<chem>C1c1c(C2=NC(C)C(=O)Nc3c2cc([N+](=O)[O-])cc3)cccc1</chem>	8.92
Nitrazepam	<chem>O=[N+](=[O-])c1cc2C(c3ccccc3)=NCC(=O)Nc2cc1</chem>	8.00
Nordazepam	<chem>C1c1cc2C(c3ccccc3)=NCC(=O)Nc2cc1</chem>	8.03
Oxazepam	<chem>C1c1cc2C(c3ccccc3)=NC(O)C(=O)Nc2cc1</chem>	7.74
Pinazepam	<chem>C1c1cc2C(c3ccccc3)=NCC(=O)N(CC#C)c2cc1</chem>	7.03
Ro 05-2904	<chem>FC(F)(F)c1cc2C(c3ccccc3)=NCC(=O)Nc2cc1</chem>	7.89
Ro 05-3061	<chem>Fc1cc2C(c3ccccc3)=NCC(=O)Nc2cc1</chem>	7.40
Ro 05-3328	<chem>C1c1cc2C(c3ccccc3)=NCC(=O)Nc2cc1</chem>	7.06
Ro 05-3590	<chem>FC(F)(F)c1c(C2=NCC(=O)Nc3c2cc([N+](=O)[O-])cc3)cccc1</chem>	8.46
Ro 05-4082	<chem>C1c1c(C2=NCC(=O)N(C)c3c2cc([N+](=O)[O-])cc3)cccc1</chem>	8.66
Ro 05-4435	<chem>Fc1c(C2=NCC(=O)Nc3c2cc([N+](=O)[O-])cc3)cccc1</chem>	8.82
Ro 05-4528	<chem>O=C1N(C)c2c(C(c3ccccc3)=NC1)cc(C#N)cc2</chem>	6.42
Ro 05-4619	<chem>C1c1c(C2=NCC(=O)Nc3c2cc(N)cc3)cccc1</chem>	7.12
Ro 05-4865	<chem>Fc1cc2C(c3ccccc3)=NCC(=O)N(C)c2cc1</chem>	7.77
Ro 05-6820	<chem>Fc1c(C2=NCC(=O)Nc3c2cc(F)cc3)cccc1</chem>	8.13
Ro 05-6822	<chem>Fc1c(C2=NCC(=O)N(C)c3c2cc(F)cc3)cccc1</chem>	8.29
Ro 06-7263	<chem>C1N1C(=O)C(C)N=C(c2ccccc2)c2c1ccc(Cl)c2</chem>	7.31
Ro 06-9098	<chem>O=[N+](=[O-])c1cc2C(c3ccccc3)=NCC(=O)N(COC)c2cc1</chem>	6.37
Ro 07-1986	<chem>C1N1C(=O)CN=C(c2c(F)cccc2)c2c1ccc(CCN)c2</chem>	8.08
Ro 07-2750	<chem>C1c1cc2C(c3c(F)cccc3)=NCC(=O)N(CCO)c2cc1</chem>	7.61
Ro 07-9957	<chem>Ic1cc2C(c3c(F)cccc3)=NCC(=O)N(C)c2cc1</chem>	8.54
Ro 08-3026	<chem>C1c1c(C2=NCC(=O)Nc3c2cc(COCCN)cc3)cccc1</chem>	7.20

Ro 08-9013	<chem>C1N1C(=O)CN=C(c2c(F)cccc2)c2c1ccc(CCOCC(=O)N)c2</chem>	7.37
Ro 11-4878	<chem>Clc1cc2C(c3c(F)cccc3)=NC(C)C(=O)Nc2cc1</chem>	8.46
Ro 11-6896	<chem>Fc1c(C2=NC(C)C(=O)N(C)c3c2cc([N+](=O)[O-])cc3)cccc1</chem>	8.15
Ro 12-6377	<chem>Fc1c(C2=NCC(=O)N(C)c3c2cc(NC(=O)NC)cc3)cccc1</chem>	6.34
Ro 14-3074	<chem>Fc1c(C2=NCC(=O)Nc3c2cc(N=[N+]=[N-])cc3)cccc1</chem>	8.28
Ro 17-2221	<chem>O=C1Nc2c(C(c3cccc3)=NC1)cc(CCN)cc2</chem>	6.59
Ro 20-1310	<chem>Clc1cc2C(c3cccc3)=NCC(=O)N(C(C)(C)C)c2cc1</chem>	6.21
Ro 20-1815	<chem>Fc1c(C2=NCC(=O)N(C)c3c2cc(N)cc3)cccc1</chem>	7.19
Ro 20-2533	<chem>O=C1Nc2c(C(c3cccc3)=NC1)cc(CC)cc2</chem>	7.44
Ro 20-2541	<chem>Fc1c(C2=NCC(=O)N(C)c3c2cc(C#N)cc3)cccc1</chem>	7.52
Ro 20-3053	<chem>Fc1c(C2=NCC(=O)Nc3c2cc(C(=O)C)cc3)cccc1</chem>	7.74
Ro 20-5747	<chem>O=C1Nc2c(C(c3cccc3)=NC1)cc(C=C)cc2</chem>	7.62
Ro 20-7078	<chem>Clc1cc2C(c3c(F)cccc3)=NC(Cl)C(=O)Nc2cc1</chem>	8.28
Ro 20-7736	<chem>Fc1c(C2=NCC(=O)N(C)c3c2cc(NO)cc3)cccc1</chem>	7.02
Ro 22-4683	<chem>Fc1c(C2=NCC(=O)N(C(C)(C)C)c3c2cc([N+](=O)[O-])cc3)cccc1</chem>	6.52
Temazepam	<chem>Clc1cc2C(c3cccc3)=NC(O)C(=O)N(C)c2cc1</chem>	7.80
Tetrazepam	<chem>Clc1cc2C(C3=CCCC3)=NCC(=O)N(C)c2cc1</chem>	7.47
<b>Test set 1,4 benzodiazepines</b>		
Molecule	Smile	log 1/C
Prazepam	<chem>C1CC1CN2C(=O)CN=C(C3=C2C=CC(=C3)Cl)C4=CC=CC=C4</chem>	6.96
Ro 05-2921	<chem>O=C1CN=C(c2cccc2)c2cccc2N1</chem>	6.45
Ro 05-4336	<chem>C1C(=O)NC2=CC=CC=C2C(=N1)C3=CC=CC=C3F</chem>	6.51
Ro 05-4520	<chem>CN1C(=O)CN=C(C2=CC=CC=C2)C3=CC=CC=C3F</chem>	7.47
7-Aminonitrazepam	<chem>C1C(=O)NC2=C(C=C(C=C2)N)C(=N1)C3=CC=CC=C3</chem>	6.41
Norfludiazepam	<chem>C1C(=O)NC2=C(C=C(C=C2)Cl)C(=N1)C3=CC=CC=C3F</chem>	8.70
<b>Training set triazolo, imidazo, and thienotriazolobenzodiazepines</b>		
Molecule	Smile	log 1/C
Hydroxytriazolam	<chem>Clc1c(C2=NCc3n(c(CO)nn3)-c3c2cc(Cl)cc3)cccc1</chem>	8.38
Adinazolam	<chem>Clc1cc2C(c3cccc3)=NCc3n(c(CN(C)C)nn3)-c2cc1</chem>	6.87
Alprazolam	<chem>Clc1cc2C(c3cccc3)=NCc3n(c(C)nn3)-c2cc1</chem>	7.70
Brotizolam	<chem>Brc1sc2-n3c(C)nnc3CN=C(c3c(Cl)cccc3)c2c1</chem>	8.92
Estazolam	<chem>Clc1cc2C(c3cccc3)=NCc3n(-c2cc1)cnn3</chem>	8.07
Etizolam	<chem>Clc1c(C2=NCc3n(c(C)nn3)-c3sc(CC)cc23)cccc1</chem>	8.51
Midazolam	<chem>Clc1cc2C(c3c(F)cccc3)=NCc3n(c(C)nc3)-c2cc1</chem>	8.32
Ro 11-1465	<chem>Clc1c(C2=NCc3n(c(C)nn3)-c3sc(Cl)cc23)cccc1</chem>	8.85
Ro 11-5073	<chem>Clc1cc2C(c3c(F)cccc3)=NC(C)c3n(c(C)nn3)-c2cc1</chem>	8.48
Ro 11-5074	<chem>Clc1c(C2=NC(SC)c3n(c(C)nn3)-c3c2cc([N+](=O)[O-])cc3)cccc1</chem>	8.47
Ro 11-6679	<chem>S(C)C1N=C(c2c(F)cccc2)c2c(-n3c(C)nnc13)ccc([N+](=O)[O-])c2</chem>	8.40
Ro 11-7800	<chem>Clc1c(C2=NCc3n(c(CN)nn3)-c3sc(Cl)cc23)cccc1</chem>	8.54



Ro 14-1636	<chem>Ic1sc2-n3c(C)nnc3CN=C(c3c(Cl)cccc3)c2c1</chem>	8.82
Ro 15-8670	<chem>Clc1cc2C(c3cccc3)=NCc3c(C(=O)OCC)ncn3-c2cc1</chem>	7.82
Ro 16-0529	<chem>Clc1c2C(c3cccc3)=NCc3c(C(=O)OCC)ncn3-c2ccc1</chem>	7.85
Ro 17-4582	<chem>Clc1c(C2=NCc3n(c(C)nn3)-c3secc23)cccc1</chem>	8.46
Ro 21-5205	<chem>Clc1cc2C(c3c(F)cccc3)=NCc3c(C(=O)OC)ncn3-c2cc1</chem>	8.13
Ro 21-8482	<chem>Clc1c(C2=NCc3c(C(=O)N)nc(C)n3-c3c2cc(Cl)cc3)cccc1.N(=C)C</chem>	7.59
Ro 22-1892	<chem>Clc1cc2C(c3cccc3)=NCc3c(C(=O)OC(C)C)ncn3-c2cc1</chem>	7.92
U-35005	<chem>Clc1c(C2=NCc3n(c(C)nn3)-c3c2cc(Cl)cc3)cccc1</chem>	8.37
<b>Test set triazolo, imidazo, and thienotriazolobenzodiazepines</b>		
<b>Molecule</b>	<b>Smile</b>	<b>log 1/C</b>
Ro 21-8137	<chem>C1C2=C(N=CN2C3=C(C=C(C=C3)Cl)C(=N1)C4=CC=CC=C4F)C(=O)N</chem>	8.46
Ro 21-8384	<chem>C1C2=C(N=CN2C3=C(C=C(C=C3)Cl)C(=N1)C4=CC=CC=C4Cl)C(=O)N</chem>	8.42
Triazolam	<chem>CC1=NN=C2N1C3=C(C=C(C=C3)Cl)C(=NC2)C4=CC=CC=C4Cl</chem>	8.4
$\alpha$ -hydroxymidazolam	<chem>C1C2=CN=C(N2C3=C(C=C(C=C3)Cl)C(=N1)C4=CC=CC=C4F)CO</chem>	8.35

*Table A.5 Statistics of the QSAR model manually calculated for 1,4-BZD, and Other-BDZ training and test sets*

Descriptors	1,4-BDZ Training set		1,4-BZD Test set
	r <sup>2</sup>	q <sup>2</sup>	r <sup>2</sup>
6	0.59	0.48	0.29
5	0.6	0.47	0.29
4	0.58	0.48	0.29
3	0.57	0.46	0.31
Descriptors	Other-BDZ Training set		Other-BDZ Test set
	r <sup>2</sup>	q <sup>2</sup>	r <sup>2</sup>
6	0.61	0.37	0.35
5	0.59	0.42	0.29
4	0.57	0.48	0.27
3	0.6	0.43	0.31

**Table A.6 Predicted value of biological activity (log1/c) for the 102 DBZDs identified by NPSfinder<sup>®</sup> calculated with the AutoQSAR model from Sec. 5.1.3. Log1/c represents the logarithm of the reciprocal of the molar inhibitory concentration (IC50)(nM) required to displace 50% of [3H]-diazepam from rat cerebral cortex. The DBZDs were divided into three biological activity groups according to the predicted log1/c values: low (5.80–6.99), medium (7.00–7.99) and high (>= 8.00). These values were chosen after the evaluation of biological activity values available for four BDZs reported in literature as high potency ones, i.e. triazolam (Halcion, log 1/c= 8.40 ), lorazepam (Ativan, log 1/c= 8.46 ), clonazepam (Klonopin, log 1/c= 8.74) and flunitrazepam (Rohypnol, log 1/c= 8.42). Note: The molecules are listed in decreasing order of predicted log1/c. The higher log1/c values should correspond to a higher biological activity**

Molecule	SMILES	Predicted log1/c
<b>High predicted biological activity</b>		
Ro 09-9212	<chem>Clc1c(C2=NCC(=O)Nc3sc(Cl)cc23)cccc1</chem>	9.40
Ro 07-5193	<chem>Clc1c(c(F)ccc1)C1=NCC(=O)Nc2c1cc(Cl)cc2</chem>	9.06
Ro 20-8065	<chem>Clc1c(Cl)cc2NC(=O)CN=C(c3c(F)cccc3)c2c1</chem>	9.04
Ro 07-5220	<chem>Clc1c(c(Cl)ccc1)C1=NCC(=O)N(C)c2c1cc(Cl)cc2</chem>	8.95
Ro 07-3953	<chem>Clc1cc2C(c3c(F)cccc3F)=NCC(=O)Nc2cc1</chem>	8.81
Flucotizolam	<chem>Clc1sc2-n3c(C)nnc3CN=C(c3c(F)cccc3)c2c1</chem>	8.77
Ciclotizolam	<chem>Brc1sc2-n3c(C4CCCC4)nnc3CN=C(c3c(Cl)cccc3)c2c1</chem>	8.77
Flubrotizolam	<chem>Brc1sc2-n3c(C)nnc3CN=C(c3c(F)cccc3)c2c1</chem>	8.67
Phenazepam	<chem>Brc1cc2C(c3c(Cl)cccc3)=NCC(=O)Nc2cc1</chem>	8.61
Ro 07-9749	<chem>Ic1cc2C(c3c(F)cccc3)=NCC(=O)Nc2cc1</chem>	8.60
Clonazolam	<chem>Clc1c(C2=NCc3n(c(C)nn3)-c3c2cc([N+](=O)[O-])cc3)cccc1</chem>	8.58
Ro 15-9270	<chem>Clc1c(C=2c3c(-n4c(C)nnc4CC=2)ccc([N+](=O)[O-])c3)cccc1</chem>	8.52
Climazolam	<chem>Clc1c(C2=NCc3n(c(C)nc3)-c3c2cc(Cl)cc3)cccc1</chem>	8.49
Flunitrazolam	<chem>Fc1c(C2=NCc3n(c(C)nn3)-c3c2cc([N+](=O)[O-])cc3)cccc1</chem>	8.47
Ro 20-8552	<chem>Clc1c(C)cc2C(c3c(F)cccc3)=NCC(=O)Nc2c1</chem>	8.42
Methyl Clonazepam	<chem>Clc1c(C2=NCC(=O)N(C)c3c2cc([N+](=O)[O-])cc3)cccc1</chem>	8.40
Reclazepam	<chem>Clc1c(C2=NCCN(C=3OCC(=O)N=3)c3c2cc(Cl)cc3)cccc1</chem>	8.39
Uldazepam	<chem>Clc1c(C2=NCC(NOCC=C)=Nc3c2cc(Cl)cc3)cccc1</chem>	8.39
Zapizolam	<chem>Clc1c(C2=NCc3n(-c4c2nc(Cl)cc4)cnn3)cccc1</chem>	8.38
Ethyl Dirazepate	<chem>Clc1c(C2=NC(C(=O)OCC)C(=O)Nc3c2cc(Cl)cc3)cccc1</chem>	8.35
Difludiazepam (RO- 07-4065)	<chem>Clc1cc2C(c3c(F)cccc3F)=NCC(=O)N(C)c2cc1</chem>	8.35
Metizolam	<chem>Clc1c(C2=NCc3n(-c4sc(CC)cc24)cnn3)cccc1</chem>	8.35
Etizolam	<chem>Clc1c(C2=NCc3n(c(C)nn3)-c3sc(CC)cc23)cccc1</chem>	8.34
Desmethyltriazolam	<chem>Clc1c(C2=NCc3n(-c4c2cc(Cl)cc4)cnn3)cccc1</chem>	8.32
Flubromazepam	<chem>Brc1cc2C(c3c(F)cccc3)=NCC(=O)Nc2cc1</chem>	8.30
Ro 13-3780	<chem>Brc1cc2C(c3c(F)cccc3F)=NCC(=O)N(C)c2cc1</chem>	8.26
Lopirazepam	<chem>Clc1c(C2=NC(O)C(=O)Nc3c2nc(Cl)cc3)cccc1</chem>	8.24
Cloniprazepam	<chem>Clc1c(C2=NCC(=O)N(CC3CC3)c3c2cc([N+](=O)[O-])cc3)cccc1</chem>	8.23
Nifoxipam	<chem>Fc1c(C2=NC(O)C(=O)Nc3c2cc([N+](=O)[O-])cc3)cccc1</chem>	8.21
Phenazolam	<chem>Brc1cc2C(c3c(Cl)cccc3)=NCc3n(c(C)nn3)-c2cc1</chem>	8.20

Diclazepam	<chem>C1c(C2=NCC(=O)N(C)c3c2cc(Cl)cc3)cccc1</chem>	8.19
4'-Chlorodiazepam	<chem>C1cc2C(c3ccc(Cl)cc3)=NCC(=O)N(C)c2cc1</chem>	8.19
3-Hydroxyphenazepam	<chem>Brc1cc2C(c3c(Cl)cccc3)=NC(O)C(=O)Nc2cc1</chem>	8.16
Benzazepam	<chem>O=C1Nc2sc3c(c2C(c2cccc2)=NC1)CCCC3</chem>	8.16
Cinazepam	<chem>Brc1cc2C(c3c(Cl)cccc3)=NC(OC(=O)CCC(=O)O)C(=O)Nc2cc1</chem>	8.16
Flualprazolam	<chem>C1c(C2=NCC3n(c(C)nn3)-c2cc1)cccc3</chem>	8.15
Metaclazepam	<chem>Brc1cc2C(c3c(Cl)cccc3)=NCC(COC)N(C)c2cc1</chem>	8.14
Fluetizolam	<chem>Fc1c(C2=NCC3n(c(C)nn3)-c3sc(CC)cc23)cccc1</chem>	8.14
Pynazolam	<chem>O=[N+](O-)c1cc2C(c3ncccc3)=NCc3n(c(C)nn3)-c2cc1</chem>	8.13
Desmethylnitrazolam	<chem>O=[N+](O-)c1cc2C(c3cccc3)=NCc3n(-c2cc1)cnn3</chem>	8.11
Nitrazolam	<chem>O=[N+](O-)c1cc2C(c3cccc3)=NCc3n(c(C)nn3)-c2cc1</chem>	8.07
Flubromazolam	<chem>Brc1cc2C(c3c(F)cccc3)=NCc3n(c(C)nn3)-c2cc1</chem>	8.00
<b>Medium predicted biological activity</b>		
Fletazepam	<chem>C1c(C2=NCC3n(c(C)nn3)-c2cc1)cccc3</chem>	7.99
7-BPDBD	<chem>Brc1cc2C(c3cccc3)=NCC(=O)Nc2cc1</chem>	7.90
Tuclazepam	<chem>C1c(C2=NCC(CO)N(C)c3c2cc(Cl)cc3)cccc1</chem>	7.88
SH-053-R-CH3-2'F	<chem>Fc1c(C2=NC(C)c3c(C(=O)OCC)nn3-c3c2cc(C#C)cc3)cccc1</chem>	7.81
Pyclazolam	<chem>C1c(C2=NCC3n(c(C)nn3)-c2cc1)cccc3</chem>	7.80
RO 21-8137	<chem>C1c(C2=NCC3n(c(C)nn3)-c2cc1)cccc3</chem>	7.79
Estazolam	<chem>O=[N+](O-)c1cc2C(c3cccc3)=NCc3n(-c2cc1)cnn3</chem>	7.78
Pyeazolam (SH-TRI-108)	<chem>C(C#C)c1cc2C(c3ncccc3)=NCc3n(c(C)nn3)-c2cc1</chem>	7.78
Flutoprazepam	<chem>C1c(C2=NCC3n(c(C)nn3)-c2cc1)cccc3</chem>	7.77
Rilmazolam	<chem>C1c(C2=NCC3n(nc(C(=O)N(C)C)n3)-c3c2cc(Cl)cc3)cccc1</chem>	7.77
Deschloroetizolam	<chem>C(C)c1sc2-n3c(C)nnc3CN=C(c3cccc3)c2c1</chem>	7.73
Zometapine	<chem>C1c(C2=NCCNc3n(C)nc(C)c23)cccc1</chem>	7.65
Pypazolam	<chem>Brc1cc2C(c3ncccc3)=NCc3n(c(C)nn3)-c2cc1</chem>	7.64
Imidazenil	<chem>Brc1c(C2=NCC3c(C(=O)N)nn3-c3c2cc(F)cc3)cccc1</chem>	7.64
Menitrazepam	<chem>O=[N+](O-)c1cc2C(C3=CCCC3)=NCC(=O)N(C)c2cc1</chem>	7.60
Bromazolam	<chem>Brc1cc2C(c3cccc3)=NCc3n(c(C)nn3)-c2cc1</chem>	7.59
MP-iii-022	<chem>Fc1c(C2=NC(C)c3c(C(=O)NC)nn3-c3c2cc(C#C)cc3)cccc1</chem>	7.58
Ro 05-4608	<chem>C1c(C2=NCC(=O)N(C)c3c2cccc3)cccc1</chem>	7.55
Cyprazepam	<chem>C1c(C2=NCC3n(c(C)nn3)-c2cc1)cccc3</chem>	7.53
Triflunordazepam	<chem>FC(F)(F)c1cc2C(c3cccc3)=NCC(=O)Nc2cc1</chem>	7.52
Quazepam	<chem>C1c(C2=NCC3n(c(C)nn3)-c2cc1)cccc3</chem>	7.51
N-Methylbromazepam	<chem>Brc1cc2C(c3ncccc3)=NCC(=O)N(C)c2cc1</chem>	7.48
Flutemazepam	<chem>C1c(C2=NCC3n(c(C)nn3)-c2cc1)cccc3</chem>	7.48
Thionordazepam	<chem>O=[N+](O-)c1cc2C(c3cccc3)=NCC(=S)Nc2cc1</chem>	7.45
Iomazenil	<chem>Ic1c2C(=O)N(C)Cc3c(C(=O)OCC)nn3-c2ccc1</chem>	7.44

QH-II-066	<chem>O=C1N(C)c2c(C(c3ccccc3)=NC1)cc(C#C)cc2</chem>	7.42
CP-1414S	<chem>O=[N+][[O-]]c1cc2N(c3ccccc3)C(=O)CC(N)=Nc2cc1</chem>	7.42
Lofendazam	<chem>Clc1cc2N(c3ccccc3)C(=O)CCNc2cc1</chem>	7.41
Tofisopam	<chem>O(C)c1c(OC)ccc(C2=NN=C(C)C(CC)c3c2cc(OC)c(OC)c3)c1</chem>	7.36
Fluadinazolam	<chem>Clc1cc2C(c3c(F)cccc3)=NCc3n(c(CN(C)C)nn3)-c2cc1</chem>	7.33
Remimazolam	<chem>Brc1cc2C(c3ncccc3)=NC(CCC(=O)OC)c3n(c(C)cn3)-c2cc1</chem>	7.32
Ethyl Carfluzepate	<chem>Clc1cc2C(c3c(F)cccc3)=NC(C(=O)OCC)C(=O)N(C(=O)NC)c2cc1</chem>	7.24
Doxefazepam	<chem>Clc1cc2C(c3c(F)cccc3)=NC(O)C(=O)N(CCO)c2cc1</chem>	7.23
Cinolazepam	<chem>Clc1cc2C(c3c(F)cccc3)=NC(O)C(=O)N(CCC#N)c2cc1</chem>	7.20
FG-8205	<chem>Clc1c2C(=O)N(C)Cc3c(-c4nc(C(C)C)on4)ncn3-c2ccc1</chem>	7.17
Ro 17-1812	<chem>Clc1c2C(=O)N3C(c4c(C(=O)OCC5CC5)ncn4-c2ccc1)CC3</chem>	7.13
Ro 15-4941	<chem>Clc1c2C(=O)N3C(c4c(C(=O)OCC)ncn4-c2ccc1)CCC3</chem>	7.09
Fluloprazolam	<chem>Fc1c(C2=NCC=3N(C(=O)C(=CN4CCN(C)CC4)N=3)c3c2cc([N+](=O)[O-])cc3)cccc1</chem>	7.08
JQ1	<chem>Clc1ccc(C2=NC(CC(=O)OC(C)(C)C)c3n(c(C)nn3)-c3sc(C)c(C)c23)cc1</chem>	7.06
PWZ-029	<chem>Clc1cc2C(=O)N(C)Cc3c(COC)ncn3-c2cc1</chem>	7.04
Arfendazam	<chem>Clc1cc2N(c3ccccc3)C(=O)CCN(C(=O)OCC)c2cc1</chem>	7.03
Flupyrzapon/ Zolazepam	<chem>Fc1c(C2=NCC(=O)N(C)c3n(C)nc(C)c23)cccc1</chem>	7.00
Sulazepam	<chem>Clc1cc2C(c3ccccc3)=NCC(=S)N(C)c2cc1</chem>	7.00
<b>Low predicted biological activity</b>		
Mexazolam	<chem>Clc1c(C23OCC(C)N2CC(=O)Nc2c3cc(Cl)cc2)cccc1</chem>	6.98
Premazepam	<chem>O=C1Nc2c(c(C)n(C)c2)C(c2ccccc2)=NC1</chem>	6.97
Ripazepam	<chem>O=C1Nc2c(C)nn(CC)c2C(c2ccccc2)=NC1</chem>	6.96
Tolufazepam	<chem>Clc1c(C2=NCC(=O)N(CCS(=O)(=O)c3ccc(C)cc3)c3c2cc(Cl)cc3)cccc1</chem>	6.95
7-Aminoflunitrazepam	<chem>Fc1c(C2=NCC(=O)N(C)c3c2cc(N)cc3)cccc1</chem>	6.95
Elfazepam	<chem>Clc1cc2C(c3c(F)cccc3)=NCC(=O)N(CCS(=O)(=O)CC)c2cc1</chem>	6.85
Clazolam	<chem>Clc1cc2c(N(C)C(=O)CN3C2c2c(ccc2)CC3)cc1</chem>	6.78
Fosazepam	<chem>Clc1cc2C(c3ccccc3)=NCC(=O)N(CP(=O)(C)C)c2cc1</chem>	6.66
Pivoxazepam	<chem>Clc1cc2C(c3ccccc3)=NC(OC(=O)C(C)(C)C(=O)Nc2cc1</chem>	6.45
Triflubazam	<chem>FC(F)(F)c1cc2N(c3ccccc3)C(=O)CC(=O)N(C)c2cc1</chem>	6.43
Gidazepam	<chem>Brc1cc2C(c3ccccc3)=NCC(=O)N(Cc(=O)NN)c2cc1</chem>	6.34
Ro 48-8684	<chem>Fc1cc2C(=O)N(C)Cc3c(-c4oc(CN(CCC)CCC)cn4)ncn3-c2cc1</chem>	6.33
Ro 48-6791	<chem>Fc1cc2C(=O)N(C)Cc3c(-c4nc(CN(CCC)CCC)on4)ncn3-c2cc1</chem>	6.29
Flutazolam	<chem>Clc1cc2C3(c4c(F)cccc4)OCCN3CC(=O)N(CCO)c2cc1</chem>	6.26
Devazepide	<chem>O=C(c2cc1cccc1[nH]2)N[C@H]3/N=C(\c4ccccc4N(C3=O)C)c5ccccc5</chem>	6.01
Zomebazam	<chem>O=C1N(C)c2n(C)nc(C)c2N(c2ccccc2)C(=O)C1</chem>	5.95
Carburazepam	<chem>Clc1cc2C(N(C(=O)N)CC(=O)N(C)c2cc1)c1cccc1</chem>	5.86

**Table A.7 Drug-like parameters for the 102 DBZDs identified by the NPSfinder. The parameters considered were : MW (molecular weight),TP vdw SA (Total polar vdw surface area ), SlogP ( Log Octanol/Water Partition Coefficient), lip\_acc (Lipinski Acceptor Count), lip\_don (Lipinski Donor Count), lip\_druglike (Lipinski Druglike test), lip\_violation (Lipinski Violation count).**

<b>Molecule</b>	<b>MW</b>	<b>TP VDW SA</b>	<b>SlogP</b>	<b>lip_acc</b>	<b>lip_don</b>	<b>lip_druglike</b>	<b>lip_violation</b>
Ro 09-9212	311.2	58.2	3.8	3	1	1	0
Ro 07-5193	323.2	70.1	3.9	3	1	1	0
Ro 20-8065	323.2	70.1	3.9	3	1	1	0
Ro 07-5220	353.6	52.5	4.5	3	0	1	0
Ro 07-3953	306.7	82.0	3.4	3	1	1	0
Flucotizolam	332.8	17.6	4.0	4	0	1	0
Ciclotizolam	461.8	5.7	6.4	4	0	1	1
Flubrotizolam	377.2	17.6	4.2	4	0	1	0
Phenazepam	349.6	58.2	3.9	3	1	1	0
Ro 07-9749	380.2	70.1	3.2	3	1	1	0
Clonazolam	353.8	46.3	3.8	7	0	1	0
Ro 15-9270	352.8	40.6	3.9	6	0	1	0
Climazolam	342.2	11.4	5.1	3	0	1	1
Flunitrazolam	337.3	58.2	3.2	7	0	1	0
Ro 20-8552	302.7	70.1	3.6	3	1	1	0
Methyl Clonazepam	329.7	93.1	3.1	6	0	1	0
Reclazepam	374.2	74.2	3.6	5	0	1	0
Uldazepam	360.2	39.3	4.6	4	1	1	0
Zapizolam	330.2	36.2	3.6	5	0	1	0
Ethyl Dirazepate	377.2	75.4	3.7	5	1	1	0
Difludiazepam (RO- 07-4065)	320.7	76.3	3.4	3	0	1	0
Devazepide	408.5	77.6	4.06	3	1	1	0
Metizolam	328.8	30.5	4.2	4	0	1	0
Etizolam	342.9	5.7	4.5	4	0	1	0
Desmethyltriazolam	329.2	30.5	4.2	4	0	1	0
Flubromazepam	333.2	70.1	3.4	3	1	1	0

Ro 13-3780	365.2	76.3	3.5	3	0	1	0
Lopirazepam	322.2	56.5	2.5	5	2	1	0
Cloniprazepam	369.8	93.1	3.8	6	0	1	0
Nifoxipam ( 3-OH-Norflunitrazepam)	315.3	103.4	1.8	7	2	1	0
Phenazolam ( Clobromazolam, DM-ii-90)	387.7	5.7	4.6	4	0	1	0
Diclazepam	319.2	52.5	3.8	3	0	1	0
4'-Chlorodiazepam	319.2	52.5	3.8	3	0	1	0
3-Hydroxyphenazepam	365.6	50.8	3.2	4	2	1	0
Bentazepam	296.4	58.2	3.4	3	1	1	0
Cinazepam	465.7	109.9	3.6	7	2	1	0
Flualprazolam	326.8	17.6	4.0	4	0	1	0
Metaclazepam	393.7	8.2	4.4	3	0	1	0
Fluetizolam	326.4	17.6	4.0	4	0	1	0
Pynazolam	320.3	52.0	2.5	8	0	1	0
Desmethylnitrazolam	305.3	71.1	2.8	7	0	1	0
Nitrazolam	319.3	46.3	3.1	7	0	1	0
Flubromazolam	371.2	17.6	4.1	4	0	1	0
Fletazepam	370.7	93.8	4.2	3	0	1	0
7-BPDBD	315.2	58.2	3.2	3	1	1	0
Tuclazepam	335.2	41.3	3.6	3	1	1	0
SH-053-R-CH3-2'F	387.4	54.1	4.2	5	0	1	0
Pyclazolam	309.8	11.4	3.2	5	0	1	0
RO 21-8137	354.8	49.8	3.4	5	2	1	0
Estazolam	294.7	30.5	3.5	4	0	1	0
Pyeazolam (SH-TRI-108)	299.3	11.4	2.6	5	0	1	0
Flutoprazepam	342.8	64.4	4.1	3	0	1	0
Rilmazolam	400.3	49.1	3.9	6	0	1	0
Deschloroetizolam	308.4	5.7	3.8	4	0	1	0
Zometapine	274.8	5.7	3.0	4	1	1	0
Pypazolam	354.2	11.4	3.4	5	0	1	0

Imidazenil	399.2	49.8	3.5	5	2	1	0
Menitrazepam	299.3	93.1	2.9	6	0	1	0
Bromazolam	353.2	5.7	4.0	4	0	1	0
MP-iii-022	372.4	55.5	3.4	5	1	1	0
Ro 05-4608	284.7	52.5	3.2	3	0	1	0
Cyprazepam	339.8	66.5	3.7	4	1	1	0
Triflunordazepam	304.3	67.2	3.8	3	1	1	0
Quazepam	386.8	26.6	5.0	2	0	1	1
N-Methylbromazepam	330.2	58.2	2.7	4	0	1	0
Flutemazepam	318.7	57.1	2.6	4	1	1	0
Thionordazepam	286.8	5.7	3.9	2	1	1	0
Iomazenil	411.2	63.0	2.5	6	0	1	0
QH-II-066	274.3	52.5	2.5	3	0	1	0
CP-1414S	296.3	72.8	2.7	7	2	1	0
Lofendazam	272.7	26.5	3.8	3	1	1	0
Tofisopam	382.5	10.0	4.4	6	0	1	0
Fluadinazolam	369.8	17.6	4.0	5	0	1	0
Remimazolam	439.3	47.8	4.3	6	0	1	0
Ethyl Carfluzepate	417.8	118.3	2.9	7	1	1	0
Doxefazepam	348.8	92.7	2.0	5	2	1	0
Cinolazepam	357.8	57.1	2.9	5	1	1	0
FG-8205	357.8	62.2	3.6	7	0	1	0
Ro 17-1812	357.8	63.0	3.1	6	0	1	0
Ro 15-4941	345.8	63.0	3.1	6	0	1	0
Fluloprazolam	448.5	90.4	2.4	9	0	1	0
JQ1	457.0	36.5	5.6	6	0	1	1
PWZ-029	291.7	34.7	2.8	5	0	1	0
Arfendazam	344.8	61.8	4.4	5	0	1	0
Flupyrazapon/ Zolazepam	286.3	64.4	2.0	5	0	1	0
Sulazepam	300.8	5.7	4.0	2	0	1	0



Mexazolam	363.2	34.7	4.2	4	1	1	0
Premazepam	253.3	58.2	2.5	4	1	1	0
Ripazepam	268.3	58.2	2.3	5	1	1	0
Tolufazepam	487.4	126.8	5.0	5	0	1	0
7-Aminoflunitrazepam	283.3	64.4	2.2	4	2	1	0
Elfazepam	408.9	152.3	3.1	5	0	1	0
Clazolam	312.8	26.5	3.4	3	0	1	0
Fosazepam	360.8	151.9	3.0	4	0	1	0
Pivoxazepam	370.8	81.6	4.0	5	1	1	0
Triflubazam	334.3	62.1	4.0	4	0	1	0
Gidazepam	387.2	79.0	1.6	6	3	1	0
Ro 48-8684	411.5	65.2	4.4	7	0	1	0
Ro 48-6791	412.5	74.2	3.8	8	0	1	0
Flutazolam	376.8	76.6	2.7	5	1	1	0
Zomebazam	284.3	53.0	2.1	6	0	1	0
Carburazepam	329.8	57.5	2.9	5	2	1	0

*Table A.8 Composition of the training and test set used to build the QSAR models in Forge™. The log 1/c data obtained from the literature (Hadjipavlou-Litina and Hansch, 1994) -were experimentally determined using spectrometric measurements of [3H]-diazepam displacement.. The predicted values (3DQSAR model from Sec. 5.2.2) of log1/c for each molecule are presented as well*

Molecule	log 1/C	3D Field QSAR	Distance to model	RVM	Sim
<b>Training set</b>					
Brotizolam	8.9	9.1	Excellent	9.0	0.9
Meclonazepam	8.9	8.9	Excellent	9.0	0.8
Ro 11-1465	8.9	8.8	Excellent	8.7	0.9
Ro 05-4435	8.8	8.8	Excellent	8.7	0.9
Clonazepam	8.7	8.8	Excellent	8.7	0.8
Flunitrazepam	8.4	8.8	Excellent	8.7	0.9
Ro 05-4082	8.7	8.7	Excellent	8.6	0.9
Norfludiazepam	8.7	8.7	Excellent	8.5	0.4
Delorazepam	8.7	8.6	Excellent	8.6	0.9
Ro 07-9957	8.5	8.6	Excellent	8.6	0.8
Ro 11-5073	8.5	8.6	Excellent	8.4	0.7
Lorazepam	8.5	8.6	Excellent	8.5	0.8
Hydroxytriazolam	8.4	8.6	Excellent	8.6	0.9
Etizolam	8.5	8.5	Excellent	8.5	0.9
Ro 11-5074	8.5	8.5	Excellent	8.5	0.8
Ro 17-4582	8.5	8.4	Excellent	8.5	0.8
Triazolam	8.4	8.4	Excellent	8.3	0.9
Ro 11-4878	8.5	8.3	Excellent	8.3	0.9
Ro 11-6679	8.4	8.3	Excellent	8.3	0.8
Midazolam	8.3	8.3	Excellent	8.2	0.9
Ro 05-6822	8.3	8.3	Excellent	8.4	0.3
Ro 14-3074	8.3	8.3	Excellent	8.3	0.8
Ro 20-7078	8.3	8.3	Excellent	8.3	0.7
4-hydroxymidazolam	8.4	8.2	Excellent	8.2	0.9
Ro 07-1986	8.1	8.1	Excellent	8.2	0.9
Ro 21-5205	8.1	8.0	Excellent	8.2	0.8
Estazolam	8.1	8.0	Excellent	8.2	0.9
Nordiazepam	8.0	8.0	Excellent	8.0	0.9
Flurazepam	7.8	8.0	Excellent	7.8	0.7
Ro 05-6820	8.1	7.9	Excellent	8.1	0.9
Ro 22-1892	7.9	7.9	Excellent	7.9	0.8
Ro 05-2904	7.9	7.9	Excellent	7.9	0.8
Ro 15-8670	7.8	7.9	Excellent	8.0	0.8
Diazepam	8.1	7.8	Excellent	7.8	0.9
Oxazepam	7.7	7.8	Excellent	7.6	0.8
Ro 16-0529	7.9	7.7	Excellent	7.5	0.8
Ro 05-4865	7.8	7.7	Excellent	7.7	0.9
Ro 20-3053	7.7	7.7	Excellent	7.6	0.8
Ro 07-2750	7.6	7.7	Excellent	7.7	0.9

Alprazolam	7.7	7.6	Excellent	7.8	0.2
Desmethylnitrazepam	7.5	7.6	Excellent	7.7	0.9
Ro 20-5747	7.6	7.5	Excellent	7.5	0.9
Ro 20-2541	7.5	7.4	Excellent	7.4	0.9
Tetrazepam	7.5	7.4	Excellent	7.4	0.9
Ro 08-9013	7.4	7.4	Excellent	7.4	0.8
Ro 05-4520	7.5	7.4	Excellent	7.3	0.9
Ro 20-2533	7.4	7.3	Excellent	7.5	0.8
Ro 06-7263	7.3	7.3	Excellent	7.6	0.8
Ro 08-3026	7.2	7.2	Excellent	7.3	0.7
Ro 20-1815	7.2	7.2	Excellent	7.2	0.7
Ro 05-4619	7.1	7.1	Excellent	7.1	0.8
Ro 20-7736	7.0	7.1	Excellent	7.2	0.9
Halazepam	7.0	7.0	Excellent	7.1	0.9
Pinazepam	7.0	7.0	Excellent	7.1	0.7
Prazepam	7.0	7.0	Excellent	6.9	0.1
Adinazolam	6.9	6.9	Excellent	6.9	0.9
Proflazepam	6.9	6.9	Excellent	6.8	0.8
Ro 05-4336	6.5	6.8	Excellent	6.7	0.9
Ro 05-2921	6.5	6.6	Excellent	6.5	0.9
Ro 05-4528	6.4	6.5	Excellent	6.5	0.9
Ro 22-4683	6.5	6.4	Excellent	6.6	0.8
Ro 12-6377	6.3	6.4	Excellent	6.3	0.8
7-Aminonitrazepam	6.4	6.4	Excellent	6.5	0.8
Ro 20-1310	6.2	6.2	Excellent	6.2	0.9
<b>Test set</b>					
Camazepam	6.1	6.1	Excellent	6.1	0.8
Ro 14-1636	8.8	8.8	Excellent	8.9	0.9
Ro 11-7800	8.5	8.7	Excellent	8.6	0.8
U-35005	8.4	8.5	Excellent	8.6	0.9
Ro 05-3590	8.5	8.4	Good	8.3	0.8
Ro 11-6896	8.2	8.3	Excellent	8.4	0.9
Nitrazepam	8.0	8.2	Excellent	8.3	0.8
Temazepam	7.8	8.2	Excellent	8.0	0.9
Ro 05-3328	7.1	7.8	Excellent	7.6	0.9
Ro 21-8482	7.6	7.7	Poor	7.4	0.8
Ro 05-3061	7.4	7.5	Excellent	7.6	0.9
Ro 17-2221	6.6	7.1	OK	7.0	0.7
Ro 06-9098	6.4	6.7	Excellent	6.7	0.8

*Table A.9 Statistics for the 20 3D Filed QSAR model generated for DBZDs. In red is highlighted the chosen model. Here are presented the statistic of the QSAR models generated in the form of: the coefficient of determination ( $r^2$ ) which indicates the goodness of fit; the cross-validated coefficient of determination ( $q^2$ ) which indicates the robustness; the coefficient of determination for the test set ( $r^2$  test), which indicates the predictive power; the root mean square error (RMSE) as reliability measure; and Tau as a further parameter to assess the predictivity of the model. As  $r^2$ , the closer the value of Tau is to one, the better the model.*

Comps	R <sup>2</sup>	Q <sup>2</sup>	Test	RMSE	Tau
0	0	-0.031	0	0.773	-0.988
1	0.636	0.393	0.553	0.593	0.46
2	0.803	0.613	0.707	0.473	0.624
3	0.851	0.636	0.775	0.459	0.648
4	0.919	0.686	0.812	0.426	0.67
5	0.957	0.698	0.799	0.418	0.695
6	0.968	0.734	0.795	0.392	0.713
7	0.974	0.745	0.785	0.384	0.717
<b>8*</b>	<b>0.981</b>	<b>0.753</b>	<b>0.815</b>	<b>0.378</b>	<b>0.72</b>
9	0.986	0.746	0.809	0.383	0.713
10	0.99	0.732	0.823	0.394	0.713
11	0.993	0.737	0.822	0.39	0.708
12	0.995	0.734	0.837	0.392	0.708
13	0.995	0.733	0.829	0.393	0.706
14	0.996	0.726	0.832	0.398	0.704
15	0.997	0.708	0.827	0.411	0.698
16	0.998	0.702	0.82	0.415	0.69
17	0.998	0.694	0.814	0.421	0.684
18	0.999	0.687	0.81	0.425	0.685
19	0.999	0.681	0.809	0.026	0.43
20	0.999	0.675	0.81	0.024	0.433

**Table A.10 Predicted values for the 102 classified/ unclassified DBZDs identified on-line with the 3D QSAR models generated with Forge™ (Sec 5.2.2). The entries are ranked for decreasing values of pred log 1/c. Note. In addition to the predicted value of log 1/c, other parameters important to evaluate each entry are included, i.e. the distance to model, which indicates how distant is the structure of the query DBZDs to those in the model; the Sim which give an indication of the quality of the alignment (1 is 100% alignment); and the logP which is an indication of the ability of that DBZDs to cross the brain barriers.**

<b>Molecule</b>	<b>3D Field QSAR</b>	<b>Distance to model</b>	<b>RVM</b>	<b>Sim</b>	<b>SlogP</b>
Flubrotizolam	9.6	Excellent	9.5	0.9	4.2
Clonazolam	9.5	Excellent	9.4	0.9	3.4
Pynazolam	9.4	Good	9.4	0.9	2.1
CP-1414S	9.4	Poor	6.4	0.7	2.5
Fluclozizolam	9.1	Excellent	9.1	0.9	4.1
MP-iii-022	9.1	Good	9.0	0.6	3.6
Ro 09-9212	9.0	Excellent	9.0	0.9	3.9
Ro 15-9270	8.9	Good	8.3	0.8	4.0
3-Hydroxyphenazepam	8.9	Excellent	8.5	0.8	3.7
Flunitrazolam	8.8	Excellent	8.7	0.9	3.1
Fluetizolam	8.8	Excellent	8.7	0.9	4.0
Desmethylnitrazolam	8.8	Excellent	8.8	0.9	2.4
Imidazenil	8.8	Excellent	8.8	0.8	3.6
Cinolazepam	8.8	Poor	8.6	0.7	3.6
Methyl Clonazepam	8.7	Excellent	8.6	0.9	3.0
Zapizolam	8.7	Excellent	8.8	0.9	3.4
Etizolam	8.7	Excellent	8.7	0.9	4.2
Flubromazolam	8.7	Excellent	8.8	0.9	4.2
Arfendazam	8.7	Excellent	7.9	0.8	4.4
Mexazolam	8.7	Poor	8.5	0.6	3.9
Triflubazam	8.7	Excellent	8.0	0.9	3.7
Bentazepam	8.6	Excellent	8.3	0.9	3.4
Bromazolam	8.6	Excellent	8.4	0.9	3.8
Metizolam	8.5	Excellent	8.7	0.9	3.9
Nifoxipam	8.5	Excellent	8.5	0.8	2.4
Nitrazolam	8.5	Excellent	8.5	0.9	2.7
Estazolam	8.5	Excellent	8.5	0.9	3.3
Deschloroetizolam	8.5	Excellent	8.5	0.9	3.6
Phenazepam	8.4	Excellent	8.3	0.9	4.0
Ro 20-8552	8.4	Good	8.4	0.8	3.9
Tofisopam	8.4	Poor	6.6	0.6	4.4
Zomebazam	8.4	Excellent	7.7	0.8	1.8
Ro 20-8065	8.3	Good	8.3	0.9	4.2
Flualprazolam	8.3	Excellent	8.3	0.9	4.0
ETHYL Carfluzepate	8.3	Excellent	7.7	0.8	3.2
Clazolam	8.3	Bad	7.8	0.6	3.3
Ro 07-3953	8.2	Excellent	8.4	0.9	4.0
Climazolam	8.2	Excellent	8.0	0.9	4.9
Desmethyltriazolam	8.2	Excellent	8.4	0.9	4.0

Thionordazepam	8.2	Excellent	8.1	0.8	4.0
Remimazolam	8.2	Good	8.3	0.6	4.3
Flutazolam	8.2	Good	7.9	0.6	3
Ro 07-5193	8.1	Excellent	8.2	0.9	4.2
Difludiazepam- 07-4065	8.1	Excellent	8.2	0.9	4.0
PHENAZOLAM CLOBROMAZOLAM DM-Ii-90	8.1	Excellent	8.2	0.9	4.4
Pyclazolam	8.1	Excellent	8.2	0.9	3.0
Flutemazepam	8.1	Excellent	8.1	0.9	3.3
Ro 07-5220	8.0	Excellent	8	0.9	4.5
Ciclotizolam	8.0	Good	8.0	0.8	6.2
Cinazepam	8.0	Bad	7.9	0.6	3.7
Pyrazolam	8.0	Excellent	8.2	0.9	3.2
Triflunordazepam	8.0	Excellent	8.0	0.8	3.5
Lofendazam	8.0	Poor	7.2	0.8	3.8
Fluloprazolam	8.0	Bad	8.0	0.7	2.5
Ro 48-6791	8.0	Bad	7.5	0.5	3.0
Menitrazepam	7.9	Excellent	7.9	0.9	2.7
Ripazepam	7.9	Excellent	7.8	0.8	2.0
Cloniprazepam	7.8	Excellent	7.7	0.9	3.8
Diclazepam	7.8	Excellent	7.7	0.9	3.9
7-Bpdbd	7.8	Excellent	7.8	0.9	3.3
Tuclazepam	7.8	Excellent	7.6	0.8	4.1
Doxefazepam	7.8	Excellent	7.5	0.9	3.0
Fg-8205	7.8	Bad	7.1	0.5	2.7
Carburazepam	7.8	Poor	8.0	0.7	2.8
Uldazepam	7.7	Poor	7.4	0.7	4.5
Ro 13-3780	7.7	Excellent	8.1	0.9	4.2
Sh-053-R-Ch3-2?F	7.7	Excellent	8	0.8	4.4
Pyeazolam	7.7	Good	8	0.9	2.4
Cyprazepam	7.7	Bad	6	0.7	3.8
Flupyrazapon / Zolazepam	7.7	Excellent	7.6	0.8	2.0
Sulazepam	7.7	Excellent	7.7	0.9	4.0
JQ1	7.6	Bad	6.7	0.6	5.6
Premazepam	7.6	Excellent	7.5	0.8	2.1
Ro 07-9749	7.5	Excellent	7.6	0.9	3.8
Reclazepam	7.5	Poor	7.7	0.8	3.6
Zometapine	7.5	Excellent	6.6	0.7	2.7
Ro 15-4941	7.5	Good	6.4	0.5	3.0
Fosazepam	7.5	Good	7.1	0.8	4.1
Ethyl Dirazepate	7.4	Good	7.5	0.8	3.8
Flubromazepam	7.4	Excellent	7.7	0.9	3.7
Lopirazepam	7.4	Excellent	7.3	0.8	2.9
Ro 21-8137	7.4	Poor	7.5	0.8	3.4
Iomazenil	7.4	OK	7.0	0.6	2.5
4'-Chlorodiazepam	7.3	Good	7.0	0.9	3.9

Fletazepam	7.3	Good	7.5	0.9	4.5
Quazepam	7.3	Excellent	7.2	0.8	5.3
QH-II-066	7.3	Good	7.4	0.9	2.6
Ro 17-1812	7.3	Bad	6.9	0.5	3.0
Ro 05-4608	7.2	Excellent	7.2	0.9	3.2
N-Methylbromazepam	7.2	Excellent	7.5	0.9	2.7
Rilmazolam	7.1	OK	7.5	0.8	3.7
Fluadinazolam	7.0	Excellent	7.1	0.9	3.8
Tolufazepam	7.0	Poor	6.9	0.8	5.0
Pivoxazepam	7.0	Poor	7.0	0.8	4.1
Metaclazepam	6.9	Excellent	6.6	0.8	4.5
Ro 48-8684	6.9	Bad	6.7	0.5	3.6
7-Aminoflunitrazepam	6.8	Excellent	7.0	0.8	2.5
Elfazepam	6.8	Good	7.0	0.9	3.4
Flutoprazepam	6.6	Excellent	6.6	0.9	4.4
Pwz-029	6.6	Poor	6.6	0.6	2.3
Devazepide	6.4	Bad	5.9	0.5	3.7
Gidazepam	6.4	Poor	6.4	0.9	1.7

*Table A.11 DBZDs docking values. The 102 DBZDs identified by NPSfinder®, were docked as described in section 4.3.8. In particular those DBZDs showing the triazole moiety were docked in PDB6HUO using the pharmacophore placement in Figure 4.15, while the others were docked in PDB6X3 using the one in Figure 4.16. For each molecule, several conformations with different S values (Kcal/mol) were returned. The ones showing the lowest S value (i.e., the lower the value, the more potent the binding) as well as the interaction with His102 were identified. The rmsd here reported measures the root mean square deviation between the pose before refinement and the pose after refinement, giving an idea of how the refined pose is close to the one suggested by the docking superposition points.*

Molecule	S	rmsd	Molecule	S	rmsd
3-Hydroxyphenazepam	-6.6	1.2	MP-III-022	-5.6	1.8
4'-Chlorodiazepam	-6.6	0.9	Menitrazepam	-5.9	1.1
7-Aminoflunitrazepam	-5.9	0.9	Metaclazepam	-6.1	1.4
7-BPDBD	-6.3	1.2	Methyl Clonazepam	-5.8	1.0
Arfendazam	-6.1	1.6	Metizolam	-6.9	0.9
Benzazepam	-6.3	1.3	Mexazolam	51.0	1.8
Bromazolam	-5.3	1.6	N-Methylbromazepam	-5.5	0.7
CP-1414S	-6.8	1.2	Nifoxipam ( 3-OH-Norflunitrazepam)	-6.9	1.6
Carburazepam	-4.9	1.3	Nitrazolam	-7.4	1.5
Ciclotizolam	-6.8	2.0	PWZ-029	-6.3	0.4
Cinazepam	-6.8	1.4	Phenazepam	-6.7	1.1
Cinolazepam	-7.0	1.3	Phenazolam	-5.7	1.6
Clazolam	-7.1	2.0	Pivoxazepam	-2.1	1.6
Climazolam	-5.0	1.8	Premazepam	-4.9	1.3
Clonazolam	-7.2	1.0	Pyclazolam	-6.9	0.7
Cloniprazepam	-6.9	1.9	Pyeazolam (SH-TRI-108)	-6.7	1.2
Cyprazepam	-5.6	2.0	Pynazolam	-7.7	0.9
Deschloroetizolam	-6.9	2.0	Pypazolam	-6.9	1.2
Desmethylnitrazolam	-7.3	0.9	QH-II-066	-6.6	1.5
Desmethyltriazolam	-7.0	1.1	Quazepam	-5.3	1.7
Devazepide	3.8	1.9	RO 21-8137	-5.2	1.5
Diclazepam	-7.0	1.7	Reclazepam	-7.1	1.0
Difludiazepam (RO- 07-4065)	-6.9	1.0	Remimazolam	-6.9	1.1
Doxefazepam	-5.3	2.0	Rilmazolam	-7.8	1.6
Elfazepam	-6.9	1.9	Ripazepam	-7.8	0.9
Estazolam	-6.6	0.8	Ro 05-4608	-4.2	1.3
Ethyl Carfluzepate	-6.6	1.8	Ro 07-3953	-5.4	1.3
Ethyl Dirazepate	-6.7	1.3	Ro 07-5193	-6.8	2.0
Etizolam	-5.9	1.7	Ro 07-5220	-4.1	1.0
FG-8205	-3.8	1.4	Ro 07-9749	-6.4	1.6
Fletazepam	-5.7	1.5	Ro 09-9212	-5.4	0.9
Fluadinazolam	-7.5	1.3	Ro 13-3780	-7.0	1.9
Flualprazolam	-6.6	1.3	Ro 15-4941	-6.7	1.8
Flubromazepam	-6.5	1.6	Ro 15-9270	-6.6	1.6
Flubromazolam	-7.4	1.3	Ro 17-1812	-7.0	1.4
Flubrotizolam	-7.1	1.3	Ro 20-8065	-5.5	1.2
Flucotizolam	-6.5	1.6	Ro 20-8552	-6.6	1.3



Fluetizolam	-7.3	1.7	Ro 48-6791	-2.4	1.7
Fluloprazolam	-7.3	1.7	Ro 48-8684	-7.6	1.7
Flunitrazolam	-7.8	0.8	SH-053-R-CH3-2'F	-4.7	1.5
Flupyrazapon	-6.0	1.6	Sulazepam	-6.7	1.0
Flutazolam	-6.0	1.8	Thionordazepam	-5.2	1.3
Flutemazepam	-5.0	1.5	Tofisopam	-7.0	1.6
Flutoprazepam	-5.5	1.3	Tolufazepam	-6.4	2.0
Fosazepam	-6.6	1.7	Triflubazam	-5.0	1.8
Gidazepam	-7.0	1.3	Triflunordazepam	-4.2	1.5
Imidazenil	-6.4	1.6	Tuclazepam	-6.6	2.0
Iomazenil	-6.1	0.9	Uldazepam	-6.0	1.2
JQ1	-6.2	1.9	Zapizolam	-6.4	1.0
Lofendazam	-4.8	1.3	Zomebazam	-5.9	1.4
Lopirazepam	-5.5	1.2	Zometapine	-5.4	1.0

*Table A.12. Ion channel ligands and GPCR-A ligands which matched the pharmacophore created by the top ten DBZDs (Figure 5.11). these hits resulted from the filtering of two databases from Zinc15, the ion channel ligands (25376 entries) and the G-protein-coupled receptors (GPCR)-A ligands (20682 entries).*

<b>Ion Channel (Zinc)</b>	
<b>ZINC_ID</b>	<b>SMILES</b>
ZINC000014211214	<chem>FC(F)(F)c1cc(C(F)(F)F)cc(CN(c2nn(C)nn2)[C@@]2c3nc(C)ccc3N(C(=O)OC(C)C)[C@](CC)C2)c1</chem>
ZINC000040952830	<chem>O(C)c1c(-c2[nH]ccn2)cc(Oc2c(N)nc(N)nc2)c(C(C)C)c1</chem>
ZINC000000000903	<chem>Clc1cc2C(c3ccccc3)=NCc3n(c(C)nn3)-c2cc1</chem>
ZINC000000000903	<chem>Clc1cc2C(c3ccccc3)=NCc3n(c(C)nn3)-c2cc1</chem>
ZINC000000002212	<chem>Clc1c(C2=NCc3n(c(C)nn3)-c3c2cc(Cl)cc3)cccc1</chem>
ZINC000095582529	<chem>Clc1cc(-c2n(CCOC)ncc2)c(Oc2c(C#N)cc(S(=O)(=O)Nc3snnc3)cc2)cc1</chem>
ZINC000095583579	<chem>S(=O)(=O)(Nc1scn1)c1cc(C#N)c(Oc2c(-c3n(C)ncc3)ccc(C)c2)cc1</chem>
ZINC000095583484	<chem>Clc1cc(Oc2c(F)cc(S(=O)(=O)Nc3scn3)cc2)c(-c2[nH]ncc2)cc1</chem>
ZINC000095581718	<chem>Clc1cc(-c2n(C)ncc2)c(Oc2c(F)cc(S(=O)(=O)Nc3snc(C)n3)cc2)cc1</chem>
ZINC000045245125	<chem>Clc1c(Cl)ccc([C@]2C(c3n(C)c4c(Cl)cccc4n3)=C(C)Nc3n2ncc3)c1</chem>
ZINC000045252889	<chem>Clc1c(Cl)ccc([C@]2C(c3n(C)c4c(n3)cc(C#N)cc4)=C(C)Nc3n2ncc3)c1</chem>
ZINC000095560528	<chem>Fc1ccc(-c2nc([C@]3N[C@](c4nc(C)on4)(c4cn(C)nc4)c4[nH]c5c(c4C3)cccc5)[nH]c2)cc1</chem>
<b>GPCR_A (Zinc)</b>	
<b>ZINC_ID</b>	<b>SMILES</b>
ZINC000000607971	<chem>Clc1c([C@](OCc2c(Cl)cc(Cl)cc2)Cn2ence2)ccc(Cl)c1</chem>
ZINC000013821393	<chem>Clc1c(C2=NCc3n(c(C)nn3)-c3sc(C#CCO)cc23)cccc1</chem>
ZINC000002570830	<chem>BrC1sc2-n3c(C)nnc3CN=C(c3c(Cl)cccc3)c2c1</chem>
ZINC000005013442	<chem>Clc1cc2C(c3c4c([nH]c3)cccc4)(c3c4c([nH]c3)cccc4)C(=O)Nc2cc1</chem>

**Table A.13. Composition of the training and test set used to build the QSAR models in Forge™ for fentanyl-like NSOs. The activity data were obtained by ChEMBL target report on MOR CHEMBL233 For this target only the Ki values were analysed and used. The biological activity Ki is identified as the ‘inhibition constant’ and indicates how potent a ligand is in inhibiting a process; Ki is the concentration required to produce half the maximum inhibition (Neubig et al., 2003). Ki is expressed in molar units (M), where 1 M is equivalent to 1 mol/L (Neubig et al., 2003). Only molecules for which the displacement of the radioligand [3H]DAMGO from the human MOR was used to determine of all of the Ki values, were selected. The binding data were converted to their negative decimal logarithm pKi (pKi = -logKi). In the table the predicted values obtained with the 3D QSAR model generated in Section 7.1.2 are reported.**

Training set						
Title	Structure	pKi	Field QSAR	Dist to model	RF	RVM
1	<chem>FCOC(=O)C1(N(c2ccccc2)C(=O)CC)CC[NH+](CC1)CCc3ccccc3</chem>	9.9	10.1	Excellent	11.2	9.9
2	<chem>O=C1[C@H](c2ccccc2N1C3CC[NH+](CC3)CCC(c4ccccc4)c5ccccc5)CC</chem>	8.7	8.9	Excellent	8.7	8.5
3	<chem>O=C1Cc2ccccc2N1C3CC[NH+](C4C5CCCC4CCC5)CC3</chem>	8.6	8.7	Excellent	8.7	8.6
4	<chem>O=C1[C@@H](c2ccccc2N1C3CC[NH+](C@@H)4c5ccc6CCC[C@H](c65)CC4)CC3)CC</chem>	8.1	8.2	Excellent	7.9	8.0
5	<chem>O=C1[C@H](c2ccccc2N1C3CC[NH+](CC3)Cc4ccc5c4cc[nH]5)CC</chem>	8.0	7.6	Excellent	7.7	7.8
6	<chem>OCCOc1ccc(-c2nc3ccccc3n2C4CC[NH+](C5(CCCCCC5)C)CC4)c1</chem>	8.0	7.6	Excellent	7.6	7.9
7	<chem>O=C1Cc2ccccc2N1C3CC[NH+](C4CCC(CC4)C(CC)(C)C)CC3</chem>	7.8	7.9	Excellent	7.9	7.8
8	<chem>O=C1Cc2ccccc2N1C3CC[NH+](C@@H)4c5ccc6CCC[C@H](c65)CC4)CC3</chem>	7.5	7.5	Excellent	7.5	7.4
9	<chem>O=C(N(C1CC[NH+](CC1)CCc2ccccc2)CCCCCCCCNC(N)=[NH2+])CC</chem>	7.4	7.5	Excellent	7.1	7.3
10	<chem>Clc1c(F)ccc(-c2nc3ccccc3n2C4CC[NH+](C5(CCCCCC5)C)CC4)c1</chem>	7.4	7.0	Excellent	7.0	7.0
11	<chem>O=C(N(C)C)[C@@H]1Cc2ccccc2N1C(=O)CC[NH+])3CCC(CC3)c4ccccc4C</chem>	7.2	7.0	Excellent	7.0	6.9
12	<chem>Clc1ccc(O)c2CN[C@@H](C[NH+])3CCC4(CC3)c5ccccc5CC4)Cc12</chem>	7.2	7.4	Excellent	7.1	7.1
13	<chem>O=C(N(C)C)[C@@H]1Cc2ccccc2N1C(=O)CC[NH+])3CCC(CC3)c4ccccc4</chem>	7.1	7.1	Excellent	7.0	7.0
14	<chem>O=C(N1c2ccccc2C[C@H]1C(=O)N(C)C)CC[NH+])3CCC(CC3)c4c(cccc4C)C</chem>	7.1	6.8	Excellent	7.0	6.8
15	<chem>O=C(N(C)C)[C@@H]1Cc2ccccc2N1C(=O)CC[NH+])3CC(CC3)c4ccccc4C</chem>	6.9	7.0	Excellent	6.8	7.0
16	<chem>OCC[NH+])1C[C@@H]2[C@H](C1)CN(C32CC[NH+](C4CCC(CC4)C(C)C)CC3)c5ccccc5</chem>	6.8	6.5	Excellent	6.7	6.5
17	<chem>O=C1c2ccccc2C[C@H](N1C)C[NH+])3CCC4(CC3)c5ccccc5CC4</chem>	6.6	6.5	Excellent	6.6	6.7
18	<chem>CC(C1CCC([NH+])2CCC3([C@H]4[C@H](C[NH+](C4)CCCC)CN3c5ccccc5)CC2)CC1)C</chem>	6.6	6.6	Excellent	6.6	6.7

19	<chem>Fc1ccc(C2CC[NH+](CC2)C[C@@H]3Cc4cccc4CN3)c(c1)C</chem>	6.5	6.7	Excellent	6.6	6.7
20	<chem>[NH+]1([C@@H]2c3cccc4cccc(C2)c43)CCC(CC1)c5c[nH]c6c5cccn6</chem>	6.4	6.4	Excellent	6.1	6.2
21	<chem>O=C(N1CCC2(CC1)c3cccc3CC2)[C@@H]4Cc5cccc5C[NH2+]4</chem>	6.4	6.2	Excellent	6.5	6.3
22	<chem>Fc1ccc2c(c(C3CC[NH+](CC3)Cc4cccc5cccc54)c[nH]2)c1</chem>	6.3	6.5	Excellent	6.5	6.8
23	<chem>Fc1ccc2c(n(C[C@H](O)C[NH+](C)C)cc2C3CC[NH+](C[C@H]4c5cccc6cccc(C4)c65)CC3)c1</chem>	6.1	6.1	Excellent	6.2	6.0
24	<chem>Fc1ccc2c([nH]cc2C3CC[NH+](C[C@H]4c5cccc6cccc(C4)c65)CC3)c1</chem>	6.1	6.5	Excellent	6.3	6.2
25	<chem>O=C(NCC1(Nc2cccc2)CC[NH+](CC1)Cc3cccc3)CNC(N)=[NH2+]</chem>	5.3	5.1	Excellent	3.9	5.3
26	<chem>[NH+]1(CC2CCCC2)CCC(CC1)c3c[nH]c4c3cccn4</chem>	5.3	5.5	Excellent	5.2	5.3
27	<chem>O=C1[C@H](c2cccc2N1C3CC[NH+](CC3)CCc4cccc4)CC</chem>	8.0	7.9	Excellent	7.9	7.7
28	<chem>CC(C1CCC([NH+]2CCC3([C@H]4[C@H](C[NH+](C4)CCN5CCOCC5)CN3c6cccc6)CC2)CC1)C</chem>	6.8	6.7	Excellent	6.7	6.7
29	<chem>Clc1ccc2c(c(C3CC[NH+](C[C@H]4c5cccc6cccc(C4)c65)CC3)c([nH]2)C)c1</chem>	6.6	6.4	Excellent	6.6	6.4
30	<chem>O=C(N1Cc2cccc2C[C@@H]1C[NH+]3CCC4(CC3)c5cccc5CC4)N</chem>	7.0	7.3	Excellent	7.4	7.2
31	<chem>OCC1([NH+]2CCC(n3c4cccc4[nH+]c3N5C[C@@H]6C[NH+](C[C@@H]6C5)Cc7cccc7)CC2)CCCCCCC1</chem>	6.9	6.9	Excellent	6.8	6.9
32	<chem>OCC1([NH+]2CCC(n3c4cccc4[nH+]c3N5C[C@@H]6C[NH2+]C[C@@H]6C5)CC2)CCCCCCC1</chem>	6.7	6.6	Excellent	6.7	6.8
33	<chem>O=C(OC)C1([NH+]2CCC(n3c4cccc4[nH+]c3N5CCN(CC5)C)CC2)CCCCCCC1</chem>	6.4	6.6	Excellent	6.5	6.6
34	<chem>C[NH+]1C[C@@H]2CN(C3([C@@H]2C1)CC[NH+](C4CCCCCCCC4)CC3)c5cccc5</chem>	7.1	7.5	Excellent	7.0	7.3
35	<chem>Clc1ccc2c(c(C3CC[NH+](CC3)Cc4cccc5cccc54)c([nH]2)C)c1</chem>	6.1	6.2	Excellent	6.0	6.5
36	<chem>[NH3+]Cc1ccc(-c2nc3cccc3n2C4CC[NH+](C5(CCCCCC5)C)CC4)c1</chem>	7.7	7.9	Excellent	7.5	7.8
37	<chem>O=C1Cc2cccc2N1C3CC[NH+](C[C@H]4c5cccc6CCC[C@@H](c65)CC4)CC3</chem>	7.1	7.1	Excellent	7.0	6.9
38	<chem>O=C1[C@H](c2cccc2N1C3CC[NH+](CC3)CCCCc4ccc(-c5cccc5)cc4)CC</chem>	6.8	6.8	Excellent	7.0	7.0
39	<chem>Clc1ccc(-c2nc3cccc3n2C4CC[NH+](C5(CCCCCC5)CO)CC4)cc1</chem>	6.8	6.9	Excellent	6.9	7.1
40	<chem>[NH+]1(C[C@@H]2Cc3cccc3CN2)CCC4(CC1)c5cccc5CC4</chem>	6.7	6.8	Excellent	6.8	6.8
41	<chem>Clc1c(F)ccc(-c2nc3cccc3n2C4CC[NH+](C5(CCCCCC5)CO)CC4)c1</chem>	6.5	6.5	Excellent	6.7	6.8
42	<chem>CCCCC[NH+]1CCC(CC1)c2c[nH]c3c2cccn3</chem>	5.3	5.7	Excellent	4.9	5.6
43	<chem>OCC1([NH+]2CCC(n3c(N4CCNC(C4)(C)C)[nH+]c5cccc53)CC2)CCCCCCC1</chem>	6.4	6.4	Excellent	6.4	6.3
44	<chem>O=C(NCC1(Nc2cc(OC)cc(OC)c2)CC[NH+](CC1)Cc3cccc3)CNC(N)=[NH2+]</chem>	6.2	6.0	Excellent	6.1	6.0

45	<chem>C[NH+]1C[C@@H]2[C@H](C1)CN(C32CC[NH+](C4CCC(CC4)C(C)C)CC3)c5ccccc5</chem>	6.5	6.4	Excellent	6.5	6.4
46	<chem>Clc1ccc2c(c(C3CC[NH+](CC3)Cc4ccccc4)c[nH]2)c1</chem>	6.6	6.6	Excellent	6.7	7.0
47	<chem>F[C@H](C(=O)N(C1(CC[NH+](CC1)CCc2cccs2)COC)c3ccccc3)C</chem>	9.9	9.5	Excellent	11.0	9.7
48	<chem>FCCCCC[NH+]1CCC(N(C(=O)CC)c2ccccc2)(CC1)C(OC)=O</chem>	9.1	9.2	Excellent	8.7	9.0
49	<chem>O=C1Cc2ccccc2N1C3CC[NH+](CC3)[C@H](c4ccccc4)C</chem>	8.6	8.5	Excellent	8.4	8.4
50	<chem>O=C1Cc2ccccc2N1C3CC[NH+](C[C@@H](C4CCCC4)C)CC3</chem>	8.5	8.4	Excellent	8.3	8.8
51	<chem>O=C1[C@H](c2ccccc2N1C3CC[NH+](C[C@H]4Cc5ccccc5CC4)CC3)CC</chem>	8.0	8.3	Excellent	8.1	8.2
52	<chem>C[NH+]1Cc2ccccc2C[C@@H]1CN3CCC4(CC3)c5ccccc5CC4</chem>	7.2	7.2	Excellent	7.0	6.9
53	<chem>O(c1ccc(C[NH+]2CCC(CC2)c3c[nH]c4c3cccn4)cc1)c5ccccc5</chem>	6.5	6.4	Excellent	6.4	6.3
54	<chem>Fc1ccc(N2C[C@H]3C[NH+](C[C@H]3C42CC[NH+](C5CCC(CC5)C(C)C)CC4)CC6CC6)cc1</chem>	6.2	6.3	Excellent	6.4	6.6
55	<chem>O=C(N(CC)C)C1(CC[NH+](CC1)CCCCC)c2cccc(O)c2</chem>	8.4	8.2	Excellent	8.3	7.9
56	<chem>OCC1([NH+]2CCC(N3C(=O)Nc4ccccc43)CC2)CCCCC1</chem>	7.8	7.8	Excellent	7.9	7.9
57	<chem>Clc1ccc(O)c2CN[C@H](C[NH+]3CCC(CC3)c4ccc(F)cc4C)Cc12</chem>	6.4	6.4	Excellent	6.5	6.2
58	<chem>O=C(N1c2ccccc2C[C@H]1C(=O)N(C)C)CC[NH+]3CCC([NH+]4CCCC4)CC3</chem>	6.4	6.3	Excellent	6.4	6.3
59	<chem>O=C1[C@H](c2ccccc2N1C3CC[NH+](C[C@H]4c5ccccc5CCC4)CC3)CC</chem>	9.0	9.0	Excellent	9.3	9.0
60	<chem>OCC1([NH+]2CCC(n3c4ccccc4[nH+]c3N5CCN(CC5)C)CC2)CCCCC1</chem>	6.6	6.2	Excellent	6.6	6.7
61	<chem>O=C(OC)[C@]1(N(c2ccccc2)C(=O)CC)CC[NH+](C[C@H]1C)CCc3ccccc3</chem>	9.9	9.8	Excellent	10.1	9.9
62	<chem>O=C(N1Cc2ccccc2C[C@@H]1C[NH+]3CCC4(CC3)c5ccccc5CC4)C</chem>	7.1	7.1	Excellent	7.2	7.0
63	<chem>CC(C1CCC([NH+]2CCC3([C@@H]4CN(C[C@@H]4CN3c5ccccc5)c6ccccc6)CC2)CC1)C</chem>	6.9	7.0	Excellent	6.9	6.9
64	<chem>O1c2ccccc2C[C@H](C[NH+]3CCC4(CC3)c5ccccc5CC4)C1</chem>	7.3	7.7	Excellent	7.5	7.4
65	<chem>CC(C1CCC([NH+]2CCC3([C@@H]4C[NH+](C[C@@H]4CN3c5ccccc5)Cc6ccccc6)CC2)CC1)C</chem>	6.8	6.9	Excellent	6.8	6.8
66	<chem>CC1([NH+]2CCC(n3c(N4C[C@@H](N[C@@H](C4)C)C)[nH+]c5ccccc53)CC2)CCCCC1</chem>	7.7	7.5	Excellent	7.4	7.3
67	<chem>Clc1c(F)ccc(-c2nc3ccccc3n2C4CC[NH+](C5(CCCCC5)CO)CC4)c1</chem>	6.4	6.4	Excellent	6.8	6.5
68	<chem>O=C1[C@@H](c2ccccc2N1C3CC[NH+](C4CCC(CC4)C(C)C)CC3)C</chem>	8.4	8.2	Excellent	8.3	8.2
69	<chem>FCCCCC[NH+]1CCC(N(C(=O)CC)c2ccccc2)CC1</chem>	7.9	7.9	Excellent	7.4	7.7
70	<chem>Oc1ccc2c1CN[C@@H](C[NH+]3CCC4(CC3)c5ccccc5CC4)C2</chem>	6.5	6.6	Excellent	6.6	6.5

71	<chem>N/C(=[NH+])c1ccc2c(nc(n2C3CC[NH+](CC3)C)Cc4ccc(OCC)cc4)c1)c5cccs5</chem>	5.5	5.6	Excellent	5.6	5.6
72	<chem>O=C1[C@H](c2ccccc2N1C3CC[NH+](C4CCCC(C4)C(C)C)CC3)CC</chem>	9.0	8.8	Excellent	8.7	8.7
73	<chem>O=C1[C@@H](c2ccccc2N1C3CC[NH+](C@H)4c5ccccc6CCC[C@H](c65)CC4)CC3)CC</chem>	8.8	8.9	Excellent	8.7	8.7
74	<chem>O=C1Cc2ccccc2N1C3CC[NH+](C4CCCC(C4)CCC)CC3</chem>	8.3	7.9	Excellent	8.2	8.0
75	<chem>CC1([NH+])2CCC(n3c(nc4ccccc43)-c5cc6ccccc6o5)CC2)CCCCCCC1</chem>	7.0	7.0	Excellent	6.9	7.2
76	<chem>Clc1ccc2c1[nH]cc2C3CC[NH+](C@H)4c5ccccc6cccc(C4)c65)CC3</chem>	6.6	6.7	Excellent	6.6	6.6
77	<chem>OCC1([NH+])2CCC(n3c(N4CCN[C@@H](C4)C)[nH+]e5ccccc53)CC2)CCCCCCC1</chem>	6.4	6.2	Excellent	6.5	6.1
78	<chem>CC(C1CCC([NH+])2CCC3([C@@H]4C[NH2+]C[C@@H]4CN3c5ccccc5)CC2)CC1)C</chem>	6.3	6.3	Excellent	6.4	6.5
79	<chem>Fc1ccc2c(c(C3CC[NH+](CC4CCCCCCC4)CC3)cn2C[C@H](O)C[NH+](C)C)c1</chem>	5.6	5.5	Excellent	5.7	5.8
80	<chem>O=C(NCC1(Nc2ccccc3ccccc32)CC[NH+](CC1)Cc4ccccc4)CNC(N)=[NH2+]</chem>	5.7	5.6	Excellent	5.5	5.9
81	<chem>Fc1ccc2c(c(C3CC[NH+](C@H)4c5ccccc6cccc(C4)c65)CC3)c[nH]2)c1</chem>	6.3	6.4	Excellent	6.3	6.5
82	<chem>O=C1Cc2ccccc2N1C3CC[NH+](C4CCCCCCC4)CC3</chem>	7.5	7.8	Excellent	7.5	7.7
83	<chem>Cn1c2c(c(C3CC[NH+](C@H)4c5ccccc6cccc(C4)c65)CC3)c1)ccn2</chem>	6.1	6.1	Excellent	5.8	6.2
84	<chem>CC1([NH+])2CCC(n3c(nc4ccccc43)-c5ccc6cc[nH]c6c5)CC2)CCCCCCC1</chem>	6.8	6.5	Excellent	6.7	6.7
85	<chem>Fc1ccc(C2CC[NH+](CC2)CCC(=O)N3c4ccccc4C[C@H]3C(=O)N(C)C)cc1</chem>	6.6	6.6	Excellent	6.7	6.6
86	<chem>CC1([NH+])2CCC(n3c4ccccc4nc3[C@H]5CCC[NH+](C5)C)CC2)CCCCCCC1</chem>	8.0	8.0	Excellent	7.5	8.0
87	<chem>[NH+])1(CC2CCCCCCC2)CCC(CC1)c3c[nH]c4c3cccn4</chem>	5.7	5.6	Excellent	5.1	5.6
88	<chem>O=C(N(C)C)[C@@H]1Cc2ccccc2N1C(=O)CC[NH+])3CCC(CC3)c4ccccc4</chem>	6.3	6.7	Excellent	6.6	7.1
89	<chem>[NH+])1(CCC(CC1)c2c[nH]c3c2cccn3)Cc4ccccc5ccccc54</chem>	6.5	6.4	Excellent	6.3	6.1
90	<chem>OCCn1c2c(c(C3CC[NH+](C@H)4c5ccccc6cccc(C4)c65)CC3)c1)ccn2</chem>	6.3	6.4	Excellent	6.2	6.4
91	<chem>Clc1ccc2c1[nH]cc2C3CC[NH+](CC4CCCCCCC4)CC3</chem>	6.4	6.6	Excellent	6.5	6.6
92	<chem>O=C1CCc2ccccc2N1C3CC[NH+](C4CCCC(C4)C(C)C)CC3</chem>	8.1	8.1	Excellent	7.8	7.9
93	<chem>Fc1ccc2c(c(C3CC[NH+](CC4CCCCCCC4)CC3)c[nH]2)c1</chem>	6.0	6.0	Excellent	6.0	6.1
94	<chem>O=C1[C@H](c2ccccc2N1C3CC[NH+](C4CCCCCCC4)CC3)C</chem>	8.0	8.1	Excellent	7.9	7.8
Training set						
1	<chem>O=C(OC)C1(N(c2ccccc2)C(=O)CC)CC[NH+](CC1)CCc3ccccc3</chem>	10.2	9.9	Excellent	10.6	10.0

2	<chem>O=C1[C@H](c2ccccc2N1C3CC[NH+](C4CCCCCCC4)CC3)CC</chem>	7.8	8.0	Excellent	7.6	8.0
3	<chem>O=C1Cc2ccccc2N1C3CC[NH+](C@H)4c5cccc6CCC[C@H](c65)CC4)CC3</chem>	7.4	7.4	Good	7.4	7.5
4	<chem>FC(F)(F)c1cccc(-c2nc3ccccc3n2C4CC[NH+](C5(CCCCCC5)C)CC4)c1</chem>	7.2	7.3	OK	7.0	7.0
5	<chem>C[NH+]1C[C@@H]2CN(C3([C@@H]2C1)CC[NH+](C@H)4CC[C@@H]5CCCC[C@@H]5C4)CC3)c6ccccc6</chem>	6.4	6.5	Excellent	6.4	6.5
6	<chem>O=C1Cc2ccccc2N1C3CC[NH+](C4CCC(CC4)C(C)C)CC3</chem>	8.1	8.1	Excellent	8.2	8.4
7	<chem>[NH+]1(C[C@H]2Cc3ccccc3CC2)CCC4(CC1)c5ccccc5CC4</chem>	6.5	6.8	Excellent	6.5	6.8
8	<chem>O=C(N(C1CC[NH+](CC1)CCc2ccccc2)CCCNC(N)=[NH2+])CC</chem>	7.6	7.3	Poor	7.6	7.6
9	<chem>Brc1ccc(O)c2CN[C@@H](C[NH+]3CCC4(CC3)c5ccccc5CC4)Cc12</chem>	6.9	6.6	Excellent	6.8	6.7
10	<chem>Oc1ccc2CN[C@H](C[NH+]3CCC4(CC3)c5ccccc5CC4)Cc2c1</chem>	6.4	6.5	Excellent	6.7	6.5
11	<chem>O=C1CCc2ccccc2N1C3CC[NH+](C4CCCCCCC4)CC3</chem>	7.3	7.3	Excellent	7.4	7.6
12	<chem>FCCOC(=O)C1(N(c2ccccc2)C(=O)CC)CC[NH+](CC1)CCc3ccccc3</chem>	8.9	8.9	OK	8.9	8.8
13	<chem>Fc1ccc(C2CC[NH+](CC2)CCC(=O)N3c4ccccc4C[C@H]3C(=O)N(C)C)c(C)c1</chem>	6.9	6.6	Good	7.0	6.8
14	<chem>O=C1C[C@H](c2ccccc2N1C3CC[NH+](C4CCCCCCC4)CC3)C</chem>	7.6	7.7	Excellent	7.7	7.9
15	<chem>F[C@H](C(=O)N(C1CC[NH+](CC1)CCc2ccccc2)c3ccccc3)C</chem>	8.7	9.1	Excellent	9.4	9.1
16	<chem>C[NH+]1C[C@@H]2CN(C3([C@@H]2C1)CC[NH+](C4CCCCCCC4)CC3)c5ccccc5</chem>	6.1	6.4	Good	6.4	6.1
17	<chem>O=C1[C@@H](c2ccccc2N1C3CC[NH+](CC3)C/C=C/c4ccccc4)CC</chem>	7.5	7.5	Excellent	7.2	7.2
18	<chem>O=C1Cc2ccccc2N1C3CC[NH+](CC3)Cc4ccccc4</chem>	7.0	7.1	Excellent	7.4	7.3
19	<chem>O=C(NCCNC(N)=[NH2+])C1(Nc2ccccc2)CC[NH+](CC1)Cc3ccccc3</chem>	6.7	7.3	Excellent	7.0	6.8
20	<chem>[O-]C(=O)C1([NH+]2CCC(n3c4ccccc4[nH+]c3N5CCN(CC5)C)CC2)CCCCCCC1</chem>	6.4	6.2	Excellent	6.9	6.8
21	<chem>C[NH+]1C[C@@H]2[C@H](C1)CN(C32CC[NH+](C4CCC(CC4)C(C)C)CC3)c5ccccc5</chem>	6.3	6.2	Excellent	6.4	6.2

*Table A.14 Statistics for the 20 3D Filed QSAR model generated for fentanyl-like NSOs. In red is highlighted the chosen model. Here are presented the statistic of the QSAR models generated in the form of: the coefficient of determination ( $r^2$ ) which indicates the goodness of fit; the cross-validated coefficient of determination ( $q^2$ ) which indicates the robustness; the coefficient of determination for the test set ( $r^2_{test}$ ), which indicates the predictive power; the root mean square error (RMSE) as reliability measure; and Tau as a further parameter to assess the predictivity of the model. As  $r^2$ , the closer the value of Tau is to one, the better the model.*

Comps	$R^2$	$Q^2$	Test	RMSE	Tau
0	0.0	0.0	-0.1	1.0	-0.9
1	0.8	0.6	0.8	0.6	0.6
2	0.9	0.7	0.9	0.6	0.6
3	0.9	0.7	0.9	0.5	0.7
4	1.0	0.7	0.9	0.5	0.7
5*	1.0	0.7	0.9	0.5	0.7
6	1.0	0.7	0.9	0.5	0.7
7	1.0	0.7	0.9	0.5	0.6
8	1.0	0.7	0.9	0.5	0.6
9	1.0	0.7	0.9	0.5	0.6
10	1.0	0.7	0.9	0.5	0.6
11	1.0	0.7	0.9	0.5	0.6
12	1.0	0.7	0.9	0.5	0.6
13	1.0	0.7	0.9	0.5	0.6
14	1.0	0.7	0.9	0.5	0.6
15	1.0	0.7	0.9	0.5	0.6
16	1.0	0.7	0.9	0.5	0.6
17	1.0	0.7	0.9	0.5	0.6
18	1.0	0.7	0.9	0.5	0.6
19	1.0	0.7	0.9	0.5	0.6
20	1.0	0.7	0.9	0.5	0.6



**Table A.15** *pKi* values prediction for the 238 fentanyl-like NSOs molecules identified. The value is presented as the average of the prediction obtained with Field QSAR and the RVM models as described in Section 7.1.2. As discussed in section 6.1.4 the biological activity *Ki* is the ‘inhibition constant’ (Neubig et al. 2003), is expressed in molar units (*M*), and calculated as the displacement of the radioligand [<sup>3</sup>H]DAMGO from the human MOR.

Title	pKi Pred	Dist to model	Sim
<b>Very high biological activity</b>			
n-(2-fluorophenyl)-n-[1-(2-phenylethyl)-4-(pyridin-2-yl)piperidin-4-yl]propanamide	10.2	Excellent	0.7
methyl 4-[phenyl(propanoyl)amino]-1-[2-(1h-pyrrol-1-yl)ethyl]piperidine-4-carboxylate	10.1	Good	0.6
2-methyl carfentanil	10.0	Good	0.7
carfentanil	10.0	Excellent	0.7
n-methyl-carfentanil	10.0	Excellent	0.6
butyryl-carfentanyl	10.0	Excellent	0.7
acetyl-carfentanil	9.9	Excellent	0.7
n-{1-[2-(4-ethyl-5-oxo-4,5-dihydro-1h-tetrazol-1-yl)ethyl]-4-(1,3-thiazol-2-yl)piperidin-4-yl}-n-(2-fluorophenyl)propanamide	9.9	Excellent	0.6
4-methoxymethylfentanyl	9.9	Excellent	0.7
n-(2-fluorophenyl)-n-{1-[2-(1h-pyrazol-1-yl)ethyl]-4-(pyridin-2-yl)piperidin-4-yl}propanamide	9.9	Excellent	0.6
n-quinolinyl-fentanyl	9.9	Excellent	0.7
n-(2-fluorophenyl)-n-[4-phenyl-1-(2-phenylethyl)piperidin-4-yl]propanamide	9.9	Excellent	0.7
4-(m-hydroxyphenyl)fentanyl	9.8	Excellent	0.7
methyl 1-[2-(2-oxo-1,3-benzoxazol-3(2h)-yl)ethyl]-4-[phenyl(propanoyl)amino]piperidine-4-carboxylate	9.8	Good	0.6
n-(2-fluorophenyl)-n-{4-(4-methyl-1,3-thiazol-2-yl)-1-[2-(1h-pyrazol-1-yl)ethyl]piperidin-4-yl}propanamide	9.8	Excellent	0.7
4-phenylfentanyl	9.8	Excellent	0.7
brifentanil	9.8	Good	0.6
methyl 4-[phenyl(propanoyl)amino]-1-[2-(pyridin-2-yl)ethyl]piperidine-4-carboxylate	9.8	Excellent	0.7
n-phenyl-n-[1-(2-phenylethyl)-4-(1,3-thiazol-2-yl)piperidin-4-yl]propanamide	9.8	Excellent	0.7
lofentanil	9.7	Excellent	0.7
methyl 1-(2-hydroxy-2-phenylethyl)-3-methyl-4-[phenyl(propanoyl)amino]piperidine-4-carboxylate	9.7	Excellent	0.7
methyl 4-[phenyl(propanoyl)amino]-1-[2-(thiophen-3-yl)ethyl]piperidine-4-carboxylate	9.7	Excellent	0.7
n-(2-fluorophenyl)-n-{4-(4-methyl-1,3-thiazol-2-yl)-1-[2-(thiophen-3-yl)ethyl]piperidin-4-yl}propanamide	9.7	Excellent	0.7
methyl 4-[phenyl(propanoyl)amino]-1-[2-(1h-pyrazol-1-yl)ethyl]piperidine-4-carboxylate	9.7	Excellent	0.6
ethyl {4-[phenyl(propanoyl)amino]-1-[2-(thiophen-2-yl)ethyl]piperidin-4-yl}methyl carbonate	9.6	Excellent	0.6

methyl 4-[phenyl(propanoyl)amino]-1-[2-(2h-tetrazol-2-yl)ethyl]piperidine-4-carboxylate	9.6	Excellent	0.6
n-(2-fluorophenyl)-n-{4-phenyl-1-[2-(thiophen-3-yl)ethyl]piperidin-4-yl}propanamide	9.6	Excellent	0.7
methyl 1-[2-hydroxy-2-(thiophen-2-yl)ethyl]-4-[phenyl(propanoyl)amino]piperidine-4-carboxylate	9.6	Excellent	0.7
n-phenyl-n-{4-phenyl-1-[2-(pyridin-2-yl)ethyl]piperidin-4-yl}propanamide	9.6	Excellent	0.7
2'-fluoro-butyrylfentanyl	9.5	Excellent	0.8
n-(2-fluorophenyl)-n-{4-phenyl-1-[2-(1h-pyrazol-1-yl)ethyl]piperidin-4-yl}propanamide	9.5	Excellent	0.6
n-[1-(2-hydroxy-2-phenylethyl)-3-methylpiperidin-4-yl]-n-(3-methoxyphenyl)propanamide	9.5	Excellent	0.6
2',2''-difluorofentanyl	9.5	Excellent	0.7
3-phenylpropanoylfentanyl	9.5	OK	0.6
4''-bromo-ohmefentanyl	9.5	Good	0.6
4'-hydroxybutyrylfentanyl	9.5	Excellent	0.7
4-methylfentanyl	9.5	Excellent	0.7
fluoropentyl-norcarfentaniol	9.5	Excellent	0.7
n-(2-fluorophenyl)-n-[1-(2-phenylethyl)-4-(1,3-thiazol-2-yl)piperidin-4-yl]propanamide	9.5	Excellent	0.7
n-(2-fluorophenyl)-n-{4-phenyl-1-[2-(thiophen-2-yl)ethyl]piperidin-4-yl}propanamide	9.5	Excellent	0.7
n-[4-(4-methyl-1,3-thiazol-2-yl)-1-(2-phenylethyl)piperidin-4-yl]-n-phenylpropanamide	9.5	Excellent	0.7
n-phenyl-n-{4-phenyl-1-[2-(thiophen-2-yl)ethyl]piperidin-4-yl}propanamide	9.5	Excellent	0.6
butyrylremifentanyl	9.4	Excellent	0.7
n-{1-[2-(furan-2-yl)-2-hydroxyethyl]-4-(methoxymethyl)piperidin-4-yl}-n-phenylpropanamide	9.4	Excellent	0.7
4''-methyl-acetylfentanyl	9.4	Excellent	0.7
butyrylfentanyl	9.4	Excellent	0.7
hexanoyl fentanyl	9.4	Good	0.7
isovaleroylfentanyl	9.4	Excellent	0.7
methyl 1-[2-[(1-methyl-1h-imidazol-2-yl)sulfanyl]ethyl]-4-[phenyl(propanoyl)amino]piperidine-4-carboxylate	9.4	OK	0.6
2'-fluoro-isobutyrylfentanyl	9.4	Good	0.8
3-allylfentanyl	9.3	Good	0.6
acetylfentanyl	9.3	Excellent	0.7
methacroylfentanyl	9.3	Excellent	0.7
3'-4'-methylenedioxyfentanyl	9.3	Good	0.6
3'-fluoro-butyrylfentanyl	9.3	Excellent	0.8
4''-methylfentanyl	9.3	Excellent	0.7

4-fluorofentanyl	9.3	Poor	0.8
benzodioxolefentanyl	9.3	OK	0.7
methyl 1-[2-(2-oxo-2,3-dihydro-1h-indol-1-yl)ethyl]-4-[phenyl(propanoyl)amino]piperidine-4-carboxylate	9.3	Excellent	0.6
n-phenyl-n-{4-phenyl-1-[2-(thiophen-3-yl)ethyl]piperidin-4-yl}propanamide	9.3	Good	0.7
ocfentanil	9.3	Excellent	0.7
trefentanil	9.3	Good	0.5
4''-fluorofentanyl	9.2	Excellent	0.7
n-(2-fluorophenyl)-n-{1-[2-(4-methyl-1,3-thiazol-5-yl)ethyl]-4-phenylpiperidin-4-yl}propanamide	9.2	Excellent	0.7
2-fluorofentanyl	9.2	Excellent	0.7
n-(2-fluorophenyl)-n-{4-(4-methyl-1,3-thiazol-2-yl)-1-[2-(4-methyl-1,3-thiazol-5-yl)ethyl]piperidin-4-yl}propanamide	9.2	Excellent	0.7
4'-chloro-cyclopropylfentanyl	9.2	Excellent	0.7
cyclobutylfentanyl	9.2	Good	0.6
4'-chloro-butyrylfentanyl	9.1	Excellent	0.7
4'-fluoro-crotonylfentanyl	9.1	Excellent	0.7
4'-fluoro-cyclopropylfentanyl	9.1	Excellent	0.7
cyclopentylfentanyl	9.1	Excellent	0.6
fentanyl	9.1	Excellent	0.7
n-[1-(2-hydroxy-2-phenylethyl)-4-(methoxymethyl)-3-methylpiperidin-4-yl]-n-phenylpropanamide	9.1	Excellent	0.7
2-methyl crotonyl fentanyl	9.1	Good	0.7
3'-me-4f-ibf	9.1	Excellent	0.7
3-fluorofentanyl	9.1	Poor	0.7
4'-methyl-furanylfentanyl	9.1	Good	0.7
acrylfentanyl	9.1	Excellent	0.7
alfentanil	9.1	Excellent	0.6
cyclopentenylfentanyl	9.1	Good	0.6
cyclopropylfentanyl	9.1	Excellent	0.7
4'-chlorofentanyl	9.0	Excellent	0.7
4'-fluoro-cyclopentylfentanyl	9.0	Excellent	0.7
4'-methylfentanyl	9.0	Excellent	0.7
benzofuranyl-fentanyl	9.0	Excellent	0.6
n-adamantyl-fentanyl	9.0	Excellent	0.8

n-furanylethylfentanyl	9.0	Excellent	0.7
3'-4'-dichloro-3''-fluorofentanyl	9.0	Excellent	0.7
3'-methyl-methoxyacetylfentanyl	9.0	Good	0.7
4'-chloro-cyclobutylfentanyl	9.0	Excellent	0.7
4'-fluoro-butyrylfentanyl	9.0	Excellent	0.7
4''-methoxyfentanyl	9.0	Excellent	0.6
crotonylfentanyl	9.0	Good	0.7
methoxyacetylfentanyl	9.0	Good	0.7
n-{1-[2-(3,5-dimethyl-1h-pyrazol-1-yl)ethyl]-4-phenylpiperidin-4-yl}-n-(2-fluorophenyl)propanamide	9.0	Excellent	0.6
<b>High biological activity</b>			
4'-methyl-methoxyacetylfentanyl	8.9	Good	0.7
4'-chloro-cyclopentylfentanyl	8.9	Excellent	0.7
m-fluoro-methoxyacetylfentanyl	8.9	Excellent	0.7
n-methyl-butyrylfentanyl	8.9	Excellent	0.6
sufentanil	8.9	Good	0.7
n-{3,5-dimethyl-1-[2-(1h-pyrazol-1-yl)ethyl]piperidin-4-yl}-2-methoxy-n-phenylacetamide	8.9	Good	0.6
n-benzoxazolyl-fentanyl	8.9	Good	0.6
3'-fluoro-isobutyrylfentanyl	8.9	Excellent	0.8
3,3-dimethylfentanyl	8.8	Excellent	0.7
3-furanylfentanyl	8.8	Poor	0.8
benzoylfentanyl	8.8	OK	0.6
mirfentanil	8.8	OK	0.7
n-(3-fluorophenyl)-n-[1-(2-hydroxy-2-phenylethyl)-3-methylpiperidin-4-yl]propanamide	8.8	Poor	0.7
n-{1-[2-hydroxy-2-(thiophen-2-yl)ethyl]-3-methylpiperidin-4-yl}-n-(3-methoxyphenyl)propanamide	8.8	Excellent	0.6
3,5-dimethyl-cyclopentylfentanyl	8.8	Excellent	0.7
methyl 1-[2-(4-methyl-1,3-thiazol-5-yl)ethyl]-4-[phenyl(propanoyl)amino]piperidine-4-carboxylate	8.8	Poor	0.7
p-fluoro-furanylfentanyl	8.8	Excellent	0.6
phenylacetylfentanyl	8.8	Poor	0.6
β-methylfentanyl	8.8	Good	0.6
2-methylfentanyl	8.7	Poor	0.8
3-ethylfentanyl	8.7	Excellent	0.6

3-methyl-furanylfentanyl	8.7	Excellent	0.7
p-fluoro-tetrahydrofuranylfentanyl	8.7	Excellent	0.6
thiophenoylfentanyl	8.7	Good	0.6
2'-isopropyl-furanylfentanyl	8.6	OK	0.7
o-methyl-benzoylfentanyl	8.6	Good	0.6
o-methyl-cyclopropylfentanyl	8.6	Poor	0.6
psicofentanil	8.6	Poor	0.6
remifentanil	8.6	Excellent	0.6
n-{1-[2-hydroxy-2-(pyridin-4-yl)ethyl]-3-methylpiperidin-4-yl}-n-phenylpropanamide	8.6	Excellent	0.6
p-bromofentanyl	8.6	Excellent	0.6
propyl-norfentanyl	8.6	Bad	0.6
3-methyl-butyrylfentanyl	8.5	Excellent	0.8
cyclohexylfentanyl	8.5	Poor	0.7
p-chloro-isobutyrylfentanyl	8.5	Excellent	0.6
p-fluoro-furan-3-ylfentanyl	8.5	Good	0.6
3-methyl-thiofentanyl	8.5	Excellent	0.6
n-[1-(2-hydroxy-2-phenylethyl)-3-methylpiperidin-4-yl]-n-(pyridin-2-yl)propanamide	8.5	Excellent	0.7
n-{1-[2-hydroxy-2-(pyridin-3-yl)ethyl]-3-methylpiperidin-4-yl}-n-phenylpropanamide	8.5	Excellent	0.6
p-fluoro-thiofentanyl	8.5	Poor	0.6
p-fluoro- $\beta$ -hydroxy-thiobutyrylfentanyl	8.5	Good	0.6
p-methoxy-butyrylfentanyl	8.5	Poor	0.6
$\alpha$ -methyl-acetylfentanyl	8.5	Good	0.6
3-methylfentanyl	8.4	Excellent	0.6
4''-fluoro-ohmefentanyl	8.4	Good	0.7
o-methylfentanyl	8.4	Good	0.6
pivaloylfentanyl	8.4	OK	0.6
valeryl fentanyl	8.4	Good	0.6
$\alpha'$ -methyl-butyrylfentanyl	8.4	Good	0.6
$\beta$ -hydroxy-3-methyl-thienylfentanyl	8.4	Excellent	0.6
p-methoxy-furanylfentanyl	8.4	OK	0.6
4'-methyl-tetrahydrofuranylfentanyl	8.4	OK	0.7

pharaohfentanyl	8.4	Excellent	0.6
o-methyl-furanylfentanyl	8.4	Good	0.6
methyl 1-[2-[5-methyl-2-(methylsulfanyl)-6-oxopyrimidin-1(6h)-yl]ethyl]-4-[phenyl(propanoyl)amino]piperidine-4-carboxylate	8.3	Good	0.6
n-[1-[2-hydroxy-2-(1-methyl-1h-pyrrol-2-yl)ethyl]-3-methylpiperidin-4-yl]-n-phenylpropanamide	8.3	Excellent	0.6
o-methoxy-furanylfentanyl	8.3	OK	0.6
p-iodofentanyl	8.3	OK	0.6
p-methoxy-acetylfentanyl	8.3	Excellent	0.6
p-methyl-acetylfentanyl	8.3	OK	0.6
$\beta$ -hydroxy-p-fluorofentanyl	8.3	Excellent	0.6
$\beta$ -hydroxy-sufentanil	8.3	Good	0.6
3-methoxyfentanyl	8.3	Excellent	0.7
tetrahydrofuranylfentanyl	8.3	Good	0.6
thenylfentanyl	8.3	Excellent	0.6
n-[1-(2-hydroxy-2-phenylethyl)-3-methylpiperidin-4-yl]-n-phenylthiophene-2-carboxamide	8.2	Good	0.7
n-methyl-acetyl-norfentanyl	8.2	Bad	0.6
$\alpha$ ,3-dimethylfentanyl	8.2	OK	0.6
$\alpha$ -methyl-acrylfentanyl	8.2	Good	0.6
p-fluoro-methoxyacetylfentanyl	8.2	Excellent	0.6
p-methoxyfentanyl	8.2	Good	0.6
tmcp-f	8.2	Excellent	0.6
furanylfentanyl	8.2	OK	0.7
furanyl-norfentanyl	8.2	Poor	0.6
methyl 1-[(2,3-dihydro-1,4-benzodioxin-2-yl)methyl]-4-[phenyl(propanoyl)amino]piperidine-4-carboxylate	8.2	Excellent	0.8
n-(4-fluorophenyl)-n-[1-(2-hydroxy-2-phenylethyl)-3-methylpiperidin-4-yl]propanamide	8.2	Excellent	0.7
n-[1-(2-cyclopropyl-2-hydroxyethyl)-3-methylpiperidin-4-yl]-n-phenylpropanamide	8.2	Excellent	0.7
p-tfm-fentanyl	8.2	Good	0.6
thiofentanyl	8.2	Good	0.6
ethyl 1-(2-hydroxy-2-phenylethyl)-3-methyl-4-[phenyl(propanoyl)amino]piperidine-4-carboxylate	8.1	OK	0.8
m-methylfentanyl	8.1	Poor	0.7
p-fluoro-isobutyrylfentanyl	8.1	Excellent	0.6

$\beta$ -hydroxy-3-methylfentanyl carbamate	8.1	Good	0.6
2,3-secofentanyl	8.1	Good	0.6
3-methyl phenoxy acetylfentanil	8.1	Poor	0.6
4"-nitrofentanyl	8.1	Poor	0.5
methyl 1-[2-(3-oxo-2,3-dihydro-4h-1,4-benzothiazin-4-yl)ethyl]-4-[phenyl(propanoyl)amino]piperidine-4-carboxylate	8.1	Poor	0.6
n-[1-(2-hydroxy-2-phenylethyl)-3-methylpiperidin-4-yl]-2-methoxy-n-phenylacetamide	8.1	Excellent	0.7
n-[1-(2-hydroxy-2-phenylethyl)-3-methylpiperidin-4-yl]-n-phenylthiophene-3-carboxamide	8.1	Excellent	0.7
n-methyl norfentanyl	8.1	Bad	0.6
p-methyl-cyclopropylfentanyl	8.1	OK	0.6
3,5-dimethylfentanyl	8.0	Excellent	0.7
ohmefentanil	8.0	Excellent	0.6
p-fluoro-furanylremifentanil	8.0	Excellent	0.6
p-methoxy-methoxyacetylfentanyl	8.0	Good	0.6
$\alpha$ -methyl-p-fluorofentanyl	8.0	Excellent	0.6
$\alpha$ -methyl-thiofentanyl	8.0	Good	0.6
alphamethylfentanyl	8.0	Poor	0.7
fentanyl	8.0	Excellent	0.7
n-[1-(2-hydroxy-2-phenylethyl)-3-methylpiperidin-4-yl]-n-phenylfuran-2-carboxamide	8.0	Excellent	0.7
n-benzylcarfentanil	8.0	Excellent	0.8
p-chloro-furanyl fentanyl	8.0	OK	0.6
phenylpropyl-norfentanyl	8.0	Poor	0.6
$\alpha$ -methyl-isobutyrylfentanyl	8.0	Good	0.6
p-chloro-methoxyacetylfentanyl	8.0	OK	0.6
<b>Medium biological activity</b>			
isobutyrylfentanyl	7.9	Poor	0.7
isocarfentanil	7.9	Excellent	0.6
o-fluoro-despropionoylfentanyl	7.9	Excellent	0.7
p-fluoro-acrylfentanyl	7.9	Excellent	0.6
$\beta$ -hydroxy-carfentanil	7.9	OK	0.6
n-[1-(2-hydroxy-2-phenylethyl)-3-methylpiperidin-4-yl]-n-phenylfuran-3-carboxamide	7.9	Good	0.7
n-phenyl-n-{4-phenyl-1-[2-(1h-pyrazol-1-yl)ethyl]piperidin-4-yl}propanamide	7.9	Good	0.6

p-fluoro-acetylfentanyl	7.9	Excellent	0.6
$\alpha$ -methyl-butyrylfentanyl	7.9	Good	0.6
$\beta$ -hydroxyfentanyl	7.9	Good	0.6
$\beta$ -hydroxy-thiofentanyl	7.9	Excellent	0.6
isofentanyl	7.8	Poor	0.7
methyl 1-[2-oxo-2-(thiophen-2-yl)ethyl]-4-[phenyl(propanoyl)amino]piperidine-4-carboxylate	7.8	Excellent	0.8
n-(2-fluorophenyl)-n-[1-(2-hydroxy-2-phenylethyl)-3-methylpiperidin-4-yl]propanamide	7.8	Excellent	0.8
furanylbenzylfentanyl	7.8	OK	0.7
acetyl-norfentanyl	7.8	Excellent	0.6
phenoxyethyl-norfentanyl	7.8	Excellent	0.6
remifentanil bis ethyl ester	7.7	Good	0.5
$\alpha'$ -methoxyfentanyl	7.7	Good	0.6
p-fluoro-furanylethylfentanyl	7.7	Poor	0.6
benzoilolbenzylfentanyl	7.7	Good	0.7
n-benzyl-butyrylfentanyl	7.7	Excellent	0.7
n-[1-(2-hydroxy-2-phenylethyl)-3-methylpiperidin-4-yl]-n-(pyridin-3-yl)propanamide	7.6	Excellent	0.7
n-{1-[(2r,3r)-3-hydroxy-1,2,3,4-tetrahydronaphthalen-2-yl]-3-methylpiperidin-4-yl}-n-phenylpropanamide	7.6	Poor	0.7
o-methyl-acetylfentanyl	7.6	Poor	0.6
p-methoxy-tetrahydrofuranyl fentanyl	7.6	OK	0.6
p-methoxy-valeryl fentanyl	7.6	OK	0.6
p-fluoro-cyclopropylbenzylfentanyl	7.6	Excellent	0.6
2-furanylbenzylfentanyl	7.5	Excellent	0.6
n-benzyl-acetylfentanyl	7.5	Good	0.7
thiafentanil	7.5	Good	0.6
benzylfentanyl	7.5	Excellent	0.7
p-fluoro-isopropylbenzylfentanyl	7.5	Excellent	0.6
4-anpp	7.4	Excellent	0.7
despropionyl-3-methylfentanyl	7.4	Excellent	0.7
n-benzyl-p-fluoro-isobutyrylfentanyl	7.2	Good	0.5
despropionyl-p-fluorobenzylfentanyl	7.1	Good	0.6



**Table A.16. Composition of the training and test set used to build the QSAR models in Forge™ for morphine-like NSOs. The activity data were obtained by ChEMBL target report on MOR CHEMBL233 For this target only the Ki values were analysed and used. The biological activity Ki is identified as the ‘inhibition constant’ and indicates how potent a ligand is in inhibiting a process; Ki is the concentration required to produce half the maximum inhibition (Neubig et al., 2003). Ki is expressed in molar units (M), where 1 M is equivalent to 1 mol/L (Neubig et al., 2003). Only molecules for which the displacement of the radioligand [3H]DAMGO from the human MOR was used to determine of all of the Ki values, were selected. The binding data were converted to their negative decimal logarithm pKi (pKi = -logKi). In the table the predicted values obtained with the 3D QSAR model generated in Section 7.1.2 are reported..**

Training set						
Title	Structure	p(Ki)	Field QSAR	Dist to model	RF	RVM
CHEMBL517567	<chem>O[C@]([C@H]1C[C@]23CC[C@]1(OC)[C@H]4[C@@]53c6c(O4)c(ccc6C[C@H]2[NH+](C5)CC7CC7)C(=O)N)(C(C)(C)C)C</chem>	9.1	8.6	Excellent	8.8	8.5
CHEMBL415284	<chem>O[C@H]1C=C[C@H]2[C@H]3Cc4ccc(O)c5c4[C@@]2(CC[NH+]3CC=C)[C@H]1O5</chem>	9.7	9.4	Excellent	10.0	9.2
CHEMBL33986	<chem>O[C@]12CCCC[C@@]32c4cc(O)ccc4C[C@H]1[NH+](CC5CCC5)CC3</chem>	9.9	9.2	Excellent	9.7	9.5
CHEMBL517779	<chem>O[C@]12CCCC[C@@]32c4cc(ccc4C[C@H]1[NH+](CC5CCC5)CC3)C(=O)N</chem>	9.8	9.3	Excellent	9.7	10.1
CHEMBL297428	<chem>O=C(N)c1ccc2c(C3(CC[NH+](C(C3C)C2)CC4CC4)C)c1</chem>	9.5	10.0	Excellent	9.5	9.4
CHEMBL80	<chem>O[C@]12CCC(=O)[C@H]3[C@@]42c5c(O3)c(O)ccc5C[C@H]1[NH+](CC4)CC=C</chem>	9.2	9.0	Excellent	8.9	8.6
CHEMBL516552	<chem>O[C@H]1C=C[C@H]2[C@H]3Cc4ccc(c5c4[C@@]2(CC[NH+]3CC=C)[C@@H]1O5)C(=O)N</chem>	7.7	7.7	Excellent	7.9	7.5
CHEMBL512526	<chem>Ic1ccc(CN(Cc2ccc(I)cc2)c3ccc4C[C@@H]5[C@@H]6CCCC[C@]6(CC[NH+]5CC7CCC7)c4c3)cc1</chem>	8.5	8.1	Excellent	8.0	8.4
CHEMBL568830	<chem>Oc1c(cc2C[C@@H]3[C@@H]4CCCC[C@]4(CC[NH+]3CC5CCC5)c2c1)C[NH3+]</chem>	6.5	6.7	Excellent	6.9	6.7
CHEMBL570225	<chem>[NH+]1(CC2CCC2)CC[C@]34c5cc(Nc6ccccc6)ccc5C[C@@H]1[C@@H]4CCCC3</chem>	8.8	9.3	Excellent	8.9	9.2
CHEMBL569725	<chem>Ic1ccc(NC(=O)Nc2ccc3c([C@]45CCCC[C@H]5[C@H]([NH+](CC4)CC6CC6)C3)c2)cc1</chem>	7.6	8.1	Excellent	8.1	8.3
CHEMBL585901	<chem>Oc1c(cc2C[C@@H]3[C@@H]4CCCC[C@]4(CC[NH+]3CC5CCC5)c2c1)/C=N\O</chem>	8.4	9.0	Excellent	8.7	8.8
CHEMBL570428	<chem>OC(CCCCCCCC)c1c(O)cc2c(C[C@@H]3[C@@H]4CCCC[C@]24CC[NH+]3CC5CCC5)c1</chem>	7.4	7.6	Excellent	7.5	7.7
CHEMBL576273	<chem>Ic1ccc(CNc2ccc3C[C@@H]4[C@@H]5CCCC[C@]5(CC[NH+]4CC6CCC6)c3c2)cc1</chem>	8.3	8.2	Excellent	8.0	8.0
CHEMBL568878	<chem>Oc1c(cc2C[C@@H]3[C@@H]4CCCC[C@]4(CC[NH+]3CC5CCC5)c2c1)CO</chem>	6.4	6.4	Excellent	6.1	6.6
CHEMBL572216	<chem>Ic1ccc(NC(=O)Nc2ccc3c([C@]45CCCC[C@H]5[C@H]([NH+](CC4)CC6CCC6)C3)c2)cc1</chem>	7.6	7.8	Excellent	7.3	7.7
CHEMBL576065	<chem>C[NH+]1CC[C@@]23CCCC[C@H]3[C@H]1Cc4cc5c(OC[NH+](C5)Cc6ccccc6)cc42</chem>	7.0	7.2	Excellent	7.2	7.4
CHEMBL569724	<chem>Ic1ccc(NC(=O)Nc2ccc3c([C@]45CCCC[C@H]5[C@H]([NH+](CC4)C)C3)c2)cc1</chem>	7.8	7.7	Excellent	7.9	8.0
CHEMBL571561	<chem>O=C(Nc1ccc2c([C@]34CCCC[C@H]4[C@H]([NH+](CC3)CC5CC5)C2)c1)Nc6ccccc6</chem>	8.4	8.1	Excellent	8.4	8.3

CHEMBL584530	OC(c1c(O)cc2c(C[C@@H]3[C@@H]4CCCC[C@]24CC[NH+]3CC5CCC5)c1)CC	6.7	6.3	Excellent	6.4	6.6
CHEMBL49269	Oc1ccc2C[C@@H]3[C@@H]4CCCC[C@]4(CC[NH+]3CC5CCC5)c2c1	10.2	10.1	Excellent	10.7	9.9
CHEMBL570654	Ic1ccc(NC(Oc2ccc3C[C@@H]4[C@@H]5CCCC[C@]5(CC[NH+]4CC6CCC6)c3c2)=O)cc1	9.0	9.0	Excellent	8.7	8.9
CHEMBL571990	COc1ccc(Nc2ccc3C[C@@H]4[C@@H]5CCCC[C@]5(CC[NH+]4CC6CCC6)c3c2)cc1	9.2	9.2	Excellent	9.1	9.3
CHEMBL570429	Ic1ccc(NC(Oc2ccc3C[C@@H]4[C@@H]5CCCC[C@]5(CC[NH+]4CC6CCC6)c3c2)=O)cc1	9.2	9.5	Excellent	9.1	9.5
CHEMBL568876	Ic1ccc(CNc2ccc3C[C@@H]4[C@@H]5CCCC[C@]5(CC[NH+]4CC6CCC6)c3c2)cc1	9.2	9.4	Excellent	9.1	9.4
CHEMBL568877	COc1ccc(CNc2ccc3C[C@@H]4[C@@H]5CCCC[C@]5(CC[NH+]4CC6CCC6)c3c2)cc1	9.5	9.0	Excellent	9.3	8.9
CHEMBL72180	Oc1ccc2c([C@@]3(CC[NH+](C[C@@H]3O2)CCc4ccccc4)CC)c1	9.2	8.6	Excellent	9.1	8.7
CHEMBL70	O[C@H]1C=C[C@H]2[C@H]3Cc4ccc(O)c5c4[C@@]2(CC[NH+]3C)[C@H]1O5	8.6	8.2	Excellent	8.5	8.2
CHEMBL568309	O[C@H](C[NH+]1CC[C@]2(c3cc(O)ccc3O[C@H]2C1)CC)c4ccccc4	8.0	8.0	Excellent	8.4	7.9
CHEMBL568076	Oc1ccc2c([C@]3(CC[NH+](C[C@H]3O2)CCc4ccccc4)CC)c1	6.7	6.9	Excellent	6.8	7.1
CHEMBL567855	Oc1ccc2c([C@@]3(CC[NH2+](C[C@@H]3O2)CC)c1	7.3	7.9	Excellent	7.9	7.5
CHEMBL566527	O[C@@H](C[NH+]1CC[C@]2(c3cc(O)ccc3O[C@H]2C1)CC)c4ccccc4	7.1	6.4	Excellent	7.1	6.8
CHEMBL598977	Oc1cccc2c1O[C@H]3C[NH+](CC[C@@]23CCc4ccccc4)C	6.1	6.9	Excellent	6.4	6.5
CHEMBL592302	Fc1ccc(CC[NH+]2CC[C@]3(c4ccccc(O)c4O[C@H]3C2)CC)cc1	6.5	6.1	Excellent	6.1	6.3
CHEMBL599175	Oc1cccc2c1O[C@H]3C[NH+](CC[C@@]23CC)CCc4ccccc4	5.8	5.9	Excellent	4.9	5.8
CHEMBL592301	Fc1ccc(C[NH+]2CC[C@]3(c4ccccc(O)c4O[C@H]3C2)CC)cc1	5.6	5.7	Excellent	4.9	5.6
CHEMBL3596371	FC(F)C[NH+]1CC[C@]23c4c5c(O)ccc4C[C@@H]1[C@]3(O)Cc6cc7ccccc7nc6[C@@H]2O5	6.0	6.4	Excellent	5.9	6.6
CHEMBL610012	O[C@]12Cc3cc4ccccc4nc3[C@H]5[C@@]62c7c(O5)c(O)ccc7C[C@H]1[NH+](CC8CC8)CC6	7.7	7.6	Excellent	8.0	8.1
CHEMBL3596367	FC(F)C[NH+]1CC[C@]23c4c5c(O)ccc4C[C@@H]1[C@]3(O)Cc6c7ccccc7[nH]c6C2O5	6.0	6.6	Excellent	6.0	5.9
CHEMBL3758348	O[C@]12CCC(=O)[C@]3([C@@]42c5c(O3)c(O)ccc5C[C@H]1[NH+](CC4)C)CO	8.5	8.4	Excellent	8.3	8.3
CHEMBL3786083	O[C@@]12CC/C(C(=O)C[C@@]31c4cc(O)ccc4C[C@H]2[NH+](CC5CC5)CC3)=C/c6ccccc6	7.3	7.1	Excellent	7.5	7.2
CHEMBL252172	O[C@]12C/C(C(=O)[C@H]3[C@@]42c5c(O3)c(O)ccc5C[C@H]1[NH+](CC6CC6)CC4)=C/c7ccccc7	8.0	8.3	Excellent	7.9	8.2
CHEMBL3785265	O[C@@]12C/C(C(=O)C[C@@]31c4cc(O)ccc4C[C@H]2[NH+](CC5CC5)CC3)=C/c6ccccc6	8.3	8.2	Excellent	8.3	8.1
CHEMBL1797689	O[C@]12CCC(=O)C[C@@]32c4cc(O)ccc4C[C@H]1[NH+](CC3)CC5CC5	9.1	8.9	Excellent	9.0	9.0
CHEMBL3787663	O[C@@]12CCc3cc4ccccc4nc3[C@@]51c6ccc(O)ccc6C[C@H]2[NH+](CC7CC7)CC5	7.8	8.0	Excellent	7.9	7.8
CHEMBL4094170	O[C@]12C/C(C(=O)[C@H]3[C@@]42c5c(O3)c(O)ccc5C[C@H]1[NH+](CC4)CCc6ccccc6)=C/c7ccccc7	7.3	7.7	Excellent	7.6	7.5
CHEMBL4457877	O[C@@]12CC(=C(O)[C@H]3[C@]41c5c(O3)c(O)ccc5C[C@]2([NH+](CC4)CC6CC6)C)C(=O)Nc7ccc(cc7)C#N	8.3	8.1	Excellent	8.1	7.8
CHEMBL4529950	O[C@]12CC(=C(O)[C@H]3[C@@]42c5c(O3)c(O)ccc5C[C@H]1[NH+](CC6CC6)CC4)C(=O)	9.0	9.5	Excellent	9.0	9.3

	Nc7ccccc7					
CHEMBL4561876	O[C@@]12CC(=C(O)[C@H]3[C@@]41c5c(O3)c(O)ccc5C[C@]2([NH+](CC6CC6)CC4)C(=O)NCc7ccccc7	9.0	8.6	Excellent	8.6	8.6
CHEMBL4445736	O[C@]12CC(=C(O)[C@H]3[C@@]42c5c(O3)c(O)ccc5C[C@H]1[NH+](CC4)CC6CC6)C(=O)NC(c7nc(no7)C)(C)C	8.1	8.2	Excellent	8.2	8.5
CHEMBL4543425	O[C@]12CC(=C(O)[C@H]3[C@@]42c5c(O3)c(O)ccc5C[C@H]1[NH+](CC4)CC6CC6)C(=O)Nc7ccccc7	8.0	7.3	Excellent	8.0	8.1
CHEMBL4439770	O[C@]12Cc3c(n[nH]c3[C@H]4[C@@]52c6c(O4)c(O)ccc6C[C@H]1[NH+](CC5)CC7CC7)C	7.6	8.0	Excellent	7.8	8.3
CHEMBL4468216	Clc1c(ccc2c1[nH]c3c2C[C@@]4(O)[C@H]5Cc6ccc(O)c7c6[C@@]4(CC[NH+]5CC8CC8)C3O7)C([O-])=O	7.7	7.8	Excellent	7.8	8.0
CHEMBL2113373	O=C(N[C@]12Cc3c4ccccc4[nH]c3[C@H]5[C@@]62c7c(O5)c(O)ccc7CC1[NH+](CC6)C)CCc8ccccc8	8.0	8.2	Excellent	8.3	8.2
CHEMBL607017	O=C1CC[C@@]2(NC(=O)/C=C/c3ccccc3C)[C@H]4Cc5ccc(OC)c6c5[C@]2([C@H]1O6)CC[NH+]4C	9.4	9.3	Excellent	8.7	8.8
CHEMBL607068	O=C1CC[C@@]2(NC(=O)/C=C\c3ccc([N+](O-])=O)cc3)[C@H]4Cc5ccc(O)c6c5[C@@]2(CC[NH+]4C)[C@H]1O6	9.7	9.8	Excellent	9.5	9.5
CHEMBL2113666	Clc1ccccc1/C=C/C(=O)N[C@]23CCC(=O)[C@H]4[C@@]53c6c(O4)cccc6C[C@H]2[NH+](C5)C	9.8	9.5	Excellent	10.3	9.5
CHEMBL611402	Clc1ccccc1/C=C/C(=O)N[C@]23CCC(=O)[C@H]4[C@@]53c6c(O4)c(O)ccc6C[C@H]2[NH+](CC7CC7)CC5	9.2	9.3	Excellent	9.2	9.3
CHEMBL607126	O=C1CC[C@@]2(NC(=O)CCc3ccc(cc3)C)[C@H]4Cc5ccc(O)c6c5[C@]2([C@H]1O6)CC[NH+]4C	9.5	9.1	Excellent	9.3	9.1
CHEMBL610883	O=C1CC[C@@]2(NC(=O)/C=C/c3ccccc3C)[C@H]4Cc5ccc(O)c6c5[C@]2([C@H]1O6)CC[NH+]4CC7CC7	9.1	9.6	Excellent	9.3	9.6
CHEMBL49143	Nc1ccc2C[C@@H]3[C@@H]4CCCC[C@]4(CC[NH+]3CC5CCC5)c2c1	8.4	9.1	Excellent	8.8	9.3
CHEMBL427862	O=C(Oc1ccc2CC3C4CCCC4(CC[NH+]3CC5CC5)c2c1)NCC	9.5	8.9	Excellent	9.3	8.9
CHEMBL592	Oc1ccc2C[C@@H]3[C@@H]4CCCC[C@]4(CC[NH+]3C)c2c1	9.7	9.5	Excellent	9.5	9.8
CHEMBL301160	Oc1ccc2C[C@@H]3[C@@H]4CCCC[C@]4(CC[NH+]3CC5CCC5)c2c1	9.6	8.9	Excellent	9.4	8.9
CHEMBL392269	OC1C[C@@]2(OC)[C@H](C[C@@]13[C@H]4Cc5ccc(O)c6c5[C@]3([C@H]2O6)CC[NH+]4C)[C@@H](O)C	7.5	8.2	Excellent	7.9	8.2
CHEMBL238017	OC1C[C@@]23C[C@@H]([C@@]1(OC)[C@H]4[C@@]53c6c(O4)c(O)ccc6C[C@H]2[NH+](CC5)C)[C@@H](O)C	7.9	7.5	Excellent	8.0	7.8
CHEMBL401245	OC1C[C@@]23C[C@@H]([C@@]1(OC)[C@H]4[C@@]53c6c(O4)c(O)ccc6C[C@H]2[NH+](CC5)C)[C@H](O)C	7.7	8.1	Excellent	7.9	8.2
CHEMBL215926	Clc1ccc(CCCCN[C@]23CCC(=O)[C@H]4[C@@]53c6c(O4)c(OC)ccc6C[C@H]2[NH+](CC7CC7)CC5)cc1	8.7	8.3	Excellent	8.6	8.4
CHEMBL217658	Clc1ccc(CCN[C@]23CCC(=O)[C@H]4[C@@]53c6c(O4)c(O)ccc6C[C@H]2[NH+](CC7CC7)CC5)cc1	9.1	9.4	Excellent	8.9	9.1

CHEMBL387101	<chem>C1c1ccc(CCN[C@]23CCC(=O)[C@H]4[C@@]53c6c(O4)c(OC)ccc6C[C@H]2[NH+](CC7CC7)CC5)cc1</chem>	8.9	9.2	Excellent	8.8	8.4
CHEMBL217479	<chem>C1c1ccc(CCCC(=O)N[C@]23CCC(=O)[C@H]4[C@@]53c6c(O4)c(O)ccc6C[C@H]2[NH+](CC7CC7)CC5)cc1</chem>	8.9	8.4	Excellent	8.7	8.7
CHEMBL216365	<chem>C1c1ccc(/C=C(CC(=O)N[C@]23CCC(=O)[C@H]4[C@@]53c6c(O4)c(OC)ccc6C[C@H]2[NH+](CC5)CC7CC7)cc1</chem>	8.1	7.6	Excellent	8.3	8.2
CHEMBL385316	<chem>O[C@]12Cc3c4CCCCc4n(c3[C@H]5[C@@]62c7c(O5)c(O)ccc7CC1[NH+](CC8CC8)CC6)CC9CCCC9</chem>	7.7	7.5	Excellent	7.8	7.7
CHEMBL221421	<chem>O[C@]12Cc3c4CCCCc4n(c3[C@H]5[C@@]62c7c(O5)c(O)ccc7C[C@H]1[NH+](CC6)C)Cc8cccc8</chem>	7.1	7.2	Excellent	7.6	7.1
CHEMBL346879	<chem>O[C@]12Cc3c(en(c3[C@H]4[C@@]52c6c(O4)c(O)ccc6CC1[NH+](CC5)CC7CC7)Cc8cccc8)-c9cccc9</chem>	7.8	7.5	Excellent	7.9	7.6
<b>Test set</b>						
Title	Structure	p(Ki)	Field QSAR	Dist to model	RF	RVM
CHEMBL56585	<chem>Oc1ccc2c([C@@]3(CC[NH+])([C@H]([C@@H]3C)C2)CC4CC4)C)c1</chem>	9.8	9.9	Excellent	10.4	9.6
CHEMBL568757	<chem>[NH+]1(CC2CC2)CC[C@]34c5cc(Nc6cccc6)ccc5C[C@@H]1[C@@H]4CCCC3</chem>	10.1	9.9	OK	9.2	9.8
CHEMBL568989	<chem>Ic1ccc(NC(Oc2ccc3C[C@@H]4[C@@H]5CCCC[C@]5(CC[NH+]4C)c3c2)=O)cc1</chem>	9.5	9.2	OK	8.9	9.0
CHEMBL571998	<chem>[NH+]1(CC2CC2)CC[C@]34c5cc(NC6cccc6)ccc5C[C@@H]1[C@@H]4CCCC3</chem>	9.6	9.0	Good	9.0	9.0
CHEMBL583265	<chem>Oc1c(C[NH2+]CCC)cc2C[C@@H]3[C@@H]4CCCC[C@]4(CC[NH+]3CC5CCC5)c2c1</chem>	6.5	6.4	Good	6.8	6.7
CHEMBL566557	<chem>O[C@@H](C[NH+]1CC[C@@]2(c3cc(O)ccc3O[C@@H]2C1)CC)c4cccc4</chem>	5.9	6.8	Good	6.9	7.0
CHEMBL430441	<chem>Oc1ccc2c([C@@]3(CC[NH+](C[C@@H]3O2)C)CC)c1</chem>	7.8	8.4	Excellent	8.7	8.1
CHEMBL567213	<chem>O[C@H](C[NH+]1CC[C@@]2(c3cc(O)ccc3O[C@@H]2C1)CC)c4cccc4</chem>	6.2	7.0	Excellent	7.5	7.4
CHEMBL589260	<chem>Oc1cccc2c1O[C@H]3C[NH+](CC[C@@]23CC)CC4CC4</chem>	5.3	6.2	Excellent	6.3	6.3
CHEMBL3596372	<chem>FC(F)(F)C[NH+]1CC[C@]23c4c5c(O)ccc4C[C@@H]1[C@]3(O)Cc6cc7cccc7nc6[C@@H]2O5</chem>	6.0	7.0	Excellent	7.4	7.0
CHEMBL3786970	<chem>O[C@@]12C/C(C(=O)C[C@@]31c4cc(O)ccc4C[C@H]2[NH+](CC5CC5)CC3)=C\c6cccc6</chem>	7.7	8.1	Poor	7.8	8.1
CHEMBL1201770	<chem>O[C@]12CCC(=O)[C@H]3[C@@]42c5c(O3)c(O)ccc5C[C@H]1[N+](CC4)(CC6CC6)C</chem>	8.3	8.5	Good	8.3	7.6
CHEMBL4521187	<chem>O[C@]12CC(=C(O)[C@H]3[C@@]42c5c(O3)c(O)ccc5C[C@H]1[NH+](CC4)CC6CC6)C(=O)N[C@@H](CO)C</chem>	7.7	8.5	OK	8.2	8.8
CHEMBL2105755	<chem>O[C@]12CC(=C(O)[C@H]3[C@@]42c5c(O3)c(O)ccc5C[C@H]1[NH+](CC6CC6)CC4)C(=O)NC(C)(C)c7nc(no7)-c8cccc8</chem>	9.0	8.9	Poor	8.6	8.7
CHEMBL2113378	<chem>Oc1ccc2CC3[C@]4(NCCCc5cccc5)Cc6c7cccc7[nH]c6[C@H]8[C@]4(CC[NH+]3C)c2c1O8</chem>	8.0	8.1	Good	8.6	7.8
CHEMBL2113380	<chem>Oc1ccc2CC3[C@]4(CCCc5cccc5)Cc6c7cccc7[nH]c6[C@H]8[C@]4(CC[NH+]3C)c2c1O8</chem>	8.3	8.2	OK	8.2	8.3
CHEMBL2113381	<chem>O=C(N[C@]12Cc3c4cccc4[nH]c3[C@H]5[C@@]62c7c(O5)c(O)ccc7CC1[NH+](CC6)C)CC</chem>	7.3	6.8	OK	7.0	7.0

CHEMBL607016	<chem>Clc1cccc1/C=C/C(=O)N[C@]23CCC(=O)[C@H]4[C@@]53c6c(O4)c(OC)ccc6C[C@H]2[NH+](CC5)C</chem>	9.2	8.6	Excellent	9.1	8.2
CHEMBL448428	<chem>Clc1ccc(CC(=O)N[C@]23CCC(=O)[C@H]4[C@@]53c6c(O4)c(O)ccc6C[C@H]2[NH+](CC7CC7)CC5)cc1</chem>	9.1	9.0	OK	8.7	9.2
CHEMBL222579	<chem>O[C@]12Cc3c4CCCCc4n(c3[C@H]5[C@@]62c7c(O5)c(O)ccc7C[C@H]1[NH+](CC6)C)CC8CCCC8</chem>	7.8	8.0	Excellent	8.1	7.8
CHEMBL222597	<chem>O[C@]12Cc3c4CCCCc4n(c3[C@H]5[C@@]62c7c(O5)c(O)ccc7C[C@H]1[NH+](CC8CC8)C6)CC9CC9</chem>	8.6	8.5	Good	8.3	8.4

*Table A.17 Statistics for the 20 3D Filed QSAR model generated for morphine-like NSOs. In red is highlighted the chosen model. Here are presented the statistic of the QSAR models generated in the form of: the coefficient of determination ( $r^2$ ) which indicates the goodness of fit; the cross-validated coefficient of determination ( $q^2$ ) which indicates the robustness; the coefficient of determination for the test set ( $r^2$  test), which indicates the predictive power; the root mean square error (RMSE) as reliability measure; and Tau as a further parameter to assess the predictivity of the model. As  $r^2$ , the closer the value of Tau is to one, the better the model.*

Comps	R <sup>2</sup>	Q <sup>2</sup>	Test	R <sup>2</sup>	RMSE	Tau
0	0	-0.027	-0.03	1.108	1.122	-0.993
1	0.646	0.474	0.663	0.659	0.803	0.437
2	0.765	0.597	0.781	0.536	0.703	0.552
3*	0.874	0.694	0.809	0.393	0.613	0.609
4	0.914	0.676	0.802	0.324	0.631	0.603
5	0.94	0.708	0.796	0.272	0.599	0.624
6	0.959	0.693	0.788	0.225	0.614	0.606
7	0.971	0.693	0.789	0.188	0.613	0.605
8	0.981	0.69	0.8	0.153	0.617	0.596
9	0.985	0.687	0.795	0.134	0.62	0.593
10	0.989	0.672	0.812	0.114	0.634	0.581
11	0.993	0.658	0.8	0.093	0.647	0.575
12	0.995	0.641	0.788	0.074	0.664	0.567
13	0.997	0.619	0.781	0.06	0.684	0.555
14	0.998	0.599	0.78	0.049	0.701	0.544
15	0.999	0.586	0.774	0.037	0.713	0.538
16	0.999	0.581	0.773	0.029	0.717	0.538
17	1	0.577	0.772	0.021	0.72	0.538
18	1	0.574	0.769	0.014	0.723	0.534
19	1	0.573	0.767	0.01	0.724	0.535
20	1	0.572	0.767	0.007	0.725	0.535

**Table A.18. Binding affinity values (S, kcal/mol) for the fentanyl-like NSOs identified by the identified by the NPSfinder® (Sec 3.3), docked as described in Section 4.3.8 in PDB5C1M (MOR). Rmsd is a measure of the variance of the pose**

MOL	S	rmsd_refine
2,3-SECOFENTANYL	-7.8	2.1
2',2''-DIFLUOROFENTANYL	-7.5	1.7
2'-FLUORO-BUTYRYLFENTANYL	-7.3	1.8
2'-FLUORO-ISOBUTYRYLFENTANYL	-7.9	2.2
2'-ISOPROPYL-FURANYLFENTANYL	-8.1	1.5
2-FURANYLBENZYL FENTANYL	-7.4	2.4
2-METHYL CARFENTANIL	-8.1	2.2
2-METHYLFENTANYL	-7.4	2.0
3,3-DIMETHYLFENTANYL	-7.6	2.2
3,5-DIMETHYL-CYCLOPENTYLFENTANYL	-7.8	1.6
3,5-DIMETHYLFENTANYL	-7.7	2.0
3'-4'-DICHLORO-3''-FLUOROFENTANYL	-8.0	1.9
3'-4'-METHYLENEDIOXYFENTANYL	-8.6	1.6
3'-FLUORO-BUTYRYLFENTANYL	-7.9	1.9
3'-FLUORO-ISOBUTYRYLFENTANYL	-8.1	2.2
3'-ME-4F-IBF	-7.8	2.4
3'-METHYL-METHOXYACETYLFENTANYL	-7.5	2.2
3-ALLYLFENTANYL	-8.5	2.6
3-ETHYLFENTANYL	-7.8	2.7
3-FLUOROFENTANYL	-7.1	3.0
3-FURANYLFENTANYL	-8.3	2.3
3-METHOXYFENTANYL	-7.8	2.1
3-METHYL PHENOXY ACETYLFENTANIL	-7.7	2.6
3-METHYL-BUTYRYLFENTANYL	-8.0	2.0
3-METHYLFENTANYL	-7.8	2.4
3-METHYL-FURANYLFENTANYL	-8.3	1.2
3-METHYL-THIOFENTANYL	-7.8	1.7
3-PHENYLPROPANOYLFENTANYL	-8.7	2.3
4-(M-HYDROXYPHENYL)FENTANYL	-8.0	2.8
4''-BROMO-OHMEFENTANYL	-8.2	2.6
4'-CHLORO-BUTYRYLFENTANYL	-7.6	1.8
4'-CHLORO-CYCLOBUTYLFENTANYL	-8.3	1.8
4'-CHLORO-CYCLOPROPYLFENTANYL	-7.6	2.1
4'-CHLOROFENTANYL	-7.4	1.0
4'-FLUORO-BUTYRYLFENTANYL	-7.5	1.6
4'-FLUORO-CROTONYLFENTANYL	-8.0	2.3
4'-FLUORO-CYCLOPENTYLFENTANYL	-8.7	2.1
4'-FLUORO-CYCLOPROPYLFENTANYL	-8.3	2.3
4''-FLUOROFENTANYL	-8.1	2.3

4''-FLUORO-OHMEFENTANYL	-7.8	1.5
4'-HYDROXYBUTYRYLFENTANYL	-8.4	1.8
4''-METHOXYFENTANYL	-8.4	1.4
4''-METHYL-ACETYLFENTANYL	-7.0	1.5
4'-METHYLFENTANYL	-7.8	2.1
4''-METHYLFENTANYL	-8.2	1.7
4'-METHYL-FURANYLFENTANYL	-8.5	2.7
4'-METHYL-METHOXYACETYLFENTANYL	-7.9	2.1
4'-METHYL-TETRAHYDROFURANYLFENTANYL	-8.4	1.5
4-ANPP	-6.7	1.9
4'-CHLORO-CYCLOPENTYLFENTANYL	-8.4	2.3
4-FLUOROFENTANYL	-8.1	2.3
4-METHOXYMETHYLFENTANYL	-8.8	2.7
4-METHYLFENTANYL	-6.7	2.6
4-PHENYLFENTANYL	-8.2	1.8
ACETYL-CARFENTANIL	-7.8	2.2
ACETYLFENTANYL	-6.9	2.0
ACETYL-NORFENTANYL	-5.9	1.1
ACRYLFENTANYL	-7.1	1.7
ALPHAMETHYLFENTANYL	-8.0	2.1
BENZODIOXOLEFENTANYL	-9.1	2.0
BENZOFURANYL-FENTANYL	-7.7	2.0
BENZOYLBENZYL FENTANYL	-8.8	1.7
BENZOYLFENTANYL	-8.3	2.6
BENZYL FENTANYL	-7.8	1.7
BUTYRYL-CARFENTANYL	-8.4	1.7
BUTYRYLFENTANYL	-7.8	2.1
CARFENTANIL	-8.4	2.9
CROTONYLFENTANYL	-7.1	1.9
CYCLOBUTYLFENTANYL	-8.5	2.7
CYCLOHEXYLFENTANYL	-8.2	1.8
CYCLOPENTENYLFENTANYL	-8.4	2.4
CYCLOPENTYLFENTANYL	-8.7	2.3
CYCLOPROPYLFENTANYL	-7.3	1.5
DESPROPIONYL-3-METHYLFENTANYL	-6.8	2.7
DESPROPIONYL-P-FLUOROBENZYL FENTANYL	-6.7	2.3
ETHYL {4-[PHENYL(PROPANOYL)AMINO]-1-[2-(THIOPHEN-2-YL)ETHYL]PIPERIDIN-4-YL}METHYL CARBONATE	-8.6	3.0
FENTANYL	-6.9	2.3
FENTRANYL	-7.0	2.3
FURANYLBENZYL FENTANYL	-8.6	1.6
FURANYLFENTANYL	-8.0	1.7
FURANYL-NORFENTANYL	-6.1	1.8
HEXANOYL FENTANYL	-6.8	1.9
ISOBUTYRYLFENTANYL	-7.0	1.9



ISOCARFENTANIL	-8.0	1.8
ISOFENTANYL	-7.8	2.4
ISOVALEROYLFENTANYL	-8.1	2.4
LOFENTANIL	-8.5	3.9
METHOXYACETYLFENTANYL	-7.5	1.8
METHYL 1-[2-(4-METHYL-1,3-THIAZOL-5-YL)ETHYL]-4-[PHENYL(PROPANOYL)AMINO]PIPERIDINE-4-CARBOXYLATE	-8.4	2.4
METHYL 1-[2-HYDROXY-2-(THIOPHEN-2-YL)ETHYL]-4-[PHENYL(PROPANOYL)AMINO]PIPERIDINE-4-CARBOXYLATE	-8.3	2.2
METHYL 1-{2-[(1-METHYL-1H-IMIDAZOL-2-YL)SULFANYL]ETHYL}-4-[PHENYL(PROPANOYL)AMINO]PIPERIDINE-4-CARBOXYLATE	-8.7	2.9
METHYL 1-{2-[5-METHYL-2-(METHYLSULFANYL)-6-OXOPYRIMIDIN-1(6H)-YL]ETHYL}-4-[PHENYL(PROPANOYL)AMINO]PIPERIDINE-4-CARBOXYLATE	-7.9	2.2
METHYL 4-[PHENYL(PROPANOYL)AMINO]-1-[2-(PYRIDIN-2-YL)ETHYL]PIPERIDINE-4-CARBOXYLATE	-8.3	2.0
M-FLUORO-METHOXYACETYLFENTANYL	-6.1	1.1
MIRFENTANIL	-7.9	2.2
M-METHYLFENTANYL	-7.7	1.5
N-(2-FLUOROPHENYL)-N-[1-(2-HYDROXY-2-PHENYLETHYL)-3-METHYLPIPERIDIN-4-YL]PROPANAMIDE	-8.4	2.1
N-(2-FLUOROPHENYL)-N-[1-(2-PHENYLETHYL)-4-(1,3-THIAZOL-2-YL)PIPERIDIN-4-YL]PROPANAMIDE	-8.3	2.1
N-(2-FLUOROPHENYL)-N-[1-(2-PHENYLETHYL)-4-(PYRIDIN-2-YL)PIPERIDIN-4-YL]PROPANAMIDE	-8.7	2.0
N-(2-FLUOROPHENYL)-N-[4-PHENYL-1-(2-PHENYLETHYL)PIPERIDIN-4-YL]PROPANAMIDE	-7.6	1.5
N-(2-FLUOROPHENYL)-N-{1-[2-(4-METHYL-1,3-THIAZOL-5-YL)ETHYL]-4-PHENYLPIPERIDIN-4-YL}PROPANAMIDE	-6.7	1.8
N-(2-FLUOROPHENYL)-N-{1-[2-(4-METHYL-1,3-THIAZOL-5-YL)ETHYL]-4-PHENYLPIPERIDIN-4-YL}PROPANAMIDE	-7.7	1.8
N-(2-FLUOROPHENYL)-N-{4-(4-METHYL-1,3-THIAZOL-2-YL)-1-[2-(THIOPHEN-3-YL)ETHYL]PIPERIDIN-4-YL}PROPANAMIDE	-8.9	2.6
N-(2-FLUOROPHENYL)-N-{4-PHENYL-1-[2-(1H-PYRAZOL-1-YL)ETHYL]PIPERIDIN-4-YL}PROPANAMIDE	-7.9	2.3
N-(2-FLUOROPHENYL)-N-{4-PHENYL-1-[2-(THIOPHEN-2-YL)ETHYL]PIPERIDIN-4-YL}PROPANAMIDE	-9.2	2.0
N-(2-FLUOROPHENYL)-N-{4-PHENYL-1-[2-(THIOPHEN-3-YL)ETHYL]PIPERIDIN-4-YL}PROPANAMIDE	-8.8	2.2
N-(3-FLUOROPHENYL)-N-[1-(2-HYDROXY-2-PHENYLETHYL)-3-METHYLPIPERIDIN-4-YL]PROPANAMIDE	-8.2	2.9
N-(4-FLUOROPHENYL)-N-[1-(2-HYDROXY-2-PHENYLETHYL)-3-METHYLPIPERIDIN-4-YL]PROPANAMIDE	-8.7	1.9

N-[1-(2-CYCLOPROPYL-2-HYDROXYETHYL)-3-METHYLPIPERIDIN-4-YL]-N-PHENYLPROPANAMIDE	-7.4	1.9
N-[1-(2-HYDROXY-2-PHENYLETHYL)-3-METHYLPIPERIDIN-4-YL]-2-METHOXY-N-PHENYLACETAMIDE	-7.5	1.7
N-[1-(2-HYDROXY-2-PHENYLETHYL)-3-METHYLPIPERIDIN-4-YL]-N-(3-METHOXYPHENYL)PROPANAMIDE	-7.7	2.2
N-[1-(2-HYDROXY-2-PHENYLETHYL)-3-METHYLPIPERIDIN-4-YL]-N-(PYRIDIN-2-YL)PROPANAMIDE	-7.7	1.6
N-[1-(2-HYDROXY-2-PHENYLETHYL)-3-METHYLPIPERIDIN-4-YL]-N-(PYRIDIN-3-YL)PROPANAMIDE	-7.9	1.6
N-[1-(2-HYDROXY-2-PHENYLETHYL)-3-METHYLPIPERIDIN-4-YL]-N-PHENYLFURAN-3-CARBOXAMIDE	-5.9	1.4
N-[1-(2-HYDROXY-2-PHENYLETHYL)-3-METHYLPIPERIDIN-4-YL]-N-PHENYLTHIOPHENE-2-CARBOXAMIDE	-8.7	2.4
N-[1-(2-HYDROXY-2-PHENYLETHYL)-3-METHYLPIPERIDIN-4-YL]-N-PHENYLTHIOPHENE-3-CARBOXAMIDE	-9.0	2.1
N-[1-(2-HYDROXY-2-PHENYLETHYL)-4-(METHOXYMETHYL)-3-METHYLPIPERIDIN-4-YL]-N-PHENYLPROPANAMIDE	-8.1	1.5
N-[4-(4-METHYL-1,3-THIAZOL-2-YL)-1-(2-PHENYLETHYL)PIPERIDIN-4-YL]-N-PHENYLPROPANAMIDE	-8.4	2.0
N-{1-[(2R,3R)-3-HYDROXY-1,2,3,4-TETRAHYDRONAPHTHALEN-2-YL]-3-METHYLPIPERIDIN-4-YL}-N-PHENYLPROPANAMIDE	-8.6	2.0
N-{1-[2-(FURAN-2-YL)-2-HYDROXYETHYL]-4-(METHOXYMETHYL)PIPERIDIN-4-YL}-N-PHENYLPROPANAMIDE	-8.3	2.0
N-{1-[2-HYDROXY-2-(1-METHYL-1H-PYRROL-2-YL)ETHYL]-3-METHYLPIPERIDIN-4-YL}-N-PHENYLPROPANAMIDE	-8.3	3.2
N-{1-[2-HYDROXY-2-(PYRIDIN-3-YL)ETHYL]-3-METHYLPIPERIDIN-4-YL}-N-PHENYLPROPANAMIDE	-8.2	2.6
N-{1-[2-HYDROXY-2-(PYRIDIN-4-YL)ETHYL]-3-METHYLPIPERIDIN-4-YL}-N-PHENYLPROPANAMIDE	-7.8	2.0
N-{1-[2-HYDROXY-2-(THIOPHEN-2-YL)ETHYL]-3-METHYLPIPERIDIN-4-YL}-N-(3-METHOXYPHENYL)PROPANAMIDE	-8.5	1.7
N-{3,5-DIMETHYL-1-[2-(1H-PYRAZOL-1-YL)ETHYL]PIPERIDIN-4-YL}-2-METHOXY-N-PHENYLACETAMIDE	-8.4	2.0
N-{3,5-DIMETHYL-1-[2-(1H-PYRAZOL-1-YL)ETHYL]PIPERIDIN-4-YL}-2-METHOXY-N-PHENYLACETAMIDE	-7.6	1.4
N-ADAMANTYL-FENTANYL	-8.7	1.7
N-BENZOAZOLYL-FENTANYL	-8.0	2.0
N-BENZYL-ACETYLFENTANYL	-7.4	1.6
N-BENZYL-BUTYRYLFENTANYL	-8.0	2.2
N-BENZYL CARFENTANYL	-8.4	2.4
N-BENZYL-P-FLUORO-ISOBUTYRYLFENTANYL	-8.1	2.5
N-FURANYLETHYLFENTANYL	-8.0	2.3

N-METHYL NORFENTANYL	-5.9	2.7
N-METHYL-ACETYL-NORFENTANYL	-5.8	1.9
N-METHYL-BUTYRYLFENTANYL	-6.3	1.8
N-METHYL-CARFENTANIL	-7.1	1.9
N-PHENYL-N-[1-(2-PHENYLETHYL)-4-(1,3-THIAZOL-2-YL)PIPERIDIN-4-YL]PROPANAMIDE	-8.2	2.6
N-PHENYL-N-{4-PHENYL-1-[2-(1H-PYRAZOL-1-YL)ETHYL]PIPERIDIN-4-YL}PROPANAMIDE	-8.9	1.9
N-PHENYL-N-{4-PHENYL-1-[2-(THIOPHEN-2-YL)ETHYL]PIPERIDIN-4-YL}PROPANAMIDE	-8.4	2.0
N-PHENYL-N-{4-PHENYL-1-[2-(THIOPHEN-3-YL)ETHYL]PIPERIDIN-4-YL}PROPANAMIDE	-6.9	1.7
N-QUINOLINYL-FENTANYL	-7.9	2.4
OCFENTANIL	-7.8	2.0
O-FLUORO-DESPROPIONOYLFENTANYL	-6.9	1.2
OHMEFENTANIL	-8.1	2.3
O-METHOXY-FURANYLFENTANYL	-8.1	1.5
O-METHYL-ACETYLFENTANYL	-7.3	2.4
O-METHYL-BENZOYLFENTANYL	-8.3	1.5
O-METHYL-CYCLOPROPYLFENTANYL	-7.1	1.8
O-METHYLFENTANYL	-7.6	1.8
O-METHYL-FURANYLFENTANYL	-7.4	1.3
P-BROMOFENTANYL	-8.0	1.9
P-CHLORO-FURANYLFENTANYL	-7.8	1.5
P-CHLORO-ISOBUTYRYLFENTANYL	-7.5	1.2
P-CHLORO-METHOXYACETYLFENTANYL	-7.8	2.2
P-FLUORO-ACETYLFENTANYL	-7.6	2.6
P-FLUORO-ACRYLFENTANYL	-7.2	1.8
P-FLUORO-CYCLOPROPYLBENZYL FENTANYL	-8.0	2.1
P-FLUORO-FURAN-3-YLFENTANYL	-8.1	2.1
P-FLUORO-FURANYLETHYLFENTANYL	-7.3	2.7
P-FLUORO-FURANYLFENTANYL	-7.8	1.3
P-FLUORO-ISOBUTYRYLFENTANYL	-8.6	1.5
P-FLUORO-ISOPROPYLBENZYL FENTANYL	-7.7	2.7
P-FLUORO-METHOXYACETYLFENTANYL	-8.3	1.9
P-FLUORO-TETRAHYDROFURANYLFENTANYL	-7.7	2.0
P-FLUORO-THIOFENTANYL	-7.0	2.4
P-FLUORO-β-HYDROXY-THIOBUTYRYLFENTANYL	-7.3	2.3
PHARAOHFENTANYL	-7.0	2.1
PHENYLACETYLFENTANYL	-8.6	1.4
PHENYLPROPYL-NORFENTANYL	-6.0	1.9
P-iodofentanyL	-8.3	3.5
PIVALOYLFENTANYL	-7.5	1.6
P-METHOXY-ACETYLFENTANYL	-7.2	1.9
P-METHOXY-BUTYRYLFENTANYL	-8.6	2.4
P-METHOXYFENTANYL	-8.8	3.0
P-METHOXY-FURANYLFENTANYL	-8.8	2.0

P-METHOXY-METHOXYACETYLFENTANYL	-8.1	1.8
P-METHOXY-TETRAHYDROFURANYLFENTANYL	-8.0	1.6
P-METHYL-ACETYLFENTANYL	-7.4	1.3
P-METHYL-CYCLOPROPYLFENTANYL	-7.7	2.1
PROPYL-NORFENTANYL	-6.9	2.3
P-TFM-FENTANYL	-7.9	2.1
SUFENTANIL	-8.5	2.1
TETRAHYDROFURANYLFENTANYL	-8.0	1.7
THENYLFENTANYL	-7.6	1.9
THIAFENTANIL	-8.4	2.5
THIOFENTANYL	-7.2	3.6
THIOPHENOYLFENTANYL	-8.1	2.2
TMCP-F	-8.2	2.1
VALERYLFENTANYL	-7.9	2.3
$\alpha$ ,3-DIMETHYLFENTANYL	-8.0	1.6
$\alpha'$ -METHOXYFENTANYL	-8.5	2.5
$\alpha'$ -METHYL-BUTYRYLFENTANYL	-8.0	2.0
$\alpha$ -METHYL-ACETYLFENTANYL	-7.5	2.9
$\alpha$ -METHYL-ACRYLFENTANYL	-5.3	1.9
$\alpha$ -METHYL-ISOBUTYRYLFENTANYL	-6.4	2.0
$\alpha$ -METHYL-P-FLUOROFENTANYL	-7.5	1.9
$\alpha$ -METHYL-THIOFENTANYL	-7.6	2.1
$\beta$ -HYDROXY-3-METHYLFENTANYL CARBAMATE	-8.4	2.2
$\beta$ -HYDROXY-3-METHYL-THIENYLFENTANYL	-7.8	2.3
$\beta$ -HYDROXY-CARFENTANIL	-8.9	2.3
$\beta$ -HYDROXYFENTANYL	-8.2	2.0
$\beta$ -HYDROXY-P-FLUOROFENTANYL	-8.0	1.8
$\beta$ -HYDROXY-SUFENTANIL	-8.4	1.6
$\beta$ -HYDROXY-THIOFENTANYL	-7.6	2.3
$\beta$ -METHYLFENTANYL	-7.1	1.6

**Table A.19** Twenty most active agonist selected from the ChEMBL Activity Database as reference compounds for the creation of the pharmacophore maps. Compounds were identified across assays to minimise biases

<b>KOR</b>		
<b>Molecule ChEMBL ID</b>	<b>SMILES</b>	<b>EC<sub>50</sub> (nM)</b>
CHEMBL4108754	<chem>O=C(N[C@@H](C(=O)N1CCC2(C(=O)NC(=O)N2)CC1)CCCCN)[C@H](NC(=O)[C@H](NC(=O)[C@H](N)Cc1cccc1)Cc1cccc1)CC(C)C</chem>	0.001
CHEMBL4108145	<chem>O=C(N[C@@H](C(=O)N1CCC2(C(=O)NCC2)CC1)CCCCN)[C@H](NC(=O)[C@H](NC(=O)[C@H](N)Cc1cccc1)Cc1cccc1)CC(C)C</chem>	0.003
CHEMBL4112470	<chem>O=C(N[C@@H](C(=O)N1CCC(n2c(C)nnc2C)CC1)CCCCN)[C@H](NC(=O)[C@H](NC(=O)[C@H](N)Cc1cccc1)Cc1cccc1)CC(C)C</chem>	0.004
CHEMBL4087151	<chem>O=C(N(C)[C@H]1[C@@H]2Oc3c(O)ccc4[C@H](O)[C@H]5N(CC6CC6)CC[C@@]2([C@@]5(O)CC1)c34)/C=C/c1sccc1</chem>	0.005
CHEMBL4115175	<chem>O=C(N[C@@H](C(=O)N1CCC(N2C(=O)Cc3c2cccc3)CC1)CCCCN)[C@H](NC(=O)[C@H](NC(=O)[C@H](N)Cc1cccc1)Cc1cccc1)CC(C)C</chem>	0.005
CHEMBL4112000	<chem>O=C(N[C@@H](C(=O)N1CCC(N2C(=O)Nc3c2cccc3)CC1)CCCCN)[C@H](NC(=O)[C@H](NC(=O)[C@H](N)Cc1cccc1)Cc1cccc1)CC(C)C</chem>	0.005
CHEMBL2338721	<chem>O(C)[C@]12[C@@H]([C@@H](O)CCC(C)C)[C@@]3([C@@H]4N(CC5CC5)CC[C@@]53[C@H]1Oc1c(O)ccc(e51)C4)CC2</chem>	0.006
CHEMBL4115104	<chem>O=C(N[C@@H](C(=O)NCc1ncc(C)nc1)CCCCN)[C@H](NC(=O)[C@H](NC(=O)[C@H](N)Cc1cccc1)Cc1cccc1)CC(C)C</chem>	0.006
CHEMBL2338723	<chem>O(C)[C@]12[C@@H]([C@@H](O)CC3CCCC3)C[C@@]3([C@@H]4N(CC5CC5)CC[C@@]53[C@H]1Oc1c(O)ccc(e51)C4)CC2</chem>	0.007
CHEMBL2338724	<chem>O(C)[C@]12[C@@H]([C@@H](O)CCC3CCCC3)C[C@@]3([C@@H]4N(CC5CC5)CC[C@@]53[C@H]1Oc1c(O)ccc(e51)C4)CC2</chem>	0.008
CHEMBL4108908	<chem>Clc1cc2NC(=O)N(C3CCN(C(=O)[C@H](NC(=O)[C@H](NC(=O)[C@H](NC(=O)[C@H](N)Cc4cccc4)Cc4cccc4)CC(C)C)CCCCN)CC3)c2cc1</chem>	0.008
CHEMBL4115212	<chem>O=C(N[C@@H](C(=O)N1CCC2(C(=O)N(C)CC2)CC1)CCCCN)[C@H](NC(=O)[C@H](NC(=O)[C@H](N)Cc1cccc1)Cc1cccc1)CC(C)C</chem>	0.008
CHEMBL2338725	<chem>O(C)[C@]12[C@@H]([C@@H](O)C3CCCC3)C[C@@]3([C@@H]4N(CC5CC5)CC[C@@]53[C@H]1Oc1c(O)ccc(e51)C4)CC2</chem>	0.010
CHEMBL2338747	<chem>O(C)[C@]12[C@@H]([C@@H](O)(CC3CCCC3)C)C[C@@]3([C@@H]4N(CC5CC5)CC[C@@]53[C@H]1Oc1c(O)ccc(e51)C4)CC2</chem>	0.011
CHEMBL4111684	<chem>O=C(N[C@@H](C(=O)N1CCC(N2C(=O)NC(c3cccc3)=C2)CC1)CCCCN)[C@H](NC(=O)[C@H](NC(=O)[C@H](N)Cc1cccc1)Cc1cccc1)CC(C)C</chem>	0.012
CHEMBL2338720	<chem>O(C)[C@]12[C@@H]([C@@H](O)CC(C)C)C[C@@]3([C@@H]4N(CC5CC5)CC[C@@]53[C@H]1Oc1c(O)ccc(e51)C4)CC2</chem>	0.013
CHEMBL4110548	<chem>O=C(N[C@@H](C(=O)N1CCC(C(=O)N2CCOCC2)CC1)CCCCN)[C@H](NC(=O)[C@H](NC(=O)[C@H](N)Cc1cccc1)Cc1cccc1)CC(C)C</chem>	0.015
CHEMBL2338753	<chem>O(C)[C@]12[C@@H]([C@@H](O)(CCc3cccc3)C)C[C@@]3([C@@H]4N(CC5CC5)CC[C@@]53[C@H]1Oc1c(O)ccc(e51)C4)CC2</chem>	0.016
CHEMBL4115291	<chem>O=C(N[C@@H](C(=O)N1CCC2(N(c3cccc3)CNC2=O)CC1)CCCCN)[C@H](NC(=O)[C@H](NC(=O)[C@H](N)Cc1cccc1)Cc1cccc1)CC(C)C</chem>	0.017
CHEMBL2338750	<chem>O(C)[C@]12[C@@H]([C@@H](O)(CC3CCCC3)C)C[C@@]3([C@@H]4N(CC5CC5)CC[C@@]53[C@H]1Oc1c(O)ccc(e51)C4)CC2</chem>	0.017
CHEMBL3359804	<chem>O=C(O[C@@H]1C(=O)[C@H]2[C@](C)([C@H](C(=O)OC)C1)CC[C@H]1C(=O)O[C@H](c3c(C#C)occ3)C[C@]21C)C</chem>	0.019
CHEMBL2338722	<chem>O(C)[C@]12[C@@H]([C@@H](O)C3CCCC3)C[C@@]3([C@@H]4N(CC5CC5)CC[C@@]53[C@H]1Oc1c(O)ccc(e51)C4)CC2</chem>	0.020
<b>DOR</b>		

CHEMBL2151735	O=C(N([C@@H](C(=O)N[C@@H]1C(=O)N(CC(=O)N)Cc2c(cccc2)C1)C)C)[C@@H]([NH3+])Cc1c(C)cc(O)cc1C	0.016
CHEMBL559518	Oc1cc2c(cc1)C[C@H]1[NH+](CC3CC3)CC[C@@]32[C@H]1Cc1c(nc2c(c1)cccc2)C3	0.018
CHEMBL552308	Oc1cc2c(cc1)C[C@H]1[NH+](C)CC[C@@]32[C@H]1Cc1c(nc2c(c1)cccc2)C3	0.047
CHEMBL8234	O=C([O-])[C@@H](NC(=O)[C@@H](NC(=O)CNC(=O)CNC(=O)[C@@H]([NH3+])Cc1ccc(O)cc1)Cc1cccc1)CC(C)C	0.080
CHEMBL3758292	O=C([C@@H]([NH3+])Cc1c(C)cc(O)cc1)N1[C@@H](C(=O)NCc2[nH]c3c(n2)cccc3)Cc2c(cccc2)C1	0.081
CHEMBL2113666	Clc1c(/C=C/C(=O)N[C@]23[C@@H]4[NH+](C)CC[C@@]52[C@H](C(=O)CC3)Oc2c5c(ccc2)C4)cccc1	0.100
CHEMBL567175	Oc1c2O[C@H]3c4[nH]c5c(c4[C@@]4(O)[C@@H]6[NH+](CC7CC7)CC[C@]34c2c(cc1)C6)cccc5	0.110
CHEMBL31421	O=C(N[C@@H]1C(C)(C)SSC(C)(C)[C@H](C(=O)[O-])NC(=O)[C@H](Cc2cccc2)NC(=O)CNC1=O)[C@@H]([NH3+])Cc1ccc(O)cc1	0.120
CHEMBL25230	O=C(N(CC)CC)c1ccc([C@@H](N2[C@@H](C)C[NH+](CC=C)[C@H](C)C2)c2cc(O)ccc2)cc1	0.120
CHEMBL2208349	O=C(NCCc1ccc(-c2c(O)cccc2)cc1)c1cc2C3(C)C(C)C([NH+](CC4CC4)CC3)Cc2cc1	0.160
CHEMBL226166	Oc1cc2c(cc1)C[C@H]1[NH+](CC3CC3)CC[C@@]32[C@H]1Cc1c2c([nH]c1C3)cccc2	0.160
CHEMBL67192	O=C(N(CC)CC)c1ccc(Cc2cccc2)=C2CC3[NH+](Cc4cc5OCOc5cc4)C(C2)CC3)cc1	0.200
CHEMBL568818	O=C(N(CC)CC)c1ccc(Nc2cc(O)ccc2)C2CC[NH+](CCc3ccc3)CC2)cc1	0.220
CHEMBL4103044	O=C(N1C2C3[C@@H](C1)CC1(C43c3c(ccc(O)c3)CC1[NH+](CC1CC1)CC4)CC2)c1ccc1	0.230
CHEMBL2179656	Clc1ccc(-c2cnc3[C@@H]4Oc5c(O)ccc6c5[C@@]54[C@](OCCc4cccc4)([C@H]([NH+](C)CC5)C6)Cc3c2)cc1	0.270
CHEMBL577615	O=C(N(CC)CC)c1ccc(Nc2cc(C(=O)N)ccc2)C2CC[NH+](Cc3cccc3)CC2)cc1	0.300
CHEMBL611932	O=C(N[C@H]1[C@@H]2Oc3c(O)ccc4c3[C@@]32[C@](O)([C@H]([NH+](CC2CC2)CC3)C4)CC1)c1ccc(C(C)(C)C)cc1	0.300
CHEMBL281986	O(C)[C@]12C3([C@H](O)CCC3)CC3(C45[C@@H]1Oc1c(O)ccc(c41)CC3[NH+](CC1CC1)CC5)C=C2	0.300
CHEMBL421520	S=C(NC(C)(C)C)NC[C@H]1N(C(=O)[C@@H]([NH3+])Cc2c(C)cc(O)cc2)Cc2c(cccc2)C1	0.320
CHEMBL4075409	O=C(N1C2C3[C@H](OC4(C53c3c(ccc(O)c3)CC4[NH+](CC=C)CC5)CC2)C1)c1cccc1	0.430
<b>MOR</b>		
CHEMBL2151735	O=C(N([C@@H](C(=O)N[C@@H]1C(=O)N(CC(=O)N)Cc2c(cccc2)C1)C)C)[C@@H](N)Cc1c(C)cc(O)cc1C	0.0017
CHEMBL4550234	O=C(NC(C(C(=O)N)=C)c1ccc1)[C@@H](NC(=O)[C@H](N(C(=O)C(N)Cc1c(C)cc(O)cc1)C)C)Cc1cccc1	0.0018
CHEMBL4521879	O=C(NC(C(C(=O)N)=C)c1cccc1)[C@@H](NC(=O)[C@H](N(C(=O)C(N)Cc1c(C)cc(O)cc1)C)C)Cc1cccc1	0.0018
CHEMBL4563672	O=C(N(c1cccc1)C1(C(=O)OC)CCN(Cc2c(O)cccc2)CC1)CC	0.0024
CHEMBL290429	O=C(N(c1cccc1)C1(C(=O)OC)CCN(Cc2cccc2)CC1)CC	0.0049
CHEMBL4463749	O=C(N(c1cccc1)C1(C(=O)OC)CCN(CC(O)c2cccc2)CC1)CC	0.0051
CHEMBL4588535	O=C(N(c1cccc1)C1(C(=O)OC)CCN(Cc2cc(O)ccc2)CC1)CC	0.0140
CHEMBL4578287	O=C(N(c1cccc1)C1(C(=O)OC)CCN(Cc2ccc(O)cc2)CC1)CC	0.0280
CHEMBL2113666	Clc1c(/C=C/C(=O)N[C@]23[C@@H]4N(C)CC[C@@]52[C@H](C(=O)CC3)Oc2c5c(ccc2)C4)cccc1	0.0400

CHEMBL607125	O=C(N[C@]12[C@@H]3N(C)CC[C@@]41[C@H](C(=O)CC2)Oc1c(O)ccc(c41)C3)/C=C/c1c(C)cccc1	0.0400
CHEMBL333357	O=C(N[C@H](C(=O)N)Cc1cccc1)[C@@H](NC(=O)[C@H]1N(C(=O)[C@@H](N)Cc2ccc(O)cc2)CCC1)Cc1cccc1	0.0400
CHEMBL2151734	O=C(N(CC(=O)N)C)[C@@H](NC(=O)[C@H](N(C(=O)[C@@H](N)Cc1c(C)cc(O)cc1C)C)C)Cc1cccc1	0.0790
CHEMBL1834247	O=C(N[C@@H](C(=O)N[C@@H]1C(=O)N(CC(=O)N)Cc2c(ccc2)C1)C)[C@@H](N)Cc1c(C)cc(O)cc1C	0.0832
CHEMBL494853	O=C(N[C@@H]1[C@@H]2Oc3c(O)ccc4c3[C@@]32[C@](O)([C@H](N(CC2CC2)CC3)C4)CC1)c1nc2c(cc1)cccc2	0.0900
CHEMBL3408737	O=C(N[C@@H]1C(=O)N(CCC(=O)N)Cc2c(ccc2)C1)[C@H](NC(=O)[C@@H](N)Cc1c(C)cc(O)cc1C)CCNC(=N)N	0.1000
CHEMBL331325	O=C(N[C@H](C(=O)N)Cc1cccc1)[C@@H](NC(=O)[C@H]1N(C(=O)[C@@H](N)Cc2c(C)cc(O)cc2C)CCC1)Cc1cccc1	0.1000
CHEMBL511142	O(C)[C@@]12[C@@H]([C@](O)(C(C)(C)C)C)[C@@]3([C@@H]4N(CC5CC5)CC[C@@]53[C@H]1Oc1c(O)ccc(c51)C4)CC2	0.1100
CHEMBL4103328	O(Cc1cccc1)[C@]12[C@@H]3N(C)CC[C@@]41[C@@H](Oc1c(O)ccc(c41)C3)CCC2	0.1300
CHEMBL13470	O=C(N(CC)CC)c1ccc([C@@H](N2[C@@H](C)CN(CC=C)[C@H](C)C2)c2cc(OC)ccc2)cc1	0.1400
CHEMBL2208351	O=C(NCCc1ccc(-c2cc3OCOc3cc2)cc1)c1cc2C3(C)C(C)C(N(CC4CC4)CC3)Cc2cc1	0.1500

Table A20. Test sets for KOR, DOR, MOR pharmacophores validation

Notes. These compounds were selected to include a variety of structures and a broad activity value set (i.e. at least four orders of magnitude). In red the compounds that were filtered by the KOR, MOR and DOR pharmacophore.

KOR		
Mol	Smiles	EC <sub>50</sub>
CHEMBL472410	<chem>O=C(N[C@H]1[C@@H]2Oc3c(O)ccc4c3[C@@]32[C@](OCC=C)([C@H](N(CC2CC2)CC3)C4)CC1)/C=C/c1cccc1</chem>	0.08
CHEMBL454018	<chem>O=[N+](([O-])c1cc(/C=C/C(=O)N[C@H]2[C@@H]3Oc4c(O)ccc5c4[C@@]43[C@](O)([C@H](N(CC3CC3)CC4)C5)CC2)ccc1</chem>	0.12
CHEMBL473362	<chem>O=C(N[C@H]1[C@@H]2Oc3c(O)ccc4c3[C@@]32[C@](O)([C@H](N(CC2CC2)CC3)C4)CC1)/C=C/c1cccc1</chem>	0.12
CHEMBL2338742	<chem>O(C)[C@]12[C@@H]([C@H](O)CC3CCCC3)C[C@@]3([C@@H]4N(CC5CC5)CC[C@@]53[C@H]1Oc1c(O)ccc(c51)C4)CC2</chem>	0.19
CHEMBL2338716	<chem>O(C)[C@]12[C@@H]([C@H](O)CCC3CCCC3)C[C@@]3([C@@H]4N(CC5CC5)CC[C@@]53[C@H]1Oc1c(O)ccc(c51)C4)CC2</chem>	0.24
CHEMBL2338740	<chem>O(C)[C@]12[C@@H]([C@H](O)C3CCCC3)C[C@@]3([C@@H]4N(CC5CC5)CC[C@@]53[C@H]1Oc1c(O)ccc(c51)C4)CC2</chem>	0.29
CHEMBL575682	<chem>O=C(N[C@]12[C@@H]3N(CC4CC4)CC[C@@]41[C@H](C(=O)CC2)Oc1c(O)ccc(c41)C3)C#Cc1cccc1</chem>	0.30
CHEMBL2338733	<chem>O(C)[C@]12[C@@H]([C@@](O)(CC3CCCC3)C)C[C@@]3([C@@H]4N(CC5CC5)CC[C@@]53[C@H]1Oc1c(O)ccc(c51)C4)CC2</chem>	0.31
CHEMBL511655	<chem>Clc1c(/C=C/C(=O)N[C@H]2[C@@H]3Oc4c(O)ccc5c4[C@@]43[C@](O)([C@H](N(CC3CC3)CC4)C5)CC2)cccc1</chem>	0.40
CHEMBL2338756	<chem>O(C)[C@]12[C@@H]([C@@](O)(C(C)C)C)C[C@@]3([C@@H]4N(CC5CC5)CC[C@@]53[C@H]1Oc1c(O)ccc(c51)C4)CC2</chem>	0.46
CHEMBL2338734	<chem>O(C)[C@]12[C@@H]([C@@](O)(CCC3CCCC3)C)C[C@@]3([C@@H]4N(CC5CC5)CC[C@@]53[C@H]1Oc1c(O)ccc(c51)C4)CC2</chem>	0.46
CHEMBL503017	<chem>O=C(N[C@H]1[C@@H]2Oc3c(O)ccc4c3[C@@]32[C@](OC(=O)C2cccc2)([C@H](N(CC2CC2)CC3)C4)CC1)/C=C/c1cccc1</chem>	0.49
CHEMBL2338737	<chem>O(C)[C@]12[C@@H]([C@H](O)C(C)C)C[C@@]3([C@@H]4N(CC5CC5)CC[C@@]53[C@H]1Oc1c(O)ccc(c51)C4)CC2</chem>	0.63
CHEMBL2338729	<chem>O(C)[C@]12[C@@H]([C@@](O)CCc3cccc3)C[C@@]3([C@@H]4N(CC5CC5)CC[C@@]53[C@H]1Oc1c(O)ccc(c51)C4)CC2</chem>	0.73
CHEMBL509552	<chem>O=C(N[C@H]1[C@@H]2Oc3c(O)ccc4c3[C@@]32[C@](OC2cccc2)([C@H](N(CC2CC2)CC3)C4)CC1)/C=C/c1cccc1</chem>	0.78
CHEMBL147511	<chem>O=C(Oc1cc2c(cc1)C[C@H]1N(CC3CCC3)CC[C@@]32[C@H]1CCCC3)CCCCCCCC(=O)Oc1cc2c(cc1)C[C@H]1N(CC3CCC3)CC[C@@]32[C@H]1CCCC3</chem>	0.85
CHEMBL513598	<chem>O=C(N[C@H]1[C@@H]2Oc3c(O)ccc4c3[C@@]32[C@](O)([C@H](N(CC2CC2)CC3)C4)CC1)/C=C/c1c(OC)cccc1</chem>	0.95
CHEMBL56585	<chem>Oc1cc2[C@@]3(C)[C@@H](C)[C@H](N(CC4CC4)CC3)Cc2cc1</chem>	1.30
CHEMBL502267	<chem>Clc1c(Cl)ccc(N(CC(=O)N2C(CN3CCCC3)CN(c3cccc3)CC2)C)c1</chem>	1.30
CHEMBL301160	<chem>Oc1cc2c(cc1)C[C@H]1N(CC3CCC3)CC[C@@]32[C@H]1CCCC3</chem>	1.30
CHEMBL503079	<chem>O=C(Cc1c2c(cc1)cccc2)N1C(CN2CCCC2)CN(c2cccc2)CC1</chem>	1.60



CHEMBL584791	O=C(Oc1c2O[C@@H]3[C@]45[C@H]([C@H](N(CC=C)CC4)Cc(c25)cc1)CCC3)CCCCCCCCC(=O)Oc1cc2c(cc1)CC1N(CC3CCC3)CC[C@@]32[C@H]1CCCC3	1.60
CHEMBL448145	O=[N+]([O-])c1c(/C=C/C(=O)N[C@H]2[C@@H]3Oc4c(O)ccc5c4[C@@]43[C@](O)([C@H](N(CC3CC3)CC4)C5)CC2)cccc1	1.90
CHEMBL503080	Clc1cc2c(CC(=O)N3C(CN4CCCC4)CN(c4ccccc4)CC3)csc2cc1	2.00
CHEMBL2338715	O=C1[C@@H]2N(CC3CC3)CC[C@@](CC)([C@@H]2C)c2c1ccc(O)c2	2.20
CHEMBL472583	O=C(N[C@H]1[C@@H]2Oc3c(O)ccc4c3[C@@]32[C@](OC(=O)C)([C@H](N(CC2CC2)CC3)C4)CC1)/C=C/c1cccc1	2.40
CHEMBL566346	O=C(Oc1cc2c(cc1)C[C@H]1N(CC3CCC3)CC[C@@]32[C@H]1CCCC3)CCCCCCCCC(=O)O	2.80
CHEMBL254154	Clc1c(Cl)ccc(N(CC(=O)N2C(CN3CCCC3)CCCC2)C)c1	3.00
CHEMBL526933	Clc1c(Cl)ccc(N(CC(=O)N2C(CN3CCCC3)CN(S(=O)(=O)C)CC2)C)c1	3.00
CHEMBL575451	O=C(N[C@]12[C@@H]3N(CC4CC4)CC[C@@]41[C@H](C(=O)CC2)Oc1c(OC)ccc(c41)C3)C#Cc1cccc1	3.18
CHEMBL526747	Clc1c(Cl)ccc(N(CC(=O)N2C(CN3CCCC3)CN(c3cc(OC)ccc3)CC2)C)c1	3.20
CHEMBL524888	FC(F)(F)c1n(CC(=O)N2C(CN3CCCC3)CN(c3ccccc3)CC2)c2c(n1)cccc2	4.00
CHEMBL524367	Clc1c(Cl)ccc(N(CC(=O)N2C(CN3CCCC3)CN(c3cc(Cl)ccc3)CC2)C)c1	4.00
CHEMBL518712	C(N1C2[C@H](C)[C@@](C)(c3c(cc4nc[nH]c4c3)C2)CC1)C1CC1	4.70
CHEMBL565679	O=C(Oc1cc2c(cc1)C[C@H]1N(CC3CCC3)CC[C@@]32[C@H]1CCCC3)C(CCCCCC(C(=O)O)C)C	4.90
CHEMBL473699	C(N1C2[C@H](C)[C@@](C)(c3c(cc4nc(C)[nH]c4c3)C2)CC1)C1CC1	5.80
CHEMBL500407	Clc1c(Cl)ccc(N(CC(=O)N2C(CN3CCCC3)CN(c3cc(F)c(F)cc3)CC2)C)c1	6.30
CHEMBL584790	O=C(Oc1cc2c(cc1)C[C@H]1N(CC3CCC3)CC[C@@]32[C@H]1CCCC3)C(CCCCCC(C(=O)Oc1cc2c(cc1)C[C@H]1N(CC3CCC3)CC[C@@]32[C@H]1CCCC3)(C)C)C	6.40
CHEMBL582930	O=C(Oc1cc2c(cc1)C[C@H]1N(CC3CCC3)CC[C@@]32[C@H]1CCCC3)C(CCCCCC(C(=O)Oc1cc2c(cc1)C[C@H]1N(CC3CCC3)CC[C@@]32[C@H]1CCCC3)C)C	7.30
CHEMBL475108	C(N1C2[C@H](C)[C@@](C)(c3c4nn[nH]c4ccc3C2)CC1)C1CC1	8.60
CHEMBL468871	O=C(N[C@H]1[C@@H]2Oc3c(O)ccc4c3[C@@]32[C@](OC(=O)c2cccc2)([C@H](N(CC2CC2)CC3)C4)CC1)/C=C/c1cccc1	9.80
CHEMBL572525	O=C(N[C@H]1C(=O)N[C@@H](Cc2cccc2)C(=O)N[C@@H](Cc2cc3c(cc2)cccc3)C(=O)N[C@H](C(=O)N)CSCSC1)[C@@H](N)Cc1ccc(O)cc1	12.0
CHEMBL578422	Clc1ccc(C#CC(=O)N[C@]23[C@@H]4N(CC5CC5)CC[C@@]52[C@H](C(=O)CC3)Oc2c(OC)ccc(c52)C4)cc1	20.0
CHEMBL474755	O=C(O[C@]12[C@@H]3N(CC4CC4)CC[C@@]41[C@H](C(=O)CC2)Oc1c(OC)ccc(c41)C3)/C=C/c1cccc1	26.0
CHEMBL441765	Clc1c(Cl)ccc(CC(=O)N(C)[C@H]2[C@H](N3CCCC3)CCCC2)c1	36.0
CHEMBL557937	Oc1cc2c(cc1)C[C@@]13[C@@]2(Cc2n(C)c4c(c2C1)cccc4)CCN(C)C3	62.1
CHEMBL562340	Oc1cc2c(cc1)C[C@@]13[C@@]2(Cc2[nH]c4c(c2C1)cccc4)CCN(CC1CC1)C3	67.1
CHEMBL515593	C(N1C2[C@H](C)[C@@](C)(c3c(cc4nn[nH]c4c3)C2)CC1)C1CC1	77.0
CHEMBL499353	Clc1c(Cl)ccc(N(CC(=O)N2C(CN3CCCC3)CN(S(=O)(=O)c3cc(OC)ccc3)CC2)C)c1	79.0
CHEMBL471543	O=C(O[C@]12[C@@H]3N(CC4CC4)CC[C@@]41[C@H](C(=O)CC2)Oc1c(OC)ccc(c41)C3)/C=C/c1ccc(C)cc1	157

CHEMBL499351	<chem>Clc1c(Cl)ccc(N(CC(=O)N2C(CN3CCCC3)CN(S(=O)(=O)c3cc(Cl)ccc3)CC2)C)c1</chem>	200
CHEMBL526913	<chem>Clc1c(Cl)ccc(N(CC(=O)N2C(CN3CCCC3)CN(S(=O)(=O)c3ccccc3)CC2)C)c1</chem>	250
CHEMBL525457	<chem>Clc1cc2N(CC(=O)N3C(CN4CCCC4)CN(S(=O)(=O)c4cc(OC)c(OC)cc4)CC3)C(=O)Oc2cc1</chem>	320
CHEMBL498314	<chem>Clc1cc2N(CC(=O)N3C(CN4CCCC4)CN(S(=O)(=O)c4cc(OC)ccc4)CC3)C(=O)Oc2cc1</chem>	320
CHEMBL496084	<chem>Clc1c(Cl)ccc(N(CC(=O)N2C(CN3CCCC3)CN(S(=O)(=O)c3cc(F)c(F)cc3)CC2)C)c1</chem>	400
CHEMBL527013	<chem>O=C(CN1C(=O)Oc2c1cccc2)N1C(CN2CCCC2)CN(c2ccccc2)CC1</chem>	400
CHEMBL70	<chem>O[C@@H]1[C@@H]2Oc3c(O)ccc4c3[C@@]32[C@H]([C@H](N(C)CC3)C4)C=C1</chem>	484
CHEMBL524546	<chem>Clc1c(Cl)ccc(N(CC(=O)N2C(CN3CCCC3)CN(C(=O)c3ccccc3)CC2)C)c1</chem>	630
CHEMBL498330	<chem>Clc1cc2N(CC(=O)N3C(CN4CCCC4)CN(S(=O)(=O)c4cc(C#N)ccc4)CC3)C(=O)Oc2cc1</chem>	630
CHEMBL525554	<chem>Br1cc(S(=O)(=O)N2CC(CN3CCCC3)N(C(=O)CN3C(=O)Oc4c3cc(Cl)cc4)CC2)c(OC)cc1</chem>	790
CHEMBL498329	<chem>Clc1cc2N(CC(=O)N3C(CN4CCCC4)CN(S(=O)(=O)c4ccccc4)CC3)C(=O)Oc2cc1</chem>	790
CHEMBL499352	<chem>Clc1c(Cl)ccc(N(CC(=O)N2C(CN3CCCC3)CN(S(=O)(=O)c3ccc(Cl)cc3)CC2)C)c1</chem>	790
CHEMBL503582	<chem>Clc1c(S(=O)(=O)N2CC(CN3CCCC3)N(C(=O)CN3C(=O)Oc4c3cc(Cl)cc4)CC2)cc(C(F)(F)F)cc1</chem>	1000
CHEMBL524288	<chem>S(=O)(=O)(N1CC(CN2CCCC2)N(C(=O)CN2C(=O)Oc3c2cccc3)CC1)c1ccccc1</chem>	1000
CHEMBL525823	<chem>Clc1cc2N(CC(=O)N3C(CN4CCCC4)CN(S(=O)(=O)c4ccc(NC(=O)C)cc4)CC3)C(=O)Oc2cc1</chem>	1300
CHEMBL505188	<chem>Br1c(OC)c(OC)ccc1S(=O)(=O)N1CC(CN2CCCC2)N(C(=O)CN2C(=O)Oc3c2cc(Cl)cc3)CC1</chem>	1300
CHEMBL503322	<chem>Clc1cc2N(CC(=O)N3C(CN4CCCC4)CN(S(=O)(=O)c4cc(C(F)(F)F)ccc4)CC3)C(=O)Oc2cc1</chem>	2000
CHEMBL497667	<chem>Clc1cc2N(CC(=O)N3C(CN4CCCC4)CN(S(=O)(=O)c4ccc(C(=O)O)cc4)CC3)C(=O)Oc2cc1</chem>	2000
CHEMBL525922	<chem>Br1c(S(=O)(=O)N2CC(CN3CCCC3)N(C(=O)CN3C(=O)Oc4c3cc(Cl)cc4)CC2)cccc1</chem>	2000
CHEMBL526842	<chem>Clc1cc2N(CC(=O)N3C(CN4CCCC4)CN(S(=O)(=O)c4ccc(OC)cc4)CC3)C(=O)Oc2cc1</chem>	2000
CHEMBL502825	<chem>Clc1c(Cl)ccc(N(CC(=O)N2C(CN3CCCC3)CN(C(=O)c3ccc(C#N)cc3)CC2)C)c1</chem>	3200
CHEMBL502819	<chem>Clc1c(Cl)ccc(N(CC(=O)N2C(CN3CCCC3)CN(C(=O)Nc3ccccc3)CC2)C)c1</chem>	4000
CHEMBL501461	<chem>Clc1c(Cl)ccc(N(CC(=O)N2C(CN3CCCC3)CN(C(=O)c3ccccc3)CC2)C)c1</chem>	7900
CHEMBL526192	<chem>Clc1cc2N(CC(=O)N3C(CN4CCCC4)CN(S(=O)(=O)c4cc(O)c(C(=O)O)cc4)CC3)C(=O)Oc2cc1</chem>	7900
CHEMBL501468	<chem>Clc1c(Cl)ccc(N(CC(=O)N2C(CN3CCCC3)CN(C(=O)c3cc(Cl)ccc3)CC2)C)c1</chem>	10000
CHEMBL526735	<chem>Clc1c(Cl)ccc(N(CC(=O)N2C(CN3CCCC3)CN(C(=O)c3cc(OC)c(OC)cc3)CC2)C)c1</chem>	10000
<b>DOR</b>		
<b>Mol</b>	<b>Smiles</b>	<b>EC<sub>50</sub></b>
CHEMBL559518	<chem>Oc1cc2c(cc1)C[C@H]1N(CC3CC3)CC[C@@]32[C@H]1Cc1c(nc2c(c1)cccc2)C3</chem>	0.02
CHEMBL552308	<chem>Oc1cc2c(cc1)C[C@H]1N(C)CC[C@@]32[C@H]1Cc1c(nc2c(c1)cccc2)C3</chem>	0.05

CHEMBL564538	Oc1cc2c(cc1)C[C@H]1N(CC(C)C)CC[C@@]32[C@H]1Cc1c(nc2c(c1)cccc2)C3	0.06
CHEMBL567175	Oc1c2O[C@H]3c4[nH]c5c(c4C[C@@]4(O)[C@@H]6N(CC7CC7)CC[C@]34c2c(cc1)C6)cccc5	0.11
CHEMBL1929365	Oc1c2c(ccc1)C[C@H]1N(CC3CC3)CC[C@@]32[C@H]1Cc1c(nc2c(c1)cccc2)C3	0.19
CHEMBL2113383	Oc1c2O[C@H]3c4[nH]c5c(c4C[C@]4(NCC)[C@]63c2c(cc1)CC4N(C)CC6)cccc5	0.33
CHEMBL25230	O=C(N(CC)CC)c1ccc([C@@H](N2[C@@H](C)CN(CC=C)[C@H](C)C2)c2cc(O)ccc2)cc1	0.40
CHEMBL249985	O=C(NCCc1ccc(-c2ccc(OC)cc2)cc1)c1cc2[C@]3(C)[C@@H](C)C(N(CC4CC4)CC3)Cc2cc1	0.68
CHEMBL327745	Oc1cc([C@@]23[C@H](CN(C)CC2)Cc2c(nc4c(c2)cccc4)C3)ccc1	0.70
CHEMBL392185	O=C(N[C@@H](C(=O)NCC(=O)N[C@H](C(=O)N1CCC(N(C(=O)CC)c2ccccc2)CC1)Cc1cccc1)C)[C@@H](N)Cc1c(C)cc(O)cc1C	0.77
CHEMBL2113378	Oc1c2O[C@H]3c4[nH]c5c(c4C[C@]4(NCCCc6cccc6)[C@]63c2c(cc1)CC4N(C)CC6)cccc5	0.87
CHEMBL2113382	Oc1c2O[C@H]3c4[nH]c5c(c4C[C@]4(NCCc6cccc6)[C@]63c2c(cc1)CC4N(C)CC6)cccc5	0.95
CHEMBL13786	S(CC[C@H](NC(=O)[C@@H](NC(=O)CNC(=O)CNC(=O)[C@@H](N)Cc1ccc(O)cc1)Cc1cccc1)C(=O)O)C	1.03
CHEMBL2113379	O=C(N[C@@]12[C@]34[C@@H](Oc5c(O)ccc(c35)CC1N(C)CC4)c1[nH]c3c(c1C2)cccc3)Cc1cccc1	1.20
CHEMBL2113373	O=C(N[C@@]12[C@]34[C@@H](Oc5c(O)ccc(c35)CC1N(C)CC4)c1[nH]c3c(c1C2)cccc3)CCc1cccc1	1.40
CHEMBL494479	O=C(N(CC)CC)c1ccc(C=2c3c(OC4(C=2)CCNCC4)ccc(O)c3)cc1	1.40
CHEMBL294616	O=C(N[C@@H]1C(C)(C)SSC(C)(C)[C@H](C(=O)O)NC(=O)[C@@H](Cc2ccccc2)NC(=O)CNC1=O)[C@@H](N)Cc1ccc(O)cc1	1.60
CHEMBL1929364	Oc1c2c(ccc1)C[C@H]1N(C)CC[C@@]32[C@H]1Cc1c(nc2c(c1)cccc2)C3	1.77
CHEMBL438871	Clc1ccc(-c2ccc(CCNC(=O)c3cc4[C@]5(C)[C@@H](C)C(N(CC6CC6)CC5)Cc4cc3)cc2)cc1	2.00
CHEMBL1929362	Oc1c2c(ccc1)C[C@H]1N(CC(C)C)CC[C@@]32[C@H]1Cc1c(nc2c(c1)cccc2)C3	2.34
CHEMBL1649939	O=C(N[C@H](C(=O)N1CCC(N(C(=O)CC)c2ccccc2)CC1)Cc1cccc1)[C@H](NC(=O)[C@@H](N)Cc1c(C)cc(O)cc1C)CCCC	2.82
CHEMBL377789	O=C(NCCc1ccc(-c2ccccc2)cc1)c1cc2[C@]3(C)[C@@H](C)C(N(CC4CC4)CC3)Cc2cc1	3.00
CHEMBL2113381	O=C(N[C@@]12[C@]34[C@@H](Oc5c(O)ccc(c35)CC1N(C)CC4)c1[nH]c3c(c1C2)cccc3)CCCC	3.30
CHEMBL573214	Oc1c2O[C@H]3c4[nH]c5[C@@H]6Oc7c(O)ccc8c7[C@@]76[C@](O)([C@H](N(CC6CC6)CC7)C8)Cc5c4C[C@@]4(O)[C@@H]5N(CC6CC6)C[C@]34c2c(cc1)C5	4.42
CHEMBL2113377	Oc1c2O[C@H]3c4[nH]c5c(c4C[C@]4(NCCCC)[C@]63c2c(cc1)CC4N(C)CC6)cccc5	4.71
CHEMBL19019	O=C1[C@@H]2Oc3c(O)ccc4c3[C@@]32[C@](O)([C@H](N(CC2CC2)CC3)C4)CC1	5.44
CHEMBL2113380	Oc1c2O[C@H]3c4[nH]c5c(c4C[C@]4(CCCc6cccc6)[C@]63c2c(cc1)CC4N(C)CC6)cccc5	7.53
CHEMBL2113376	Oc1c2O[C@H]3c4[nH]c5c(c4C[C@]4(N)[C@]63c2c(cc1)CC4N(C)CC6)cccc5	8.60
CHEMBL250993	BrC1cc(CCNC(=O)c2cc3[C@]4(C)[C@@H](C)C(N(CC5CC5)CC4)Cc3cc2)ccc1	14.0
CHEMBL13470	O=C(N(CC)CC)c1ccc([C@@H](N2[C@@H](C)CN(CC=C)[C@H](C)C2)c2cc(OC)ccc2)cc1	15.7
CHEMBL556648	O=C(N(CC)CC)c1ccc([C@@H]2c3c(OC4(C2)CCNCC4)cccc3)cc1	16.0
CHEMBL401278	O=C(NCCc1cc(-c2ccccc2)ccc1)c1cc2[C@]3(C)[C@@H](C)C(N(CC4CC4)CC3)Cc2cc1	18.0

CHEMBL494462	O=C(N(CC)CC)c1ccc(C=2c3c(OC4(C=2)CCNCC4)cccc3)cc1	19.0
<b>CHEMBL2113372</b>	O=C(N[C@@]12[C@]34[C@@H](O)c5c(O)ccc(c35)CC1N(C)CC4)c1[nH]c3c(c1C2)cccc3)CCCCC	19.0
CHEMBL563893	O=C(N(CC)CC)c1ccc(C=2c3c(OC4(C=2)CCNCCC4)cccc3)cc1	20.0
<b>CHEMBL249567</b>	Br1ccc(CCNC(=O)c2cc3[C@]4(C)[C@@H](C)C(N(CC5CC5)CC4)Cc3cc2)cc1	20.0
CHEMBL494480	O=C(N(CC)CC)c1ccc(C=2c3c(O)cccc3OC3(C=2)CCNCC3)cc1	20.0
CHEMBL557121	O=C(N(CC)CC)c1ccc(C2c3c(OC4(C2)CCNCC4)cccc3)cc1	21.0
<b>CHEMBL557458</b>	O=C(N(CC)CC)c1c(O)cc(C=2c3c(OC4(C=2)CCNCC4)cccc3)cc1	26.0
CHEMBL1649945	Clc1ccc(C[C@H](NC(=O)[C@H](NC(=O)[C@@H](N)Cc2c(C)cc(O)cc2C)C(=O)N2CCC(N(C(=O)CC)c3cccc3)CC2)cc1	26.0
CHEMBL556439	O=C(N(CC)CC)c1ccc(C=2c3c(OC4(C=2)CNCC4)cccc3)cc1	28.0
CHEMBL551613	O=C(N1Cc2c(cccc2)C1)c1ccc(C=2c3c(OC4(C=2)CCNCC4)cccc3)cc1	45.0
CHEMBL561882	O=C(N(C(C)C)C(C)C)c1ccc(C=2c3c(OC4(C=2)CCNCC4)cccc3)cc1	47.0
CHEMBL562873	Fe1c(C(=O)N(CC)CC)ccc(C=2c3c(OC4(C=2)CCNCC4)cccc3)c1	66.0
CHEMBL550472	O=C(N(CC)CC)c1sc(C=2c3c(OC4(C=2)CCNCC4)cccc3)cc1	69.0
CHEMBL561805	O=C(N(C)C)c1ccc(C=2c3c(OC4(C=2)CCNCC4)cccc3)cc1	81.0
CHEMBL494265	O=C(OC)c1ccc(C=2c3c(OC4(C=2)CCNCC4)cccc3)cc1	81.0
<b>CHEMBL494275</b>	O=C(N(CC)CC)c1ccc(C=2c3c(OC4(C=2)CCN(C)CC4)cccc3)cc1	89.0
<b>CHEMBL551412</b>	O=C(NCC)c1ccc(C=2c3c(OC4(C=2)CCNCC4)cccc3)cc1	90.0
CHEMBL562280	O=C(N(CC)CC)c1ncc(C=2c3c(OC4(C=2)CCNCC4)cccc3)cn1	92.0
CHEMBL561339	O=C(N(CC)CC)c1cc(O)c(C=2c3c(OC4(C=2)CCNCC4)cccc3)cc1	94.0
CHEMBL550261	O=C(N1CCCCC1)c1ccc(C=2c3c(OC4(C=2)CCNCC4)cccc3)cc1	100
CHEMBL551536	O=C(N(Cc1ccccc1)C)c1ccc(C=2c3c(OC4(C=2)CCNCC4)cccc3)cc1	100
<b>CHEMBL551413</b>	O=C(NC)c1ccc(C=2c3c(OC4(C=2)CCNCC4)cccc3)cc1	110
CHEMBL550063	O=C(N)c1ccc(C=2c3c(OC4(C=2)CCNCC4)cccc3)cc1	110
CHEMBL495094	O=C(N(CC)CC)c1ccc(C=2c3c(OC4(C=2)CCNCC4)cc(O)cc3)cc1	140
CHEMBL557054	O=C(N(CC)CC)c1ncc(C=2c3c(OC4(C=2)CCNCC4)cccc3)cc1	150
CHEMBL551615	O=C1N(CC)CCc2c1ccc(C=1c3c(OC4(C=1)CCNCC4)cccc3)c2	190
CHEMBL495073	O(C)c1ccc(C=2c3c(OC4(C=2)CCNCC4)cccc3)cc1	190
<b>CHEMBL235743</b>	O=C(N[C@@H](C(=O)NCC(=O)N[C@H](C(=O)N)Cc1ccccc1C)[C@@H](N)Cc1ccc(O)cc1	190
CHEMBL564922	O=C(N1CCCC1)c1ccc(C=2c3c(OC4(C=2)CCNCC4)cccc3)cc1	200
CHEMBL495278	N#Cc1ccc(C=2c3c(OC4(C=2)CCNCC4)cccc3)cc1	200

CHEMBL495074	<chem>Oc1ccc(C=2c3c(OC4(C=2)CCNCC4)cccc3)cc1</chem>	220
CHEMBL494266	<chem>O=C(O)c1ccc(C=2c3c(OC4(C=2)CCNCC4)cccc3)cc1</chem>	220
CHEMBL551414	<chem>O=C(N1CCOCC1)c1ccc(C=2c3c(OC4(C=2)CCNCC4)cccc3)cc1</chem>	240
CHEMBL561138	<chem>O=C(N(CC)CC)c1cnc(C=2c3c(OC4(C=2)CCNCC4)cccc3)cc1</chem>	270
CHEMBL562478	<chem>O=C(N(CC)CC)c1cc(C)c(C=2c3c(OC4(C=2)CCNCC4)cccc3)cc1</chem>	360
CHEMBL562898	<chem>O=C(N(CC)CC)c1scc(C=2c3c(OC4(C=2)CCNCC4)cccc3)c1</chem>	370
CHEMBL492447	<chem>c1(C=2c3c(OC4(C=2)CCNCC4)cccc3)cccc1</chem>	380
CHEMBL550471	<chem>O=C(N(CC)CC)c1ccc([C@H]2c3c(OC4(C2)CCNCC4)cccc3)cc1</chem>	420
CHEMBL563700	<chem>O=C(N(CC)CC)c1ccc(C=2c3c(OC4(C=2)CNCCC4)cccc3)cc1</chem>	480
CHEMBL492448	<chem>Cc1ccc(C=2c3c(OC4(C=2)CCNCC4)cccc3)cc1</chem>	810
CHEMBL559414	<chem>Fe1c(C=2c3c(OC4(C=2)CCNCC4)cccc3)ccc(C(=O)N(CC)CC)c1</chem>	980
CHEMBL550669	<chem>O=C(N(CC)CC)c1oc(C=2c3c(OC4(C=2)CCNCC4)cccc3)cc1</chem>	980
CHEMBL38874	<chem>O=C(NCCO)[C@@H](N(C(=O)CNC(=O)[C@H](NC(=O)[C@@H](N)Cc1ccc(O)cc1)C)C)Cc1cccc1</chem>	10000
CHEMBL440765	<chem>O=C(N(C)[C@@H]1[C@@H](N2CCCC2)C[C@@]2(OCCC2)CC1)Cc1cccc1</chem>	10000
<b>MOR</b>		
<b>Mol</b>	<b>Smiles</b>	<b>EC<sub>50</sub></b>
CHEMBL19019	<chem>O=C1[C@@H]2Oc3c(O)ccc4c3[C@@]32[C@](O)([C@H](N(CC2CC2)CC3)C4)CC1</chem>	0.38
CHEMBL3339378	<chem>O=C(NC1cccc1)C=1[C@@]2(O)C3Oc4c(O)ccc5c4C43[C@](N=1)(C(N(CC1CC1)CC4)C5)CC2</chem>	0.40
CHEMBL267495	<chem>O=C(N(C)[C@H]1[C@@H]2Oc3c(O)ccc4c3[C@@]32[C@](O)([C@H](N(CC2CC2)CC3)C4)CC1)/C=C/c1cccc1</chem>	0.72
CHEMBL1852788	<chem>Clc1nccc(C(=O)N[C@H]2[C@@H]3Oc4c(O)ccc5c4[C@@]43[C@](O)([C@H](N(CC3CC3)CC4)C5)CC2)c1</chem>	0.83
Fentanyl	<chem>O=C(N(c1cccc1)C1CC[NH+](CCc2cccc2)CC1)CC</chem>	1.00
Carfentanyl	<chem>O=C(N(c1cccc1)C1(C(=O)OC)CC[NH+](CCc2cccc2)CC1)CC</chem>	1.00
α-methylfentanyl	<chem>O=C(N(c1cccc1)C1CC[NH+](C@@H)(Cc2cccc2)C)CC1)CC</chem>	1.00
β-hydroxyfentanyl	<chem>O=C(N(c1cccc1)C1CC[NH+](C[C@@H](O)c2cccc2)CC1)CC</chem>	1.00
CHEMBL3339379	<chem>O=C(NCCc1cccc1)C=1[C@@]2(O)C3Oc4c(O)ccc5c4C43[C@](N=1)(C(N(CC1CC1)CC4)C5)CC2</chem>	1.09
CHEMBL1852558	<chem>O=C(N[C@H]1[C@@H]2Oc3c(O)ccc4c3[C@@]32[C@](O)([C@H](N(CC2CC2)CC3)C4)CC1)c1cc(C)ncc1</chem>	1.13
CHEMBL1852385	<chem>Brc1nccc(C(=O)N[C@H]2[C@@H]3Oc4c(O)ccc5c4[C@@]43[C@](O)([C@H](N(CC3CC3)CC4)C5)CC2)c1</chem>	1.19
CHEMBL1852602	<chem>Brc1c(C(=O)N[C@H]2[C@@H]3Oc4c(O)ccc5c4[C@@]43[C@](O)([C@H](N(CC3CC3)CC4)C5)CC2)ccnc1</chem>	1.31
CHEMBL1852555	<chem>O=C(N[C@H]1[C@@H]2Oc3c(O)ccc4c3[C@@]32[C@](O)([C@H](N(CC2CC2)CC3)C4)CC1)CCc1cnc1</chem>	1.46
CHEMBL1852393	<chem>O=C(N[C@H]1[C@@H]2Oc3c(O)ccc4c3[C@@]32[C@](O)([C@H](N(CC2CC2)CC3)C4)CC1)c1c(C)cncc1</chem>	1.52

CHEMBL301160	Oc1cc2c(cc1)C[C@H]1N(CC3CCC3)CC[C@@]32[C@H]1CCCC3	1.60
CHEMBL2397022	O=C(N[C@]12[C@@H]3N(CC4CC4)CC[C@@]41[C@H](C(=O)CC2)Oc1c(O)ccc(c41)C3)c1cnc1	1.67
CHEMBL3264748	O=C1N(CCc2ccccc2)[C@@]23OCOc4c(O)ccc5c4[C@@]46[C@@H]2[C@@H]1O[C@@]4([C@H](N(CC1CC1)CC6)C5)CC3	2.10
CHEMBL2179656	Clc1ccc(-c2enc3[C@@H]4Oc5c(O)ccc6c5[C@@]54[C@](OCCc4cccc4)([C@H](N(C)CC5)C6)Cc3c2)cc1	2.15
CHEMBL3264746	O=C1N(Cc2ccccc2)[C@@]23OCOc4c(O)ccc5c4[C@@]46[C@@H]2[C@@H]1O[C@@]4([C@H](N(CC1cccc1)CC6)C5)CC3	2.30
CHEMBL1852672	Clc1c(C(=O)N[C@H]2[C@@H]3Oc4c(O)ccc5c4[C@@]43[C@](O)([C@H](N(CC3CC3)CC4)C5)CC2)ccnc1	2.32
CHEMBL1852814	O=C(N[C@H]1[C@@H]2Oc3c(O)ccc4c3[C@@]32[C@](O)([C@H](N(CC2CC2)CC3)C4)CC1)Cc1cnc1	2.32
CHEMBL3217271	Oc1cc([C@@]23[C@H](C)CN(CCCc4cccc4)[C@@H](C[C@H](N(CC4CC4)C)C2)C3)ccc1.Cl.Cl	2.70
CHEMBL3264745	O=C1N(Cc2ccccc2)[C@@]23OCOc4c(O)ccc5c4[C@@]46[C@@H]2[C@@H]1O[C@@]4([C@H](N(CC=C)CC6)C5)CC3	2.70
CHEMBL3264742	O=C1N(Cc2ccccc2)[C@@]23OCOc4c(O)ccc5c4[C@@]46[C@@H]2[C@@H]1O[C@@]4([C@H](N(CC1CC1)CC6)C5)CC3	2.80
CHEMBL2397018	O=C(N[C@]12[C@@H]3N(CC4CC4)CC[C@@]41[C@H](C(=O)CC2)Oc1c(O)ccc(c41)C3)c1enc2c(c1)cccc2	2.81
CHEMBL1852458	O=C(N[C@H]1[C@@H]2Oc3c(O)ccc4c3[C@@]32[C@](O)([C@H](N(CC2CC2)CC3)C4)CC1)CNC(=O)c1cnc1	2.84
CHEMBL566346	O=C(Oc1cc2c(cc1)C[C@H]1N(CC3CCC3)CC[C@@]32[C@H]1CCCC3)CCCCCCCC(=O)O	3.00
CHEMBL56585	Oc1cc2[C@@]3(C)[C@@H](C)[C@H](N(CC4CC4)CC3)Cc2cc1	4.00
CHEMBL2179655	Clc1ccc(-c2enc3[C@@H]4Oc5c(O)ccc6c5[C@@]54[C@](OC/C=C/c4cccc4)([C@H](N(C)CC5)C6)Cc3c2)cc1	4.27
CHEMBL2387196	O=C1N(C2CCN(C3CCC(C(C)C)CC3)CC2)c2c(C1CC)cccc2	4.70
CHEMBL1852475	O=C(N[C@H]1[C@@H]2Oc3c(O)ccc4c3[C@@]32[C@](O)([C@H](N(CC2CC2)CC3)C4)CC1)C1CCN(C)CC1	5.08
CHEMBL3216613	Oc1cc([C@@]23[C@H](C)CN(CCCc4cccc4)[C@@H](C[C@H](N(C)C)C2)C3)ccc1.Cl.Cl	6.50
CHEMBL2397015	O=C(N[C@]12[C@@H]3N(CC4CC4)CC[C@@]41[C@H](C(=O)CC2)Oc1c(O)ccc(c41)C3)c1cccc1	7.20
CHEMBL2178341	O=C(N[C@H]1[C@@H]2Oc3c(O)ccc4c3[C@@]32[C@](O)([C@H](N(CC2CC2)CC3)C4)CC1)c1ncnc1	7.49
CHEMBL3264747	O=C1N(c2ccccc2)[C@@]23OCOc4c(O)ccc5c4[C@@]46[C@@H]2[C@@H]1O[C@@]4([C@H](N(CC1CC1)CC6)C5)CC3	9.00
CHEMBL518712	C(N1C2[C@H](C)[C@@](C)(c3c(cc4nc[nH]c4c3)C2)CC1)C1CC1	9.80
CHEMBL2177697	O=C(N[C@H]1[C@@H]2Oc3c(O)ccc4c3[C@@]32[C@](O)([C@H](N(CC2CC2)CC3)C4)CC1)c1cc(C#N)nc1	10.0
CHEMBL2397019	O=C(N[C@]12[C@@H]3N(CC4CC4)CC[C@@]41[C@H](C(=O)CC2)Oc1c(O)ccc(c41)C3)c1cc2c(cc1)cccc2	11.1
CHEMBL565679	O=C(Oc1cc2c(cc1)C[C@H]1N(CC3CCC3)CC[C@@]32[C@H]1CCCC3)C(CCCCCC(C(=O)O)C)C	13.0
CHEMBL3217272	Oc1cc([C@@]23[C@H](C)CN(CCCc4cccc4)[C@@H](C[C@H](N)C2)C3)ccc1.Cl.Cl	15.0
CHEMBL70	O[C@@H]1[C@@H]2Oc3c(O)ccc4c3[C@@]32[C@H]([C@H](N(C)CC3)C4)C=C1	15.6
CHEMBL386272	Clc1ccc(/C=C/C(=O)N[C@]23[C@@H]4N(CC5CC5)CC[C@@]52[C@H](C(=O)CC3)Oc2c(OC)ccc(c52)C4)cc1	17.8
CHEMBL473699	C(N1C2[C@H](C)[C@@](C)(c3c(cc4nc(C)[nH]c4c3)C2)CC1)C1CC1	18.0
CHEMBL3215960	Oc1cc([C@@]23[C@H](C)CN(CCCc4cccc4)[C@@H](C[C@H](NCCC)C2)C3)ccc1.Cl.Cl	18.0

CHEMBL3216611	Oc1cc([C@@]23[C@H](C)CN(CCCc4cccc4)[C@@H](C[C@H](N)C2)C3)ccc1.Cl.Cl	19.5
CHEMBL3086465	Oc1cc([C@]23[C@@H](C)CN(CCCc4cccc4)[C@H](C[C@@H](N)C2)C3)ccc1	20.6
CHEMBL2387191	O=C1N(C2CCN(C(C)C3CCCC3)CC2)c2c(cccc2)C1	28.0
CHEMBL2178340	O=C(N[C@H]1[C@@H]2Oc3c(O)ccc4c3[C@@]32[C@](O)([C@H](N(CC2CC2)CC3)C4)CC1)c1enncc1	28.3
CHEMBL102900	O=C1N(C2CCN(C3C4CCCC3CC4)CC2)c2c(cccc2)C1	29.0
CHEMBL562340	Oc1cc2c(cc1)C[C@@]13[C@@]2(Cc2[nH]c4c(c2C1)cccc4)CCN(CC1CC1)C3	33.0
CHEMBL3217051	Oc1cc([C@]23[C@H](C)CN(CCCc4cccc4)[C@@H](C[C@H](NCC)C2)C3)ccc1.Cl.Cl	33.0
CHEMBL474755	O=C(O[C@]12[C@@H]3N(CC4CC4)CC[C@@]41[C@H](C(=O)CC2)Oc1c(OC)ccc(c41)C3)/C=C/c1cccc1	34.4
CHEMBL2387197	O=C1N(C2CCN(C3CCCC3)CC2)c2e(C1CC)cccc2	37.3
CHEMBL2397017	O=C(N[C@]12[C@@H]3N(CC4CC4)CC[C@@]41[C@H](C(=O)CC2)Oc1c(O)ccc(c41)C3)c1nc2c(cc1)cccc2	38.8
CHEMBL2179662	Clc1ccc(-c2nc3[C@@H]4Oc5c(O)ccc6c5[C@@]54[C@](OC(=O)CCc4cccc4)([C@H](N(C)CC5)C6)Cc3c2)cc1	48.0
CHEMBL2387192	O=C1N(C2CCN(C(C)c3cccc3)CC2)c2c(cccc2)C1	50.6
CHEMBL38874	O=C(NCCO)[C@@H](N(C(=O)CNC(=O)[C@H](NC(=O)[C@@H](N)Cc1ccc(O)cc1)C)C)Cc1cccc1	55.0
CHEMBL2387200	O=C1N(C2CCN(C3CCCC3)CC2)c2e(C(C)C1)cccc2	58.0
CHEMBL3217050	Oc1cc([C@@]23[C@H](C)CN(CCCc4cccc4)[C@@H](C[C@H](N(CC)C)C2)C3)ccc1.Cl.Cl	60.0
CHEMBL2387198	O=C1N(C2CCN(C3CCC(C(C)C)CC3)CC2)c2c(cccc2)CC1	68.0
CHEMBL2387187	O=C1N(C2CCN(C3CCC(C(C)C)CC3)CC2)c2c(cccc2)C1	73.5
CHEMBL2179661	Clc1ccc(-c2nc3[C@@H]4Oc5c(O)ccc6c5[C@@]54[C@](OC(=O)Cc4cccc4)([C@H](N(C)CC5)C6)Cc3c2)cc1	87.0
CHEMBL2387195	O=C1N(C2CCN(C3CCCC3)CC2)c2e(C1C)cccc2	94.0
CHEMBL101454	O=C1N(C2CCN(C3CCCC3)CC2)c2c(cccc2)C1	99.0
CHEMBL3264743	O=C1N(Cc2cccc2)[C@@]23OCOc4c(O)ccc5c4[C@@]46[C@@H]2[C@@H]1O[C@@]4([C@H](N(C)CC6)C5)CC3	113
CHEMBL2387194	O=C1N(C2CCN(C3CCC(C(C)C)CC3)CC2)c2e(C1C)cccc2	120
CHEMBL2387193	O=C1N(C2CCN(C3c4c5[C@@H](CC3)CCCc5ccc4)CC2)c2c(cccc2)C1	129
CHEMBL3217273	Oc1cc([C@]23[C@H](C)CN(CCCc4cccc4)[C@@H](C[C@H](NCC4CC4)C2)C3)ccc1.Cl.Cl	130
CHEMBL557937	Oc1cc2c(cc1)C[C@@]13[C@@]2(Cc2n(C)c4c(c2C1)cccc4)CCN(C)C3	174
CHEMBL2387189	O=C1N(C2CCN(C3CCC(C(CC)(C)C)CC3)CC2)c2c(cccc2)C1	189
CHEMBL3264744	O=C1N(Cc2cccc2)[C@@]23OCOc4c(O)ccc5c4[C@@]46[C@@H]2[C@@H]1O[C@@]4([C@H](N(CC(C)C)CC6)C5)CC3	223
CHEMBL2179654	Clc1ccc(-c2nc3[C@@H]4Oc5c(O)ccc6c5[C@@]54[C@](OCc4cccc4)([C@H](N(C)CC5)C6)Cc3c2)cc1	301
CHEMBL2179653	Clc1ccc(-c2nc3[C@@H]4Oc5c(O)ccc6c5[C@@]54[C@](OC)([C@H](N(C)CC5)C6)Cc3c2)cc1	379
CHEMBL2387188	O=C1N(C2CCN(C3CCC(CCC)CC3)CC2)c2c(cccc2)C1	595

<a href="#">CHEMBL320874</a>	<chem>O=C1N(C2CCN(Cc3ccccc3)CC2)c2c(cccc2)C1</chem>	1981
<a href="#">CHEMBL2179660</a>	<chem>Clc1cc(-c2nc3[C@@H]4Oc5c(O)ccc6c5[C@@]54[C@](OC(=O)c4ccccc4)([C@H](N(C)CC5)C6)Cc3c2)cc1</chem>	4623



**Table A.21 Results of the docking studies for the filtered DBZDs and identified reference compounds. For each OR a total of five reference agonist binders, i.e. the co-crystallised ligand plus four molecules identified from ChEMBL database, were used. Pharmacophore mapping studies identified 18 molecules for MOR, 22 for KOR and 25 for DOR.**

<b>MOR</b>		
Molecule	SMILESs	S (Kcal/mol)
<b>BU72</b>	<chem>O(C)[C@]12[C@]3(C)[C@@H](c4ccccc4)[NH2+][C@H]1[C@@]14c5c(ccc(O)c5)C[C@@H]([NH+](C)CC1)[C@@]4(C=C2)C3</chem>	-10.15
Fentanyl	<chem>O=C(N(c1ccccc1)C1CC[NH+](CCc2ccccc2)CC1)CC</chem>	-8.44
Carfentanyl	<chem>O=C(N(c1ccccc1)C1(C(=O)OC)CC[NH+](CCc2ccccc2)CC1)CC</chem>	-9.59
$\alpha$ -methylfentanyl	<chem>O=C(N(c1ccccc1)C1CC[NH+](C[C@@H](Cc2ccccc2)C)CC1)CC</chem>	-8.99
$\beta$ -hydroxyfentanyl	<chem>O=C(N(c1ccccc1)C1CC[NH+](C[C@@H](O)c2ccccc2)CC1)CC</chem>	-8.79
Ciclotizolam	<chem>Brc1sc2-n3c(C4CCCC4)nnc3C[NH+]=C(c3c(Cl)cccc3)c2c1</chem>	-8.30
Cloniprazepam	<chem>Clc1c(C2=NCC(=O)N(CC3CC3)c3c2cc([N+](=O)[O-])cc3)cccc1</chem>	-7.78
Deschloroetizolam	<chem>C(C)c1sc2-n3c(C)nnc3C[NH+]=C(c3ccccc3)c2c1</chem>	-7.14
FG-8205	<chem>Clc1c2C(=O)N(C)Cc3c(-c4nc(C(C)C)on4)ncn3-c2ccc1</chem>	-7.77
Fluloprazolam	<chem>Fc1c(C2=NCC=3N(C(=O)C(=CN4CC[NH+](C)CC4)N=3)c3c2cc([N+](=O)[O-])cc3)cccc1</chem>	-9.33
Flunitrazolam	<chem>Fc1c(C2=NCc3n(c(C)nn3)-c3c2cc([N+](=O)[O-])cc3)cccc1</chem>	-7.50
Metizolam	<chem>Clc1c(C2=[NH+]Cc3n(-c4sc(CC)cc24)cnn3)cccc1</chem>	-7.08
Mexazolam	<chem>Clc1c(C23OCC(C)N2CC(=O)Nc2c3cc(Cl)cc2)cccc1</chem>	-7.29
Nitrazolam	<chem>O=[N+](O)c1cc2C(c3ccccc3)=NCc3n(c(C)nn3)-c2cc1</chem>	-6.95
PWZ-029	<chem>Clc1cc2C(=O)N(C)Cc3c(COC)ncn3-c2cc1</chem>	-6.26
Phenazolam	<chem>Brc1cc2C(c3c(Cl)cccc3)=NCc3n(c(C)nn3)-c2cc1</chem>	-6.80
Pynazolam	<chem>O=[N+](O)c1cc2C(c3ncccc3)=NCc3n(c(C)nn3)-c2cc1</chem>	-7.33
Ro 05-4608	<chem>Clc1c(C2=NCC(=O)N(C)c3c2ccccc3)cccc1</chem>	-6.37
Ro 15-9270	<chem>Clc1c(C=2c3c(-n4c(C)nnc4CC=2)ccc([N+](=O)[O-])c3)cccc1</chem>	-7.55
Ro 17-1812	<chem>Clc1c2C(=O)N3C(c4c(C(=O)OCC5CC5)ncn4-c2ccc1)CC3</chem>	-8.09
Ro 48-6791	<chem>Fc1cc2C(=O)N(C)Cc3c(-c4nc(CN(CCC)CCC)on4)ncn3-c2cc1</chem>	-9.02
Ro 48-8684	<chem>Fc1cc2C(=O)N(C)Cc3c(-c4oc(C[NH+](CCC)CCC)en4)ncn3-c2cc1</chem>	-9.36
Tuclazepam	<chem>Clc1c(C2=[NH+]CC(CO)N(C)c3c2cc(Cl)cc3)cccc1</chem>	-7.18

<b>KOR</b>		
<b>MP11 04</b>	C1CC1CN2CC[C@]34[C@@H]5[C@H]2CC6=C3C(=C(C=C6)O)O[C@H]4[C@@H](C=C5)NC(=O)C7=CC(=CC=C7)I	-9.79
CHEMBL503080	Clc1cc2c(CC(=O)N3[C@H](C[NH+]4CCCC4)CN(c4cccc4)CC3)csc2cc1	-9.00
CHEMBL526933	Clc1c(Cl)ccc(N(CC(=O)N2[C@H](C[NH+]3CCCC3)CN(S(=O)(=O)C)CC2)C)c1	-9.24
CHEMBL526747	Clc1c(Cl)ccc(N(CC(=O)N2[C@H](C[NH+]3CCCC3)CN(c3cc(OC)ccc3)CC2)C)c1	-9.01
CHEMBL499351	Clc1c(Cl)ccc(N(CC(=O)N2[C@H](C[NH+]3CCCC3)CN(S(=O)(=O)c3cc(Cl)ccc3)CC2)C)c1	-9.74
CHEMBL525457	Clc1cc2N(CC(=O)N3[C@H](C[NH+]4CCCC4)CN(S(=O)(=O)c4cc(OC)c(OC)cc4)CC3)C(=O)Oc2cc1	-9.81
Arfendazam	Clc1cc2N(c3cccc3)C(=O)CCN(C(=O)OCC)c2cc1	-7.84
Ciclotizolam	Brc1sc2-n3c(C4CCCC4)nnc3C[NH+]=C(c3c(Cl)cccc3)e2c1	-8.39
Cinazepam	Brc1cc2C(c3c(Cl)cccc3)=NC(OC(=O)CCC(=O)[O-])C(=O)Nc2cc1	-8.34
Clonazolam	Clc1c(C2=NCc3n(c(C)nn3)-c3c2cc([N+](=O)[O-])cc3)cccc1	-7.45
Cloniprazepam	Clc1c(C2=NCC(=O)N(CC3CC3)c3c2cc([N+](=O)[O-])cc3)cccc1	-7.79
Devazepide	O=C(N[C@@H]1C(=O)N(C)c2c(C(c3cccc3)=N1)cccc2)c1[nH]c2c(c1)cccc2	-8.21
FG-8205	Clc1c2C(=O)N(C)Cc3c(-c4nc(C(C)C)on4)ncn3-c2ccc1	-8.24
Fluadinazolam	Clc1cc2C(c3c(F)cccc3)=NCc3n(c(C[NH+](C)C)nn3)-c2cc1	-7.46
Fluloprazolam	Fc1c(C2=NCC=3N(C(=O)C(=CN4CC[NH+](C)CC4)N=3)c3c2cc([N+](=O)[O-])cc3)cccc1	-8.80
Flutazolam	Clc1cc2C3(c4c(F)cccc4)OCCN3CC(=O)N(CCO)c2cc1	-6.86
Iomazenil	Ic1c2C(=O)N(C)Cc3c(C(=O)OCC)ncn3-c2ccc1	-7.87
JQ1	Clc1ccc(C2=[NH+]C(CC(=O)OC(C)(C)C)c3n(c(C)nn3)-c3sc(C)c(C)c23)cc1	-8.24
PWZ-029	Clc1cc2C(=O)N(C)Cc3c(COC)ncn3-c2cc1	-7.10
Pivoxazepam	Clc1cc2C(c3cccc3)=NC(OC(=O)C(C)(C)C)C(=O)Nc2cc1	-8.05
Remimazolam	Brc1cc2C(c3ncccc3)=NC(CCC(=O)OC)c3n(c(C)cn3)-c2cc1	-7.94
Rilmazolam	Clc1c(C2=NCc3n(nc(C(=O)N(C)C)n3)-c3c2cc(Cl)cc3)cccc1	-8.31
Ro 15-4941	Clc1c2C(=O)N3C(c4c(C(=O)OCC)ncn4-c2ccc1)CCC3	-8.01
Ro 15-9270	Clc1c(C=2c3c(-n4c(C)nnc4CC=2)ccc([N+](=O)[O-])c3)cccc1	-7.23
Ro 17-1812	Clc1c2C(=O)N3C(c4c(C(=O)OCC5CC5)ncn4-c2ccc1)CC3	-7.70
Ro 48-6791	Fc1cc2C(=O)N(C)Cc3c(-c4nc(CN(CCC)CCC)on4)ncn3-c2cc1	-8.51
Ro 48-8684	Fc1cc2C(=O)N(C)Cc3c(-c4oc(C[NH+](CCC)CCC)cn4)ncn3-c2cc1	-8.15
Tofisopam	O(C)c1c(OC)ccc(C2=NN=C(C)C(CC)c3c2cc(OC)c(OC)c3)c1	-8.91
<b>DOR</b>		

<b>DPI-287</b>	<chem>O=C(N(CC)CC)c1ccc([C@@H](N2[C@@H](C)C[NH+](CC=C)[C@H](C)C2)c2cc(O)ccc2)cc1</chem>	-8.58
CHEMBL2151735	<chem>O=C(N([C@@H](C(=O)N[C@@H]1C(=O)N(CC(=O)N)Cc2c(cccc2)C1)C)C)[C@@H]([NH3+])Cc1c(C)cc(O)cc1C</chem>	-9.44
CHEMBL8234	<chem>O=C([O-])[C@@H](NC(=O)[C@@H](NC(=O)CNC(=O)CNC(=O)[C@@H]([NH3+])Cc1ccc(O)cc1)Cc1cccc1)CC(C)C</chem>	-10.43
CHEMBL3758292	<chem>O=C([C@@H]([NH3+])Cc1c(C)cc(O)cc1)N1[C@@H](C(=O)NCc2[nH]c3c(n2)cccc3)Cc2c(cccc2)C1</chem>	-9.70
CHEMBL2113666	<chem>Clc1c(/C=C/C(=O)N[C@]23[C@@H]4[NH+](C)CC[C@@]52[C@H](C(=O)CC3)Oc2c5c(ccc2)C4)cccc1</chem>	-7.26
Midazolam	<chem>Clc1cc2C(c3c(F)cccc3)=NCc3n(c(C)[nH+])c3)-c2cc1</chem>	-6.76
Arfendazam	<chem>Clc1cc2N(c3cccc3)C(=O)CCN(C(=O)OCC)c2cc1</chem>	-7.54
Ciclotizolam	<chem>Brc1sc2-n3c(C4CCCC4)nnc3C[NH+]=C(c3c(Cl)cccc3)c2c1</chem>	-8.45
Cloniprazepam	<chem>Clc1c(C2=NCC(=O)N(CC3CC3)c3c2cc([N+](=O)[O-])cc3)cccc1</chem>	-7.72
Devazepide	<chem>O=C(N([C@@H]1C(=O)N(C)c2c(C(c3cccc3)=N1)cccc2)c1[nH]c2c(c1)cccc2</chem>	-7.41
Elfazepam	<chem>Clc1cc2C(c3c(F)cccc3)=NCC(=O)N(CCS(=O)(=O)CC)c2cc1</chem>	-8.24
Ethyl Carfluzepate	<chem>Clc1cc2C(c3c(F)cccc3)=N[C@H](C(=O)OCC)C(=O)N(C(=O)NC)c2cc1</chem>	-7.56
FG-8205	<chem>Clc1c2C(=O)N(C)Cc3c(-c4nc(C(C)C)on4)ncn3-c2ccc1</chem>	-7.79
Fluadinazolam	<chem>Clc1cc2C(c3c(F)cccc3)=NCc3n(c(C[NH+](C)C)nn3)-c2cc1</chem>	-7.47
Fluloprazolam	<chem>Fc1c(C2=NCC=3N(C(=O)/C(=C/N4CC[NH+](C)CC4)/N=3)c3c2cc([N+](=O)[O-])cc3)cccc1</chem>	-8.59
Iomazenil	<chem>Ic1c2C(=O)N(C)Cc3c(C(=O)OCC)ncn3-c2ccc1</chem>	-7.60
JQ1	<chem>Clc1ccc(C2=[NH+][C@H](CC(=O)OC(C)C)c3n(c(C)nn3)-c3sc(C)c(C)c23)cc1</chem>	-8.62
MP-iii-022	<chem>Fc1c(C2=N[C@H](C)c3c(C(=O)NC)ncn3-c3c2cc(C#C)cc3)cccc1</chem>	-7.31
Metaclazepam	<chem>Brc1cc2C(c3c(Cl)cccc3)=[NH+][C@H](COC)N(C)c2cc1</chem>	-7.57
PWZ-029	<chem>Clc1cc2C(=O)N(C)Cc3c(COC)ncn3-c2cc1</chem>	-6.19
Pivoxazepam	<chem>Clc1cc2C(c3cccc3)=N[C@H](OC(=O)C(C)C)C(=O)Nc2cc1</chem>	-7.19
Remimazolam	<chem>Brc1cc2C(c3ncccc3)=N[C@H](CCC(=O)OC)c3n(c(C)cn3)-c2cc1</chem>	-7.70
Rilmazolam	<chem>Clc1c(C2=NCc3n(nc(C(=O)N(C)C)n3)-c3c2cc(Cl)cc3)cccc1</chem>	-8.03
Ro 15-4941	<chem>Clc1c2C(=O)N3[C@H](c4c(C(=O)OCC)ncn4-c2ccc1)CCC3</chem>	-6.85
Ro 17-1812	<chem>Clc1c2C(=O)N3[C@H](c4c(C(=O)OCC5CC5)ncn4-c2ccc1)CC3</chem>	-7.57
Ro 48-6791	<chem>Fc1cc2C(=O)N(C)Cc3c(-c4nc(CN(CCC)CCC)on4)ncn3-c2cc1</chem>	-8.23
Ro 48-8684	<chem>Fc1cc2C(=O)N(C)Cc3c(-c4oc(C[NH+](CCC)CCC)cn4)ncn3-c2cc1</chem>	-8.70
SH-053-R-CH3-2'F	<chem>Fc1c(C2=N[C@H](C)c3c(C(=O)OCC)ncn3-c3c2cc(C#C)cc3)cccc1</chem>	-7.64
Tolufazepam	<chem>Clc1c(C2=NCC(=O)N(CCS(=O)(=O)c3ccc(C)cc3)c3c2cc(Cl)cc3)cccc1</chem>	-8.67
Uldazepam	<chem>Clc1c(C2=NC/C(=N\OCC=C)/Nc3c2cc(Cl)cc3)cccc1</chem>	-7.35



Table A.22. Details of ligand interaction for the top-three scoring DBZDs on each ORs

Notes. The ligand columns display which is the ligand atom involved in the binding; the receptor column which is the amino acid residues involved in the binding; the interaction column describe the type of interaction/binding; the distance column display the distance between the two ligand and the receptor atoms; the E column display the energy of the interaction, the lower the value, the stronger the binding.

<b>MOR</b>					
<b>BU72</b>					
Ligand	Receptor		Interaction	Distance	E (kcal/mol)
N 32	MET	151	H-donor	3.54	-3.8
C 34	ASP	147	H-donor	2.67	-0.4
C 38	HOH	548	H-donor	3.22	-0.8
O 48	HOH	525	H-donor	2.61	-2.1
N 32	ASP	147	Ionic	3.53	-3.1
6-ring	ILE	144	pi-H	4.05	-0.4
6-ring	MET	151	pi-H	4.92	-0.3
6-ring	VAL	300	pi-H	4.68	-0.2
6-ring	VAL	300	pi-H	4.06	-0.8
<b>JQ1</b>					
Ligand	Receptor		Interaction	Distance	E (kcal/mol)
C 5	ASP	147	H-donor	3.29	-0.7
N 9	ASP	147	Ionic	3.20	-3.3
<b>R0 48-8684</b>					
Ligand	Receptor		Interaction	Distance	E (kcal/mol)
N 24	ASP	147	H-donor	3.35	-2.1
C 39	HIS	54	H-donor	3.30	-0.3
C 42	CYS	217	H-donor	4.80	-0.2
C 50	MET	151	H-donor	4.54	-0.4
N 24	ASP	147	Ionic	3.35	-3.9
C 56	HIS	297	H-pi	3.40	-0.4
6-ring	MET	151	pi-H	4.40	-0.2
6-ring	VAL	300	pi-H	4.00	-0.2
<b>Fluloprazolam</b>					
Ligand	Receptor		Interaction	Distance	E (kcal/mol)
N 23	ASP	147	H-donor	3.58	-1.0
N 23	ASP	147	Ionic	3.58	-1.6
C 54	TYR	148	H-pi	3.79	-0.5
<b>KOR</b>					
<b>MP1104</b>					
Ligand	Recepto		Interaction	Distance	E (kcal/mol)
C 3	ASP	138	H-donor	3.27	-0.5
C 14	MET	142	H-donor	4.13	-0.5

I 16	THR	111	H-donor	4.04	-0.4
I 16	THR	111	H-donor	4.44	-0.2
N 26	ASP	138	H-donor	3.02	-2.0
N 26	ASP	138	H-donor	2.8	-10.8
C 27	ASP	138	H-donor	3.34	-0.4
C 27	MET	142	H-donor	3.38	-1.5
N 26	ASP	138	Ionic	3.02	-6.0
N 26	ASP	138	Ionic	2.80	-7.8
C 21	TYR	139	H-pi	4.02	-0.3
C 29	TYR	320	H-pi	3.55	-0.3
6-ring	ILE	294	pi-H	4.83	-0.3
<b>Ro 48-8684</b>					
Ligand	Receptor		Interaction	Distance	E (kcal/mol)
C 29	SER	323	H-donor	3.00	-0.2
C 36	MET	142	H-donor	3.61	-0.3
C 39	ASP	138	H-donor	3.00	-0.2
O 7	HIS	291	H-acceptor	3.77	-0.2
N 24	ASP	138	Ionic	3.92	-1.6
C 46	TYR	320	H-pi	3.88	-0.2
6-ring	ILE	294	pi-H	4.13	-0.7
5-ring	GLY	319	pi-H	4.78	-0.2
<b>JQ1</b>					
Ligand	Receptor		Interaction	Distance	(kcal/mol)
C 3	CYS	210	H-donor	3.72	-0.4
N 9	ASP	138	H-donor	3.02	-10.0
C 27	MET	142	H-donor	3.91	-0.3
C 53	ASP	138	H-donor	3.11	-0.6
N 9	ASP	138	Ionic	3.02	-6.0
<b>Ciclotizolam</b>					
Ligand	Receptor		Interaction	Distance	E (kcal/mol)
C 38	ILE	316	H-donor	3.55	-0.2
C 42	ASP	138	H-donor	3.26	-0.5
N 30	ASP	138	Ionic	4.07	-1.2
N 30	ASP	138	Ionic	3.35	-4.0
6-ring	ILE	290	pi-H	4.47	-0.2
5-ring	ILE	294	pi-H	4.80	-0.5
5-ring	ILE	294	pi-H	3.63	-0.2
6-ring	ILE	316	pi-H	3.65	-0.2
5-ring	TYR	139	pi-pi	3.61	0.2
<b>DOR</b>					
<b>DPI-287</b>					
Ligand	Receptor		Interaction	Distance	E (kcal/mol)
C 44	MET	132	H-donor	3.34	-0.7
C 49	ASP	128	H-donor	3.24	-0.3
C 53	ASP	128	H-donor	2.97	-2.0

N 62	ASP	128	H-donor	2.72	-10.9
N 62	ASP	128	H-donor	2.92	-6.1
N 42	ASP	128	Ionic	3.87	-1.8
N 62	ASP	128	Ionic	2.72	-8.5
N 62	ASP	128	Ionic	2.92	-6.7
C 5	TRP	284	H-pi	4.17	-0.3
C 5	TRP	284	H-pi	3.88	-0.3
C 12	TRP	284	H-pi	4.55	-0.4
C 58	TYR	308	H-pi	4.97	-0.3
6-ring	MET	132	pi-H	4.08	-0.4
6-ring	MET	132	pi-H	4.93	-0.2
6-ring	VAL	281	pi-H	3.94	-0.6
<b>Ro 48-8684</b>					
Ligand	Receptor		Interaction	Distance	E (kcal/mol)
C 21	MET	132	H-donor	4.33	-0.9
C 26	ASP	128	H-donor	3.23	-0.4
C 36	ASP	128	H-donor	3.12	-0.3
C 36	MET	132	H-donor	3.65	-0.5
N 24	ASP	128	Ionic	3.20	-4.8
N 24	ASP	128	Ionic	3.56	-2.9
<b>Ro 48-6791</b>					
Ligand	Receptor				
C 13	TYR		Interaction	Distance	E (kcal/mol)
C 21	MET	129	H-donor	2.98	-0.4
N 24	ASP	132	H-donor	3.81	-0.8
N 24	ASP	128	H-donor	3.11	-7.9
C 29	ASP	128	H-donor	3.57	-1.0
O 7	LYS	128	H-donor	3.16	-0.5
O 7	LYS	214	H-acceptor	3.68	-0.2
N 24	ASP	214	H-acceptor	3.21	-0.4
N 24	ASP	128	Ionic	3.11	-5.4
C 36	TYR	128	Ionic	3.57	-2.9
<b>Fluloprazolam</b>					
		308	H-pi	3.50	-0.3
Ligand	Receptor		Interaction	Distance	E (kcal/mol)
C 29	ASP	128	H-donor	2.77	-0.7
C 29	MET	132	H-donor	4.58	-0.7
C 48	MET	132	H-donor	3.75	-0.5
O 42	LYS	214	H-acceptor	3.09	-0.2
O 43	PHE	218	H-acceptor	3.28	-0.2
N 23	ASP	128	Ionic	3.61	-2.7
C 32	TYR	308	H-pi	4.28	-0.2
6-ring	PHE	133	pi-H	4.93	-0.2
6-ring	VAL	217	pi-H	3.75	-0.2
6-ring	VAL	217	pi-H	4.13	-0.5

6-ring	VAL	281	pi-H	3.89	-0.2
--------	-----	-----	------	------	------



## Appendix B

### Appendix B

Site	Size	PLB	Hyd	Side	Residues
1	245	3.62	88	150	1:(GLY52 SER53 HIS54 SER55 YCM57 TYR58)
2	87	0.56	27	61	1:(THR103 MET161 ASP164 ARG165 ALA166)
3	43	-0.13	8	25	1:(SER55 LEU56 YCM57 PRO58 GLN59 THR100)
4	36	-0.14	18	28	1:(ASN109 LEU112 ALA113 LEU116 ILE117)
5	20	-0.19	6	21	1:(THR101 ALA102 THR103 ASP164 ALA166)
6	54	-0.21	14	39	1:(GLY52 SER53 YCM57 PRO58 TRP226)
7	19	-0.22	15	23	1:(LEU158 ILE248 VAL285 VAL286 VAL287)
8	10	-0.24	13	16	1:(PHE84 PHE87 LEU88 MET90 TYR91)
9	14	-0.33	12	19	1:(MET99 ILE105 PHE108 ASN109 LEU110)
10	11	-0.35	12	17	1:(GLN59 PRO63 ALA68 MET72 TYR128 LEU129)

*Figure B.1 MOE Site Finder application. This application is used to calculate possible active sites in a receptor (the atoms button) from the 3D atomic coordinates of the latter. The Atoms options is used to control the interpretation of the atoms currently loaded in MOE, i.e. the receptor which need investigation. . To start the search apply is pressed, and a list of calculated sites will be summarized in the list. For each site the following information became available, the size which indicates the number of alpha spheres comprising the site, the PLB which is the Propensity for Ligand Binding, the Hyd which indicates the number of hydrophobic contact atoms in the receptor, the Side which indicates the number of sidechain contact atoms in the receptor. The Residues column list all the residues comprised in the calculated site in the format chain:residue-name.*

## Scoring function

The definition for the scoring function were taken as reported in the MOE manual.

### London dG Scoring

The London dG scoring function estimates the free energy of binding of the ligand from a given pose. The functional form is a sum of terms:

$$\Delta G = c + E_{\text{flex}} + \sum_{\text{h-bonds}} c_{\text{HB}} f_{\text{HB}} + \sum_{\text{m-lig}} c_{\text{M}} f_{\text{M}} + \sum_{\text{atoms } i} \Delta D_i$$

where  $c$  represents the average gain/loss of rotational and translational entropy;  $E_{\text{flex}}$  is the energy due to the loss of flexibility of the ligand (calculated from ligand topology only);  $f_{\text{HB}}$  measures geometric imperfections of hydrogen bonds and takes a value in  $[0,1]$ ;  $c_{\text{HB}}$  is the energy of an ideal hydrogen bond;  $f_{\text{M}}$  measures geometric imperfections of metal ligations and takes a value in  $[0,1]$ ;  $c_{\text{M}}$  is the energy of an ideal metal ligation; and  $D_i$  is the desolvation energy of atom  $i$ . The difference in desolvation energies is calculated according to the formula

$$\Delta D_i = c_i R_i^3 \left\{ \iiint_{u \notin A \cup B} |u|^{-6} du - \iiint_{u \notin B} |u|^{-6} du \right\}$$

where  $A$  and  $B$  are the protein and/or ligand volumes with atom  $i$  belonging to volume  $B$ ;  $R_i$  is the solvation radius of atom  $i$  (taken as the OPLS-AA van der Waals sigma parameter plus 0.5 Å); and  $c_i$  is the desolvation coefficient of atom  $i$ . The coefficients  $\{c, c_{\text{HB}}, c_i\}$  were fitted from approximately 400 X-ray crystal structures of protein-ligand complexes with available experimental  $\text{pK}_i$  data. Atoms are categorized into about a dozen atom types for the assignment of the  $c_i$  coefficients. The triple integrals are approximated using Generalized Born integral formulas.

### GBVI/WSA dG Scoring

The GBVI/WSA  $\Delta G$  is a forcefield-based scoring function which estimates the free energy of binding of the ligand from a given pose. It has been trained using the MMFF94x and AMBER99 forcefield on the 99 protein-ligand complexes of the SIE training set [Naim]. The functional form is a sum of terms:

$$\Delta G \approx c + \alpha \left[ \frac{2}{3} (\Delta E_{\text{Coul}} + \Delta E_{\text{sol}}) + \Delta E_{\text{vdW}} + \beta \Delta S_{A_{\text{weighted}}} \right]$$

where:

- $c$  represents the average gain/loss of rotational and translational entropy.
- $\alpha, \beta$  are constants which were determined during training (along with  $c$  and are forcefield-dependent. If not using an AMBER forcefield, the parameters will be set by default to the MMFF trained parameters.
- $E_{\text{Coul}}$  is the coulombic electrostatic term which is calculated using currently loaded charges, using a constant dielectric of  $\epsilon_r=1$ .
- $E_{\text{sol}}$  is the solvation electrostatic term which is calculated using the GBVI solvation model. For more information on the GBVI solvation model, please see [Potential Energy Selection and Configuration](#).
- $E_{\text{vdW}}$  is the van der Waals contribution to binding.
- $S_{A_{\text{weighted}}}$  is the surface area, weighted by exposure. This weighting scheme penalizes exposed surface area.

## *Psychonauts' psychedelics: a systematic, multilingual, web-crawling exercise*

### *Abstract*

Psychedelics alter the perception of reality through agonist or partial agonist interaction with the 2A serotonergic receptor. They are classified as phenethylamines, tryptamines and lysergamides. These classes, according to the United Nations Office on Drugs and Crime (UNODC) and European Monitoring Centre for Drugs and Drug Addiction (EMCDDA), account for an important percentage of the new psychoactive substances (NPS) current scenario.

The paper aimed at: a) identifying and categorise psychedelic molecules from a list of psychonaut websites and NPS online resources; and b) comparing the NPSfinder® results with those from the European and United Nations databases. A crawling software (i.e. 'NPSfinder®') was created to automatically scan, 24/7, a list of URLs and to extract a range of information (chemical/street names, chemical formulae, etc.) to facilitate NPS identification. Data collected were manually analysed and compared with the EMCDDA and UNODC databases.

The overall number of psychedelic NPS detected by NPSfinder® (November 2017-February 2020) was 1344, almost ten-times higher than that reported by the UNODC and EMCDDA combined. Of these, 994 previously unknown molecules were identified as (potential) novel psychedelics, suggesting a strong discrepancy between online and real-world NPS scenarios.

The results show the interest of psychonauts, and maybe of the much larger community of 'recreational' drug users, towards psychedelics. Moreover, examining online scenarios may help in assessing the availability in the real world of psychedelic NPS; understanding drug trends; and in possibly predicting future drug scenarios.

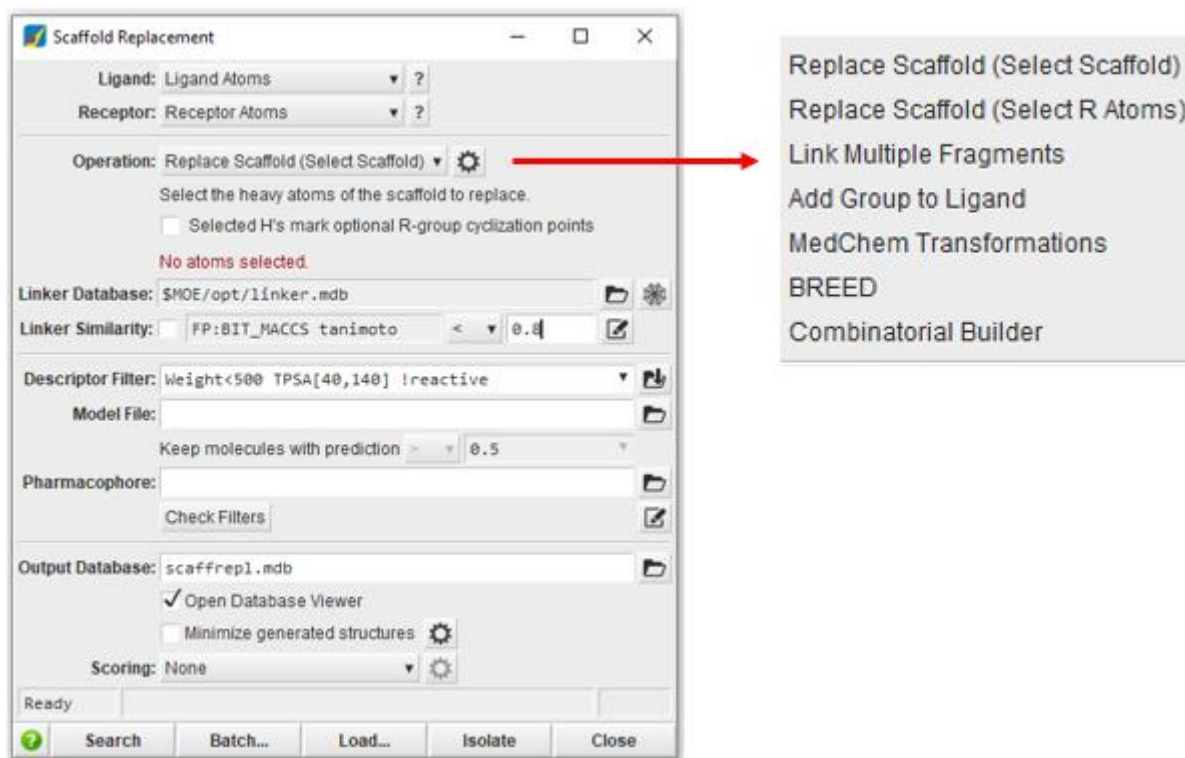


*Figure B.2* Fragment application tools interface in MOE®.

**Table B.1. Overview of the 3D and machine learning QSAR model used with Forge™. The information here presented are extrapolated from Forge™ user manual.**

<b>3 Field QSAR</b>
<p>3 Field QSAR in Forge™ is a regression method based on Partial Least Squares analysis (Wold 2001), specifically with the use of SIMPLS algorithm (deJong 1993). The latter has the advantage of using as many descriptors as the user requires, this because the latter can be correlated one to another differently to what reported for Ordinary Least Squares methodologies. The original descriptors are represented by latent variables, i.e. variables that can only be inferred indirectly through a mathematical model from other observable variables. These variables provide an equation (QSAR model) which predicts the activity as a linear combination and provide a visual interpretation of the model (electrostatic and hydrophobic coefficients).</p>
<p>To choose the number of latent variable a cross validation is carried out by progressively removing more latent variables and then choose the numbers of the latter which provide the best cross-validation output (<math>q^2</math>). The cross validation is carried out to avoid overfitting the method, i.e producing very accurate results which cannot be applied as well to new molecules well. When the performance gets worse while extracting an extra variable, the system stops and use the previous model. Default variation for cross-validation we use in Field QSAR is leave one out cross-validation (LOO CV). To assess the lack of overfitting a further validation step is carried out automatically with scramble sets (Klopman 1985). A scramble set randomly shuffles the biological activities associating them with random descriptors and generating pairs which should not be correlated. this should result in a very unproductive model, usually showing negative <math>q^2</math> values.</p>
<p>The resulting validated equation should look like</p> $y_i = \beta_{e1}e_{i1} + \beta_{e2}e_{i2} + \dots + \beta_{en}e_{in}$ <p>with <math>y_i</math> is the activity of molecule <math>i</math>, <math>e_{i1}</math> is the electrostatic potential evaluated for molecule <math>i</math> at electrostatic probe 1, <math>\beta_{e1}</math> is the regression coefficient that applies to electrostatic probe 1, and so on. This equation calculates the contribution from each sample point location to the final predicted activity. Displaying the 'field contributions to predicted activity' sizes the descriptor points by this contribution value, to see which points are increasing the predicted activity and which are decreasing it.</p>
<b>Machine Learning methods</b>
<p>All of the machine learning methods are supervised learning methods, i.e. the predictive model is built from training molecules for which we know the activity value or class</p>
<b>Random Forest</b>
<p>Random Forest (Breiman 2001) is a regression method based upon decision trees, which involve several splits for the data for a selected descriptor to fit a regression line. Random forests continue the splitting process recursively until the maximum tree depth is reached and it uses an ensemble of decision trees built from a random sample of the original descriptors. This very complex machine learning approach is based on number of trees (the most important parameter), the fraction of the total descriptors and the minimum samples per leaf, i.e. the minimum node size.</p>
<b>Relevance Vector Machines</b>
<p>Relevance Vector Machines (Michael Tipping 2000) plots descriptors for the Training Set molecules as points in <math>n</math>-dimensional space, where '<math>n</math>' is the number of descriptors. One advantage of this method is that it can deal with non-linear relationships between molecular descriptors and activity data. If the data points cannot be separated linearly, a transformation can be applied to the points so that they can be represented in a higher dimensional space, in which they may be separable. This is known as 'the kernel trick' (Aizerman 1964) and the functions that perform this operation are known as 'kernels. the training process training process uses Bayesian interference</p>

## Achievements

In this section is presented a series of the screenshots of each article, oral presentation and poster I published/presented during my PhD programme. The titles of the two successful experimental thesis I supervised at the Faculty of Pharmacy at the University of Padova are reported as well together with the image representing my research project, with which I won the first prize at the 2022 Vision and Voice competition at the University of Hertfordshire.

## Articles

ORIGINAL RESEARCH article

Front. Psychiatry, 09 February 2021  
Sec. Addictive Disorders  
<https://doi.org/10.3389/fpsyt.2020.632405>

This article is part of the Research Topic  
Drug and Behavioral Addictions During Social-Distancing  
for the COVID-19 Pandemic  
[View all 51 Articles >](#)

[Download Article](#) ▾

---

**Identifying New/Emerging Psychoactive Substances at the Time of COVID-19; A Web-Based Approach**

**22,045**   
total views

[View Article Impact](#)



European Neuropsychopharmacology

Volume 49, August 2021, Pages 69-92



## Psychonauts' psychedelics: A systematic, multilingual, web-crawling exercise

Valeria Catalani <sup>a</sup> , John Martin Corkery <sup>a</sup> , Amira Guirguis <sup>a, b</sup> , Flavia Napoletano <sup>c</sup> , Davide Arillotta <sup>a</sup>   
, Caroline Zangani <sup>d</sup> , Alessandro Vento <sup>e, f, g</sup> , Fabrizio Schifano <sup>a</sup> 

[Show more](#) ▾

[+](#) Add to Mendeley [🔗](#) Share [🗒](#) Cite

<https://doi.org/10.1016/j.euroneuro.2021.03.006>

[Get rights and content](#)



- Submit to this Journal
- Review for this Journal
- Edit a Special Issue

Open Access Article

## The Psychonauts' Benzodiazepines; Quantitative Structure-Activity Relationship (QSAR) Analysis and Docking Prediction of Their Biological Activity

by Valeria Catalani<sup>1</sup>, Michelle Botha<sup>1</sup>, John Martin Corkery<sup>1</sup>, Amira Guirguis<sup>1,2</sup>, Alessandro Vento<sup>3,4,5</sup>, Norbert Scherbaum<sup>6,\*</sup> and Fabrizio Schifano<sup>1</sup>

<sup>1</sup> Psychopharmacology, Drug Misuse & Novel Psychoactive Substances Research Unit, School of Life & Medical Sciences, University of Hertfordshire, College Lane Campus, Hatfield AL10 9AB, UK



Current Pharmaceutical Design

Editor-in-Chief >>

ISSN (Print): 1381-6128  
ISSN (Online): 1873-4286

Back Journal Subscribe

Research Article

### Designer Benzodiazepines' Activity on Opioid Receptors: A Docking Study

Author(s): Valeria Catalani\*, Michelle Botha, John Martin Corkery, Amira Guirguis, Alessandro Vento and Fabrizio Schifano

Volume 28, Issue 32, 2022

Published on: 22 September, 2022

Page: [2639 - 2652]

Pages: 14

DOI: [10.2174/1381612828666220510153319](https://doi.org/10.2174/1381612828666220510153319)

Advertiser

CHEMICAL BIOLOGY & DRUG DESIGN



RESEARCH ARTICLE

### *In silico* studies on recreational drugs: 3D quantitative structure activity relationship prediction of classified and *de novo* designer benzodiazepines

Valeria Catalani✉, Giuseppe Floresta, Michelle Botha, John Martin Corkery, Amira Guirguis, Alessandro Vento, Vincenzo Abbate, Fabrizio Schifano

First published: 15 July 2022 | <https://doi.org/10.1111/cbdd.14119>

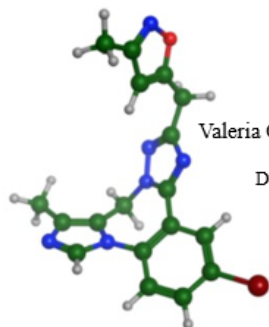


Advertisement

## Oral presentations

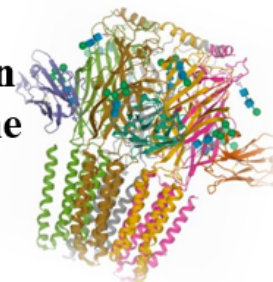


### Cognitive Enhancers: computational models on Benzodiazepines and Racetams identified online



Valeria Catalani<sup>1</sup>, Flavia Napoletano, Michelle Botha, Amira Guirguis, John Corkery, Alessandro Vento, Fabrizio Schifano

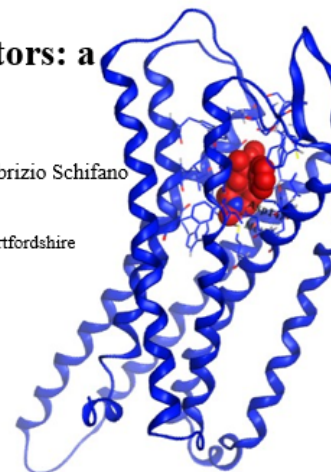
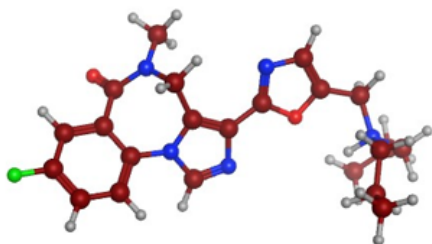
Department of Clinical and Pharmaceutical Sciences, School of Life and Medical Science, University of Hertfordshire



### Designer benzodiazepines activity on opioids receptors: a docking study.

Valeria Catalani<sup>1</sup>, Flavia Napoletano, Michelle Botha, Amira Guirguis, John Corkery, Alessandro Vento, Fabrizio Schifano

Department of Clinical and Pharmaceutical Sciences, School of Life and Medical Science, University of Hertfordshire

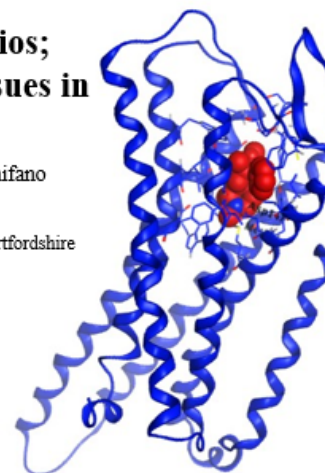
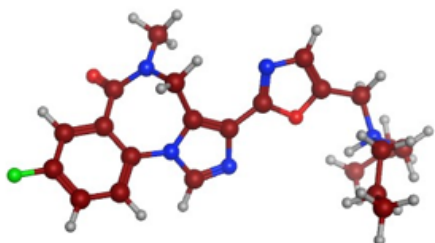




# Analysing and assessing the current web-based NPS scenarios; drafting an ad-hoc theoretical model to predict future drug issues in the real world

Valeria Catalani<sup>1</sup>, Michelle Botha, Amira Guirguis, John Corkery, Alessandro Vento, Fabrizio Schifano

Department of Clinical and Pharmaceutical Sciences, School of Life and Medical Science, University of Hertfordshire



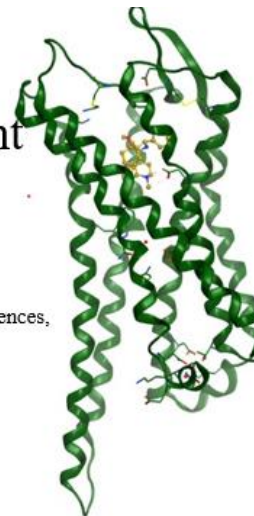
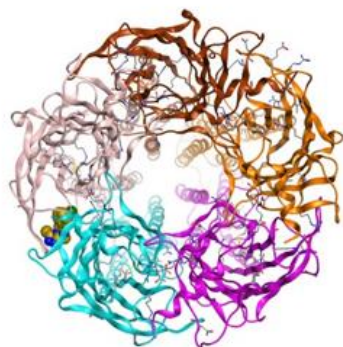
University of  
Hertfordshire **UH**



# In silico technologies: preliminary (risk)assessment on New Psychoactive Substances

Valeria Catalani<sup>1</sup>, Michelle Botha, John Martin Corkery, Amira Guirguis, Fabrizio Schifano

Psychopharmacology, Drug Misuse & Novel Psychoactive Substances Research Unit, School of Life & Medical Sciences,  
University of Hertfordshire, College Lane Campus, Hatfield, United Kingdom



University of  
Hertfordshire **UH**

# In silico studies on recreational drugs: 3D-QSAR prediction of classified and de novo designer benzodiazepines

Valeria Catalani<sup>1</sup>, Giuseppe Floresta, Michelle Botha, Amira Guirguis, John Corkery, Alessandro Vento, Vincenzo Abbate, Fabrizio Schifano

Department of Clinical and Pharmaceutical Sciences, School of Life and Medical Science, University of Hertfordshire



## Posters

### NPSfinder<sup>®</sup> designer benzodiazepines: QSAR and Docking studies.

Catalani, V. Schifano, F. Botha, M. Corkery, J. Guirguis, A  
Psychopharmacology, Drug Misuse & Novel Psychoactive Substances Research  
Unit, School of Life & Medical Sciences, University of Hertfordshire  
College Lane, AL10 9AB, United Kingdom



#### 1. Introduction

In 2017 the UNODC reported the non-medical use of benzodiazepines (BZD) as a threat to public health, with 40 United Nation member reporting them as the most used recreational sedatives/tranquillisers<sup>1</sup>. This concern increased throughout 2020, when a rise in the use of designer/NPS benzodiazepine was reported<sup>2</sup>. In April 2020, the UK Advisory Council on the Misuse of Drugs (ACMD) published evidences of health and social harms associated with their use/abuse<sup>3</sup>. In parallel UNODC reported an increase benzodiazepine-like NPS in toxicological, post-mortem and driving under the influence medical reports. BZDs are strong CNS depressants and when used in combination with other drugs cause serious toxicity with profound sedation, respiratory depression, coma, and death<sup>4</sup>.

At date, the number of NPS benzodiazepines (fig.1) identified and reported by the UNODC<sup>5</sup> and the EMCDDA<sup>6</sup> account for 31. However, results from a web crawling exercise over the surface web identified a higher number of NPS benzodiazepines, precisely 131, of which 94 unknowns. This result amplifies the concern towards unknown composition/potency of the designer benzodiazepine, making it necessary to try and understand the possible threat associated. The aim of this study was to use computational models ,QSAR and Docking, to investigate/predict the biological activity of these unknow molecules on the GABA-A benzodiazepine receptor.

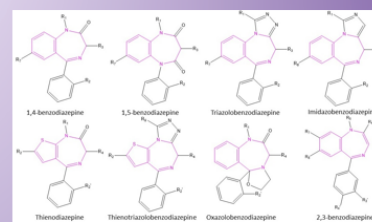


Figure 1: Common chemical backbone for NPS benzodiazepines

## Supervised experimental thesis at the Faculty of Pharmacy



**UNIVERSITA' DEGLI STUDI DI PADOVA**

**DIPARTIMENTO DI SCIENZA DEL FARMACO**

**CORSO DI LAUREA MAGISTRALE IN FARMACIA**

**TESI DI LAUREA**

**METODI COMPUTAZIONALI APPLICATI ALLO STUDIO  
DELLE NUOVE SOSTANZE PSICOATTIVE IDENTIFICATE  
ONLINE: PREDIZIONE DEL PROFILO FARMACOLOGICO  
DELLE FENETILAMMINE SINTETICHE**

**RELATORE: PROF.SSA MIOLO GIORGIA**

**CO-RELATORE: DOTT.SSA CATALANI VALERIA  
PROF. SCHIFANO FABRIZIO**

**LAUREANDO: TOSATO FILIPPO**

**ANNO ACCADEMICO 2021/2022**



**UNIVERSITA' DEGLI STUDI DI PADOVA**

**DIPARTIMENTO DI SCIENZE DEL FARMACO**

**CORSO DI LAUREA MAGISTRALE IN FARMACIA**

**TESI DI LAUREA**

**METODI COMPUTAZIONALI APPLICATI ALLO STUDIO DELLE  
NUOVE SOSTANZE PSICOATTIVE IDENTIFICATE ONLINE:  
PREDIZIONE DEL PROFILO FARMACOLOGICO DEI CANNABINOIDI  
SINTETICI**

**RELATORE: PROF.SSA CHILIN ADRIANA**

**CO-RELATORI: DOTT.SSA CATALANI VALERIA  
PROF. SCHIFANO FABRIZIO**

**LAUREANDO: CHIARO NICOLA**

**ANNO ACCADEMICO 2021/2022**

## 1<sup>st</sup> Prize at the 2022 Vision and Voice Competition



Novel Psychoactive Substance (NPS) are becoming more and more popular, and can be found in a variety of forms, including gummies. NPS, also known as legal highs, are psychotropic substances that interfere with the central nervous system causing effects comparable to the classic drugs of abuse (i.e. cocaine, heroin, MDMA, cannabis, LSD, etc). However, being them novel, their possible sought-after effects are unknown, as well as their possible side effects. This represents a serious risk and threat to public health. One way to try and tackle the issue is to proceed to an evaluation of their pharmacological/toxicological profiles. Current *in vitro* and *in vivo* methodologies are struggling to keep the pace with the speed at which NPS enter the market, hence other means need to come in support. *In silico* methodologies have been suggested for preliminary risk assessment as they are able to predict the NPS receptor profile, their binding affinity and biological activity. The current project applies computational power (Quantitative Structure Activity Relationships (QSAR), Docking studies, and Pharmacophore mapping) to predict the biological activity of designer benzodiazepines and new synthetic opioids, assess their binding profile and provide an educated guess of their potential threat.

Beware of what you eat